EXTREME WIND CLIMATE OF URUGUAY

by

VALERIA DURAÑONA

A thesis submitted to

Facultad de Ingeniería, Universidad de la República

for the degree of

Doctora en Mecánica de los Fluidos Aplicada

Thesis Director: Prof. Christopher J. Baker

University of Birmingham, United Kingdom

November, 2015

Esta tesis se la dedico a aquellos que en mi niñez
me enseñaron a apreciar los detalles
de la naturaleza,
a mirar al cielo y observar las nubes,
escuchar al viento,
estudiar la lluvia
y no tenerle miedo a las tormentas;
y a Nacho,
cuya curiosidad de niño
me ha permitido revivir esas
experiencias con él

Abstract

Uruguay belongs to the second most prone region of the world to the occurrence of severe convective storms, and to the region of South America that presents the highest frequency of occurrence of intense cyclogenesis events. Both meteorological processes produce high winds in the country, which represent a risk for the physical integrity and lives of the population, produce losses and damage to their properties and to critical infrastructure; impact the agronomic, energy, insurance and construction sectors. In particular, wind loading is the dominant environmental loading for buildings and structures in Uruguay.

Extra-tropical cyclones can produce extensive wind damage and sustain high winds speeds in large parts of the country over several hours; however, research carried out for specific sectors of the country showed that intense convective activity had been responsible for most of the wind damage and incidences reported in their cases.

The analysis of 4 years of meteorological data from 25 automatic weather stations distributed across the country also showed the significance of intense convective activity in the extreme wind climate of Uruguay: the highest wind gusts, as well as the highest 10min mean wind speeds, presented distinctive non-synoptic and transient characteristics, and usually occurred under intense convection. On the other hand, the geographic behaviour of high winds found differed from the geographic distribution presented in the official national extreme wind map, established by the national code UNIT 50-84 Wind actions on structures: the highest wind gusts would not occur along the South Atlantic and Río de la Plata coastlines and along the border with Argentina. Instead, more high wind events with higher wind speeds would be registered toward the northwest of the country. In this area, wind gusts of 40m/s were measured several times at 10m height at fixed locations in open terrain in just 4 years. In addition, a clear seasonal trend was found in wind gust speeds as well as in 10min mean wind speeds, with the highest wind speeds mainly occurring from October to March, and especially in November and February, in accordance with the behaviour of severe convective activity in the region. It could also be verified that intense convective activity as well as synoptic high wind events generate their highest wind speeds mainly from the southwest quadrant.

A similar seasonal trend was found in the 10min mean wind speeds annual maxima measured along 35 years at the official meteorological station at Carrasco airport in Montevideo, capital city of Uruguay, implying that convective activity, apart from producing the highest wind gusts across all the country, would also dominate the maxima 10min mean wind speeds measured at 10m height for longer return periods. In addition, it could be observed that the extreme value distribution of 10min mean wind speeds annual maxima for Montevideo may be adequately modelled by a Gumbel distribution, while the UNIT 50-84 wind code proposes a Frechet distribution for wind gust speeds extreme statistics.

The characteristics of non-synoptic high wind events, generally related to the occurrence of intense convective activity, should be considered in national and regional wind codes. In particular, extreme wind maps should be directly based in measurements of wind gust speeds, as there is not a direct relation between mean and wind gust speeds during severe convection. For these studies, the wind gust averaging period, the time response of the wind measuring system, as well as the quality of the wind data should be considered and carefully analysed.

In order to recommend adequate models for the flow structure of strong convective outflows for national and regional wind codes, calculations, and physical and numerical simulations, additional research and full-scale measurements would be needed. Besides the international recognition of the necessity of more full-scale measurements, these models may need to consider regional characteristics. Other aspects of the Uruguayan wind code for actions on structures are also discussed, and the necessity of their review and update is emphasised.

Resumen

Uruguay se encuentra en la segunda región del mundo de mayor ocurrencia de tormentas convectivas severas, y en la región de América del Sur con mayor frecuencia de formación de ciclones extratropicales intensos. Ambos procesos meteorológicos producen vientos intensos en el país, los cuales representan un riesgo para la integridad física de la población, producen pérdidas y daños materiales a sus propiedades y a infraestructuras críticas, e impactan sectores como el agronómico, de la energía, seguros y construcción del país. En particular, la acción del viento es la carga ambiental que domina el diseño estructural en Uruguay.

Los ciclones extratropicales pueden generar importantes daños por viento y velocidades elevadas en una amplia zona del país durante varias horas. Sin embargo, estudios realizados para sectores específicos nacionales mostraron que la actividad convectiva intensa había sido responsable de la mayor parte de los daños e incidencias por viento informadas en esos casos.

El análisis de 4 años de datos meteorológicos de 25 estaciones automáticas distribuidas en el país también indica que las tormentas convectivas intensas dominan su clima de vientos extremos: las ráfagas de viento más intensas y las mayores velocidades promediadas en 10min corresponden a eventos no sinópticos, con marcadas características transitorias, y generalmente ocurren durante actividad convectiva intensa. Por otra parte, se encontró que el comportamiento geográfico de los vientos fuertes difiere del indicado en el mapa nacional de vientos extremos dado por la norma de viento UNIT 50-84: las ráfagas de viento más intensas no ocurrirían cerca de la franja costera del país o de la frontera con Argentina, sino que se registrarían velocidades más intensas más frecuentemente hacia el noroeste del país. En varios puntos de esa zona se midieron varias veces ráfagas de viento de 40m/s a 10m de altura en 4 años. También se identificó una clara tendencia estacional tanto en las mayores velocidades de ráfaga como en las mayores velocidades medias en 10min, con valores más altos entre octubre y marzo, y sobre todo en noviembre y febrero, coincidiendo con el comportamiento de la actividad convectiva severa en la región. Así mismo, se verificó que tanto las tormentas convectivas intensas como los eventos de viento intenso de escala sinóptica producen sus vientos más fuertes del cuadrante suroeste.

Se encontró una tendencia estacional similar en los máximos anuales en 10min medidos durante 35 años en la estación de Carrasco, Montevideo, implicando que la actividad convectiva también dominaría las máximas velocidades medias en 10min a 10m de altura, para periodos de retorno mayores. Adicionalmente, se pudo observar que la estadística de vientos extremos promediados en 10min para Montevideo puede ser modelada adecuadamente por una distribución Gumbel, mientras que la norma UNIT 50-84 propone una distribución Frechet para las ráfagas de viento.

Las características de los vientos no sinópticos, generalmente relacionados a la ocurrencia de actividad convectiva intensa, y con marcadas características transitorias, deberían considerarse en las normas de acción del viento nacionales y regionales. Al no existir una relación directa entre la velocidad media y de ráfaga durante los mismos, los mapas de vientos extremos deberían basarse en medidas de velocidades de ráfagas. Para ello, los tiempos de promediación de las ráfagas, el tiempo de respuesta de los sistemas de medición y la calidad de los datos de viento utilizados deben ser tenidos en cuenta y analizados cuidadosamente.

Para recomendar modelos de la estructura del flujo durante eventos convectivos intensos para normas de viento nacionales y regionales, cálculos y simulaciones físicas y numéricas, se necesitaría realizar investigaciones y medidas de velocidad adicionales. Internacionalmente se reconoce la necesidad de contar con más medidas de campo, y por otra parte, estos modelos pueden necesitar considerar características particulares de la región. Se discute también otros aspectos de la norma UNIT 50-84 y se enfatiza su necesidad de revisión y actualización.

Acknowledgments

My most special gratitude to my thesis director, Prof. Christopher Baker, from the University of Birmingham, United Kingdom, without whom this thesis would not have been possible: first of all for receiving me at Birmingham during the first years of this PhD research; and throughout the different stages of the research and the writing up of this thesis, for all his help, advice, time, support, insight and encouragement.

Thanks to my parents for taking care of my son through different periods of this research.

Different wind databases were analysed during this research, and access to them are gratefully acknowledged: to the DNM, currently INUMET, and its personnel, for access to data and metadata of Carrasco and Antepuerto stations, to historical literature on meteorological measurements in Uruguay, and to bulletins from the Observatory of Prado station; to UTE, for access to data and metadata from its network of automatic meteorological stations, and to the ANP, for access to data and metadata from an automatic anemometer located in the Port of Montevideo. Information and advices from José Cataldo during the process of accessing and analysing meteorological data and metadata are also gratefully acknowledged.

During the search for information and different analyses required for this PhD research, several researchers were consulted. I would like to thank all of them for their time, insight, comments on various aspects of this work and for supplying copy of papers.

A special thank to Gustavo Necco, for having guided me through different analyses of meteorological data, and especially when trying to interpret the first results obtained from the analysis of data from UTE, and for sharing with me his deep insight on the extreme wind climate of the region, and to Rafael Terra, Gabriel Cazes and Gabriel Pisciottano, for discussions on this topic and suggestions of meteorological information and literature sources.

I would also like to thank Jon Wieringa, for discussion on the estimation of z_o values for Carrasco station, and for providing me with literature on homogenisation and data quality; Gonzalo Perera, for discussions on different techniques for carrying out extreme value analyses; John Holmes, for his additional encouragement to study the extreme wind climate of Uruguay, discussions on wind gust averaging periods and for supplying related literature on this topic and on historical downburst measurements; Bob Cechet and Augusto Sanabria, for receiving me in Australia and visiting Uruguay for discussing research on severe winds; Bruno Natalini, for sharing his experience on the study of damaging wind events in north eastern Argentina, for discussions on the regional extreme wind climatology, and for providing me with literature from Argentina; Ernani Nascimento and Jorge Riera, for discussions on the extreme wind climate of the south of Brazil, and for providing me with literature from Brazil; Giovanni Solari, for kindly sharing with me his deep knowledge on non-synoptic high winds in Italy; Mario Bidegain, Andrés Silva and M[a] Luisa Altinger de Schwarzkopf, for providing me with meteorological information and literature on high wind events that took place in Uruguay, and Rosario Casanova, for the estimation of the measurement height of Antepuerto station.

During the final stage of the writing-up of this thesis, exchanges with Christopher Baker, Giovanni Solari, John Holmes, Andries Kruger, Madeleine Renom and Gustavo Necco were extremely valuable. I would like to thank them for their time and advice along that stage.

I would also like to thank the economic support from the Program PDT from CONICYT, AlBan from the European Union, and the University of Birmingham, UK, which made my visits to the University of Birmingham possible, and from the School of Engineering, UdelaR, and IMFIA through different stages of this PhD research and the writing up of this thesis.

Table of Contents

1. Introduction 1
   1.1. Background, motivation and expected contributions of this work 1
   1.2. Research aims and objectives 4
   1.3. Thesis structure 5
2. Literature review 9
   2.1. Introduction 9
   2.2. Mean and extreme wind climates 9
      2.2.1. Scales of atmospheric motions, laws for flows of Atmospheric Boundary Layer type and conditions for their validity 11
         2.2.1.1. Scales of atmospheric motions 11
         2.2.1.2. The Atmospheric Boundary Layer (ABL) 15
         2.2.1.3. Flows of ABL type and models for their mean wind speed profile 15
         2.2.1.4. Wind gust speeds and gust factors 20
      2.2.2. Main characteristics of the general circulation of the atmosphere and average sea-level pressures 26
      2.2.3. High wind events 29
         2.2.3.1. Synoptic high winds 30
         2.2.3.1.1. Intense extra-tropical cyclones 30
         2.2.3.1.2. Hurricanes and tropical storms 34
         2.2.3.1.3. Subtropical cyclones 37
         2.2.3.2. Non-synoptic high winds 38
         2.2.3.2.1. Intense convective activity 38
      2.2.4. Topography and wind climate of South America 59
         2.2.4.1. Mean wind climate of SESA 63
         2.2.4.2. Extreme wind climate of SESA 66
         2.2.4.2.1. Synoptic high winds in SESA 66
         2.2.4.2.1.1. Extra-tropical cyclones in SESA 66
         2.2.4.2.2. Non-synoptic high winds in SESA 70
         2.2.4.2.2.1. Severe convective activity in SESA 70
      2.2.5. Geography and climate of Uruguay 83
         2.2.5.1. Mean wind climate of Uruguay 85
         2.2.5.2. Extreme wind climate of Uruguay 88

2.2.5.2.1. Synoptic high winds in Uruguay 91
2.2.5.2.1.1. Extra-tropical cyclones in Uruguay 91
2.2.5.2.1.2. Other synoptic weather patterns that generate high winds of synoptic temporal scale in Uruguay 95
2.2.5.2.2. Non-synoptic high winds in Uruguay 98
2.2.5.2.2.1. Severe convective activity in Uruguay 98
2.3. Data quality considerations 109
2.4. Extreme wind value analysis 114
2.4.1. Methods to calculate extreme wind speeds 114
2.5. Extreme winds in wind codes 121
2.5.1. Some international wind codes 124
2.5.2. Regional wind codes 126
2.5.2.1. CIRSOC 102 – Argentinian wind code for actions on structures 126
2.5.2.2. NBR 6123 – Brazilian wind code for actions on structures 129
3. Wind measurements in Uruguay and stations metadata 132
3.1. Introduction 132
3.2. Background on wind measurements in Uruguay 132
3.3. Network of automatic meteorological stations 134
3.3.1. Description of the stations 135
3.4. Station at Carrasco airport, Montevideo 141
3.4.1. Location and available periods of measurements 141
3.4.2. Procedure for the retrieval of wind data and metadata of Carrasco station 143
3.4.3. Metadata of Carrasco first measurement period 148
3.4.4. Metadata of Carrasco second measurement period 151
3.4.5. Metadata of Carrasco third measurement period 153
3.4.6. Metadata of Carrasco fourth measurement period 155
3.5. Observatory of Prado station, Montevideo 158
3.5.1. Metadata of Observatory of Prado station 158
3.5.2. Available information from Observatory of Prado station 161
3.6. Satellite images and other meteorological data and information 162
4. Vulnerability of Uruguay to high winds 163
4.1. Introduction 163

4.2. Background and motivation 163
4.3. Main aim and objectives of this research 167
4.4. Methodology 167
4.5. Results 170
4.5.1. General results 170
4.5.2. Correlation between wind gust speed and type of damage 171
4.5.3. Size of affected areas 172
4.5.4. Verification 172
4.6. Example: severe extra-tropical cyclone of August 23rd, 2005 174
4.7. Example: severe convective activity (MCC) on March 10th, 2002 181
4.8. Example: wind events affecting high voltage transmission lines 183
4.9. Discussion 187
5. Analysis of meteorological data from UTE network of automatic stations 195
5.1. Introduction 195
5.2. Special characteristics of this network 195
5.3. Main objectives of this analysis 198
5.4. General methodology 198
5.5. Analysis of high wind gust speeds 200
5.5.1. Methodology 200
5.5.2. Results 205
5.6. Analysis of high 10min mean wind speeds 244
5.6.1. Methodology 244
5.6.2. Results 245
5.7. Discussion 251
6. Extreme wind value analyses of 10min mean wind speed registered at Carrasco station 255
6.1. Introduction 255
6.2. Wind data homogenisation 256
6.3. Extreme wind value analysis 259
6.4. Seasonal distribution 262
6.5. Discussion 265

7. Review of wind speeds for structural design and extreme wind map of Uruguay, established in the wind code UNIT 50-84 268
7.1. Introduction 268
7.2. Background and motivation 268
7.3. Wind speeds for structural design 269
7.4. Metadata of Antepuerto station 272
7.5. Development of the national extreme wind map 273
7.6. Analysis of the wind data used, procedures and hypotheses made 275
7.7. Discussion 279
8. Summary discussion 283
9. Conclusions and recommendations for future work 296
9.1. Conclusions 296
9.2. Recommendations for future work 303
10. List of references 307
11. Annexes 2
A.1 General circulation of the atmosphere and average sea-level pressures 2
A.2 10 highest wind gust events registered at Pintado station 12
A.3 Highest wind gust events at Pintado at 45m, complete years, from the 11th case 22
A.4 Highest 10min mean wind events at Pintado at 45m, complete years 48

List of Tables

Table 2.1 Stages from tropical depressions to hurricanes (Muzeau et al., 2007) 36
Table 2.2 Saffir-Simpson hurricane scale (Schott et al., 2012) 37
Table 2.3 Fujita intensity scale for tornadoes (Holmes, 2007) 57
Table 3.1 Characteristics of the automatic stations of UTE network 137
Table 3.2 Additional characteristics of the automatic stations of UTE network 138
Table 3.3 Main characteristics of the different measurement periods at Carrasco station 143
Table 3.4 Wind sectors and corresponding wind directions 147
Table 6.1 Lower bounds for z_0 ($z_{0\ min}$) 258
Table 6.2 Upper bounds for z_0 ($z_{0\ max}$) 258
Table 6.3 Estimated parameters for the GEV and Gumbel distributions and results of statistical tests, for both sets of homogenised annual maxima 10min mean wind speed from Carrasco station 260
Table 6.4 Comparison of 10min mean wind speeds obtained for different return periods, corresponding to different measurement periods and length homogenisations (km/h) .. 262

List of Figures

Figure 1.1 Location of Uruguay (adapted from Wikipedia)....1
Figure 2.1 Names of different regions of the world and approximate corresponding latitudes (from Ahrens, 2009)....10
Figure 2.2 Length and time scales of different atmospheric motions (Markowski and Richardson, 2010)....12
Figure 2.3 Length and time scales of different atmospheric motions (from Ahrens, 2009)....12
Figure 2.4 Horizontal and depth scales of different atmospheric motions (from Markowski and Richardson, 2010)....13
Figure 2.5 Average sea-level pressure distribution and surface wind-flow patterns for (a) January and (b) July (adapted from Ahrens, 2009)....27
Figure 2.6 Distribution of cyclogenesis (individual systems) for SH winter (adapted from Taljaard, 1967)....33
Figure 2.7 Regions of the Earth where hurricanes usually originate (from University_of_Illinois, 2010)....35
Figure 2.8 Average number of tropical storms (in yellow) and hurricanes (in red) formation per year (from Guin and Saxena, 2002)....36
Figure 2.9 Downdraft at the mature stage of a convective storm (from Hermant, 2000)....41
Figure 2.10 Downburst model (Fujita 1985)....41
Figure 2.11 Expected wind speed profiles for (a) a flow of ABL type and (b) a downdraft outflow (from Lin, 2010)....44
Figure 2.12 Expected wind speed profile for a downburst outflow from a stationary storm (from Holmes, 2007)....45
Figure 2.13 Typical wind structure, pressure, wind speed, direction and temperature evolution during the passage of a downburst (from Markowski and Richardson, 2010)....45
Figure 2.14 Stages of an isolated cell (Markowski and Richardson, 2010)....46
Figure 2.15 Multicellular convection (from Markowski and Richardson, 2010)....47
Figure 2.16 MCSs sub-classification (from Markowski and Richardson, 2010)....49
Figure 2.17 Cold front passage and associated cumulonimbus (CB) clouds (Bidegain, 2007)51
Figure 2.18 Temperature and 2.5min-mean horizontal (u) and vertical (y) wind speed at 12m height, during the passage of a MCS organised in a line in Switzerland (adapted from Schmid et al., 2000)....51
Figure 2.19 Global distribution of MCCs at their maximum extent (adapted from Laing and Fritsch, 1997)....54
Figure 2.20 Number of 6h periods per year prone to the occurrence of (a) severe convective storms and (b) significant tornadoes (updated from Brooks et al., 2003 in Beniston et al., 2008)....56
Figure 2.21 South America topography (adapted from Lydolph, 1985)....60
Figure 2.22 South American main semi-permanent highs and lows, surface wind flows and ocean currents that influence SESA wind climate (fromVeblen et al., 2007)....61
Figure 2.23. Definition of South Eastern South America (SESA) and regional topography (from Salio et al., 2007)....62
Figure 2.24 Average sea-level pressure distribution for January and July for part of South America (adapted from Celemín, 1984)....64
Figure 2.25 Isolines of annual frequency of cyclogenesis (adapted from Gan and Rao, 1991) 67
Figure 2.26 Typical trajectories of extra-tropical cyclones centres in South America for (a) SH winter and (b) SH summer (adapted from Wölcken, 1954)....68

Figure 2.27 Trajectories of all cyclonic systems originating in the cyclogenesis region near 30°S over South America (from Hoskins and Hodges, 2005).....69
Figure 2.28 Map of the approximate geographical region of South America where severe convective activity is more frequent (adapted from Nascimento and Doswell, 2006).....71
Figure 2.29 Location of the most intense convective storms (from Zipser et al., 2006).....72
Figure 2.30 Location of the 1% most intense convective storms (from Zipser et al., 2006) ...72
Figure 2.31 Location of the 1% most intense convective storms (from Zipser et al., 2006) ...73
Figure 2.32 Number of high wind gusts generated by severe convective activity in the south of Brazil between 2005 and 2013 (adapted from Ferreira, 2014) 74
Figure 2.33 Geographic distribution of the passage of squall lines in Argentina (adapted from Lichtenstein and Schwarzkopf, 1970).....75
Figure 2.34 Geographic distribution of tornadoes in Argentina (adapted from Schwarzkopf and Rosso, 1993) 79
Figure 2.35 Updated geographic distribution of tornadoes in Argentina (adapted from Schwarzkopf, 2010).....80
Figure 2.36 Tornadoes occurrence presented in Dyer, 1991.....81
Figure 2.37 Location and geography of Uruguay (adapted from ElUruguayo.com, 2010) 84
Figure 2.38 Topography of Uruguay (adapted from Cataldo, 2010).....85
Figure 2.39 Annual mean wind speeds at different heights (adapted from Cataldo et al., 2010b).....86
Figure 2.40 Wind speed distribution at Florida, Uruguay, at 45.4m height (from Cataldo, 2010).....87
Figure 2.41 Wind roses for different sites and heights at the southern centre of Uruguay (from Cataldo, 2010) 88
Figure 2.42 Extra-tropical cyclone over Uruguay (adapted from Celemín, 1984).....94
Figure 2.43 Wind evolution in Montevideo during the passage of an extra-tropical cyclone over Uruguay in July, 1923 (adapted from Vieira, 1969) 94
Figure 2.44 Synoptic weather pattern associated to a 'sudestada' in Montevideo and Rio de la Plata (adapted from García, 1970).....95
Figure 2.45 Synoptic weather pattern associated to a typical 'pampero' wind in Uruguay (adapted from García, 1970).....96
Figure 2.46 Synoptic weather pattern that can cause high wind speeds from the south in Uruguay (adapted from Celemín, 1984).....97
Figure 2.47 Severe convective storm passing over Montevideo (from D'Angelo, 2013) 100
Figure 2.48 Conceptual model of a low pressure system crossing the Andes in the southern region of South America (adapted from Vera et al., 2006) 102
Figure 2.49 Locations of MCCs over SESA at their greatest extent along 2 years, and corresponding season of occurrence (adapted from Velasco and Fritsch, 1987) 103
Figure 2.50 Tracks of mid-latitudes MCCs in November along two warm seasons (adapted from Velasco and Fritsch, 1987) 104
Figure 2.51 (a): Downburst in Maryland, USA, on August 1st, 1983 (adapted from Wakimoto, 2001); (b) and (c): Downburst in Montevideo, Uruguay, on July 8th, 1935 (from Morandi, 1938) 105
Figure 2.52 Some tornadoes in Uruguay: (a) F3 tornado in Florida, April 21st, 1970 (picture taken by Juan Pastorino Torena, 2011) (b) tornado in Rocha, October 23rd, 2012 during the passage of an extra-tropical cyclone (from BluchannelTV, 2012).....107
Figure 2.53 Some waterspouts in Uruguay: (a) in Colonia, 1988, (b) in Montevideo, November 24th, 2012 (from BluchannelTV, 2012) 108

Figure 2.54 A hundred years long wind data series spoiled by gradual changes in toposcale surroundings (from Wieringa, 1996) 113
Figure 2.55 Extreme wind map in the current Argentinian wind code CIRSOC, 2005a (3s gusts with 50-year return period, values in m/s) 127
Figure 2.56 Values of the reference wind gust speed (β, values in m/s) in Argentinian wind code IRAM:11-700, 1979 (adapted from Chamlian, 1993) 128
Figure 2.57 Extreme wind map in the current Brazilian wind code, adapted from NBR:6123, 1988a 129
Figure 2.58 Proposed extreme wind map for Brazil (adapted from Beck and Correa, 2012) 131
Figure 3.1 (a) Analysed stations from UTE network, (b) Analysed stations from UTE network, Carrasco ('Aeropuerto'), Observatory of Prado ('Prado') and Antepuerto stations (images adapted from Google Earth) 136
Figure 3.2 Tower and location of anemometers at 40 and 86m height at Pintado station (adapted from Cataldo et al., 2010a) 139
Figure 3.3 Tower and anemometer at Pintado station (images from UTE) 140
Figure 3.4 Locations of main anemometers at Carrasco airport from 1960 to 2009 (adapted from Google Earth, image of 2010) 142
Figure 3.5 Format of Carrasco books between 1996 and 2009 145
Figure 3.6 Surroundings of Carrasco station, aerial picture of 1966 148
Figure 3.7 Surroundings of the control tower of Carrasco airport (Google Earth image of 2000) 149
Figure 3.8 Surroundings of the control tower of Carrasco airport taken by V. Durañona in 2007 149
Figure 3.9 View of the airport building and the control tower from the east before 1971 (FAU archive) 150
Figure 3.10 View of the airport building and the control tower from the west, 1948 (FAU archive) 150
Figure 3.11 Surroundings of Carrasco anemometer from 1977 to 1994 (Google Earth image of 2004) 151
Figure 3.12 Closer view of the surroundings of Carrasco anemometer from 1977 to 1994 (Google Earth image of 2000) 152
Figure 3.13 View from the southwest of the location of Carrasco anemometer from 1977 to 1994, picture taken by V. Durañona in 2007 152
Figure 3.14 Tower of Carrasco anemometer from 1977 to 1994, picture taken by V. Durañona in 2011 153
Figure 3.15 Surroundings of Carrasco anemometer from 1995 to 2006 (Google Earth image of 2000) 154
Figure 3.16 Closer view of the surroundings of Carrasco anemometer from 1995 to 2006 (Google Earth image of 2000) 154
Figure 3.17 Tower of Carrasco anemometer from 1995 to 2006, picture taken by V. Durañona in 2011 155
Figure 3.18 Surroundings of Carrasco anemometer from 2007 to 2009 (Google Earth image of 2006) 156
Figure 3.19 Closer view of the surroundings of Carrasco anemometer from 2007 (Google Earth image of 2009) 156
Figure 3.20 Tower, anemometer and wind vane at Carrasco from 2007 to 2009, picture taken by V. Durañona in 2011 157
Figure 3.21 Observatory of Prado station in 1901 (from Morandi, 1901) 159

Figure 3.22 Surroundings of Observatory of Prado station around 1915 (from Morandi, 1917b) 160
Figure 3.23 Observatory of Prado station around 1915 (from Morandi, 1917b) 160
Figure 4.1 (a): Isobars; (b) and (c): GOES satellite images at 21h local time during the passage of the extra-tropical cyclone of August 23rd, 2005 (from CPTEC/INPE, 2012) 175
Figure 4.2 10min mean wind speeds, wind direction and pressure evolution in Montevideo during the passage of the severe extra-tropical cyclone of August 23rd, 2005 (adapted from Cataldo and Durañona, 2005) 177
Figure 4.3 Wind gust speeds, wind direction and pressure evolution in Montevideo during the passage of the severe extra-tropical cyclone of August 23rd, 2005 179
Figure 4.4 10min mean wind speed, gust factors, temperature and pressure evolution during the passage of the severe extra-tropical cyclone of August 23rd, 2005 180
Figure 4.5 Supercell over the Río de la Plata on March 10th, 2002 182
Figure 4.6 Satellite images of the MCC of March 10th, 2002 (adapted from DNM, 2002) ... 182
Figure 4.7 Localisation of line failures and sites where wind damage was reported (adapted form Durañona and Cataldo, 2009) 184
Figure 5.1 Example of high correlation during abrupt increase in wind gust speed at heights between 10 and 75m 208
Figure 5.2 Wind speed, temperature and direction evolution at station José Ignacio during the entrance of a cold air mass on September 27th, 2009 209
Figure 5.3 Synoptic weather chart some hours before the entrance of a cold air mass into Uruguay on September 27th, 2009 (CPTEC/INPE, 2012) 210
Figure 5.4 Infrared image from GOES 10 satellite (adapted from CPTEC/INPE, 2012) at 15:15h local time on September 27th , 2009 211
Figure 5.5 Examples of events that presented wind gust speed with: (a) a very pronounced peak, (b) a pronounced peak 214
Figure 5.6 Examples of events that presented wind gust speed with: (a) an abrupt increase and gradual decrease, (b) an increase and decrease within several hours 215
Figure 5.7 GOES satellite images corresponding to the events illustrated in Figure 5.5 and Figure 5.6 (adapted from CPTEC/INPE, 2012) 217
Figure 5.8 Wind speed, temperature and direction evolution at station Valentines during the passage of a cold front on January 16th, 2011 219
Figure 5.9 Maximum wind gust speed registered at each station during the passage of a cold front during April 4th and 5th, 2012 (*) 223
Figure 5.10 Maximum wind gust speed registered at each station during the passage of an intense extra-tropical cyclone on September 19th, 2012 (**) 226
Figure 5.11 Wind speed, temperature and direction evolution at the station that registered the highest wind gust in Uruguay during the passage of the intense extra-tropical cyclone of September 19th, 2012 227
Figure 5.12 Characteristics of high wind gust events at 45m at station 11-Pintado 233
Figure 5.13 Characteristics of high wind gust events at 45m height in the network 236
Figure 5.14 Characteristics of events with wind gust speeds > 80km/h at 45m height 239
Figure 5.15 Characteristics of events with wind gust speeds > 104km/h at 45m height 241
Figure 5.16 Characteristics of high 10min mean wind events at 45m at station 11-Pintado . 248
Figure 5.17 Characteristics of high 10min mean wind events at 45m in the network 250
Figure 6.1 Monthly distribution of the 10min mean wind speed annual maxima from Carrasco station, homogenised with z_{0min} 264

Figure 6.2 Monthly distribution of the 10min mean wind speed annual maxima from Carrasco station, homogenised with z_{0max}.....264
Figure 7.1 Annual maxima wind gust speeds registered at Antepuerto station from 1906 to 1969 (km/h) 270
Figure 7.2 Antepuerto station and surroundings (from IMM data).....272
Figure 7.3 Current Uruguayan extreme wind map: values of the reference wind speed (β, in m/s, at 10m height) in the Uruguayan wind code UNIT:50-84.....274
Figure 7.4 Antepuerto station and surroundings 278
Figure 7.5 Location of anemometers at Antepuerto station (image from DNM).....278
Figure 8.1 Main mechanism for the development of MCSs in SESA (Vera et al., 2006) 284

List of acronyms

ABL	Atmospheric Boundary Layer
ACER	Average conditional exceedances rate method
ANP	National Administration of Ports
ANTEL	National Administration of Telecommunications
BSE	State Insurance Bank
CPTEC	Centre for Weather Prediction and Climate Studies, from Brazil
DNE	National Directorate of Energy
DNM	National Directorate of Meteorology (former)
FAU	Uruguayan Air Force
GEV	General Extreme Value
GPD	Generalised Pareto distribution
IAWE	International Association of Wind Engineering
IMFIA	Institute of Fluid Mechanics and Environmental Engineering
IMM	Municipal City Council of Montevideo
INMET	Brazilian National Institute of Meteorology
INUMET	National Institute of Meteorology (current)
ITCZ	Intertropical Convergence Zone
LLJS	Low-level jet stream
MCC	Mesoscale convective complex
MCS	Mesoscale convective system
MGAP	Ministry of Agriculture, Livestock and Fishing
MIEM	Ministry of Industry, Energy and Mining
MIS	Method of independent storms
ML	Maximum Likelihood

NH	Northern Hemisphere
NOAA	National Oceanic and Atmospheric Administration
POT	Peak-over-threshold
PWM_s	Probability weighted moments
SA	South America
SALLJ	South American low-level jet
SE	Standard error
SESA	South Eastern South America
SH	Southern Hemisphere
SINAE	National Emergency System
SST	Sea surface temperature
ST	Subtropical cyclone
TRMM	Tropical Rainfall Measuring Mission
UdelaR	University of the Republic (Uruguay)
UTC	Universal time coordinated
UTE	National Administration of Power Stations and Electrical Transmissions
WGWS	Working Group on Wind Structure set up by IAWE
WGF	Working Group on Extreme Wind Prediction and Zoning set up by IAWE

List of notation

b	Empirical parameter for estimating height of logarithmic sub-layer
d	zero plane displacement
D	Depth scale of an atmospheric motion
F	Cumulative distribution function
f	Coriolis parameter
H	High pressure area
i.i.d.	Independent and identically distributed
k	Shape parameter of the GEV distribution
κ	von Karman's constant
L	Low pressure area
L	Horizontal length scale of an atmospheric motion
Ln	Natural logarithm
n	Power lax exponent or potential index
N	Number of elements in an extreme data series
N	Brunt-Vaisala frequency
t	Time
T	Temperature
T	Return or recurrence period
U	Mean horizontal wind speed
U_{gust}	Horizontal wind gust speed
$U_{gust\ 10m}$	Horizontal wind gust speed at 10m height
$U_{gust\ 45m}$	Horizontal wind gust speed interpolated at 45m height
U_{max}	Maximum horizontal wind speed registered in a period of 10min

U_{ref}	Mean horizontal wind speed registered at height z_{ref}
U_{10min}	Mean horizontal wind speed averaged in 10min
$U_{10min\ 45m}$	Mean horizontal wind speed averaged in 10min at 45m height
u_*	Friction velocity
V	Vertical mean wind speed
x_i	Maximum wind speed during period i
X_T	Wind speed exceeded on average once every *T* years
y	Reduce variate for extreme statistics analysis
z	Height above ground
z_g	Gradient height
z_L	Height of logarithmic sub-layer
z_r	Height of roughness sub-layer
z_{ref}	Height at point of reference
z_0	Surface roughness length

Greek letters

β	Reference wind speed for Frechet distribution
δ	Atmospheric Boundary Layer (ABL) height
δ_I	Internal sub-layer height after a change in roughness
γ	Shape factor for Frechet distribution
μ	Location parameter of extreme value distribution
σ	Scale parameter of extreme value distribution

Chapter One

Introduction

1.1. Background, motivation and expected contributions of this work

Uruguay is located in the south eastern region of South America (SA) (Figure 1.1), between the latitudes of 30° and 35º south and the longitudes of 53º and 58º west, being part of the mid-latitudes. It has an area of approximately 175,000 km^2 and a population of around 3.3 million people, of whom 1.3 million live in Montevideo city, its capital.



Figure 1.1 Location of Uruguay (adapted from Wikipedia)

The extreme wind climate in this region of the world is principally governed by severe convective activity, and by extra-tropical cyclones that intensify during their trajectory (Durañona, 2010; Schwarzkopf and Rosso, 1993; Loredo-Souza, 2012) with a predominant translation direction toward the southeast.

Uruguay belongs to the region most affected by severe convective events in South America (SA) (Nascimento and Doswell, 2006), and also to one of the regions of the Southern Hemisphere (SH) that experiences significant cyclogenesis events over land more frequently (Gan and Rao, 1991; Seluchi, 1995). As a consequence of its strong extreme wind climate, damaging wind events of different length and time scales occur rather frequently, ranging from intense synoptic winds to more localised high winds, as downdraft outflows, and in some cases, tornadoes (Durañona, 2010; Nascimento and Doswell, 2006; Schwarzkopf and Rosso, 1993).

These events represent a risk for the lives of the population, produce losses and damage to their properties and to critical infrastructure, as for example to that belonging to the electrical or communication areas. High winds impact on different economic sectors of Uruguay (Durañona, 2011b): in the energy sector they are responsible for interruptions and damage to the electric transmission and distribution systems; in the agronomic sector, they produce crops, fruits, trees, forests and greenhouses damage and losses; in the construction sector, they cause failures of buildings and structures of different kind; in the maritime transport of goods and people, they affect ships and harbour operations, to cite some examples.

There exist many reports of high winds in Uruguay and of their associated damage (Durañona, 2010), although this documentation has not been systematic (Durañona, 2011b) as it is usually the case in this region of the world (Nascimento and Doswell, 2006). The analysis and documentation of existent and new data can assist with the prevention and/or mitigation of the effects of the Uruguayan extreme wind climate on different areas, as well as with the improvement of the safety of its population. These topics are addressed in Chapters 4 to 6 of this thesis.

The necessity and relevance of reviewing and updating extreme wind value analyses is also widely recognised. In particular, wind is the most critical environmental loading affecting the structural design in many parts of the world, and extreme wind climatology provides information on the extreme winds that might affect a structure during its lifetime, which is required for making rational decisions on the magnitude of the wind loads to be used in design (Simiu and Scanlan, 1996).

In Uruguay, the national wind code for actions on structures UNIT:50-84, 1984 is the official source of extreme wind information for structural design, as well as for any controversy that may arise related to high wind events in the country. However, the design wind speeds and extreme wind map for wind loading calculations presented in this code were obtained with wind data measured from 1906 to 1969 at a non-standard exposure, and with the knowledge and tools available more than 30 years ago. Several hypotheses were made during its establishment, and the document that described these processes already recognised that they should be reviewed when more information were available. Advances in the last decades in the wind engineering and regional meteorology fields have brought concerns on several

assumptions made during these developments. In spite of this, and of the multiple and significant consequences of the impact of high winds in Uruguay, neither the characterisation of the extreme wind climate of the whole country nor the necessity to review the national design wind speeds and extreme wind map were addressed during the last decades. Chapters 4 to 6 present useful information for the characterisation of the extreme wind climate of Uruguay, while Chapter 7 analyses the extreme wind map and design winds established in the national wind code.

The PhD research presented in this thesis aimed at covering this lack of information with a wind engineering approach, through the search, documentation and analysis of historical and current high wind events in Uruguay and related wind data literature, and through the analysis and discussion of the data, metadata and procedures applied to obtain the design wind speeds and extreme wind map established in the wind code UNIT:50-84, 1984.

On the other hand, the vulnerability of Uruguay to high winds has increased in the last few decades as a direct consequence of the growth of exposed resources, such as taller and more expensive buildings of different shapes in Montevideo and other areas, many of them built with glass curtain wall facades; bigger ships visiting the country; more tall antennas and solar collectors over the roofs of buildings in populated areas; the continuous increase of medium and low-voltage distribution lines; the recent growth of wind farms installations or the exponential increase of productive forest plantations in different regions of the country. This in turn has increased the hazard that high winds represent for the population. It is then a matter of concern to search, analyse and keep up to date as much information as possible on the highest wind speeds that occur in the country, as this information will allow a better understanding of the actual vulnerability to extreme winds, as a first step towards prevention.

The results obtained from this PhD research can contribute to the revision of the national extreme wind map, the update of the national wind code, the development of specific wind codes that Uruguay lacks of, the improvement of measures taken during the occurrence of high wind events, the improvement of management of existing insurances, the creation of new insurance products, as well as other important issues needed to be addressed in order to accompany the increase of vulnerability to high winds.

Last but not least, the information presented in this thesis may help policy and decision-makers becoming more aware of the strong extreme wind climate of Uruguay and of its different impacts, and of the necessity of counting with reliable meteorological data and other sources of information to analyse this climate, enough funding for research on extreme winds and their effect on different sectors of the country, new prevention and mitigation plans, updates of existing wind codes and/or the creation of new ones that the country may need.

1.2. Research aims and objectives

The main aims of the PhD research presented in this thesis are summarised below.

1. To identify and characterise the main types of high wind events that determine the extreme wind climate of the country, their relative contribution to it, and the most common types of wind damage produced.

2. To document and analyse the main characteristics of available wind databases and sources of information on high wind events, current as well as historical, and discuss the type of wind measurements required to adequately characterise the extreme wind climate of Uruguay, and in particular, the one needed to update the national extreme wind map, established in the wind code UNIT:50-84, 1984 Wind action on structures.

To achieve these aims, a number of objectives were set and are presented below.

1. Conduct a search and analyse available sources of information regarding damaging wind events that occur in Uruguay, generate a database with the main characteristics of these events and their effects, and estimate a threshold wind speed for wind damage.

2. Conduct a search and analyse available historical and current wind measurements, and the quality of the data and metadata of the corresponding meteorological stations.

3. Analyse the high wind events that cause wind damage in the country, and describe their main characteristics, such as wind speed evolution with time, expected wind speed values,

frequencies of occurrence, predominant wind directions, seasonal distribution, gust factors, wind speed distribution with height, typical trajectories, etc. Compare and link these results with information presented in historical literature and with national, regional and international research in the fields of meteorology and wind engineering.

4. Perform extreme wind value analysis on available wind data series of adequate length and quality, and estimate the frequency of occurrence of potential damaging wind events in the case of short records.

5. Describe and discuss the characteristics of the wind data, corresponding metadata and procedures applied for determining the design wind speeds for Uruguay and developing the national extreme wind map established in the national wind code UNIT:50-84, 1984. Compare and discuss the probability and geographical distributions of extreme winds presented in this code with those obtained from other wind databases studies.

1.3. Thesis structure

The thesis is organised into 9 chapters, including the current chapter, Chapter 1, which presents the background and general aims of this PhD research.

Chapter 2 presents a review of the literature on scales of atmospheric motions, the main characteristics of Atmospheric Boundary Layer (ABL) flows, wind gust speed measurements and gust factor values during convective and non-convective high winds, a basic description of the global circulation of the atmosphere, a classification of extreme wind events and a review of the prior knowledge on regional and national mean and extreme wind climate. It also presents a review on data quality considerations, extreme wind value analyses, and the main characteristics of current international and regional wind codes.

Chapter 3 describes the main wind databases analysed during this research and their corresponding metadata.

Chapter 4 presents a first research carried out to identify the most common types of wind damage produced in Uruguay, including as examples the description and consequences of two

different extreme wind events, and an analysis of the effect of high wind events on high voltage transmission lines.

Chapter 5 describes the methodology and results obtained from the analysis of relatively recent installed automatic meteorological stations, which continuously measure different meteorological parameters at heights from 10 to 100m across the country.

Chapter 6 presents the methodology and results obtained from the extreme value analysis of a 35 years long 10min mean wind database from Montevideo.

Chapter 7 reviews and discusses the procedures, assumptions and information used to obtain the design wind speeds for Uruguay and the national extreme wind map established in the national wind code UNIT:50-84, 1984.

Chapter 8 discusses the whole thesis research, and especially the results obtained in Chapters 4 to 7 and the links among them. It also compares and relates them to previous information on the extreme wind climate of Uruguay reviewed in Chapter 2, taking also into account the current knowledge on the extreme wind climate of the region. The importance of considering wind data quality and metadata during extreme wind research is stressed, and the necessity of reviewing and updating the national wind code is justified.

Finally, Chapter 9 presents the main conclusions of the research presented in this thesis and several recommendations for future work.

Along the time this PhD research was conducted, the available information to characterise the extreme wind climate of Uruguay gradually increased, both quantitative and qualitatively, changing the type of results that could be obtained from its analysis.

In the beginning, it mainly consisted in the description of damaging wind events available principally in newspapers, in isolated reports of high wind events usually prepared by meteorologists, and in wind data records of relatively short length from few meteorological stations. Consequently, this PhD research focused on characterising the damaging wind events that occur in Uruguay and the principal features of the vulnerability of the country to high wind events, through the generation of a comprehensive database of wind damage

information, giving also place to several publications. This research is presented in Chapter 4 of this thesis.

After some time, access to two important wind databases was granted or obtained. These databases presented different characteristics, and their analyses allowed a more detailed description of the main characteristics of the potential damaging wind events that occur in Uruguay. These analyses, whose results have been also published and presented in Conferences, are described in Chapters 5 and 6.

This thesis tries to link these different types of research conducted along the years, and to present their results in the context of the current knowledge of the regional extreme wind climatology, giving also a historical perspective of intense wind events that have been documented in Uruguay and in South Eastern South America during the last century.

It is worth pointing out that this thesis contains a series of original contributions for the field of wind engineering, in particular in relation to the characteristics of non-synoptic high wind events. The analysis of this type of high wind events is of current international interest for the wind loading of structures in regions where severe convective activity is a dominant feature of their extreme wind climates, as it was found it was the case of Uruguay, as well as for the estimation of design wind loads for long return periods worldwide. It has been widely and internationally recognised the lack of full-scale measurements of this type of high winds for their study, and the data gathered during this PhD research may offer a rich and invaluable source of information on this type of event. In particular, Annexes A.2 to A.4 were especially included in this thesis as examples of the type of information that can be obtained from the meteorological stations from UTE network, whose characteristics may be unique.

On the other hand, Chapter 5 offers a first characterisation of actual measurements of high wind events in Uruguay, applying a novel approach, and points out the significance of non-synoptic high winds in the extreme wind climate of the country. In particular, it illustrates their distinctive transient characteristics and their tendency to occur under intense convective activity. It also proposes a method to analyse the time evolution of high wind events at fixed points in the country, as well as their time evolution over the country.

The important differences found between the characteristics of synoptic and non-synoptic high winds highlights the relevance of reviewing the scheme for wind loading calculation outlined in the national wind code for structures, UNIT:50-84, 1984, as well as the national extreme wind map. In particular, the presented research shows a different geographic behaviour of high winds from the one proposed in the national extreme wind map, with more high wind events toward the northwest of the country instead than along its coastline and border with Argentina, as well as a distinctive seasonal behaviour, with higher wind speeds registered in spring and summer than in other seasons of the year, characteristics that may be relevant for different wind engineering applications.

Results described in Chapter 5 and 7 also suggest the importance of carrying out new extreme value analysis on wind gust speed records of verified quality, with the aim of recalculating design wind speeds values for different regions of Uruguay; while Chapter 5 and 6 show that non-synoptic high winds would also have an effect on extreme 10min mean wind speeds. The lack of correlation between high wind gust speeds and their corresponding 10min mean wind speeds is highlighted in Chapter 5.

On the other hand, Chapter 4 presents a preliminary characterisation of the impact of high wind events on different sectors of Uruguay, and a description of the most common types of damage that high winds produce in the country, which may help improving the awareness of the general public and local governments to these potential threats to human lives and properties, and lead to the improvement of policies for the prevention and management of these risks and economic losses.

Finally, Chapter 9 proposes a number of new lines of research to continue investigation under the light of the main findings obtained during this PhD research.

Chapter Two

Literature review

2.1. Introduction

In this chapter, Section 2.2 provides an overview of the different scales of atmospheric motions, of the global and regional mean and extreme wind climates, of how extreme winds are usually characterised in the wind engineering field, of the national mean wind climate and of the previous knowledge on the Uruguayan extreme wind climate. Section 2.3 justifies the importance of analysing the quality and homogeneity of wind databases used for research on extreme wind and the necessity of counting with adequate metadata; while Section 2.4 reviews and describes the most common methods used to perform extreme wind value analyses in the wind engineering field. Finally, Section 2.5 provides an overview of the main international and regional wind codes currently in use. Information on how the Uruguayan wind extreme map was developed and the design wind speeds calculated is presented and discussed in Chapter 7.

2.2. Mean and extreme wind climates

In this section, Sub-section 2.2.1 introduces general concepts for the development of the following sub-sections and sections. Different scales of atmospheric motions are defined, as well as the terms ‘synoptic’ and ‘non-synoptic’, for its use in the context of this thesis. This sub-section also describes the main characteristics of the Atmospheric Boundary Layer (ABL) and of flows of ABL type. The concepts of wind gust speeds and gust factors are introduced, and, in particular, a distinction is made between gust factors generated by convective and by non-convective extreme winds.

Sub-section 2.2.2 presents general concepts of the global mean wind climate, while Sub-section 2.2.3 describes different mechanisms and weather systems that generate extreme winds of different scales worldwide.

The main features of South America topography and climate that influence the extreme wind climate of South Eastern South America (SESA), region to which Uruguay belongs, and the mean and extreme wind climate of this region are presented in Sub-section 2.2.4. Sub-section 2.2.5 describes the main features of the geography and climate of Uruguay that influence its

extreme wind climate, and summarises the main characteristics of its mean wind climate and the previous knowledge of its extreme wind climate.

As different regions of the world present distinctive meteorological behaviours depending on their latitudes, and references to these regions are made along this thesis, Figure 2.1 indicates the names that apply to them and their approximate latitudes.

The Equatorial region is limited between 10°N and 10°S latitudes, while the tropical regions would correspond to latitudes between 10° and 23°. The subtropics are located roughly between latitudes 23° and 35°, while mid-latitudes can be considered to lay between latitudes 23.5° and 66°, or between 30° and 50°, depending on the bibliographical reference.

As indicated in Section 1.1, Uruguay is located between latitudes 30°S and 35ºS, therefore belonging to the mid-latitudes and also to the subtropics. This part of the world experiences a wide variety of fast changing weather, as cold air masses from the poles and warm air masses from the tropics reach this region, sometimes alternating within hours of each other.

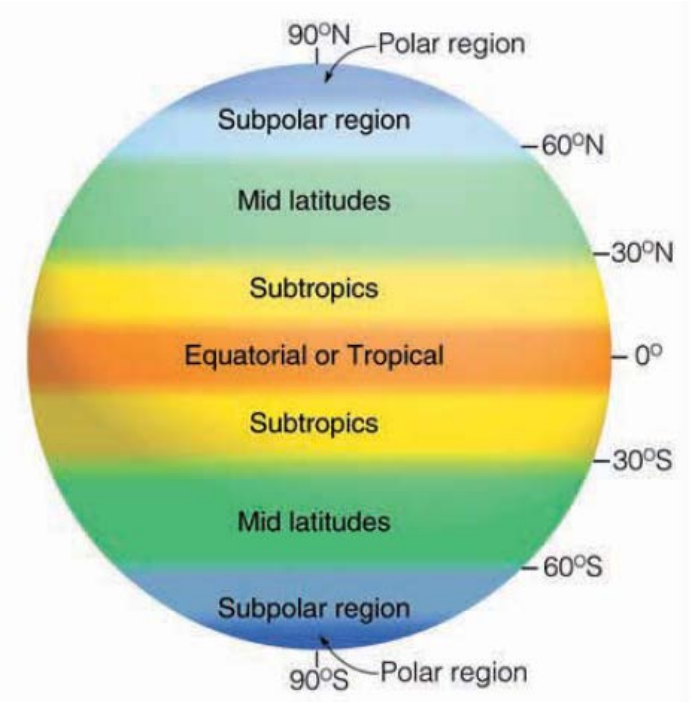


Figure 2.1 Names of different regions of the world and approximate corresponding latitudes (from Ahrens, 2009)

2.2.1. Scales of atmospheric motions, laws for flows of Atmospheric Boundary Layer type and conditions for their validity

2.2.1.1. Scales of atmospheric motions

Wind is air in motion. The movement of air transports heat and moisture and moves storms and large fair-weather systems around the globe from one area to another. Wind speed is a meteorological variable dependent on height, location and time; very influenced by nearby obstacles, as mountain ranges, forests, cities, hills, trees, buildings in a wide range of scales, and can also vary very fast with time under certain weather conditions. These characteristics make its study and description quite complex.

Atmospheric motions take place within a range of space and time scales. The rotation and differential heating of the Earth, as well as the interaction between atmospheric motions and sea surface and topography determine the global, regional and national mean and extreme wind climates.

The mean free path of molecules and the circumference of the Earth place lower and upper bounds on the length scales of atmospheric motions. The time scales of atmospheric motions can range from tenths of seconds, in the case of small scale turbulent motions, to as long as weeks in the case of planetary scale waves (Markowski and Richardson, 2010).

Meteorological phenomena having short temporal scales tend to have small spatial scales, and vice versa. Figure 2.2 illustrates this concept, showing that the ratio of horizontal lengths to time scales is of the order of ∼10m/s for most meteorological phenomena (Markowski and Richardson, 2010). This figure also shows the definition of different scales according to Orlanski, 1975 and Fujita, 1981 classification schemes. In this figure N stands for the Brunt-Vaisala frequency, and f is the Coriolis parameter, as indicated in Markowski and Richardson, 2010.

Figure 2.3 is similar to Figure 2.2, with the differences that it includes some meteorological phenomena that do not appear in Figure 2.2, it lacks of others shown in Figure 2.2, and presents other definitions for the synoptic scale, the mesoscale and the microscale. On the other hand, Figure 2.4 illustrates typical depth (D) and horizontal length scales (L) of some atmospheric motions.

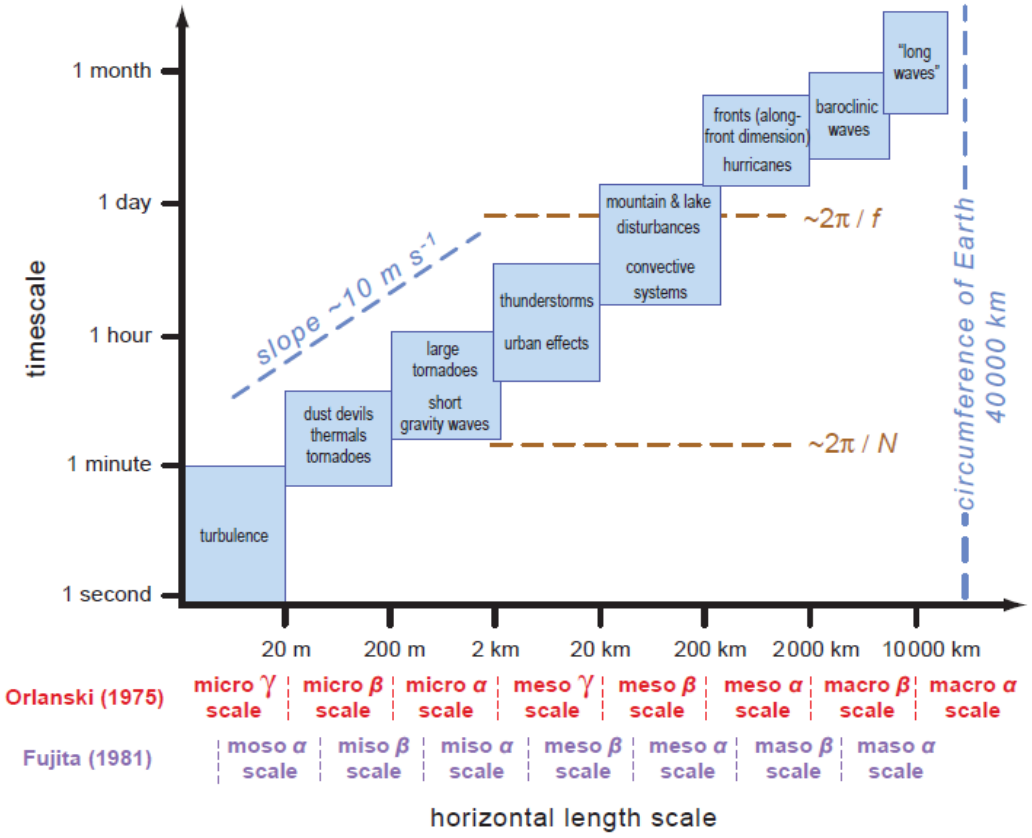


Figure 2.2 Length and time scales of different atmospheric motions (Markowski and Richardson, 2010)

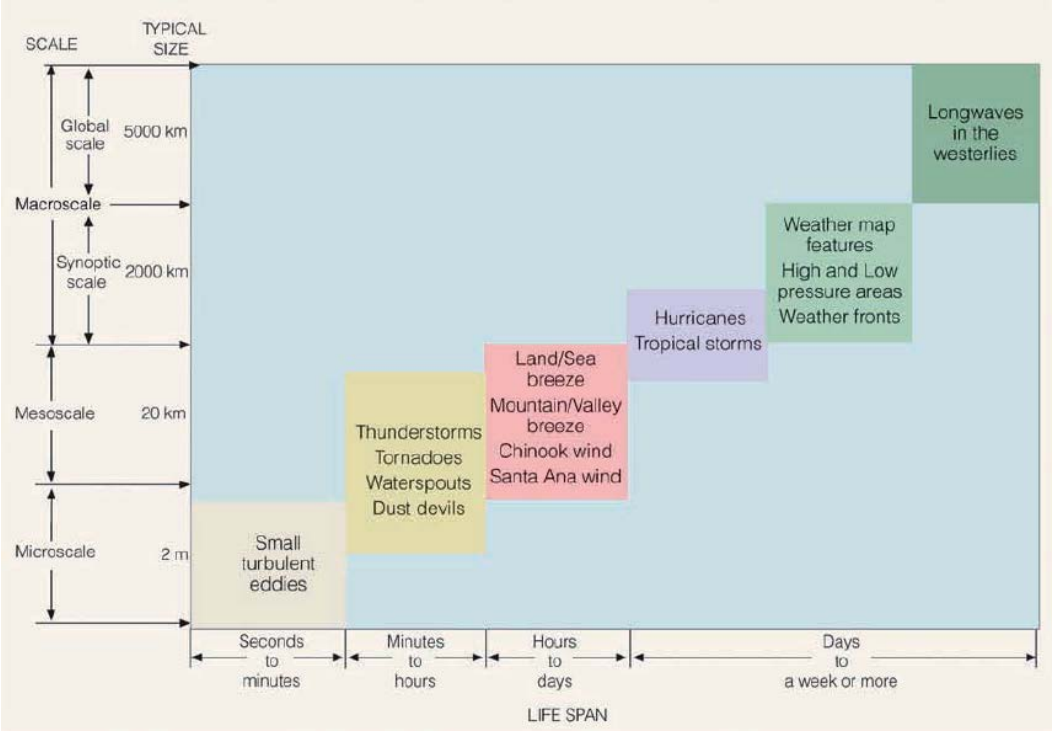


Figure 2.3 Length and time scales of different atmospheric motions (from Ahrens, 2009)

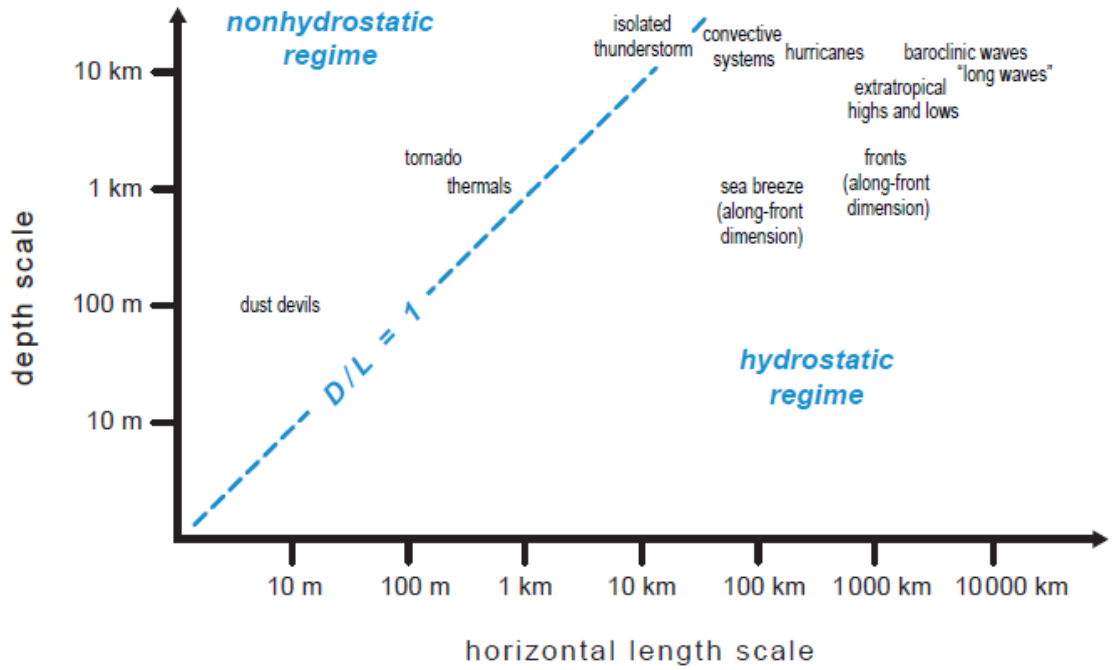


Figure 2.4 Horizontal and depth scales of different atmospheric motions (from Markowski and Richardson, 2010)

Along this thesis, the terms ‘synoptic’ and ‘non-synoptic’ will be used. According to Figure 2.2 and Figure 2.3, winds from high and low pressure areas, as anticyclones and cyclones (including extra-tropical cyclones, hurricanes and tropical storms, described in Sub-section 2.2.3.1) can be classified as synoptic, as well as other weather map features. The horizontal length scales of these atmospheric motions range from several hundreds of kilometres to few thousands kilometres. It is worth mentioning that there is more complete understanding of the synoptic scale meteorology than that on scales smaller than synoptic (Doswell, 2003b).

In this thesis, non-synoptic winds will refer to the atmospheric motions that cannot be classified as synoptic, in particular to atmospheric motions caused by convective storms (also referred to as thunderstorms in the literature), land/sea and mountain/valley breezes; downslope winds and mountain waves, among others. These atmospheric motions have length scales usually smaller than hundreds of kilometres and are described in Sub-section 2.2.3.2. In particular, a general description of severe convective storms is presented in Sub-section 2.2.3.2.1.

Due to the characteristics of the meteorological data available for conducting the research presented in this thesis, high wind events are classified as synoptic or non-synoptic according to their time scales as registered at a fixed point. Along this thesis high events are considered to have the characteristics described in Sub-section 4.5.1. Synoptic high wind events are considered to be those that sustain high wind speeds during at least around half a day, while non-synoptic winds are considered as those that sustain high wind events along less than few hours. These time scales would be related to the length scale of the atmospheric motions and to their translational speeds, as well as to the lifespan of each atmospheric motion, in the sense that if high wind speeds cease, they would no longer be registered at any point.

It is worth noting that along this thesis the term mesoscale is also used. This scale of motion is smaller than the synoptic scale and larger than the microscale, and therefore it is classified as non-synoptic in this thesis. Different definitions of the mesoscale and microscale are shown in Figure 2.2 and Figure 2.3. According to Markowski and Richardson, 2010, the Lagrangian (following a particle) time scales of mesoscale phenomena in mid-latitudes range from 10min on average to approximately 17 hours. Typical length scales of mesoscale events range from few kilometres to few hundreds kilometres (Ahrens, 2009; Markowski and Richardson, 2010).

Examples of mesoscale events that can develop high wind speeds are mesoscale convective systems (MCSs), ranging from groups of convective storms of length scales of about 100km, to huge mesoscale convective complexes (MCCs) (Velasco and Fritsch, 1987; Markowski and Richardson, 2010); downslope winds, land/sea breezes or mountain/valley circulations under certain circumstances, among others. Fronts are considered to be mesoscale events in this thesis, taking into account the length scale of their width, which allows them to sustain high winds during tens of minutes to sometimes several hours during their passage at a particular point. A general description of these air motions is presented in Sub-section 2.2.3.2.

At the mesoscale, air motions are driven by a variety of mechanisms: they can be either entirely topographically forced or thermally driven, or produced by any combination of instabilities that operate on the mesoscale.

Although definitions for different scales of atmospheric motions exist, it should be reminded that circulations of all sizes simultaneously take place within the atmosphere and may influence each other. Small eddies form inside larger ones, which in turn encompass

meteorological phenomena of even larger length scales. Mesoscale processes like downslope winds, fronts, etc., often operate in association with synoptic-scale systems, and may act as intermediaries between the microscale and the synoptic scale (Doswell and Bosart, 2001).

It is a general principle in meteorology that, as the size of a weather system decrease, the severity of the weather it can create increases. Although synoptic scale systems can produce widespread damage, it is not usually the most intense. However, the conditions within such storms can result in smaller concentrations of severe weather that become even more potentially hazardous. For example, tornadoes and downbursts are usually embedded into larger convective systems; regions of higher winds as downbursts, sting jets, or even tornadoes, may be found inside extra-tropical cyclones; tornadoes can occur inside hurricanes, etc. The definition and a conceptual model of a downburst can be found in Sub-section 2.2.3.2.1.

2.2.1.2. The Atmospheric Boundary Layer (ABL)

The Earth's surface exerts a drag force on the moving horizontal air, whose effect is to retard the flow (see for example Simiu and Scanlan, 1996). This effect is diffused by turbulent mixing throughout a region referred to as the Atmospheric Boundary Layer (ABL). The term 'boundary layer' is used in this case to refer to the region of the wind flow where the friction at the Earth's surface affects its wind speed, and it is considered to be similar in many aspects to the turbulent boundary layer that develops over a flat plate (Holmes, 2007). For large storms such as extra-tropical cyclones, this region can extend up to 500–1,000m high.

2.2.1.3. Flows of ABL type and models for their mean wind speed profile

Usually in the field of wind engineering, and along this thesis, a flow of ABL type is considered to have characteristics similar to those of boundary layers developing over rough surfaces. In these cases, and under neutral atmospheric conditions (see e.g. Rogers and Yau, 1989), mean wind speed variation with height can generally be modelled by Equations (2.1) and (2.5), as it will be seen below.

Regarding the distribution of mean wind speed with height inside an ABL flow, three sub-layers can be defined, as for turbulent flows (Schlichting, 1979; Raupach et al., 1991): a roughness sub-layer, a logarithmic sub-layer and a wake sub-layer.

According to Raupach et al., 1991, the roughness sub-layer depth is around 1 to 5 times the mean height of the roughness elements. The flow in this region is three-dimensional, very heterogeneous and highly dependent on the geometry of the obstacles.

Above the roughness sub-layer, a logarithmic sub-layer can be found, as presented for example in Schlichting, 1979. In this sub-layer, the mean wind speed profile for neutrally stratified flows approximately follows a logarithmic law, as shown by Equation (2.1):

$$U(z) = \frac{u_*}{\kappa} \cdot \mathrm{Ln}\left(\frac{z-d}{z_0}\right) \tag{2.1}$$

where U is the mean wind speed at height z; u_*, the friction velocity; Ln, the natural logarithm; κ = 0.4, the von Karman's constant; and d and z_0, the zero plane displacement height and roughness length of the upwind surface, respectively.

Plate, 1982 and Simiu and Scanlan, 1996, among other authors, present laws for the wind speed profile in the logarithmic sub-layer for other conditions of atmospheric stability.

Physically, z_0 is related to the total magnitude of the shear forces acting on the surface, while d would scale the vertical distribution of these forces in the surface canopy (Wieringa, 1993). d cannot be disregarded above dense high vegetation or over built-up areas (Wieringa, 1992), where it can take values of about three-quarters of the general rooftop height, while for surfaces with low z_0 values it is usually considered to be zero.

The logarithmic sub-layer height, z_L, can be estimated to be around 15% of δ, and an expression for its height can be found for example in Simiu and Scanlan, 1996:

$$z_L = \left(\frac{b.u_*}{f}\right) \tag{2.2}$$

where b would be an empirical coefficient with values between 0.015 and 0.03 and f, the Coriolis parameter. According to Equation (2.2), z_L could vary from 60 to 120m above a rural terrain in Uruguay for latitudes around 35º (south), for example.

From the previous calculation, it can be concluded that for high winds during flows of ABL type, the range of heights that usually involves the logarithmic sub-layer is of interest for many wind engineering applications.

As it is usually required to characterise the wind speed at sites and heights different from those where it is measured, it is necessary to know the relation between the measured wind speed, U_1 at height z_1 and the wind speed U_2 that would be measured at a nearby place at height z_2. The typical heights for performing wind measurements and those of interest in wind engineering would generally place these wind speeds, for flows of ABL type, inside the logarithmic sub-layer. The calculation of the relation between these wind speeds during flows of ABL type would therefore involve Equation (2.1) in the case of neutrally stratified flows, and require information on roughness of both upwind terrains, which are usually obtained estimating the corresponding values of z_{01} and z_{02}, and the values of d_1 and d_2.

Counihan, 1975; Wieringa, 1992; Wieringa, 1993; Simiu and Scanlan, 1996; Davenport et al., 2000 and Holmes, 2007 among others, present values for z_0 and d for different upwind surfaces, which may vary with wind direction for a specific site.

Additionally, Simiu and Scanlan, 1996 presents the following relationship between u_{*1}/u_{*2} and z_{01}/ z_{02}, which would also be needed when applying Equation (2.1) to two different sites:

$$\frac{u_{*1}}{u_{*2}} = \left(\frac{z_{01}}{z_{02}} \right)^{0.0706} \tag{2.3}$$

From Equation (2.3) and Equation (2.1) it is then possible to calculate the relation between U_1 and U_2, which yields:

$$\frac{U_2(z_2)}{U_1(z_1)} = \frac{\mathrm{Ln}\left(\frac{z_2 - d_2}{z_{02}} \right)}{\mathrm{Ln}\left(\frac{z_1 - d_1}{z_{01}} \right)} \times \left(\frac{z_{02}}{z_{01}} \right)^{0.0706} \tag{2.4}$$

As adequate z_0 measurements are seldom available in practical situations, it is often necessary to assign roughness values to parcels of terrain either by eye, from photos or from land-use maps. Such visual estimation of terrain roughness requires guidance from a roughness classification, based on good experiments over well-defined terrains. In particular, Wieringa, 1993 presents a summary of reviewed z_0 values for homogeneous natural surfaces. For the evaluation of surface homogeneity, this author advises to use a fetch-to-observation height ratio of the order of 100 -dependent on local roughness; and to consider an area of several kilometres squared for roughness integration.

Inhomogeneous terrains would consist of surface patches of different roughness, some of which can contain scattered obstacles such as shelterbelts or houses. In this case, as rougher patches contribute relatively more to the value of z_0, z_0 will never be less than the area-weighted arithmetical average of individual patches of homogeneous z_0, and it will be significantly higher than the z_0 values corresponding to the open patches. Wieringa, 1992 offers a list of z_0 values for terrains of increasing inhomogeneity.

Reviewed values of z_0 and d for homogeneous and inhomogeneous surfaces are presented in Davenport et al., 2000.

On the other hand, in the wake sub-layer, the distribution of the mean wind speed with height approximately follows a power law. This sub-layer occupies most of the ABL and its expression is presented in Equation (2.5):

$$\frac{U(z)}{U_{ref}} = \left(\frac{z}{z_{ref}} \right)^n \tag{2.5}$$

where U is the mean wind speed at height z, U_{ref}, the mean wind speed at height z_{ref}; and n the power law exponent, an empirical parameter that depends on the surface roughness, which may vary with wind direction for a specific site.

Counihan, 1975; Bietry et al., 1978; Simiu and Scanlan, 1996 and Holmes, 2007, as well as other authors, present values for the power law exponent, n, for different surfaces.

A thorough description of the different sub-layers of flows of ABL type can be found for example in Durañona, 2003.

It is worth noting that not all authors have used or use at present this model for the mean wind speed profiles of flows of ABL type, as mentioned in Section 2.5. On the other hand, in the field of meteorology, different types of atmospheric boundary layers can be defined (Markowski and Richardson, 2010).

It should also be remembered that the distributions of the mean wind speed with height presented in Equations (2.1) and (2.5) correspond to a horizontal flow that develops over a rough surface without any other disturbance, whose mean horizontal wind speed does not

vary with time, where thermal effects can be neglected, and whose vertical mean wind speed is zero, as it is the case of ABL flows simulated in wind tunnels (Durañona, 2003). As it has also been said, this wind speed profile is a mean wind speed profile, and it may differ from instantaneous wind speed profiles. Atmospheric high wind speed flows do occur under other conditions, as for example, when non-synoptic high winds take place.

When mechanically generated turbulence dominates the vertical air movement, thorough turbulent mixing tends to produce a neutrally stable atmosphere (Cook, 1985; Simiu and Scanlan, 1996). According to Cook, 1985, this condition is usually met for flows of ABL type with hourly-mean wind speeds exceeding 10m/s at 10m above the ground.

Therefore, high wind speed flows of ABL type would tend to occur under neutrally stable conditions, and would not include flows that present thermal components, such as those generated by convective storms (Harris and Deaves, 1980), katabatic winds (Holmes, 2007), sea breezes (Wallace and Hobbs, 2006), etc. In these cases, the flow does not resemble a flow of ABL type and the atmosphere is not neutrally stable, either. As a result, the wind distribution with height can greatly differ from that expected for a flow of ABL type, as already mentioned in Cataldo and Durañona, 2008.

For example, measurements and models of the flow structure during the occurrence of downbursts and tornadoes are presented by Fujita, 1981; Fujita, 1985; Hjelmfelt, 1988; Fujita, 1990; Walker, 1992; Cermak, 1998; Wood et al., 1999; Savory et al., 2001; Holmes et al., 2005a; Chay et al., 2006a; Chay et al., 2006b; Holmes, 2007; Orwig and Schroeder, 2007; Lombardo and Smith, 2009; Riera and Ponte, 2012; Gunter and Schroeder, 2013, among many other authors.

It is worth noting that there is a tendency for severe wind events of small scales not to be very well observed, and the physical processes behind them not completely understood (Stensrud et al., 2003). Current knowledge of the flow structures and profiles with height for some non-synoptic winds is discussed in Sub-section 2.2.3.2.

On the other hand, as the wind flow during extra-tropical cyclones has been studied for more than 40 years, in the wind engineering field it is assumed that their characteristics are generally well understood, at least over flat homogeneous terrain. It is also usually assumed

that their flows are of ABL type (Cermak et al., 1998; Holmes, 2007), away from the fronts that form part of these systems (Doswell, 2003b).

For the case of hurricanes, also called tropical cyclones or typhoons depending on the region of the world where they occur, although wind measurements are extremely limited, according to Holmes, 2007 it can be considered that the wind exhibits a steep logarithmic-type profile up to a certain height (60–200m), followed by a layer of strong convection, with nearly constant mean wind speed. Harper et al., 2010 also assumes that the flow for typical hurricane wind speeds (> 17m/s), away from convectively-driven phenomena such as downbursts, gust fronts, tornadoes, or flow instabilities such as boundary layer rolls, may be considered to be of ABL type up to a height of 100m.

The two latter synoptic high wind events are presented in Sub-section 2.2.3.1.

2.2.1.4. Wind gust speeds and gust factors

In many wind codes and applications, the calculation of wind gust speeds for different return periods, instead of mean wind speeds, is required for the calculation of wind loads and risk levels, as indicated in Section 2.5. Wind gust speeds are wind speeds averaged over short periods of time, e.g. 3s, while mean wind speeds are wind speeds averaged over longer periods, e.g. 10min, 1 h. The definition of return period is presented in Section 2.4.

On the other hand, it has long been recognised that the analysis of 10min mean or hourly mean wind speeds would not be adequate for the evaluation of extreme winds in places where convective storms are a dominant feature of their extreme wind climate, as indicated in e.g. Wieringa,1973; Riera et al., 1977; or Holmes et al., 2005b, among others.

These are the main reasons to present a review and discussion on wind gust speeds and gust factors in this chapter.

The WMO recommended in 2008 (WMO, 2008) to measure wind gust speeds with a 3-second moving average, and this recommendation has tended to be adopted worldwide in digitally-processed automatic weather stations. Sometimes, this average is actually calculated during the stated short period of time, but in many other cases, registered wind gust speeds correspond in fact to peak wind speeds (the highest wind speed values capable of being

registered by an anemometer and its recording system). For example, in the field of wind engineering it is not unusual to assume that the registered peak wind speeds correspond to wind gust speeds averaged over 3s, and are thus referred to as 3s gusts.

The actual averaging period of any peak wind speed depends on the time response of the anemometer at that wind speed, and on the frequency response of the measurement and recording system. This averaging period, as it will be seen later in this sub-section, can greatly differ from 3s.

Many authors have supposed that peak wind speeds just picked off from an anemograph trace would represent a 3s gust, as already indicated by Deaves, 1993 or more recently by Holmes and Ginger, 2012. In some automatic meteorological stations, even recorded peak wind speeds have been assumed to represent 3s gusts.

On the other hand, a 3s moving average truncates a large part of the turbulent wind spectrum at typical design wind speeds, and the equivalent spatial filter has a frontal area about that of a large tall building (i.e., 3,200m^2 at a mean wind speed of 30m/s), length that can be too high depending on the wind engineering application (Holmes et al., 2014). In this sense, Holmes and Ginger, 2012 proposed the use of a moving average time of 0.2s to define a basic maximum wind gust speed in the Australian and New Zealand wind code AS/NZS:1170.2, 2011. This avoids the need for a gust effect factor for small buildings, and assumes that a dynamic response factor calculation is carried out for large buildings, which incorporates a factor that takes into account the filtering effect of a large frontal area (Holmes et al., 2014).

On the other hand, sometimes wind gust speeds used for calculating wind loads, or for wind risk assessments, are estimated from measurements of mean wind speeds averaged over longer periods of time, e.g. 10min or 1h. Cook, 1985 and ISO:4354, 2009, for example, present relationships between wind gust speeds and hourly mean wind speeds for different gust averaging periods, heights and roughness lengths of the upwind surface in the first case, and for different gust averaging periods in the second one. In both cases, the relationships presented are only valid for flows of ABL type, but it has long been pointed out that many researchers from the wind engineering field assume that the highest wind gusts occur during flows of ABL type, as described in Collier et al., 1994, and apply these relations without considering that this hypothesis might not be valid.

As indicated in this sub-section, there would not exist a parametrical relationship that would link mean and gust wind speeds produced by convective storms, as wind gust speeds depend on many parameters on these cases, ranging from characteristics of the microstructure of the cumulus cloud that generates the outflow boundary responsible for the wind gust speed under consideration, thermodynamics properties of the environment and characteristics of the wind field up to several kilometres height (Rogers and Yau, 1989; Markowski and Richardson, 2010), to geometric variables as the height of the cloud, the relative distance to the point where the downdraft impacts the ground, the diameter of the impinging downdraft jet, the height at which the wind gust speed needs to be evaluated (Riera and Rocha, 1998; Chay et al., 2006a; Riera and Ponte, 2012), among others. This makes direct and good-quality measurements of wind gust speeds essential in regions prone to severe convective activity, in order to obtain adequate information on their extreme wind climate and reliable extreme wind statistics.

Apart from the averaging period corresponding to the wind gust speed used for either the calculation of wind loads or for wind risk assessment, another important issue that has to be taken into account is how the wind gust speed profile, i.e., the variation of wind gust speed with height, is modelled. This profile strongly depends on the type of flow assumed for the calculation (Holmes et al., 2005a; Riera and Ponte, 2012). Quite frequently, a flow of ABL type is assumed, and if this hypothesis is correct, the wind gust speed profile may be calculated from the mean wind speed profile expected for the roughness length (z_0) of the upwind surface.

When the wind gusts are generated by convective activity, there is not a consensus on how the wind gust speed profile could be modelled yet, as presented by Letchford, 2015; although there exist a series of models proposed to address this issue, as indicated in Sub-section 2.2.3.2 (e.g. Holmes et al., 2005a). Measurements of wind gust profiles generated by convective activity can be found in a series of papers, for example in the well-known work of Hjelmfelt, 1988; in Choi, 2004; or in the more recent work by Gunter and Schroeder, 2013 and Gunter and Schroeder, 2015, which present very interesting results, among others.

One of the landmark references in wind gust speeds and gust factors is that of Wieringa, 1973, working at that moment at the Royal Netherlands Meteorological Institute. In this paper, he presented a careful and exhaustive study of previous analyses of gusts of different duration,

taking care that the gust durations were properly identified. The gust factor is the ratio of the highest wind gust speed averaged over a short period of time, to the mean wind speed, averaged over a longer period (WMO, 2008; Harper et al., 2010). Wieringa, 1973 also presented very valuable results from some of his own studies, and his paper found its way into the field of wind engineering, making accessible very useful results from researches carried out in the field of meteorology on the subject of wind gusts.

In this paper he establishes the importance of counting with adequate metadata to infer the averaging period of the measured gusts, giving the example that at high winds, the time response of a cup anemometer to a gust may range from 0.2 to 20s with an analogue output, depending on the type of analogue recorder; and that the response of a standard Pitot tube could be between 2 and 5s. Much more recently, Holmes and Ginger, 2012 compared the averaging period of wind gust speeds measured by Dines anemometers and those measured by cup anemometers, as concerns appeared about a possible decrease in the measured wind gust speeds in Australia after Dines anemometers were switched to cup anemometers in the early 1990s in this country. It is then essential to register and take into account changes in instrumentation, recording system and/or measurement techniques in any research based in historical wind data measurements, as they can introduce an important bias in the data and consequently, significant errors in extreme wind value~~s~~ analyses, which usually require long wind data series, of good quality.

Wieringa, 1973 also concluded that for wind gust speeds measured during convective storms, it would not be easy to define an unique representative averaging period for the mean wind speed for the calculation of gust factors, as these wind gust speeds depend much more on the local stability of the whole troposphere and, therefore, would not present a consistent relation with the measured mean wind speeds.

Prof. Wieringa also indicated that for high wind gust speeds generated by convective activity, averaging periods for the mean wind speed of e.g. 10min would tend to yield higher gust factors than for high wind gust speeds measured during flows of ABL type.

Higher gust factors than those expected for ABL flows were also reported during severe convective activity in Bradbury et al., 1994 and Bradbury and Deaves, 1994, among other more recent papers. For example, since the 1990s, Prof. Choi has been studying the

importance of convective and non-convective wind gusts in the extreme wind climate of Singapore, and, in particular, the different values of gust factors usually measured in each case. Choi, 2000 reports gust factors referred to hourly mean wind speeds from 2.6 to 2.9 for non-convective gusts, and from 3.7 to 5.8 for convective gusts; in both cases at 10m height and with gust averaging periods of around 0.3s. However, Choi, 1999 recognises that convective gusts can yield hourly based gust factors around 65% higher than the corresponding 10min-based gust factors, but that the latter would still be higher than the typical values of 10min-based gust factors for non-convective gusts. This paper, as well as Choi and Hidayat, 2002, suggest an averaging period of 10min for the mean wind speed in order to calculate convective gust factors. On the other hand, Solari et al., 2015a report from measurements carried out with ultrasonic anemometers in Italy, with sampling frequencies of 10Hz, higher gust factors for convective (thunderstorms) than for non-convective (synoptic) when wind gusts are averaged over periods of 1s and mean wind speeds are averaged with moving average periods of 10 and 60min. When mean wind speeds are averaged with a moving average period of 30s, they report similar gust factor values (of around 1.2 in average), for convective and non-convective wind gusts. As a reference, with gusts averaged over 1s and mean wind speeds averaged with moving average periods of 10min, they find mean gust factor values for synoptic winds of around 1.5.

On the other hand, Prof. Wieringa (Wieringa, 1973) additionally reports the occurrence of sudden and large accelerations at the beginning and also sometimes at the end of convective storm episodes, in accordance with results also shown in previous papers of other authors, as well as in many and much more recent papers. In relation to these large accelerations, Bradbury et al., 1994 suggests that they may increase the wind loads on structures due to extra inertial effects, and thus, that it should be analysed if they need to be considered for wind loading calculations.

Wieringa, 1973 also mentions that in some cases, a leader gust is found to precede the beginning of a convective storm by about 10s. These leader gusts have been found to be basically ‘pressure jumps’, with no horizontal or vertical wind direction change.

In Wieringa, 1973, Prof. Wieringa also summarises quality checked results for non-convective wind gusts in a diagram for gust sizes from 1 to 150m, and height to z_0 relations from $z = 15.z_0$ to $1x10^6.z_0$, which shows gust factor values of up to around 2. The gust factors

presented in this diagram are median values corresponding to 10min mean wind speeds greater than 8m/s and valid for heights up to 50m. For non-convective gusts, the relationship between gust factors based in mean wind speeds averaged over 1 hour and those averaged over 10min is estimated to be around 1.10 in the Netherlands and countries with similar climates.

From the analyses presented in Wieringa, 1973, Prof. Wieringa concludes that the occurrence of convective gusts needs to be considered in the description of the extreme wind climate in regions where severe convective activity is significant.

In that sense, Collier et al., 1994 pointed out that it had been recognised for many years that downbursts, described in Sub-section 2.2.3.2.1, were able to produce important wind gust speeds in mid-latitudes, and the work of Riera and Rocha, 1998 drew attention to the same subject.

Useful concepts and guidelines on the measurement of wind gusts, and definitions of wind gust speed, peak gust speed, wind gust averaging periods and gust factors can also be found for example in Harper et al., 2010.

2.2.2. Main characteristics of the general circulation of the atmosphere and average sea-level pressures

Most processes related to the generation of extreme winds depend on the characteristics of the mean wind climate itself, which in turn are related to the general circulation of the atmosphere.

The global mean wind climate may be considered as the background wind field upon which transient weather systems are superimposed. When winds throughout the world are averaged over a long period of time, the local wind patterns vanish, and what remains is a picture of the winds on a global scale — what is commonly called the general circulation of the atmosphere (Ahrens, 2009). Actual winds at any one place and at any given time may vary considerably from this average. Nevertheless, the average can answer why and how the winds blow around the world the way they do. The average can also give a picture of the driving mechanisms behind these winds.

The general circulation of the atmosphere is mainly caused by the unequal heating of the Earth's surface between the poles and the equator, the rotation of the Earth, the geographical distributions of continents, their topography and oceans, and their interaction with the atmosphere at different length scales, as well as to the existence of different seasons due to the inclination of the Earth.

Unequal heating of the surface generates differences in atmospheric pressures, which in turn give rise to atmospheric motions on a wide range of scales, with both horizontal and vertical orientations, generally from high pressure to low pressure areas. The rotation of the Earth generates additional forces that influence the movement of the air. As Holmes, 2007 indicates, all these features set up large scale circulation systems in the atmosphere, with easterly prevailing wind directions in the tropics and near the poles, and dominating westerly winds in mid-latitudes. Annex A.1 describes the general circulation of the atmosphere with more detail, and the regions of the world that, as a result, present pressure systems that tend to persist throughout the year. These semi-permanent high and low pressure areas will sometimes be referred to as 'lows' (L) and 'highs' (H), respectively, along this thesis. Figure 2.5 illustrates the actual average sea-level pressure distribution and surface wind-flow patterns for (a) January and (b) July (adapted from Ahrens, 2009).

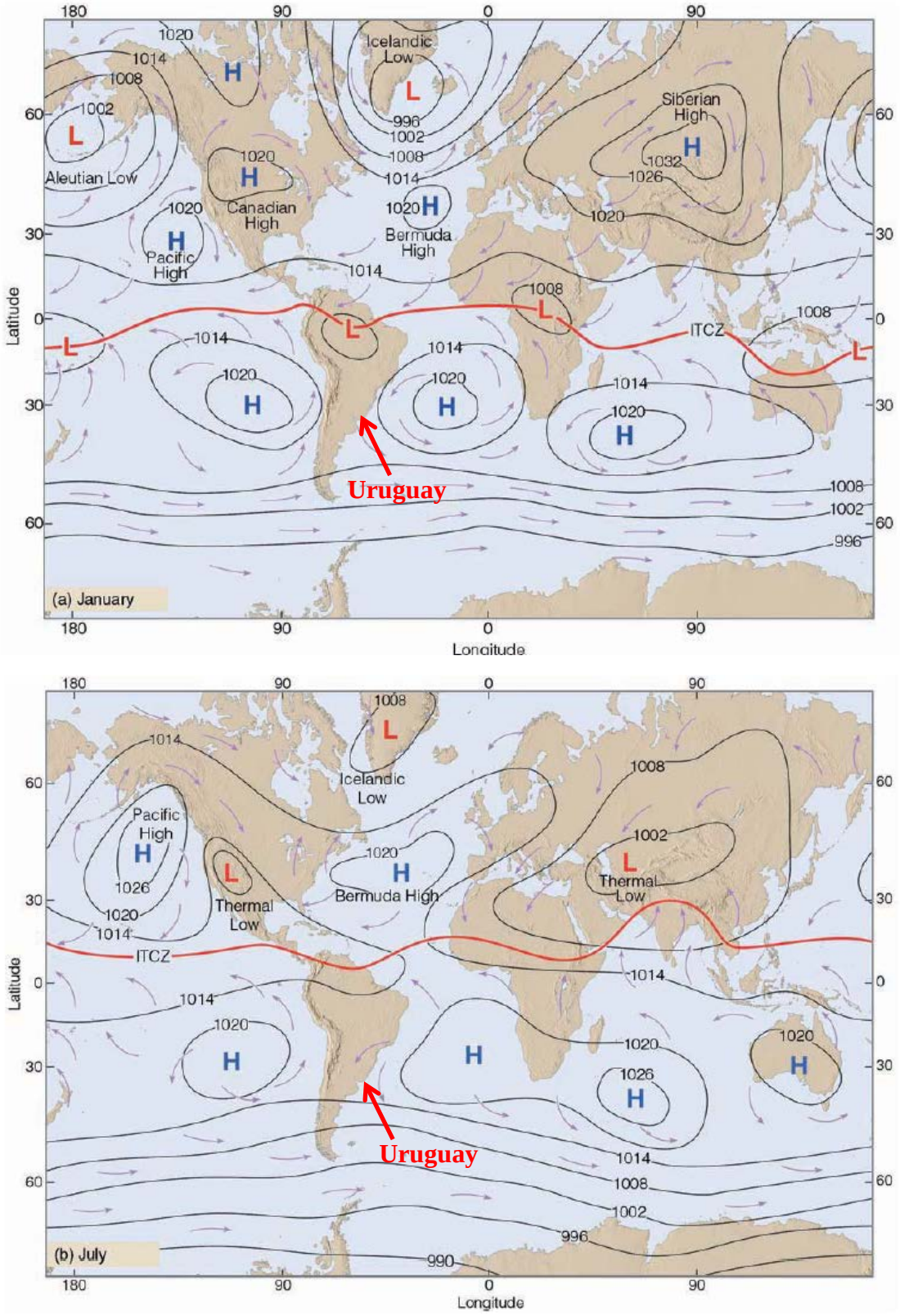


Figure 2.5 Average sea-level pressure distribution and surface wind-flow patterns for (a) January and (b) July (adapted from Ahrens, 2009)

In this figure, the pressure field is represented as isobars, and local maxima are referred to as high pressure areas or simply ‘highs’ (H) and minima, as ‘lows’ (L). It can be seen that, with the exception of the equatorial belt (10°S-10°N), the surface wind in the Earth’s atmosphere is quite parallel to the isobars.

As Figure 2.5 shows, the main characteristics of the general circulation of the atmosphere (at surface level) are:

- easterly prevailing wind directions in the tropics, with an intertropical convergence zone (ITCZ) located in average along about 7°N latitude
- dominating westerly winds in mid-latitudes, especially in the Southern Hemisphere (SH), centred around 45°N and 50°S latitudes
- semi-permanent highs in mid-latitudes over the Atlantic and Pacific Oceans located between latitudes 25° and 35° in both hemispheres
- a subpolar low pressure belt (polar front) in the SH, and two semi-permanent subpolar lows in the Northern Hemisphere (NH) between latitudes 40° and 65°. In these zones of cyclonic activity, numerous storms, having travelled eastward, tend to converge especially in winter
- in summer (winter) some pressure systems that are not semi-permanent form because surface low (high) pressure areas appear over warm (cool) lands. These are called thermal lows (highs)
- major pressure systems, wind belts, and ITCZ shift toward the south in January and toward the north in July
- in winter, the polar fronts with their cold air can move into subtropical latitudes, producing cold polar outbreaks

2.2.3. High wind events

Human society is particularly vulnerable to extreme weather and climate events, which cause damage to property and infrastructure, injuries, and in some cases, losses of lives. Various societal changes, such as increased populations in coastal and urban areas as well as its greater dependence on complex technology-based infrastructures, have made the global population potentially more vulnerable to such events and increased the risk exposure.

Regarding what an extreme or severe event is, there is no universal unique definition. For example, according to Doswell and Bosart, 2001 the definition of a severe convective event is arbitrary: a phenomenon may be classified as severe in certain region of the world if it meets some specified criteria, but these criteria may vary around the world. Tornadoes are generally an exception, as a convective storm producing any sort of tornado is usually considered to be severe. However, even this can become somewhat arbitrary. When a tornado occurs over water, i.e., a waterspout, the associated deep convective storm that produces it is not usually classified as severe (Doswell, 2003b).

Non-convective high winds are not rigorously defined either (Knox et al., 2011). Some studies employ for their definition a sustained 1min-mean wind speed of 18m/s (64km/h) or higher at 10m height for at least 1 hour, or a wind gust speed of 26m/s (94km/h) of any duration. Other studies use hurricane-force maximum winds of 33m/s (119km/h) as measured by satellites, while some others refer to damaging winds without any specific definition or threshold for wind speed values, although a value of 40m/s is sometimes used.

Beniston et al., 2008, for example, propose different definitions for severe, rare, extreme and high-impact events. In turn, this reference classifies extreme events into acute or chronic.

Extreme events also have a variety of different attributes such as rate of occurrence, magnitude (or intensity), temporal duration and timing, spatial scale (footprint) or multivariate dependencies, which need to be described in order to adequately characterise them. For instance, the temporal duration of extreme wind events can play an important role in the exposure and hence in total losses; if they are accompanied by intense rain can produce more damage if they are not, etc.

Throughout this thesis, a high wind event is considered as one that represents a potential hazard to public safety and/or property, and will be mainly defined by its intensity. The rest of its attributes will be analysed and characterised when possible.

To define the intensity of a wind event, a way of measuring it and a threshold value need to be chosen (Doswell, 2003b). Its intensity could be defined by its associated wind speed, or even taking into account injuries, lives and economic losses. As wind speed is usually the most rapidly and precise magnitude available, its measure is used to define the intensity of a high wind event along this thesis, taking into account its averaging period, as mentioned in Sub-section 2.2.1.

In the next sub-sections, high wind events widely recognised as representing hazard for the population and/or properties are described. The meteorological processes that generate them and the wind speed values that they usually develop are characterised, as well as their typical length scales, trajectories or other important attributes when this information is available.

As it was indicated in Sub-section 2.2.1, high wind events are classified in this thesis as synoptic or non-synoptic, although it is important to bear in mind that processes of different scales may act simultaneously during a high wind event, as also mentioned in that sub-section. Other classifications exist, e.g. some authors classify high wind events as convective or non-convective (Knox et al., 2011).

2.2.3.1. Synoptic high winds

2.2.3.1.1. Intense extra-tropical cyclones

Extra-tropical cyclones are synoptic-scale regions of low sea-level pressure with upward vertically wind speed and cyclonically rotating winds that form outside the tropics (see Figure 2.1). The upward vertical wind speed supports clouds, precipitation and sometimes convective storms. They usually form between latitudes 30° and 60°, and their trajectories may have preferred directions depending on the region of the world under consideration. Their lives during their movement along their trajectories can range from less than a day to more than two weeks, being the most common period one week (Stull, 2000), although winds do not blow continuously at their maximum intensity during all the time. Wind direction at a specific site can remain quite constant over many hours.

Extra-tropical cyclones can have horizontal length scales of about 500 to 2,500km, they may span the depth of the troposphere (~10km) (Hakim, 2003) and affect large areas during their passage. Damaging winds may extend over many hundreds of kilometres and last in any one place for around a day or more.

During the formation and amplification of these cyclones, regions of bands a few tens of kilometres wide, characterised by sharp horizontal gradients, and sometimes by outright discontinuities in wind and temperature (Wallace and Hobbs, 2006), develop. These regions are called fronts, and are the leading edges of the cold air flowing equatorward and of the warm air flowing poleward (Doswell, 2003b) that are part of these cyclones, as described in Annex A.1. Most of the fronts are characterised by high clouds and intense precipitation features, and much of the significant weather associated with extra-tropical cyclones occurs within them. They can generate high wind events of smaller scale, as downbursts and tornadoes produced by severe convective storms forming inside them. Cold fronts, in particular, can trigger severe convection, which in turn may generate strong downdraft outflows and gust front structures at the surface.

In the wind engineering field, it is considered that the flow associated to extra-tropical cyclones is reasonably well-understood, and that the flow in areas away from their fronts can be modelled as an Atmospheric Boundary Layer (ABL) flow (Cermak and Isyumov, 1998), as mentioned in Sub-section 2.2.1.3.

It is quite usual to find intense convective storms in the warm sector of rapidly deepening extra-tropical cyclones (Wallace and Hobbs, 2006) in winter. In the warm season, severe convection can spread well poleward of the warm sector of these cyclones. The summer extra-tropical cyclones are not as intense as the winter ones, but can have easy access to abundant moisture and instability, with a correspondingly large frequency of intense convective storms. Such events can sometimes become derechoes (Doswell and Bosart, 2001), which are defined later in this chapter.

While downdrafts generated inside extra-tropical cyclones may transport strong winds to the surface, several explanations for the occurrence of other types of localised high surface winds during the passage of extra-tropical cyclones have been also investigated, as those corresponding to the ‘sting jet’ theory. The presence of a ‘sting jet’ might bring very high

winds down to ground level, as explained in e.g. Browning, 2004 and Knox et al., 2011, among others.

According to Sinclair, 1995, extra-tropical cyclones form and develop within mid-latitudes and migrate eastward and poleward during their lives. Preferred regions for their origin and evolution include eastern coasts of South America and Australia in winter, and leeward of the Andes and near the baroclinic zones associated with the principal tropospheric jet streams year round. Details of these and other features of the general circulation of the atmosphere are described in Annex A.1. Other regions are the Pacific, near the Asian coast; the Atlantic, Greenland and the North American coasts (Guin and Saxena, 2002). Those affecting Europe typically originate to the east of North America or Greenland and subsequently move eastward across Europe. Over open water, winter cyclones tend to form and intensify near zones of strongest average sea surface temperature (SST) gradient.

Figure 2.6 illustrates for the SH winter how many more cyclones form over the South American continent, and particularly over South Eastern South America (SESA), than in any other continent of the SH (Taljaard, 1967). More recent studies, as the one of Hoskins and Hodges, 2005 have confirmed these results.

Although extra-tropical cyclones can occur every month of the year, since the polar jet stream is stronger and moves equatorward in winter, they are better developed and move faster during the colder months. Therefore, their intensification into significant extra-tropical storms almost always occurs during the late fall, winter, or early spring.

In some cases, extra-tropical cyclones can become particularly intense, and the pressure at their cores can become quite low in comparison to the average. Those that present rapidly falling pressures are sometimes called ‘bombs’. Rapid cyclogenesis is most frequent east of SA, southeast of Africa, south of Australia, and near New Zealand. In the SH, near Australia and Tasmania, results indicate a maximum in frequency of explosive cyclogenesis from June to August, i.e., during SH winter (Knox et al., 2011).

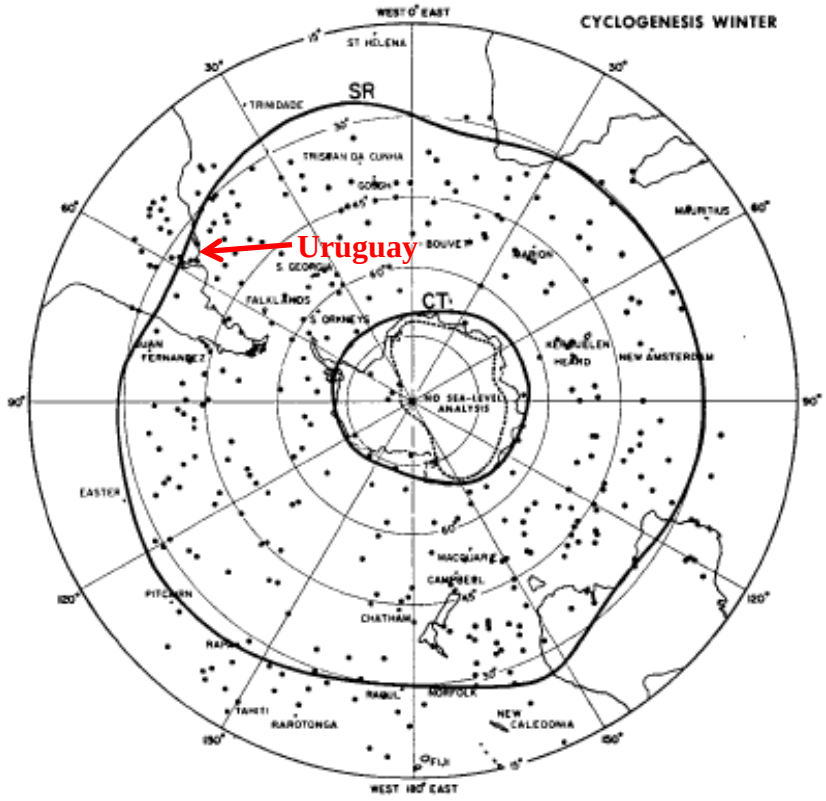


Figure 2.6 Distribution of cyclogenesis (individual systems) for SH winter (adapted from Taljaard, 1967)

Intensifying extra-tropical cyclones can cause sudden extreme winds and heavy rain over a wide region, floods, blizzards, wind chills, and hazardous travel conditions over thousands of square kilometres (Stull, 2000; Doswell, 2003b). The result of their widespread damage can be overwhelming to emergency services, and power outages can last for days. In addition to direct wind deaths and damage, the combined action of wind and water can lead to high seas and seiches causing additional damage and losses of lives (Knox et al., 2011). When they affect coastal areas, large waves can produce beach erosion, and at sea, they can represent hazards to ships of all sorts.

During these high wind events in USA, most fatalities occur in vehicles (often due to trees fallen onto them), while boating, or outdoors. Europeans have a long history of nautical disasters (Knox et al., 2011) and on average, 25 storms form each year in Europe, of which five have the potential to cause substantial damage (Guin and Saxena, 2002).

2.2.3.1.2. Hurricanes and tropical storms

When tropical cyclones develop high winds, they are known as hurricanes in America, cyclones in the Indian Ocean and Australia, or typhoons in the tropical Pacific. They are intense low-pressure cyclonic systems that occur over the tropical oceans, mainly in late summer and autumn, when rising warm air near the ocean's surface creates an area of low pressure. They are driven by the latent heat of the oceans and require a minimum sea temperature of about 26°C to be sustained. In consequence they rapidly degenerate when they move over land or into cooler waters (Guin and Saxena, 2002; Holmes, 2007). As a result, their full effects are primarily felt within about 50 to 100km from the coastline. Their most active months are January and February in the SH, and August and September in the NH. More details of their formation and characteristics can be found in e.g. Ahrens, 2009.

According to Doswell, 2003b; Marks, 2003a and Muzeau et al., 2007, tropical cyclones can be considered to reach hurricane category when 10min mean wind speeds are greater than about 33m/s. Peak sustained winds can approach 90m/s in extreme cases. The size of the region of damaging winds can vary considerably from one event to another, but mean wind speeds exceeding 'hurricane force' (>~33m/s) are usually found within a region from few tens to 100km from their centre of rotation. The central region of a hurricane, where winds are light, is known as the 'eye' of the hurricane, and can persist in the same site for many hours. As a hurricane becomes stronger, the eye diameter tends to decrease (Cermak and Isyumov, 1998).

Hurricanes have smaller horizontal length scales than extra-tropical cyclones, as suggested by Figure 2.4, but their effects can also be felt along several hundred kilometres. They are also more axisymmetric. Fully developed hurricanes have typical diameters in the range of a few hundred kilometres.

The circulation inside a hurricane has a radial component towards its eye, whose diameter can range between 8 and 80km. Outside the eye, there is a region of intense thermal convection with air currents spiralling upwards, while inside it there is a relative calm with slowly sinking air. The strongest winds occur just outside the eye wall (Holmes, 2010).

As hurricanes are the result of the large-scale integration of convective processes, they exhibit evidence of local convection, such as downbursts or gust fronts, and they can even pack

embedded tornadoes. They also present flow instabilities such as boundary layer rolls. As mentioned in Sub-section 2.2.1.3, the flow inside a hurricane up to a height of around 100m and away from these phenomena can be considered of ABL type for wind engineering applications, with a steep logarithmic-type profile for the eye wall region over the ocean or the adjacent coastline corresponding to an estimated z_0 of around 0.01cm (Franklin et al., 2003). Above that height, there would be a layer of strong convection, with nearly constant mean wind speeds (Holmes, 2007; Harper et al., 2010).

For the same reason, convective, or at least non-mechanical turbulence processes, probably play a more significant role in turbulence intensities in hurricanes than in extra-tropical cyclones (Harper et al., 2010).

Hurricanes do not form within about 5° of the equator and do not reach full strength until they reach at least 10° latitude. They are usually at full strength between 20° and 30° latitude, but can travel to higher latitudes if there are warm ocean currents to sustain them (Holmes, 2010). Although Atlantic Ocean hurricanes receive a lot of attention, only 12% of worldwide hurricanes take place there, according to University_of_Illinois, 2010, as also indicated by Figure 2.8. In the SH, they are usually confined to the Western Pacific and Indian Oceans, as Figure 2.7 and Figure 2.8 show.

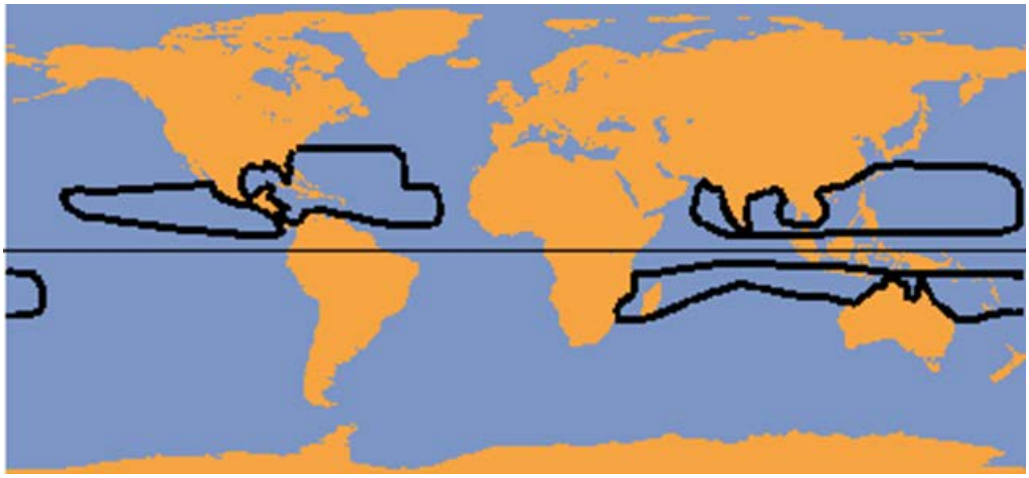


Figure 2.7 Regions of the Earth where hurricanes usually originate (from University_of_Illinois, 2010)

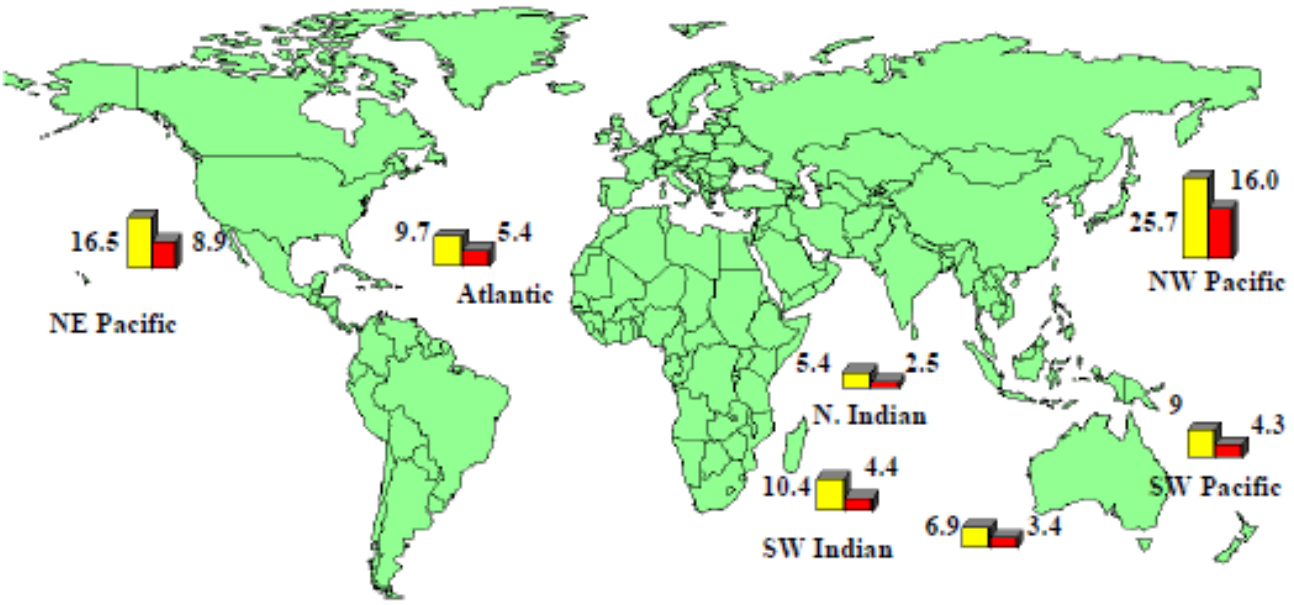


Figure 2.8 Average number of tropical storms (in yellow) and hurricanes (in red) formation per year (from Guin and Saxena, 2002)

Figure 2.8 indicates the average number of tropical storms formation per year in each of the world's major ocean basins. The number given on the left bar for each basin includes all cyclone formation of tropical storm strength or greater, whereas the number given on the right side bar indicates those that reached or exceeded hurricane strength.

Before a low pressure system is classified as a hurricane (or cyclone or typhoon, depending on the region of the world where it is developing), it goes through different stages, which may be summarized as in Table 2.1.

Name	Sustained winds speed (km/h) (a 10-minute average)	
	Atlantic & East Pacific	West Pacific
Tropical depression	≤ 62	≤ 62
Tropical storm	63-117	63-88
Severe tropical storm		89-117
Cyclones or typhoons	Tropical cyclones ≥ 118	Typhoons ≥ 118

Table 2.1 Stages from tropical depressions to hurricanes (Muzeau et al., 2007)

Category	1min-mean sustained wind speeds (km/h)	Wind damage related to flying debris and trees
I	119-153	Possible injuries for flying or falling debris; large branches of trees will snap, and shallow rooted trees can be toppled
II	154-177	Substantial risk of injury for flying and falling debris; many shallowly rooted trees will be snapped or uprooted and block numerous roads
III	178-209	High risk of injury for flying and falling debris; many trees will be snapped or uprooted, blocking numerous roads
IV	210-249	Very high risk of injury for flying and falling debris; most trees will be snapped or uprooted, and power poles downed. Fallen trees and power poles will isolate residential areas
V	>249	Very high risk of injury for flying and falling debris, even indoors; nearly all trees will be snapped or uprooted, and power poles downed. Fallen trees and power poles will isolate residential areas

Table 2.2 Saffir-Simpson hurricane scale (Schott et al., 2012)

Several scales for classifying hurricane intensities exist, one very well-known being the Saffir-Simpson hurricane wind scale reproduced in Table 2.2. This scale is especially developed for North Atlantic and Caribbean hurricanes (Schott et al., 2012), and involves the maximum 1min-mean wind speed measured at 10m height over open and level terrain. This table also shows the expected wind damage related to wind-borne debris and trees.

Hurricane sustained high winds together with wind-borne debris, downed trees and poles, intense rain and floods represent hazards for people lives, and can produce important damage to buildings and infrastructure. Wind damage can also be produced by severe wind events of smaller length scale, as strong downbursts and tornadoes. In coastal zones, extensive damage and loss of lives can be caused by the storm surge, i.e., the local rise in sea level associated with the hurricane landfall (Marks, 2003b).

2.2.3.1.3. Subtropical cyclones

There exists another category of synoptic low sea-level pressure systems called ‘subtropical cyclones’. Subtropical cyclones are cyclones that share some characteristics of tropical cyclones with others of extra-tropical cyclones. In particular, they do not present weather fronts, as extra-tropical cyclones do (Roth, 2002).

2.2.3.2. Non-synoptic high winds

Non-synoptic high winds considered in this thesis are divided into those produced by intense convective activity; those driven by thermal circulations, as katabatic winds or sea/land breezes; and those forced by topography, as downslope winds or mountain waves.

The most common types of non-synoptic high winds worldwide are generated by intense convective activity, and especially, by the strong outflow boundaries that it produces, and are presented in the following sub-section.

2.2.3.2.1. Intense convective activity

This sub-section presents a description of severe convective storms, which may be found a bit basic by meteorologists, but not so by wind engineers. Convective storms form when warm humid air is driven upwards in an unstable atmosphere. They can only take place when the atmosphere is conditionally unstable, enough moisture is present, and sufficient lifting occurs to bring air parcels to saturation.

When the ascendant flow is fortified by one or more mechanisms, a severe convective storm can form, producing large hailstones, intense rain and violent gusts. High wind events associated with these storms are mostly related to strong downburst outflows, and sometimes, to tornadoes, can have length scales from several hundred metres to a few hundred kilometres, and time scales from few minutes to several hours, as presented in Figure 2.2 and Figure 2.3. Severe convective storms can occur as isolated events or in more or less organised groups, all of them capable of producing strong downbursts. They pose a significant hazard to life and property in many places of the world, especially during the spring and summer months, more than extra-tropical cyclones according to Wallace and Hobbs, 2006.

Severe convective storms typically produce some of the fiercest weather on Earth, including intense rain, surface winds sometimes greater than 50m/s, hail, frequent lightning and tornadoes. In the USA, a convective wind event is considered severe when wind gusts exceeding 25m/s, hailstones with diameters greater than 2cm or tornadoes are produced (Doswell, 2003b).

Convection is the transfer of heat by the mass movement of a fluid (in this case, air), which happens naturally in the atmosphere. Meteorologists usually restrict the term convection to the process of rising and sinking air parcels (Ahrens, 2009).

There are different synoptic and mesoscale processes that can act to provide the adequate environment conditions for convection to initiate. Air can start moving upwards due to unequal heating, unequal moisture or vegetation type of the surface, due to topography features, the lifting of warm air along an air mass boundary such as a cold front, a dryline (defined in e.g. Grasso, 2003), outflow boundaries from previous convective cells, gust fronts, sea/ or lake/land breezes, due to converging surface winds, colliding or intersecting low-level perturbations (Johnson and Mapes, 2001; Markowski and Richardson, 2010) and/or by the appearance of a cooler and/or drier air mass aloft. Most of these aspects are described in this and following sub-sections.

Once convection initiation has begun, the interaction of convection with the environment can lead to the development of different types of severe convective storms. A wide variety of processes that can precondition the atmosphere for severe convective storm occurrence and different triggering mechanisms are described for example in Johnson and Mapes, 2001. The type of severe convective storm, and therefore, its intensity, length and time scales would depend on the origin of the process that preconditions the environment and/or on the triggering mechanism.

In the following paragraphs, the most common types of severe convective storms and their main characteristics are described, especially those characteristics that can help identifying the occurrence of such storms from meteorological records, and those related to their temporal wind speed evolution and wind structure for wind engineering applications. The development of the different stages of an isolated convective cell is described with certain detail, as the behaviour of wind speeds near the surface during this type event would present common characteristics with winds produced by other types of more complex severe convective storms. Multi-cell convective storms, supercells and different mesoscale convective systems (MCSs) are also described.

Isolated convective cells have generally horizontal length scales from 5 to 30km, lifetimes from 30-40min to greater than 6h (Weisman, 2003c) and can develop hail and gusty winds, although these occurrences are typically not severe in this type of cells, as they rarely produce strong winds or large hail. If they generate a tornado, it is usually relatively weak and short-lived, and sometimes referred to as a landspout.

These cells consist of only one updraft and do not initiate subsequent convection in any organized manner. Their life cycle may be divided into three stages.

The first stage is known as the cumulus stage. As humid air rises, it cools and condenses into a single cumulus cloud that may show extensive vertical development in just a few minutes, giving place to a cumulus nimbus cloud. This updraft keeps water droplets and ice crystals suspended within the cloud, and as the cloud builds above the freezing level, the cloud particles grow larger and become heavier. The height of these clouds is of the order of 10km, as Figure 2.4 and Figure 2.9 illustrate.

Eventually, the rising air is no longer able to keep these water and ice particles suspended, and they begin to fall through the updraft. While this is happening, drier air from around the cloud is being drawn into it in a process called entrainment, which evaporates some of the raindrops, chilling the air. The air, colder and heavier than its surrounding, begins to descend as a downdraft, which may be enhanced as falling precipitation of raindrops and ice particles drags some of the air along it (Ahrens, 2009).

The appearance of the downdraft marks the beginning of the mature stage, at which the storm is usually more intense. The updraft and the downdraft reach their greatest strength in the middle of the cloud, and heavy rain and occasionally small hail fall from the cloud. The rain may or may not reach the surface, depending on the relative humidity beneath the cloud, but the downdraft of cold air that forms with the onset of precipitation reaches the surface, sometimes as a strong wind gust, which spreads laterally with the downdraft outflow as in the model presented in Figure 2.10, and cools the surface up to some hundred metres height. This stage is illustrated in Figure 2.9. Sometimes, the air temperature lowers about 10°C in few minutes. This process creates a cold pool, which may last several hours after the storm has dissipated.

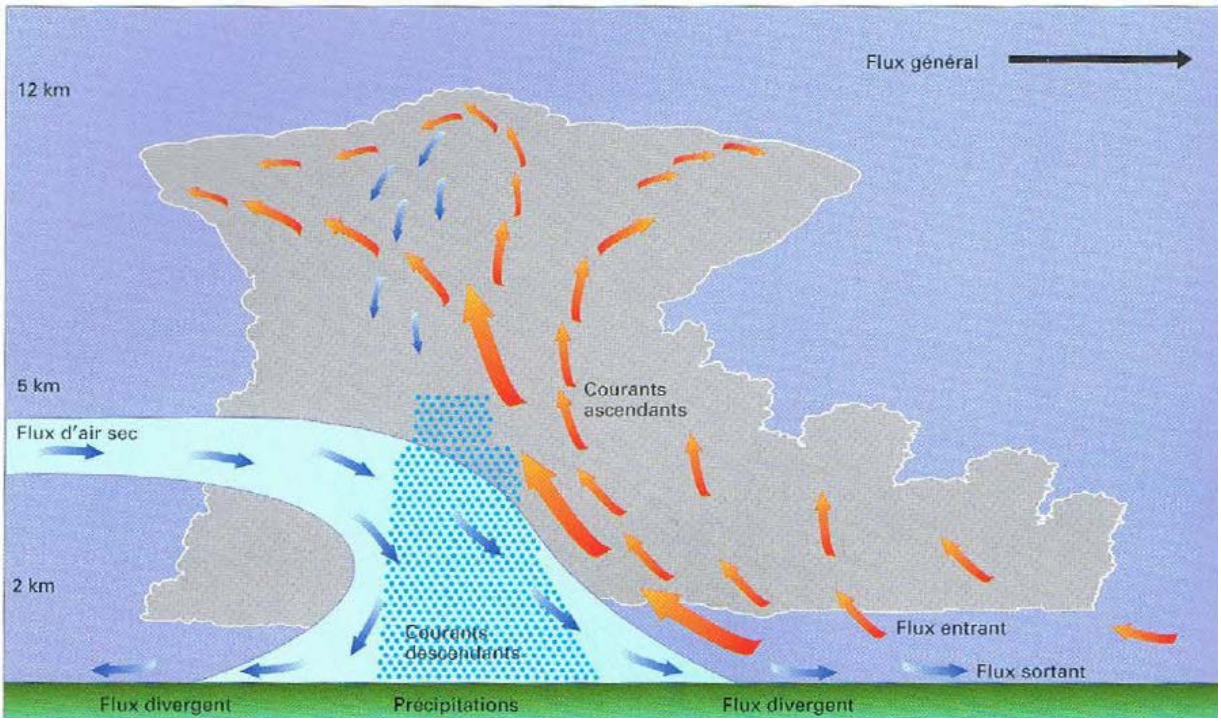


Figure 2.9 Downdraft at the mature stage of a convective storm (from Hermant, 2000)

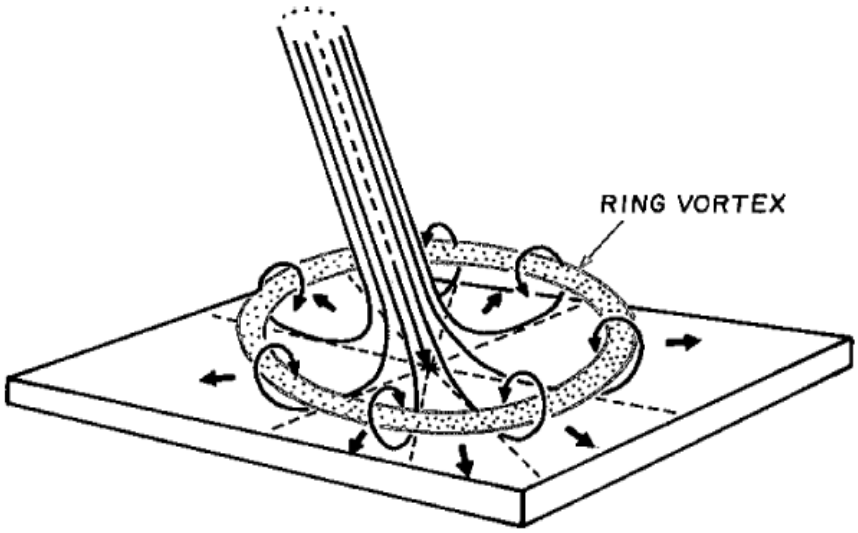


Figure 2.10 Downburst model (Fujita 1985)

The downdraft behaves as a jet of fluid impinging on a surface, as indicated by Figure 2.10. High horizontal wind speeds occur close to the surface as the downdraft impinges upon the ground, diverges and tends to form a ring vortex, which travels away as an outflow (Gunter and Schroeder, 2013). The highest wind speeds are usually found in the inferior region of the ring vortex, where outflow wind speeds are enhanced by the circulation of the ring. The horizontal wind speeds would vary approximately linearly from its centre until a radius where the wind speed is maximum, and then would decay with increasing radius. The forward velocity of the moving convective storm can be a significant component of the total wind speed produced at ground level, and must be added as a vector component to the wind speed produced by the outflow of the downdraft (Holmes, 2007).

The leading edge of the downdraft outflow is called the gust front, which can typically be from 100m to 1km high, last from 2 to 20min and spread with speeds of 5 to 15m/s.

High winds generated by severe convective storms are usually associated with the strong outflows of these downdrafts. These downdrafts are usually referred to as downbursts, and when the length scale of the area affected by high winds is characterised, they are sometimes referred to as microbursts or macrobursts. Weisman, 2003c, for example, defines a downburst as an event that presents diverging outflows with wind speeds greater than 90km/h (25m/s).

According to Fujita, 1985, these outflows have typical length scales from 40m to 40km, time scales of some minutes, and can reach wind speeds of up to 270km/h (75m/s). Downbursts are capable of inflicting severe damage to structures, trees and crops and also represent a hazard for the population.

Strong downburst outflows dominate the extreme wind climate in relation to wind loading of structures in many parts of the world (Holmes et al., 2005), especially in mid-latitudes, as in some regions of North America (Vega and Letchford, 2009), South America (Durañona, 2011b; Natalini et al., 2011; Riera, 2013), South Africa (Kruger et al., 2010), Australia or New Zealand (AS/NZS:7000, 2010). More recently, it has been recognised that even at higher latitudes they may define the design wind speeds for longer return periods (Letchford, 2015). After the recognition of the relevant role that downbursts can play in the definition of design wind speeds, their research received special attention in the area of overhead transmission lines (Riera and Ponte, 2012).

Although many research efforts have been carried out to understand the evolution of wind speed, turbulent characteristics and wind profiles of severe convective outflows, these still remain poorly understood (Gunter and Schroeder, 2013). The lack of data on the wind structure of these events is presently being addressed by several measurement programmes and research activities worldwide.

During the study of downbursts, several models have been developed as part of overhead transmission lines and/or wind engineering research projects (e.g. Savory et al., 2001; Holmes et al., 2005a; Chay et al., 2006a; Chay et al., 2006b; Riera and Ponte, 2012, etc.). These models usually offer different expressions for estimating the slowly varying part of the horizontal wind speeds near the ground produced by downbursts, as a function of the position from the centre of the downdraft, time and height, velocity of the storm, among other parameters.

As the origin of wind gusts from downbursts is a downdraft of cold air of finite width emerging as a horizontal gust front near ground level, the wind structure presents significant differences from that of flows of ABL type, as Figure 2.11 and Figure 2.12 illustrate.

According to Holmes et al., 2005a some of the principal differences between both types of flows are that: downburst wind speeds do not increase monotonically to heights beyond the thickness of the original downdraft jet; the effects of terrain and topography on wind speed values and on their profiles with height are very different; and the largest downburst wind gust speeds are probably well correlated over both horizontal and vertical distances, significantly more than for flows of ABL type. The latter property was illustrated by the gust structure of a supercell rear-flank downburst measured at Lubbock, Texas, over seven anemometers at heights between 3m and 15m, spaced over a distance of 1.6 km (Gast and Schroeder, 2003). A measurement of the integral length scale calculated over the peak 2 minutes of the storm gave a value of 350 m, a much higher value than that found in synoptic storms at the same height. The recorded peak gust speeds up to 15m, showed very little variation with height during this storm in, − a result which may be significant for low-rise buildings.

According to Holmes, 2007, for downdraft outflows, it is usually considered that at the horizontal location where the maximum wind gust occurs, wind speed increases from ground

level up to a maximum value at a height of 50–100m, as Figure 2.12 suggest. Above this height, the wind speed would decrease. More recent research has measured the highest wind speeds at higher heights (Gunter and Schroeder, 2015).

Other relevant characteristics of downburst outflows are the sharp wind speed increase that occurs during the passage of the gust front, usually associated with rapid changes of temperature and wind direction. An example of this behaviour is illustrated in Figure 2.13.

Depending upon the intensity of the severe convective storm, wind gust speeds can increase from 3 to 30m/s in few to around tens of minutes according to e.g. Colmer, 1971 and Sinclair et al., 1973, while their decrease is usually slower (Wallace and Hobbs, 2006).

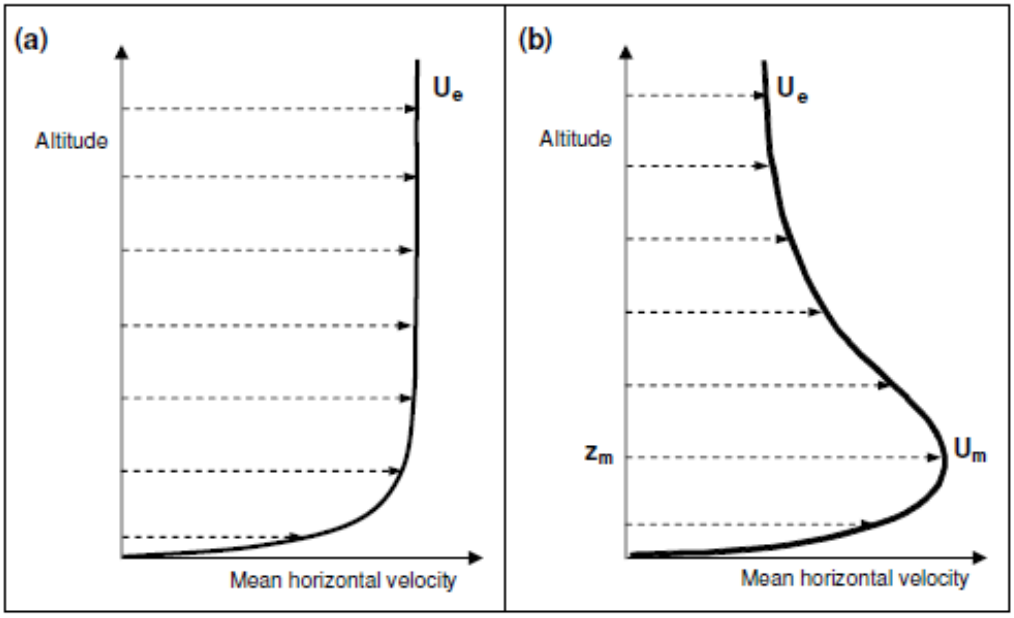


Figure 2.11 Expected wind speed profiles for (a) a flow of ABL type and (b) a downdraft outflow (from Lin, 2010)

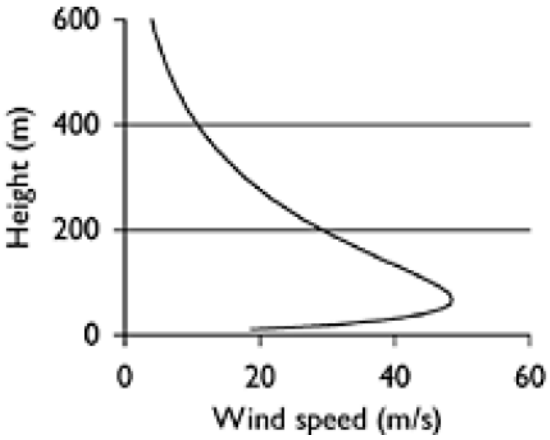


Figure 2.12 Expected wind speed profile for a downburst outflow from a stationary storm (from Holmes, 2007)

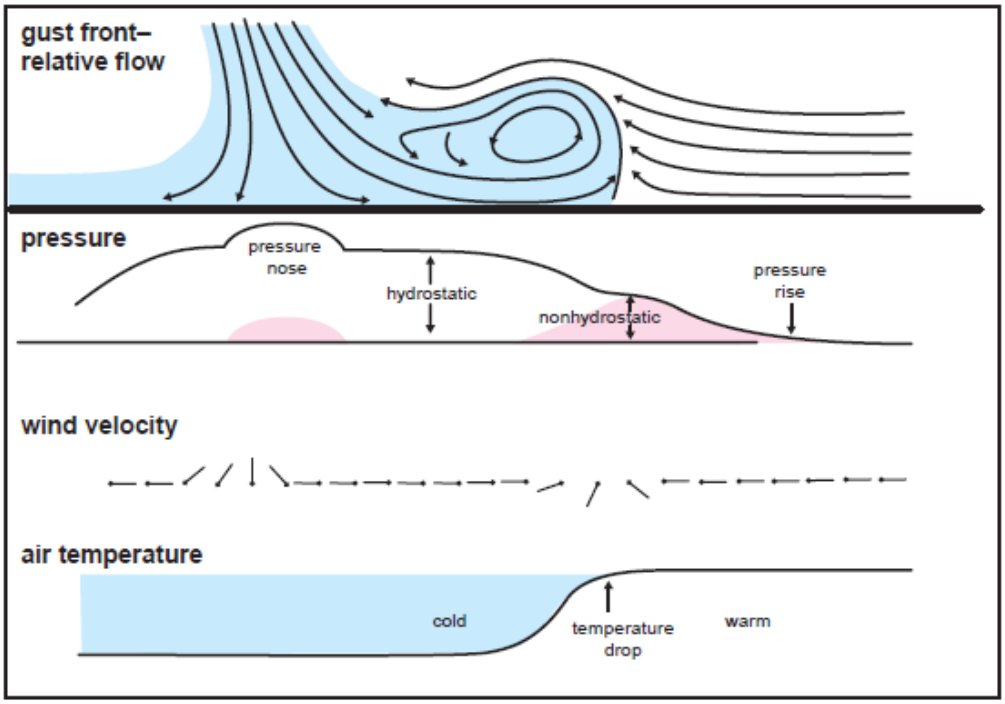


Figure 2.13 Typical wind structure, pressure, wind speed, direction and temperature evolution during the passage of a downburst (from Markowski and Richardson, 2010)

It is worth pointing out that for an observer on the ground, the passage of a gust front may resemble that of a cold front that presents severe convective activity along its front, as in both cases wind gusts can sharply increase, and occasionally exceed 100km/h (~28m/s) according to Ahrens, 2009; temperature can present an abrupt decrease, with changes as high as 10°C in just a few tens of minutes, and wind direction may present a shift.

As it is later described in this sub-section, cold fronts may be preceded by one or more lines of severe convective storms, called squall lines, which generate gust fronts and are usually parallel to the cold front. An example of changes in wind speed and temperature measured during the passage of a line of severe convective storms is presented in Figure 2.18.

Continuing with the third and last stage in the evolution of an isolated convective cell after its mature stage, during which the downdraft is generated and its outflow spreads, the storm enters into its dissipating stage, which may take from 15 to 30min. If severe weather occurs, it usually takes place near the transition from the mature to dissipating stages, or about the time when the maximum fallout of precipitation occurs. During the dissipating stage, the downdraft tends to cut off the supply of warm humid air required to form cloud droplets. In the case of isolated cells, the precipitation falls through the updraft rather than being deposited away from the updraft, and the associated hydrometeor loading reduces updraft buoyancy. The updraft then weakens and the downdraft tends to dominate the cell.

The three stages of development of an isolated convective cell are illustrated in Figure 2.14.

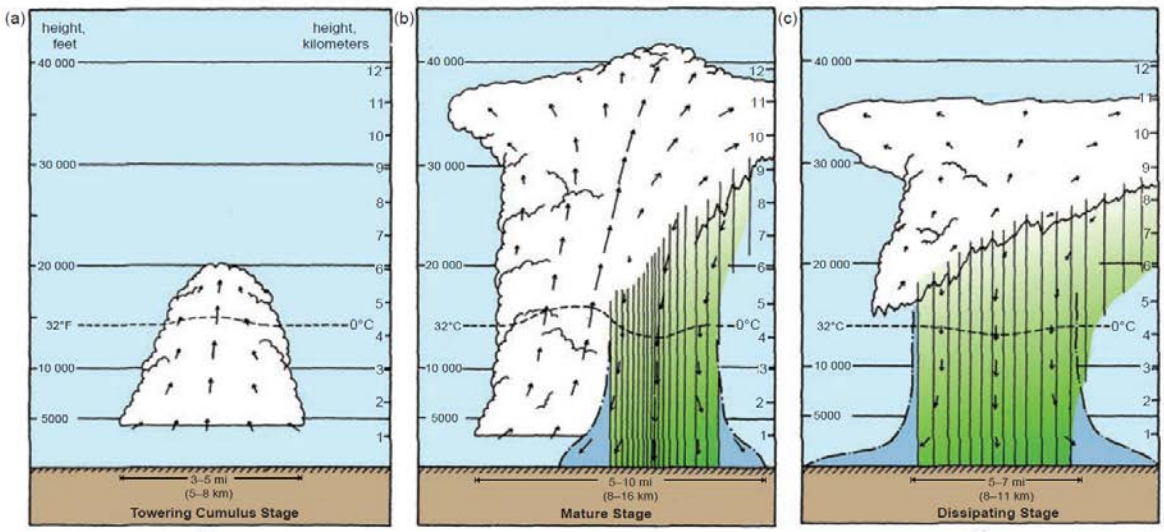


Figure 2.14 Stages of an isolated cell (Markowski and Richardson, 2010)

Multicellular convection appears when atmospheric conditions are adequate for isolated convective cells to trigger the formation of new cells. In this case, downburst winds usually less than 110km/h (~30m/s) and weak tornadoes can occur, according to Markowski and Richardson, 2010.

In this type of convective storm, each cell behaves as a single cell, but when a cell matures, a new one is triggered along its gust front, where the forced ascent is sufficient to lift air parcels. The cold downdraft of the first cell, upon reaching the surface, forces warm, moist surface air upwards, which condenses and gradually builds into a new cell. A series of cells then grow in clusters or in lines, each in a different stage of development. In this way, a highly organized cluster or line of cells is maintained for a much longer period of time than the typical lifetime of an individual cell. This mechanism is illustrated in Figure 2.15, and according to Markowski and Richardson, 2010, this is probably the most common form of convection in mid-latitudes.

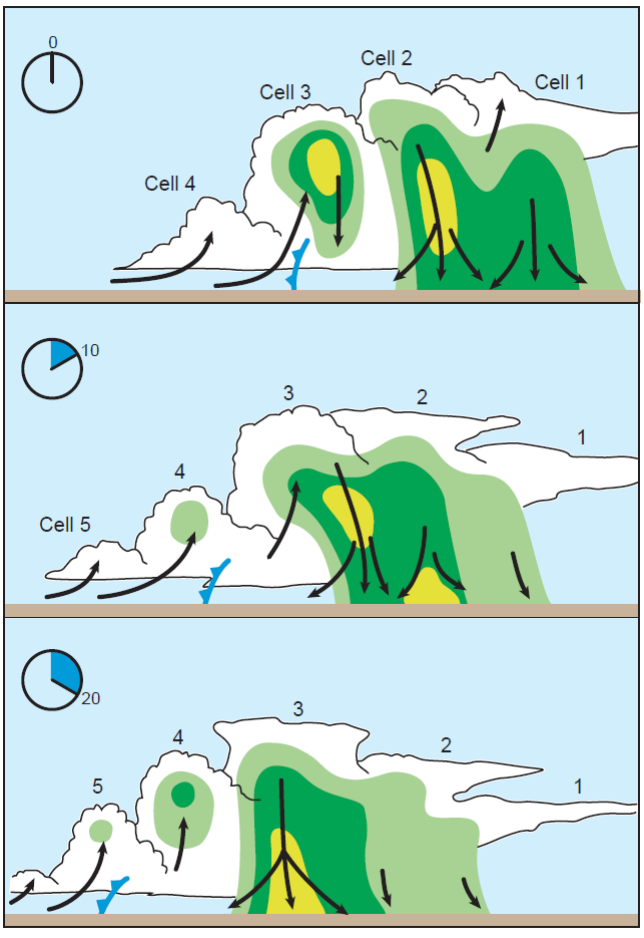


Figure 2.15 Multicellular convection (from Markowski and Richardson, 2010)

The most severe forms of multicellular convection can last for hours, as previously shown in Figure 2.2, and produce large swaths of damaging straight line winds, and hail up to the size of golf balls.

Supercells

The supercell is potentially the most dangerous convective storm, often producing downdrafts with outflow wind speeds greater than 180km/h (50m/s), large hail and violent and long-lived tornadoes, all of which pose a high threat to life and property. They are large and highly organised rotating storms that can persist for many hours. Their distinguishing characteristics are their rotating updrafts and a persistent separation between the primary updraft and downdraft currents (Weisman, 2003c). Markowski and Richardson, 2010, for example, presents a detailed description of this type of convective storm.

Convective storms do not typically occur as isolated events. Instead, they tend to form in groups, in either lines or in clusters of individual cells. In these cases, they have an identity of their own that transcends the cells of which they are made up. The most common grouping is in lines, sometimes referred to as squall lines (Doswell, 2003b).

When groups of convective cells become organized into large systems, they can be classified as **mesoscale convective systems (MCSs)**. The American Meteorological Society's Glossary of Meteorology defines a MCS as any ensemble of convective storms producing a contiguous precipitation area with a horizontal scale on the order of 100km or more in at least one direction. Their typical horizontal length scales were illustrated in Figure 2.2 and Figure 2.4.

MCSs can take a variety of forms (Holton, 2003) and can be, for example, classified according to Figure 2.16 (Markowski and Richardson, 2010).

Squall lines are MCSs that organise in lines, as their name suggests. Bow echoes are arc-shaped structures that can form within squall lines. Multiple bows embedded within a single line form a line-echo wave pattern, while mesoscale convective complexes (MCCs) have a fairly circular anvil (Markowski and Richardson, 2010).

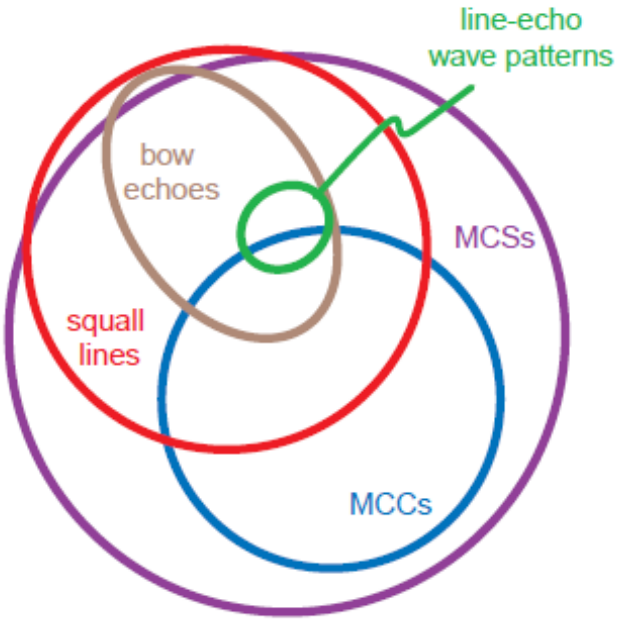


Figure 2.16 MCSs sub-classification (from Markowski and Richardson, 2010)

MCSs can extend over hundreds of kilometres and, in some cases, can last for several days (Weisman, 2003c). Wind and hail events produced by such grouping of convective storms are intermittent, rather than prolonged (as supercells), as cells form and decay.

The interaction between individual cells in lines and clusters of convective storms is often complicated, hard to predict and not completely understood, but those interactions are responsible for severe weather (Doswell, 2003b).Warm season convection in mid-latitudes, as well as tropical convection, is most often organised into MCSs with length scales of 100-1,000km and typical lifetimes of 6-12h. They have a strong impact on severe weather and heavy rainfall in these areas (Laing, 2003).

Several studies have shown that the presence of a low level jet stream (LLJS -defined in Annex A.1) parallel to mountain ranges favours the development of MCSs, as in the case of the Great Plains of USA (Maddox, 1983; Cotton et al., 1989), or in mid-latitudes in South America (Velasco and Fritsch, 1987), as described in Annex A.1.

A **squall line** is a group of convective storms arranged in a line, behind a long, continuous gust front (Wallace and Hobbs, 2006). This term applies to any line of rapidly moving convective storms, including large multicellular convective storms (Laing, 2003). Their longitudinal length scale is usually from 100 to 1,000km.

Squall lines are the most common type of mid-latitude MCSs. Severe convective storms in the form of lines are most frequent in spring and summer, producing twice as many tornadoes, high winds and hail as more circular MCSs (Laing, 2003). They can persist for many hours, and generate damaging winds and hail during their lifetimes. Since the squall line by its nature lives much longer than its constituent cells, these systems are the producers of copious rain, and, frequently, of severe weather such as high winds, tornadoes and flash floods (Rotunno, 2003). They occur over parts of the tropics as well. Tropical squall lines usually propagate westward, whereas mid-latitude squall lines usually propagate eastward.

Updrafts, and therefore, new cells, continually re-form at the leading edge of these systems with rain and hail following behind. Individual updrafts and downdrafts along the line can become quite strong, resulting in episodes of strong outflow winds and large hail, which move rapidly ahead of the system. While tornadoes can occasionally form on the leading edge of squall lines, the latter primarily produce straight-line wind damage from their downdrafts outflows.

Sometimes, a frontal zone, i.e., a surface dividing air masses of different characteristics, is composed of a number of rain bands, aligned almost parallel to the front, whose nature can resemble that of a squall line. Cold fronts, in particular, tend to trigger cumulonimbus convection, as Figure 2.17 illustrates, which in turn generates strong downdrafts and gust front structures at the surface. According to Wallace and Hobbs, 2006, squall lines are sometimes observed in the warm sector in advance of, and oriented parallel to, a cold front, 100 to 300km ahead of it (Ahrens, 2009). Baines, 2003 mentions that cold fronts usually contain one or more squall lines.

An example of the sudden changes in wind speed and temperature that can be experienced during the passage of a MCS organised in a line is shown in Figure 2.18. This figure presents simultaneous measurements of temperature and 2.5min-mean horizontal and vertical wind

speed at 12m height during the passage of such a system at a site in Switzerland (Schmid et al., 2000).

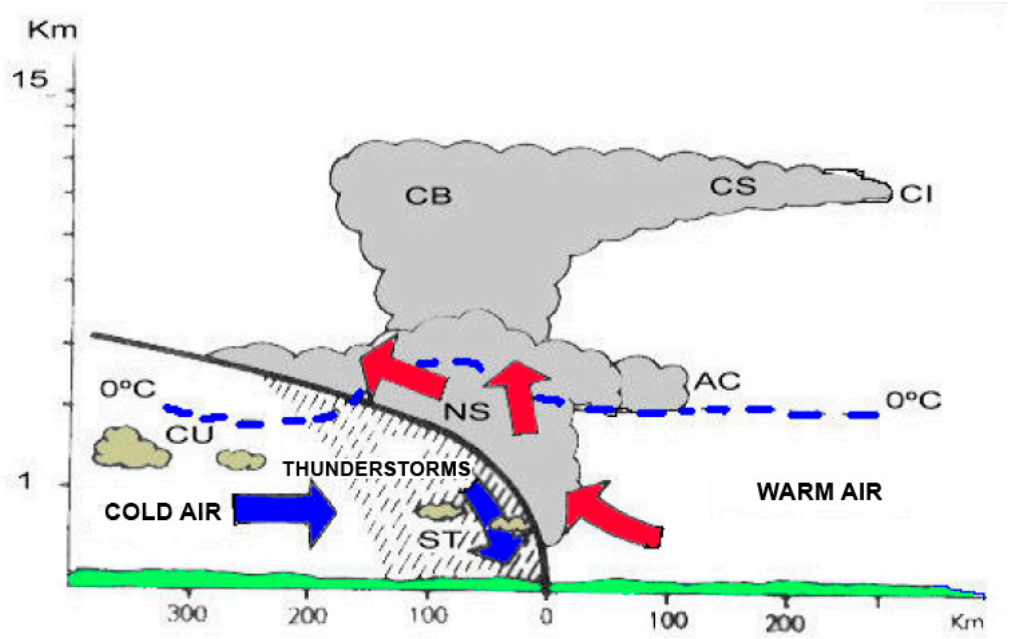


Figure 2.17 Cold front passage and associated cumulonimbus (CB) clouds (Bidegain, 2007)

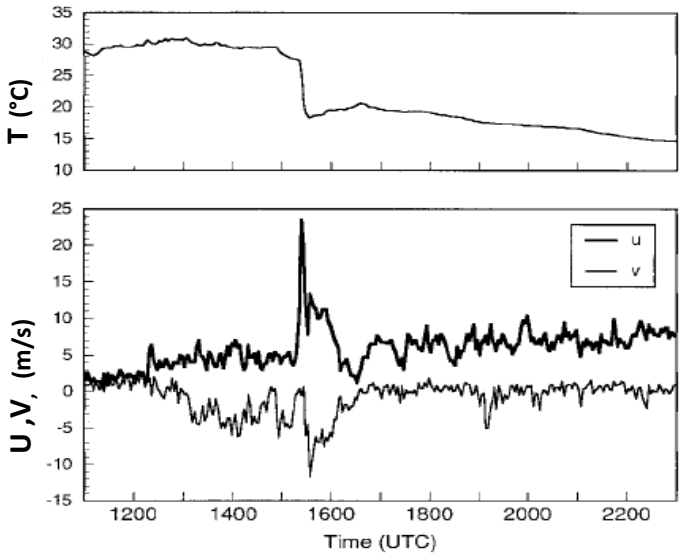


Figure 2.18 Temperature and 2.5min-mean horizontal (u) and vertical (y) wind speed at 12m height, during the passage of a MCS organised in a line in Switzerland (adapted from Schmid et al., 2000)

A temperature drop of about 10-12°C with a simultaneous sudden increase in wind speed can be noticed around 15:30 UTC in this figure. 2.5min-mean wind speeds of 24m/s were measured at 12m height, and a 10s averaged wind gust speed of 43.8m/s was measured at 74m height. In some stations, a shift of wind direction was also recorded. During this study it was also observed that the overall duration of strong gustiness was longer than that expected for a pure microburst as presented in the work of Fujita, 1985. Looking at Figure 2.18, it can also be noticed that wind speeds returned to their previous values after around one hour of their sudden increase.

Long-lived strong squall lines are sometimes called ‘derechoes’ (Spanish word for ‘straight’). Derechoes can travel many hundreds of kilometres and can produce considerable widespread damage from wind and hail.

According to Weisman, 2003a, the term derecho is used to describe convective systems that produce straight-line wind gust speeds greater than 26m/s within a concentrated area with a major axis length of at least 400km. Wind gust speeds must also show a systematic pattern of progression, with no more than 3h elapsing between successive wind damage events. Such systems have been observed to have lifetimes as long as 18h and produce a swath of damaging winds hundreds of kilometres wide and up to 1,000km long. In the USA, the duration of derechoes has been observed to range from 2.3 to 20h, with an average lifetime of 9.2h. They are the largest and most long-lived of the convective systems.

On the other hand, a **bow echo** usually begins as a strong convective cell or a short line of convective cells that may be either isolated or embedded within a more extensive squall line. As strong surface winds develop, the initial cell evolves into a bow-shaped line segment of cells, with the strongest winds occurring near the apex of the bow (Weisman, 2003a).

Bow echoes represent one of the primary convective structures associated with derecho events, but severe bow echoes occur much more frequently than derechoes. They produce damaging surface winds over more limited regions and for shorter time periods.

MCCs

Mesoscale convective complexes (MCCs) are large convective systems, with horizontal length scales that may range from 250 to 2500km, which exhibit a circular, long-lived, cold cloud shield. Beneath the nearly circular cirrus canopy, the organization of the convection may be much more linear. Thus, many squall lines and bow echoes can also be classified as MCCs, as illustrated by Figure 2.16.

These systems generally undergo merging and splitting throughout their life cycles; usually move slowly (at speeds less than 40km/h, i.e., ~11m/s); often exist for periods exceeding 12h and can produce a wide variety of severe weather, as hail, high winds, flash floods and tornadoes. Velasco and Fritsch, 1987 indicate that, for North and South America, the strongest convection inside a MCC usually occurs at its western and equatorward portion. In the USA, about 25% of all MCCs produce damaging straight-line winds or derechoes (Ahrens, 2009).

The definition of MCCs strongly depends on the available information from satellites. The reference used to classify a MCS as a MCC is the maximum infrared temperature of a black body, -32°C, which represents in average the initiation of convective precipitation. A MCC can be defined as a system that presents an area greater than 50,000 km^2 with a temperature lower than -52°C, so as to be convectively active and produce rainfall over a significant area (Necco, 1988). Different authors may use different definitions, for example Salio et al., 2007 identify the initiation of a MCC when the area enclosed by the -55°C isotherm exceeds a value of 50,000 km^2.

Doswell and Bosart, 2001 show the distribution of MCCs along the world in a map adapted from Laing and Fritsch, 1997, which is reproduced in Figure 2.19, after adding the location of Uruguay.

Velasco and Fritsch, 1987 indicate that MCCs tend to be concentrated immediately downwind of major mountain ranges, for mid-latitudes as well as for low latitudes, and that during the NH summer, MCCs in the USA shift strongly poleward with the polar jet stream, while in the SH summer, South American MCCs stay quasi-stationary with the subtropical jet stream.

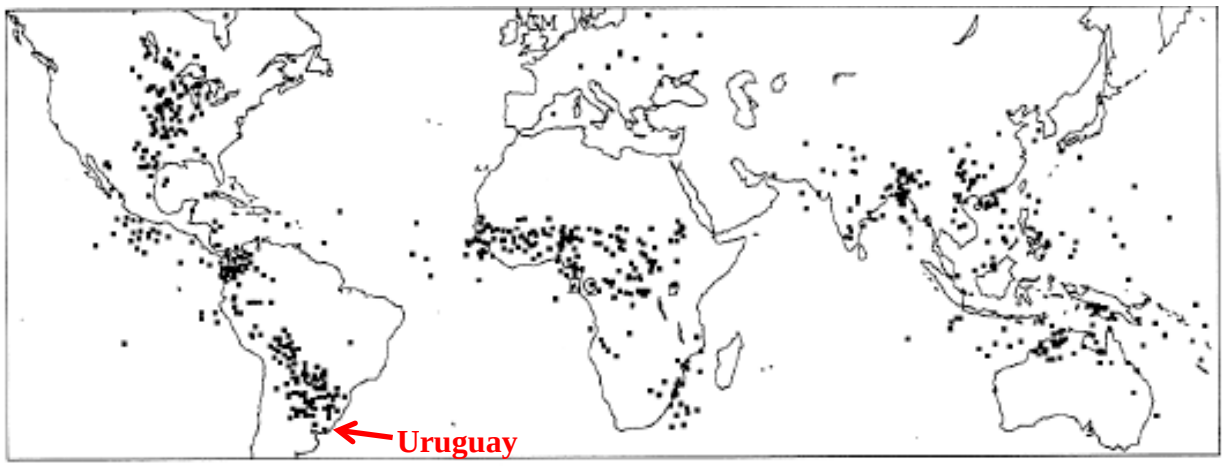


Figure 2.19 Global distribution of MCCs at their maximum extent (adapted from Laing and Fritsch, 1997)

According to Laing, 2003, mid-latitude MCCs in the NH are most frequent from June to August, while Velasco and Fritsch, 1987 indicates that for South America the months with more frequent MCC activity are November to April. Other difference is that MCCs in South America tend to be around 60% larger than in the USA.

For further information on the characteristics of tropical MCCs, the reader is referred to e.g. Velasco and Fritsch, 1987 or Laing and Fritsch, 1997.

Tornadoes, landspouts and waterspouts

Tornadoes are rapidly rotating columns of air in contact with the ground, with typical widths between 100m and 3km, time scales from just few seconds to, in rare instances, an hour or more. Most tornadoes rotate cyclonically, many have lifetimes of tens of minutes, and their average path length is about 7km, although some tornadoes have been reported of having travelled for hundreds of kilometres (Bluestein, 2003; Ahrens, 2009). Their depth ranges from only hundreds of meters to 10km. Their time and length scales were illustrated in Figure 2.2 to Figure 2.4. Theories of tornado formation and models of their structure can be found for example in Bluestein, 2003.

Horizontal wind speeds in tornadoes may vary from 18 to around 120m/s, while vertical wind speeds may be almost as intense as the horizontal wind speeds (Bluestein, 2003). In the most intense 2% of tornadoes, horizontal wind speeds may exceed 90m/s, but over 50% of them have peak wind speeds less than about 40 to 50m/s. The highest wind speeds occur over an area generally less than 20% of the tornado damage path (Cermak et al., 1998). Tornadoes represent a hazard for population and properties, and can produce devastation and many losses of lives if they strike in populated areas.

From a wind engineering approach, as the probability for a point target to be hit by a tornado is not high, tornado winds do not generally influence the wind hazard curve for point targets and small buildings for return periods less than 1,000 years. This number depends on the region of the world under consideration, but it is always high. As a consequence, tornado occurrence is usually just considered for the design of critical structures, such as nuclear power plants (Cermak et al., 1998), and sometimes when their impact on linear structures, such as high voltage transmission lines, or in large areas (e.g. large cities or towns) needs to be analysed.

Tornadoes occur mainly in large continental plains such as in the USA, South America, Russia and South Africa (Holmes, 2007). Figure 2.20 presents, for example, the number of 6h periods with environmental conditions prone to the occurrence of (a) severe convective storms and (b) significant tornadoes formation worldwide, updated from the study performed by Brooks et al., 2003 based on reanalysis data from NCAR/NCEP. This figure shows that SESA, and in particular, Uruguay, are located in the second region of the world with more frequent severe convective activity, after the Great Plains of USA. It can also be seen that these regions are concentrated downstream of high terrains, and poleward of moisture sources in the form of warm water or rain forest.

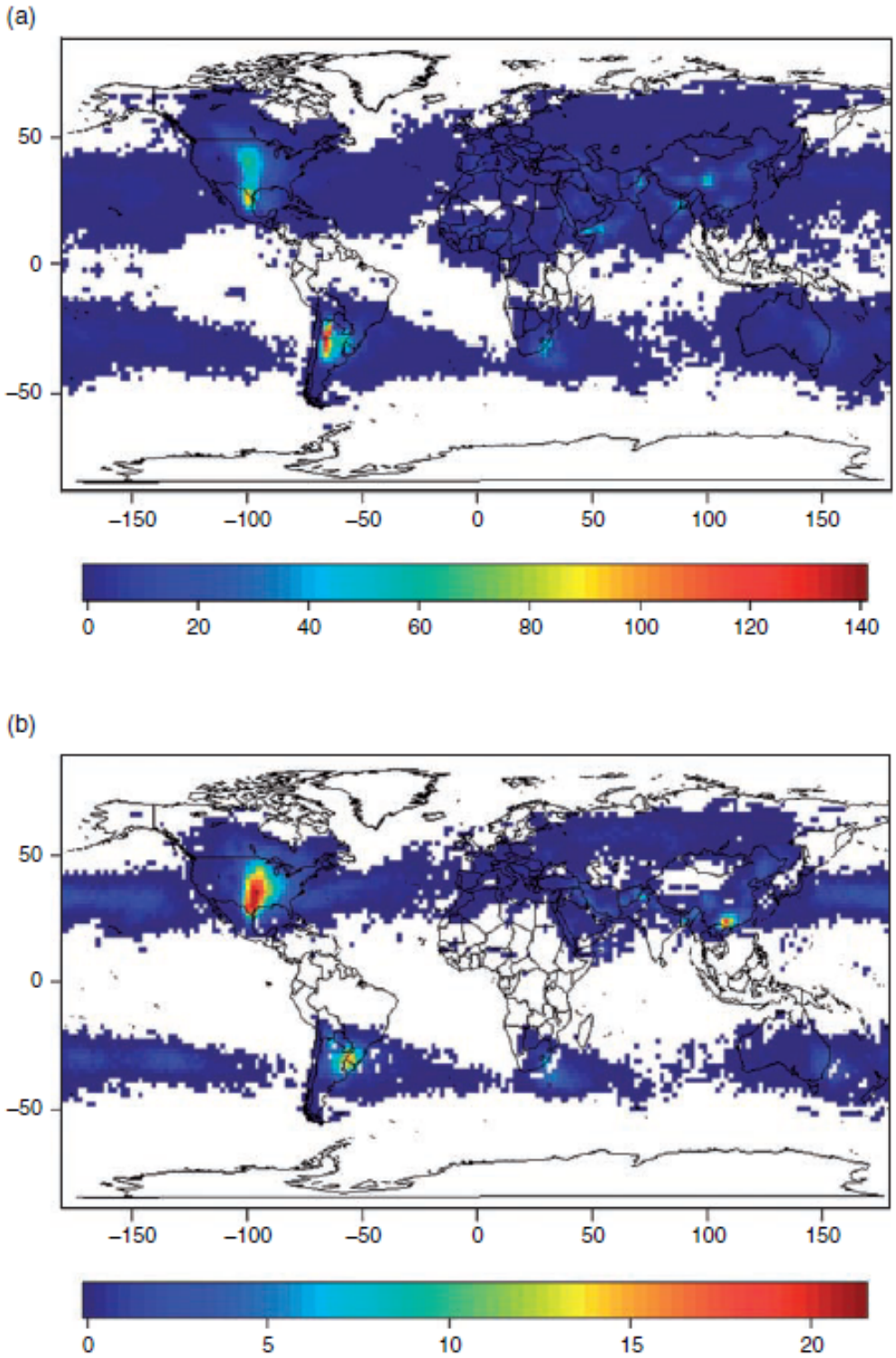


Figure 2.20 Number of 6h periods per year prone to the occurrence of (a) severe convective storms and (b) significant tornadoes (updated from Brooks et al., 2003 in Beniston et al., 2008)

Category	*Original wind speed range (m/s)*	*Proposed wind speed range (m/s)*
F0	18–32	29–38
F1	33–50	39–49
F2	51–70	50–61
F3	71–92	62–74
F4	93–116	75–89
F5	117–142	90–105

Table 2.3 Fujita intensity scale for tornadoes (Holmes, 2007)

An intensity scale for tornadoes was originally proposed in 1971 by Fujita (Fujita, 1971), ranging from F0 to F5 tornado categories. Each F-scale is associated with a specific wind speed range, although in practice, classifications are applied based on observed damage to buildings and other structures. The original scaling has been criticized by engineers for several reasons, e.g. for failing to take into account variations in the quality of constructions, as well as in their types, which may greatly differ among different regions of the world, and for not having been based on a proper correlation between damage descriptions and wind speeds. The original scale, and a scale proposed by McDonald et al., 2006, the enhanced-Fujita scale (EF-Scale) are shown in Table 2.3. These wind speed values would correspond to 3s gusts.

On the other hand, the term **landspout** is sometimes used to refer to relatively weak, short-lived tornadoes generated by isolated convective cells (Weisman, 2003c).

Finally, **waterspouts** are tornadoes that form over water, more frequently in mid-latitudes and during the warm season. They can have diameters ranging from a few meters up to 100m or more and average lifetimes of 5 to 10min. Large waterspouts may persist for up to 1h and are the most hazardous. Waterspouts have also been reported to occur in groups or sequential families of up to nine generating from a single cumulus cloudline over a 90min period.

The primary risk from waterspouts is to residents, mariners and structures in sea and large inland lakes and coastal areas. There are some well documented cases of large vessels being capsized or de-masted, and reports of boats of 25ton being lifted and turned round by large waterspouts (Golden, 2003). More details of this type of severe wind event can be found in this last reference, or in e.g. Markowski and Richardson, 2010.

2.2.4. Topography and wind climate of South America

As indicated in previous sub-sections, topography has a direct impact on mean and extreme regional wind climates as a result of its interaction with atmospheric wind flows and its direct influence on the general circulation of the atmosphere, as detailed in Annex A.1.

Figure 2.21 gives a qualitative description of the topography of South America (SA) (Lydolph, 1985), while Figure 2.22 additionally shows some climatic characteristics that also influence the mean and extreme wind climates of different regions of SA (Veblen et al., 2007), such as the location of the ITCZ, semi-permanent areas of high and low pressure, typical surface wind flows (described in Annex A.1 and indicated in Figure 2.5, and in Figures A.3 and A.4), ocean currents, etc.

The Andes Cordillera (hereafter called the Andes), shown in Figure 2.21 and Figure 2.22, act like an 8,500km long 'climatic wall', being the most continuous mountain barrier on Earth. They extend from latitude 12°N to 56°S and vary in width from 250 to 750km (Veblen et al., 2007). Southward from the Equator their elevation is between 4,000 and 7,000m, presenting their highest point at about 32°S latitude. Peaks above 5,000m are found up to about 35°S latitude, south of which they lower and eventually become dissected by glacial fiords. The Andes drop off very abruptly on both sides; on the west they often plunge steeply to the Pacific Ocean, while on the east they plunge to low-lying basins (Lydolph, 1985).

Due to the Andes location, great part of SA is mostly exposed to Atlantic influences, with only a narrow western coastal strip in the south directly influenced by the Pacific Ocean. The Andes also produce major atmospheric perturbations that allow the greatest meridian penetration of air masses anywhere in the SH (Lydolph, 1985). Although a large part of the Andes is located in the tropics, they have a great effect in the atmospheric circulation of the southern part of SA, as it is described in this sub-section.

Figure 2.21 also shows the broader Guyana and Brazilian highlands, most of which lie between 500 and 2,000m above sea level, presenting peaks up to almost 3,000m in both cases. They tend to block the circulation over part of SA. Thus, a low, interior and continuous flow corridor of warm and humid air from the equatorial Atlantic Ocean starts between the Guyana and Brazilian highlands on the east, and attracted by deep seasonal convection over the

Amazonia, whose river is also indicated in Figure 2.21 provides easy access for these moist surface winds to go inland toward the Andes on the west (Lydolph, 1985).

A LLJS, described in Annex A.1, deflects this moisture southward into the Chaco or the Altiplano regions (shown in Figure 2.22) and acts as a triggering mechanism for the formation of severe convective activity over SESA, as it provides heat and moisture to mid-latitudes, generating conditions for a convectively unstable atmosphere (Salio et al., 2007).

According to Veblen et al., 2007 this LLJS takes place especially during the summer, while Salio et al., 2007 indicates that it is present throughout the year, with an intense maximum during spring.



Figure 2.21 South America topography (adapted from Lydolph, 1985)

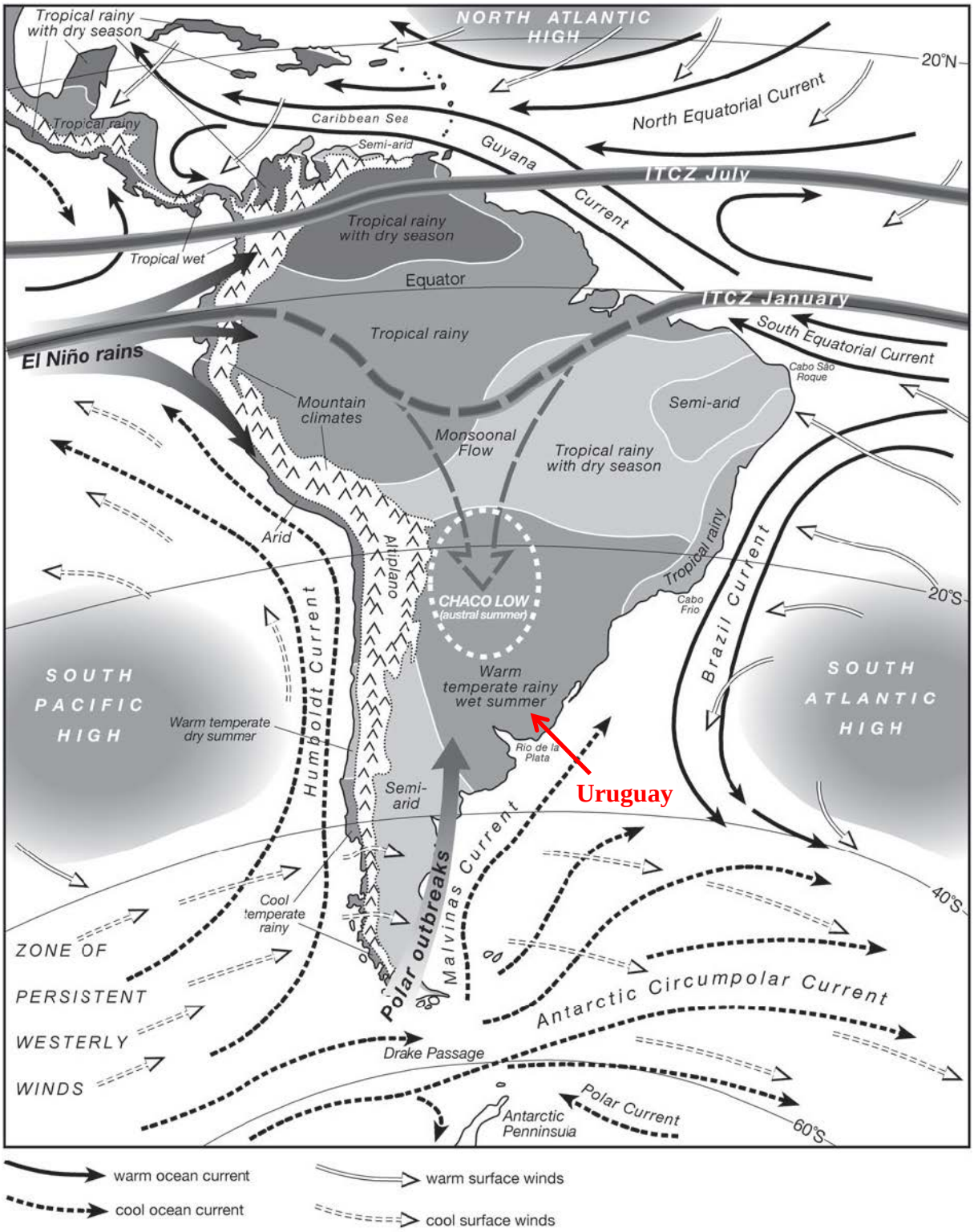


Figure 2.22 South American main semi-permanent highs and lows, surface wind flows and ocean currents that influence SESA wind climate (fromVeblen et al., 2007)

In this thesis, SESA region is defined by the rectangle shown in Figure 2.23, as in Salio et al., 2007. This region includes Uruguay, north eastern Argentina, southern Brazil and southern Paraguay, and it mostly covers the continental latitudes to the east of the Andes between 23° and 40°S, as it can be seen in this figure. Figure 2.23 also indicates the most relevant features of SESA topography and its surroundings, where the presence of the Andes, Sierras de Córdoba in Argentina, and the Brazilian highlands can be noticed. Contours corresponding to heights in meters are indicated by the grey bar of this figure.

SESA region has distinct climatological properties from the rest of SA regarding its extreme wind climate. As it is shown in Sub-section 2.2.4.2, this region concentrates most of the severe convective weather episodes in this continent (e.g. Nascimento and Doswell, 2006; Brooks et al., 2003), as already illustrated in Figure 2.19 and Figure 2.20, and also experiences one of the most significant cyclogenesis activities of SA (Gan and Rao, 1991; Seluchi, 1995, among others).

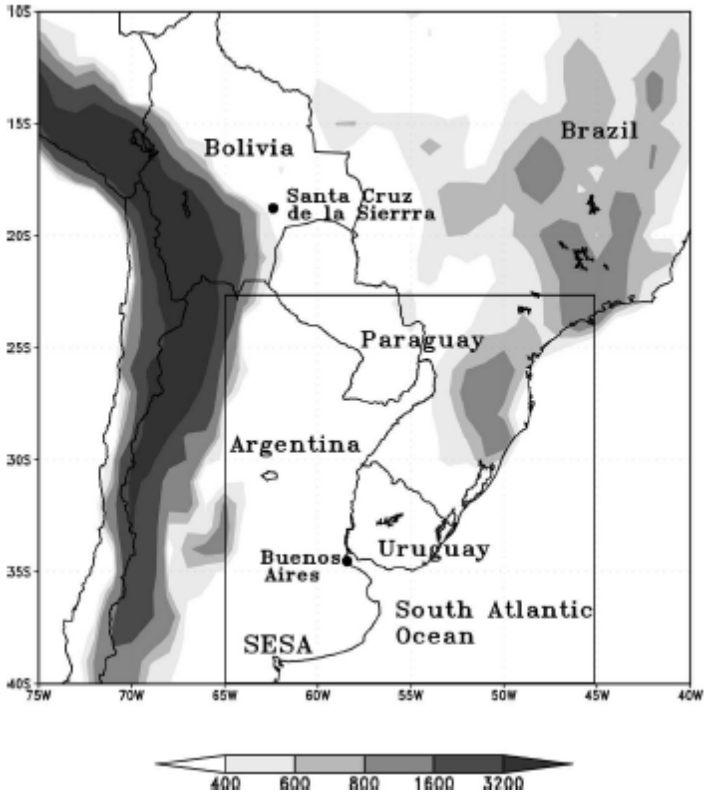


Figure 2.23. Definition of South Eastern South America (SESA) and regional topography (from Salio et al., 2007)

As indicated in Figure 2.22, SESA wind climate is also influenced by ocean currents along the continent's eastern margin. In a more localised way, the presence of the relatively warmer waters of the Río de la Plata (Figure 2.22) and of the rivers Paraguay, Parana and Uruguay, act as local sources of humidity (Prohaska, 1976). On the other hand, Sierras de Córdoba, a mountain range located southward of the Chaco and eastward of the Andes foothills, approximately between 29° and 33°S latitude and 64° and 66°W longitude, could be responsible for triggering convection initiation in some cases or acting as a barrier for the warm humid air coming from the tropics (Schwarzkopf and Rosso, 1993). The location of these Sierras, whose height varies between 1,000 and almost 3,000m, can be noticed in Figure 2.21 and Figure 2.23.

2.2.4.1. Mean wind climate of SESA

The average wind conditions of SESA are mainly controlled by three circulation systems: the circulation within and between the South Pacific anticyclone and the South Atlantic anticyclone, the wind system that develops according to the intensity of the quasi-stationary Chaco low, and the prevailing westerlies of mid-latitudes. Details of these features can be found in Annex A.1. Local winds as land and sea breezes define the mean wind climate in certain regions of SA (Schwerdtfeger, 1976), especially in summer.

As a result of the general circulation of the atmosphere described in Annex A.1 and the features of SA previously outlined, the average sea-level pressure distribution is that shown in Figure 2.24 for the months of January (SH summer) and July (SH winter) (Celemín, 1984). In this figure, letters 'A' and 'B' stand for high- and low-pressure systems (anticyclones and cyclones), respectively. For brevity they will be referred to as 'highs' and 'lows'.

Figure 2.24 presents the same pattern of pressure distribution as Figure A.4(a) and (b), but with more degree of detail.

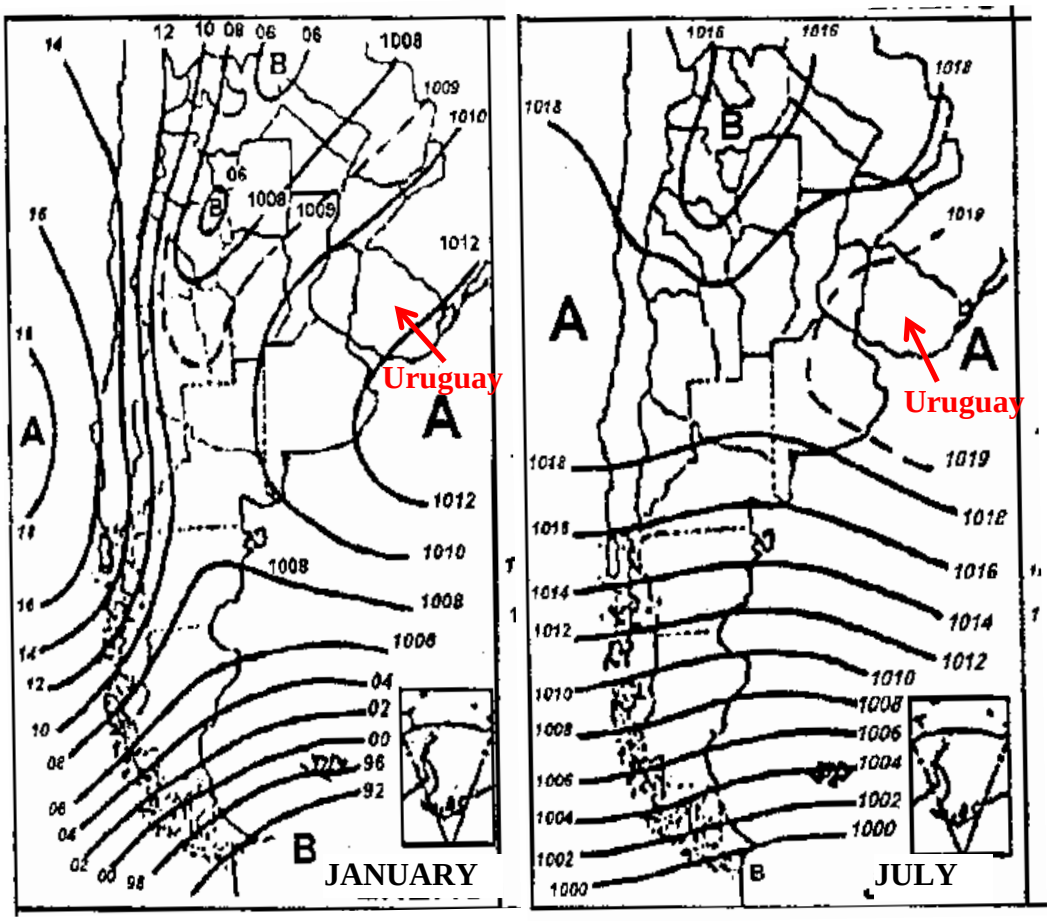


Figure 2.24 Average sea-level pressure distribution for January and July for part of South America (adapted from Celemín, 1984)

The main characteristics shown in Figure 2.24 are:

- The South Pacific and South Atlantic Oceans anticyclones, also shown in Figure 2.22, with relatively warm and dry air masses.

  The first one is generally stable, centred at approximately 32°S and 26°S latitude during SH summer and winter, respectively, although in winter it tends to weaken (Veblen et al., 2007). The second one moves throughout the year, covering in average most of the mid-latitude South Atlantic Ocean during SH summer (January graph), and becomes smaller and moves to the east and northward during SH winter (July graph).

- The Chaco thermal low, also shown in Figure 2.22, is a semi-permanent thermal-orographic low located in north western Argentina, more intense during SH summer, with an average position of around 30°S latitude and 65°W longitude.

  Its origin would be the already described advection of warm, humid (and therefore less dense) air from the equatorial Atlantic Ocean through the corridor between the Guyana and Brazilian highlands (shown in Figure 2.21) and the Andes; reinforced by the diurnal warming of this region, as it usually presents clear skies in summer, and by the Andes acting as an orographic barrier that results in lower pressures on its lee side. The zonda wind over the eastern side of the Andes, i.e., local downslope wind of foehn type (Durran, 2003), could also contribute to its intensification, as mentioned in Necco, 1988. The pressure gradient between the South Atlantic anticyclone and the Chaco low also reinforces the easterly flow of tropical air that is being channelled over the Amazon basin to turn southward. The Chaco low acts then as an 'entrance door' for tropical air into SA mid-latitudes (Celemín, 1984).

- The westerlies over the southern tip of SA and the adjacent South Pacific Ocean, also shown in Figure 2.22.

  These winds from the west are strongest during the SH summer, peaking between 45° and 55°S. During the SH winter, as the subtropical tropospheric jet stream moves northward at about 30°S latitude, the westerlies follow it and expand equatorward (Garreaud et al., 2009).

According to CLIVAR, 2006, during April and May, the southward flow of tropical warm and humid air from the Amazonia weakens, as more frequent incursions of drier and cooler air from mid-latitudes begin to occur over the interior of subtropical SA, and convection shifts gradually northward toward the equator.

2.2.4.2. Extreme wind climate of SESA

Migratory cyclones and anticyclones account for much of the short-term 'weather variations' in mid-latitudes (Sinclair, 1996), which can lead to extreme wind events.

Severe convective activity, which generates downbursts and sometimes, tornadoes (Schwarzkopf and Rosso, 1993; Riera and Rocha, 1998; Durañona, 2010; Natalini et al., 2011; Loredo-Souza, 2012), and extra-tropical cyclones that intensify during their trajectory are the main meteorological events that characterise the extreme wind climate of SESA, as it will be described in the next sub-sections.

2.2.4.2.1. Synoptic high winds in SESA

2.2.4.2.1.1. Extra-tropical cyclones in SESA

One of the regions of the SH with the highest rate of production of extra-tropical cyclones is located in the South American continent between 25º and 40ºS latitude, and in the adjacent. South Atlantic Ocean, as Figure 2.25, from Gan and Rao, 1991, shows. This figure indicates the average number of cyclogenesis events per year, and, if compared with Figure 2.23, it can be seen that this region is contained inside SESA region.

Figure 2.25 also indicates a maximum of cyclogenesis events over Uruguay, whose location Gan and Rao, 1991 relate to lee cyclogenesis due to the presence of the Andes, as it is widely recognised that cyclogenesis is commonly observed downwind of synoptic obstacles. The generation of the second maximum shown in Figure 2.25, i.e., around 40°S latitude and to the east of SA, would be caused by other meteorological reasons.

In a similar sense, Sinclair, 1995 suggested that the maximum found around 30°S latitude could be related to the flow of humid and warm air of the easterlies coming from the tropical Atlantic Ocean, and then deflected southward by the Andes into the mid-latitudes westerlies, as described in previous sub-sections.

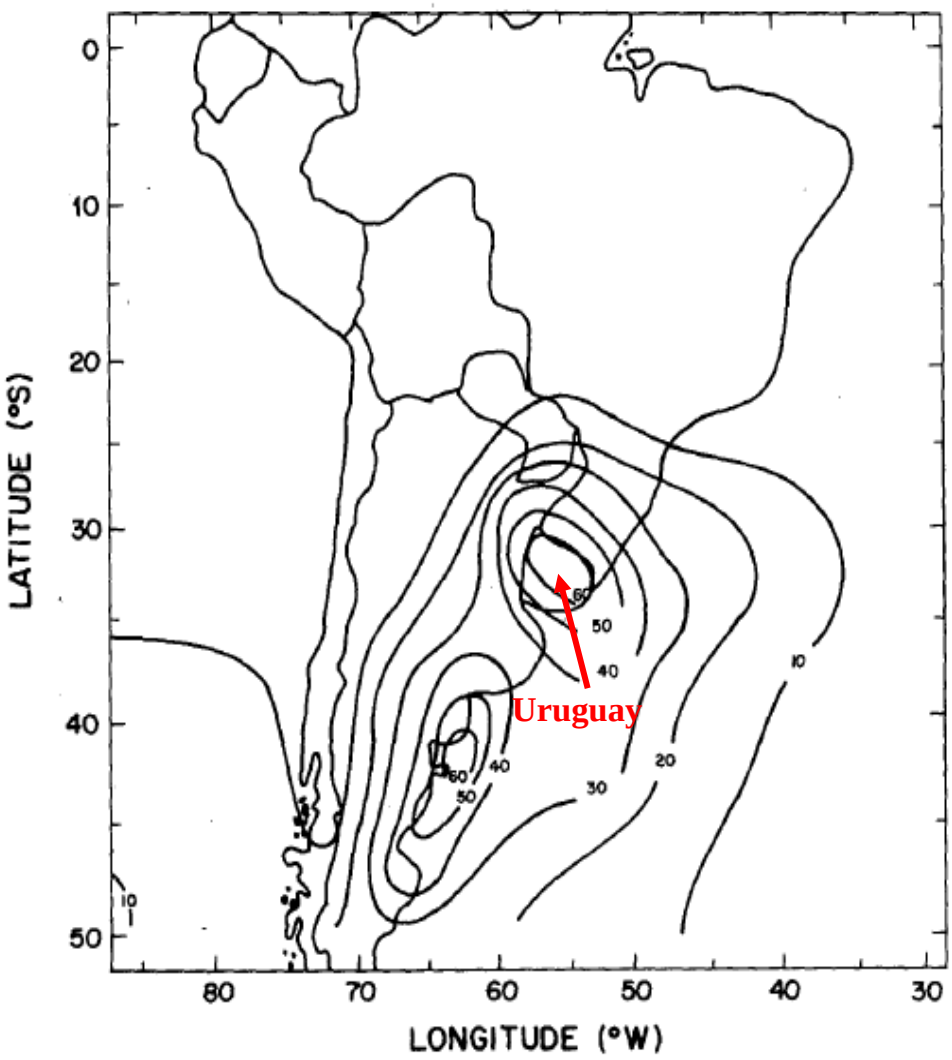


Figure 2.25 Isolines of annual frequency of cyclogenesis (adapted from Gan and Rao, 1991)

Regarding seasonal behaviour, Gan and Rao, 1991 indicate that extra-tropical cyclones over SA are more frequent in winter than in any other season. Accordingly, Necco, 1982a concludes that cyclogenesis over the continent in SESA region is more frequent in SH winter than in SH summer, while Sinclair, 1995 shows that most of the strong extra-tropical cyclones in SA occur in winter.

This behaviour could be explained by the fact that during SH summer, the South Pacific anticyclone occupies a broad latitudinal range and tends to block the westerly flow of humid air masses moving across the Pacific Ocean (Veblen et al., 2007) as suggested in Sub-section 2.2.4.1 and shown in Figure 2.24 for January, thus impeding the northward migration of the

westerlies (Sylvestre, 2009). During SH winter, however, this high weakens and usually moves equatorward, as shown in Figure 2.24 for July (Veblen et al., 2007), allowing northward penetration of westerly storm tracks to latitudes as far north as 31°S (Sylvestre, 2009).

Necco 1982b indicates that half of the cyclones originated north of 35°S latitude and west of 30°W longitude could be categorised from moderate to intense, and its figure 4 (not reproduced here) illustrates that of these, those that formed over the continent were generated inside SESA. He also shows that those initiated in the continent in winter usually present a trajectory toward the south-east, in agreement with Wölcken, 1954 (Figure 2.26(a)).

Figure 2.26(a) and (b) present typical trajectories of low pressure systems in SA for SH winter and summer, respectively, with the width of the broader arrows related to the number of these systems that tended to move with the approximate indicated trajectory. In particular, this figure illustrates the typical behaviour of extra-tropical cyclones initiated in SESA, as well as that of the Chaco low and of the subpolar lows.

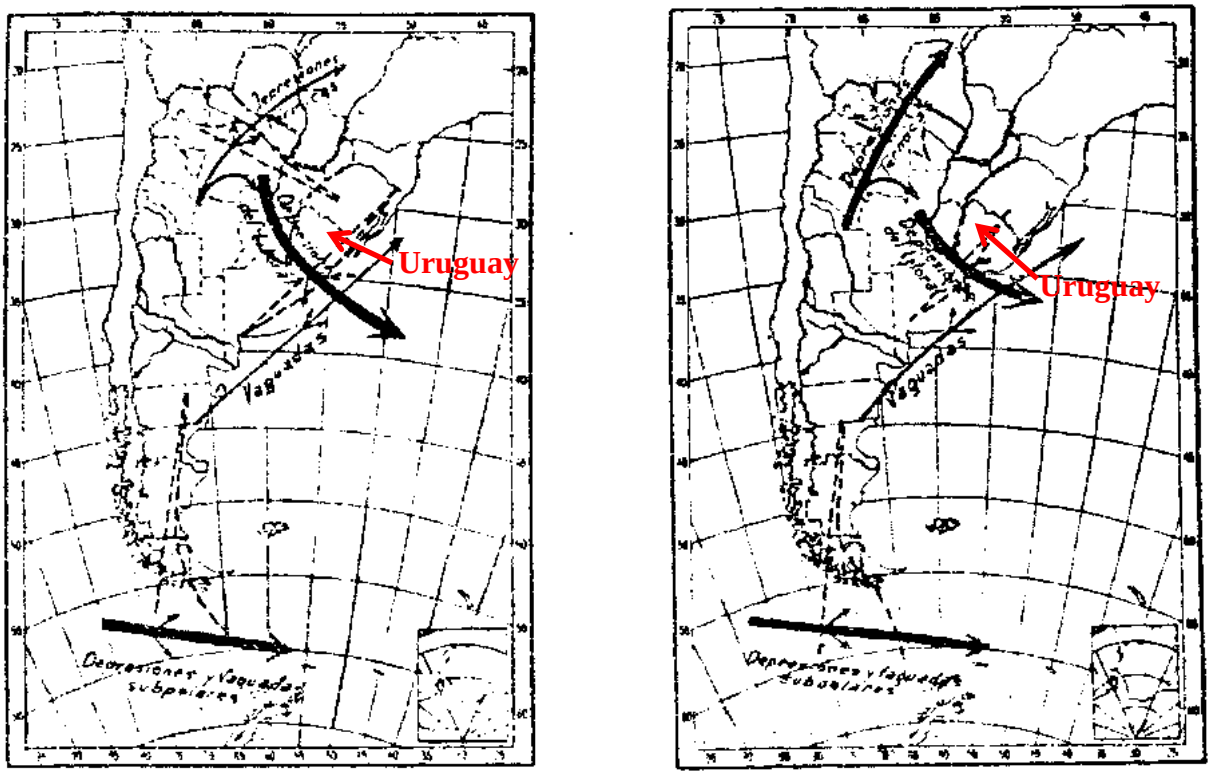


Figure 2.26 Typical trajectories of extra-tropical cyclones centres in South America for (a) SH winter and (b) SH summer (adapted from Wölcken, 1954)

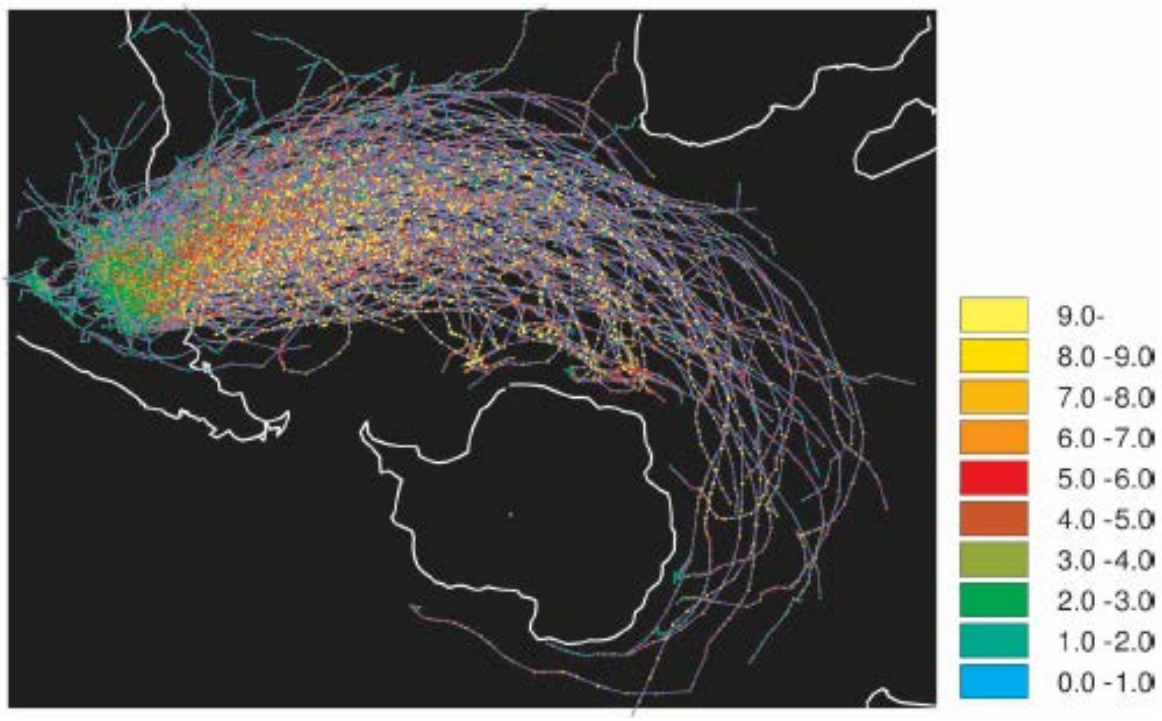


Figure 2.27 Trajectories of all cyclonic systems originating in the cyclogenesis region near 30°S over South America (from Hoskins and Hodges, 2005)

Much more recent results, as the ones presented in Hoskins and Hodges, 2005 from 40 years of re-analysis confirm the trend shown in Figure 2.26(a), as illustrated by Figure 2.27, which shows the trajectories of winter cyclones originated in the cyclogenesis region near 30°S latitude over SA. In this figure, the dots show the position and their colour the intensity of each system every 6h. Higher numbers in the colour bar of this figure correspond to higher intensities.

Likewise, Sinclair, 1995 shows in his figure 11 (not included here) a tendency for intense cyclones to generate to the northwest of Uruguay, with increasing frequency toward the southeast and with a maximum over the South Atlantic Ocean. Results shown in Necco, 1982a would suggest that the most intense extra-tropical cyclones would generate more frequently over Uruguay and toward its northwest.

In relation to rapid cyclogenesis, Sinclair, 1995 indicates that one of the areas where rapidly intensifying cyclones are most frequent is the east of SA along 35°S latitude. This is illustrated in its figure 12 (not included), which shows that Uruguay belongs to that area.

Veblen et al., 2007 observes that the increasing availability of moist air toward the east coast of SESA could contribute to storm intensification, relating this fact to the more frequent explosive cyclogenesis found near this region between 25 and 35°S latitude, especially in spring and fall.

Sinclair, 1995 indicates a translational speed for the rapidly intensifying cyclones between 15 and 20m/s, and preferred directions toward the east and southeast, with the most intense events tending to move toward the southeast.

On the other hand, Schwarzkopf, 1997 indicates that in Argentina strong winds are dominated between 35° an 55°S latitude by large extra-tropical cyclones, which tend to move to west to east; and in its north-central area, by dynamic depressions, which form mainly in winter and early spring and move towards the south-east.

2.2.4.2.2. Non-synoptic high winds in SESA

2.2.4.2.2.1. Severe convective activity in SESA

As shown in Figure 2.28, SESA has been identified as the region most affected by severe convective activity in SA (e.g. Nascimento and Doswell, 2006; Vera et al., 2006, among others), and as the second worldwide after the Great Plains of USA (e.g. Zipser et al., 2006), as illustrated by Figure 2.29 and Figure 2.30. The lower density of population of great part of SA and the fewer instrumentation available than in USA may contribute to an underestimation and unawareness of the significance of severe convective activity in the generation of extreme winds in SESA.

The region inside the dark line of Figure 2.28 corresponds to the area where the most significant severe weather episodes associated with large hail, damaging winds and tornadoes concentrates in SA. It is approximately located within the 20-40°S latitude range, and east of

the Andes (Nascimento and Doswell, 2006), thus being quite similar to the SESA region defined in Figure 2.23.

On the other hand, Figure 2.29 and Figure 2.30 show the location of the most intense convective storms on Earth studied during the Tropical Rainfall Measuring Mission (TRMM), indicating the events with maxima flash rates. In the first figure, the colours categorise these events from the most extreme to the least extreme ones, while Figure 2.30 indicates the location and number of flashes per minute for the 1% most extreme events (Zipser et al., 2006).



Figure 2.28 Map of the approximate geographical region of South America where severe convective activity is more frequent (adapted from Nascimento and Doswell, 2006)

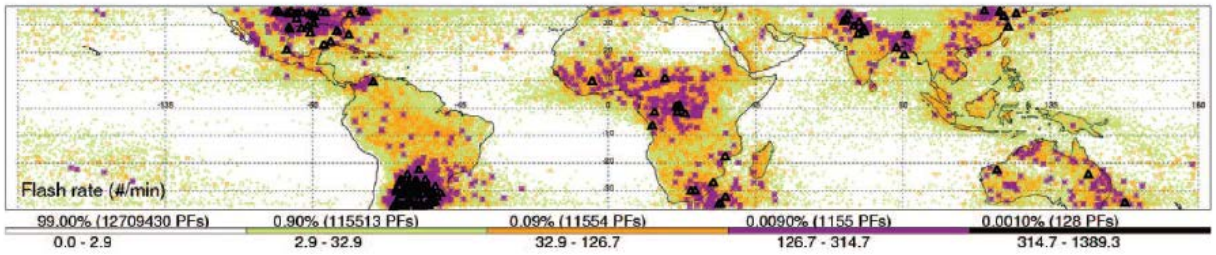


Figure 2.29 Location of the most intense convective storms [1] (from Zipser et al., 2006)

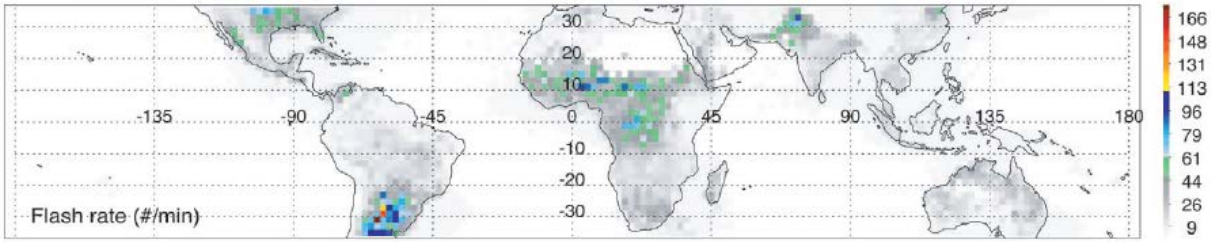


Figure 2.30 Location of the 1% most intense convective storms (from Zipser et al., 2006)

The lower limit of SESA region coincides with the lower limit of the last two figures. It can be clearly noticed that SESA corresponds to one of the regions that develops the most intense thunderstorm activity worldwide.

According to Nascimento and Doswell, 2006, the combination of ingredients for severe convection (humidity, convective instability and vertical wind shear) is frequently found in SESA region, especially from late September to May. This would be in accordance with the results from Zipser et al., 2006 shown in Figure 2.31, which indicates the seasonal distribution of the two most extreme categories defined during the TRMM research. In this figure, a tendency for most extreme events to occur more frequently from September to November may be noticed, followed by the months from December to February.

This seasonal behaviour agrees with the findings of Laing, 2003, presented in Sub-section 2.2.3.2, that indicate that squall lines are more frequent in spring and summer, and with those of Velasco and Fritsch, 1987 that show that in mid-latitude SA most MCCs are found from

[1] The most intense events are represented by black, purple, orange and green colors. The black color corresponds to the category of the most extreme events, while the green color corresponds to the least intense category.

November to April. The period of the year mentioned by Zipser et al., 2006 would also be in accordance with that indicated by Veblen et al., 2007, and with the finding presented in Sub-section 2.2.4 of Salio et al., 2007 and Veblen et al., 2007, that the South American LLJS would be stronger in spring and summer.

From the wind engineering field, Natalini et al., 2011 found that in north eastern Argentina, between 22.5° and 28°S latitude and 57.5° and 63.5°W longitude, strong winds are mainly caused by severe convective activity, produced by MCCs or the passage of either cold fronts or squall lines. During studies of damaging wind events that occurred between 2006 and 2010, several of them including field surveys, it was found that virtually all of the events that produced damage to civil structures corresponded to severe convective activity, and indicated that this is a distinctive characteristic of this region. Of 34 events studied in Chaco, Argentina, which belongs to the analysed area, 56% took place in spring, 35% in summer, 3% in autumn and 6% in winter, and high winds occurred simultaneously with rain in 79% of the cases, with heavy rain in 29%, with hail in 32%, and with rain and hail in 29% of them.

For northern Patagonia, a region of Argentina to the south of SESA, Natalini et al., 2011 reported significantly fewer events related to convective activity, as most of the damaging wind events studied were caused by the passage of extra-tropical cyclones from the South Pacific Ocean to southern SA, which produced specific synoptic weather patterns with strong isobaric gradients.

On the other hand, Schwarzkopf, 1997 indicates that in the centre and north-east of Argentina strong winds are dominated by squall lines, which sweep from south to north, and that severe storms caused by convective cells occur in Argentina north of 45ºS.

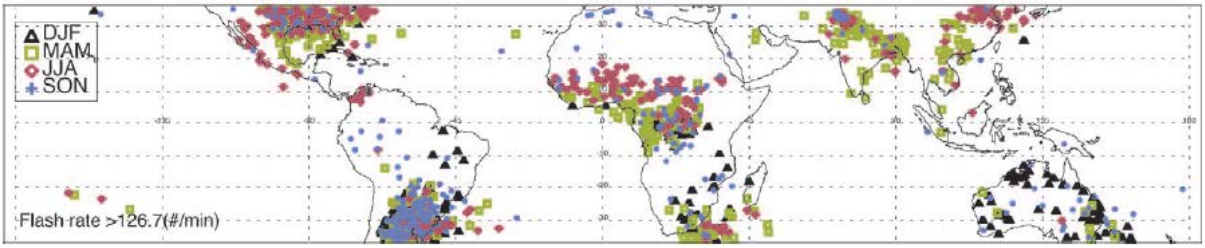


Figure 2.31 Location of the 1% most intense convective storms (from Zipser et al., 2006)

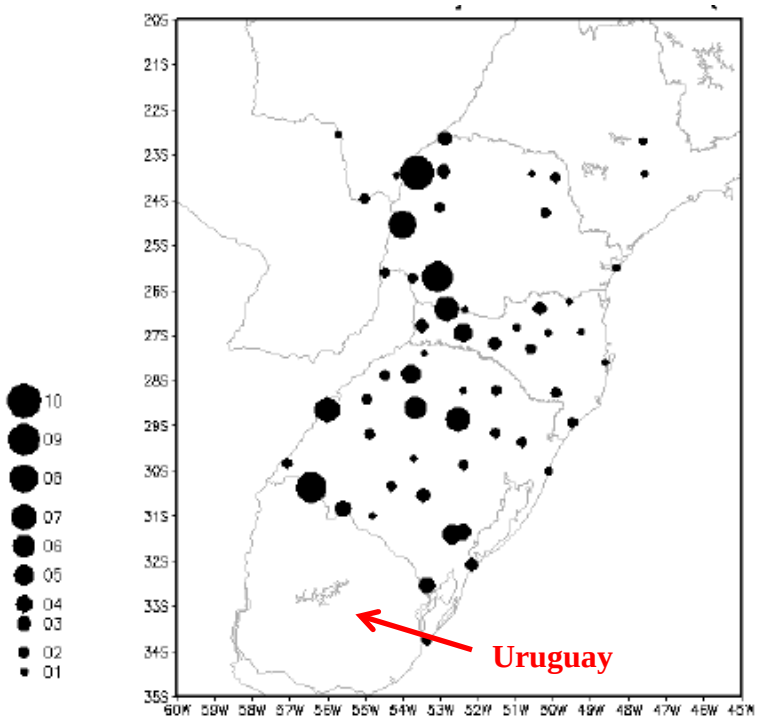


Figure 2.32 Number of high wind gusts generated by severe convective activity in the south of Brazil between 2005 and 2013 (adapted from Ferreira, 2014)

For the south of Brazil, Ferreira, 2014 analyzed the number of high wind gust speeds (>25m/s) generated by severe convective storms between 2005 and 2015 registered by automatic stations of INMET. This result is shown in Figure 2.32.

MCSs

Mesoscale convective systems (MCSs) were defined in Sub-section 2.2.3.2.1. As mentioned in that sub-section, SESA region is one of the regions of the world with the largest frequency of MCSs. This would principally involve the occurrence of MCCs (Figure 2.19) and squall lines, as suggested by Laing, 2003 for mid-latitudes MCSs. The main mechanism beyond the generation of MCSs in this region was explained in Sub-section 2.2.4 and would be related to the entrance of tropical warm humid air to mid-latitudes through the LLJS and the Chaco low.

Squall lines

Baines, 2003 indicates that cold fronts usually contain one or more squall lines. As the passage of cold fronts has been recognised as being rather frequent for eastern Argentina and Uruguay (Nobre et al., 2006), squall lines would be expected to be a common characteristic of the extreme wind climate of this area, which belongs to SESA region. This is verified by Schwarzkopf, 1997, who indicates that squall lines sweeping from south to north dominate the occurrence of strong winds in the centre and north-east of Argentina, and by Natalini et al., 2011, who report the passage of either cold fronts or squall lines as main causes of strong winds in north eastern Argentina, as mentioned before.

Figure 2.33 indicates the number of squall lines that passed over Argentina during a 10-year period (1952-1961), adapted from Lichtenstein and Schwarzkopf, 1970.

The passage of squall lines and cold fronts in Uruguay are further described in Sub-section 2.2.5.2.

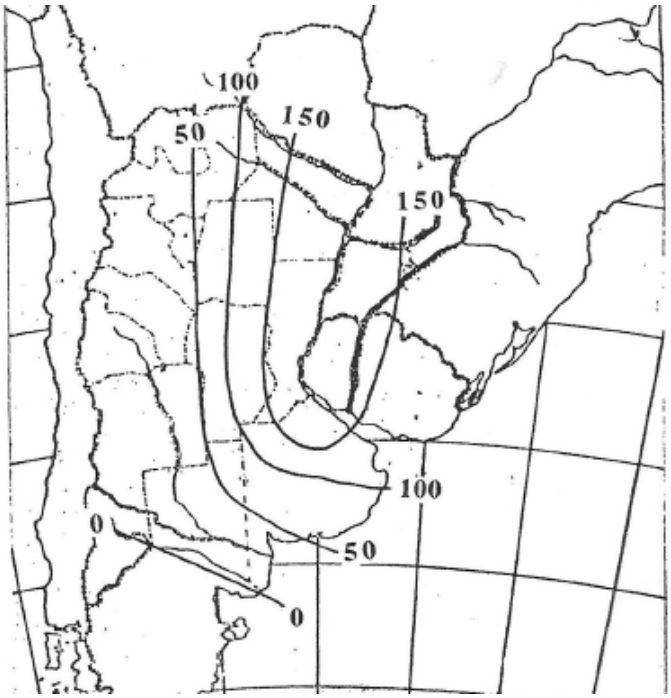


Figure 2.33 Geographic distribution of the passage of squall lines in Argentina (adapted from Lichtenstein and Schwarzkopf, 1970)

MCCs

Mesoscale convective complexes (MCSs) were defined in Sub-section 2.2.3.2.1. For mid-latitude SA, Velasco and Fritsch, 1987 observe that the region with most frequent occurrence of MCCs is slightly shifted to the north in relation with the region that tends to experience the most severe convective activity in SA, with MCCs rarely occurring south of 35°S latitude. This can also be noticed if Figure 2.19 and Figure 2.28 are compared. This reference indicates that the centroid for the occurrence of MCCs is usually found to the equatorward side of the subtropical jet stream.

Regarding seasonal behaviour, mid-latitude MCCs in SA would tend to occur mostly between November and April and would present a principal maximum in November, and a secondary maximum in April, with cases also observed in September-October and May-June in SESA (Velasco and Fritsch, 1987).

In relation to MCCs tracks, these authors report a slight shift from east-west tracks in late spring, to more equatorward tracks during midsummer, back to east-west by midfall.

Natalini et al., 2011 also reports MCCs as one of the main causes of strong winds in north eastern Argentina.

Downbursts and tornadoes

There exist many reports on the occurrence of downbursts and tornadoes in SESA, especially in Argentina, Brazil and Uruguay, although most of this information has not been systematically documented, as already pointed out by Nascimento and Doswell, 2006 and other authors, or is not publicly available.

In the next paragraphs, a number of these studies are briefly described, in particular those more related to wind engineering applications. The information corresponding to Uruguay is presented with more detail in Sub-section 2.2.5.2.

Due to the relative small scale of downbursts and tornadoes, their comprehensive study usually needs more surface measurements and the use of specific instrumentation than other types of research that may be accomplished with satellite data, for example. The number of Doppler radars, rawinsondes and other specific instruments required to obtain adequate information on these events (e.g. Wakimoto and Bringi, 1988; Kingsmill and Wakimoto, 1991, among many others) have delayed their studies in SA, where funding and access to the required resources have been usually scarce, as mentioned by Velasco and Fritsch, 1987, among others.

Some special efforts made in the last decades to describe with more detail meteorological processes that take place in SA offer valuable information for wind engineering applications. Although research with a more specific approach might be needed, and the available information would still require some sort of systematisation in order to be able to be directly applied to the field of wind engineering, it may be a question of time to count with a characterisation of downbursts and tornadoes occurrence in SESA more similar to the one that USA has, especially for its Great Plains and its so-called 'tornado alley'. This characterisation would be extremely valuable and could be applied to several regional wind engineering needs (Durañona, 2014a).

More recently, several efforts to overcome these difficulties in certain regions of the world have enabled a better understanding of regional meteorological processes. For example, CLIVAR (Variability and predictability of the ocean-atmosphere system), which is one of the four core projects of the World Climate Research Programme (WCRP), has as one of its missions to facilitate observation analysis, while its structure promotes international collaboration and cooperation, increasing the global scientific capacity beyond regional and institutional capabilities (CLIVAR, 2013).

Currently, an international project named RELAMPAGO is planned for 2017-2018 to study intense continental convective systems in subtropical SA, to understand their interactions with local and regional meteorology, topography; to place extreme continental convection in context with regional and global climate, among other objectives (WMO, 2015).

On the other hand, field surveys conducted by specialists help characterising downbursts and tornadoes, as their associated wind speed values, dimensions of affected areas, predominant

directions, etc. Of these field surveys, the research carried out by Mª Luisa Altinger de Schwarzkopff to describe and characterise the occurrence of downbursts and tornadoes in Argentina (e.g. Schwarzkopf and Rosso, 1993), deserves to be highlighted due to its systematisation, degree of detail and consistency throughout a period of several decades (1971 up to date) (Schwarzkopf, 2015).

Schwarzkopf and Rosso, 1993 present research conducted since 1971 to estimate the frequency of occurrence of downbursts and tornadoes and their main characteristics for different regions of Argentina. These authors organised a database of damaging wind events that took place in Argentina, starting in 1930 and comprising more than 50 years, along more than 20 years of research. As part of it, systematic searches were organised in several national and local newspapers, looking for high wind events corresponding to severe convective activity, combined with field surveys of places that have suffered wind damage and interviews with witnesses (Schwarzkopf, 1984-1993). In this work, downbursts were characterised by their wind speed, length, width and probability of occurrence, while tornadoes were characterised by their wind speed, radius and length of their tracks. For the classification of downbursts and tornadoes, these authors followed the work of Fujita, 1985, briefly summarised in Sub-section 2.2.3.2.1. These characterisations have been updated but have not been published in journals, and the generated database belongs to the team led by Schwarzkopff, who has been working as a private consultant for many years. According to Schwarzkopf and Rosso, 1993, tornadoes occur in all Argentina except in central and south Patagonia - a region located at the southern end of this country, and in 90% of the cases they take place to the east of 65°W longitude, with the most violent ones north of 35°S latitude. This location agrees with the definition of SESA region. These authors suggest that the presence of Sierras de Córdoba, illustrated in Figure 2.23, may be influencing their geographical distribution, acting as a barrier for the warm humid air that comes from the tropics or is generated over the basin of Paraná River.

Figure 2.34 presents the geographic distribution of the frequency of tornadoes in Argentina proposed in Schwarzkopf and Rosso, 1993, where the highest probability of occurrence of tornadoes would correspond to region A, while region B would exhibit half of that probability, and region C, a quarter of it. According to this work, tornadoes would have a tendency to occur more often in the province of Córdoba, located in region A in this figure.

The geographic distribution of the frequency of occurrence of tornadoes in Argentina updated in 2010 is presented in Figure 2.35.

This distribution would strictly be valid for Argentina, as this study did not involve a thorough analysis of tornadoes occurrence in Uruguay, Brazil or Paraguay. In fact, these authors recognise the existence of a region prone to the occurrence of violent tornadoes over the Paraguayan rain-forest, as also mentioned in Dyer, 1991.

In relation to downbursts, these authors could relate patterns of damage compatible with the occurrence of travelling microbursts, cyclonically curved (clockwise in the SH) wind flows, and micro and macrobursts, as defined by Fujita, 1985, in some cases associated with the occurrence of bow echoes and tornadoes.

Regarding their seasonal distribution, Schwarzkopf and Rosso, 1993 found that most downbursts and tornadoes occur in Argentina between October and March. They also identified a typical translational direction for most severe convective storms in this region

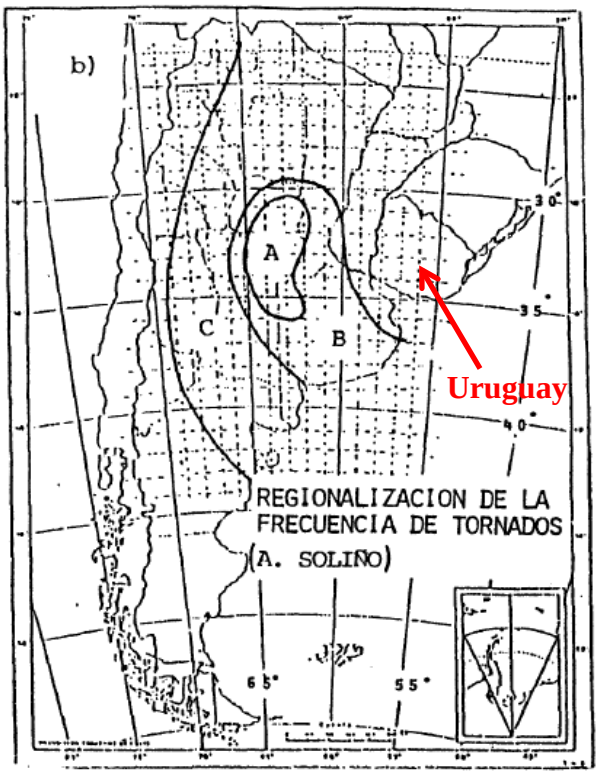


Figure 2.34 Geographic distribution of tornadoes in Argentina (adapted from Schwarzkopf and Rosso, 1993)

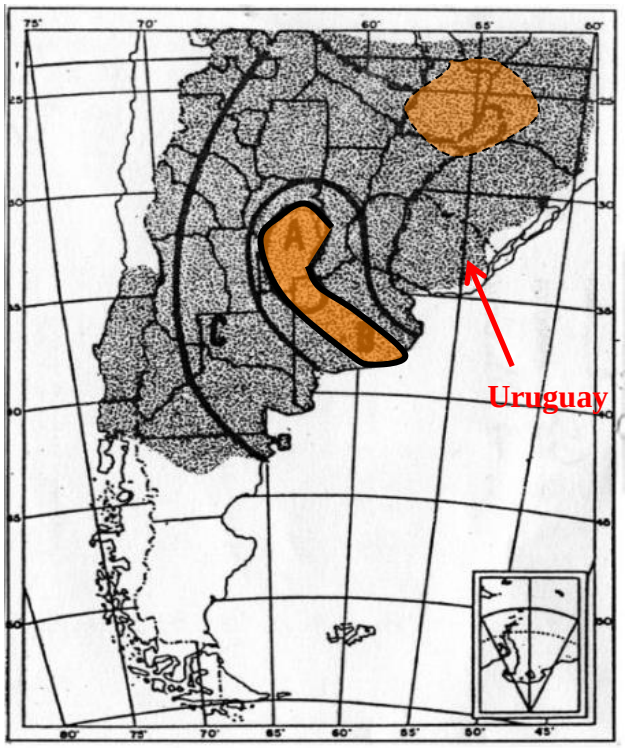


Figure 2.35 Updated geographic distribution of tornadoes in Argentina (adapted from Schwarzkopf, 2010)

from southwest to northeast, or from west to east; and that most of the intense wind gusts mainly came from the southwest sector.

There seems to exist relatively more reports on tornadoes than on downbursts in SESA, perhaps because damage caused by verified tornadoes tends to be more impressive than the one produced by downbursts, or because they exert a greater impact on the public, or due to the fact that they can sometimes be visually identified more easily. In fact, many tornadoes have been studied in Argentina, Paraguay and Brazil (Dyer, 1991; Oliveira, 2004; Schwarzkopf and Rosso, 1993), mainly in areas belonging to SESA; as well as in Uruguay (DNM, 2002; Torena, 2003a; Vecino and Torena, 2008; Torena, 2009, among others).

Dyer, 1991 describes a number of tornadoes that occurred in south western Brazil, eastern Paraguay and north eastern Argentina around 1965, reporting tracks as long as 70km and as wide as 2km. Most of them occurred in forested areas and were identified by aerial photographs studying the region between 24° and 27°30'S latitude and 52° to 56°30'W

longitude, thus belonging to SESA (Figure 2.23). This paper also mentions a tornado that occurred in 1984 and others that took place during 1987 in southern Brazil. According to this author, tornadoes occurrence in Paraguay has not been properly documented, although it is an area recognised by regional specialists as being prone to the development of violent tornadoes, as one that occurred in 1926.

Figure 2.36 reproduces a map of several tornadoes documented in SESA, as presented in Dyer, 1991.

This figure is in accordance with Figure 2.20(b), Figure 2.28, Figure 2.29 and Figure 2.30, although it may not reflect the actual and probability of occurrence in some areas of this region due to the lack of proper detection documentation of tornadoes occurrence.

In Brazil, Oliveira, 2004 for example, presents an analysis on the occurrence of tornadoes from 1976 to 2000 in the State of Santa Catarina, southern Brazil, located approximately between 26º and 29ºS latitude and 48º and 53ºW longitude. Figure 2.23 shows that this area is inside SESA. This author also presents a literature review on the study of tornadoes in Brazil.

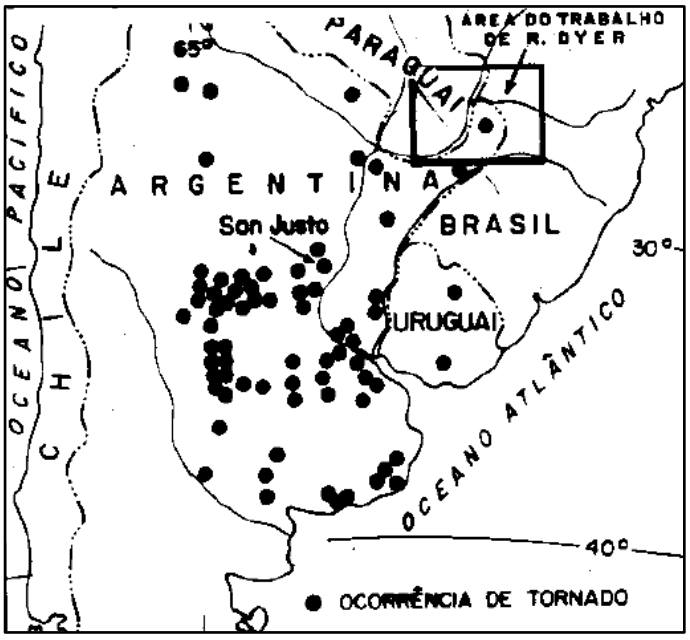


Figure 2.36 Tornadoes occurrence presented in Dyer, 1991

On the other hand, the work presented in Ferreira, 2007 describes a series of tornadoes and downbursts that occurred between 1991 and 2006 in the northern area of Brazil inside SESA, and cites a number of studies carried out in Brazil on severe convective events.

More recently, Loredo-Souza, 2012 indicates that Brazilian tornadoes have been mainly registered in the States of Rio Grande do Sul, Santa Catarina, Paraná, Mato Grosso do Sul and São Paulo, all of which belong entirely or partially to SESA. Most of the observed tornadoes were classified as F1 in Fujita scale, but this author points out that observations of F3 tornadoes have been increasing, and that one F4 tornado was registered in 1991.

For north eastern Argentina, region also belonging to SESA, Natalini et al., 2011 indicate that the relatively frequent severe convective activity sometimes ends up in tornadoes. These authors mention that every year, non-qualified eye witnesses report the occurrence of tornadoes, principally in rural and forest areas, and indicate that if one of these events took place in populated areas, damage could be overwhelming. As an example, they present details of a tornado that on October 21st, 2010 passed through a village called Pozo Del Tigre, in Formosa, with a population of 4,000 people. From damage patterns and witnesses reports, the tornado diameter was estimated to be between 20 and 40m at ground level and its lifetime of less than 15min, during which it produced strong winds, intense and dense hail, and caused 200 injured people, four deaths and 850 homes badly affected by the fall of masonry walls, debris and hail.

2.2.5. Geography and climate of Uruguay

Uruguay is located in the south eastern region of SA bordering the South Atlantic Ocean, as shown in Figure 2.23, inside the region defined as SESA in that figure and in this thesis. As indicated in Sub-section 2.2.4.2, due to its location, Uruguay is prone to the occurrence of severe convective activity and also to the passage of intense extra-tropical cyclones. In Figure 1.1, and with more detail in Figure 2.37, it can be seen that Uruguay is bounded to the north and northeast by Brazil, to the west, by Argentina, and to the southeast and south by the South Atlantic Ocean and the Río de la Plata. It is located approximately between 30º and 35ºS latitude and 53º and 58 ºW longitudes.

Figure 2.37 and Figure 2.38 show the topography of Uruguay with their height scale in meters, and illustrate how the terrain varies from rolling plains in the east, south and west borders, to low plateaus and hills. As these figures and Figure 2.21 illustrate, Uruguay would be a transition zone from the Pampas plains to the hilly uplands of Brazil. Its main topographic features are the Cuchilla Grande and Cuchilla de Haedo shown in Figure 2.37, two low ranges of hills located to the southeast and north of the country, respectively. They are the highest areas of Uruguay, whose maximum altitude is around 500m high.

According to Schwerdtfeger, 1976, Uruguay is characterised by its high degree of humidity and the absence of significant orographic barriers, which helps this humid air to travel along the country and makes most locations potentially vulnerable to high winds and to rapid changes in weather, as different types of storms sweep across the country.

The eastern coastline of Uruguay frequently receives winds from the northeast and east due to the presence of the South Atlantic anticyclone, which also brings great content of humidity from the ocean to the country. The presence of the relatively warmer waters of the Río de la Plata to the south of Uruguay, whose effects in humidity can be felt up to a distance of about 100km (Prohaska, 1976), the systems of the rivers Uruguay and Paraná located to the west, and a series of rivers as Río Negro, lakes and lagoons in the interior of the country also collaborate with the high level of humidity that Uruguay usually presents.



Figure 2.37 Location and geography of Uruguay (adapted from ElUruguayo.com, 2010)

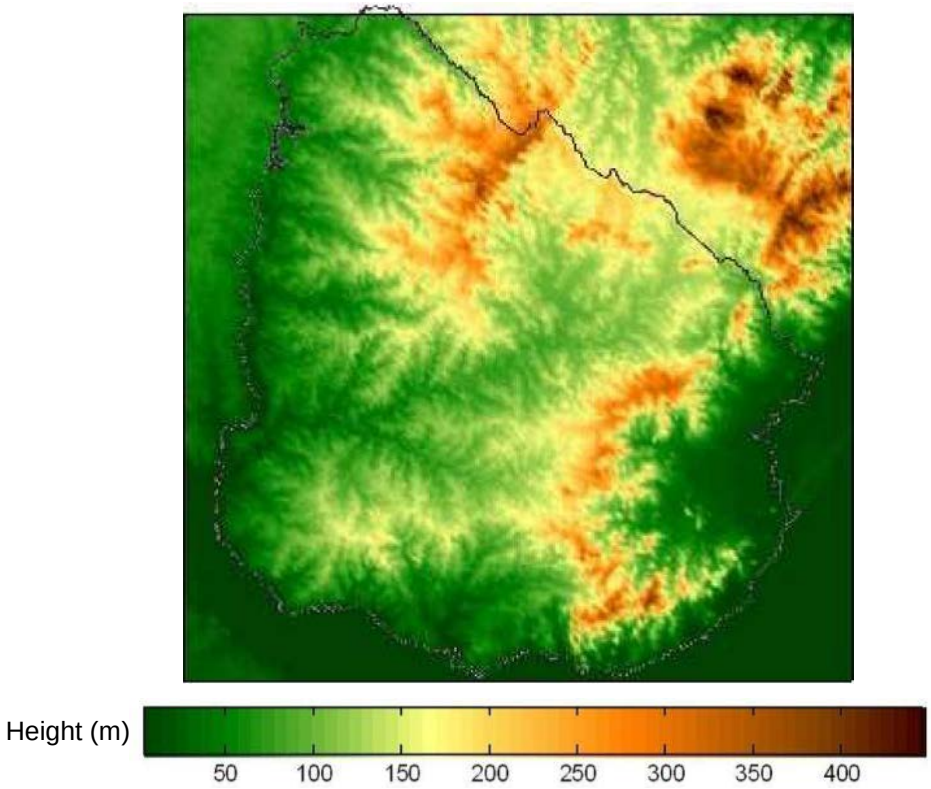


Figure 2.38 Topography of Uruguay (adapted from Cataldo, 2010)

2.2.5.1. Mean wind climate of Uruguay

According to Schwerdtfeger, 1976, surface mean winds in Uruguay depend primarily on the topography and on the position and intensity of the South Atlantic anticyclone, which would explain that in south western Uruguay, north and northeast winds prevail throughout the year, while in north eastern Uruguay east to southeast winds appear in spring and summer due to the southward displacement of the main features of the global circulation, and in particular, of this high.

Schwerdtfeger, 1976 observes an increase in mean wind speed from September to December, and higher mean wind speeds and a more pronounced sea/land breeze circulation along the Atlantic coast (i.e., departments of Maldonado and Rocha, as shown in Figure 2.37). Depending on the direction of the coastline, sea breeze winds would generally be registered from the northeast to southwest, more commonly from the northeast; while land breeze winds would mostly take place from west through north; more frequently from the northwest.

Studies from the first half of last century show similar characteristics for the most frequent wind directions in Montevideo and for the effect of the sea breeze in the first kilometres inland (Morandi, 1939). An annual mean wind speed for Montevideo of 14km/h (3.9m/s) was reported, and the spring months were also identified as the months with highest mean wind speeds (Morandi, 1921; Morandi, 1952).

According to Bidegain, 2001, usually lower mean wind speeds are found toward the north and east of the country along the year, while the coastlines of the Río de la Plata and the South Atlantic Ocean tend to experience higher mean wind speeds. In areas of complex topography, mean wind speeds can vary significantly from one location to another.

Bidegain, 2001 also indicates that mean wind speeds at 10m height can be of the order of 15km/h (4.2m/s), and that although the variability of the mean wind speed along the year is not very pronounced, spring can be regarded as the windiest season.

From more recent studies, annual mean wind speeds in Uruguay can be considered to be between 3 and 6m/s (11 and 22km/h, respectively) at 15m height above ground, depending on the location, as shown in Cataldo et al., 2010b and reproduced in Figure 2.39. Comparing this figure with Figure 2.38, the influence of Uruguayan topography on mean wind speeds can be noticed at this height. At higher altitudes, this effect is also perceived, but it is more geographically distributed.

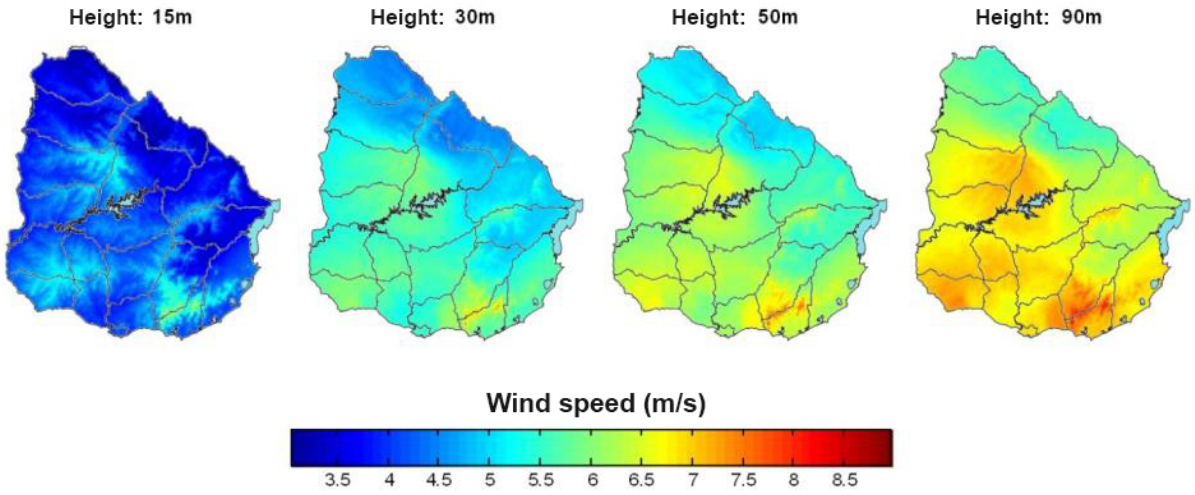


Figure 2.39 Annual mean wind speeds at different heights (adapted from Cataldo et al., 2010b)

As an example, Figure 2.40 shows the frequency distribution of mean wind speed at 45.4m height at a site in the southern centre of the country, in the department of Florida indicated in Figure 2.37.

The dots in Figure 2.40 show the experimental frequency distribution, while the line illustrates that this distribution can be adequately modelled by a Weibull probability distribution. For the definition of Weibull probability distribution, the reader can be referred to e.g. Holmes, 2007. Similar results are obtained for wind speeds distributions at other sites of the country, which follow Weibull functions quite closely within a range of Weibull parameters.

On the other hand, Figure 2.41 indicates the wind direction distribution at different heights for a series of sites located in the southern centre of the country, in level terrains and open exposures. The location of most of these sites is presented in Figure 3.1 in Section 3.3. As it can be seen in Figure 2.41, these sites show predominant wind directions from the north trough northeast, as expected from their relative position to the South Atlantic anticyclone.

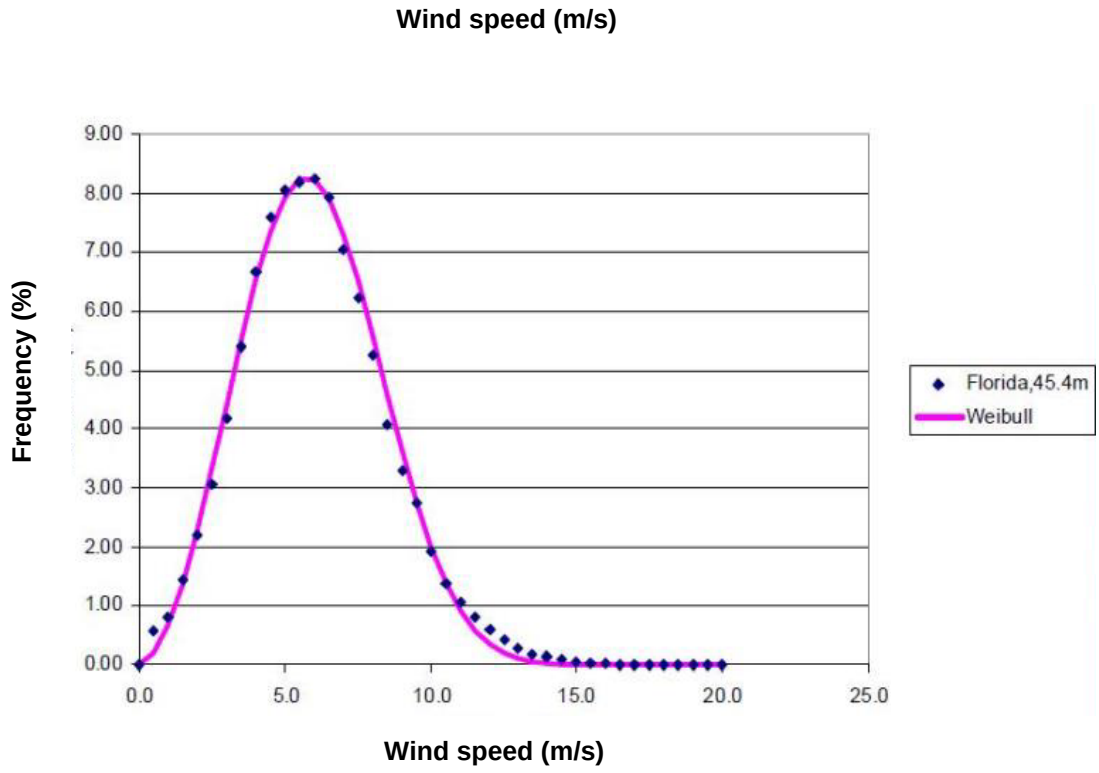


Figure 2.40 Wind speed distribution at Florida, Uruguay, at 45.4m height (from Cataldo, 2010)

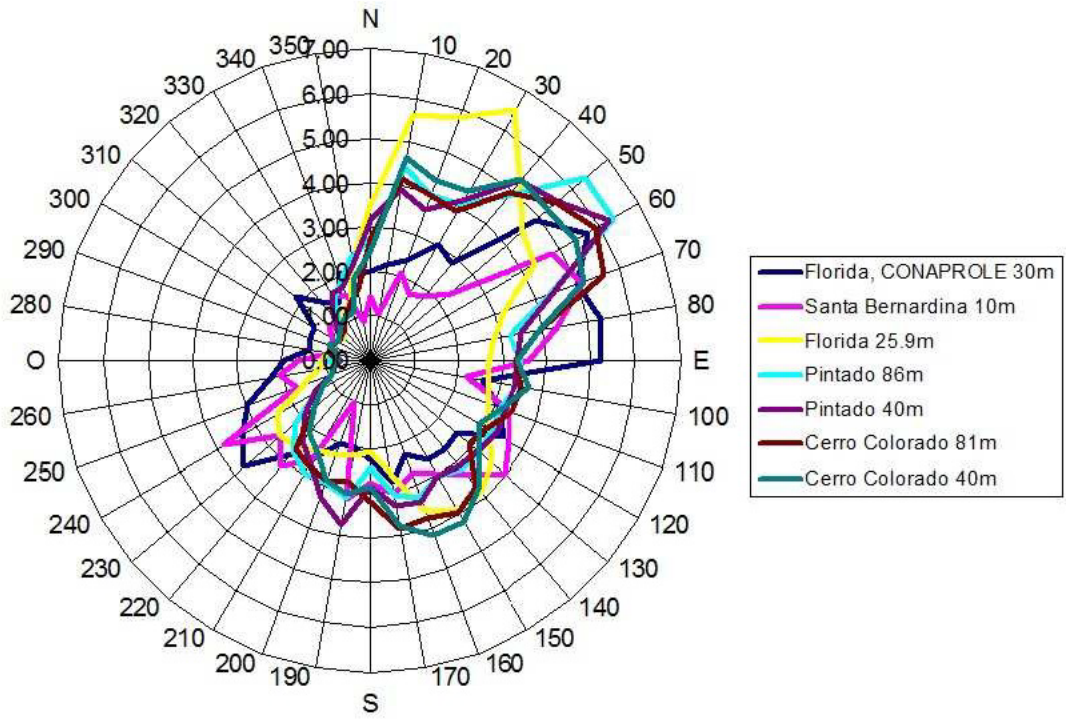


Figure 2.41 Wind roses for different sites and heights at the southern centre of Uruguay (from Cataldo, 2010)

2.2.5.2. Extreme wind climate of Uruguay

As indicated in Sub-section 2.2.2, the mean wind climate may be considered as the background wind field upon which transient weather systems, responsible in some cases of extreme winds, are superimposed (Wallace and Hobbs, 2006).

Being part of the mid-latitudes, Uruguay experiences a wide variety of fast changing weather, as cold air masses from the poles and warm air masses from the tropics are able to travel to these latitudes and sometimes alternate within hours of each other (Lutgens et al., 2001). As a result, severe convective activity, weather fronts and extra-tropical cyclones are usual characteristics of its weather (Satyamurty et al., 1998), which in turn characterise the Uruguayan extreme wind climate. In fact, the sudden changes of weather in the country have

been regarded as one of the main features of its climate since 1850's (Morandi, 1952; Boerger, 1953).

Uruguayan extreme wind climate can be considered to be rather severe, especially due to its location inside SESA, where severe convective activity tends to occur quite frequently (e.g. Nascimento and Doswell, 2006), and also because it belongs to the area with the most intense and frequent cyclogenesis in SA (e.g. Gan and Rao, 1991), as illustrated in Figure 2.28 and Figure 2.25, and as described in Sub-sections 2.2.3.2 and 2.2.4.2.

These characteristics are also cited by Nobre et al., 2006, who indicate that Uruguay is affected by the passage of cold fronts, together with eastern Argentina, and by the frequent development of intense extra-tropical cyclones. Schwerdtfeger, 1976 also mentions periodic northward advections of polar air masses as an additional cause of high wind events in the country, which under certain conditions may produce intense winds from the south.

An important difference between mean and extreme winds in Uruguay is their predominant wind direction. While mean winds blow mostly from the northeast through east directions, extreme winds usually blow from directions between the southeast and west (clockwise), mainly from the southwest quadrant. This is usually valid for the highest winds generated by extra-tropical cyclones (Cataldo and Durañona, 2005; Durañona, 2014b) as well as for those generated by convective activity (Durañona and Cataldo, 2007; Cataldo and Durañona, 2008).

According to e.g. Bidegain, 2001, the South Atlantic anticyclone can bring air masses of tropical origin from the northeast to Uruguay, while the position of the South Pacific anticyclone may be frequently related to the intrusion of polar air masses toward these lower latitudes. The interaction between these two air masses of different characteristics is responsible for the passage of cold and warm fronts across the country, which may lead to very variable weather conditions and high winds, and also for generating particular positions of highs and lows over or near Uruguay, which may lead to steadier but sometimes still strong winds, as in northern Patagonia, Argentina (Natalini et al., 2011).

To the author's knowledge, the last systematic studies of the extreme wind climate of Uruguay, apart from those carried out at the Institute of Fluid Mechanics and Environmental

Engineering (IMFIA) of the School of Engineering, UdelaR since 1996, were those presented in Morandi, 1944; Vieira, 1949; Hernández, 1971; Ricaldoni, 1979; Serrentino, 1981 and Chamlian, 1993, the last three related to the development of the national extreme wind map and extreme wind statistics for the national wind code UNIT:50-84, 1984, still in use.

Morandi, 1944 presents the analysis of 29 years of hourly mean wind speeds higher than 47km/h (13m/s) measured at Observatory of Prado station, in Montevideo, between 1901 and 1939, and gives some examples of the most intense wind speeds measured there and at other sites of Montevideo. This station is described in Section 3.5.

Vieira, 1949 characterises the main synoptic conditions when high wind events were registered at Antepuerto station, located in front of the Port of Montevideo, from 1936 to 1945. Some metadata of this station is presented in Section 7.4. Hernández, 1971 presents an analysis of the maxima wind gust speeds measured at this station from 1906 to 1969.

On the other hand, Ricaldoni, 1979 presents the basis for the study of the extreme winds in Uruguay for the development of the national wind code UNIT:50-84, 1984 and describes the main wind databases used for this purpose, -principally data from Antepuerto station from 1906 to 1969, as well as the main hypothesis made during this work. In the report of Serrentino, 1981, results of an extreme value analysis carried out on the monthly maxima wind gusts measured at Antepuerto station during that period are outlined, and compared with estimations from another stations. Finally, the work of Chamlian, 1993 presents a comparison of the design wind gust speeds proposed in the national wind code UNIT:50-84, 1984 and in the Argentinian and Brazilian wind codes in use at that time.

More recently, research on extreme winds and wind damage in Uruguay carried out at IMFIA showed that intense extra-tropical cyclones had the potential to sustain high winds during several hours in great part of the country and produce extensive wind damage (Cataldo and Durañona, 2005; Durañona, 2014b), but when e.g. wind incidences in high-voltage transmission lines (Durañona and Cataldo, 2008) or wind damage in fruit trees were analysed (Durañona and Cataldo, 2007), severe convective activity was found to be responsible for most of the wind damage and incidences reported (Durañona, 2011b).

In addition, studies of specific severe wind events that occurred in the country in the last decades have been performed by several meteorologists, mostly Uruguayan. These studies

usually focus on the description of the meteorological characteristics of the events, sometimes performing additionally field surveys to gather more information on them and on the wind damage they produced. In some cases, pictures, newspaper information and interviews to witnesses are included in their reports, and altogether they represent useful information for wind engineering purposes. Most of the studied events correspond to severe convective activity that caused intense wind damage in certain areas of the country, in general related to the occurrence of tornadoes (DNM, 2002; Torena, 2003a; Vecino and Torena, 2008; Torena, 2009), severe downbursts (Silva et al., 2008) or large hail (Silva, 2008), while some few analysed the development of intense extra-tropical cyclones (Possia et al., 2003; UdelaR, 2005).

Although a national systematic database on high wind events does not exist, the SINAE (National Emergency System) has a list of several high wind events that occurred in Uruguay (SINAE, 2011).

Apart from this, a series of websites and Facebook pages created by meteorologists, and sometimes by individuals interested in meteorology, offer information of different type about damaging wind events, which can also be useful for wind engineering analysis (e.g. Torena, 2013 and D'Angelo, 2013).

2.2.5.2.1. Synoptic high winds in Uruguay

2.2.5.2.1.1. Extra-tropical cyclones in Uruguay

As presented in Sub-section 2.2.4.2., Uruguay belongs to a region of the SH that experiences one of the most significant cyclogenesis activities (e.g. Gan and Rao, 1991; Seluchi, 1995), where extra-tropical cyclones occasionally intensify during their passage over the country and can generate damaging winds in part of it during several hours. In particular, there is a maximum for genesis of extra-tropical cyclones over Uruguay, as shown previously in Figure 2.25. According to Sinclair, 1995, Uruguay also belongs to a region where rapidly intensifying cyclones are most frequent (east of SA along 35° latitude).

Usually, the extra-tropical cyclones that form to the northwest or over Uruguay move to the southeast and reach their maximum depression over the South Atlantic Ocean (Seluchi, 1995).

Nobre et al., 2006, among others, also indicate that Uruguay and eastern Argentina are regions frequently affected by this type of cyclones. This is also supported by Wölcken, 1954 and shown in Figure 2.26. This last figure illustrates that extra-tropical cyclones pass rather frequently over Uruguay, being their most common direction toward the southeast (in accordance with results from e.g. Gan and Rao, 1991 or Seluchi, 1995), with trajectories ranging from south to east (anticlockwise)**.**

According to Gan and Rao, 1991, extra-tropical cyclones would be more frequent in winter, while Sinclair, 1995 indicates that most of the strong extra-tropical cyclones occur in winter. On the other hand, Seluchi, 1995 identifies winter as the preferred season for the occurrence of extra-tropical cyclones, and spring for intense cyclogenesis events.

Several intense extra-tropical cyclones that formed near or over Uruguay have been studied, some of them due to their associated wind damage (UdelaR, 2005; Cataldo and Durañona, 2005; Possia et al., 2011; Durañona, 2014b) and others due to the flooding of lowland areas in the coastal areas of Buenos Aires, Argentina (Seluchi et al., 2001; Possia et al., 2003). These last events are usually called ‘sudestadas’ and occur when strong winds from the southeast are sustained in the Río de la Plata for a relative long period of time.

During the passage of an extra-tropical cyclone, the direction of the wind at a particular time and site of the country depends on the location of the centre of low pressure of the extra-tropical cyclone in relation to the site. Figure 2.42(a) and (b) illustrates this concept. In this figure, as well as in Figure 2.44 to Figure 2.46, ‘B’ stands for ‘low’ and ‘A’ for ‘high’ (pressure areas). In Figure 2.42(a), the centre of low pressure would be close to the centre of Uruguay, and the wind in Montevideo would approximately come from the southeast (quite parallel to the isobars, with an inward component toward the low pressure centre). Figure 2.42(b) shows how due to their typical trajectories, the extra-tropical cyclone moved to the southeast over the South Atlantic Ocean. In this location, the wind direction in Montevideo would be from the southwest, or west-southwest; after rotating clockwise from the southeast.

Therefore, the evolution of wind direction and wind speed at a site in Uruguay during the passage of an extra-tropical cyclone is very dependent on the trajectory of its centre, its diameter, translational speed and on how close the isobars are to each other (e.g. Morandi, 1944; Vieira, 1949). As extra-tropical cyclones in this region of SA usually intensify along

their trajectory to the southeast and over the ocean, the highest winds in Uruguay would be registered close to the coast, and would tend to occur when the centre of low pressure is over the ocean but still close to the coast, as extra-tropical cyclones usually present their strongest winds quite close to their centres of low pressure (Sinclair, 1996).

If the trajectory of the centre is shifted parallel and slightly to the east in comparison with the one corresponding to Figure 2.42, the highest winds in Montevideo may be experienced from the south direction (as presented in Figure 2.43), instead than from the southwest or west-southwest. This last figure shows the wind speed and direction measured in Montevideo during the passage of an extra-tropical cyclone between July, 9th and 11th, 1923, which produced the highest wind speeds from the south, with registered values of almost 150km/h (41m/s). In this figure the arrows represent wind direction; the height of each vertical bar, the wind speed for each 1h period, and the days are labelled from 9 to 11 (July 9th and 11th).

This extra-tropical cyclone affected many buildings in Montevideo, especially close to the coast, as well as its port and ships due to the combination of intense winds, high sea and waves.

As mentioned in Sub-section 2.2.4.2., Uruguay also belongs to an area prone to explosive cyclogenesis, defined in Sub-section 2.2.3.1. These cyclones intensify rapidly after they form, thus reaching rather low central pressures and high wind speeds closer to the continent, and can be associated to significant inland wind damage. According to Knox et al., 2011, these events would be more frequent from June to August.

The highest wind speeds caused by an extra-tropical cyclone in Uruguay in the last decades correspond to an explosive cyclogenesis, or 'bomb', that occurred on August 23rd, 2005 and whose main characteristics are briefly described in Section 4.6. As expected, it moved to the southeast (e.g. Wölcken, 1954; Necco, 1982b; Gan and Rao, 1991) with intensifying wind speeds along its trajectory, and occurred in August, thus coinciding with the expected time of the year for the occurrence of the most intense extra-tropical cyclones (Sinclair, 1995; Knox et al., 2011 among others). Another example of a recent intense extra-tropical cyclone is presented in Sub-section 5.5.2.

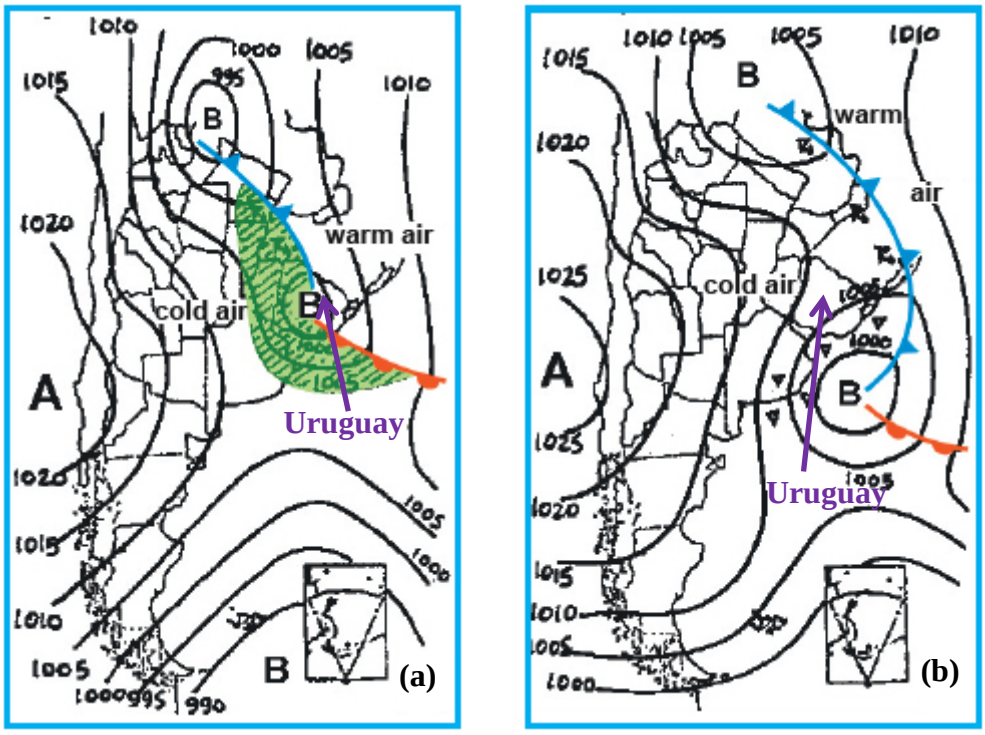


Figure 2.42 Extra-tropical cyclone over Uruguay (adapted from Celemín, 1984)

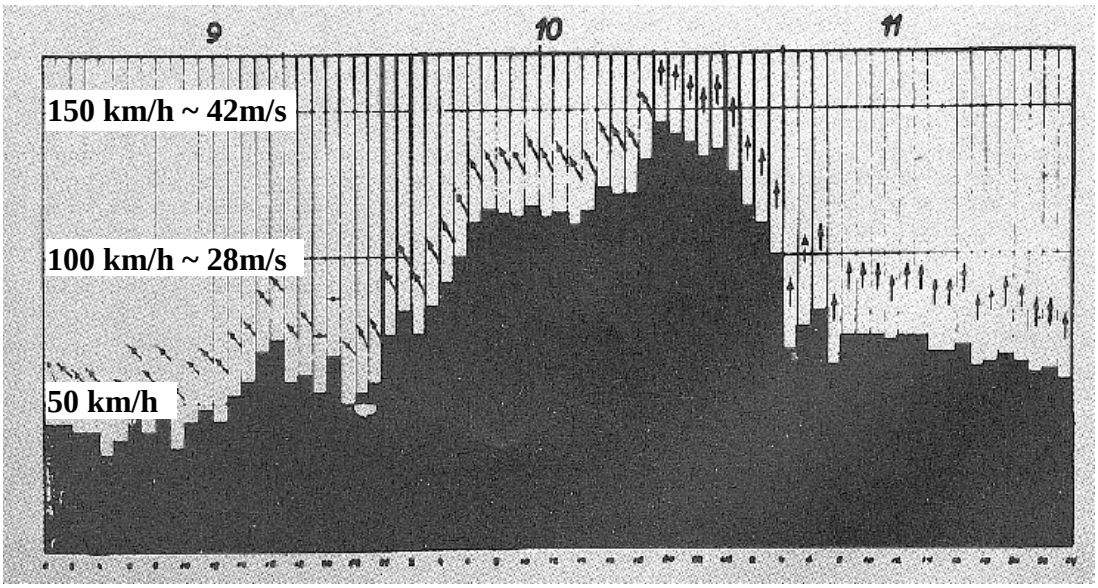


Figure 2.43 Wind evolution in Montevideo during the passage of an extra-tropical cyclone over Uruguay in July, 1923 (adapted from Vieira, 1969)

2.2.5.2.1.2. Other synoptic weather patterns that generate high winds of synoptic temporal scale in Uruguay

Certain synoptic weather patterns corresponding to different positions of highs and lows over or close to SA can lead to high synoptic winds experienced in Uruguay. As indicated by Schwerdtfeger, 1976, some of these synoptic winds receive local names, as the 'sudestada' or the 'pampero', which produce high winds in Uruguay and surroundings.

The 'sudestada' would correspond to a situation when winds from the southeast blow over the Rio de la Plata and south western Uruguay, as in Figure 2.42(a), during an extended period of time. According to Possia et al., 2003, this situation usually occurs related to extra-tropical cyclones located between 30° and 35°S latitude and 52° to 58°W longitude, and to associated anticyclones centred at about 45°S, 65°W, as illustrated by Figure 2.44.

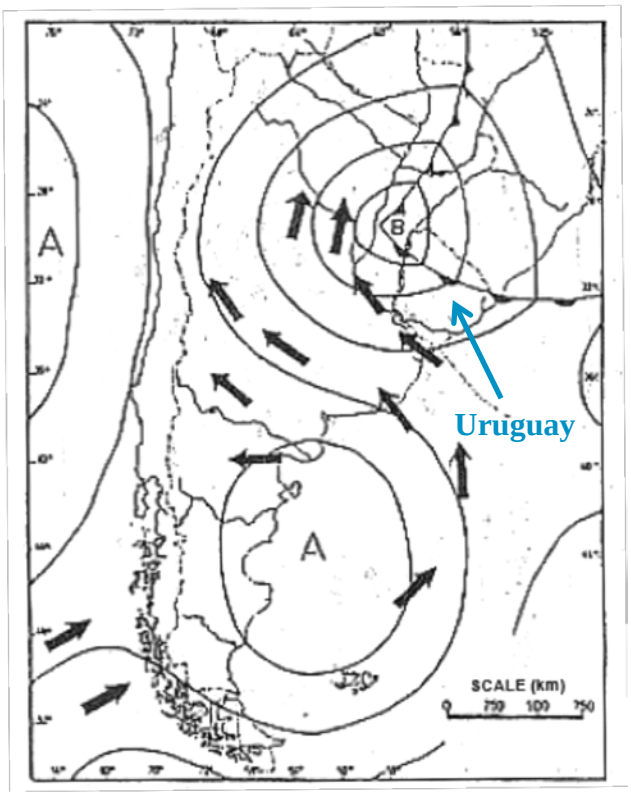


Figure 2.44 Synoptic weather pattern associated to a 'sudestada' in Montevideo and Rio de la Plata (adapted from García, 1970)

On the other hand, the term ‘pampero’ refers to persisting high winds from the southwest quadrant, which usually blow after the passage of a cold front, as indicated in Figure 2.45. This type of wind corresponds to the entrance of a cold air mass into Uruguay.

Sometimes, cold air masses can arrive with wind directions closer to the south, as Figure 2.46 shows. These polar outbreaks, also shown in Figure 2.22, occur when cold dense polar air masses pass beneath warmer tropical air masses, and may produce under certain circumstances high synoptic winds, relative steady in terms of wind speed values and direction. According to Sinclair, 1996 belts of strong winds can be found around the peripheries of highs.

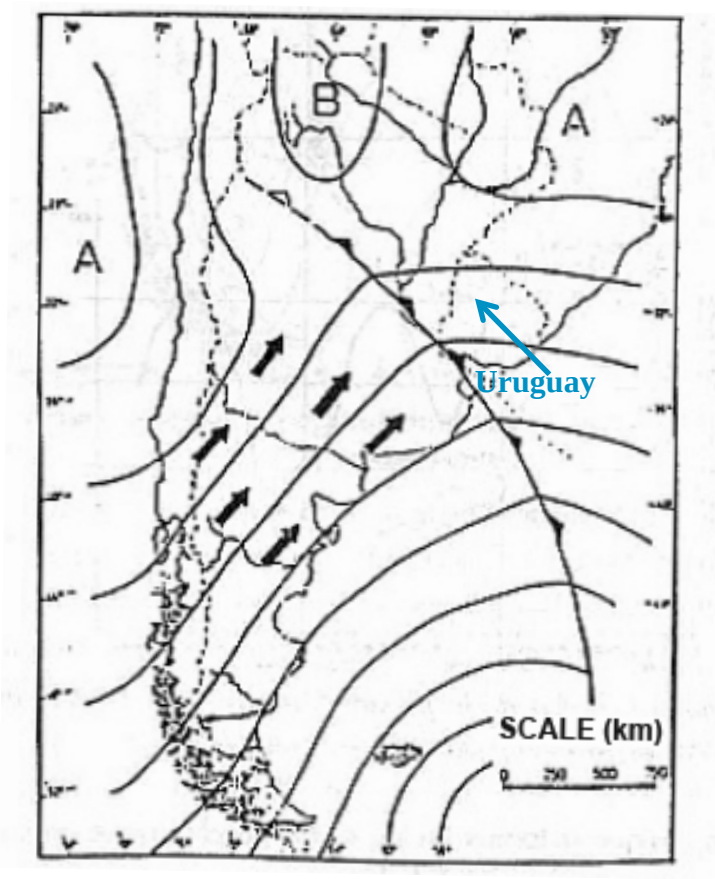


Figure 2.45 Synoptic weather pattern associated to a typical ‘pampero’ wind in Uruguay (adapted from García, 1970)

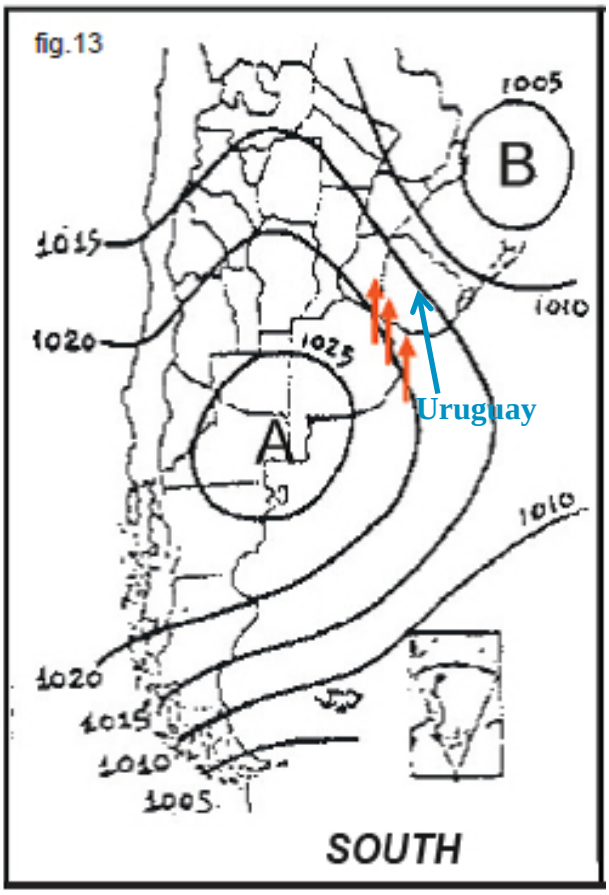


Figure 2.46 Synoptic weather pattern that can cause high wind speeds from the south in Uruguay (adapted from Celemín, 1984)

2.2.5.2.2. Non-synoptic high winds in Uruguay

2.2.5.2.2.1. Severe convective activity in Uruguay

As mentioned in Sub-section 2.2.4.2, Uruguay belongs to the region most affected by severe convective activity in SA (Nascimento and Doswell, 2006), which generate intense and localised damaging winds as downbursts and tornadoes, and to the second worldwide after the Great Plains of USA (Zipser et al., 2006).

There exist many reports on high wind events in Uruguay related to severe convective activity. However, documentation of such events has been far from systematic or complete (Durañona, 2011b), as it is usually the case in this region of the world (Nascimento and Doswell, 2006).

Celemín, 1984 indicates that severe convective activity in the Río de la Plata basin can be associated to the passage of cold fronts or squall lines, usually moving to the northeast; to warm fronts that generally move to the southwest; or that it can be generated in an independent way, with usual trajectories from west to east. He also observes that cold fronts produce higher wind gusts than warm fronts, and that they can stop their movement and become stationary fronts.

As described in Sub-section 2.2.3.2, severe convective activity is usually related to abrupt increases in wind gust speed, significant and sudden drops of temperature, intense rain, changes in wind direction and occasionally, to the occurrence of hail and tornadoes.

Reports on abrupt and significant decreases in temperature, accompanied by high wind gusts, wind direction shifts, intense rain and occasional hail can be found in different papers presented in the 'Revista Meteorológica' ('Journal of Meteorology' in Spanish), a journal edited and printed in Uruguay that published research work on South American weather and climate from 1942 to 1956 (e.g. Morandi, 1942; Boerger, 1946; Boerger, 1953), and also referred to events that had happened many decades before that period.

Many events of convective characteristics were also described in periodic bulletins from the Observatory of Prado station, station described in Section 3.5. Luis Morandi, an outstanding meteorologist who was in charge of this station from 1901 to 1925, measured, verified, processed and published meteorological data in a series of bulletins between at least 1901 and

1917 (Morandi, 1901 - 1917). Many of these bulletins contain hourly data of wind speed and direction, temperature, pressure, as well as a description of the main weather events that were observed in this station, and particular, of those that exceeded wind gust speeds of around 50km/h (13m/s).

The frequent and sudden decreases of temperature that usually occur in Uruguay caught the attention of common people and scientists as early as in the 1850's, and were considered one of the main features of the Uruguayan climate (Morandi, 1921). They would be related to the frequent passage of fast cold fronts or squall lines in the region, as presented in Celemín, 1984. In this sense, Vieira, 1949 already identified the passage of cold fronts as one of the two main meteorological events responsible for high winds in Montevideo.

Many reports on the occurrence of hail in Uruguay- another sign of severe convective activity- occasionally as big as apples, sometimes with diameters of around 4 to 5cm, can also be found in the 'Revista Meteorológica'.

Different documentation from the beginning of last century already indicated the significance of convective activity in the extreme wind climate of Uruguay (Morandi, 1901 - 1917; Morandi, 1944; Vieira, 1949; Vieira, 1969, among others). For example, in Morandi, 1901 - 1917 high wind events of relative short duration measured at the Observatory of Prado station, occurring suddenly and simultaneously with intense rain and/or hail, and/or with shifts in wind direction, were often reported. In these bulletins, more high wind events (i.e., with wind speeds higher than 50km/h, i.e., ~14m/s) of relative small time scales were reported in comparison with those that lasted for a day or so. These events usually sustained high winds during several minutes, and many, during periods from tens of minutes to few hours.

More recent reports on high wind events in Uruguay are indicated along this sub-section.

As an example of convective activity in Uruguay, Figure 2.47 illustrates the passage over Montevideo of a small supercell on January, 24th, 2012 reported e.g. in Silva, 2012, which came from the south and moved over the departments of San José, Montevideo and Canelones (indicated in Figure 2.37). Several images and information on this storm, and of many others, are available in national websites, such as D'Angelo, 2013 or Torena, 2013.



Figure 2.47 Severe convective storm passing over Montevideo (from D'Angelo, 2013)

MCSs

According to Vera et al., 2006, Uruguay is located inside a region affected by the frequent development of MCSs.

As mentioned in Sub-section 2.2.4.2.2.1, the occurrence of MCSs in this region, and severe convective activity in general, is associated with the South American LLJS that tends to occur east of the Andes, which brings tropical warm and humid air from the Amazonian region southward, setting the conditions for the development of severe convective activity over SESA, and therefore, over Uruguay. As indicated in that sub-section, according to Salio et al., 2007 and Veblen et al., 2007, this LLJS would be stronger in spring and summer.

Squall lines

The fast passage of cold fronts, and of the sometimes associated squall lines, are responsible for rapid changes in weather, high wind gusts, wind direction shifts, intense rain and sometimes hail in Uruguay (e.g. Vieira, 1949; Celemín, 1984), especially when the warm air mass that is being displaced over the country is very humid and unstable.

According to Celemín, 1984, one out of four cold fronts in summer, either moving to the northeast or while being stationary, generates a squall line ahead of it, i.e., a thin line of cumulus nimbus clouds that produce downbursts. These squall lines would be more frequent in spring and summer, especially between November and March. They usually adopt a NW-

SE orientation and move toward the northeast for several hundred kilometres, usually reaching central and northern Argentina and Uruguay, and if they do not dissipate before, also southern Brazil and Paraguay. Their translational speed would be between 30 and 60km/h (8 to 17m/s), and their lifetimes from few hours to 12 or even 20h.

Celemín, 1984 also indicates that before the passage of a squall line or a cold front at a site, the wind usually comes from a direction between the northwest and northeast (clockwise), and that after its passage, the wind direction generally changes to a direction between south and west (clockwise), accompanied by sudden high wind gusts and temperature drops. According to this author, in the area of the Río de la Plata, 4 to 5 squall lines are generated every summer, which would produce high wind gusts during 15 to 30min at a specific site.

On the other hand, Vieira, 1949 identified two typical synoptic weather patterns for the generation of high winds near the Río de la Plata, analysing events measured at Antepuerto station between 1936 and 1945 that presented mean wind speeds averaged over 2 hours higher than 75km/h (21m/s). One of the patterns corresponds to the presence of an extra-tropical cyclone with its low pressure centre located close to or over Uruguay, and the other, to the passage of a cold front over the country. For this last case, this author observes winds from N to NW directions (anti-clockwise) before the passage of the front, and high wind gusts with wind direction shifts to the southwest quadrant during its passage, together with intense rain and sometimes hail, in agreement with e.g. Celemín, 1984 or Schwarzkopf and Rosso, 1993, among others.

According to Vera et al., 2006, Figure 2.48 may illustrate the origin of many cold fronts that pass over Uruguay associated to the eastward movement of a low pressure system across the southern region of SA. In this figure, solid lines represent isobars at the surface; Hs stands for subtropical semi-permanent high; Hm, for migratory high; L, for migratory low; LT, for a lee trough, while CL, for a coastal low. The LLJS (LLJ in this figure) that commonly forms to the east of the Andes is also shown in Figure 2.48(b). Surface cold fronts are indicated with solid lines with filled triangles; warm fronts, with solid lines with filled semicircles, and the path of a cold air surge, with a shaded arrow pointing northward in Figure 2.48(d).

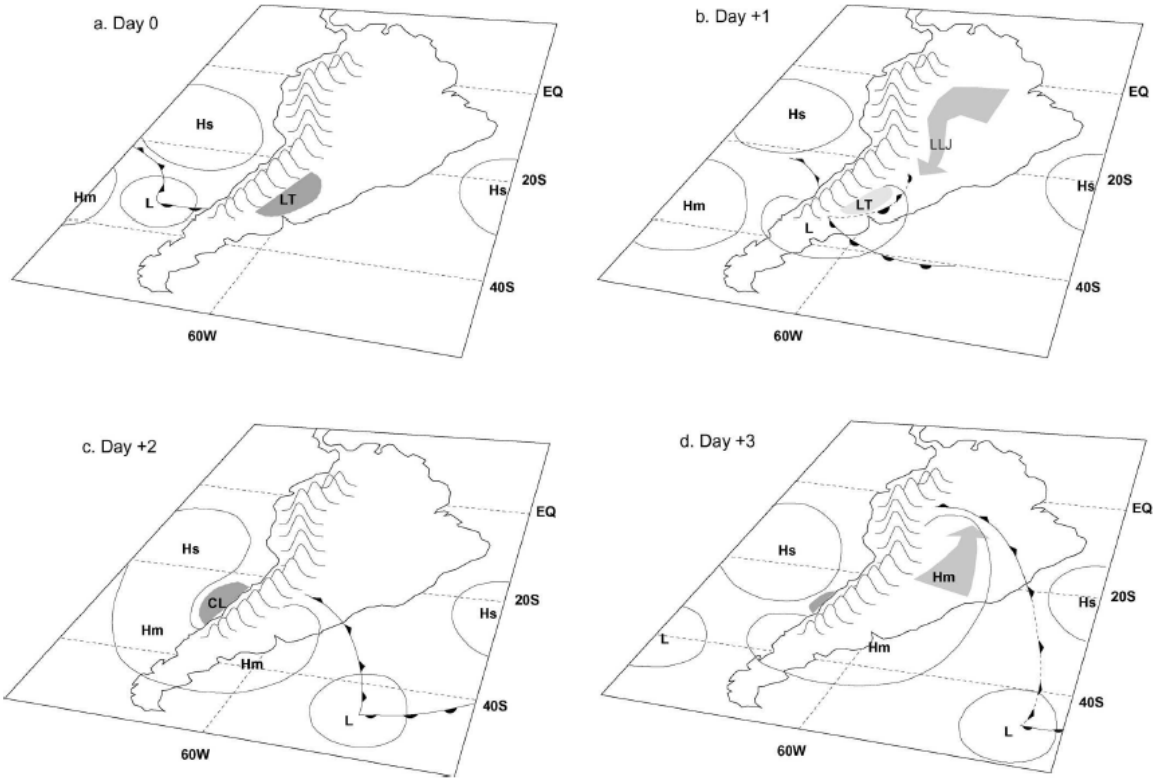


Figure 2.48 Conceptual model of a low pressure system crossing the Andes in the southern region of South America (adapted from Vera et al., 2006)

As shown in Figure 2.48(a), the persistent Pacific high over the South Pacific Ocean limits the equatorward extent of the migratory low L indicated in this figure to about 35°S, while the blocking effect of the Andes eventually allows the passage of the low through the southern tip of the continent. At the same time, strong westerly winds over the Andes produce lee-side subsidence in western-central Argentina, leading to the formation of a thermal-orographic depression (LT). This later effect produces the advance of the migratory low toward lower latitudes (Figure 2.48 (b)).

Experience shows that cold fronts become weakened as they approach the Andes and intensify on their lee side (Gan and Rao, 1994). Accompanying the movement of the migratory low, the cold front moves across SESA (Figure 2.48 (c)), followed by a cold dry air surge that moves equatorward between the Andes and the Brazilian plateau, as shown by the shaded arrow in Figure 2.48 (d). Bands of deep convection can accompany its leading edge.

During the warm season, the lee-side subsidence deepens the climatological Chaco low, which in turn intensifies the transport of moist, warm air from the Amazon basin toward SESA through the LLJS, fuelling severe storms in the form of prefrontal squall lines or other MCSs.

MCCs

In relation to MCCs, Figure 2.19 showed their relative frequent occurrence over Uruguay. In that figure, the small squares represent the location of the centre of each MCC at the time of its maximum extent.

As indicated in Sub-section 2.2.4.2, MCCs occur mostly from November to April in SESA. Figure 9 from Velasco and Fritsch, 1987 (not shown here) indicates that there would be more MCCs over or close to Uruguay in November than in other months. This month also presents the maximum number of mid-latitudes MCCs. Figure 2.49, adapted from Velasco and Fritsch, 1987, offers a closer view of MCCs over Uruguay along 2 years of observations, and shows with more detail their seasonal behaviour. This figure would indicate a tendency of MCCs to reach their greatest extent in Uruguay during the warm season (November to April), although some cases in May or June were also detected.

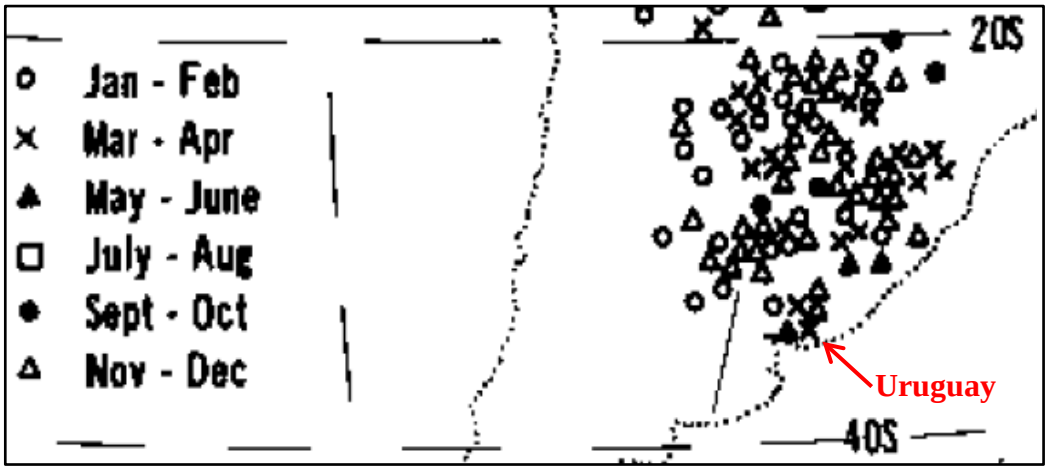


Figure 2.49 Locations of MCCs over SESA at their greatest extent along 2 years, and corresponding season of occurrence (adapted from Velasco and Fritsch, 1987)

The tracks of MCCs that took place in November along two warm seasons of observations are shown in Figure 2.50. This figure suggests that most of the MCCs passing over Uruguay would tend to come from Argentina and move toward Brazil with a northeast trajectory, principally affecting the northwest of the country.



Figure 2.50 Tracks of mid-latitudes MCCs in November along two warm seasons (adapted from Velasco and Fritsch, 1987)

Downbursts, tornadoes and waterspouts

On July 8th, 1935, while the meteorologist and Professor Luis Morandi was in charge of a meteorological station at the School of Agronomy, UdelaR in Sayago, Montevideo, a non-synoptic high wind event was recorded, with a maximum wind gust speed of almost 200km/h (55m/s) (Morandi, 1944).

The temporal evolution of the wind speed registered during this event is presented in Figure 2.51(b). High winds were accompanied by large hailstones that covered extensive areas, an indication of the occurrence of severe convective activity. The described wind damage

presented characteristics similar to downbursts foot-prints produced by a convective storm in movement (e.g. Schwarzkopf, 1984-1993; Pita and de Schwarzkopf, 2016): "In a park, populated with trees of the same species, tens of trees were damaged in different areas, while some hundreds meters from those places no damage was produced. This pattern was repeated with intermittency in sites located at a considerable distance from the previously damaged place, always in the trajectory of the storm" (Vieira, 1969).

The temporal evolution of wind speed during this event presents similar characteristics to those of downbursts registered in different parts of the world. For example, Figure 2.51(a) presents wind speed and wind direction measurements during a downburst that occurred in Maryland, USA in 1983 (Wakimoto, 2001) and had a maximum recorded wind gust of 240km/h (67m/s). This figure is presented with its horizontal axis reversed and both axes scaled, for a better comparison with Figure 2.51(b). Although the time scales and wind speed values of these two non-synoptic high wind events would be different, the qualitative behaviours of wind speed with time are very similar.

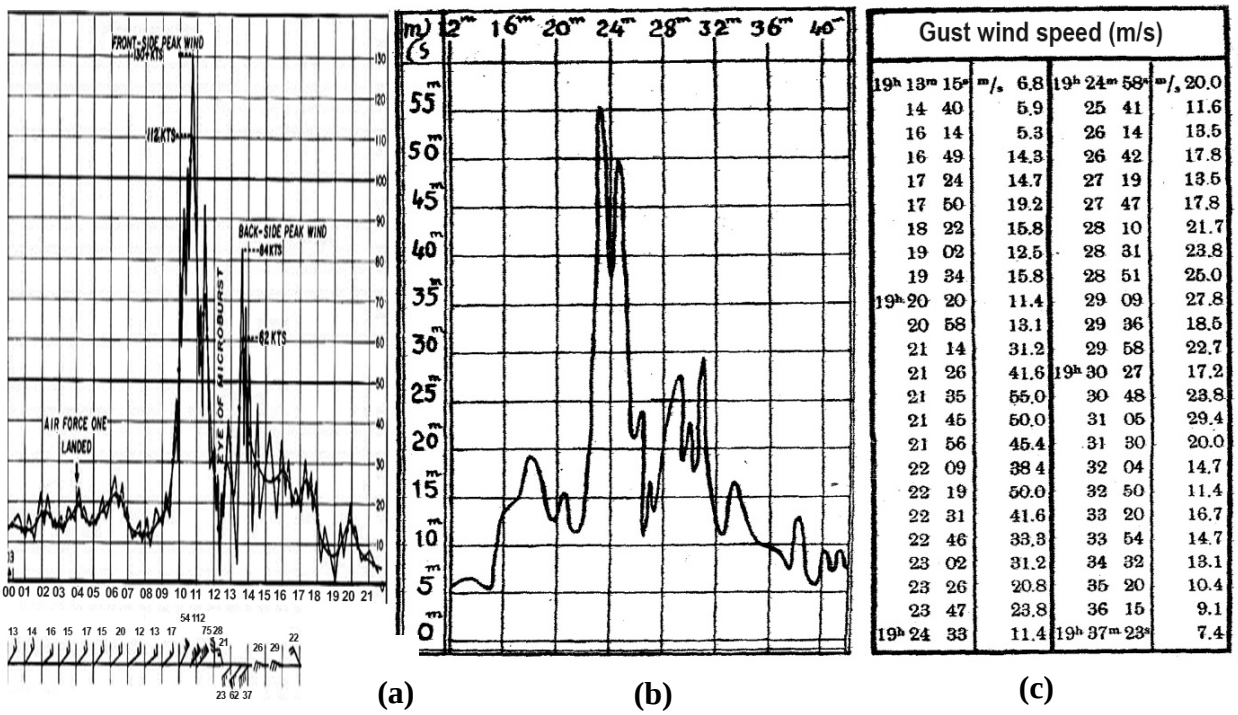


Figure 2.51 (a): Downburst in Maryland, USA, on August 1st, 1983 (adapted from Wakimoto, 2001) (b) and (c): Downburst in Montevideo, Uruguay, on July 8th, 1935 (from Morandi, 1938)

These findings, together with the characteristics of the generated wind damage, would indicate that the evolution of wind speed during the passage of very strong downburst and/or corresponding downdraft outflow was registered in Montevideo as early as in 1935. Morandi, 1938 indicates that the wind speed shown in Figure 2.51(b) was registered with an electric Robinson-Fuess anemometer of short arms that averaged half kilometre, thus, its time response may have been lower than the one corresponding to Figure 2.51(a), fact also suggested by the more rapid wind speed fluctuations shown in this last figure. It is then possible that the maximum recorded wind gust could have been higher than 55m/s, if it had been registered with a higher frequency response anemometer. On the other hand, wind speed may have been even higher at higher altitudes, or at other horizontal locations.

Figure 2.51(c) indicates the wind speed values measured during the non-synoptic high wind event registered in Montevideo in m/s, and the local time of each measurement indicating the corresponding hour, minute and second of each register. It is worth noting that during this event the wind speed increased from 13m/s (47km/h) at local time 19h 20min 58s, to 55m/s (198km/h) at 19h 21min 35s, i.e., it increased 150km/h (42m/s) in around half a minute. According to this register, wind speeds higher than 150km/h were sustained for approximately 40-60s.

The severe convective storm that produced this non-synoptic high wind event affected different areas of Montevideo, as its centre where several roofs, doors, windows, light poles, electricity cables, trucks and trees were blown down, and its port, as mentioned in Vieira, 1969.

It is worth noting that there are still not many registers of wind speed measurements during the passage of downbursts and/or their corresponding downdraft outflows around the world with a measurement frequency that allows a good description of this type of event, and that the event registered in Montevideo in 1935 may be the first documented presenting such high wind speeds, to the author's knowledge. A downburst that occurred exactly 1 month later in Great Britain (August 8th, 1935) is reported in Gold, 1936, but reached a much lower wind gust speed (96km/h, i.e., ~27m/s). Examples of wind speeds measured during the passage of other downbursts registered around the world are presented in figures 4a-c in Durañona, 2013 (not shown here), as those corresponding to one that took place in Texas, USA in 2002 (Holmes et al., 2008), and to other in Sydney, Australia in 2001 (Holmes, 2004).

Quite recently, Prof. Solari from the University of Genoa, Italy has been measuring non-synoptic high wind events with ultrasonic anemometers registering at 10Hz (Solari et al., 2015a), showing the importance of describing these events with a high temporal resolution. He also reported fast increases in wind gust speed in just few tens of seconds during these events.

In relation to tornadoes, there exist several reports on tornadoes that occurred in Uruguay, usually performed by independent Uruguayan meteorologists or by the National Institute of Meteorology (INUMET), formerly named DNM. These reports usually describe the event from a meteorological point of view, sometimes performing additionally field surveys to gather more information about it and its related wind damage. Some examples of such reports are DNM, 2002; Torena, 2003; Vecino and Torena, 2008 and Torena, 2009.

Figure 2.52 shows images of two out of many tornadoes that have been registered in Uruguay. Figure 2.52(a) corresponds to a F3 tornado that caused widespread damage in the department of Florida, Uruguay on April 21st, 1970, while Figure 2.52(b) shows a more recent tornado that formed in the department of Rocha, which was embedded in an intense extra-tropical cyclone that passed over the country on October 23rd, 2012.

Waterspouts are occasionally observed close to the Uruguayan coastline. Figure 2.53(a) shows a series of waterspouts that formed near the south western coast of Uruguay, over the Río de la Plata, in front of the department of Colonia in 1988, while Figure 2.53(b) corresponds to a waterspout observed from the coast of Montevideo on November 24th, 2012.



Figure 2.52 Some tornadoes in Uruguay: (a) F3 tornado in Florida, April 21st, 1970 (picture taken by Juan Pastorino Torena, 2011) (b) tornado in Rocha, October 23rd, 2012 during the passage of an extra-tropical cyclone (from BluchannelTV, 2012)



Figure 2.53 Some waterspouts in Uruguay: (a) in Colonia, 1988 (b) in Montevideo, November 24th, 2012 (from BluchannelTV, 2012)

2.3. Data quality considerations

As Wieringa and Rudel, 2002 indicate, the basic assumption of many wind data users is that official station observations conform closely to the rules of instrumentation, exposure and siting given in the World Meteorological Organization (WMO)-CIMO Guide. However, this is not often the case for different reasons.

According to Aguilar et al., 2003, in order to extract accurate conclusions from wind data analysis, high quality and homogeneous long-term datasets are needed, but these data are influenced by a wide variety of observational practices. As wind data depend on the measurement instrument, its exposure, recording procedures and many other factors, in order to provide high quality datasets it is crucial to maintain comprehensive station documentation and to keep it updated. Such station documentation is information about the data, or data about the data, which is called metadata. Metadata should reflect how, where, when and by whom information was collected, and all the changes a station has undergone during its lifetime, composing what is called the station history.

The importance and necessity of metadata can also be understood by quoting one of the GCOS Climate monitoring principles (WMO, 2002): "The details and history of local conditions, instruments, operating procedures, data processing algorithms and other factors pertinent to interpreting data (i.e., metadata) should be documented and treated with the same care as the data themselves."

However, Wieringa and Rudel, 2002 indicate that in most countries metadata about station siting and exposure are not usually archived, even when good records on the technical state of the instrumentation exist. The information usually available is the geographical coordinates of the station and the elevation above sea level, and therefore, most wind data users need to deal with metadata and homogeneity to some extent.

According to the WMO, wind measurements should be carried out at 10m height over level and open terrain; open terrain meaning an area where the distance between the anemometer and any obstruction is at least ten times the height of the obstruction. The anemometer exposure is affected by the instrument height above ground, the roughness and topography of the surrounding terrain, as well as the size, shape, porosity, distribution and distance of the

upwind obstacles over which the wind must blow. An example of how surroundings can greatly affect wind measurements is presented in Durañona and Cataldo, 2001.

When the exposure of the station is not standard (WMO, 2006), models of the ABL are usually applied to correct its exposure - as those presented in Sub-section 2.2.1, assuming that the flow is of ABL type. In this case, the minimum information required would be the actual observation height, the roughness length(s) of its surroundings (z_0), and location of obstacles around the station.

If it is necessary to correct wind measurements due to differences in surface roughness from the standard exposure, the effective roughness z_0 in the nearest kilometres upwind may be estimated for example from visual appraisal of available information in maps, surface or aerial photos, and classifications of effective terrain roughness such as those presented in Davenport et al., 2000.

According to Wieringa and Rudel, 2002, some other problems that may arise with wind data are: unavailability of observers during certain periods of the day, or of power supply; instruments mounted in undesirable or unexpected positions; wind masts that claim to be located in open locations but are actually seriously sheltered and underestimate the wind by for example 20 or 30% relative to really open terrain. Other errors in wind records may appear due to the use of non-calibrated instruments, reading mistakes or wrong digitisation when the station is not automatic. A situation commonly encountered in practice is one in which, while the anemometer may not have been moved, the roughness of the terrain surrounding the anemometer has changed significantly over the years, as for example a result of extensive land development. In such situations, the adjustment of the data to a common roughness may pose insurmountable problems, unless detailed information on the phases of the land development is available. This is of vital importance when long data series need to be analysed.

Aguilar et al., 2003 gives detailed information on the metadata needed to assess the quality and homogeneity of long-term datasets. These metadata should include:

- station identifiers
- geographical data of the station, latitude and longitude, elevation above mean sea level and relocations

- information on the local environment: mapping of the mesoscale region at a scale of about 1:100,000 and toposcale map (~ 1:5,000) updated each year; photos of the station taken from all points of the compass with enough distance and of instrument positions, updated upon significant changes; a microscale map of the instrument positions, updated when individual instruments are relocated or other significant changes occur
- information on the local land use/land cover: proximity and size of large water surfaces, urbanised areas, mountain ranges, terrain slope with both steepness and direction; forests, crops and other roughness; nearby obstacles such as trees or houses; at airports: airplanes
- information on the type of instruments: instrument manufacturer, model of instrument with size and identification, output type and sensitivity, transducer type if applicable, response time if applicable, time and method of azimuth alignment for wind direction, response time of the anemometer and of the recording chain, and how these were determined
- information on instrument mounting such as height above surface, where it is mounted
- information on data recording and transmission, such as scale units and resolution, range of recorded variations, response time and/or sampling time, averaging period if applicable
- information on observing practices: observers, observed elements, observing times, corrections made by observers
- routine maintenance, as routine checks
- data processing

About the most common sources to obtain and gather metadata, Aguilar et al., 2003 suggests:
- contacting the meteorological office or other responsible institutions
- visiting the meteorological site, as mapping and photographing the meteorological site provides a great amount of information about the recording conditions
- looking for information in the data themselves, as they are an excellent source of metadata like station codes, location, observing times, missing data, etc.
- interviewing current and former observers and/or local experts, who can add useful information
- consulting archives, libraries, newspaper archives, etc., as those sources may help to recover historical information of the station, and provide data for population and urban growth or historical events
- consulting instrument manufacturers

Regarding homogeneity, Aguilar et al., 2003 indicate that unfortunately most long-term climatological time series have been affected by a number of non-climatic factors that make these data unrepresentative of the actual climate variation occurring over time. These factors may include changes in instruments, observing practices, station locations, formulae used to calculate means, and station environment, among others. Some changes cause sharp discontinuities, while other changes, such as change in the environment around the station, can cause gradual biases in the data. As changes in instruments can have a great impact on data homogeneity, it is crucial to note in the metadata the exact date of the replacement. All of these inhomogeneities can bias a time series and lead to misinterpretations of the studied climate. It is important, therefore, to remove the inhomogeneities or at least determine the possible error they may cause.

On the other hand, Simiu and Scanlan, 1996 indicate that in order to provide useful information on the wind climate at a given location, wind speed data recorded at that location must be reliable and must constitute a micrometeorologically homogeneous set.

For these authors, wind speed data may be considered to be reliable if:

- the instrumentation used for obtaining the data (i.e., sensor and recording system) may be assumed to have performed adequately and was properly calibrated. If it can be determined that the calibration was not adequate, the data must be adjusted whenever the information needed for that purpose is available
- the sensor was exposed in such a way that it was not influenced by local flow effects due to the proximity of an obstruction (e.g. building top or instrument support).

Regarding homogeneity, a set of wind speed data would be considered to be homogeneous if all the data belonging to the set have been obtained under identical or equivalent conditions, taking into account:

- averaging time (i.e., whether highest gust, fastest mile; 1, 5 or 10min average, etc. was recorded)
- height above ground
- roughness of surrounding terrain (exposure)

A good example of the concepts summarised in this section is given by Figure 2.54, which shows how inhomogeneous a long series of wind observations can become. This figure presents the evolution with time of the annual mean wind speed measured at a station of New Zealand along 100 years, and its relation with changes of its surroundings and with relocations of the anemometer. A significant variability on annual mean wind speed can be observed, which is mainly due to non-climatic causes. Without counting with adequate metadata, this behaviour may have been attributed to climate change or climate variability.

As indicated by Wieringa, 1996, wind observations are very sensitive to changes in the surroundings, much more than observations of rainfall, temperature, or radiation. Therefore, most station wind series show gradual or sharp changes because of nearby vegetation growth, building activity, and/or relocation of the wind mast. As many climatologists require 'long-term representativity', it is essential to keep records of these changes so they can be accounted for before arriving at erroneous conclusions.

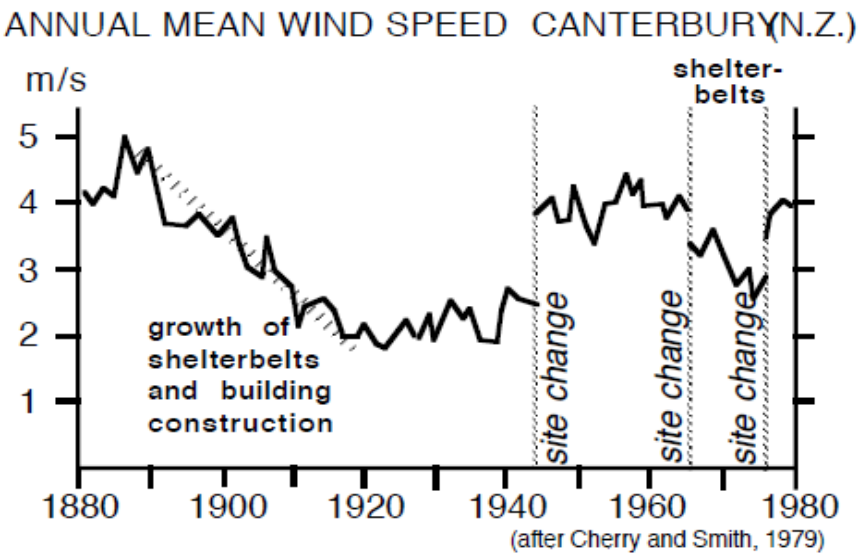


Figure 2.54 A hundred years long wind data series spoiled by gradual changes in toposcale surroundings (from Wieringa, 1996)

2.4. Extreme wind value analysis

As indicated in Palutikof et al., 1999, high wind speeds pose a threat to the integrity of structures, particularly to those at exposed sites, such as wind turbines or radio masts. In any design project, safety considerations must be balanced against the additional cost of overdesigning, and accurate estimation of the occurrence of extreme wind speeds is an important factor in achieving the correct balance.

Estimates of the 50-year return period wind speeds are typically required for design applications, and many times the available wind data series have lengths between 10 and 20 years. A theoretical distribution is usually fitted to the extreme wind speed values in order to calculate the quantiles X_T, i.e., the maximum wind speed which is exceeded, on average, once every T years, being T the return or recurrence period.

As indicated in Wieringa, 1996; Aguilar et al., 2003 and summarised in the previous section, the quality of any wind data series and of its associated metadata is essential to obtain reliable results, especially when analysing long wind data sets for estimates of wind speeds of long return periods.

In addition, the averaging period of the wind speed values used to perform extreme wind value analysis needs to be clearly known or specified (Holmes and Ginger, 2012), as the registered wind speeds may vary with the averaging period, as discussed in Sub-section 2.2.1. Knowledge of the frequency response of the wind measurement system is thus required.

2.4.1. Methods to calculate extreme wind speeds

The estimation of wind speeds of long return periods from observed data for design purposes has been the subject of extensive research over many years, as indicated in Karpa and Naess, 2013. Cook, 1985; Simiu and Scanlan, 1996; Palutikof et al., 1999 and ASCE:7-10, 2010 for example, present different methods for this estimation, and discuss their main advantages and disadvantages.

According to Karpa and Naess, 2013, there would not be a general agreement on a preferred method for extreme wind value estimation. Standard methods for estimating extreme wind

speeds from limited sets of observed data are commonly based on assuming an asymptotic domain for the distribution of extreme values, generally corresponding to a Gumbel or Type I distribution; or adopting a peaks-over-threshold (POT) approach, usually assuming that the exceedances above high thresholds follow a generalized Pareto distribution (GPD).

One of the distributions more widely used for extreme wind value analysis is the Generalized Extreme Value distribution, or GEV. This distribution is based on the results of Fisher and Tippett, 1928, which showed that if a sample is chosen from a parent distribution, and the maximum (or minimum) of each sample is selected, then the distribution of the maxima (or minima) approaches one of three limiting forms, as the size of the samples increases. These three families were combined into a single distribution, now known as GEV, which has the following cumulative distribution function shown in Equations (2.6):

$$F(x) = e^{\left[-(1-k\cdot y)^{1/k}\right]} \qquad k \neq 0$$

$$F(x) = e^{\left[-e(-y)\right]} \qquad k = 0 \tag{2.6}$$

where k is a shape parameter, which determines the type of extreme value distribution, and y is the standardized or reduced variate, defined as:

$$y = \frac{x-\mu}{\sigma} \tag{2.7}$$

where μ is the mode or location parameter of the extreme value distribution, and σ is the dispersion or scale parameter.

Fisher-Tippet Type I, II and III distributions, also known as the Gumbel, Frechet and Weibull distributions, present values of $k = 0$, $k < 0$ and $k > 0$, respectively. Type III distribution is bounded at the upper end, while Types I and II are unbounded at the upper end, with Type II having a thicker tail than Type I.

The aim of the classical extreme value theory is to define the form of the limiting distribution and estimate its parameters. Cook, 1985 suggests that at least 20 extreme values should be used in order to obtain reliable results, and states that this method should not be employed with less than 10.

There are several graphical and numerical methods for estimating the distribution and the corresponding parameters that best fit the extreme wind data.

Graphical methods are based on the fact that $F(x)$, the probability that an annual maximum wind speed is less than x, can be estimated for each of the observed annual maxima by simply ordering the extreme wind data series from the smallest (x_1) to the largest (x_N) wind speed value, and calculating an empirical value of $F(x_i)$ from the ranked position of x_i. These estimates are known as the plotting positions. Choosing plotting positions which lead to unbiased quantile estimates is not straightforward.

According to Gringorten (Gringorten, 1963), for the Gumbel distribution, an almost unbiased plotting position is given by:

$$F(x_i) = \frac{i - 0.44}{\mathrm{N} + 0.12} \tag{2.8}$$

where i is the position of the annual maximum wind speed value x_i in the sorted annual maximum wind speed series, and N in this case is the length in years of the extreme data series.

Then, a graph can be constructed and linearized by plotting the reduced variate, y, against values of x, and a straight line may be fitted to the plotted points, by e.g. using least-squares fit. From this fit, the parameters μ and σ can be calculated.

Among the numerical methods for the determination of the GEV parameters for extreme wind value analysis, the most commonly used are the probability weighted moments (PWMs) and the maximum likelihood (ML) methods. The method of moments is one of the simplest to apply, but its bias and efficiency are not easy to evaluate.

The principal drawback to the classical GEV method is that only one maximum (or minimum) value is selected per sample or epoch. As the extreme data series needs to be i.i.d. (independent and identically distributed) according to Fisher and Tippett, 1928, and extreme wind data may exhibit seasonal variability, they are usually constructed from yearly maxima. It then follows that in order to have an extreme wind data series with 20 data, as suggested by

Cook, 1985, 20 years of wind data are needed. To overcome this difficulty, alternative approaches have been developed, as presented in Palutikof et al., 1999.

One of these methods consists in extending the concept of a single extreme per epoch to include the r-largest values. To apply this method, it is necessary to decide how to maintain the independence of extremes and the size of r.

Another option is to apply the method of independent storms (MIS), which uses a lull, or period of wind speeds below a selected (low) threshold, to separate storms, and then extracts the maximum wind speed from each storm.

A third method consists in extracting peak-over-threshold (POT) maxima in order to produce a series of extreme values above a chosen (high) threshold. The generalised Pareto distribution (GPD) is generally used to describe the behaviour of the events above the specified threshold.

The great advantage of using the GEV distribution with annual maxima is that few decisions are required for the calculation of the distribution parameters, while with the alternative approaches, decisions must be made which can have a strong impact on the estimated values of the distribution parameters. For the r-largest method it is necessary to decide on the size of r, while for the MIS and POT methods a threshold value has to be selected.

The precision of the estimates of the distribution parameters and quantiles is expressed by the standard error, which is the square root of the variance of the error in the estimates. Small standard errors are an important criterion in assessing the success of an extreme value analysis. Uncertainty in the estimation of distribution parameters arises from, for example, an arbitrary choice of the statistical model and inefficiencies in the determination of its parameters.

The standard error (SE) of the quantiles estimates for the GEV distribution with $k = 0$ can be obtained from:

$$SE[\hat{X}_T] = \left[\frac{\mu^2}{\mathrm{N}} \cdot \left(0.608 \cdot \mathrm{Z}^2 - 0.514 \cdot \mathrm{Z} + 1.109 \right) \right]^{\frac{1}{2}} \tag{2.9}$$

where N is the length of the extreme data series and Z is:

$$Z=\mathrm{Ln}\left[-\mathrm{Ln}\left(1-\frac{1}{T}\right)\right] \tag{2.10}$$

For both statistical and meteorological reasons, longer records will usually produce more accurate estimates of extreme winds, assuming that the wind climate itself is not significantly changing. Statistically, since the standard error is inversely proportional to the sample size, larger samples imply smaller standard errors.

Regarding the choice of the statistical model, several goodness of fit tests exist to aid model selection, as presented in Durañona, 2012b.

According to Palutikof et al., 1999, extreme gust and mean wind speed data for temperate latitudes have been traditionally fitted to a Type I distribution. However, some decades ago, several wind codes adopted a Type II distribution for their extreme winds (Ricaldoni, 1979; Chamlian, 1993; Natalini and Natalini, 2010), as the Uruguayan, Argentinian and Brazilian wind codes UNIT:50-84, 1984; IRAM:11-700, 1979 and NBR:6123, 1988a respectively. Palutikof et al., 1999 indicate that a Type II distribution is seldom found, and according to several authors, as Gomes and Vickery, 1978 and Cook, 1985, it is generally indicative of a mixed wind series, i.e., when more than one meteorological type of event dominates the extreme wind climate. The usual current choice is regarded by Palutikof et al., 1999 to be between the Type I (Gumbel) and Type III (Weibull) distributions, but some regional authors still find that in some stations, a Type II distribution yields a better fit (e.g. Beck and Correa, 2012, as presented in Sub-section 2.5.2.2). In other cases, a Type I distribution has been chosen without comparing its goodness of fit to the extreme wind data series, with the goodness of fit of other distributions, as for the development of the current extreme wind map of Argentina (Natalini and Natalini, 2010).

When the choice is between a Type I and a Type III distribution, as the first is unbounded at the upper end, and the last is bounded from above, the Type I distribution is often chosen by those that argue that there is no natural upper bound for wind speed. The assumption of a Type I distribution has the added attraction that, since *k* is set equal to zero, the solution is simpler. Another argument for this choice is that as the Type III will normally give lower

extreme wind speeds for a given return period, thus, selecting a Type I distribution would make allowance for margins of errors associated with different sources of uncertainties.

Apart from deciding on the distribution model, the method for estimating the parameters needs to be selected. According to Palutikof et al., 1999, the ML methods introduce negligible bias for sample sizes between 30 and 1,000, and in cases where the shape parameter, *k*, has a non-zero value, the PWM methods will be severely biased for large positive values ($k > +0.2$), although no examples of such large values were found by these authors in the literature on extreme winds. In addition, the ML method has been reported to yield much more stable parameter estimates than the PWM methods in GPD analysis of wind speeds over a range of thresholds.

In order to comply with the i.i.d. requirements for the application of Fisher and Tippett, 1928 results, homogeneity of the data series is needed.

Non-stationarity on the data might appear due to natural causes, or due to human error/activity. For example, if data from a period of low wind speeds is used, the extremes may be underestimated. Changes in observers can influence the homogeneity of a series, as until relatively recently wind records were compiled from chart recorders or dials, procedure that introduces a strong subjective element in the measurement of wind speed. Changes of instrument types, faulty instrumentation or changes in the surroundings of the station may also produce inhomogeneities in the wind data series, and attention should be paid to these factors when analysing extreme wind statistics.

Different techniques to assess, and when possible, to correct the resulting inhomogeneities, are available. A simple time series plot of the data may be sufficient to reveal the presence of trends or step jumps.

On the other hand, when more than one meteorological mechanism dominates the extreme wind climate in a region, it is advised to treat the data produced by the different phenomena in a separate way.

According to Palutikof et al., 1999, if a long time series is available, the most commonly used distribution in extreme wind value analysis is the GEV Type I (Gumbel), applied to a set of annual maxima.

Although techniques such as the r-largest, the MIS, and POT methods have the advantage that for a given time series more points are selected for analysis, and therefore, the standard errors should be lower than for an annual maxima analysis performed on the same data set, more decisions are required, such as on the threshold value and minimum separation distance, which can have a very large impact on the final parameter estimates. Thus, the results would not be as reliable as those from analyses based on the GEV distribution or GPD applied to a long data set.

On the hand, a short data set would imply large standard errors and, in the presence of a mixed climate, a likely failure to capture the full range of extremes.

More recent methods have been proposed for extreme value analysis such as the ACER (Average Conditional Exceedances Rate) method described in Karpa and Naess, 2013. These authors claim that this method is better than the GEV applied to annual maxima and than the POT method, indicating in particular that it has been studied in-depth on synthetic data with known extreme value distribution, carrying out Monte Carlo simulations to produce 100 data samples. They observed that the predicted 100-year return period levels were consistently better for the ACER method than for both the POT and GEV methods, and indicated that these results would be published in a forthcoming paper.

In particular, they say that ACER provides a non-parametric representation of the exact extreme value distribution inherent in the data, avoiding invoking the ultimate asymptotic distributions, and trying to capture to some extent also the sub-asymptotic behaviour of extreme value data if appropriate, but in a manner that is asymptotically consistent.

Karpa and Naess, 2013 state that this method can be applied to non-stationary series, as seasonal effects are automatically accounted for; and to non-independent series, so an initial separation of extreme wind data caused by different meteorological mechanisms would not be required. They also say that this method is not sensitive to outliers and offers a more robust solution for the estimation of extreme value statistics.

2.5. Extreme winds in wind codes

The assessment of wind loads on a building during its design stage requires an adequate estimation of the maximum wind speed to which the building will be exposed during its lifetime. Wind climatology provides the designer and the code writer with information on the extreme winds that might affect a structure during its lifetime. Such information is required for making rational decisions on the magnitude of the wind loads to be used in design (Simiu and Scanlan, 1996). This information is usually provided in the form of extreme wind maps, which are generally part of the national codes of wind actions on buildings and structures.

As presented in Sections 2.3 and 2.4, the reliability of climatological assessments based on the analysis of extreme wind speed data can be greatly affected by the quality of the data (Simiu and Scanlan, 1996; Wieringa, 1996).

On the other hand, most design techniques and wind codes evaluate wind loads on structures assuming that the wind flow is of ABL type, despite increasing recognition of the relevance of non-synoptic winds produced by severe convective activity for the definition of design wind speeds in many regions of the world (Chay et al., 2006a).

As it has long been recognised, the analysis of wind gust speeds is necessary for the evaluation of extreme winds in places where convective storms are a dominant feature of their extreme wind climate (Riera et al., 1977; Holmes et al., 2005b), and extreme 10min mean wind speeds would not offer enough information to describe the extreme wind speeds.

According to Holmes et al., 2005, in the beginning of wind engineering the main way in which the wind speed distribution with height above ground level was specified was through the use of a power law, as in Equation (2.5), Sub-section 2.2.1. Although this law does not have a theoretical basis and offers a poor fit close to ground level, its use continues in a significant number of national wind codes due to its extreme simplicity and usability.

Other codes adopted the logarithmic wind speed profile presented in Equation (2.1), Sub-section 2.2.1, as it offers a better approximation close to ground level and has theoretical background. However, this approach tends to provide a poor fit to experimental data for heights greater than 30 to 50m, as expected from what was exposed in Sub-section 2.2.1. To remedy this, a number of wind codes added linear and non-linear terms to the logarithmic law,

like the formula presented by Harris and Deaves, 1980, providing a better fit to the wind speed profile over a large height range with just one formula.

As Holmes et al., 2005a indicates, the International Association for Wind Engineering (IAWE) set up in 1999 the Working Group on Wind Structure (WGWS), one of the International Codification Working Groups to review and make recommendations for harmonisation in international codification for wind loads. This WGWS recommends for use in codes and standards the logarithmic law or the related Deaves/Harris expression, as models of the wind speed distribution with height for synoptic winds. The Deaves/Harris model is presented in Equation (2.11):

$$U(z) = 2.5 \cdot u_* \cdot \mathrm{Ln}\left(\frac{z}{z_g}\right) + 5.75 \cdot \left(\frac{z}{z_g}\right) - 1.88 \cdot \left(\frac{z}{z_g}\right)^2 - 1.33 \cdot \left(\frac{z}{z_g}\right)^3 + 0.25 \cdot \left(\frac{z}{z_g}\right)^4 \qquad (2.11)$$

where U is the mean wind speed at height z; u_*, the friction velocity and z_g, the gradient height.

On the other hand, this Working Group recognises that the flow structure during hurricanes and during severe convective activity is not usually taken into account in wind codes and standards. Regarding severe convective activity, the WGWS states that there is an urgent need to incorporate the wind structure of downbursts into codes and standards, given the importance of these extreme winds in many regions of the world. In the same sense, Holmes et al., 2005a recognised that although severe downburst winds dominate the wind design of structures in many parts of the world, no code or standard at that time addressed the wind structure of these flows, such as their wind gust profile for design applications, and proposed an expression for the wind gust profile of downbursts until the required full-scale data is available.

Another working group set up by IAWE to review and make recommendations for harmonisation in international codification for wind loads was the Working Group WGF, Extreme Wind Prediction and Zoning (Holmes et al., 2005b), with the aim of covering topics as international database of extreme winds, quality assurance and data quality, averaging times, return periods, probability distributions and fitting methods, mixed wind climates,

directionality effects, the influence of orography, rare events and simulation methods, long-term climate change, and zoning and mapping.

In relation to the averaging time, Holmes et al., 2005b indicate that its choice may depend on the type of meteorological event that generates the extreme winds in the analysed region. Where downbursts are the dominant meteorological mechanism, the use of a 2 or 3s gust is usual, as 1h or 10min mean wind speeds have little or no relation with the maximum wind gust developed. Where synoptic winds dominate the extreme wind climate, a longer averaging time gives mores stability to values used in extreme wind value analyses, being the most common averaging periods 10min and 1h.

Holmes et al., 2005b also indicates that wind gust speeds are usually measured continuously, and are therefore truly representative of the wind gust speed climate at a particular location, but the same does not necessarily occur with mean wind speeds. Some countries measure mean wind speed continuously, as the UK, the Netherlands and Switzerland, but most stations around the world only measure it during a period immediately before the reporting hour. This is the case of the National Institute of Meteorology of Uruguay (INUMET), whose stations usually measure 10min mean wind speeds before the hour.

Thus, for many countries, the 10min mean wind speed is representative of the conditions during the 10min period immediately before the reporting hour, with no information about the mean wind speed over the preceding 50min. As a result, the reported 10min mean wind speed is not necessarily representative of the maximum 10min mean wind speed over that hour, and any extreme wind occurring during the unrecorded 50min will not be represented in the station records.

In relation to return periods for the definition of design wind speeds in wind codes, the most common choice is 50 years, although the Australian/New Zealand building codes recommend a value of 500 years for normal structures, in common with earthquake engineering practice; and lately, ASCE:7-10, 2010 is basing its basic wind speed in return periods spanning from 300 to 1,700 years.

The WGF also advises the use of extreme wind data series with record lengths of at least 30 years for the analysis of individual stations, unless aggregation of stations into ‘superstations’ is adopted.

About mixed extreme wind climates, the WGF recognises the existence of three possible different situations: **(a)** extreme winds generated by different meteorological types of event, but with one of them clearly more dominating than the others; **(b)** different meteorological types of events have stronger winds over different ranges of the probability domain, e.g. event 'A' is stronger over the lower return period range whereas event 'B' develops stronger winds over the higher return period range, and **(c)** the different meteorological types of event have stronger winds over different averaging periods, e.g. event 'A' is stronger for a longer averaging period (hourly mean), whereas event 'B' presents stronger winds for a shorter averaging period (gust).

For scenario **(a)**, the WGF indicates that the usual extreme analysis method (without separation of storm types) can be used without introducing much error, but that for case **(b)**, a separate extreme analysis for each of the different meteorological types of event should be carried out, and a combination of their resulting distributions is needed. For case **(c)** the WGF recommends to perform a careful analysis, and indicates that although results obtained from the usual extreme wind value analysis would be more or less similar to those obtained from the separate analysis method, they could introduce inconsistency to other wind characteristics (e.g. gust factor) (Holmes et al., 2005b).

As a general recommendation, the WGF proposes to carry out separate extreme wind value analyses for extreme wind speeds measured during storms of different types, when possible and known to be a feature of particular stations or regions.

2.5.1. Some international wind codes

This sub-section briefly describes the main characteristics of several international wind codes for action on structures, and in particular, their definition of reference (or basic) wind speed for wind loading calculations, suggested wind speed profiles with height, and meteorological events considered to cause extreme winds.

In particular, the main characteristics of the wind codes Eurocode1, 2004; ISO:4354, 2009; ASCE:7-10, 2010 and AS/NZS:1170.2, 2011 are presented.

For the definition of basic or reference wind speed, averaging times vary among the different wind codes and within them, as presented in Bashor and Kareem, 2009. Eurocode1, 2004 for example, bases its basic wind speed in 10min mean wind speeds, while ISO:4354, 2009 allows the use of either 3s gusts or 10min mean wind speeds. ASCE:7-10, 2010 and AS/NZS:1170.2, 2011 are based on 3s wind gusts.

In Eurocode1, 2004, the basic wind speed is defined as the 10min mean wind speed at 10m height over flat and open terrain with a return period of 50 years.

ISO:4354, 2009 defines a reference wind speed as the 10min mean or 3s gust wind speed at 10m height over flat and open terrain with a return period that can be chosen. For flows of ABL type, this wind code provides relationships between mean and gust wind speeds for different averaging times, heights and roughness lengths, and takes into account downburst winds proposing a different wind gust profile.

The basic wind speed in ASCE:7-10, 2010 is defined as a 3s gust at 10m height in open and level terrain with a return period that depends on the use of the building or structure under study. These return periods span from 300 to 1,700 years.

On the other hand, AS/NZS:1170.2, 2011 defines a site wind speed for each of the 8 wind directions covering the wind rose, as the regional 3s wind gust speed with a recurrence period that can be chosen. In this code, Australia and New Zealand are divided into several regions that have different extreme wind climates. In particular, this code classifies regions as non-cyclonic or cyclonic regions, with different wind gust speed profiles each.

In relation to wind speed profiles, Eurocode1, 2004; ISO:4354, 2009 and AS/NZS:1170.2, 2011 propose the use of logarithmic laws, as Equation (2.1), whereas the rest use power laws, like Equation (2.5). ISO:4354, 2009 also provides power law fits to the profiles. All these codes assume that extreme winds occur during flows of ABL type, except for ISO:4354, 2009, which additionally consider downbursts as another type of flow capable of generating extreme winds.

2.5.2. Regional wind codes

This sub-section briefly presents how Argentinian and Brazilian wind codes for actions on structures define their reference wind speeds, and how their extreme wind maps were obtained.

2.5.2.1. CIRSOC 102 – Argentinian wind code for actions on structures

The current extreme wind map for Argentina is presented in the Argentinian wind code for actions on structures CIRSOC, 2005a and shown in Figure 2.55. This figure indicates the expected 3s wind gust speeds at 10m height in open and level terrain, for a recurrence period of 50 years, which varies between 36 and 66m/s, with values between 46 and 48m/s close to the border of Uruguay.

Natalini and Natalini, 2010 indicate that this map is based on the work of Viollaz of 1997, who calculated the corresponding wind speeds for 70 meteorological stations; and on a report from María Luisa Altinger de Schwarzkopf (Schwarzkopf, 1997), who proposed lines of equal wind speeds taking into account the results from Viollaz, and the typical meteorological events that take place in different regions of Argentina.

At each station, a Type I (Gumbel) distribution was assumed and the parameters μ and σ were calculated applying the method of moments (described for example in Simiu and Scanlan, 1996) to annual maxima wind gust speeds mainly registered between 1967 and 1990. After that, a global σ was estimated for all Argentina. The final value of the local σ was calculated as the mean of the global and local σ, and from this value, a local μ was estimated (Natalini and Natalini, 2010).

This wind code proposes a power law similar to the one presented in Equation (2.5) for the wind gust speed profile with height, thus assuming flows of ABL type for all extreme winds.

CIRSOC, 2005a was based on the wind code ASCE 7-95, except, of course, for its extreme wind map.

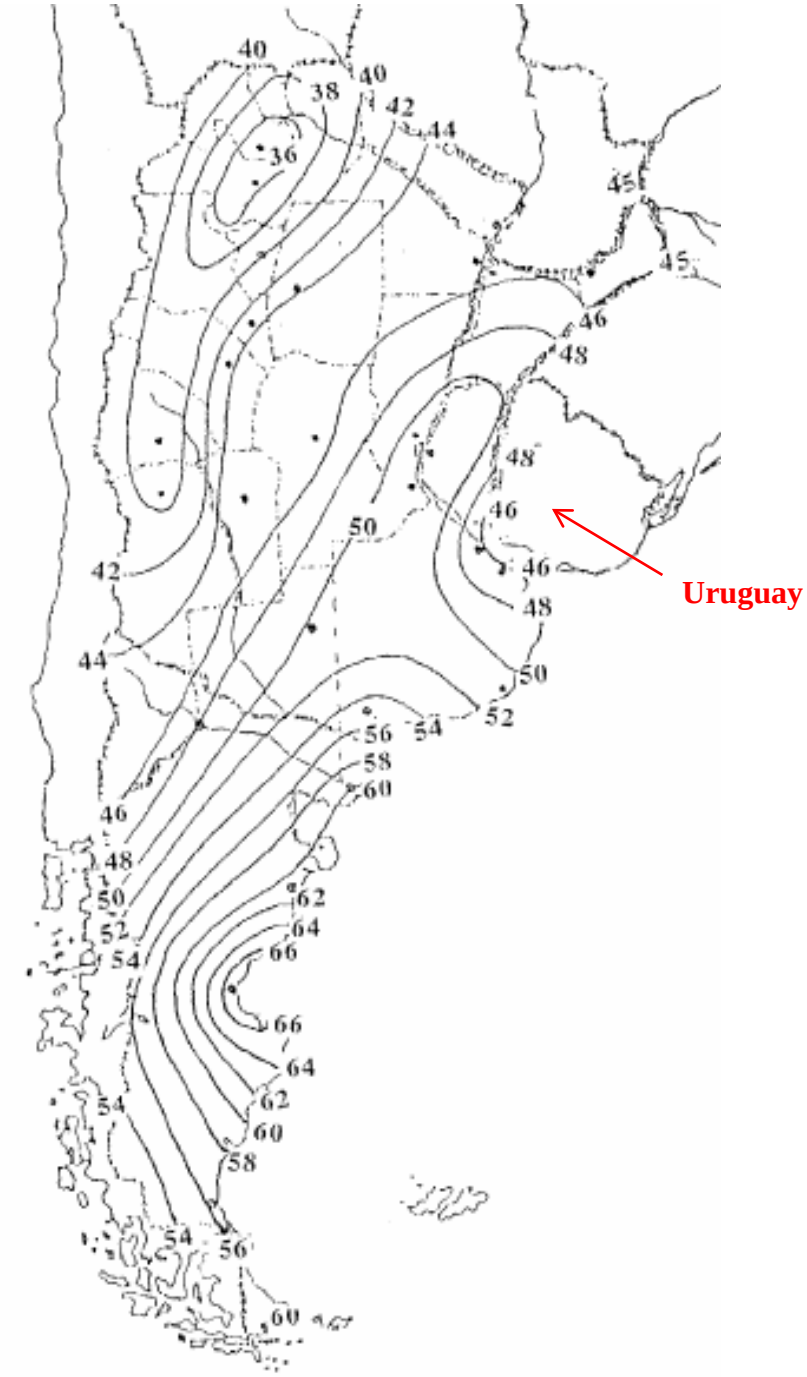


Figure 2.55 Extreme wind map in the current Argentinian wind code CIRSOC, 2005a (3s gusts with 50-year return period, values in m/s)

The previous extreme wind map for Argentina was obtained from studies of Riera, Viollaz and Reimundin, 1977 and Viollaz, Riera and Reimundin, 1975 (Natalini and Natalini, 2010), and presented in the Argentinian wind code, IRAM:11-700, 1979.

In the latter case, it was assumed that extreme winds followed a Type II (Frechet) distribution, as this distribution seemed to offer a better fit to extreme wind records, and also because it yielded more conservative wind speeds than the Type I distribution.

According to Chamlian, 1993, the probability that the annual maximum wind gust were higher than v_o was calculated with Equation (7.1) from Section 7.3 with γ = 8.22 for all Argentina, and β varying with location as presented in Figure 2.56. γ and β are the parameters of the Frechet distribution, respectively known as the shape factor and the reference wind speed.

At present, there are more than 20 years of new wind data series since the current extreme wind map was developed, and improved techniques to perform extreme value analyses are available. A review and update of this map has therefore been strongly suggested (Natalini and Natalini, 2010).

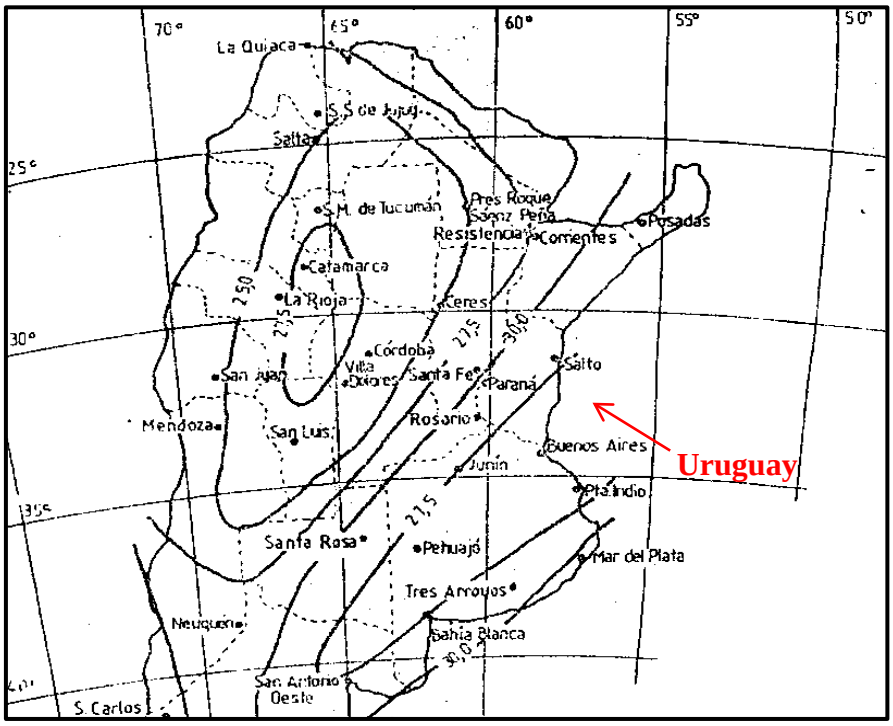


Figure 2.56 Values of the reference wind gust speed (β, values in m/s) in Argentinian wind code IRAM:11-700, 1979 (adapted from Chamlian, 1993)

2.5.2.2. NBR 6123 – Brazilian wind code for actions on structures

The current extreme wind map for Brazil is given in the Brazilian wind code for actions on structures NBR:6123, 1988a, and shown in Figure 2.57. In this figure, wind speed values correspond to the expected 3s wind gust speeds at 10m height in open terrain with 50-year return period, and vary from around 30m/s in the north half of Brazil to 50m/s at its extreme south, with values around 45 to 50m/s near the border with Uruguay.

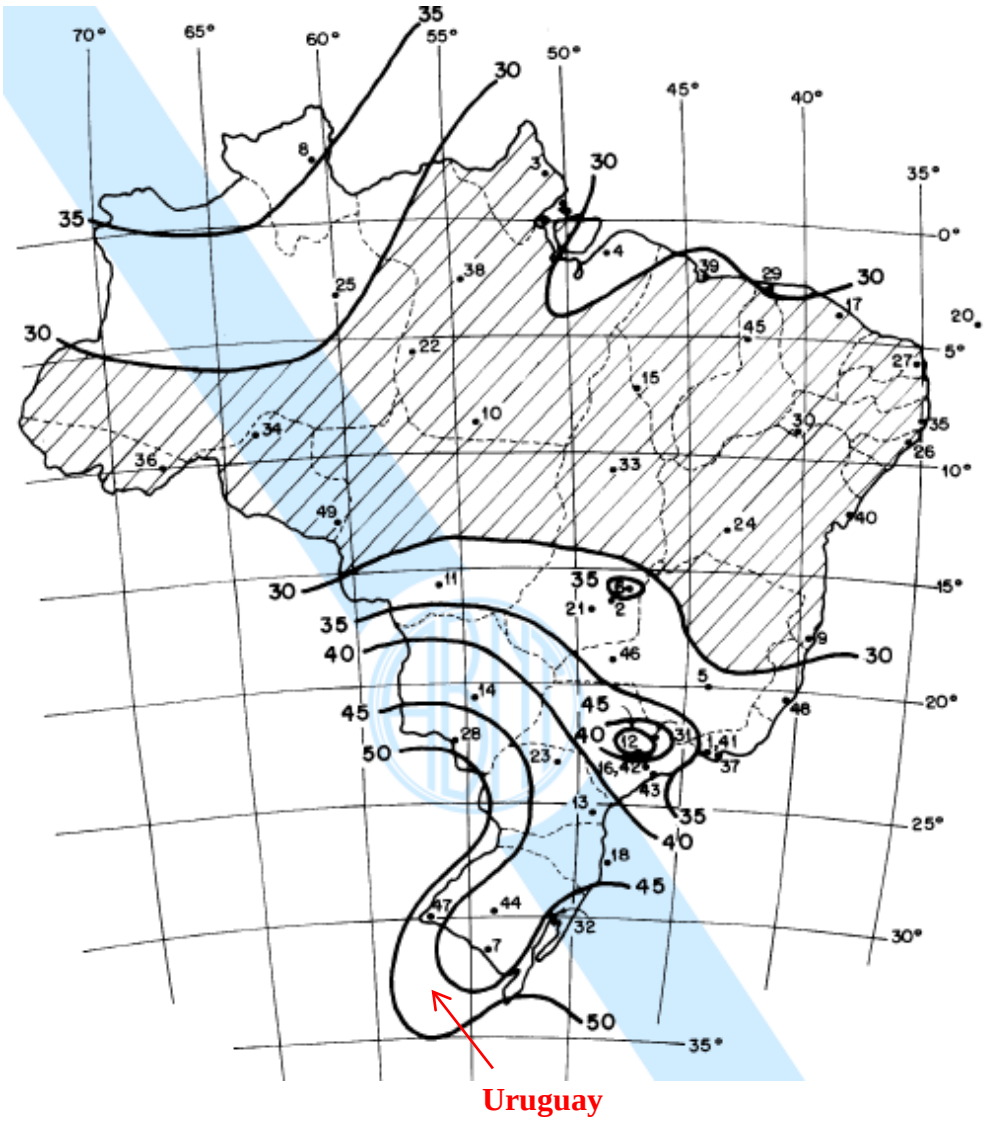


Figure 2.57 Extreme wind map in the current Brazilian wind code, adapted from NBR:6123, 1988a
(3s gusts with 50-year return period, values in m/s)

The current Brazilian wind map is based in the work of Paradatz of 1977, who analysed annual maximum wind speed measured at 49 meteorological stations between 1950 and 1974. The length of each record was between 8 and 25 years, and the analysed data summed up a total of 919 stations×years (Beck and Correa, 2012). These stations registered wind gusts averaged over 30s, and these values were multiplied by 1.15 to obtain the corresponding 3s gust. Wind speeds generated by different types of meteorological events were not differentiated.

Although statistical studies carried out as part of two Master theses showed that in some stations Frechet distribution offered a better fit than Gumbel distribution, while in others the Gumbel distribution gave a better adjustment, it was assumed that the extreme winds followed a Type II (Frechet) distribution in all the stations. The choice for a Frechet distribution was based on the fact that it yields higher wind speeds than the Gumbel distribution for the same return period, making allowance for uncertainties related to the short lengths of the wind data series used, of around 20 years at each station (Riera, 2013).

The profile of wind gusts with height proposed in this wind code follows a power law, similar to the one presented in Equation (2.5), thus assuming flows of ABL type for all extreme winds.

According to Riera, 2013, Riera and Nanni studied later the statistical distribution of the annual maxima wind speeds produced by extra-tropical cyclones and by convective storms in a separate way. The type of event was classified according a series of criteria developed for the available meteorological data in Brazilian airports, which register the duration of extreme winds and simultaneous occurrence of rain, hail, thunder, etc. Nanni conducted statistical tests that showed that both series were different, and that a Type I distribution (Gumbel) yielded a better adjustment for each meteorological type of event, but not for the mixed series. These results were not incorporated in the current Brazilian wind code.

On the other hand, Beck and Correa, 2012 analysed 37 years of additional wind records from 104 meteorological stations at airports, together with the original data studied by Padaratz, in order to update the design wind speeds for Brazil. The analysed data corresponded to 4,142 station×years. For each station and year, each data consisted in the annual maximum of the

30s mean wind speed multiplied by 1.15, or the maximum between this value and the maximum annual wind gust, when these last measurements were available.

Gumbel distributions were fitted to the annual maximum wind speed data series of each station, and 3s wind gust speeds with 50-year return period were obtained. These results are shown in Figure 2.58. These authors report higher wind speeds for significant areas of Brazil, as in its centre, northeast and north, and the same or lower wind speeds for some areas of the south and southeast of the country, as it can be seen if Figure 2.57 and Figure 2.58 are compared.

Statistical tests showed that the Gumbel distribution gave a better adjustment in 87 of the 104 stations, against 21 stations where Frechet distribution yielded a better fit.

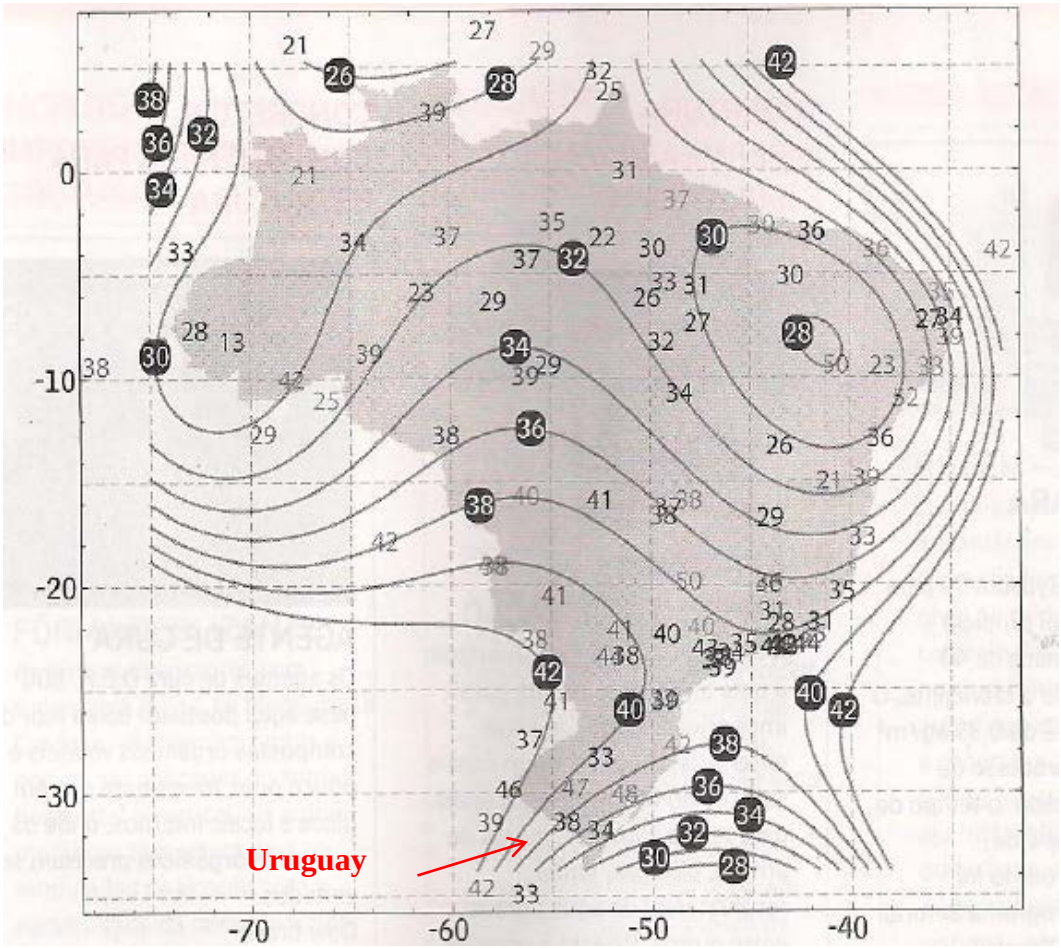


Figure 2.58 Proposed extreme wind map for Brazil (adapted from Beck and Correa, 2012)
(3s gusts with 50-year return period, values in m/s)

Chapter Three

Wind measurements in Uruguay and stations metadata

3.1. Introduction

This chapter presents and describes three different databases of wind speed measurements in Uruguay that were analysed with varying degrees of depth along this thesis, which altogether cover the period from 1901 to date.

Each of these databases has distinct characteristics, which range from different recording systems, averaging periods, types, heights and exposure of anemometers to their sample frequencies and lengths of records.

Section 3.2 briefly describes the history of wind measurements in Uruguay. Taking into account the relevance of counting with adequate metadata, as emphasised in Section 2.3, during this PhD research the search and documentation of the metadata from the analysed stations was conducted with particular care and personal effort by the author of this thesis, and Sections 3.3 to 3.5 present the type of data and metadata available from these stations. Finally, Section 3.6 indicates other meteorological data and information analysed during this PhD research.

3.2. Background on wind measurements in Uruguay

During this PhD research, the author of this thesis did not find a comprehensive document on the history of wind measurement in Uruguay, and the summary presented in this sub-section is a compilation of information from different sources.

Wind speed started to be measured in Uruguay around 1883 at the Observatory of Pío College of Villa Colón, where it was automatically registered by an anemograph, simultaneously with rain intensity and duration (Morandi, 1917a).

From that year until 1938, Prof. Luis Morandi, an outstanding and methodical meteorologist, was in charge of different meteorological stations in Montevideo, where he personally took care of the quality of the measurements, paying attention to the state of the instruments, the exposure of the anemometers and wind vanes, how the readings were performed, studying the

correlation between measurements at different sites and along the time, etc. He also registered the metadata of those stations, and specifically maintained an archive with the occurrence of high wind events, registering simultaneously different meteorological parameters.

In Morandi, 1939, for example, he presents the main features of Montevideo climate through the analysis of 56 years of observations carried out under his direction at the Observatory of Pío College, Villa Colón from 1883 to 1900; at the Observatory of Prado from 1901 to 1921; at a station from the School of Agronomy from 1921 to 1928, and at a station located in the military airport of Montevideo from 1929 to 1938. In particular, he published monthly bulletins with hourly wind measurements from the Observatory of Prado, the first meteorological station of the country described in Section 3.5, and many reports and papers in journals with his main findings and conclusions.

The meteorological data carefully analysed by Morandi show several important characteristics of the extreme wind climate of Uruguay during the first half of last century.

Wind was also registered from 1906 to 1969 with anemographs at Antepuerto station, which belonged to the National Institute of Meteorology of that time and was located in front of the port of Montevideo. The characteristics of its measurements and corresponding metadata are described and discussed in Sections 7.3 and 7.4. The national extreme wind map and design wind speeds proposed in the wind code UNIT:50-84, 1984 were mainly obtained from these measurements, and the corresponding discussion is presented in Section 7.7.

Along time, other meteorological stations were gradually installed across the country by the National Institute of Meteorology. At present, of these stations, the station with the longest wind record corresponds to the station located at Carrasco airport, in Montevideo, currently belonging to INUMET, former DNM. As described in Section 3.4, it carries out hourly measurements during the last 10min of each hour since 1960, being the station with the longest series of 10min mean wind speeds that is currently measuring 24 hours a day. According to Section 2.4, the length of its wind record would be adequate for performing extreme wind value analysis, which is presented in Chapter 6.

More recently, a network of automatic meteorological stations began to be installed in 2008 by the National Administration of Power Stations and Electrical Transmissions (UTE) at different sites in Uruguay, for wind power assessment of the country (Cataldo et al., 2010b).

These stations measure mean, standard deviation, maximum and minimum values of wind speed, direction and temperature every 10min at several heights, as illustrated by Table 3.1. Between 2010 and 2011, 4 additional stations with similar characteristics were installed by the DNE, the National Direction of Energy, from the Ministry of Industry, Energy and Mining.

The length of the data series of these stations was not enough for a proper extreme wind value analysis at the time the research presented in this thesis was carried out, but the number of stations installed allowed performing a first description of the main characteristics of the high wind events that occur in Uruguay, as their typical temporal and spatial scales, their wind evolution with time, correlation among different heights, seasonal distribution, highest wind speeds measured, geographic distribution, as well as of the main associated meteorological events that produce the highest winds in the country. This analysis is presented in Chapter 5.

3.3. Network of automatic meteorological stations

In 2008, UTE began installing a network of automatic meteorological stations, motivated by the research on wind power resource assessment for the whole country. During those years, the National Direction of Energy, DNE, from the Ministry of Industry, Energy and Mining started a program to promote the use of wind energy in Uruguay, and installed 4 additional meteorological stations between 2010 and 2011 in places not covered by UTE at that time, which later on were transferred to UTE. All these stations register a series of meteorological parameters at different heights and automatically transmit the mean, standard deviation, maximum and minimum values of wind speed, wind direction and temperature every 10 minutes. In some stations, relative humidity and/or solar radiation are also measured. Some additional stations have been installed, especially in the northwest of Uruguay, after the analysis presented in Chapter 5 started in July, 2012, while some of the analysed stations have been dismounted by the time this thesis is being written.

3.3.1. Description of the stations

The stations selected for the analysis presented in Chapter 5 corresponded to those measuring in open and level terrain during the period 2008-2012, without significant obstacles in their surroundings that could influence their wind measurements.

There were 25 stations complying with these conditions, generally surrounded by rural terrain. These stations are those shown in the darkest colour in Figure 3.1(a), and their main characteristics are indicated in Table 3.1. Each station originally installed by UTE is identified by a number (2-5, 7-18, 20, 23, 33, 34 and 36) and a name, while the stations installed by the DNE are identified by three letters or by two letters and a number (ARN, EGA, LC2 and ITP), and a name.

Figure 3.1(b) is similar to Figure 3.1(a), but it also shows the topography of Uruguay and the location of three additional stations already mentioned in this thesis, indicated in orange in this figure: Carrasco station (called 'Aeropuerto' in this figure), Observatory of Prado station, and Antepuerto station.

The stations shown in light violet in Figure 3.1(b), i.e., 33, 34 and 36, were not considered for most of the analysis described in Chapter 5, as they had measured less than 1 year by the time of that analysis; while the stations shown in dark violet, i.e., 3, 13 and 15, had measured in the past and were not currently operative at that time. The height scale for the topography of Uruguay, in meters, is indicated in the upper right of Figure 3.1(b). The highest point of the country is around 500m high, as indicated in Sub-section 2.2.5.

Figure 3.1(b) illustrates that the locations of the analysed meteorological stations cover most of the country, with some areas with relatively less stations than others, as in the northwest and northeast. As the maximum distance between two points of Uruguay is less than 600km, the density of these stations would allow an adequate analysis of the trajectories and main characteristics of different weather systems that generate high winds in Uruguay.

The columns of Table 3.1 show, for each station, its number and name, the analysed measurement period, the corresponding number of complete years of measurements, and the measurement heights for each type of sensor. In the case of the anemometers, the number of sensors at each height or the orientation when there was only one anemometer is shown in



Figure 3.1 (a) Analysed stations from UTE network, (b) Analysed stations from UTE network, Carrasco ('Aeropuerto'), Observatory of Prado ('Prado') and Antepuerto stations (images adapted from Google Earth)

N°	Station	Measurement period	Complete years at 3/07/2012	Anemometers heights (m)	Wind vanes heights (m)	Thermometer heights (m)	Hygrometer height (m)	Solarimeter height (m)
2	Bonete	31/7/2008 - 3/7/2012	3	50 (2), 25 (S) , 10 (E)	50, 25	4	-	9
3	Florida	24/4/2008 - 26/8/2009	1	45 (2), 26 (W), 10 (W)	45.4, 25.9	10	-	-
4	Peralta	6/5/2008 - 3/7/2012	4	74.5 (2), 41.5 (W), 10 (W)	74.5, 41.5	4	-	-
5	Valentines	13/5/2008 - 3/7/2012	4	76.5 (2), 41.5 (E), 10 (E)	76.5, 41.5	8	-	-
7	Rosario	27/5/2008 - 3/7/2012	4	65 (2), 44 (W), 10 (W)	65, 44	4	-	7
8	Artilleros	17/6/2008 - 3/7/2012	4	46.6 (2), 27.3 (E), 11.2 (S)	46.6, 27.3	6	-	-
9	Piedras de Afilar	1/7/2008 - 3/7/2012	4	64.4 (2), 37 (2)	64.4, 37	8	-	-
10	Arroyo Cañas	10/7/2008 - 3/7/2012	4	60 (2), 37 (2)	60, 37	5	-	-
11	Pintado	15/7/2008 - 3/7/2012	4	86 (2), 40 (2), 72 (2)	86, 40	13	-	-
12	Cerro Colorado	24/7/2008 - 3/7/2012	3	81 (2), 40 (2)	81, 40	8	-	-
13	Palmar	1/8/2008 - 9/8/2009	1	58 (2), 40 (2)	58, 39	-	-	-
14	Andresito	19/08/2008 - 3/7/2012	3	87 (2), 39 (2)	87, 39	17	-	-
15	Tupambaé	10/9/2008 - 23/8/2010	2	79 (2), 39 (2)	79, 39	-	-	-
16	Pampa	7/10/2008 - 3/7/2012	3	72 (2), 30 (2), 92 (2)	54, 30	9, 53	-	-
17	Buena Unión	08/10/2008 - 3/7/2012	3	66 (2), 28 (2)	58, 28	10	-	11
18	José Ignacio 1	17/10/2008 - 3/7/2012	3	54 (2), 24 (2)	54, 24	8	-	-
20	Rocha	1/7/2009 - 3/7/2012	3	74 (2), 31 (2)	70, 31	12	-	-
23	Mc. Meekan	12/11/2010 - 3/7/2012	1	60 (2), 40 (2)	60, 40	10	-	-
33	B. Brum	15/2/2012 - 3/7/2012	0	73 (2), 40 (2)	72, 40	73	-	6
34	J. Otamendi	15/3/2012 - 3/7/2012	0	101 (2), 80 (2), 60 (2)	100, 60	100	-	5
36	Colonia Terra	31/05/2012 - 3/7/2012	0	58 (2), 35 (2)	58, 35	58	-	-
40-ARN	Arroyo Negro	7/10/2010 - 3/7/2012	1	75 (S), 55 (2), 20(S)	75	75, 3	3	-
41-EGA	Egaña	1/10/2010 - 3/7/2012	1	72 (S), 55 (2), 21 (S)	73, 3	73	3	-
42-LC2	Lascano	27/9/2010 - 3/7/2012	1	72.3 (S), 55 (2), 21.3 (S)	73, 3	72.8	-	-
43-ITP	Itapebí	6/4/2011 - 3/7/2012	1	75 (2), 55 (S), 20 (S)	75, 3	75	3	-

Table 3.1 Characteristics of the automatic stations of UTE network

brackets. As this table indicates, the measurement periods of these stations ranged from few months to more than 4 years at July, 2012.

This table also shows that every station measures wind speed at two or three heights, wind direction at usually two heights, and temperature at one height. When humidity and/or solar radiation are recorded, they are measured at one height. The anemometers heights vary among the different stations, ranging from 10 to 100m.

Wind speed is measured with 3-cup anemometers model 40C from NRG Systems, with a distance constant of 2.6m and a measurement range between 1 and 96m/s. Wind direction is measured with wind vanes model 200P from NRG Systems. Wind data is registered at 1 sample/second (1Hz). For the definition of the distance constant of an anemometer, the reader can be referred for example to Brock and Richardson, 2001.

N°	Station	Tower height (m)	Tower section	Length of the side (m)	Latitude (S)	Longitude (W)
2	Bonete	48	triangular	0.45	32°48´0,4´´	56°24´56,4´´
3	Florida	60	-	-	34°05´54,4´´	56°08´28,8´´
4	Peralta	88	triangular	1.1	32°34´42,2´´	56°24´46,9´´
5	Valentines	91	triangular	1.1	33°15'52,9"	55°06'4,3"
7	Rosario		triangular	1.1	34°16'32,6"	57°20'6,3"
8	Artilleros	64	triangular	1.5	34°23'14,5"	57°33'27,3"
9	Piedras de Afilar	75	triangular	1.1	34°40´56,1´´	55°34´31,2´´
10	Arroyo Cañas	70	triangular	1.1	34°34'14,9"	54°50'11,9"
11	Pintado	94	triangular	1.1	33°55'17,0"	56°17'57,3"
12	Cerro Colorado	94	triangular	1.1	33°43´34,4´´	56°47´43,6´´
13	Palmar	60	circular	10" y 8"	33°04´04,1´´	57°27´33,2´´
14	Andresito	130	triangular	1.1	33°09´26,0´´	57°08´17,5´´
15	Tupambaé	100	triangular	1.1	32°50´06,5"	54°45´10,7"
16	Pampa	90	triangular	1.1	32°14´48,1"	56°12´53,0"
17	Buena Unión	80	triangular	1.1	31°03´30,4"	55°36´06,7"
18	José Ignacio 1	70	triangular	1.1	34°51´32,4"	54°43´54,7"
20	Rocha	81	triangular	1.1	34°05´38,2"	53°38´57,3"
23	Mc. Meekan	60	circular	10" y 8"	34°37´14,2"	56°43´04,3"
33	B. Brum	80	triangular	1.1	31°44,85´	57°52,12´
34	J. Otamendi	100	triangular	0.45	32°08,528´	54°25,267´
36	Colonia Terra	60	triangular	1.5	30°26´57,00"	56°35´13,00"
40-ARN	Arroyo Negro				32°30´34.86´´	58°0´41.46"
41-EGA	Egaña				33°36´25.44´´	57°41´3.72"
42-LC2	Lascano				31°20´1.56´´	57°25´23.70"
43-ITP	Itapebí				33°33´3.00´´	53°56´31.86"

Table 3.2 Additional characteristics of the automatic stations of UTE network

These sensors were installed in towers with triangular or circular section; the anemometers, at the extreme end of 1.52m long horizontal supports, while the wind vanes, facing north. Table 3.2 indicates, for each station, the maximum height of each tower, the shape of its section, the characteristic dimension of its section, and its latitude and longitude.

Most of these towers have triangular sections with different dimensions and porosities. The sides of each triangular tower have equal dimensions, with lengths between 0.45 and 1.5m, being 1.1m the most common. The porosities of the towers range mainly from 69 to 78%. The circular towers have diameters between 0.20 and 0.25m.

The potential effect of each tower on wind speed measurements was analysed, and found to be smaller than 3% for the wind directions that placed the anemometer outside the wake of the tower. It is assumed that wind direction measurements are not affected by the presence of the tower.

Figure 3.2 shows, as an example, the geometry of the tower and position and support of the anemometers at 40 and 86m height at Pintado station (station number 11 in Table 3.1), while Figure 3.3 shows pictures of the tower and of one of the anemometers of this station.

Information on other stations can be found, for example, in Cataldo et al., 2010a, Cataldo, 2011 or at UTE.

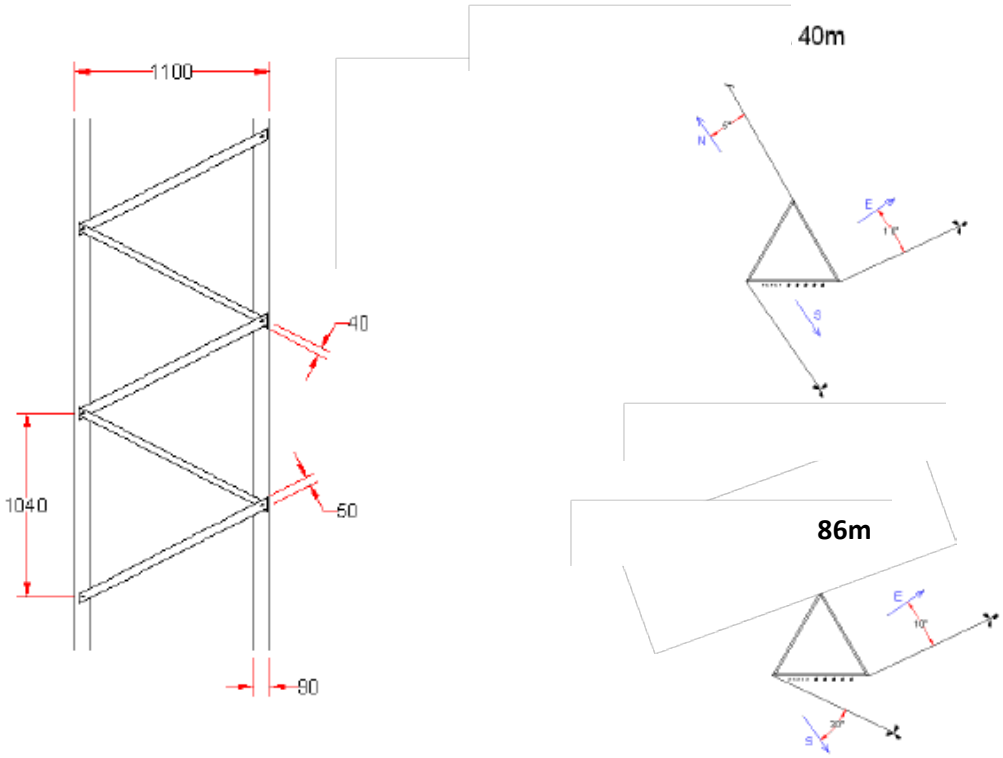


Figure 3.2 Tower and location of anemometers at 40 and 86m height at Pintado station (adapted from Cataldo et al., 2010a)



Figure 3.3 Tower and anemometer at Pintado station (images from UTE)

As indicated in Table 3.1, the stations installed by UTE have two anemometers at the highest altitude, and one or two anemometers at the other heights. When there are two anemometers at the same height, they are installed with an angle between them as close to 90° as possible. The wind speed series are generated by a software program from UTE, using for each 10min interval, the wind speed measurements from the anemometer least affected by the tower, fact that varies with time as it depends on the wind speed direction.

The four stations installed by the DNE have all similar characteristics: one anemometer and one wind vane at the highest altitude, of around 75m; two anemometers at 55m height; one anemometer at 20m height; two thermometers: one at 3m height and the other at 75m height, and a relative humidity sensor at 3m height. The sensors are from Metone, the model of the anemometers is 010C-1, and the model of the wind vanes is 020C-1.

3.4. Station at Carrasco airport, Montevideo

Carrasco station, located at the international airport of Carrasco, Montevideo, has been measuring wind speed and direction, among other meteorological variables, since 1960. Its main wind records consist in hourly 10min mean wind speed and direction measured during the last 10min of each hour. Wind gusts have been, and are, occasionally registered following criteria that have changed over time, which would not allow performing extreme value analysis on this data.

The registers of this station currently constitute the longest source of wind data measured in open terrain in Uruguay. Although the location of the anemometers of this station has changed several times inside the airport, as described in Sub-sections 3.4.3 to 3.4.6, their surroundings have remained mainly open and level.

A summary of the main metadata of this station is presented in Sub-section 3.4.1, while the procedure for the retrieval of the wind data and metadata from this station is described in Sub-section 3.4.2.

The retrieval and analysis of the quality of the wind data from this station for the period between 1960 and 2009, and the search and documentation of the corresponding metadata, i.e., the historical description of the anemometers used, their locations, heights of measurement, surroundings, etc. as recommended in Section 2.3, was carried out by the author of this thesis during 2011. The analysis of its wind data, presented in Chapter 6, was performed during 2012.

3.4.1. Location and available periods of measurements

Figure 3.4 shows the main locations of the anemometers that have measured at Carrasco station since 1960, in an image of Carrasco airport and its surroundings of 2010.

Between 1960 and 1976, the anemometer of Carrasco station was installed over the control tower (‘Torre de control’ in Spanish) of the airport, after which it was located above the roof of the station building (‘Anemómetro sobre techo de estación’ in Spanish) until 1994. Since 1995 it has been installed in independent towers: from 1995 to 2006 it was located between

the station building and the 24 runway head ('Anemómetro Sainco10m' in Spanish), while from 2007 to 2009 it was moved closer to the 24 runway head ('Anemómetro cabecera 24' in Spanish), as Figure 3.4 shows.

In the lower left of this figure, a scale 2km long helps estimating distances in this image. Taking that into account, it can be seen that the airport has the coast of the Río de la Plata to its southeast, at a distance of about 3km. The first kilometres to the west correspond mainly to rural terrain, while there are suburbs to the north, with low houses, trees and fields. The area to the east of the airport is at present more built-up than in the 1960's, especially in the strip closer to the coast, with many one- and two-storey houses and trees. Some lakes and a park with high trees (mainly eucalyptuses and pines) are located to the south and southeast of the airport.

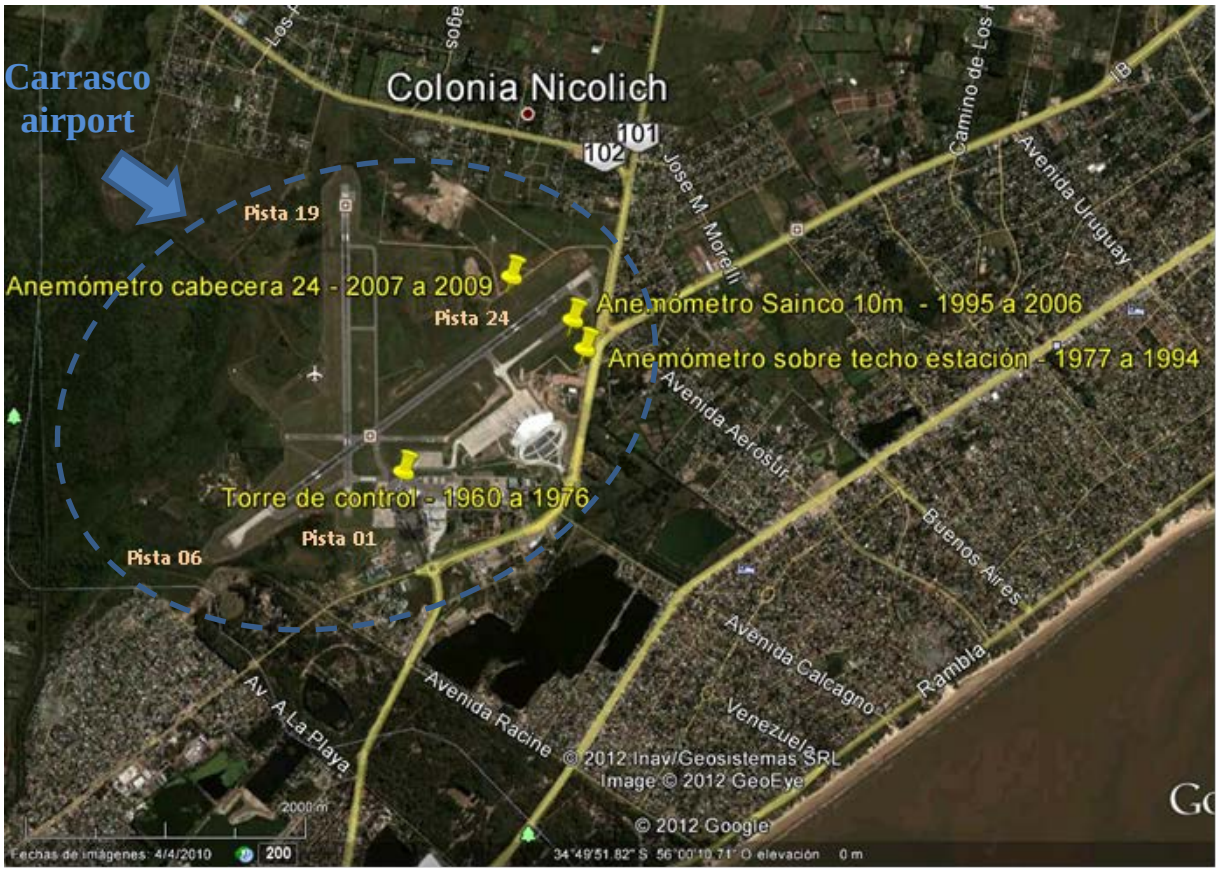


Figure 3.4 Locations of main anemometers at Carrasco airport from 1960 to 2009 (adapted from Google Earth, image of 2010)

Measurement period	Anemometer brand	Type of anemometer	Location	Height above ground (m)
1/1/1960 to 2/3/1977	Lambrecht	Cup anemometer and wind vane, with dial indicators	Over the control tower of 21.2m height, in a tower 2m high	24m
3/3/1977 to 1994	Casella	Cup anemometer and wind vane, with dial indicators	Over the roof of the station building, in a tower	10m
1995 to 2006	Sainco	Cup anemometer and wind vane, with dial indicators	Near the 24 runway head and near the station building, in a tower	10m
2007 to 2009	Allweather Inc.	Cup anemometer and wind vane, with automatic mean and register	Near the 24 runway head, in a tower	10m

Table 3.3 Main characteristics of the different measurement periods at Carrasco station

In Figure 3.4, four labels identify the different runway heads ('Pista' in Spanish: 01, 06, 19 and 24) of the airport, and four pins mark the sites where the anemometers measured along the different periods.

Table 3.3 summarises the main metadata of the different periods of measurement, indicating the starting and ending dates of each period, the brand and type of the anemometer used, a brief description of the site where it measured and the height of the anemometer above the ground.

3.4.2. Procedure for the retrieval of wind data and metadata of Carrasco station

Wind data quality needs to be verified before being used in any research, even more when a long term data series is required for extreme value analysis. The corresponding metadata is as important as the data itself, and it needs to be documented, and also analysed before the wind data is used for research.

Carrasco station has been measuring hourly 10min mean wind speeds since 1960 to date. The IMFIA had bought in the past 16 years of wind data from this station, corresponding to the

periods 1979 to 1995, 1999 and 2000. During 2011, wind data from 2001 to 2010 from several meteorological stations were being digitised by the School of Engineering, UdelaR, with other research purposes, and access to hourly 10min mean wind data of Carrasco station from those years was granted by the DNM (currently INUMET) to the author of this thesis. The rest of the data of this station had not been digitised and remained in the original station books until 2011, when the DNM also granted access to them to personnel of IMFIA for research purposes. It was then decided that wind data from the periods from 1960 to 1978 and from 1996 to 1998 would be digitised under the supervision of the author of this thesis.

Different book formats for registering wind speed and direction had been used, and the units and resolution of the wind speed and direction measurements had also experienced some changes. During some periods, the value of the registered wind speed did not correspond to the direct measurement because a unit conversion had been applied beforehand, in some cases losing accuracy and introducing some bias to the wind data.

Therefore, hourly 10min mean wind speed and direction were digitised, or its quality verified in the case of the 16 years the IMFIA already had, directly from the original handwritten books of records of Carrasco station, which were available at the central office of DNM in Montevideo. Figure 3.5 is an example of one of the formats used in these books.

For using wind data from Carrasco station, the following general criteria was set:

- Years of wind data with less than 90% of hourly 10min mean wind records would be disregarded
- Wind data without adequate metadata would be disregarded
- Wind data of inadequate quality would be disregarded

As already indicated, hourly 10min mean wind data from 1960 to 1978 were digitised from the original books of the station. Of this period, the book of 1968 only had records of wind measurements until the end of July, while during 1971, wind speed had been registered only 4 times a day. As it had been decided that only years with more than 90% of their data were going to be analysed, these two years were not taken into account for the analysis presented in Chapter 6.

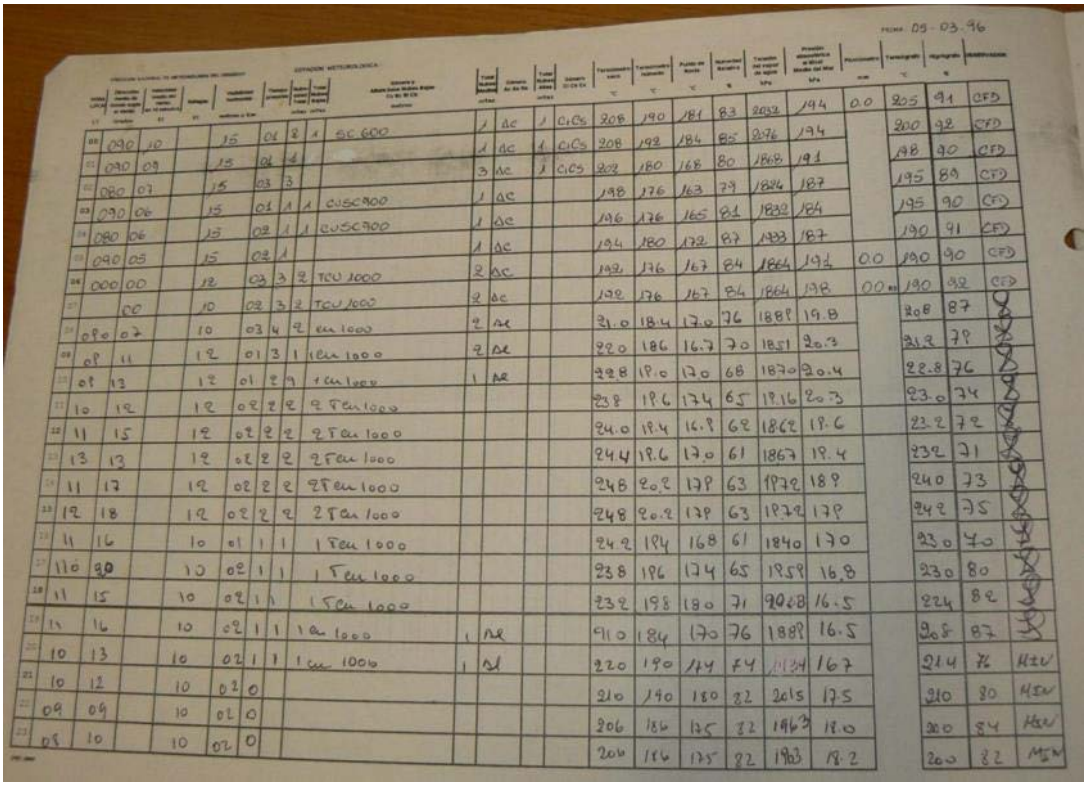


Figure 3.5 Format of Carrasco books between 1996 and 2009

In relation to the wind data the IMFIA already had, the period from 1979 to 1991 was not taken into account for the analysis presented in Chapter 6 either, for the following reasons:

- The original books of the station from 1979 to 1981 were not found, and the wind data values that the IMFIA had from these years could not be checked.
- While verifying the values of the hourly 10min mean wind data from 1982 to 1986, comparing the original registers of the station wind data with the data the IMFIA had, it was found that during high wind events, the wind speed that IMFIA had was an average between the mean wind speed and the wind gust measured during that hour, making it impossible to retrieve the corresponding 10min mean wind speeds without digitising this data again.
- When comparing the wind data the IMFIA had from 1987 to 1989 with the original records, it was found that the digitised data had been converted from knots to km/h in a way that introduced errors of up to 7% depending on the wind speed value. As there was not a biunivocal relationship between both values, the original records could not be recovered.
- The years from 1990 and 1991 had less than 90% of the expected wind data registers.

The wind data the IMFIA already had from 1992 to 1995, 1999 and 2000 could be compared with the registers of the station books and were found to be the same, and there were therefore included for the analysis presented in Chapter 6.

As a result of this verification of wind data quality, the data series considered for the extreme wind value analysis presented in Chapter 6 contained 35 years of hourly 10min mean wind data measured between 1960 and 2009, corresponding to the following years: 1960 to 1967, 1969, 1970, 1972 to 1978 and 1992 to 2009.

On the other hand, the metadata are as important as the wind data themselves, as already indicated in Section 2.3. Any trend or jump in the data not related to wind climate can have a significant effect in the computation of the extreme wind statistics and may introduce errors difficult to be estimated, which may lead to erroneous conclusions. However, if a jump or trend is a direct result of the relocation of an anemometer, change of its surroundings, etc. and this information is available, those changes can be taken into account to obtain an homogeneous wind data set, which would represent the history of the wind itself, not affected by the history of the station.

As there was no comprehensive information on the metadata of Carrasco station at the beginning of this PhD research, these issues motivated the author of the thesis to conduct a careful search for the metadata of this station for the period between 1960 and 2009. This work was carried out along 2011, during which the author of this thesis reconstructed the history of this station for that period searching for information in different sectors of DNM, organising a visit to the station and to the different locations inside the airport where the anemometers had measured, talking with previous and current observers of the station, and searching for pictures and aerial photographs that could allow the description of the change of its surroundings with time, as recommended in Section 2.3. The information of the different locations of the anemometers and their surroundings was complemented with technical information on the instruments and other type of metadata found in historical documents and books of the station in different sections of the central office of DNM in Montevideo. This work was documented in Durañona, 2011a and take into account during the analysis of wind speeds measured at Carrasco station (Chapter 6).

From this search for metadata, it could be concluded that the anemometer had experienced several changes in location, height, surroundings, brand and in the methods of measuring and registering wind speed and direction along the analysed 50 years period. A summary of the main metadata found was presented in Sub-section 3.4.1. All these changes were taken into account in order to generate a homogeneous wind data set of 10min mean wind speed, as summarised in Section 6.2, and presented with more detail in Durañona, 2011a and taken into account during the analysis of wind speeds measured at Carrasco Station (Chapter 6).

In the following sub-sections, information on the location of the anemometers and on their surroundings is presented for each measurement period shown in Table 3.3. The identification of the sites where the anemometers measured was possible due to a visit to Carrasco station organised in October, 2011. The visit to the station and the retrieval of important information was possible thanks to the coordination of Met. José Luis Castro, meteorological observer since 1979 and in charge of Carrasco station between 2002 and April, 2011, and to the guide of the chief of the station at the moment of the visit, the aeronautic meteorological observer Met. Rodolfo Lares, who are gratefully acknowledged.

The surroundings of the stations were divided into 8 different sectors for the analysis presented in Chapter 6. These are indicated in Table 3.4, corresponding to the following wind directions:

Sector number	**Wind directions**
1	NNW-N (north-northwest – north)
2	NNE-NE (north-northeast – northeast)
3	ENE-E (east-northeast – east)
4	ESE-SE (east-southeast – southeast)
5	SSE-S (south-southeast – south)
6	SSW-SW (south-southwest – southwest)
7	WSW-W (west-southwest – west)
8	WNW-NW (west-northwest – northwest)

Table 3.4 Wind sectors and corresponding wind directions

3.4.3. Metadata of Carrasco first measurement period

From January 1st, 1960 to March 2nd, 1977 wind speed and direction were measured with a Lambrecht cup anemometer and a wind vane installed over the control tower of the airport at 24m height. The height of the control tower was 21.2m. Wind speed and direction were visually averaged in dial indicators graduated in knots and degrees. The resolution of the measurements was 1kt and 10°, respectively.

Figure 3.6 shows an aerial picture of the surroundings of the airport in 1966 which belonged to DNM, now INUMET. The runways are labelled with numbers and the control tower is indicated with a cross.

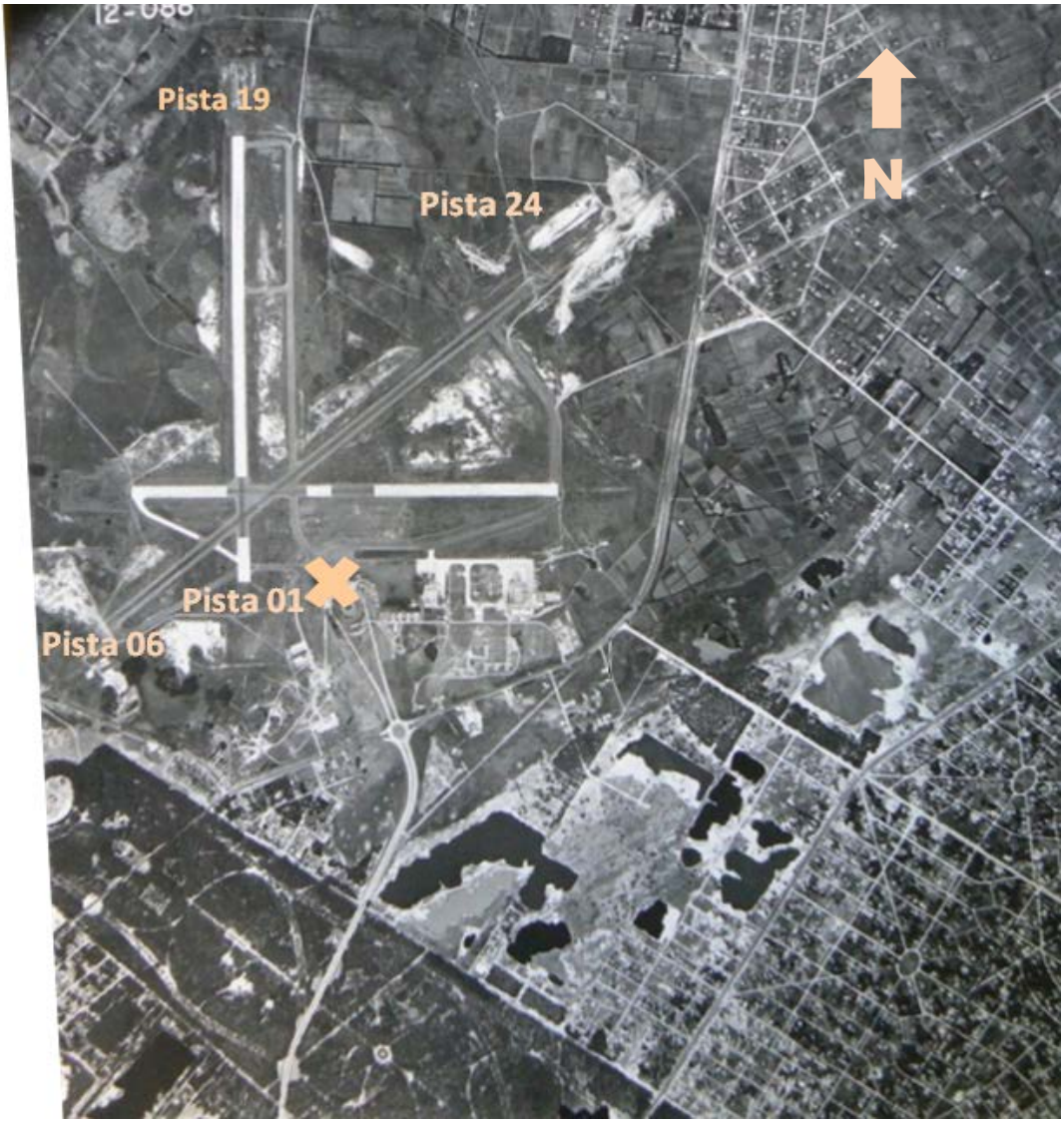


Figure 3.6 Surroundings of Carrasco station, aerial picture of 1966

The location of the control tower ('Torre de control') is also shown in Figure 3.7 and Figure 3.8.



Figure 3.7 Surroundings of the control tower of Carrasco airport (Google Earth image of 2000)

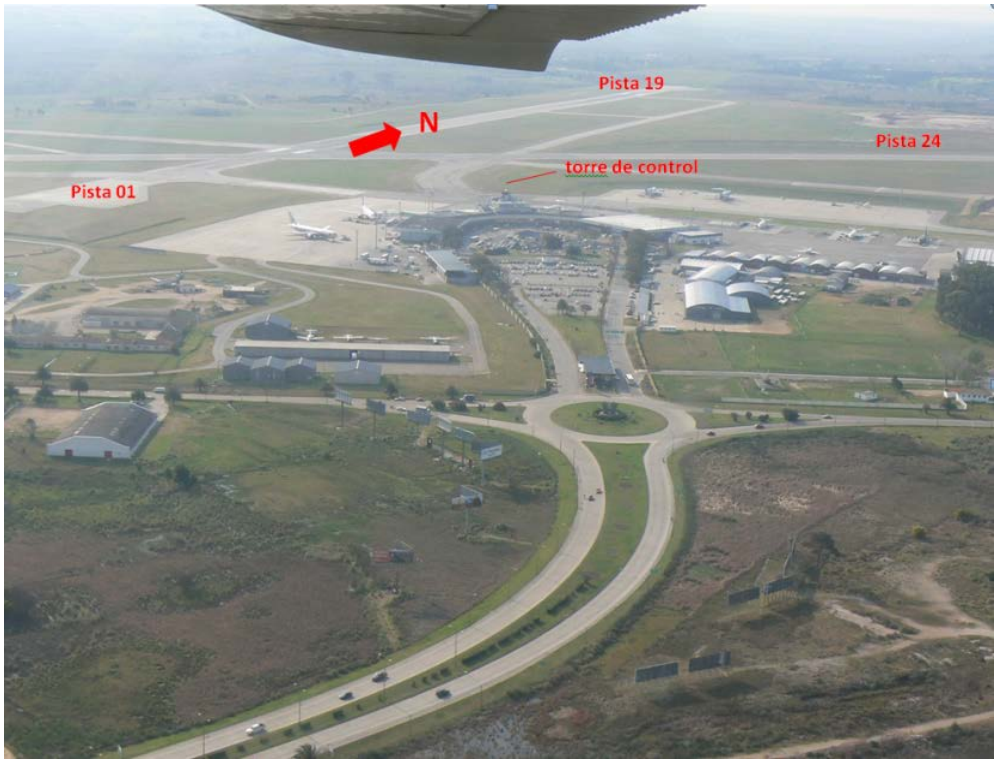


Figure 3.8 Surroundings of the control tower of Carrasco airport taken by V. Durañona in 2007

Figure 3.7 presents a circle centred in the control tower of Carrasco airport, which corresponds to a radius of 2km, and it is divided in 8 sectors numbered 1 to 8, each of them corresponding to the two wind directions shown in this figure and in Table 3.4. The letter 'O' that appears in some sectors in this figure and others, as well as in Table 3.4, stands for west 'W' Figure 3.8 shows the airport and its control tower from the southeast.

Since this first period ranged from 1960 to 1977, a search for older pictures was performed. Figure 3.9 and Figure 3.10 show the control tower and its surroundings before 1970.



Figure 3.9 View of the airport building and the control tower from the east before 1971 (FAU archive)

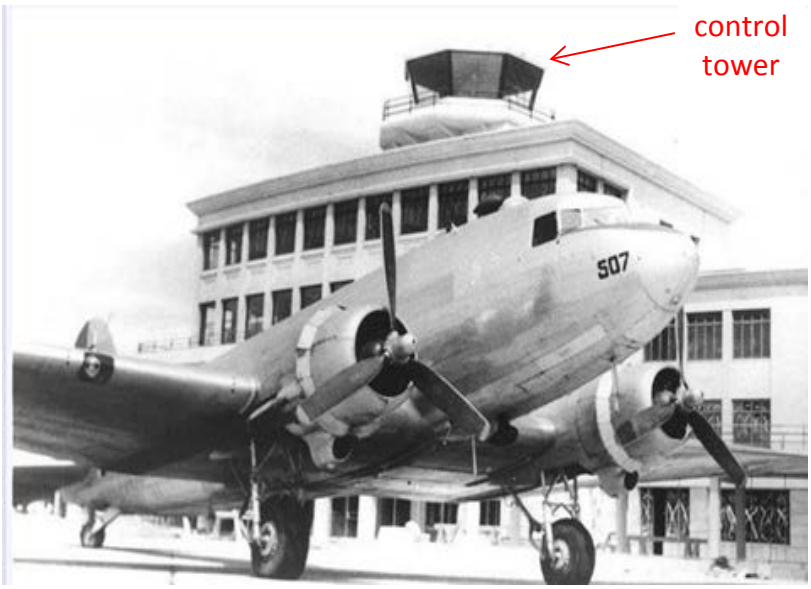


Figure 3.10 View of the airport building and the control tower from the west, 1948 (FAU archive)

3.4.4. Metadata of Carrasco second measurement period

At the beginning of this period, which spans from March 3rd, 1977 to 1994, the anemometer was installed 1,600m to the northeast from its previous location, near the 24 runway head and over the station building, at 10m height, as indicated in Table 3.3. The coordinates of this location were 34°50'00'S latitude and 56°00'7''W longitude, and its height over mean sea level, 32.88m.

Wind speed and direction were measured with a Casella cup anemometer and wind vane, and the measurements were visually averaged in dial indicators with resolutions of 1kt and 10°, respectively.

Figure 3.11 shows the surroundings of this anemometer, with a circle of 2km radius centred on its location and the 8 wind sectors indicated in Table 3.4. Additionally, Figure 3.12 and Figure 3.13 present a closer view of the surroundings and a view of the station building from the southwest, respectively. In this last figure, the location of the station building is indicated with a cross. On the other hand, Figure 3.14 shows the tower installed above the roof of the station building, where the anemometer measured during this period.



Figure 3.11 Surroundings of Carrasco anemometer from 1977 to 1994 (Google Earth image of 2004)



Figure 3.12 Closer view of the surroundings of Carrasco anemometer from 1977 to 1994 (Google Earth image of 2000)



Figure 3.13 View from the southwest of the location of Carrasco anemometer from 1977 to 1994, picture taken by V. Durañona in 2007



Figure 3.14 Tower of Carrasco anemometer from 1977 to 1994, picture taken by V. Durañona in 2011

3.4.5. Metadata of Carrasco third measurement period

From 1995 to 2006 wind speed and wind direction were measured with a Sainco cup anemometer and wind vane at 10m height, in a tower located between the 24 runway head and the station building. The measurements were visually averaged in dial indicators, with a resolution of 1kt and 10°, respectively.

Figure 3.15 shows the surroundings of this anemometer in a circle with a radius of 2km and the 8 wind sectors indicated in Table 3.4. On the other hand, Figure 3.16 presents a closer view of its surroundings, and Figure 3.17, a picture of the actual tower where wind was measured during this period.

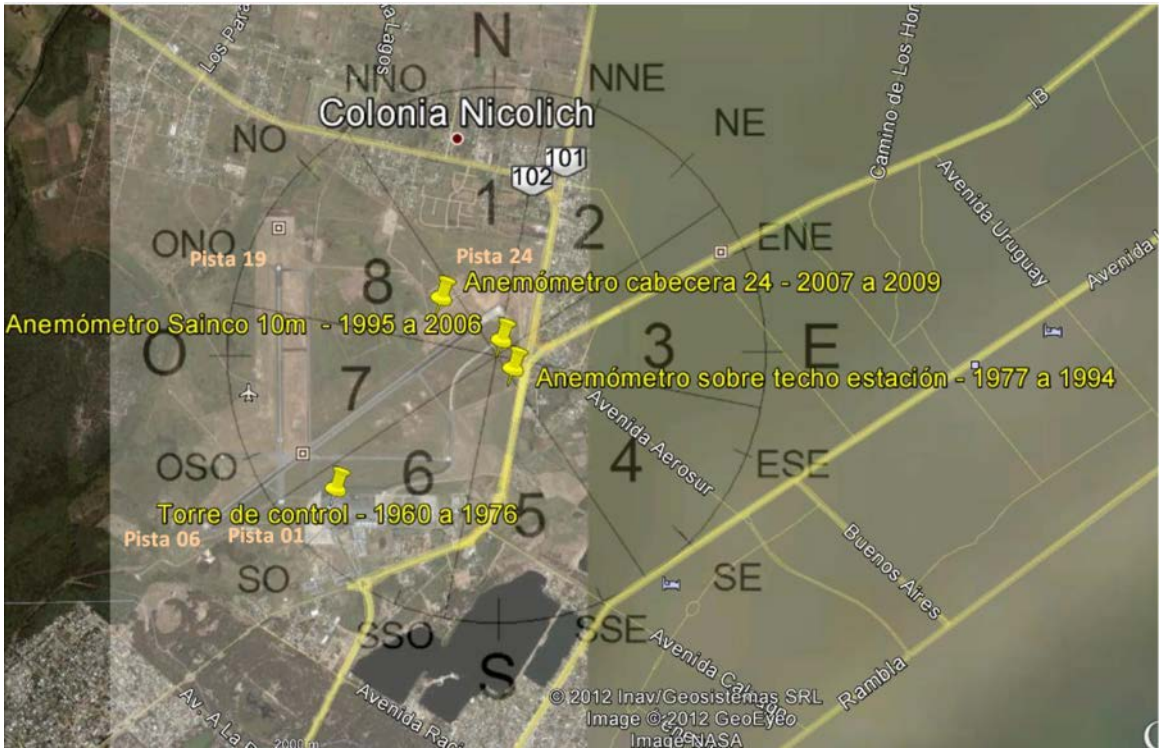


Figure 3.15 Surroundings of Carrasco anemometer from 1995 to 2006 (Google Earth image of 2000)



Figure 3.16 Closer view of the surroundings of Carrasco anemometer from 1995 to 2006 (Google Earth image of 2000)



Figure 3.17 Tower of Carrasco anemometer from 1995 to 2006, picture taken by V. Durañona in 2011

3.4.6. Metadata of Carrasco fourth measurement period

In 2007 the anemometer was relocated closer to the 24 runway head. Figure 3.18 indicates this new location, with a circle of 2km radius centred on it, and again the 8 sectors indicated in Table 3.4, while Figure 3.19 shows a closer view of its surroundings. Wind speed and direction were measured with an Allweather Inc. anemometer and wind vane, which automatically registered their mean values. The anemometer and wind vane were installed in a tower at 10m height, as illustrated in Figure 3.20.



Figure 3.18 Surroundings of Carrasco anemometer from 2007 to 2009 (Google Earth image of 2006)



Figure 3.19 Closer view of the surroundings of Carrasco anemometer from 2007 (Google Earth image of 2009)





Figure 3.20 Tower, anemometer and wind vane at Carrasco from 2007 to 2009, picture taken by V. Durañona in 2011

3.5. Observatory of Prado station, Montevideo

During the search for metadata of Carrasco station along 2011, historical measurements carried out at the Observatory of Prado station, located in Montevideo, and reports and handwritten materials from Prof. Luis Morandi were found at the central office of INUMET.

This observatory was the main meteorological station of Uruguay in the beginning of last century, directed from its foundation in 1900, until 1923, by Prof. Luis Morandi, an outstanding and methodical meteorologist and researcher, as mentioned in Sub-section 3.2. This station started as a municipal observatory, but 5 years later was nationalised under the name of the Physic-Climatological National Institute.

Monthly and annual bulletins containing 24 measurements per day of hourly wind speed, wind direction, temperature and other meteorological variables carried out from 1901 to 1917 at this station are available, together with metadata that allows evaluating the quality of these measurements. These bulletins also contain valuable information on high wind events, when the hourly mean wind speed was higher than 47km/h (13m/s), or sudden increases in wind speed occurred, as they detail the event as a whole, describing how the wind direction changed, if intense rain, hail and/or thunder occurred, indicating the values of the highest wind gusts, their duration, the time the whole event lasted, etc.

In this section, Sub-section 3.5.1 characterises the location of this station, its wind sensors, and describes how measurements were performed, while Sub-section 3.5.2 gives a brief account of the available meteorological information.

In Chapter 4, some meteorological information from this station is analysed, while in Chapter 8, some measurements carried out at the Observatory of Prado, and conclusions on the climate of Montevideo derived from them, are discussed and compared with other results obtained from this PhD research, offering a historical perspective and comparison.

3.5.1. Metadata of Observatory of Prado station

The Observatory of Prado station was located 5km to the north of the centre of Montevideo, occupying an area of 500m^2 inside a terrain of 7,000m^2 with coordinates 34°52’48”S latitude

and 58°32’19”5°W longitude. It was situated in the highest area between the small rivers Miguelete and Quitacalzones, with an altitude of 42m above mean sea level, near the intersection of Suárez Ave. and Millán Ave.

In this meteorological station, wind speed and direction were measured with one Richard anemometer with electric independent register of wind speed and direction, and one Denza anemometer with mechanic register.

The building of this station was 17m high and surrounded by open terrain (Morandi, 1944), as shown by Figure 3.21 to Figure 3.23.

It had a square base and consisted in two floors and a tower. The dimensions of the second floor were 6m x 6m, and there was a small tower above it, where two anemometers were installed in two diagonal corners, 1.20m above the parapet of the tower, and a wind vane was located 3m above the roof. These instruments are indicated by arrows in these figures.

Figure 3.21 corresponds to the first year of measurement of the station, while Figure 3.22 and Figure 3.23 show the station and its surroundings some years later.



Figure 3.21 Observatory of Prado station in 1901 (from Morandi, 1901)



PABELLÓN SEÍSMICO, CASILLA METEOROLÓGICA Y OFICINAS CENTRALES
DEL INSTITUTO NACIONAL F. CLIMATOLÓGICO
PRADO — MONTEVIDEO

Figure 3.22 Surroundings of Observatory of Prado station around 1915 (from Morandi, 1917b)

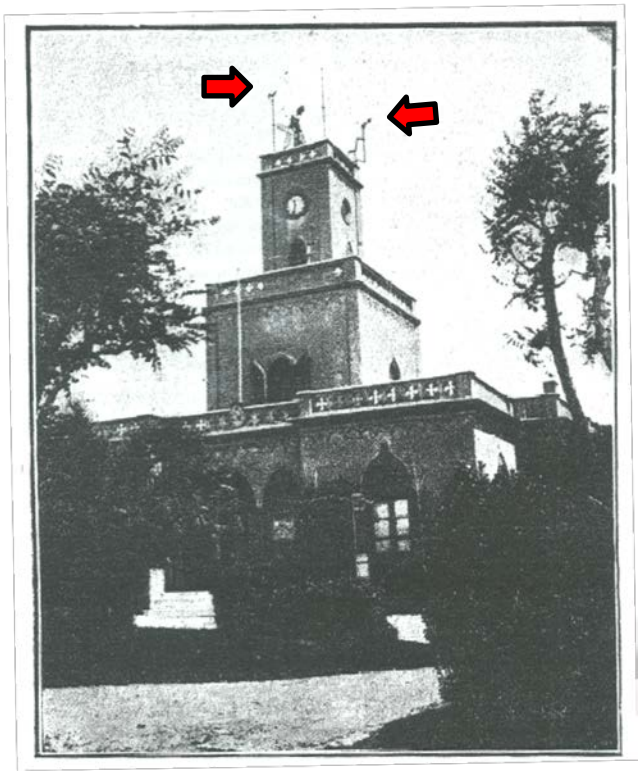


Figure 3.23 Observatory of Prado station around 1915 (from Morandi, 1917b)

3.5.2. Available information from Observatory of Prado station

There are monthly, annual, 5-year and 10-year bulletins from Observatory of Prado station from 1901 to 1917 at the INUMET office in Montevideo, but there would exist monthly and annual bulletins until 1921 according to Morandi, 1938.

In monthly bulletins, 24 measurements of hourly mean wind speed and direction, temperature and pressure are presented for each day of the month, and when the wind speed exceeded 50km/h (14m/s), a detail of the meteorological conditions and time evolution of wind gusts, wind direction, rain, hail, etc. were also included in these reports. When high wind gusts occurred, wind measurements were carried out directly on the anemograph during short periods of time (between 1 and 5min), and the evolution of the wind speed with time was described.

These bulletins also informed about sudden decreases in temperature, with simultaneous register of wind speed, indicating if wind direction shifts, intense rain and/or hail had occurred, and describing the duration of these conditions.

Every month, the predominant wind direction, mean wind speed, maximum wind speed of short duration, number of hours with wind speed higher than 40km/h (11m/s) and 60km/h (17m/s), number of days with thunder, hail, and rain were reported. Observations of the size of hail, sea and land breeze, as well as of wind speed, wind direction and pressure during synoptic high wind events can also be found in these bulletins. In each bulletin, different meteorological variables were reported for the corresponding observational period, such as mean wind speed, wind rose for all wind speeds and for those above certain threshold, and compared with measurements from previous reported periods.

As examples of the available information, until 1917 the highest registered wind speed of short duration had been 45m/s (160km/h) in 1914, while the highest 1h mean wind speed corresponded to 103km/h (29m/s), with wind gusts of up to 145km/h (40m/s). In 1907, analysing 5 years, hourly mean wind speeds higher than 60km/h corresponded to W and SW directions in 71% of the cases. Hourly mean wind speeds higher than 47km/h (13m/s) were found to occur 0.8% of the time. In 1916, a sudden temperature decrease of 16.3° with simultaneous occurrence of hail and rain was registered (Morandi, 1952). The rain of highest intensity reported was 20mm in 4min.

3.6. Satellite images and other meteorological data and information

Other sources of data were used during this PhD research, especially for the analysis of the main meteorological conditions and wind damage during specific dates. These consisted in infrared images from GOES 10 and GOES 12 satellites, synoptic charts, information on wind damage and characteristics of high wind events reported in newspapers and in web sites as the ones mentioned in Sub-section 2.2.5.2 and other regional blogs (e.g. Celemín, 2008). YouTube videos were sometimes used to analyse high wind events, as well as images and videos from national TV channels.

The images from GOES satellite were obtained from CPTEC/INPE (Centre for Weather Prediction and Climate Studies, Brazil) web page (CPTEC/INPE, 2012), and used in particular to confirm if there was significant convective activity over Uruguay, associated to the development of clouds with high vertical extent; and in that case, to analyse how the convective activity moved over the country, especially around the time and location where the maximum wind speeds were registered; if a relationship between the main characteristics of the convective activity and the main characteristics of the wind speeds generated across the country could be found, etc. The CPTEC infrared images database usually consisted in one image every 30min or 1h. In these images, different colours are assigned to clouds of different height, taking into account the temperature of the top of the clouds. The colder this temperature, the higher the top of the clouds, implying a higher potential to give place to severe convective activity. The assigned colours correspond with temperatures of their tops lower than -80°C, between -80°C and -70°C, -70°C and -60°C, -60°C and -50°C, -50°C and -40°C, and between -40°C and -30°C.

In relation to newspaper reports, as it is described in the next chapter, before the data from the network of stations of UTE were available, a systematic search on one of the main national newspapers was conducted in order to obtain a first description of the vulnerability of Uruguay to high winds, threshold wind speeds for damage to start, typical types of damage caused, main types and characteristics of meteorological events; to analyse if any inhomogeneity in the geographical distribution of high wind events or wind damage could be detected, etc.

Chapter Four

Vulnerability of Uruguay to high winds

4.1. Introduction

In this chapter, research conducted between 2005 and 2010 by the author of this thesis that contributed to obtaining a first picture of the characteristics of high wind events responsible for wind damage in Uruguay and of their effects is described. Part of this work was presented in Durañona and Cataldo, 2007; Durañona and Cataldo, 2008; Durañona and Cataldo, 2009; Durañona, 2010 and Durañona, 2011b.

Section 4.2 provides the background and motivation for conducting research on damaging wind events and their effects on the country, and presents an overview of the knowledge the national wind engineering community had on the extreme wind climate of Uruguay around 2005; Section 4.3 outlines the main aim and objectives of this research, while Section 4.4 presents a methodology employed to characterise the most frequent damaging wind events and their associated damage in the country, whose results are indicated in Section 4.5. Sections 4.6 and 4.7 respectively describe the main characteristics and effects of one of the most severe extra-tropical cyclones and of one of the most severe convective events that caused significant wind damage in Uruguay in the last decades, while Section 4.8 show how high winds from severe convective activity can disconnect high-voltage transmission lines and cause important outages in the country. Finally, the main results of this research are discussed in Section 4.9.

4.2. Background and motivation

As mentioned in Sub-section 2.2.5, the absence of significant topography in Uruguay makes most locations potentially vulnerable to high winds and to rapid changes in weather. Its coastline, home of a great percentage of the country's population, is especially vulnerable to intense extra-tropical cyclones, which intensify while moving toward the South Atlantic Ocean.

High winds threaten people lives and their properties, and represent a potential risk for structures, critical infrastructure, telecommunications, transmission and distribution energy

systems, as well as for ports and boats of different sizes. Wind energy is an important renewable energy resource for Uruguay (Cataldo et al., 2010b), and wind turbines and wind farms are also subject to potentially damaging high wind events (Durañona, 2012a).

On the other hand, the agro-alimentary sector represents around 25% of Uruguay's gross domestic product and 70% of the total exportations, being most of it exposed to environmental risks. In particular, the occurrence of high winds is one of the most important and least studied risks in several areas of the agronomic sector, mainly due to the lack of the required information on the extreme wind climate of Uruguay (Durañona, 2010).

In spite of the impact high winds have in different sectors and at different levels in the country, there was little knowledge on the extreme wind climate of Uruguay by the time this PhD research started, at least from a wind engineering perspective. This PhD research thus principally aimed at starting covering this lack of information.

The research described in this chapter was mostly conducted between 2005 and 2010, before the author of this thesis had access to the meteorological data listed in Sections 3.3 to 3.5.

Before that time, factors as the relative small length and time scales of high winds produced by severe convective activity usually mentioned in the wind engineering literature, the internationally widespread use of ABL wind tunnels, as well as the few full-scale measurements and data available on the wind structure of severe convective winds (Holmes et al., 2005a) may have contributed to the general assumptions, with few exceptions (Riera and Rocha, 1998; Choi, 1999; Holmes, 1999), that intense extra-tropical cyclones were responsible for most of the highest wind speeds registered in mid-latitudes, and that their flow could be adequately modelled as an ABL flow.

In accordance with the previous paragraph, and as the length and time scales of extra-tropical cyclones and those of other synoptic weather patterns that can cause high winds are large enough to allow them to be registered by conventional meteorological stations, i.e., stations that measure the last 10min of each hour, it was also assumed in the beginning of this research that most of the damaging wind events occurring in Uruguay would be registered by any DNM (currently INUMET) station relatively close to the site(s) where wind damage was reported.

In 2002, a MCC, described in Section 4.7, produced severe wind damage in an area around 12km wide and 100km long, 30km north of Montevideo, causing losses estimated in US$ 27 million (US dollars). Wind damage also occurred along some other hundreds of kilometres more within a relative narrow path, until it reached the eastern coast of Uruguay. This was considered an exceptional episode in the country because of its violence, and the relative large size of the areas severely affected by wind damage in comparison with other events of smaller scales. The highest hourly 10min mean wind speed recorded at Carrasco station (station described in Section 3.4) for that year was around 60km/h (17m/s) and it was registered during this event, with a wind gust speed of 87km/h (24m/s). It is worth mentioning that this station was located around 30km from the severely affected areas, and that wind measurements were carried out visually at that time.

On the other hand, in 2005 an extra-tropical cyclone that suddenly deepened over Uruguay affected the south and east of the country and generated economic losses of around US$ 40 million. It corresponded to one of the most intense of these events of the last decades, and the wind damage it produced and the size of the affected areas reinforced the idea that extra-tropical cyclones were the most significant high wind events regarding wind vulnerability of Uruguay. The highest hourly 10min mean wind speed recorded at Carrasco station for that year was 98km/h (27m/s), and it was registered during the passage of this extra-tropical cyclone, with a wind gust speed of 174km/h (48.3m/s).

Some years later, during 2007 and 2008, the author of this thesis participated in a study for the development of a new insurance for fruit fall events due to high winds for the State Insurance Bank (BSE) (Durañona and Cataldo, 2007), and in an assessment for the National Administration of Power Stations and Electrical Transmissions (UTE) (Cataldo and Durañona, 2008), to evaluate the reasons why the two 500kV transmission lines Palmar-Montevideo were failing more often than expected.

The BSE and UTE provided the author of this thesis with several dates when fruit fall and failures in the high-voltage transmission lines had occurred. As part of these studies, she analysed 25 dates in order to characterise the high wind events that had occurred, and the wind speed values that produced the type of damage or failure under study. Part of this research is presented in Sections 4.7 and 4.8.

In a first stage of these researches, 10min mean wind speeds measured at the closest DNM stations (the available meteorological registers at that time, as described in Chapter 3) from the reported damage or failure were analysed. It was soon found that high winds were not usually registered in these stations during the occurrence of these damaging wind events, which had been quite significant for the agronomic and energy sectors.

These findings made the author of this thesis question herself if the main wind data sources generally used for wind engineering research in Uruguay, i.e., wind data from conventional meteorological stations, measuring 10min mean wind speeds during the last 10min of each hour, might be missing important information regarding wind vulnerability of the country, and if the analysis of other sources of data might be required for a better wind damage evaluation.

As funding was not forthcoming to investigate these potential problems with the depth they deserved, the understanding of their relevance provided the author with the motivation to include these topics in this PhD research. As at the beginning of this PhD research the network of UTE stations described in Section 3.3 had not been installed, she started searching for other sources of information on damaging winds occurring in Uruguay, and devising a qualitative study to evaluate the effects of high winds on the country.

More recently, similar questions arose in the North Regional Division of UTE (Larguero, 2014), when personnel in charge of informing outages causes realised that many electric poles could fall near a meteorological station that had not measured significant high winds.

It was expected that results from this research could help policy and decision-makers becoming more aware of the wind vulnerability of Uruguay to high wind events and the necessity of its study, as a first step towards prevention and mitigation of its effects.

The following sections, Sections 4.3 to 4.5, present the principal objectives of this study, its methodology and the preliminary results obtained, research summarised in Durañona, 2011b.

4.3. Main aim and objectives of this research

The research presented in this chapter aimed at obtaining the main characteristics of the vulnerability of Uruguay to high winds. The objectives set were to identify threshold wind speed values for the occurrence of wind damage, and the main characteristics of this damage, to obtain a relation between wind speeds and types and intensities of damage, to investigate the existence of particular patterns in the geographic distribution of the affected areas, and describe the main meteorological events that generate high winds in the country.

4.4. Methodology

During the search for wind damage information and wind data sources, the author consulted several national organisations and companies about the existence of registers of damaging wind events, but found that this information was not systematically recorded, or was not available for research. Public companies as UTE or ANTEL did not have a systematic register of the events that produced wind damage in their infrastructure at that time, except for failures of high-voltage transmission lines in the case of UTE.

Rural associations, forest companies and the Ministry of Agriculture, Livestock and Fishing (MGAP) were also consulted for wind damage information, but it was found that their registers were rather scarce.

The most important insurance companies of Uruguay were also contacted during this search, but the author of this thesis was told that they did not keep a systematic register of damaging wind events, and that this type of information was usually private and generally not available for research.

As a result of these enquiries, some damaging wind events and their dates could be identified, but the gathered information regarding vulnerability of Uruguay to high winds from these sources did not give a comprehensive picture of the problem.

While carrying out the research for the BSE described in Sub-section 4.2 and in Durañona and Cataldo, 2007, the author of this thesis found that the wind events that had produced significant fruit fall had received considerable media coverage, and detailed descriptions of

the related meteorological events and of the corresponding wind damage were relatively easy to find. On the contrary, information on the meteorological conditions during the dates when the high-voltage transmission lines Palmar-Montevideo had failed was more limited, maybe due to the fact that they crossed areas of Uruguay that were scarcely populated. During the research for UTE, newspapers were identified as the most complete source of information regarding damaging wind events, as they tend to report high winds causing damage in the country giving details of the types of damage that occurred, locations and areas affected, if intense rain (and/or hail) happened during the events, and quite often they also describe how the increase of wind speed with time was, the duration of the high winds, and/or cited wind speed values measured at or near the affected areas. When this information existed, it was straightforward to identify if the high wind event had passed over the high-voltage transmission lines in the date and time of an incidence, to classify it as a synoptic or non-synoptic high wind event as defined in Sub-section 2.2.1.1, and to know if it presented the distinctive features of convective activity described in Sub-section 2.2.3.2, characteristics usually informed in newspapers. This allowed for a primary classification of the damaging wind events into synoptic and non-synoptic.

As other available sources of wind vulnerability information presented different characteristics and their registers were not systematic, it was decided to use newspaper information as the main source for creating a primary database of damaging wind events. This method for retrieving information on wind damage has been used by different authors, Schwarzkopf and Rosso, 1993; Blackmore, 2003, and it is also mentioned in Nascimento and Doswell, 2006, among others.

A digital systematic search was then carried out on one of the main national newspapers (El País), looking for news that included the words in Spanish meaning ‘storm’, ‘wind’ and ‘tornado’ in this newspaper between 2006 and 2010. After identifying articles containing the selected keywords in this newspaper, relevant information such as date of occurrence of the reported high wind event, affected locations, measured wind speeds, description of wind damage and of other meteorological events that had taken place during its occurrence (as intense rain, hail, etc.) was extracted. The measurement height was not usually indicated, while the duration of the event was sometimes mentioned. In this way, many high wind events were found and characterised.

This information could sometimes be complemented with reports from different institutions and/or meteorologists, information from local or regional web pages, as described in Sub-section 2.2.5.2; YouTube videos of severe weather episodes, etc. These other sources of information contained in many cases pictures taken, witnesses description of the characteristics of the events and of the damage produced, which could also help classifying the events and estimating the highest wind speeds that had occurred.

Sometimes the newspapers cited wind measurements carried out in known stations whose wind data could be checked, while in other cases the mentioned wind speed values could be verified with other reliable wind measurements carried out close to the affected sites at the time of the events, or estimated from the description of the damage caused to trees, electric lines, poles, houses, buildings, etc. As newspapers usually cite the maximum wind speed measured, it was decided to use the wind gust speed as the reference wind speed for this study.

After the validation of several cited wind speed values, the relation between wind gust speed values and type and level of damage was analysed using the generated database.

Information from two other sources of wind damage was added to this database. One of them corresponded to historical damaging wind events that took place during the last century in the country, reported and described either in papers, such as Morandi, 1944 and Vieira, 1949, in journals, as 'Revista Meteorológica', journal already described in Sub-section 2.2.5.2.2 (Morandi, 1901 - 1917) or in books, as Vieira, 1969.

The second one consisted in a list of convective storms that had occurred in Uruguay (Schwarzkopf and Ramis, 2010) that María Luisa Altinger de Schwarzkopf, whose work was described in Sub-section 2.2.4.2.2.1, kindly sent to the author of this thesis. She had gathered part of this information while carrying out her work and completed it with information on a series of other events that Guillermo Ramis, an Uruguayan meteorologist, had given to her.

With all this information, the generated database of high wind events that had taken place in Uruguay gathered descriptions of about 200 intense convective events that produced high winds, wind damage, tornadoes and/or large hail in Uruguay between 1891 and 2011.

4.5. Results

4.5.1. General results

It was found that when wind damage was informed, wind gust speed values were usually reported. Additionally, when wind damage was informed, almost all reported wind speeds were 80km/h (22.2m/s) or higher. This result is discussed in Section 4.9.

Wind gust speed was therefore selected as the magnitude to characterise a high wind event in this PhD research, taking into account what was expressed in Section 2.2.3 (Doswell, 2003b). A wind gust speed value of 80km/h was selected as the threshold for wind damage, and for classifying a wind event as a 'high wind event' in the rest of this thesis.

On the other hand, the digital search for high wind events that occurred between 2006 and 2010 (5 complete years) in Uruguay, described in Section 4.4, yielded 84 different dates when this type of event had been reported.

The obtained results suggested that high wind events related to intense convective activity produce significant wind damage with higher frequency than synoptic high events, as e.g. those generated by extra-tropical cyclones. In average, 16 days with wind damage occurring under typical conditions of intense convective activity, as those described in Sub-section 2.2.3.2, were found to be reported per year in one of the main national newspapers, while the frequency of reported extra-tropical cyclones causing wind damage was estimated to be about one per year in average. Given the relative smaller length scales of the areas affected by intense convective activity, as indicated in Sub-section 2.2.1.1, it would be reasonable to expect that many intense convective events go unreported.

These results highlighted the significance of convective activity in the extreme wind climate of Uruguay, as expected from Sub-section 2.2.5.2.2, and reinforced the decision of selecting wind gust speeds (and not mean wind speeds) as the magnitude to characterise high wind events in the country, as recommended by different authors (e.g. Wieringa,1973; Riera et al., 1977; Holmes et al., 2005b, among others) and mentioned in Sub-sections 2.2.1.4 and Section 2.5.

The maximum wind gust speed reported in the 5-year long analysed period was 145km/h (40m/s). It was estimated that 90% of the reported events exceeded wind gusts of 90km/h (25m/s), 65% exceeded 100km/h (28m/s), 30% exceeded 110km/h (31m/s) and 10% exceeded 120km/h (33m/s).

It was found that wind direction during these damaging wind events, when reported, was usually from the southwest quadrant.

It was also found that in 80% of the cases, intense rain had been reported together with the occurrence of high winds, while in 60% of the cases, hail had been reported.

From this analysis, it could be verified that high wind speed events in Uruguay are responsible for great losses in the agroindustry, interruptions and damage to the electric transmission and distribution systems, and affect a variety of buildings and structures. In particular, they can produce important damage and losses of crops, fruits, forest woods, urban trees; damage and failures of high voltage transmission lines and towers and medium voltage distribution lines and poles, affect low and high-rise buildings, sheds, silos, greenhouses, telecommunication antennas and signs among other structures; produce pedestrian risk situations and affect ports and ships.

4.5.2. Correlation between wind gust speed and type of damage

It is worth mentioning that although the reported wind speeds might have not been the highest wind speeds occurring during the damaging wind events, as the anemometers may have not been located in the area affected by the highest wind speeds, a clear trend was found between wind speed values and levels of damage, with more significant damage reported and more robust structures affected at higher reported wind speeds.

After analysing all the gathered information, it was found that at reported wind gust speeds of:

• 80km/h (22.2m/s) and higher, blown down trees and damaged roofs were the most common damage reported. The tree genus more often mentioned as being uprooted was the eucalyptus.

• 90km/h (25m/s), poles, antennas and electricity cables were also reported to be blown down, the number of affected houses and trees rose, and when the events struck in rural areas, sheds and greenhouses were also damaged.
• 100km/h (28m/s), silos, signs and other structures, as well as ships, were reported to be affected.
• 120km/h (33m/s), incidences in medium voltage distribution lines were usually reported and information of fruit fall was found.
• At 130km/h (36m/s), some houses and service stations could be blown down.

4.5.3. Size of affected areas

It was found, as expected, that in most of the analysed damaging wind events not all the country was affected, and that the intensity of the damage varied with location. Several cases with very localised high wind speeds reported were found, one of them affecting an area as small as 300 to 400m wide and 2.5km long. In the analysed period of 5 years (2006-2010), at least 8 tornadoes were reported.

After analysing the dimensions of the affected areas, it was estimated that in around 55% of the identified damaging wind events, damage was reported in less than 5% of the country, that around 22% of the events affected between 5 and 10% of the country and that about 15% of them generated damage in 10 to 15% of the country. Damage was less reported to the east of the country, along the South Atlantic coast. During the analysed period, at least two intense extra-tropical cyclones occurred, affecting around one third of the country, specially the south eastern coast.

A more detailed analysis of the geographic behaviour and of the typical dimensions of the areas affected by high wind events is presented in Chapter 5.

4.5.4. Verification

In order to verify some of the results presented in Sub-section 4.5.1, it was decided to analyse some wind databases that were available by the time that research was conducted. With that aim, wind gust speed values obtained from the search for damaging wind events in the

newspaper El País, described in Section 4.4, were compared with wind gust speeds higher than 80km/h measured at two different sites in Montevideo, along different periods of time.

One corresponded to the registers of an automatic meteorological station located in the port of Montevideo, which belongs to the National Administration of Ports (ANP), and started measuring in 2005. This station registers the mean and maximum values of wind speed and wind direction every minute, as well as other meteorological variables, as temperature and rain. This station is located quite close to the 'Antepuerto' station described in Section 7.4.

Metadata of this station is described in e.g. Cataldo and Durañona, 2005. A search for wind gust speeds higher than 80km/h was performed on 3 complete years of measurements of this station from the period between 2006 and 2010. In the 3 analysed years, 5 events with wind gust speeds higher than 80km/h were found: wind gust speeds exceeded 110km/h (31m/s) during the passage of an extra-tropical cyclone; they reached 90km/h (25m/s) during short periods of time in 2 different days, and exceeded 80km/h during short periods of time in another 2 days.

The second wind database used for verification of the results presented in Sub-section 4.5.1 corresponded to that of the Observatory of Prado station, station described in Section 3.5. A search for wind gust speeds higher than 80km/h measured at this station was performed employing some of the reports from Morandi, 1901 - 1917. 5 complete years belonging to the period 1901 to 1917 were selected for this analysis, and a total of 7 of these events were found: 1 event with wind gusts that reached 144km/h (40m/s); 1 with sustained winds of 114km/h (32m/s) during 6min and an average of 84km/h (23m/s) in 20min; one that developed wind gusts between 90 and 115km/h (25 and 32m/s) along 3h; one with 1min mean between 96 and 108km/h (27 and 30m/s); and three that developed wind gusts between 80 and 90km/h for short periods of time.

From both analyses, it was estimated that at least one damaging wind event would occur every year at any open site in Montevideo, and that it would not be unusual to find registers of wind gust speeds of 145km/h (40m/s) when analysing a period of few years of wind observations.

The wind direction reported in both stations during most of the identified high wind events was in agreement with the typical wind direction found during the search for damaging wind events in the database described in Section 4.4, i.e., from the SW quadrant.

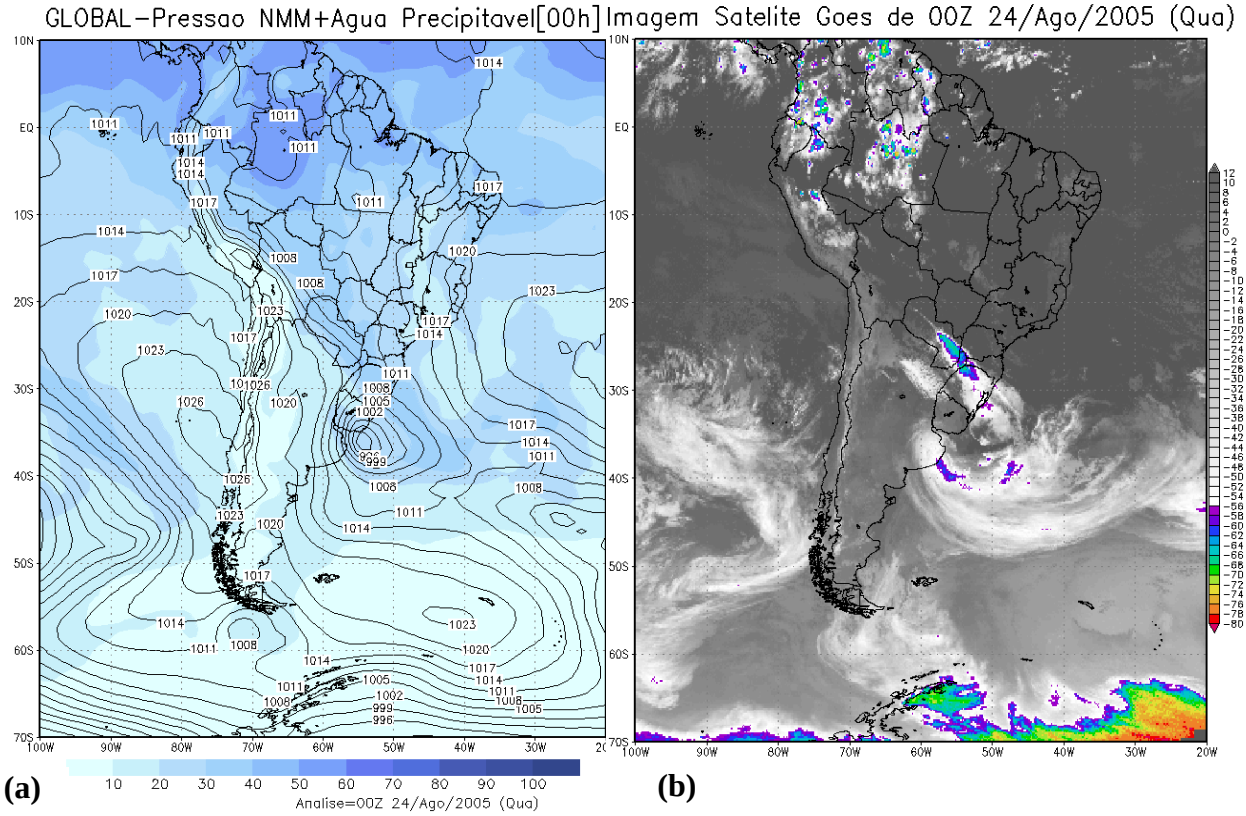
Although few years of data were analysed, the comparison between high wind events found in wind records from Montevideo from the beginning of last century and from the beginning of the current century would not suggest an increasing trend in the frequency or in the values of the highest wind gust speeds.

The description of most of the high wind events reported in Morandi, 1901 - 1917, i.e., measured at a fixed and open site in Montevideo, also showed the significance of intense convective activity in the extreme wind climate of Montevideo. Most of these high wind events presented the typical characteristics of intense convective activity indicated in Sub-section 2.2.3.2, such as sudden wind gust speed increases, abrupt temperature decreases, shifts in wind direction, highest wind gusts from the SW quadrant, simultaneous occurrence of intense rain and/or hail, among others. These characteristics were also commonly found in the high wind events identified during the search described in Section 4.4.

4.6. Example: severe extra-tropical cyclone of August 23rd, 2005

On August 23rd, 2005 an atmospheric depression strongly deepened over Uruguay while moving to the southeast, causing a fast pressure decrease and a strong pressure gradient that produced intense winds from the southwest. This rapid and intense cyclogenesis was described as ‘explosive’ by several authors (e.g. Possia et al., 2011). Wind damage was principally reported in the departments of the country located in the southern and eastern areas, especially along the coastline.

Figure 4.1(a)-(c) shows the isobars and images of SA and Uruguay from GOES satellite at 21h local time. The wind speed registers available during the passage of this extra-tropical cyclone indicated that the highest 10min mean wind speeds and highest wind gusts were measured in Montevideo between 22 and 22.35h local time, when 10min mean wind speeds of almost 100km/h (28m/s) and wind gusts between 130 and 174km/h (36 and 48.3m/s) were registered at 10m height.



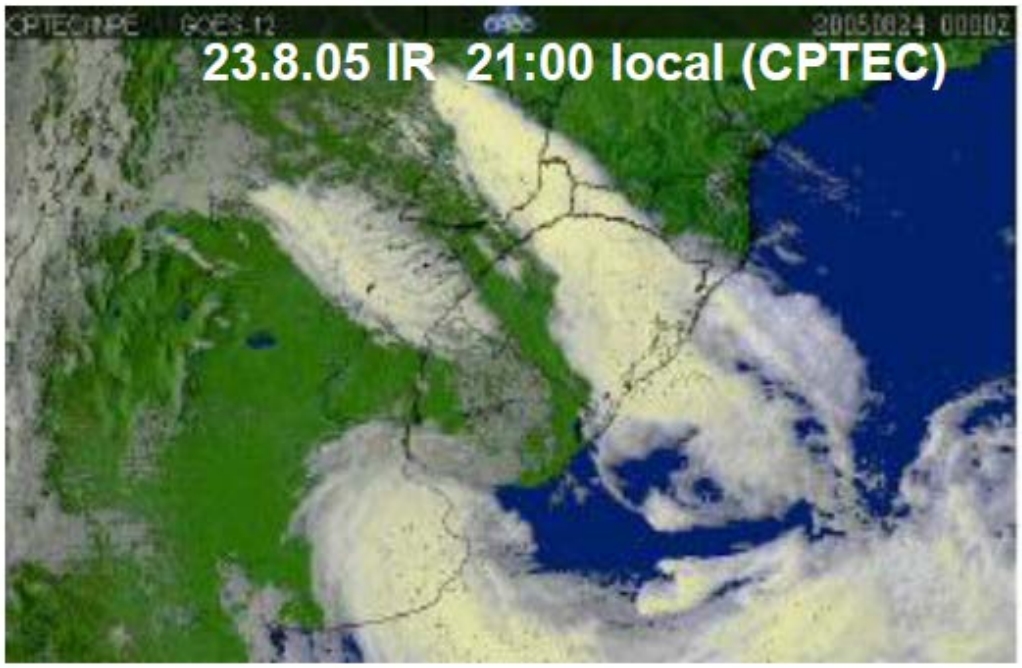


Figure 4.1 (a): Isobars; (b) and (c): GOES satellite images at 21h local time during the passage of the extra-tropical cyclone of August 23rd, 2005 (from CPTEC/INPE, 2012)

The closer isobars seen to the west of the low pressure centre in Figure 4.1(a) would be expected to be responsible for the generation of the highest wind speeds, and as the trajectory of this extra-tropical cyclone was approximately toward the southeast, the highest wind speeds in Uruguay would be expected to occur along the southern and eastern coastlines of the country, with wind directions from the southwest quadrant, as commented in Sub-section 2.2.5.2, and illustrated in Figure 4.2 and Figure 4.3.

This severe extra-tropical cyclone blew down thousands of trees and destroyed hundreds of houses. 2,000 people had to be evacuated, 28 were injured and two died. The emergency line received 20,000 calls for help principally due to blown roofs and cables, and trees uprooted or fallen onto buildings and vehicles. Most of the national routes west of Montevideo were blocked by trees and cables, and more than 100,000 clients experienced blackouts and interruptions of telephone and internet services. A FM antenna fell down in one of the most urbanised areas of Montevideo and some kiosks were blown more than two blocks away. Ports were also affected: a floating crane broke moorings and crashed into one of the harbour docks, several containers were blown, and many ships were damaged and others sank. Losses were estimated to be around U$S 40 million (US dollars).

Figure 4.2 indicates the evolution of different meteorological parameters along the 23rd and 24th of August, 2005 at two stations located in Montevideo: the station located at the Port of Montevideo (ANP station) described in Sub-section 4.5.4, and Carrasco station, located approximately 20km to the east-northeast from ANP station and described in Sub-section 3.4.5.

The analysed stations have different types of surroundings and measurements heights. The roughness length values of the surroundings of each station (z_0) were estimated for the different wind directions, and the measured wind speeds at ANP station were translated into Carrasco's conditions assuming a flow of ABL type, applying Equation (2.4) presented in Sub-section 2.2.1.3. More details of the metadata and surroundings of ANP station, roughness length estimations, and of the indicated procedure are presented in Cataldo and Durañona, 2005.

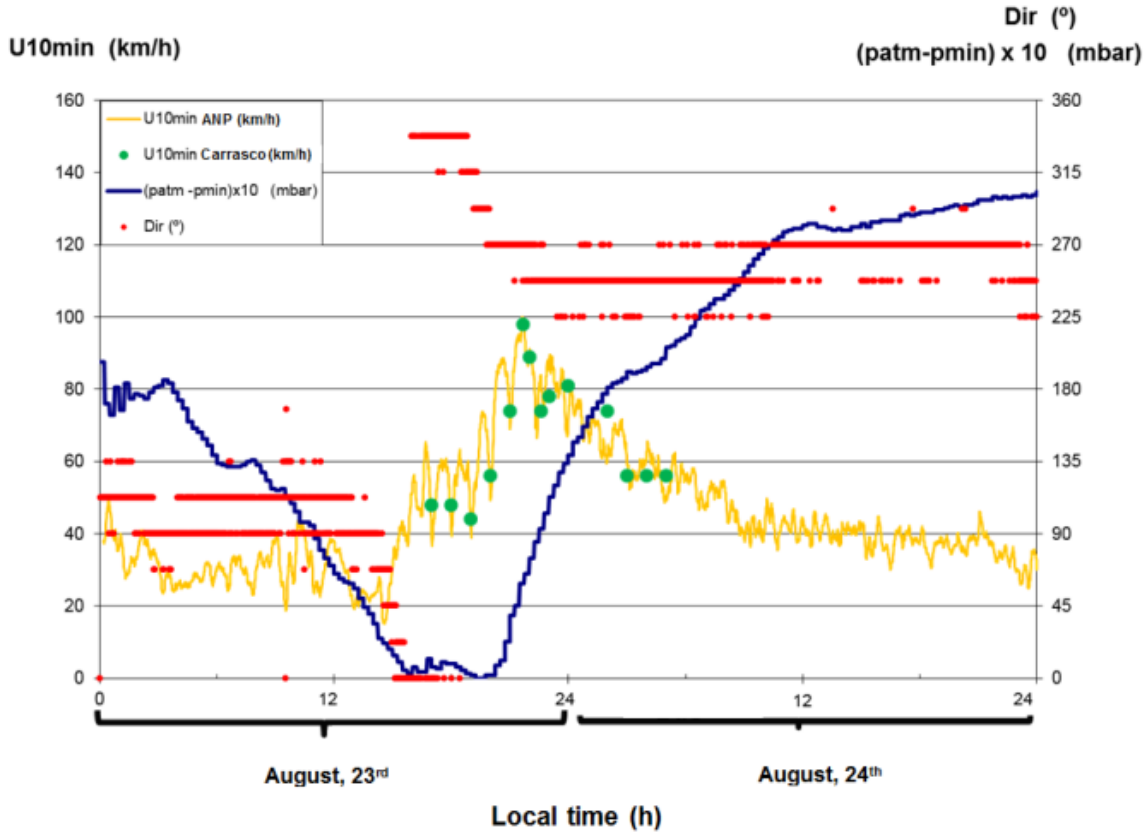


Figure 4.2 10min mean wind speeds, wind direction and pressure evolution in Montevideo during the passage of the severe extra-tropical cyclone of August 23rd, 2005 (adapted from Cataldo and Durañona, 2005)

The horizontal scale of Figure 4.2, which covers 2 complete days, 23rd and 24th of August, 2005, indicates the local time in a 24h format. The vertical scale to the left shows the 10min mean wind speeds measured at Carrasco station ($U_{10min\ Carrasco}$) and the 10min mean wind speeds measured at ANP station translated into Carrasco's conditions ($U_{10min\ ANP}$), both in km/h. Wind speeds at ANP station are presented as 10min mean running averages, and plotted in a continuous line, while wind speeds at Carrasco station are indicated by circular dots.

The vertical scale to the right shows the wind direction in degrees and the atmospheric pressure scaled in order to present it in the same scale as the wind direction, as Equation (4.1) indicates:

$$p_{atm}(\text{mbar}) = p_{min}(\text{mbar}) + \frac{(read\ value)}{10} \tag{4.1}$$

where p_{min} is the minimum pressure registered during this event (992mbar) and p_{atm} is the atmospheric pressure measured at ANP station during the event. Wind direction is plotted with small circles and atmospheric pressure with a continuous line. Both registers are from ANP station.

A good agreement between the corresponding 10min mean wind speeds of both stations can be noticed in Figure 4.2. The maximum U_{10min} at Carrasco station was 98km/h (27.2m/s), while the maximum U_{10min} at ANP station translated into Carrasco's conditions was estimated to be around 100km/h (27.8m/s). This figure also shows the passage of the low pressure region of the extra-tropical cyclone in Montevideo, and the characteristic variation of wind direction with time for these events, from east to southwest in this case (clockwise).

On the other hand, Figure 4.3 shows the wind gust speeds measured at both stations ($U_{gust\ ANP}$ and $U_{gust\ Carrasco}$) in the vertical scale to the left of this figure, instead of the 10min mean wind speeds shown in Figure 4.2. Wind gusts measured at ANP station were approximated to Carrasco's conditions applying Equation (2.4). Wind direction and pressure measured at ANP station are again shown in the vertical scale to the right, with the pressure scaled with Equation (4.1).

A relative good agreement between wind gust speeds from both stations can also be noticed, except for the highest wind gust speed registered at Carrasco station, which was 174km/h (48.3m/s) at 22:34h local time, highlighted with a circle in this figure. The maximum wind gust speeds registered at ANP station and translated into Carrasco's conditions corresponded to values between 136 and 140km/h (37.8 and 38.9m/s), and were occasionally registered from 22:29h to 23:29h local time.

To the author's knowledge, no similar value of wind gust speed as the one registered at Carrasco station was measured at other stations in the country during the passage of this extra-tropical cyclone. Such relative high value, and the fact that it was measured in just one of two stations only 20km apart, could be related to some type of non-synoptic high wind event embedded into this extra-tropical cyclone.

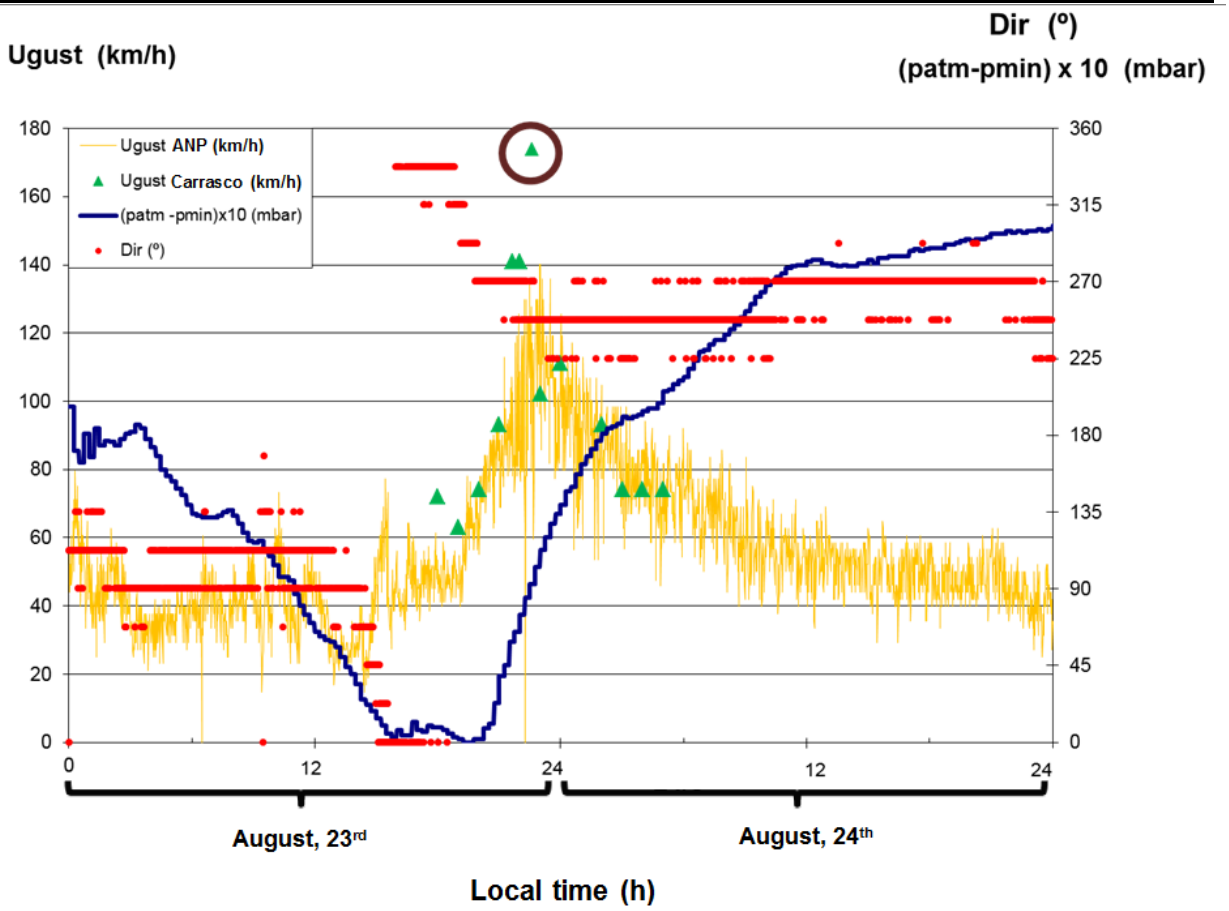


Figure 4.3 Wind gust speeds, wind direction and pressure evolution in Montevideo during the passage of the severe extra-tropical cyclone of August 23rd, 2005 (adapted from Cataldo and Durañona, 2005)

A comparison among different meteorological parameters measured at ANP and Carrasco stations are presented in Figure 4.4. This figure shows in its left vertical scale the 10min mean wind speeds measured at ANP station translated into Carrasco's conditions (in km/h), and the temperature measured at ANP station, scaled in order to present it in the same scale (the actual measured temperature in °C is the read value divided by 4). The vertical scale to the right indicates the pressure measured at ANP station scaled as in Figure 4.2 and Figure 4.3, and the actual gust factors measured at each station multiplied by 100. Gust factors were calculated as $U_{gust}/U_{10min.}$ They are shown with a continuous thin line for the whole set of wind measurements at ANP station, and with crosses for Carrasco station. At Carrasco station, the maximum gust factor (2.35) is indicated with the biggest cross, while the rest are shown with smaller crosses and corresponded to values between 1.3 and 1.6. The gust factors for ANP station presented values between 1.3 and 1.75 from 22:29h to 23:29h local time, with an average value of 1.54.

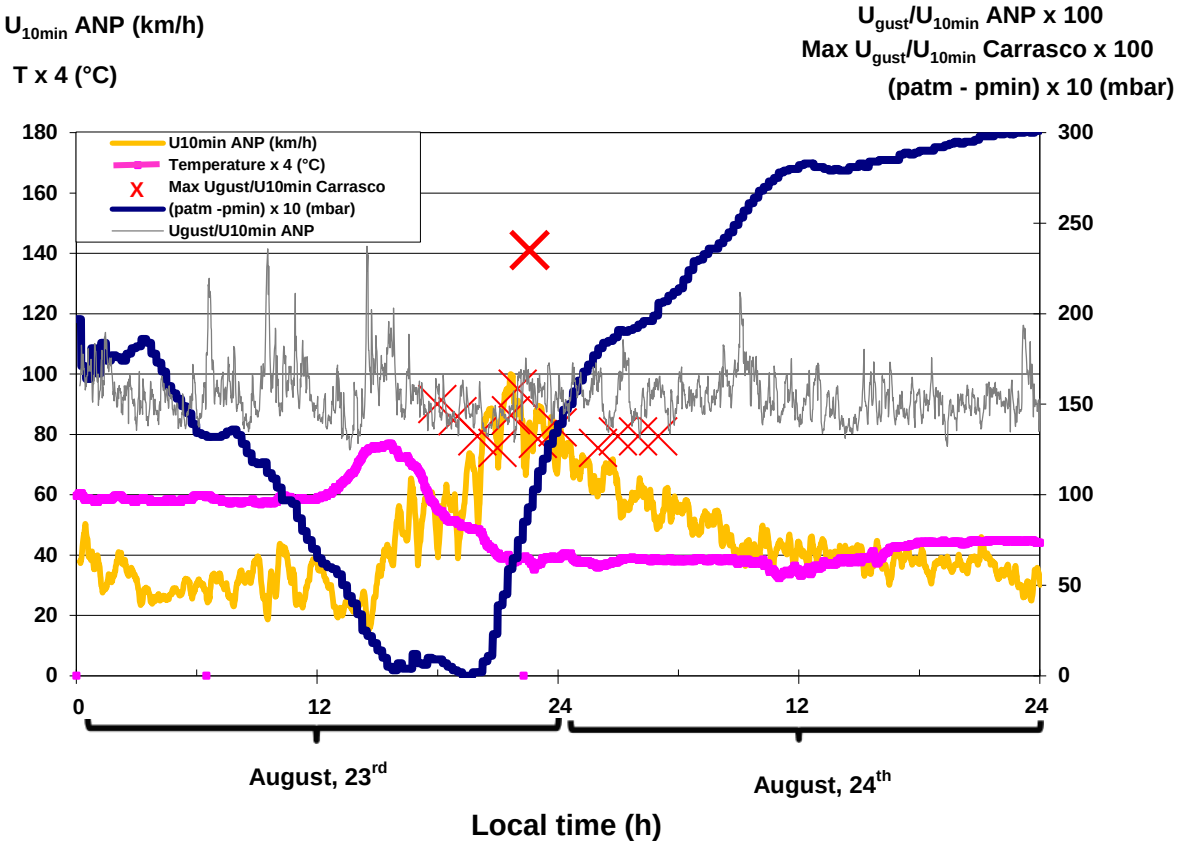


Figure 4.4 10min mean wind speed, gust factors, temperature and pressure evolution during the passage of the severe extra-tropical cyclone of August 23rd, 2005 (adapted from Cataldo and Durañona, 2005)

The meteorological parameters presented in Figure 4.4 help illustrating the characteristics of the passage of this explosive extra-tropical cyclone over Montevideo. In particular, it can be seen that the gust factor values calculated for ANP station during the register of the higher wind speeds (with a mean of around 1.5), correspond to typical values found for synoptic winds (e.g. Solari et al., 2015a cite mean gust factor values of 1.5 for gusts averaged over 1s and mean wind speeds averaged with moving average periods of 10min, as indicated in Sub-section 2.2.1.4), while the gust factor calculated for the maximum wind gust speed registered at Carrasco station (174km/h) was 2.35.

One explanation for the high wind gust measured at Carrasco station and not at ANP station might be the occurrence of a sting jet, as mentioned in Sub-section 2.2.3.1.1, which may bring very high winds down to ground level. Some similarities between this explosive extra-tropical

cyclone and others studied in Europe (e.g. Browning, 2004; Clark et al., 2005) pointed out by Necco, 2015 may support this hypothesis.

As presented in Sub-section 2.2.3.1, it is common for extra-tropical cyclones to embed high wind events of relative small length scales. A more recent intense extra-tropical cyclone that generated high winds over Uruguay on October 23rd, 2012 embedded a tornado, as shown in Figure 2.52(b) in Sub-section 2.2.5.2.

4.7. Example: severe convective activity (MCC) on March 10th, 2002

One of the most damaging events that occurred in Uruguay in the last years took place when a MCC generated at least one tornado, violent downbursts, hail and intense rain in the south of the country on March 10th, 2002, between 15:00h and 17:30h local time (UTC-3) (DNM, 2002; Torena, 2003b; Durañona and Cataldo, 2007; Durañona, 2010; Durañona, 2011b).

The data and description presented in this section were obtained from several reports that included field surveys and analysis of information from witnesses, and from newspaper articles. It is worth mentioning that the network of stations of UTE described in Section 3.3 had not been installed by that time.

This MCC developed a supercell (DNM, 2002), shown in Figure 4.5 over the Río de la Plata. Figure 4.6 illustrates how this MCC approached Uruguay from the southwest, with a series of satellite images from 14:39h to 16:09h local time. The supercell travelled from the southwest and entered Uruguay through its south western coast as indicated in Figure 4.6. When the most intense winds took place, the approximate area of the MCC was 178,000km^2 (DNM, 2002).

Violent downbursts and at least one tornado produced the most important damage in a strip from west to east, approximately 10 to 15km wide and 60 to 200km long (DNM, 2002), 30km north of Montevideo. The storm travelled during 2½ hours at a mean wind speed of 85km/h (24m/s), affecting 5 departments in the south of the country and an area of 6,500km^2 along its trajectory. Wind gusts of up to 124km/h (34m/s) were measured, but in some areas the wind speed was estimated to be around 200km/h (56m/s) from the level of damage. One



Figure 4.5 Supercell over the Río de la Plata on March 10th, 2002 (picture of Ignacio Landini)

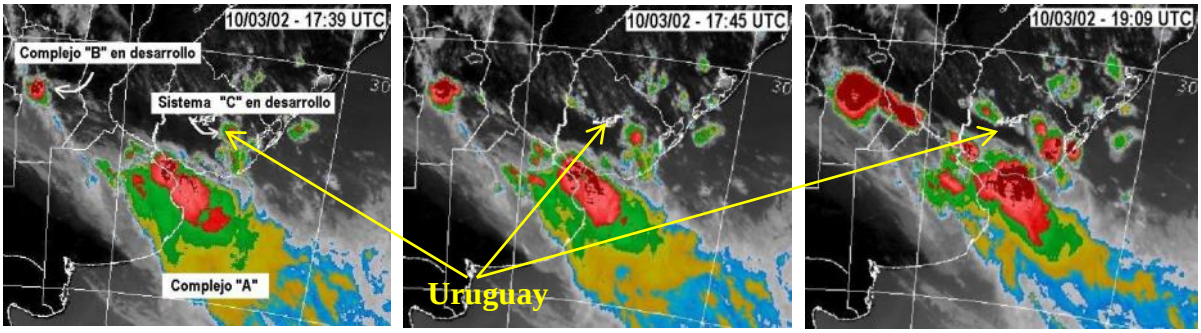


Figure 4.6 Satellite images of the MCC of March 10th, 2002 (adapted from DNM, 2002)

tornado was categorised as an F3 and associated with the occurrence of micro and macrobursts. Its diameter was estimated in 80m, and its path, around 50km (DNM, 2002).

As a consequence of this event, 19 towers of 500kV and 48 towers of 150kV fell down, 700 buildings were destroyed, many crops were lost and two people died (El País, 2002-2015; Durañona and Cataldo, 2007). Many people lost all their belongings. Along the path of the storm, roofs of 1,250 houses and of 38 schools were damaged within a few minutes, windows were broken, walls brought down and metal sheets scattered within a 5km radius. Cables and poles fell down and many trees were blown down or cut at mid-height. Entire wood forests and crops from more than 1,000 producers were affected, and farms, greenhouses, fruit and

agriculture business experienced total losses. Many telephone lines and poles were damaged. The repair of the high voltage transmission towers cost U$S 2 million (US dollars), and the use of thermal power generation during the outage cost U$S 10 million, while the agroindustry lost at least U$S 15 million. It was estimated that this event caused a total loss of U$S 27 million to the country (Durañona and Cataldo, 2007; El País, 2002-2015).

4.8. Example: wind events affecting high voltage transmission lines

In 2007, UTE had been studying for some time a series of disconnections experienced during the passage of storms over the main high-voltage transmission lines that supply energy to Montevideo, capital city of Uruguay, where around half of its population lives.

These lines correspond to two 500kV lines that go from a hydroelectric dam located in Palmar, approximately 300km northwest of Montevideo, to Montevideo, as shown in Figure 4.7. The hydroelectric generation is the cheapest energy source for the country.

During some meteorological phenomena, these lines had simultaneously failed producing extensive blackouts that affected great part of the country. The characteristics of these failures pointed out to the wind as one possible cause of these failures. It was suspected that the wind generated loads that produced excessive conductor sway angles, bringing the conductors close enough to the transmission towers to produce a discharge and disconnect the lines, but when the calculation of the sway angles of the conductors was reviewed, taking into account international transmission lines wind design codes and the official extreme wind statistics presented in the national wind code for actions on structures UNIT:50-84, 1984, no explanation was found for the relative high frequency of these failures. For this reason, UTE consulted the IMFIA about this problem.

An analysis of the weather conditions during 23 dates provided by UTE when failures in the 500kV Palmar-Montevideo transmission lines had occurred between 2000 and 2007 was carried out by the author of this thesis, as presented in Durañona and Cataldo, 2008. In particular, newspapers were used to look for damaging wind events reported during the days when incidences in the transmission lines had occurred, as conventional meteorological

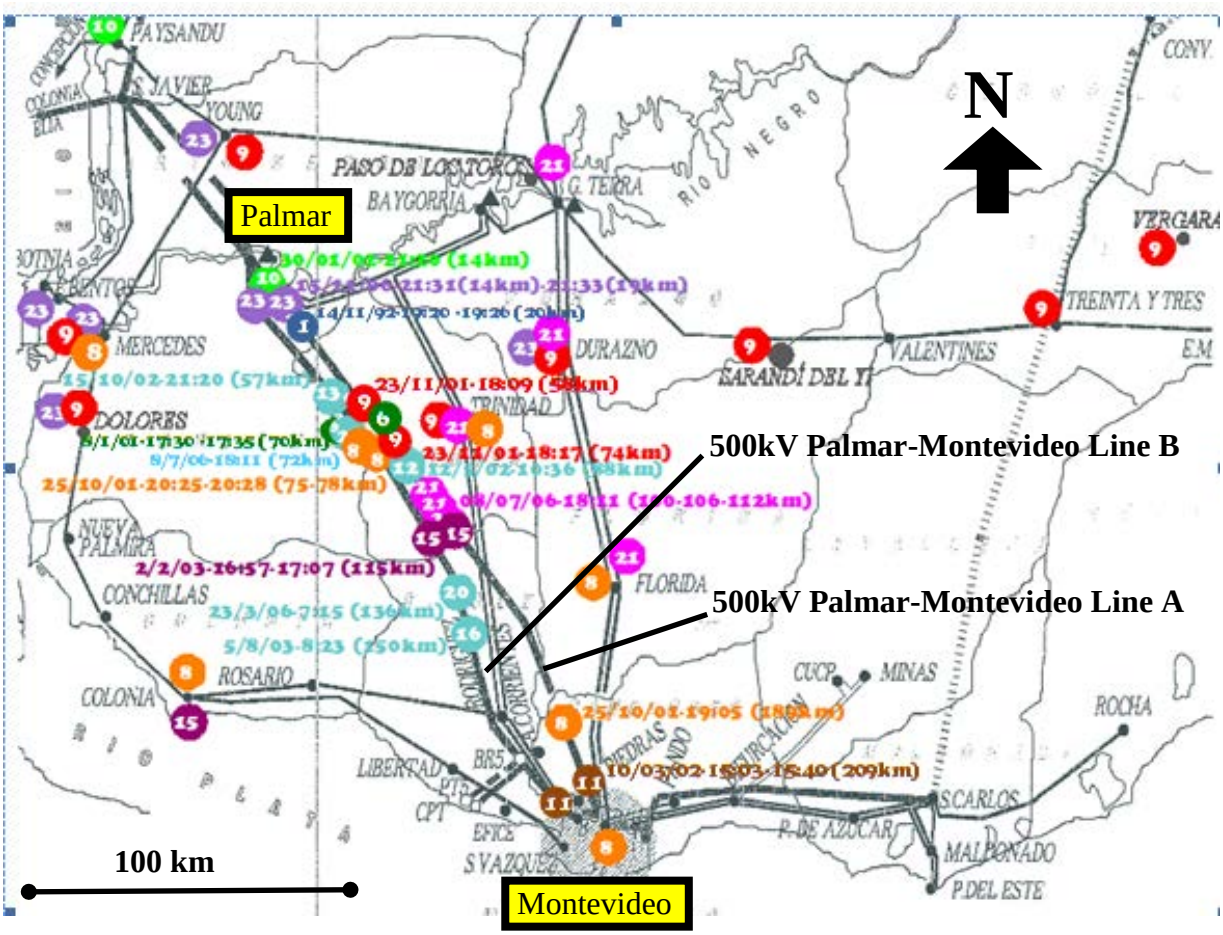


Figure 4.7 Localisation of line failures and sites where wind damage was reported (adapted form Durañona and Cataldo, 2009)

stations did not usually report high winds during those days. It is worth mentioning that the network of stations of UTE described in Section 3.3, had not started to be installed at that time. Information regarding the occurrence of high winds, intense winds of short duration, hail and/or intense rain during those days were collected, which could imply the occurrence of intense convective storms over the transmission lines, as indicated in Sub-section 2.2.3.2.

Out of the 23 studied dates when line disconnections had taken place, 16 corresponded to days when localised high winds, hail and/or intense rain had been reported to occur in areas close to these failures, supporting the hypothesis that most of them had been caused by intense convective activity (Durañona and Cataldo, 2008). The frequency distribution of the months of the year when these failures had occurred matched the expected distribution for

severe convection in this region, as presented in Sub-section 2.2.4.2.2.1. On the other hand, when the time of the day when high wind, hail and/or intense rain had been registered, a high correlation was found between this time and the time of occurrence of the line disconnection. Moreover, when the localisation of the failure in the transmission line was registered, it was found that many times the disconnection of the line had occurred between areas that had reported the most intense wind damage, as illustrated by Figure 4.7.

In this figure, the location of several failures experienced by both 500KV lines are identified over the lines with numbers inside circles when this information was available. For each number, the date and time of occurrence, as well as the distance from Palmar, are indicated in a text nearby in the same colour. For the same dates, the places of the country affected by high winds, hail and/or intense rain, indicating the occurrence of intense convective activity and the high probability of downbursts occurrence (or other types of strong outflow boundaries generated by deep convection), are identified with the same number and colour than the corresponding line failure.

Analysing this figure, it could also be verified for the storms whose trajectories could be studied, that they mainly moved from the southwest to northeast, and sometimes from west to east, as expected for convective activity organised in lines for the region (see e.g. Sub-section 2.2.4.2.2.1), with translational wind speeds between 50 and 90km/h (14 and 25m/s). The most intense wind gusts recorded during these events were between 90 and 145km/h (25 and 40m/s) at 10m height, and their directions mainly corresponded to directions from southwest through west (clockwise). These values and directions are also characteristic of winds produced by downbursts in the region, as indicated in Schwarzkopf and Rosso, 1993. It is worth mentioning that the developed wind gust speeds could have been more intense than the ones registered, as the places most affected by the storms may not have had an anemometer nearby to register wind speeds.

When information on the dimensions of the areas that had suffered wind damage, and/or on the duration of the high wind events, was available, their relative small length and time scales could also be verified, reinforcing the hypothesis that wind damage had been caused by strong downbursts generated by severe convective activity in those places.

On the other hand, personnel from UTE indicated that during several line failures, a manual reconnection of the affected line(s) was attempted without success during several minutes, after which the line(s) could be connected again. This period matches the typical time scales of the most intense wind speeds produced by e.g. downdraft outflows. These wind speeds would produce loads high enough to maintain the conductors close to the towers, and prevent the reconnection until the wind speed has not fallen to lower values. The estimation of wind loads and their corresponding sway angles were presented in Durañona and Cataldo, 2009.

In addition, in the cases when both lines were disconnected, it could be verified that the distance between them was short enough to be able to be affected by the same downdraft outflow, or by other types of strong outflow boundaries generated by intense convection. In these cases, line B, as identified in Figure 4.7, was the first line to fail, after which Line A was disconnected, indicating a storm translational direction from west to east. Besides, the failures occurred in the west cantilever of the lines in 85% of the cases when this information was available. This is another indication that most of the failures were produced by wind, as the most intense wind gust speeds caused by intense convective activity in the region are from southwest through west directions (clockwise), according to e.g. Schwarzkopf, 1984-1993, and it is in the west cantilever where the wind force would move the conductors toward the tower, thus producing the disconnection of that line.

From this analysis it could also be verified that there would be several events per year crossing these high-voltage transmission lines with wind speeds greater than 100km/h (28m/s) at 10m height.

The main reason why transmission lines fail in downburst winds is that the span reduction factor that should be applied to design wind loads is much greater than in synoptic winds for which they have been designed. This is discussed in Holmes et al., 2008 and is nowadays well accepted by the industry in Australia and North America.

4.9. Discussion

The results presented in Section 4.5 are useful for a preliminary characterisation of the impact of high wind events on Uruguay.

As indicated in Section 4.5.1, analysing the wind damage database described in Section 4.4, a wind gust speed value of about 80km/h (22.2m/s) was estimated as the wind gust speed threshold at which wind damage starts being reported. It is worth mentioning that this wind gust speed value (22.2m/s) is similar, although a bit lower, than the value mentioned in Knox et al., 2011 for considering a non-convective high wind event as severe (26m/s), by Doswell, 2003a for considering a convective event as severe (25m/s), and by Weisman, 2003b for identifying the occurrence of a derecho (26m/s), as described in Sub-section 2.2.3.

It could be verified that wind is responsible for many crops, trees and forests losses in the country, interruptions and damage to the electric transmission system, widespread outages, damage to buildings and structures, pedestrian non-comfort and risk situations, and that it can also affect ships of different size and harbour operations, among other effects. In particular, an example of its impact on crops and agriculture was presented in Section 4.7, and on high-voltage transmission lines, in Section 4.8.

It was found that if a high wind event stroke in rural areas, damaged sheds, greenhouses and silos, as well as fall of fruits from trees were usually reported; if it took place in urbanised areas, many buildings and signs were generally affected; if there were ports located along its trajectory, ships could be damaged or passengers could be put in risky situations; if it crossed medium to low voltage energy distribution lines, power outages were very likely to occur in the affected areas. If intense convective storms produced intense downdraft outflows or other non-synoptic high winds over the Palmar-Montevideo high-voltage transmission lines, widespread blackouts affecting highly populated areas of the country could occur.

The impact of a high wind event in Uruguay is thus very dependent on its trajectory, length scale and exposed resources, goods and infrastructure in the areas affected by the highest wind speeds, which can significantly vary in Uruguay within tens of kilometres in some cases, both due to differences in land use and to different damage patterns for different types of high wind events. One example of this was presented in Sub-section 4.7, where the effects of

severe convective activity (MCC) that generated a supercell were described. As its highest winds occurred in areas with intensive production systems, the most significant economic losses were experienced by the agronomic sector, while the second most affected sector corresponded to the generation of energy, mainly due to the falling of several high-voltage transmission towers of Palmar-Montevideo lines, which are quite perpendicular to the typical direction of the highest winds produced by severe convective activity in the region. If this event had occurred in a non-productive and scarcely populated area, and without crossing transmission lines, it could have not affected the population in such a significant way, and reached the media as it did.

It was found that intense extra-tropical cyclones caused more widespread damage in the southern and eastern areas of the country, where they tend to intensify and to produce their highest wind speeds. An example of the evolution and effects of an intense extra-tropical cyclone over Uruguay was presented in Section 4.6.

As indicated in Sub-section 4.5.3, wind damage information suggested that a single event or a succession of events related to intense convective activity would tend to affect less than 15% of the territory, while around one third of the country could be affected during the passage of an intense extra-tropical cyclone. This is an example of the kind of information from this type of research that could be useful for e.g. insurance companies or other sectors requiring wind risk analysis.

Blown down roofs and trees were identified as the most common types of wind damage produced, both starting to be reported at about 80km/h. These results are in close agreement with those presented in Natalini et al., 2011.

Many of the blown down roofs corresponded to light metallic roofs, while the simultaneous occurrence of high wind and rain in 80% of the cases might lower the value of wind speed required to blow down a tree. Other types of roofs, trees in dry soil or with deeper roots, may be blown down or fall at higher wind speeds. The wind speed threshold for damage would then depend on the characteristics of the constructions, tree genus and meteorological events simultaneously occurring with high winds, such as intense rain and/or hail, although 80km/h was the lowest wind speed consistently reported together with wind damage.

Wind debris was also found to represent a risk of injury for the population, mainly coming from trees branches and metallic sheets from roofs.

On the other hand, buildings and other structures can greatly modify wind speed values at pedestrian level, causing particular areas of cities and towns to represent greater risks for pedestrians, especially if the streets are parallel to the direction of the highest wind speeds, as it occurred during an intense extra-tropical cyclone on September 19th, 2012, which produced its highest wind speeds from the south in Montevideo. High-rise buildings, as well as some constructions with certain configurations can also produce localised areas of very intense winds. An extreme case occurred during the severe extra-tropical cyclone of August 23rd, 2005, when a car, parked at one of the most dangerous sites of Montevideo for intense winds coming from the southwest, was lifted and impacted the tallest building of the city, 160m high, when this extra-tropical cyclone generated its highest wind speeds from this direction (Cataldo and Durañona, 2005).

It was found that the newspapers were a good source of information on wind damage. Although the reported wind speeds might have not been the highest wind speeds occurring during the informed damaging wind events, as the anemometers may have not been located in the area affected by the highest wind speeds, a clear trend was found between reported wind speed values and levels of damage, with more significant levels of damage reported and more robust structures affected at higher reported wind speeds.

A preliminary analysis of high wind events registered at heights around 10m at open and fixed locations in Montevideo (as shown for the Observatory of Prado and ANP stations) verified that wind gusts higher than 80km/h (22.2m/s) could occur more frequently than once a year, and that wind gusts higher than 100km/h may occur once every two years in average. It also illustrated that along just few years, intense convective activity could be the cause of the highest registered winds at fixed locations. This relatively high probability could be explained by the fact that Uruguay is located in the second most prone region of the world to severe convective activity, as indicated in Sub-section 2.2.5.2.2.1.

Analysing one of the main national newspapers, an event with wind gusts exceeding 120km/h (33m/s) was found to be reported every year in some place of the country. Above this wind

speed, apart from reports of widespread damage to trees and roofs, many poles, electricity cables and some antennas were also informed to be considerably damaged.

Attention is drawn to the very rich source of information on high wind events in all the documentation from Morandi, and especially in the bulletins of the Observatory of Prado station (Morandi, 1901 - 1917), station described in Section 3.5, which covered continuous measurements of wind speed, and reported with detail all high wind events exceeding 50km/h (~14m/s), including wind gusts and their duration, information that it is not usually available, and which was partially used in Sub-section 4.5.4.

The research presented in this chapter also showed the relevance of the impact of intense convective activity on several sectors of the Uruguayan economy as the energy, agronomic and insurance sectors. When specific high wind events that caused great losses in crops (Section 4.7) or important disruption on the electric transmission system (Section 4.8) were analysed, convective activity was found to be responsible for most of them, developing wind speeds exceeding 100km/h (28m/s) many times a year across the country. Gusts of 130 to 145km/h (36 to 40m/s) have also been reported several times in the last decade, in agreement with values of wind speeds informed 100 years ago. As part of the study carried out for UTE (Durañona and Cataldo, 2008), tracks of the damage produced by several convective storms could also be analysed, verifying that they mainly travelled from southwest to northeast or from west to east, as indicated by Celemín, 1984. A summary of this work is presented in Durañona and Cataldo, 2009.

One important finding from the research conducted for the BSE (Section 4.7) and UTE (Section 4.8) was that wind data from a conventional meteorological station nearby a wind damaged site may not be an adequate source of information for the evaluation of a particular damaging wind event. This could be explained by the fact that most damaging wind events would tend to present smaller length scales than the distance between the damaged sites and the nearby station(s). The stations may register relative high winds in some cases, but not necessarily, and usually not, the highest wind speeds produced by a particular storm.

Another fact that should be taken into account is that conventional meteorological stations do not measure continuously, and although intense convective winds might be registered, these stations miss 50min of data every hour, during which non-synoptic high winds may occur. On

the other hand, carrying out averages of wind speeds during 10min would lower the highest winds produced by convective activity, whose maxima wind speeds typically take place during few minutes.

Both facts should be further analysed if extreme winds expected at a specific site are estimated for different engineering applications from 10min mean wind records, or from meteorological stations not measuring continuously, or from relatively short wind records.

It was found that damaging winds were reported many times a year in Uruguay, mostly during the occurrence of intense convective activity over the country, and occasionally but affecting wider areas, due to the intensification of extra-tropical cyclones near its coast. These results are in agreement with wind measurements carried out at the beginning of last century, and also with recent measurements.

As indicated by Blackmore, 2003, the actual number of damaging wind events may be higher than the ones estimated from newspapers and reports, and in particular for non-synoptic high winds. For example, the occurrence of the severe convective activity of March 10th, 2002 over an important productive area, may have been more noticeable than other similar events that could have taken place on areas with fewer resources exposed to winds. Thus, the actual frequency of occurrence of damaging wind events in Uruguay may have been underestimated during the analysis carried out on the generated database presented in this chapter in Section 4.4, and consequently, the numbers cited would represent lower bounds.

Therefore, if wind measurements from conventional meteorological stations do not adequately describe the highest wind speeds nor the frequency of occurrence of high winds associated with intense convective activity, and newspapers and reports may underestimate the frequency of occurrence of non-synoptic high wind events, wind data series from stations that measure continuously, with averaging periods smaller than at least half the duration of the highest wind speeds generated by intense convective activity, would be needed for analysis, in order to arrive at quantitatively more accurate results.

It is also worth taking into account that intense extra-tropical cyclones in Uruguay can embed high wind speed events of smaller length and time scales than the typical scales of extra-tropical cyclones, and that the highest wind speeds measured during an extra-tropical cyclone

may in fact correspond to these smaller events, as suggested by the findings of Section 4.6. As suggested in that section, it could be worth exploring with a meteorological approach, the hypothesis of development of sting jets (and other non-synoptic high wind events) inside intense extra-tropical cyclones passing over Uruguay.

In addition, it seems that tornadoes can be generated in any place of the country, mostly associated with the occurrence of severe convective activity, but sometimes developing inside intense extra-tropical cyclones, as the event that took place in the southeast of Uruguay on October 23rd, 2012 (Figure 2.52).

As previously mentioned, it was found that great part of the electric transmission system failures would be caused by high wind events, and in particular, by intense convective activity. Although the probability of occurrence of a downdraft outflow at a specific site is usually considered not to be high, the probability of one of these events (or of other strong outflow boundaries generated by deep convection) crossing an electrical transmission system would be more significant due to the important extension of such systems (Holmes, 2007). In spite of this, most design codes calculate the wind loads on these systems assuming ABL flows, hypothesis that usually leads to an important underestimation of these loads, especially due to the lower correlation this type of flow would present for the highest wind gusts along conductor spans. In the case of Uruguay, the direction of the main high-voltage transmission lines that supply energy to Montevideo, quite perpendicular to the typical directions of the highest wind gusts produced by intense convective activity in the region, presents the worst scenario.

It is therefore advised for the calculation of wind loads on conductors in Uruguay, and especially for high-voltage transmission lines, due to their potential national impact in case of failure, to take into account the differences between the characteristics of downdraft outflows and flows of ABL type, as the higher correlation over longer horizontal distances and heights of the first ones, as indicated in Sub-section 2.2.3.2. What is also true is that there is no general consensus yet on how a typical downdraft outflow profile may be (Holmes et al., 2005a).

It is worth mentioning that the Emergency National System (SINAE) was created in 2009, with the aim of protecting people, significant goods and the environment from disaster

situations, and that it is still consolidating its infrastructure. By the time the information regarding wind vulnerability was processed with the methodology described in Section 4.4, the SINAE did not have registers of damaging wind events. At present, the SINAE offers some partial information on a series of damaging wind events that affected Uruguay, covering mainly the period between the years 2000 and 2011, with some additional historical events that occurred since 1968 (SINAE, 2011). This information was gathered as part of the United Nations Project ONU/09/000K carried out from January to October, 2011 in order to create a national disaster inventory of meteorological events. This inventory, available at SINAE web page, was also based mainly on newspaper information (SINAE, 2011). This technique was similar to the one used by Maria Luisa Altinger de Schwarzkopf in order to characterise non-synoptic high wind events in Argentina (Schwarzkopf, 1984-1993; Schwarzkopf and Rosso, 1993). Studies of this type have also been carried out in periodic basis in the UK (Blackmore, 2003) as mentioned before, and are aligned with the methodology applied to generate the database of damaging wind events that occur in Uruguay presented in Section 4.4.

It also deserves attention the fact that a search for damaging wind events and severe convective activity carried out along just few years, provided information on about 200 cases from 1900's to date, in a country with an area of around 175,000 km^2 where these events are not systematically reported or registered.

As part of its duties, the SINAE coordinates assistance when severe wind events affect anywhere in the country. To the author's knowledge, during this assistance the SINAE system does not register the dates of those events nor the damage involved. However, as Nascimento and Doswell, 2006 points out, information collected in situ by emergency management personnel is an excellent support for severe weather documentation, as they usually represent the first technical personnel to arrive at affected places, when the destruction signature is still very clear. This documentation can offer valuable information for future planning, prevention and mitigation of their effects. In this case, recommendations given for conducting field surveys, as in Bunting and Smith, 1993 could be worth taking into account.

For example, it would be very valuable to systematically analyse and register if different wind damage generated during high wind events are caused either by non-synoptic or synoptic high wind events. This classification is relevant for wind engineering, as pointed out by Solari et

al., 2015b. Convective and synoptic high wind speed events present important differences on their wind flow and turbulent structures, not to mention on their expected seasonal and statistical distributions. To achieve this objective, the participation of meteorologists would be essential.

The creation of a comprehensive national database with damaging wind events would collaborate in the evaluation of the vulnerability of different sectors of Uruguay to high winds, gaining further insight into the potential risks and economic consequences of high winds in Uruguay.

Chapter Five

Analysis of meteorological data from UTE network of automatic stations

5.1. Introduction

In this chapter, Section 5.2 gives details of the special characteristics of the network of automatic meteorological stations of UTE described in Section 3.3 in relation to other available measurements, while Section 5.3 briefly outlines the objectives of the research carried out on meteorological data from this network; Section 5.4 presents the general methodology applied for the study of the highest gust and 10min mean wind speeds registered by this network. Section 5.5 describes the analysis carried out on the highest wind gust speeds and the results obtained, while Section 5.6 shows the analysis and results of the study of the highest 10min mean wind speeds. Finally, Section 5.7 discusses these results and links them to material presented in the literature review.

The analysis of this database started in 2012, but the interpretation of the obtained results represented a challenge for the knowledge on the extreme wind climate of Uruguay from a wind engineering perspective at that time, and required a series of discussions with local and regional meteorologists and wind engineers, which are still going on, and a deeper review of the meteorological characteristics of the region, as presented in Sub-section 2.2.4.2. The results presented in Sub-sections 5.5.2 and 5.6.2 correspond to the analysis of data measured by this network until July, 2012, but the insight gained into this topic until 2015 is present in some comments in these sections and in the discussion outlined in Section 5.7, as well as in Chapters 8 and 9. An update of part of this research has been recently presented (Durañona et al., 2015).

5.2. Special characteristics of this network

As indicated in Sub-section 3.3.1, 25 stations from this network, shown in Figure 3.1 and listed in Table 3.1, located in open and level terrain, were selected for the analysis presented in this chapter. These stations register the mean, standard deviation, maximum and minimum values of wind speed, wind direction and temperature every 10min, and of relative humidity

and/or solar radiation in the stations equipped with these sensors. As already mentioned, wind speed at these stations is measured with 3-cup anemometers model 40C from NRG Systems.

Along this entire chapter, the wind direction values presented are values averaged over 10min although they are also used to assign direction to wind gust speeds. On the other hand, in part of the analysis, wind gust speeds are shown at different heights for the same 10min interval, although they may have not occurred simultaneously. Due to the type of available information, wind gust speeds are defined in this chapter as the maximum values of the wind speeds measured over 10min intervals at the specified sampling frequency (1 sample per second) by the corresponding anemometer(s) of this network, as registered in the database of UTE.

As the stations of this network have been gradually installed, the lengths of their analysed records varied from few months to about four years by July, 2012. It is worth mentioning that altogether these data series generated a database for analysis representing a volume of 850 months of measurement of each meteorological parameter every 10min.

The density of stations of this network, as well as the frequency of their measurements, allows the description of the evolution in space and time of synoptic weather systems and eventually non-synoptic features that produce high winds up to 100m height as they move across the country, and of the characteristics of high wind events generated at specific sites. Having stations not further than about 100km from any point of the country, registering every 10min measurements sampled at 1Hz, allows the analysis of high wind events with a detail that was not possible before the installation of this network, as already commented in Chapter 4.

Furthermore, personnel from UTE methodically verifies the quality of the data measured by all the stations of the network before including it in this database, and continuously keep registers of their metadata. To carry out the analysis presented in this chapter, it is required that more than 20 stations measure with good quality data along several years, and to have access to adequate metadata to arrive at valid conclusions, as emphasised in Sections 2.3 and 2.4 .

The importance of counting with reliable data and metadata was specifically presented in Section 2.3, and different examples have been given in other sections of this thesis that

illustrate the good results that can be obtained from high quality measurements, and the problems that may arise when analysing wind data of unverified or poor quality.

In the case of this network:

- Many stations were sited so as not to be influenced by topography or surroundings, and different evaluations were carried out to verify this, and to assess on the possible influence of the towers on wind measurements, as presented in Section 3.3.
- The characteristics of the sensors, their locations and orientation are known for a particular time and station, their surroundings are monitored, and measurements compared among different stations to detect erroneous measurements due to faulty sensors or measurement systems, or changes in the surroundings. When an error is detected, the situation is evaluated and corrected when necessary, and if it is not possible, then the data is not taken into account, while changes are registered in the metadata.
- The calibrations of the sensors are kept up to date.
- The percentage of missing data is very low.
- Automatic measurements avoid inhomogeneities and errors that may be introduced when readings are carried out by observers, as commented in Section 2.3.

As also indicated in that section, it is not usual to have a network of stations complying with all the above characteristics.

In addition, other features of this network make the analysis of its measurements unprecedented to the author's knowledge, at least in the region:

- Simultaneous measurements of wind speed, direction and temperature provide relevant information that can help identifying high winds produced by convective activity, as they are characterised by concurrent sudden increases in wind speed, wind direction shifts and temperature drops (as presented in Sub-section 2.2.3.2 and illustrated in Figure 2.13 and Figure 2.18).
- Measurement of wind gust and wind direction at different heights, and in some cases, up to 100m height, may offer valuable information on the structure of non-synoptic high wind events.

5.3. Main objectives of this analysis

The principal aim of the research presented in this chapter was the identification and characterisation of the main types of high wind events that occur in Uruguay, as the meteorological conditions related to their occurrence, their typical temporal and spatial scales; trajectories, geographic, seasonal and frequency distribution of high wind speeds; behaviour of wind speed and direction with time at fixed locations under high wind events, correlation among wind speeds measured at different heights, etc., in order to make the best use of the potential of this network.

5.4. General methodology

First of all, the data and metadata of the 25 stations selected for this research were gathered and prepared for their analysis. All the meteorological measurements performed every 10min since the installation of each station, until the beginning of their preparation for analysis (July 3rd, 2012), were downloaded from UTE database or supplied by the DNE and arranged to have all the same format. Information on their metadata was obtained directly from UTE and from the downloaded database. Secondly, a decision was made on how to define a high wind event, and a procedure to perform the search for this type of events on the analysed database of UTE was outlined. Matlab software was used to identify and characterise each high wind event.

Thus, a series of Matlab codes were specifically written to search and analyse the characteristics of the meteorological events that generate high winds in Uruguay during different stages of this research.

When a high wind event was identified in the analysed database, gust and 10min mean wind speeds data series were analysed at each measurement height, together with wind direction, temperature and solar radiation data when this last measurement was available. One of the first analyses included the simultaneous study of the temporal evolution of these variables during a period of 10h centred at the time of the register of the highest wind speed (either gust or 10min mean) generating figures and spread sheet files with the main results.

When comparing measurements from different stations, only complete years were analysed, in order to take into account the probable seasonality in the occurrence of high wind events, as expected from Sub-section 2.2.5.2; and to obtain more homogeneous results across the country. From Table 3.1, it can be seen that the stations that measured less than one year during the analysed period were stations 33, 34 and 36. Thus, the analysis of characteristics such as the number of high wind events per year measured at each station, their seasonal behaviour, wind roses of high wind events, etc. was carried out in data series from the rest of the 22 stations, comprising 696 months of measurements.

With the same aim of obtaining more homogeneous results among the different stations, it was decided to interpolate wind speed measurements at 45m height, as almost all stations measured above and below this height, as Table 3.1 indicates. A linear interpolation was selected after looking at the wind speed values measured below and above this heights during many high wind events. From this previous analysis, it could be seen that the difference between these values around the time the highest wind speed was measured was usually not significant and that the corresponding wind speed profiles could even present a negative slop, especially in the case of wind gust speeds. This behaviour can be observed looking at the first two graphs of the last row of figures shown in Annexes A.2, A.3 and A.4.

For certain specific days when high wind events occurred in a number of stations, data series from all the available stations were used to describe the trajectory and evolution of high winds over a map of Uruguay. In these cases, a figure was generated every 10min during the event, containing the most relevant meteorological information measured at each station during that period.

In the aforementioned cases, the sequences of the generated figures and their evolution with time, combined with satellite images, as those mentioned in Section 3.6, were analysed in order to obtain more comprehensive information on the meteorological event that was producing high winds, than just looking at records from each station in a separate way. Sometimes synoptic charts as those mentioned in Section 3.6 were useful, especially for the analysis of extra-tropical cyclones or of specific synoptic weather patterns that were producing high winds over Uruguay.

5.5. Analysis of high wind gust speeds

In this section, the analysis carried out to characterise events presenting wind gust speeds with the potential of producing wind damage in Uruguay is described.

As a wind speed of 80km/h (22.2m/s) was identified in Section 4.5 as the threshold for wind damage to start being reported, this value was chosen as the threshold for analysing wind gust speeds measured by the UTE network of automatic weather stations. In this way, it was expected that this analysis could characterise damaging wind events and allow the comparison of these results with those outlined in Section 4.5.

5.5.1. Methodology

a) As a first approach to describe the main characteristics of the events producing the highest wind gust speeds in Uruguay, wind gusts higher than 80km/h registered in any of the 25 stations indicated in Figure 3.1 at any height, during any 10min interval of the measurement periods listed in Table 3.1, were identified. This corresponded to the analysis of a data series 850 months long of wind gusts registered every 10min, as commented before.

In this thesis, a high wind event was defined as any causing a wind gust speed higher than 80km/h at any station and at any height in a period of 10 hours (h), centred in the time the highest wind gust was registered. Thus, if during his 10h period, several wind gusts higher than this threshold were registered at a station at any height period, they were all counted as one event.

For each event, two figures were generated: one with the evolution at each available height of: the 10min mean wind speed together with the wind gust registered, the temperature and wind direction, during the analysed 10h period; and a second figure containing the evolution with time at different heights during the analysed 10h period of: 10min mean wind speed, wind gust speed, wind direction, standard deviation divided the 10min mean wind speed for each 10min interval, wind gust speed divided by the 10min mean wind speed for each 10min interval, i.e., the gust factor; temperature, and profile with height of: 10min mean wind speed, wind gust speed, and wind direction.

In addition, for each station, a spread sheet with the main characteristics of all the events presenting wind gust speeds higher than 80km/h was generated.

b) As almost 1,000 events in total were identified in the analysed database as a result of **a)**, it was decided to study the four highest wind speeds registered at each station i.e., around 100 events, to obtain a first characterisation of the most intense wind gust events.

For each of these events, the station, date, time of occurrence, value of the highest wind gust and height at which the highest wind gust was registered were identified. After a qualitative examination of these events, it could be noticed that the time behaviour of wind speed, wind direction and temperature tended to group them into few categories, as described in Sub-section 5.5.2, paragraph b).

For the characterisation, it was then taken into account if wind speed and/or wind direction showed a sudden, gradual or non-significant change, if the temperature increased, decreased or did not show any change; as well as the value of the mean wind direction registered during the 10min interval when the highest wind gust speed was measured.

After this characterisation, the frequency of occurrence of events presenting different behaviours was evaluated with the aid of the generated figures.

The presence of significant convective activity over Uruguay was evaluated with images of GOES satellites from CPTEC web page (CPTEC/INPE, 2012), and it was qualitatively analysed if there was a relation between the intensity of the convective activity and the characteristics of the wind gust speed evolution with time, e.g. if higher wind gust speeds, or high wind events of smaller time scales were related to higher tops of the clouds.

For some events, surface synoptic weather charts were taken into account to help describing the meteorological conditions that accompanied some types of high wind events identified, e.g. a surface synoptic weather chart may show if a low pressure system is producing high winds in the country, if a sudden irruption of a cold air mass from the south is generating synoptic high winds, or indicate the location of a cold front responsible for severe convective activity along it.

c) As it was found that several of the events identified in **b)** occurred the same day in certain number of stations, it was decided to study with more detail the seven dates that produced wind gusts higher than 80km/h in the greatest amount of stations.

A Matlab code was written to create, for each date, a figure every 10min, simultaneously showing all the stations over a map of Uruguay, and the values of the wind gust speed interpolated at 45m height, its corresponding wind direction and temperature for all the stations that were operative during each particular event. The highest wind gust speed at 45m height for each 10min interval, and the station where it was calculated were identified in the title of each figure, together with the date of the event and the time corresponding to the analysed 10min interval.

For each of these dates, the program additionally generated a spread sheet containing its main characteristics along time, and a figure summarising the most relevant meteorological information obtained over a map of Uruguay that helped characterising the meteorological phenomenon. Each of these seven figures show the location of all the stations, the maximum wind gust speed calculated at 45m height at each station during each date, and the corresponding wind direction and temperature. The title of these figures also indicates the highest wind gust speed at 45m height registered along each date, and the corresponding station.

Figure 5.9 and Figure 5.10 are examples of this type of analysis. Figure 5.10 corresponds to an extra-tropical cyclone that affected Uruguay on September 19th, 2012, date outside the analysed periods, as shown by Table 3.1.

For all these seven dates, satellite images from CPTEC web page (CPTEC/INPE, 2012), synoptic weather charts and other meteorological information were collected and analysed to improve the understanding of these high wind speed phenomena. Satellite images could many times verify the presence of clouds with high vertical extent, related to intense convection, in the dates and times when these high wind events had occurred. The analysis of the animated sequence of these images also helped to visualise the movement of these clouds over Uruguay and the reason why the highest wind gust registered at each station had occurred at a particular time. The cause of the occurrence of some other high wind events could be identified with synoptic weather charts. Technical meteorological reports

and newspaper information with descriptions of some of these high wind events and related wind damage also contributed to this characterisation.

After these analyses, the main characteristics of the wind events that produced the highest wind gusts in large areas of the country could be described: the typical directions of the highest wind gusts, if they tended to present wind direction shifts or temperature drops, geographic patterns of the trajectories of the highest wind gusts across Uruguay, their translational wind speeds, if they were associated with severe convection, extra-tropical cyclones or other synoptic weather patterns, etc.

d) After arriving at these conclusions, a more quantitative analysis was carried out to compare results from different stations in a more homogeneous way, analysing only complete years and with the highest wind gusts interpolated at 45m height at each station. This is the type of information also analysed in **e)** to **g)**.

This time, wind gust speed measurements carried out at different heights were interpolated at 45m height for each 10min interval of the 696 months data series corresponding to complete years of measurements. These data correspond to the 22 stations that measured the complete years shown in Table 3.1. Then, the events that presented wind gust speeds higher than 80km/h at 45m height ($U_{gust\ 45m} \geq$ 80km/h) were identified and characterised with the aid of Matlab codes. One of the codes generated a figure per each high wind event, showing in each of them the evolution with time of the actual measurements of both gust and 10min mean wind speeds, with one graph for each different measurement height, and three more graphs with temperature, wind direction, and gust and 10min mean wind speeds interpolated at 45m height. For the stations where solar radiation or humidity was measured, the time evolution of these variables was also indicated in these figures. As mentioned in **a)** these graphs describe the time evolution along 10h, centred at the time the highest wind gust at 45m height was calculated.

The code additionally generated a spread sheet for each station, where the main characteristics of each high wind event and the values interpolated at 45m height were stored.

e) To process all this information in a more comprehensive way, different graphs and tables were produced with new Matlab codes.

As a first step, a figure per station with different graphs characterising the highest wind gusts interpolated at 45m height was produced. This figure contained a bar graph indicating the frequency of occurrence of $U_{gust\ 45m} \geq 80$km/h for different wind gust speeds intervals, and another showing the monthly distribution of these events; a wind rose with the events presenting $U_{gust\ 45m} \geq 80$km/h, and a second wind rose with the highest wind gust speed events, the latter with the aim of easily showing the direction from which the highest wind gusts tended to come from.

f) After **e)**, several graphs (and spread sheets) summarising the previous information for the whole country were generated: a bar graph with the frequency of occurrence of all $U_{gust\ 45m} \geq$ 80km/h regardless the station for different wind gust speeds intervals; a second bar graph with the monthly distributions of these wind gust events, and a series of wind roses that characterised the wind direction distribution of the events that presented $U_{gust\ 45m}$ higher than 80, 104, 120 and 140km/h (22.2, 29, 33 and 39m/s).

g) In addition, part of this information was presented over maps of Uruguay to analyse the geographic distribution of different variables:

A Matlab code was developed to generate one figure that gives information on the events that presented $U_{gust\ 45m} \geq 80$km/h across the country. This figure shows for each station, the predominant wind direction and month of the year when these events mostly occurred, together with the mean value of $U_{gust\ 45m} \geq 80$km/h and the monthly frequency of these high wind events. This figure identifies in its title the station where the highest mean of these wind gust speeds was calculated and its value, the station where the maximum monthly frequency of occurrence of these events was found, and the corresponding mean number of events per month that occurred at that station.

A second figure characterising the events with $U_{gust\ 45m} \geq 104$km/h (29m/s) across the country was also generated. For each station, the predominant wind direction and season of the year when these events mostly took place is shown, together with the mean of the $U_{gust\ 45m} \geq 104$km/h and the annual frequency of these higher wind events. This figure also

identifies in its title the station where the highest mean of these wind gust speeds was calculated and its value, and the station where the maximum annual frequency of occurrence of these events was found, with the corresponding mean number of events per year that occurred at that station.

h) Final analyses were carried out to investigate the values of gust factors at 10m height during convective activity, the characteristics of the events that presented $U_{gust} \geq 40$m/s (144km/h) at any height, and wind gust speed measurements in those stations that had anemometers installed at 10m height.

5.5.2. Results

In the next paragraphs, the results of the analyses described in the previous sub-section are presented, following the methodologies described in **a)** to **h)**.

a) Analysing the 850 months corresponding to the whole available database, 966 different 10h periods presenting $U_{gust} \geq 80$km/h were identified in 24 of the 25 stations. The only station that did not register any $U_{gust} \geq 80$km/h was station 36, which had measured only 1 month during June, 2012.

As an example, the ten highest wind gust events registered at Pintado station are presented in Annex A.2.

The figures in Annex A.2 show, in their title, from left to right, the number and name of the station where the measurements were carried out, the measurement period analysed for that station, the number of the event for that station in descending order according to the value of the high wind gust speed registered (for each station, Event 1 corresponds to the event that registered the maximum wind gust speed at that station; Event 2 to the second largest, and so on); the corresponding value of the high wind gust speed measured, the date and local time when it was measured and the length of the timeseries in months used for the analysis.

As it can be seen in this annex, there are two different figures for each event, both of them showing the temporal evolution of different meteorological variables during the event. In

the graphs, the vertical dotted line corresponds to the time when the maximum wind gust speed was registered and the horizontal axis shows the previous and following five hours.

In the first figure, the three graphs in the first row simultaneously show the gust and 10min mean wind speeds in m/s, each at a different height. The darkest line corresponds to the wind gust speed, while the lightest, to the 10min mean wind speed. These graphs are shown in descending order with height from left to right. The graph of the second row shows the evolution of the temperature with time, in °C, while the graphs in the last row correspond to the wind direction measured at different heights, with the corresponding height indicated in the vertical axis.

In the second figure, the first row has three graphs, each simultaneously showing a different meteorological variable at several heights along the 10h period around the high wind gust speed registered. From left to right, they correspond to the 10min mean wind speed, wind gust speed and wind direction, and their legends indicate the colour that corresponds to each height. The second row shows from left to right the temporal evolution at different heights: of the standard deviation of the wind gust speed divided by the 10min mean wind speed; of the gust factor, i.e., the wind gust speed divided by the 10min mean wind speed, and of the temperature. Finally, the last row has also three graphs, which show the temporal evolution of different profiles with height, corresponding from left to right to the 10min mean wind speed, the wind gust speed and the wind direction.

Looking at these figures, several characteristics can be noticed, which are shared with most of the events corresponding to the highest wind gust speeds measured at other stations: most of the events (and especially, the highest ones) presented very distinctive transient features, as sudden increases in gust and 10min mean wind speeds, simultaneously with temperature drops, in some cases more abrupt than in others, and wind direction shifts, also in some cases, more abrupt than in others. A specific example of this type of behaviour is presented later particularly in Figure 5.6(a), corresponding to the highest wind gust speed measured at station 4-Peralta during the analysed period. The commentaries previously made for the first figures of Pintado apply to this figure in relation to its title, vertical dotted line, horizontal axis and description of the graphs.

The events corresponding to the highest wind gust speeds registered at all the stations also present a similar evolution with time of the wind gust speed at different heights, and the same is valid for the 10min mean wind speed and for the wind direction. A correlation between the time evolution of the gust and 10min mean wind speeds can be appreciated at each height, but around the time the maximum wind gust speed is measured, the wind gust is usually significantly higher than the 10min mean wind speed, thus increasing the value of the gust factor, in some cases considerably more than in others. Near that time, wind gust speeds at different heights also tend to be relatively more similar among them than the corresponding 10min mean wind speeds at those heights. This high similarity among the wind gust speed values registered at different heights was found at all the stations of UTE network, at all the highest wind gust speed events registered, even in those stations with measurement heights spanning from as low as 10m to around 75m, as illustrated by Figure 5.1, which corresponds to the high wind gust event of Figure 5.6(a).

The commentaries previously made for the second figures of Pintado, apply to this figure in relation to its title, vertical dotted line, horizontal axis and description of the graphs. In this figure, it is clearly seen how the wind gust speeds at different heights abruptly increase during the same 10min interval, reach similar values and start decreasing again simultaneously.

The high correlation of the increase and decrease of wind gust speed among different heights spanning several tens of meters, as shown in Figure 5.1, and in Annex A.2 for Pintado, suggests that the flow structure that produces these high wind events has vertical length scales of at least several tens of meters.

As shown in Figure 5.1, and in most of the cases with measurements at 10m height, it could be noticed that the wind gust speed measured at 10m height presented quite similar values to those measured at 40 or even at 80m height.

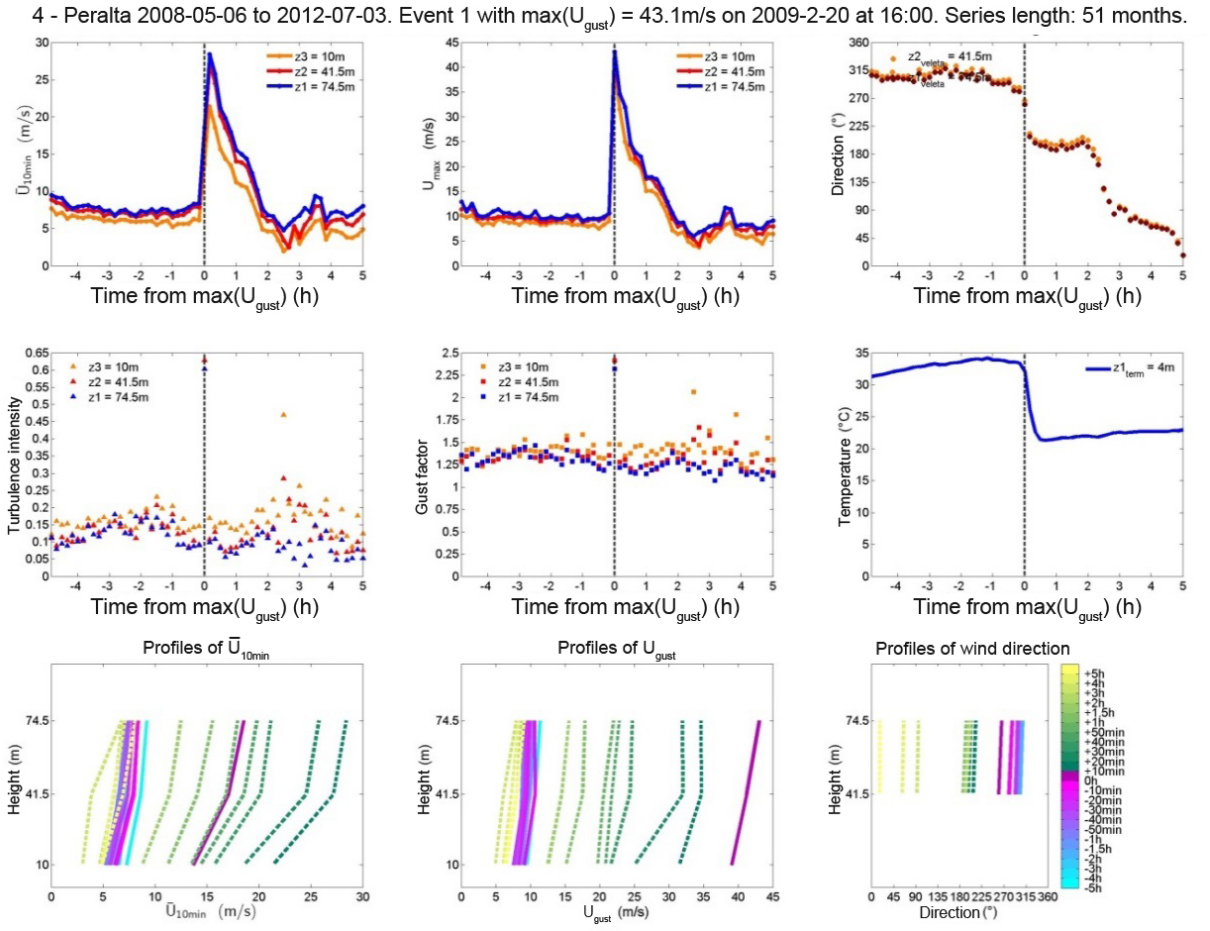


Figure 5.1 Example of high correlation during abrupt increase in wind gust speed at heights between 10 and 75m

On the other hand, in all the stations, events with slower increases and decreases in wind speed, which took place along several hours, generated less intense high winds. Due to their temporal scale as registered at a fixed location, they are referred to in this thesis as synoptic high winds, while the rest are referred to as non-synoptic high winds. These events did not usually present significant changes in temperature or wind direction. When studied, it was found that they were usually driven by synoptic weather patterns, some of them corresponding to the intensification of extra-tropical cyclones in their trajectory over the country, while others, to the presence of high and low pressure systems in particular configurations near or over Uruguay.

One main difference found between synoptic and non-synoptic high wind events was that the first usually presented smaller variations in wind speed, direction and temperature, and along significantly longer time scales.

One example of a synoptic high wind event (registered at station 18-José Ignacio at 15:10h on September 27th, 2009) is shown in Figure 5.2, which is related to the synoptic condition illustrated in Figure 5.3. The latter is a synoptic chart from CPTEC/INPE, 2012 at 21:00h local time of the previous day, i.e., 18h before the highest wind gust indicated in Figure 5.2 was registered), where it can be seen that a very intense high pressure system over the South Pacific Ocean, is collaborating with the entrance of a cold air mass in the southern region of SA. The line in blue with triangles (cold front) shown in this figure, represents the limit of the cold air mass, which is moving toward the northeast. The arrival of this cold air mass produced high winds in Uruguay from the south on September 27th, 2009, as illustrated in Figure 5.2.

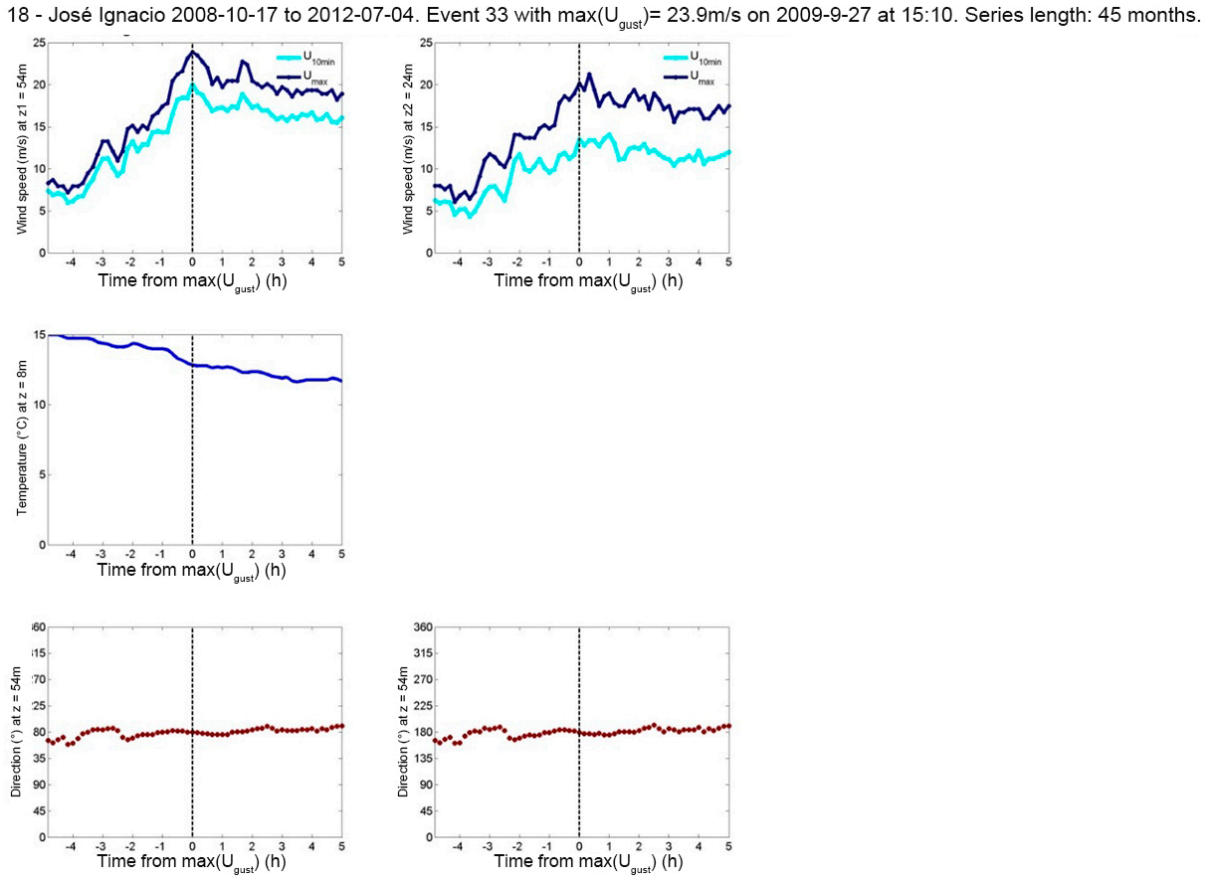


Figure 5.2 Wind speed, temperature and direction evolution at station José Ignacio during the entrance of a cold air mass on September 27th, 2009

On the other hand, Figure 5.4 is an infrared satellite image from GOES 10 (CPTEC/INPE, 2012) at 15:15h local time of September 27th, 2009, i.e., around the time the highest wind gust shown in Figure 5.2 was registered at station 18-José Ignacio.

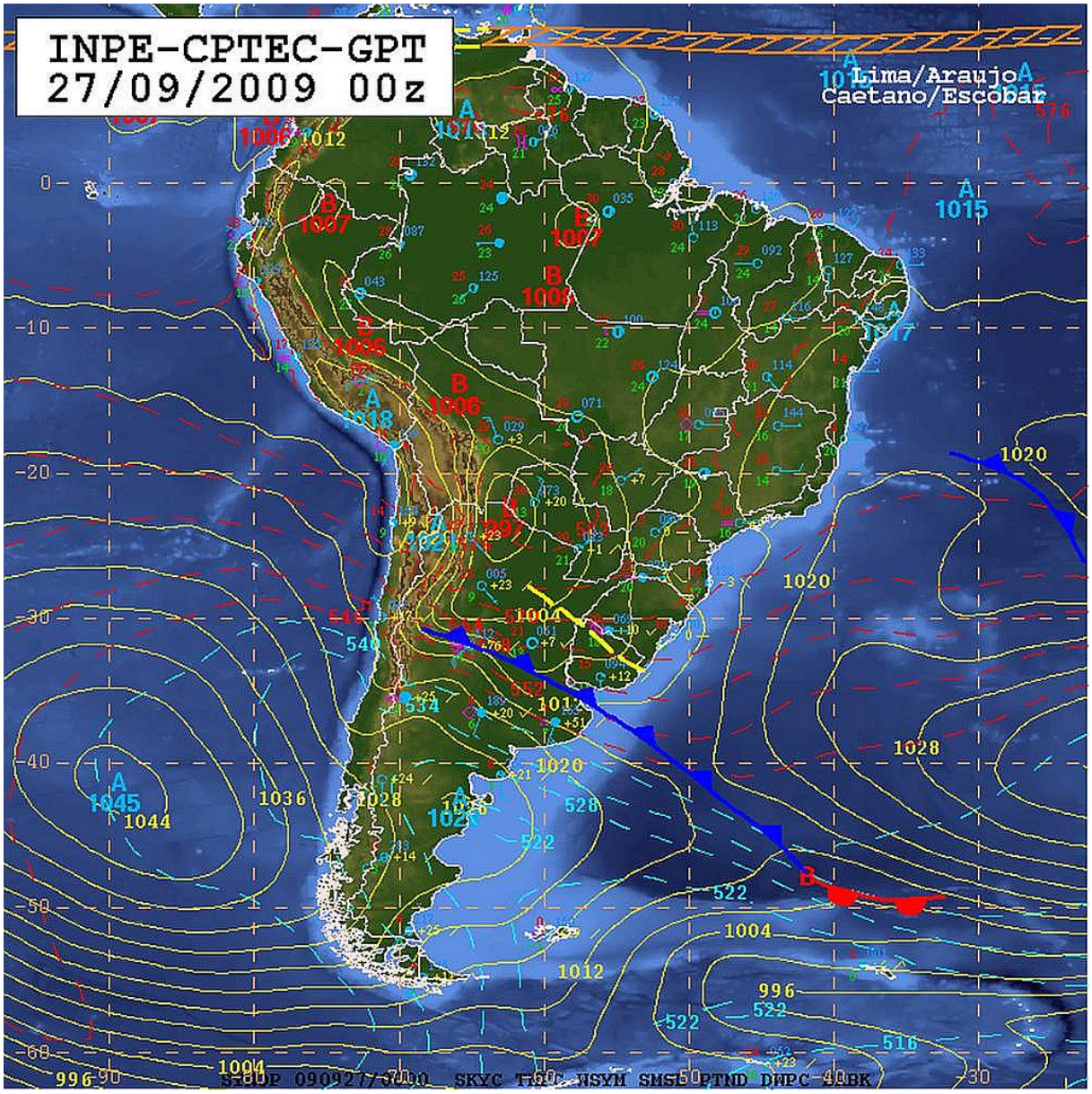


Figure 5.3 Synoptic weather chart some hours before the entrance of a cold air mass into Uruguay on September 27th, 2009 (CPTEC/INPE, 2012)

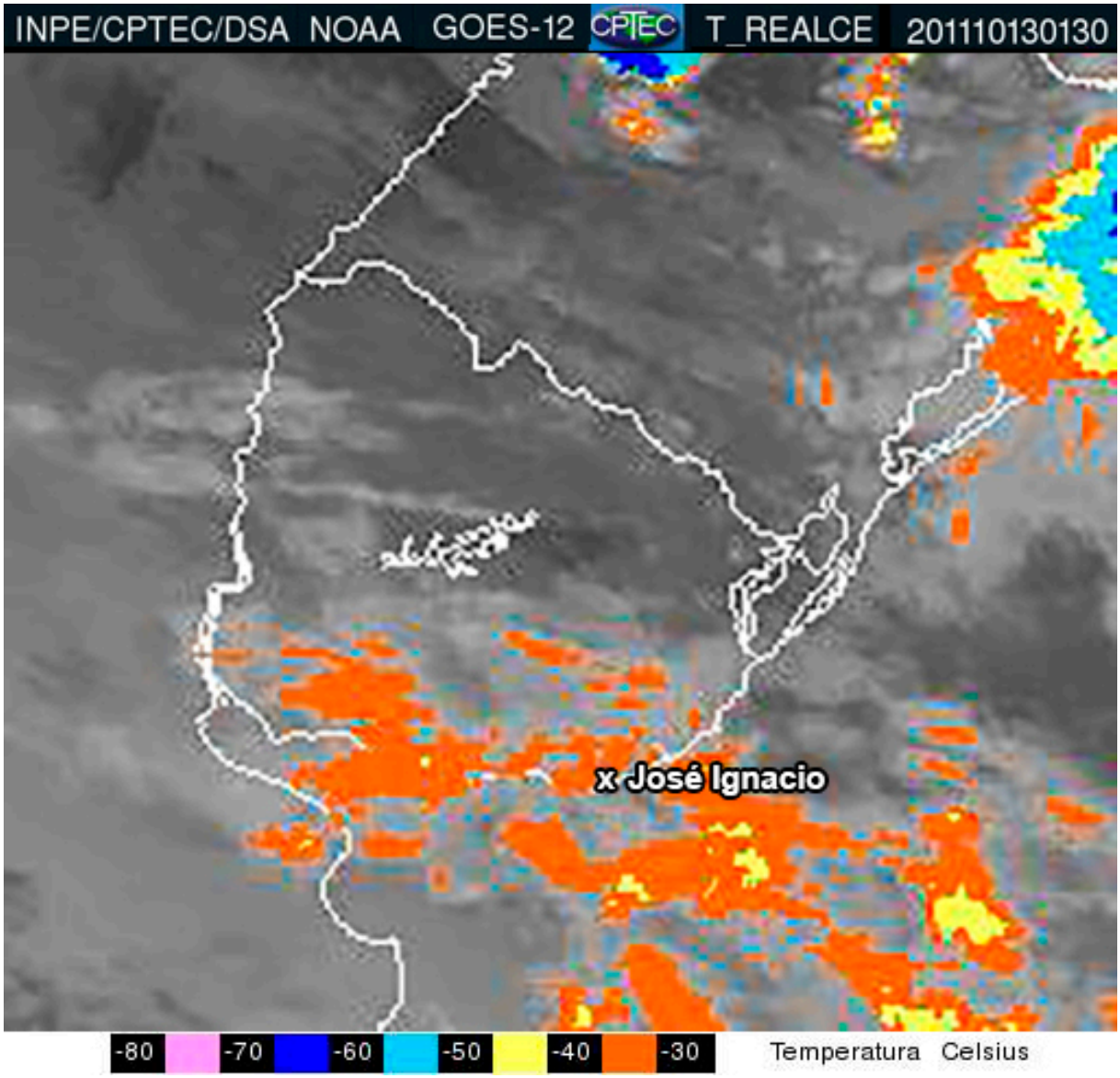


Figure 5.4 Infrared image from GOES 10 satellite (adapted from CPTEC/INPE, 2012) at 15:15h local time on September 27th , 2009

Another cause found for the generation of synoptic high winds in Uruguay during the analysis of the database of UTE corresponded to the passage of intense extra-tropical cyclones over the country. A typical case occurred 2 months after the end date of the analysed period, on September 19th, 2012, but its study was also included in this PhD research due to its intensity and the wind damage that caused in the country (see e.g. Durañona, 2014b). The highest wind gust registered during this event by the network of stations of UTE was measured at station 8-Artilleros, as it will be shown later in Figure 5.11, and corresponded to a gust of 36m/s. This figure also illustrates the smaller variations

in wind speed, wind direction and temperature that present synoptic high winds in comparison with non-synoptic high winds, variations that additionally take place along significantly longer time scales.

b) Analysing the four events that presented the highest wind gusts at each of the 24 stations mentioned in **a)**, 93 events with $U_{gust} \geq$ 80km/h were identified, which corresponded to 47 different dates. It was found that only at 2 of these 24 stations there were less than four events with $U_{gust} \geq$ 80km/h.

Looking at the figures generated for these 93 events (which are not included in this thesis except those of Pintado station, shown in Annex A.2) it could be concluded that in around 80% of the cases, the temperature decreased close to the 10min interval when the maximum wind gust occurred, sometimes as much as 15° in 30min; it increased in 4% of them but mostly just few Celsius degrees (less than 5° C in 1 hour), while in the remaining 16% of the cases the temperature did not present an appreciable change, e.g., it did not vary more than 2°C in 1 hour.

In also around 80% of the 93 events, significant variation of the wind direction took place around the time the maximum wind gust was registered. 50% of these 93 events presented abrupt wind direction changes (e.g. Figure 5.5, Figure 5.6(a) and Figure 5.8), while 30% presented gradual wind direction changes (e.g. Figure 5.6(b)). When significant wind direction change occurred, in 85% of the cases the maximum wind gust speed was registered with wind speeds from the southwest quadrant (including the south and west directions); in 10% of them, from the northwest quadrant and in the remaining 5%, from the southeast quadrant. The events without significant wind direction change presented winds from the W, E, SW and S in 30, 30, 15 and 15% of the cases, respectively.

The temporal evolution of the wind gust speed was also analysed for the 93 events, and for most of them, intense convective activity over the station was usually confirmed by GOES satellite images (CPTEC/INPE, 2012). In most cases, these images showed clouds with high vertical extent over the corresponding stations and times of the high wind events. The temporal behaviour of the wind gust speed, wind direction and temperature would match the expected characteristics of non-synoptic winds caused by strong outflow boundaries

generated by intense convection, such as downdraft outflows, gust fronts and other convective-related high wind events, as presented in Sub-section 2.2.3.2.

One finding of this analysis was that most of the events that took place under the occurrence of intense convective activity presented different behaviours of their wind gust speed with time, and that many of them could be described by one of the following behaviours:

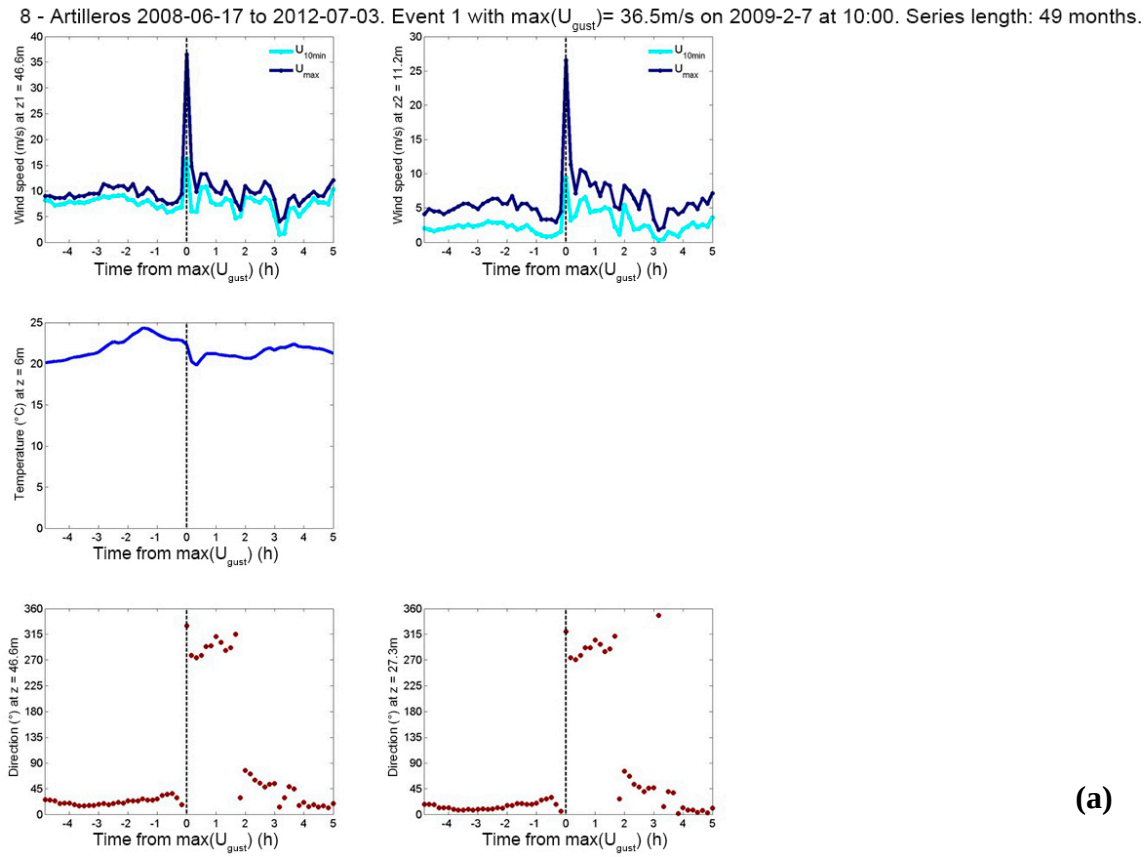
1 – Wind gust speed presenting a very pronounced peak, increasing and decreasing in half an hour or less, generally associated with temperature drop and abrupt wind direction change, as shown in Figure 5.5(a).

2 – Wind gust speed presenting a pronounced peak, increasing and decreasing in one hour or less; also associated with drop in temperature and generally abrupt wind direction change, as illustrated by Figure 5.5(b).

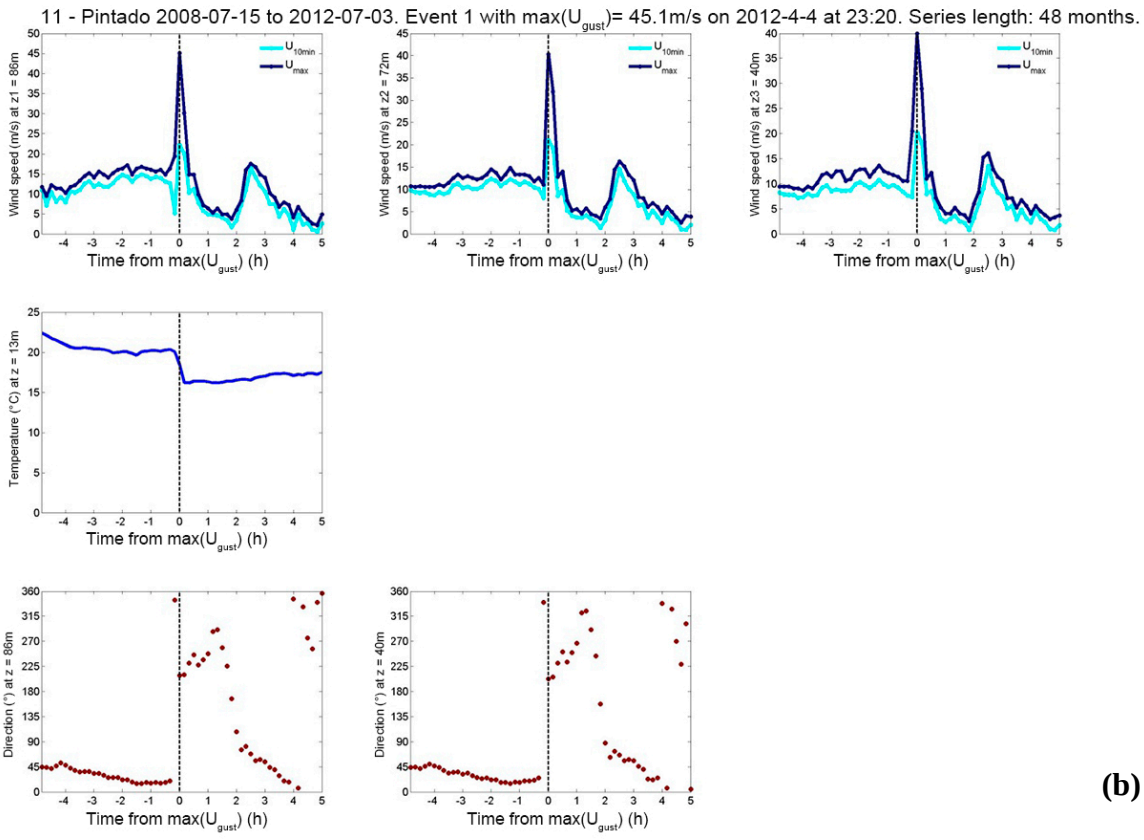
3 – Wind gust speed presenting an abrupt increase, while the decrease was gradual and could span several hours; as in Figure 5.6(a).

4 – Wind gust speed presenting an increase and decrease that generally took between 1 and 3h each; as in Figure 5.6(b).

The same commentaries made in paragraph **a)** of this sub-section for the figures shown in Annex A.2, apply to Figure 5.5 and Figure 5.6 in relation to their title, the vertical dotted line, the horizontal axis; and to the description of all the graphs of Figure 5.5 and Figure 5.6(a), and to the first row of the graphs of Figure 5.6(b). The central row of Figure 5.6(b), corresponding to station 40-ARN, shows the evolution of temperature with time for the two thermometers indicated in Table 3.1; while in the last row, the graph to the left corresponds to the wind direction measured at 75m height.

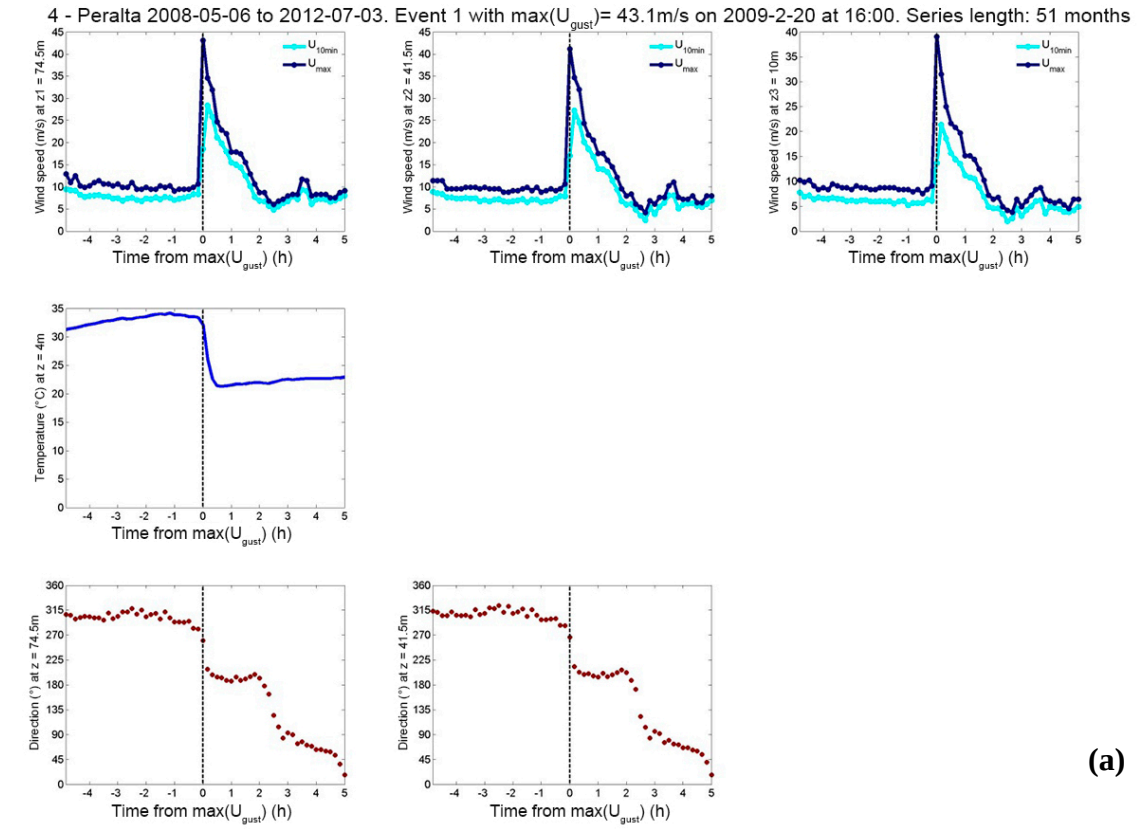


(a)

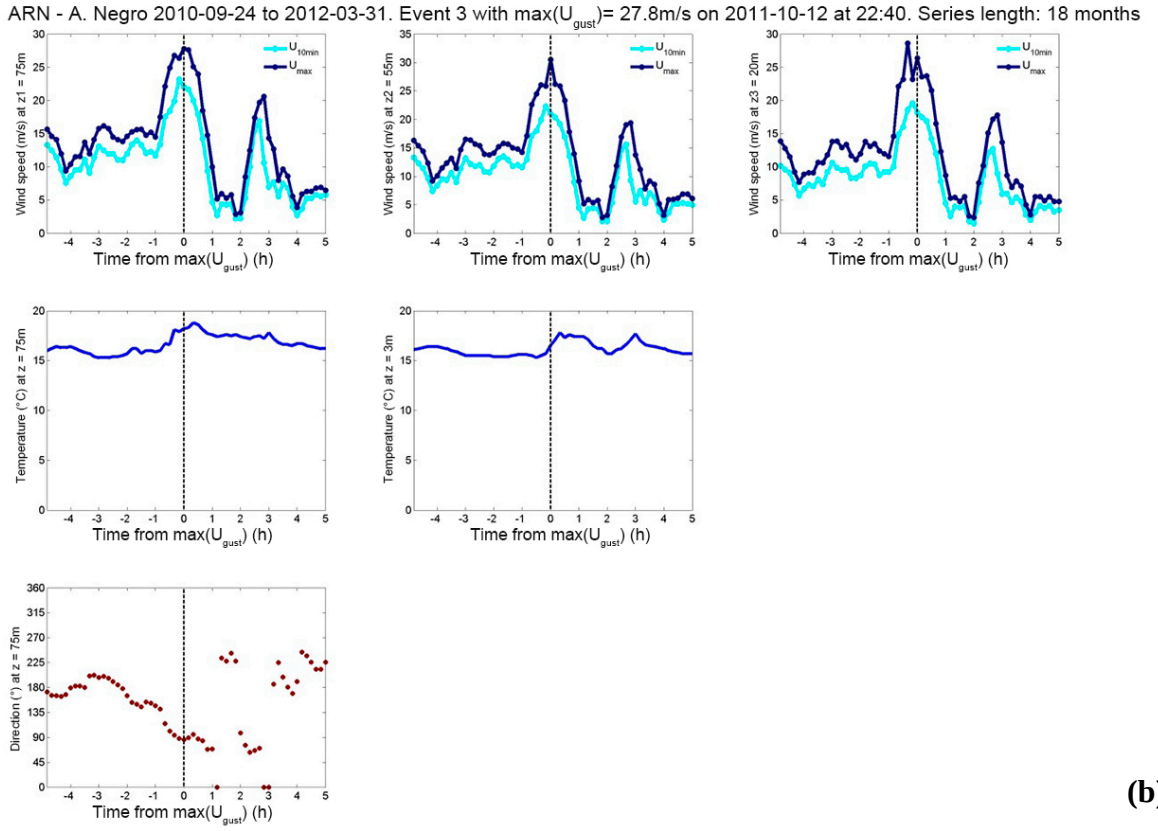


(b)

Figure 5.5 Examples of events that presented wind gust speed with: (a) a very pronounced peak, (b) a pronounced peak



(a)



(b)

Figure 5.6 Examples of events that presented wind gust speed with: (a) an abrupt increase and gradual decrease, (b) an increase and decrease within several hours

On the other hand, in Figure 5.5(a), corresponding to the station 8-Artilleros, the wind speed at 27.3m height was not plotted because this anemometer is oriented to the east, as shown in Table 3.1, and part of the wind measurements registered after the maximum wind gust speed came from the west and may have been influenced by its tower. In all these events, the commentaries made in paragraph **a)** of this sub-section, related to the correlation between wind gust and 10min mean wind speed, between gust and 10min mean wind speeds at different heights, and those related to the gust factor are valid, except for the gust factor evolution and gust factor values corresponding to Figure 5.6(b), as it will be explained below.

The gust factor values corresponding to Figure 5.6(b) were similar to typical gust factors values for flows of ABL type over rural terrain at those heights (as those cited by e.g. Cook, 1985); while the gust factor values corresponding to Figure 5.5(a)-(b) and Figure 5.6(a) were similar to those measured during convective gusts (as those indicated by e.g. Choi, 1999 and Choi, 2000). When the maximum wind gust corresponding to Figure 5.5(a) was measured, the gust factor reached a value of 2.5 at 46.6m height. The gust factor value corresponding to the highest wind gust of Figure 5.5(b) was around 2 at the three heights shown, and around 2.3 at the three heights for the case of Figure 5.6(a). Figure 5.6(b) yielded the minima gust factor values: between 1.3 and 1.5 at the three heights when the maximum gust was registered. Other differences among the four cases shown as examples in Figure 5.5 and Figure 5.6 are the behaviour of the wind direction and temperature with time close to the moment the maximum wind gust was registered. The first three cases presented temperature drops when the wind gust speed increased - the largest one corresponding to Figure 5.6(a), with a sharp decrease of around 10°C in 20min at 4m height; while Figure 5.6(b) shows a slight increase in temperature. In relation to wind direction, the three first cases show abrupt to moderate wind direction changes when the maximum wind gust occurs, while in the last case, the change of wind direction is not so clear.

As Figure 5.7 illustrates with images of GOES satellites from CPTEC web page for the events shown in Figure 5.5 and Figure 5.6 as examples, convective activity seemed to be more intense during the high wind events corresponding to the first three types of behaviour previously described (1-, 2- and 3-) than during the events corresponding to the

fourth type of behaviour (4-). Usually the first three types of behaviour presented lower temperatures of the top of the clouds at the corresponding sites and times of the highest wind gusts, than at those corresponding to the fourth type of behaviour, meaning that the first three types of behaviour could tend to correspond to higher tops of the clouds and consequently, would have more potential to produce intense convective high wind speeds (Rogers and Yau, 1989).

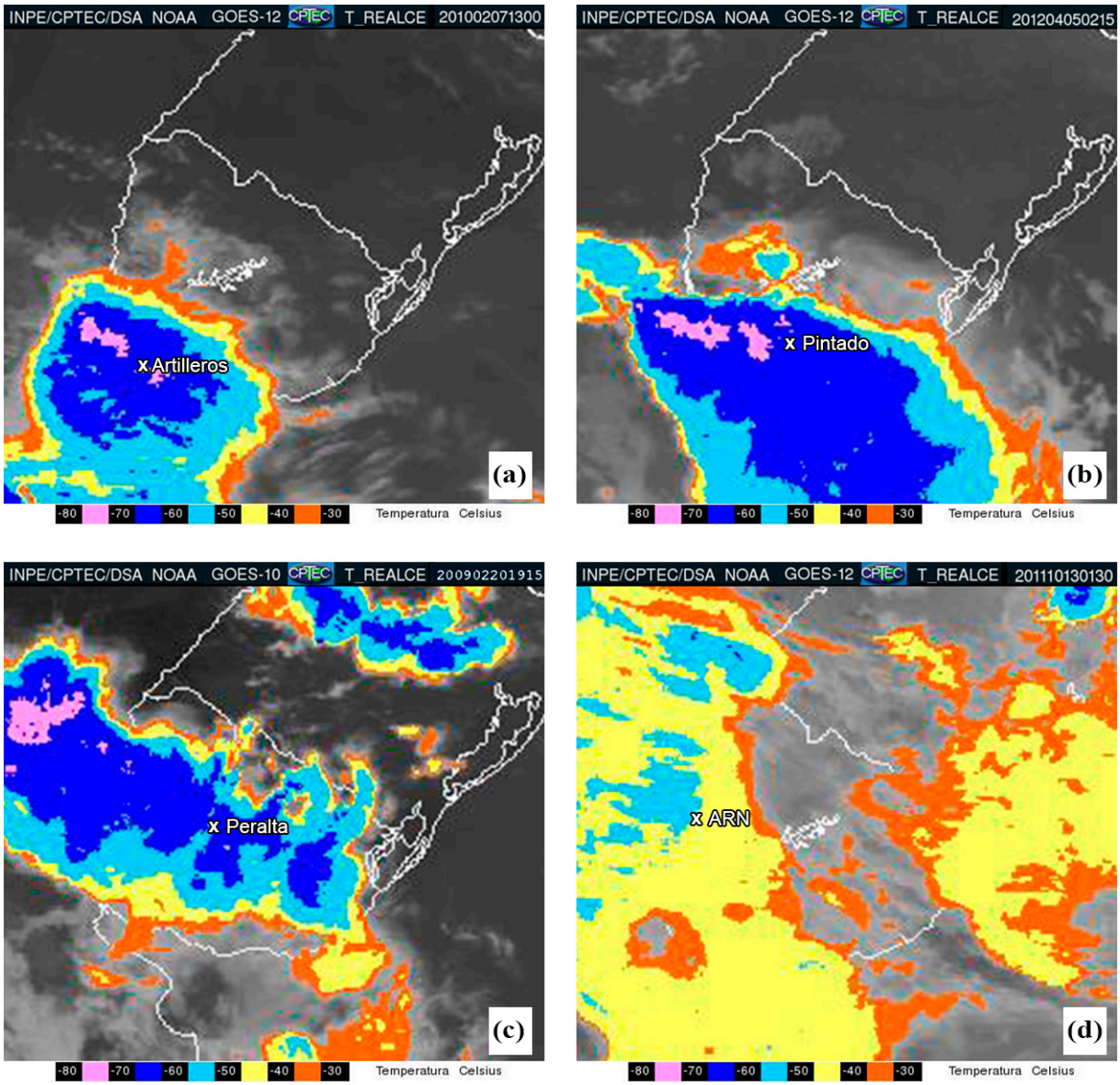


Figure 5.7 GOES satellite images corresponding to the events illustrated in Figure 5.5 and Figure 5.6 (adapted from CPTEC/INPE, 2012)

The increase in wind gust speed shown by the first three types of behaviour, as well as the time scale of that increase, would match the observations of Colmer, 1971 and Sinclair et al., 1973, mentioned in Sub-section 2.2.3.2, that during intense convective activity wind gust speed can increase from 3 to 30m/s in few to around tens of minutes.

As previously indicated, the cases that presented temperature increase when the wind gust increased were very few, around 4%. They usually corresponded to more gradual increases in wind speeds, as illustrated by figure Figure 5.6(b), if compared with Figure 5.5(a) and (b) and Figure 5.6(a). Also, increases in temperature were usually of few degrees (less than 5°C), while decreases in temperature could reach up to 15°C, as illustrated by e.g. Figure 5.6(a).

It is worth comparing Figure 5.6(a) with Figure 2.18 from Sub-section 2.2.3.2, the latter corresponding to the passage of a MCS organised in a line (Schmid et al., 2000) and presenting simultaneous measurements of temperature and 2.5min-mean wind speed measured at 12m height, where a temperature drop of around 10°C was measured with a simultaneous and sudden increase in wind speed. These similarities may suggest that the event shown in Figure 5.6(a) could correspond to a strong outflow boundary of similar characteristics to the one reported by Schmid et al., 2000.

On the other hand, the significant temperature drop shown in Figure 5.6(a), i.e., 10°C in 20min, is not an isolated case. 28 of the 93 analysed events presented temperature drops of 10°C or higher, some more abrupt than others. These 28 events corresponded to 14 different dates.

For example, on January 16th, 2011, UTE network registered the passage of a cold front over Uruguay (CPTEC/INPE, 2012), recording temperature drops of 10°C and more in 9 stations, and one of the four highest wind gust speeds measured by these 9 stations during the analysed periods indicated in Table 3.1. The highest wind gust speed interpolated at 45m height during that date corresponded to station 5-Valentines with a value of 41.3m/s and a direction from the WSW. This was the second largest wind gust speed registered at that station along the analysed 4 years. The meteorological variables measured at this station during that event are presented in Figure 5.8, where an abrupt temperature drop of more than 10°C and an abrupt wind direction shift from NNW to SW can be noticed.

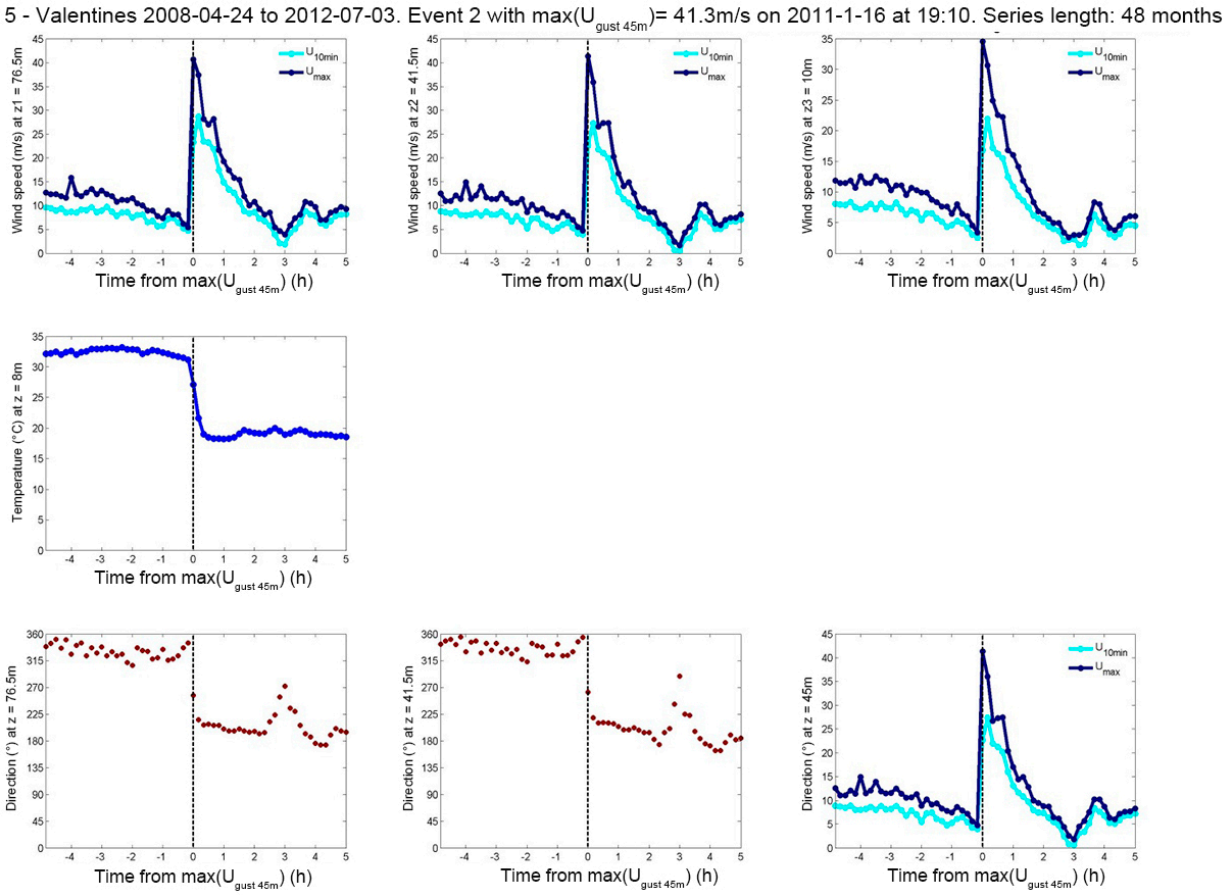


Figure 5.8 Wind speed, temperature and direction evolution at station Valentines during the passage of a cold front on January 16th, 2011

The highest and most abrupt temperature drop corresponded to around 15°C in half an hour, and was registered at station 11-Pintado on December 10th, 2010. This event is presented in Annex A.2, as 'Event 2', which means it was the second largest wind gust speed measured at Pintado station along the analysed 4 years: 41.8m/s from the WSW at 86m height.

During the high wind events previously indicated, wind gust speeds were quite similar along a range of heights during the 10min interval when the highest wind gust speed was registered. At station 5-Valentines, the highest wind gust measured at 76.5m height was 40.7m/s, and 41.4m/s at 41.5m height, while at station 11-Pintado, the highest wind gust speed was 41.8m/s at 86m height and 40m/s at 40m height. Thus, in both cases a wind gust speed difference of less than 2m/s between 40 and 80m height was registered, while in one

of them, the maximum wind gust speed was recorded at the lowest height of measurement. This occurred in many of the analysed high wind events.

It is also worth reminding from Sub-section 2.2.5.2 that significant and sudden temperature drops as those recently mentioned were frequently reported across all Uruguay (Morandi, 1952; Boerger, 1953), and considered since 1850's one of the main features of the Uruguayan climate (Morandi, 1921).

As commented before, very few of the analysed 93 events did not show significant change in wind direction or temperature, and it was found that they were usually driven by synoptic weather patterns, some of them corresponding to the intensification of extra-tropical cyclones in their trajectory over the country, while others, to the presence of high and low pressure systems in particular configurations near or over Uruguay.

The comparison among the characteristics shown by convective activity during a synoptic high wind event (Figure 5.4) and during non-synoptic high wind events (Figure 5.7(a)-(d)) is an example of the use of images from GOES satellites, and illustrates the differences found between these two different types of high wind events.

c) As indicated in paragraph **c)** of the previous sub-section, the seven dates that produced the 4 highest wind gust events at each station in the greatest amount of stations were analysed, representing meteorological phenomena that affected large areas of the country with high winds. They corresponded to the following dates: 4th and 5th of April, 2012; January 16th, 2011 and March 5th, 2012, when 7 to 9 stations registered one of their 4 highest wind gusts during those days; and December 10th, 2010; February 28th, 2012; October 30th and 31st, 2009 and October 7th, 2011, when 4 stations registered one of their 4 highest wind gusts during those days.

As explained before, for these dates and others, the meteorological information provided by UTE every 10min was analysed, and the study of the animated sequence of these figures, together with the study of the animated sequence of infrared images from GOES satellites (CPTEC/INPE, 2012), helped understanding the behaviour of different meteorological phenomena that generate high winds in Uruguay.

With the aid of satellite images animation, it could be seen that in the first 4 dates the convective activity was organised in the form of lines, in some cases wider than others, oriented from northwest to southeast, which generally moved to the northeast, and registers from UTE database indicated that it occurred associated with significant drops in temperature. In these 4 dates, the observed drops in temperature, their typical organisation in lines and direction of translation would be consistent with the characteristics related to the passage of cold fronts or squall lines in this region described by Celemín, 1984, as presented in Sub-section 2.2.5.2.

In fact, Rosso et al., 2012 studied wind damage that occurred in Buenos Aires, Argentina in the evening of April 4th, 2012, and indicated that it was produced by severe convective activity generated by the passage of a cold front. This cold front reached Uruguay and continued its movement toward the northeast during April 5th (CPTEC/INPE, 2012).

Likewise, during January 16th, 2011 a cold front moved from Argentina toward the south of Brazil, passing over Uruguay (CPTEC/INPE, 2012) and generating wind damage related to the occurrence of intense convective activity (El País, 2002-2015). On the other hand, between October 30th and 31st, 2009, a cold front entered Uruguay from its southwest, moved toward the northeast and became a stationary front over Uruguay, according to information from DNM presented in El País, 2002-2015. Later on, it moved toward the southwest as a warm front. During its movement, it produced wind damage in Uruguay related to the occurrence of intense convective activity (El País, 2002-2015).

In Uruguay, Vieira, 1949 also identified the passage of cold fronts as one of the two main meteorological phenomena responsible for high winds in Montevideo.

It is also worth reminding from Sub-section 2.2.3.2 that most high winds along a squall line are caused by strong downdraft outflows, which move rapidly ahead of the system. On the other hand, intense cold fronts may trigger cumulonimbus convection, which in turn may generate strong downdrafts and gust front structures at the surface. They can even trigger squall lines ahead of them. The wind structure during these events is therefore rather different from that of flows of ABL type (defined in Sub-section 2.2.1.3) as indicated in Sub-section 2.2.3.2.

The 5th date (February 28th, 2012) corresponded to the occurrence of intense convective activity over the southwest and south of Uruguay, accompanied by important lightning activity (CPTEC/INPE, 2012 and El País, 2002-2015), while during the 6th date (October 30th and 31st, 2009), the convective activity remained over Uruguay along both days, as described before, and as it can also be seen in satellite images from CPTEC/INPE, 2012, generating at least one tornado the last day (El País, 2002-2015), behaviours also described by Celemín, 1984.

The remaining date (October 7th, 2011) corresponded to the occurrence of intense convective activity affecting different areas of the country (CPTEC/INPE, 2012; El País, 2002-2015).

The fact that the highest wind events that affected the greatest amount of stations in an analysed period of 4 years were associated to intense convective activity, without involving the occurrence of extra-tropical cyclones, was another indicator that non-synoptic high winds related to convective activity could generate higher wind gusts in great part of Uruguay, and more frequently, than synoptic high winds generated by extra-tropical cyclones, at least for return periods of few years.

As two examples of many analysed dates, Figure 5.9 and Figure 5.10 present results obtained from the study of two meteorological phenomena that produced high wind events over many of the analysed stations, and affected great part of Uruguay, driven by some of the meteorological phenomena recognised as typical causes for the occurrence of high winds in the country.

In these figures, the maximum wind gust speed from UTE database interpolated at 45m height that was reached during each date at each station is presented, together with its time of occurrence, wind direction and temperature. The modulus of the wind direction arrow represents the value of the wind gust speed; and its colour, the value of the temperature in °C. The corresponding scale for the temperature is shown in the colour bar to the right of each figure.

Figure 5.9 illustrates some of the main characteristics of the already mentioned passage of an intense and organised cold front over Uruguay between 4th and 5th of April, 2012. It can

be seen in this figure that its trajectory was approximately from southwest to northeast, entering the country at its southwest on April 4th, 2012 around 21:40h (local time) and leaving it on April 5th around 4:50h at its northeast, thus affecting different areas of Uruguay along 7h.

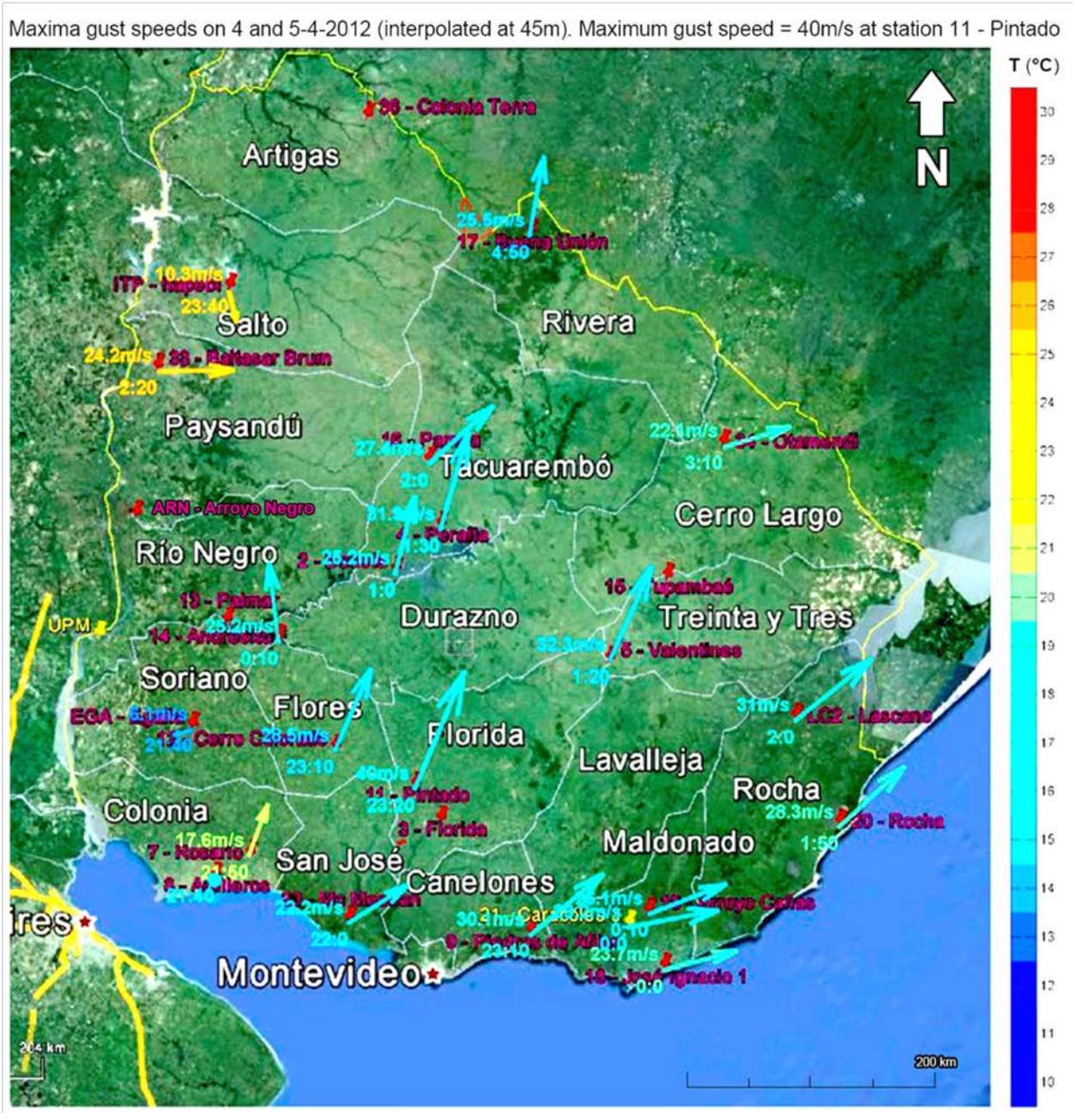


Figure 5.9 Maximum wind gust speed registered at each station during the passage of a cold front during April 4th and 5th, 2012 (*)

(*) This figure presents the maximum value of the wind gust speed registered at each station of UTE along the 4th and 5th of April, 2012, together with its corresponding time of occurrence, wind direction, and temperature (shown in the colour bar)

With this figure and the animated sequence of figures obtained from UTE and GOES satellite images databases, the translational speed of this system was estimated around 60km/h (17m/s).

The maximum wind gust speed interpolated at 45m height along those days corresponded to 40m/s at station 11-Pintado, at 23:20h local time. Figure 5.5(b) showed the gust and 10min mean wind speed, temperature and wind direction registered at this station during this high wind event. The maximum wind gust speed of 45.1m/s indicated in this last figure is the highest wind gust registered by UTE network of stations during the analysis presented in this chapter, and it was measured at a height of 86m.

Analysing the animated sequence of figures generated with information from UTE and GOES satellite images databases, as well as after looking at the time of occurrence of the maximum wind gust shown for each station in Figure 5.9, it could be seen that the cold front moved in the form of a line oriented northwest-southeast, with its trajectory perpendicular to this orientation. It was observed that during its passage, the maximum wind gust speed at a particular station occurred simultaneously with drop in temperature, as the modulus and colour of the arrows changed simultaneously.

Looking at Figure 5.9, it can also be concluded that the maxima wind gusts in all the stations came mostly from the southwest quadrant, with values from 20 to 40m/s, and that the highest wind gust speeds took place in the centre of the country. The direction of translation of this system and that of its highest wind gusts is also in agreement with the directions cited by different authors for cold fronts and squall lines affecting this region (Schwarzkopf and Rosso, 1993; Celemín, 1984).

After its passage, the wind speed decreased fast, generating peaks in the registers of wind gust speeds more or less pronounced, and the temperature stayed low for at least 5h (as seen in e.g. Figure 5.5(b)).

In some other cases of intense organised convection, after a sudden increase, wind gust speeds stayed high during longer periods, with wind gust evolution with time as that shown by Figure 5.6(a) and Figure 5.8.

On the other hand, Figure 5.10 shows the main characteristics associated to the passage of the already mentioned strong extra-tropical cyclone over Uruguay on September 19th, 2012, as seen by UTE stations. The analysis of the spatial evolution of the wind gust speeds registered at each station with an animated sequence of images every 10min was compatible with the passage over Uruguay of an extra-tropical cyclone from northwest to southeast. Its trajectory could also be verified with synoptic charts (CPTEC/INPE, 2012). Figure 5.10 shows a summary of this analysis, indicating the maximum wind gust and corresponding wind direction measured at each station on that day, and illustrates that the highest wind gusts were organised in cyclonic streamlines, as expected for an extra-tropical cyclone, where the winds are relatively parallel to the isobars, and rotate clockwise in the SH.

Figure 5.10 additionally shows that the passage of this extra-tropical cyclone affected the whole country, as all the stations registered their highest wind gusts with values higher than 25m/s. It also illustrates that its passage took around 9.5h, as the first highest wind gust was measured at 9:30h (local time) in the northwest of the country, and the last highest wind gust was measured near 19:00h in the southeast.

Some of these characteristics could also be noticed looking at animated sequences of infrared images from GOES 12 satellite (CPTEC/INPE, 2012). Taking the animated sequences of images from UTE and GOES into account, the translational speed of this system was roughly estimated as 50km/h (14m/s). This value is in good agreement with results presented in Sinclair, 1995, which estimated an average translational speed for extra-tropical cyclones (during their stages of cyclogenesis and maturity) of 13m/s.

The pattern of intensification of wind speed during the passage of this extra-tropical cyclone over Uruguay corresponded to the typical behaviour of strong extra-tropical cyclones in this region described by e.g. Seluchi, 1995 and cited in Sub-section 2.2.5.2, as they usually move to the southeast and intensify along its trajectory. Wind speeds also tend to be stronger along the coast and to the southeast of the country, characteristics also shown by the winds generated by this extra-tropical cyclone.

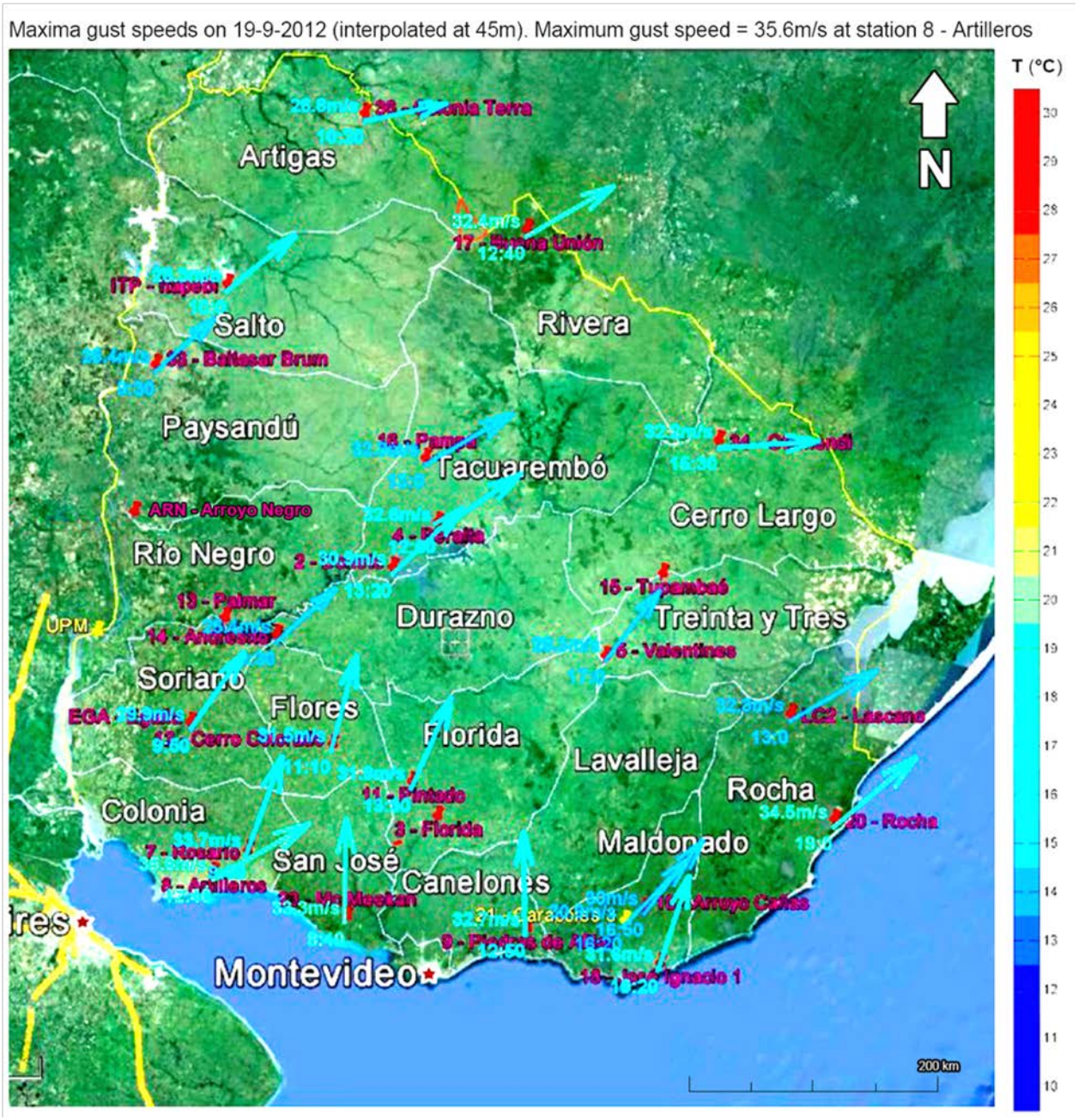


Figure 5.10 Maximum wind gust speed registered at each station during the passage of an intense extra-tropical cyclone on September 19th, 2012 (**)

(**) This figure presents the maximum value of the wind gust speed registered at each station of UTE on September 19th, 2012, together with its corresponding time of occurrence, wind direction, and temperature (shown in the colour bar)

In this case, the highest wind gust speed calculated at 45m height in the stations from UTE network corresponded to 128km/h (35.6m/s) at station 8-Artilleros at 12:40h, with a direction from the SW. This station is located few kilometres from the coast in the south western area of Uruguay.

Figure 5.11 shows the time evolution of the gust and 10min mean wind speed, temperature and wind direction 5h before and 5h after the maximum wind gust was registered at this station.

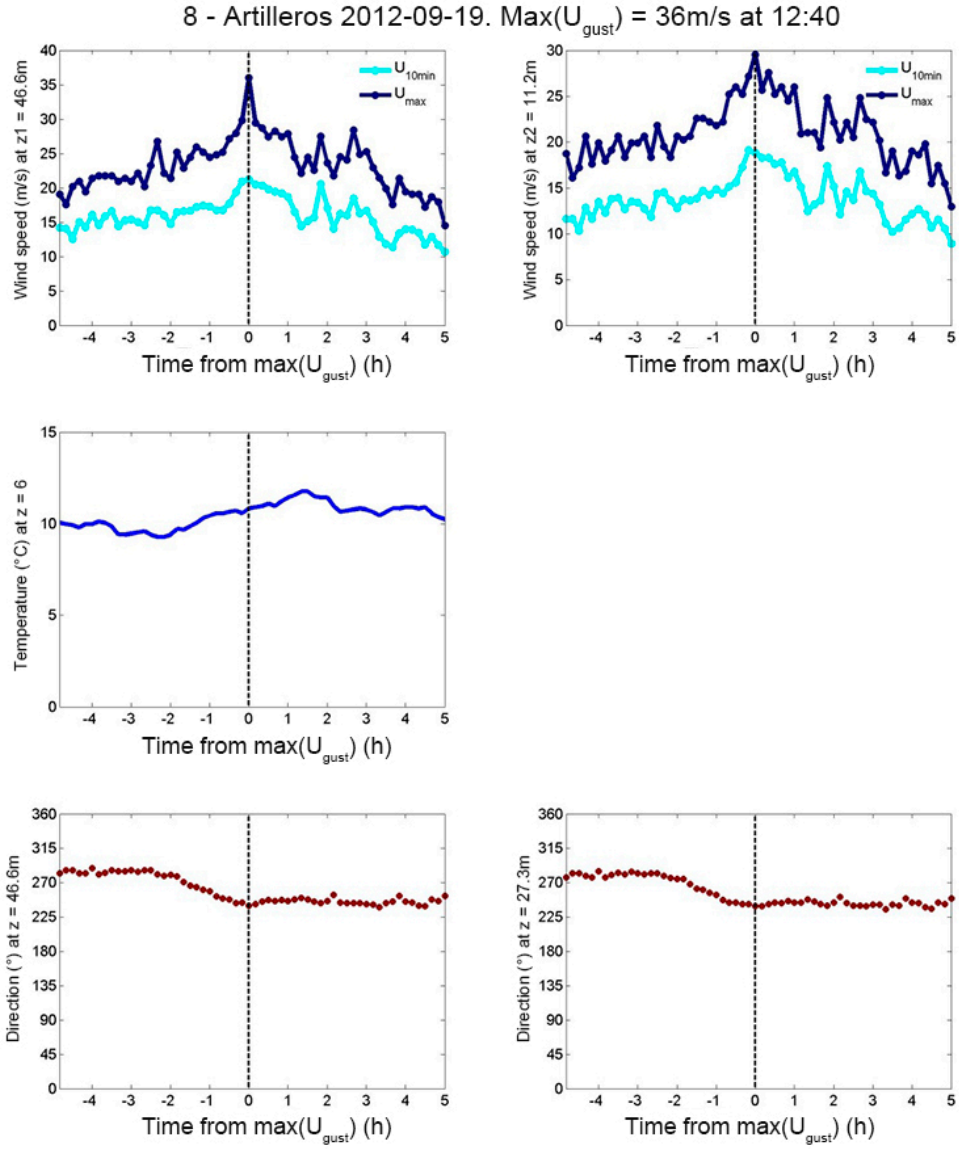


Figure 5.11 Wind speed, temperature and direction evolution at the station that registered the highest wind gust in Uruguay during the passage of the intense extra-tropical cyclone of September 19th, 2012

The maximum wind gust at this station was registered at its maximum measurement height, 46.6m. Variations in wind speed, wind direction and temperature were much more gradual than those presented in Figure 5.5 and Figure 5.6, as already mentioned.

The second highest wind gust at 45m height registered by the network of UTE during the passage of this extra-tropical cyclone corresponded to 124km/h (34.5m/s) at station 20-Rocha at 19:00h, with a direction also from the SW. This station is located in the south eastern region of the country, also few kilometres from the coast. It was thus verified that this extra-tropical cyclone produced higher wind gust speeds along the Uruguayan coast, not only in the southeast of the country, but also along its southwestern coast.

SW and S directions are usually quoted in the literature as the wind directions from where the highest winds are expected during the passage of intense extra-tropical cyclones in Uruguay (Vieira, 1969; Celemín, 1984).

Figure 5.10 and the animated sequence of figures from UTE corresponding to that date seemed to indicate that the highest wind gust measured at Rocha station at 19:00h occurred after the centre of this extra-tropical cyclone left land. This was verified looking at synoptic charts from CPTEC/INPE, 2012.

Analysing the highest wind gust speeds calculated at 45m height for each station, it could be concluded that the lowest of these values corresponded to stations 14-Andresito and 33-B. Brum, with values of 91km/h (25.4m/s) in both cases. These stations are located in the centre western area of Uruguay, as Figure 3.1 shows, and their maximum wind gusts were registered around 9:00h. From the analysis of UTE database it could also be seen that $U_{gust\ 45m} \geq$ 80km/h started to be measured at these stations between 5:00 and 7:00h. On the other hand, at the northwest of the country $U_{gust\ 45m} \geq$ 80km/h started to be registered around 1:00h.

For the two weather systems illustrated in Figure 5.9 and Figure 5.10, the analysis of the time evolution of wind gust speeds, wind directions and temperature during their passage, with a temporal resolution of one image every 10min and data from 25 stations, allowed a good description of the type of meteorological phenomenon that was affecting the country.

During the passage of the extra-tropical cyclone illustrated in Figure 5.10 well as in other analysed cases not shown in this thesis, high wind speeds were sustained during several hours at each station. The maxima wind gust speeds came from the southwest quadrant, in the analysed case corresponding to values between 25 and 36m/s with the highest ones registered along the coast and to the southeast of the country.

It could also be noticed that during the passage of cold fronts over the country as illustrated by Figure 5.9 the maxima wind gust speeds registered at most stations also tend to come from the southwest quadrant.

d) Analysing only wind gust data series from complete years, which corresponded to a database 696 months long, and identifying events with wind gust speeds interpolated at 45m height ($U_{gust\ 45m}$) higher than 80km/h for each station, 558 high wind events were found in the registers of the network of stations of UTE.

From this analysis, similar conclusions as those described in **a)** could be derived, i.e., most of the high wind speed events presented sudden increase in wind speed accompanied by temperature drop and wind direction shift, and in these cases, gust and 10min mean wind speeds showed similar time evolution at different heights, with higher gust factors usually occurring during the 10min interval when the highest wind gust was measured.

Also, similar conclusions to those mentioned in **b)** can be inferred in relation to the behaviour during these events of the wind gust speed the wind direction and temperature near the time the highest wind gust speed was registered; in relation to the typical wind directions registered when the highest wind gust speeds took place, and in relation to the presence of intense convective activity over Uruguay during most of these events. Significant drops in temperature were also a frequent characteristic, and in every station, the events that presented the highest wind gusts corresponded to conditions of intense convective activity.

Events with $U_{gust\ 45m} \geq$ 80km/h that corresponded to synoptic high winds, as due to the passage of intense extra-tropical cyclones, or those related to special synoptic weather patterns that generate high winds, also presented lower $U_{gust\ 45m}$ and accounted for fewer

cases of high wind events than those related to convective activity. It could also be noticed that in these cases convective activity seemed to be less intense or that it was not present at all at the time highest wind gusts were registered.

For every station, the order of the events according to their highest wind gusts could change a little when sorting them by the highest wind gust interpolated at 45m height, but at the end, the detected trends and conclusions were similar to the previous ones.

In all the analysed stations, it was found that non-synoptic high winds, mostly related to the presence of intense convective activity caused the highest wind gust speeds until certain wind gust speed value. Below that value, synoptic high wind events started to appear, in combination with non-synoptic high winds. For example, out of the 36 events with $U_{gust\ 45m} \geq$ 80km/h identified for station 11-Pintado, the ten highest $U_{gust\ 45m}$ were non-synoptic events that presented characteristics that corresponded with the occurrence of intense convective activity, while the 11th highest $U_{gust\ 45m}$ corresponded to a synoptic high wind event. From this event onwards, synoptic and non-synoptic high wind events were identified. The same applies to the results obtained from the analysis described in **a)** for this station.

The events that presented high $U_{gust\ 45m}$ at this station, during complete years of analysis, are presented in Annex A.3, starting at the 11th highest wind gust speed. As illustrated in this annex, along the 4 years of records analysed for this station, 36 events with $U_{gust\ 45m} \geq$ 80km/h were identified.

From the figures shown in Annexes A.2 and A.3, the main differences between synoptic and non-synoptic high wind events can also be clearly noticed. Synoptic high wind events present relative steady wind direction, temperature, and gust factor values, the latter being usually between 1.2 and 1.5 (defined over 10min) at 45m height for the stations analysed during this research. Although gust factor values vary with height, it was found that for the range of heights of the analysed stations, i.e., between 10 and 90m, synoptic high wind events typically presented gust factors values, within those quoted at the 10min interval when the highest wind gust was measured, with higher values at the lower heights. The gust factor values identified for synoptic high wind events in this research would be a bit lower than those suggested in Sub-section 2.2.1 from the results of Choi, 1999 and Choi,

2000, and consistently lower than those presented by the non-synoptic high wind events identified during this research.

On the other hand, in most of these synoptic events, gust and 10min mean wind speeds increased with height, i.e., they did not present a maximum at an intermediate height, while during the non-synoptic events, the highest wind gust speed could be measured at an intermediate height.

Typical examples of synoptic high wind events at station 11-Pintado are Events 13, 16, 25 and 31 shown in the pages A.24, A.27, A.36 and A.42 of Annex A.3. These events presented wind directions from the W, S, W and S, respectively.

The dominance of non-synoptic over synoptic high winds, in relation to their higher wind gust speed values and frequency of occurrence, can be appreciated from the figures shown in Annexes A.2 and A.3. As all the stations presented this behaviour, it can be concluded that although Uruguay would be in a region that presents a mixed extreme wind climate, i.e., extreme winds are generated by different meteorological types of events, the greatest influence of convective activity both in wind gust speed values and in frequency may allow conducting a statistical analysis without separation of storm types, as indicated by Holmes et al., 2005b and cited in Section 2.5. This hypothesis should be verified, though.

Reports on measurements of high winds in Uruguay 100 years ago already suggested that intense convective activity caused higher wind speed values and with more frequency than synoptic winds (Morandi, 1901 - 1917).

The figures from these annexes also show that during high wind events, increases in temperature, are not as common as decreases in temperature, and tend to produce lower wind gust speed values, as for example Event 35 shown in page A.46 of Annex A.3. This corresponds with the observation of Celemín, 1984 that cold fronts produce higher wind gusts than warm fronts.

From Annex A.2 and A.3, it can also be noticed that non-synoptic high wind events may produce their highest wind gust speeds within a wide range of values. In the case of station 11-Pintado, these values spanned from 45m/s to the threshold of 22.2m/s selected for this analysis.

Analysing the figures shown in Annex A.3, it could be verified that the interpolation of gust and 10min mean wind speeds at 45m height, shown in the bottom right graph of the first figure of each event, seems to adequately represent the analysed events.

e) As indicated in **e)** of the previous sub-section, the characteristics of the highest wind gust events were summarised in bar graphs and wind roses for each station. The events characterised were those that presented wind gust speeds interpolated at 45m height ($U_{gust\ 45m}$) higher than 80km/h, i.e., 22.2m/s, along the complete years indicated by Table 3.1. The analysed periods are also shown in the title of each graph.

As an example, the graphs for station 11-Pintado are indicated in Figure 5.12(a)-(d). For this station, the analysed period comprised from July, 2008 to June, 2012, as shown in the titles of these graphs.

Figure 5.12(a) illustrates the frequency of occurrence of the events with $U_{gust\ 45m} \geq$ 80km/h along the 4 years analysed, according to the value of their highest wind gust. In this graph, the abscissa axis shows $U_{gust\ 45m}$ in km/h, while the ordinate axis indicates the frequency of occurrence in percentage. It can be seen that the maximum $U_{gust\ 45m}$ corresponded to a value between 140 and 150km/h (38.9 and 41.7m/s).

Annex A.3 shows that station 11-Pintado registered 36 events with $U_{gust\ 45m} \geq$ 80km/h during this period, thus, from Figure 5.12(a), it is possible to calculate the number of events corresponding to each wind gust speed category. As 2/36 = 5.6%, there would be 2 events with $U_{gust\ 45m}$ between 140 and 150km/h in this station along the 4 years of measurement, and 2 other events with $U_{gust\ 45m}$ between 130 and 140km/h (36.1 and 38.9m/s). The number of events along the 4 years that presented $U_{gust\ 45m}$ between 80 and 90km/h (22.2 and 25m/s) would be around 15 (15/36 = 41.2%). This can be verified looking at the figures presented in Annex A.3.

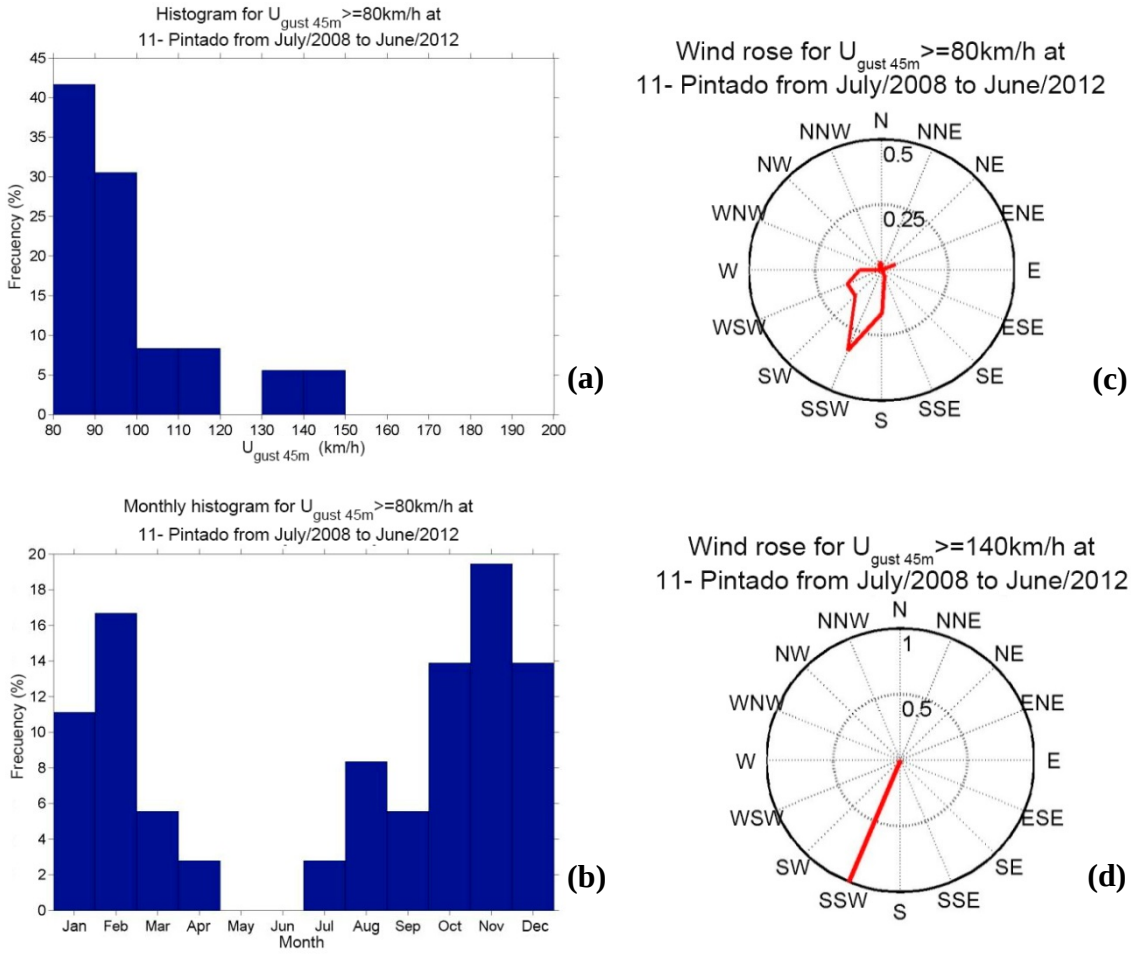


Figure 5.12 Characteristics of high wind gust events at 45m at station 11-Pintado

Also, from Annex A.2 and A.3, it can be easily seen that more than 10 events related to intense convective activity and matching the characteristics associated with the occurrence of strong outflow boundaries associated with deep convection (e.g. downdraft outflows, gust fronts and others) were registered at this station in a period of 4 years. This number would yield a frequency of around 2.5 non-synoptic high wind events per year.

On the other hand, Figure 5.12(b) describes the seasonal distribution of the events with $U_{gust\ 45m} \geq$ 80km/h registered at station 11-Pintado. The months are presented in the abscissa axis ordered from left to right, the first corresponding to January and the last one to December. This graph clearly shows the high seasonality of the events with the potential of generating damaging wind gust speeds, and that they occurred more frequently from

October to February, with a main peak in November and a secondary peak in February in this station. Analysing this graph, it can be concluded that around 50% of these events took place in spring (from October to December), and about 30% between January and February, while May and June presented the lowest frequency.

These results are consistent with those of many researchers who have studied seasonal characteristics of severe convective activity in SESA. As shown in paragraph **b)** of this sub-section, most of the high wind events identified at the network of stations occurred during intense convective activity over the country, thus, it is reasonable that the seasonal behaviour of the analysed events resembles that of severe convection in the region.

For example, results from Zipser et al., 2006 shown in Figure 2.31 in Sub-section 2.2.4.2 suggest that most extreme convective events in this region would tend to occur more frequently from September to November, followed by the months from December to February. On the other hand, Laing, 2003 indicated that squall lines would be more frequent in spring and summer, while Velasco and Fritsch, 1987 found that most MCCs would occur from November to April. This seasonal behaviour would be explained by the fact that the LLJS described in Sub-section 2.2.4, which favours the development of MCSs in this region, would be strongest in summer and spring. Velasco and Fritsch, 1987 found a maximum of MCCs occurrence in November, which coincides with the month with more high wind events registered at Pintado station.

For north eastern Argentina, Natalini et al., 2011 indicates that damaging winds are almost always caused by severe convective activity, mostly produced by MCCs and by the passage of either cold fronts or squall lines, with 56% occurring in spring and 35% in summer, as presented in Sub-section 2.2.4.2. These figures are in close agreement with those found for Pintado and presented in Figure 5.12(b). Also for Argentina, Schwarzkopf and Rosso, 1993 found that severe convective activity mostly takes place between October and March, similar to the monthly distribution shown by Figure 5.12(b).

In addition, Figure 5.12(c) and Figure 5.12(d) show the wind rose for the 558 events that presented $U_{gust\ 45m} \geq$ 80km/h, and the wind rose for those events with $U_{gust\ 45m} \geq$ 140km/h (38.9m/s), respectively. It can be concluded from Figure 5.12(c) that the great majority of the events with $U_{gust\ 45m} \geq$ 80km/h presented wind directions from the SW quadrant,

especially from directions around the SSW. During the analysed period, around 33% of these events came from the SSW; 22%, from the S; approximately 14%, from the SW, and a similar percentage, from the WSW. The W accounted for around 8% of the cases, while the ENE represented 5% of the cases, and the N, around 2%.

The seasonal behaviour of the highest wind gusts and other previous observations made on the analysis of wind gusts measured by the UTE network, suggest that non-synoptic winds are the most frequent damaging winds registered at any station in Uruguay, and in particular, intense convective activity generating flows with characteristics resembling the occurrence of strong outflow boundaries associated with deep convection would be the direct cause of these high winds.

It is worth mentioning that information on wind direction distribution, as that offered by Figure 5.12(c) and Figure 5.12(d), does not allow differentiating between synoptic and non-synoptic winds, as e.g. an intense extra-tropical cyclone, the most common synoptic meteorological event identified in the literature as responsible for producing high winds in Uruguay, typically generate their highest wind speeds from the southwest quadrant, as severe convective activity usually does, too. The same occurs with the fast entrance of a cold air mass, another synoptic event identified during this research es producing damaging wind gust speeds in Uruguay, usually from the south.

In Figure 5.12(d) it can be seen that all the events with $U_{gust\ 45m} \geq$ 140km/h (38.9m/s) at Pintado station presented a wind direction from the SSW. According to Figure 5.12(a), 2 events of this type would have been registered at Pintado, as commented before.

The same analysis illustrated for station 11-Pintado was conducted for the rest of the stations, yielding quite similar results.

f) As indicated in paragraph **f)** of the previous sub-section, the results obtained from the analyses of all the stations, as that shown for Pintado, were summarised in bar graphs and wind roses, which would describe the typical characteristics of the events that present $U_{gust\ 45m} \geq$ 80km/h in Uruguay. These results are shown in Figure 5.13(a)-(d).

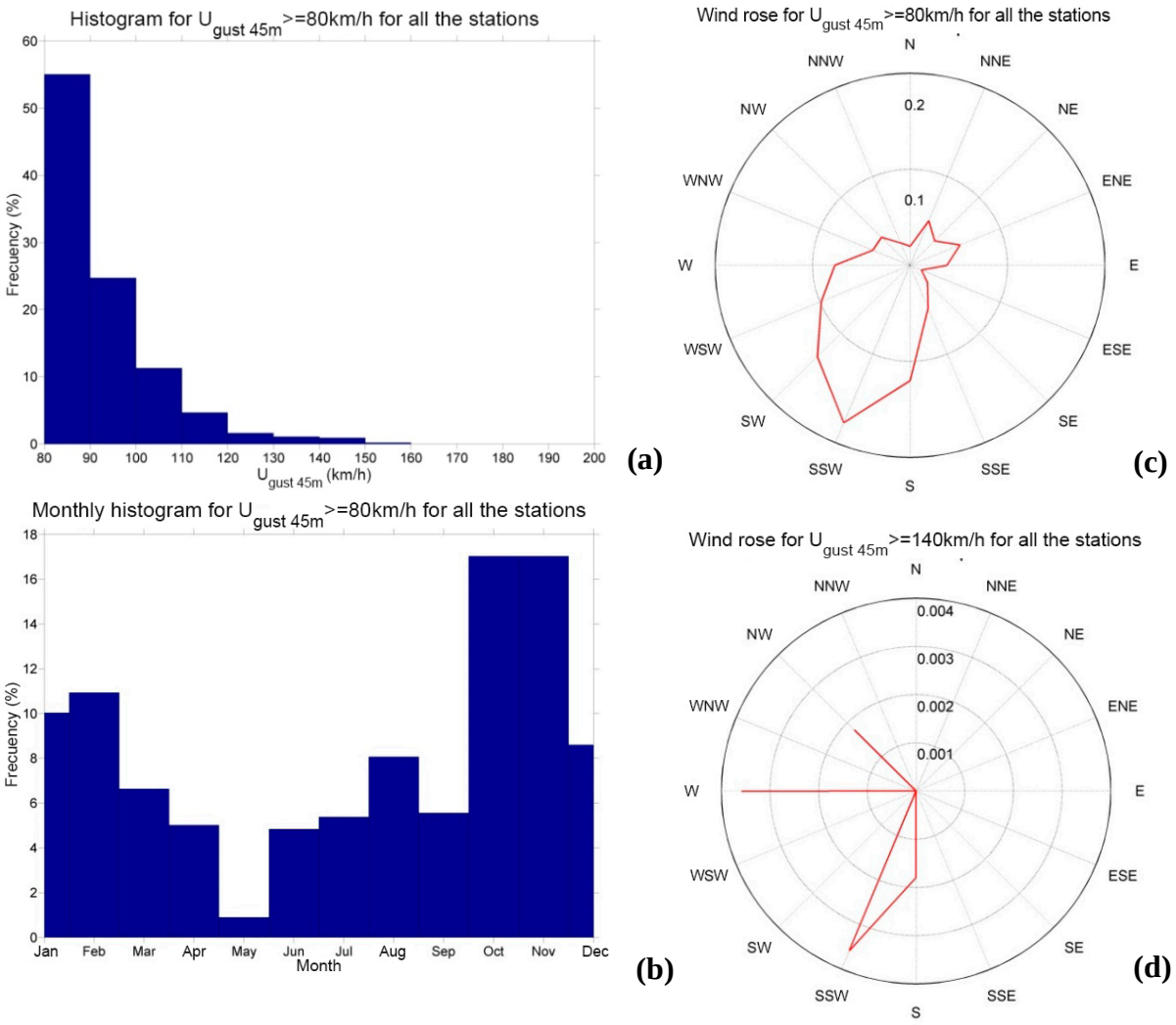


Figure 5.13 Characteristics of high wind gust events at 45m height in the network

Figure 5.13(a) shows the frequency of occurrence, according to the value of their $U_{gust\ 45m}$, of the 558 events with $U_{gust\ 45m} \geq$ 80km/h from all the stations of the network of UTE that had measured at least during a whole year. As in Figure 5.12(a), this figure shows in the abscissa axis different categories for $U_{gust\ 45m}$ in km/h, while the ordinate axis indicates their corresponding frequencies in percentage.

Looking at Figure 5.13(a), it can be seen that around 20% of these events presented $U_{gust\ 45m} \geq$ 100km/h (27.8m/s), i.e., 0.2x558=112 events, from a register corresponding to 696 months, which would yield an average of around 2 events per year per station presenting $U_{gust\ 45m} \geq$ 100km/h, most of them related to intense convective activity, as suggested

before. The maximum $U_{gust\ 45m}$ from the whole network during the analysed periods corresponded to a value of 42m/s (150km/h) and was registered at station 5-Valentines. Similar values corresponded to station 4-Peralta (41.4m/s) and 14-Andresito (41.2m/s). $U_{gust\ 45m} \geq$ 130km/h (36.1m/s) also occurred several times in one or more stations since the network started operating, as shown in Figure 5.13(a).

As in **e)**, Figure 5.13(b) describes the monthly distribution of these 558 events, where the months are identified as in Figure 5.12(b). The high seasonality of these events is again clearly shown. The months from October to February show a clear higher frequency than the rest of the months, too, with a main peak in October and November, a decrease in December and from that month, an increase until a secondary peak is found in February. May and June are again the months with fewer events, but with many less events in May than in June. Spring would be the season presenting the greatest frequency of occurrence as for station 11-Pintado, in this case representing around 40% of the events. The second season in relation to frequency occurrence would be summer, with 27% of the events. At this point, it is worth reminding that very few stations had been operative during complete years in the northwest of the country by the time the analysis of the database of UTE started, as indicated by Table 3.1 and Figure 3.1.

The seasonal behaviour illustrated in Figure 5.13(b) might be explained with findings of e.g. Salio et al., 2007 that the SALLJS (South American LLJS), which favours the development of MCSs in SESA, presents an intense maximum during spring, and with those from CLIVAR, 2006 that observes that in SA convection shifts gradually northward toward the equator between March and May, and that during April and May, the southward flow of tropical warm and humid air from the Amazonia weakens, as more frequent incursions of drier and cooler air from mid-latitudes begin to occur over the interior of subtropical SA. Maybe May corresponds with a month where intense convective activity has weakened, but other types of high wind events have not started to act as frequently or as intensely as they do during the winter months, as e.g. extra-tropical cyclones or fast intrusions of cold air masses from the south.

On the other hand, Figure 5.13(c) and Figure 5.13(d) show the wind rose for the 558 events presenting $U_{gust\ 45m} \geq$ 80km/h, and the wind rose for the 6 events that presented $U_{gust\ 45m} \geq$ 140km/h (38.9m/s), respectively.

From Figure 5.13(c) it can also be concluded that most of the events with $U_{gust\ 45m} \geq$ 80km/h presented wind directions from the SW quadrant, with the highest frequency corresponding again to the SSW direction. During the analysed period, around 17% of these events came from the SSW; 14%, from the SW; approximately 12%, from the S, and 10% from the WSW. The W accounted for around 7-8% of the cases, while the three directions between the NNE and ENE registered about 12% of these events

Looking at Figure 5.13(d) it can be seen that the events presenting $U_{gust\ 45m} \geq$ 140km/h (38.9m/s) mostly presented directions from the SW quadrant. From the 558 events identified, 6 presented $U_{gust\ 45m} \geq$ 140km/h: one corresponded to an event that occurred with wind from the S; two, from the SSW; two, from the W and one from the NW.

g) The results described in **e)** were also presented over maps of Uruguay, to analyse the geographic distribution of different characteristics of the events with high $U_{gust\ 45m}$ occurring in Uruguay, as outlined in **g)** of the previous sub-section. This is shown in Figure 5.14 and Figure 5.15.

Figure 5.14 characterises the 558 events corresponding to $U_{gust\ 45m} \geq$ 80km/h (22.2m/s) identified in the analysed 696 months database of complete years. In this figure, the modulus of each arrow represents the mean of $U_{gust\ 45m} \geq$ 80km/h for each station, value also indicated in m/s next to each station; its direction, the most frequent wind direction of these events at each station; and their colour, the most frequent month when these events occurred at each station. The bar to the right of this figure indicates the colour corresponding to each month. They are indicated in order, the one in the top corresponds to December, and the bottom one, to January. Another number next to each station indicates the average monthly frequency of the events presenting $U_{gust\ 45m} \geq$ 80km/h at each station.

Figure 5.14 also illustrates the strong tendency for this type of event to occur mostly between October and February, as shown in **f)** for Pintado and in **g)** for the whole country.

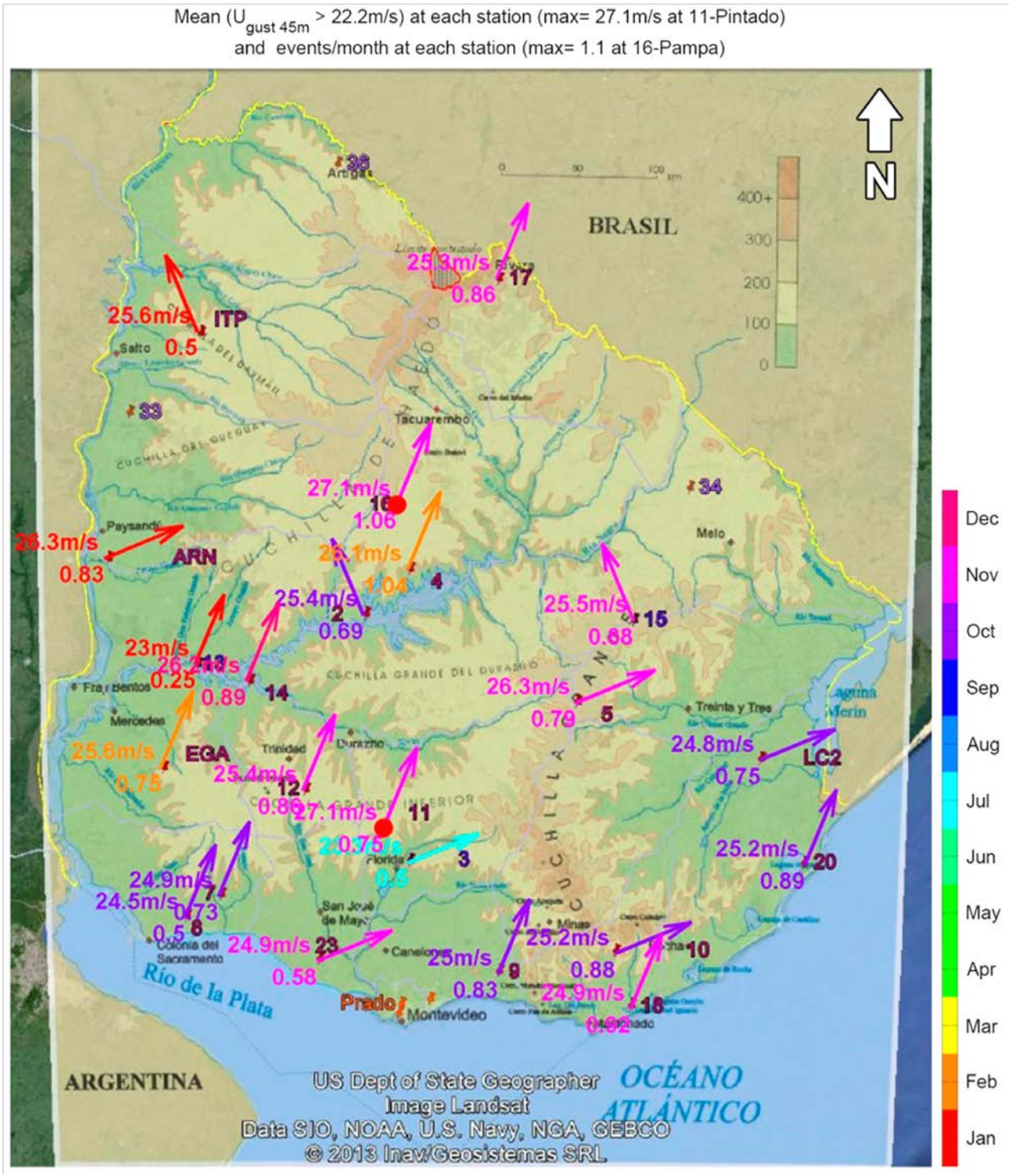


Figure 5.14 Characteristics of events with wind gust speeds > 80km/h at 45m height

Figure 5.12(b) indicated that the most frequent month presenting $U_{gust\ 45m} \geq$ 80km/h at station 11-Pintado was November, in accordance with Figure 5.14. This figure suggests that to the northwest of the country, these events would occur more frequently in summer, especially in January, while to the south and east of the country, spring months would present the highest frequency of occurrence, especially October and November.

In relation to typical wind directions, this figure clearly shows the high predominance of occurrence of high wind gusts from the southwest quadrant, being the SSW the most common wind direction at most stations.

Figure 5.14 also illustrates that the average monthly frequency of events with $U_{gust\ 45m} \geq$ 80km/h during the analysed period was between 0.5 and 1.06 at each station; i.e., in average one wind event with the potential of causing damage (at 45m height) occurred every one to two months at each of the analysed stations. Analysing the available database with complete years until July, 2012, the highest rate of occurrence was found in a central area of Uruguay; in particular, two stations, stations 16-Pampa and 4-Peralta, presented in average one event per month.

It is worth mentioning at this point that just 1 year of meteorological registers was available at that time for the northwest of Uruguay (station 43-ITP as shown in Table 3.1), that stations 40 to 43 were lately found to experience quality data problems, and that due to its particular location, station 17-Buena Unión tended to underestimate high wind events (Decaro, 2015).

On the other hand, during this analysis, it was found that station 13-Palmar exhibited a different behaviour from those of nearby stations, with lower $U_{gust\ 45m}$ and lower number of high wind events per month, and its data was not taken into account for the following analyses.

In a similar way to Figure 5.14, Figure 5.15 characterises the events that presented $U_{gust\ 45m} \geq$ 104km/h (29m/s) in the analysed database. In this figure, the modulus of each arrow represents the mean of the wind gust speeds higher than that threshold for each station, value also indicated in m/s next to each station; the direction of the arrows, the most frequent wind direction of these events at each station; and their colour, the most frequent

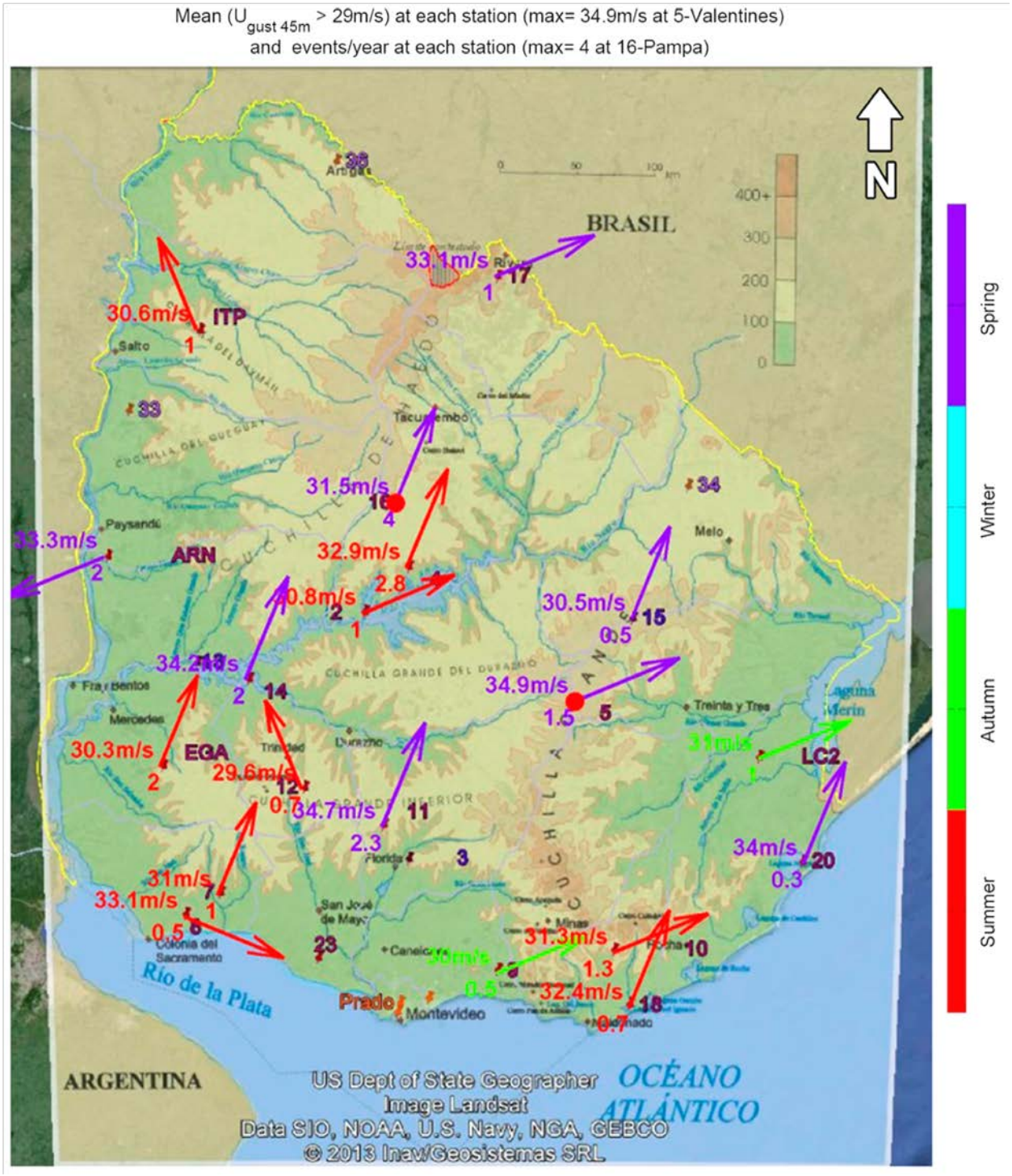


Figure 5.15 Characteristics of events with wind gust speeds > 104km/h at 45m height

season when these events occurred at each station. The bar to the right of this figure indicates the four seasons of the year; corresponding from top to bottom, to spring (considering October, November and December), winter (July, August and September), autumn (April, May and June) and summer (January, February and March).

Figure 5.15 would indicate that these higher wind gust events would occur mostly in summer and spring across the country, with some fewer events in autumn. Comparing this figure with Figure 5.14, it seems that in some areas there would be more high wind events (i.e., $U_{gust\ 45m} \geq$ 80km/h) in spring, but that the most intense events would tend to take place in summer. On the other hand, in the southeast of Uruguay some of the most intense wind gust events took place in autumn during the analysed period. These trends have been confirmed in updated analyses (Durañona, 2015).

Typical wind directions for these higher wind gust events are also from the southwest quadrant, and in particular, from the SSW as before.

In relation to the average annual frequency of occurrence of events with $U_{gust\ 45m} \geq$ 104km/h per station, this value ranged from 0.3 to 4 for each station during the analysed period. The highest rate of occurrence was found again in a central area of Uruguay for the analysed database. In particular, in the same two stations mentioned before, i.e., 16-Pampa and 4-Peralta, the rate of occurrence found was highest, registering in average around 3 to 4 of these events per year. More recent analyses of new stations installed in the northwest of Uruguay have confirmed these general comments, yielding annual frequencies between 3 and 4.5 for these events in the northwest of the country, as shown in Figure 2 of Durañona et al., 2015, not reproduced here.

h) Values of gust factors at 10m height were calculated at all the stations of the network that had anemometers installed at that height. These stations were: 4-Peralta, 5-Valentines, 7-Rosario and 8-Artilleros. Gust factors were calculated for the events that presented wind gust speeds at 10m height ($U_{gust\ 10m}$) higher than 80km/h (22.2m/s); for those that presented $U_{gust\ 10m} \geq$ 104km/h (29m/s), and for the highest $U_{gust\ 10m}$ measured at each station. The gust factor was calculated for each event as the maximum wind gust speed registered at 10m height

during the event, divided by the 10min mean wind speed registered at 10m height during the same 10min interval.

The events with $U_{gust\ 10m} \geq$ 80km/h presented gust factors ranging from 2 to 2.5, with a mean value of 2.2. The second type of event had gust factors between 1.8 and 2.9, with an average value of 2.3, while the highest $U_{gust\ 10m}$ measured at all the stations presented gust factors between 1.5 and 3.8, with a mean value of 2.6.

From these results, it could be observed that there would be a trend for events with higher $U_{gust\ 10m}$ to present higher gust factors in average, with increasing variability in their values. These results might be explained by the fact that high wind events of smaller scale tend to present higher wind speed values, as indicated in Sub-section 2.2.1, and would therefore produce higher gust factors. As shown in that sub-section, events with higher gust factors have a more frequent convective origin, and according to Wieringa, 1973 convective gusts and their corresponding 10min mean wind speeds would not have a consistent physical link; thus it seems reasonable that the correlation between the highest wind gusts and their corresponding 10min mean wind speeds is smaller, and therefore, that their gust factors present a wider range of values.

The comparison between these gust factor values and those estimated from Choi, 1999 and Choi, 2000 suggest that the three types of analysed high wind events registered at 10m height would mainly have a convective origin. This was also verified in many of these cases looking at GOES satellite images during those events and/or analysing the characteristics of the simultaneous behaviour of wind speed, wind direction and temperature.

On the other hand, there were six events that presented $U_{gust} \geq$40m/s (144km/h) in the analysed database. These wind gust values were registered at least at two heights during these events. Two of them occurred in station 11-Pintado, two in station 5-Valentines, while another event took place in station 4-Peralta, stations that had four years long data series. The other event was registered in station 14-Andresito, with three years of data available for analysis. As Figure 3.1 shows, these sites are located in the southern centre of Uruguay.

These stations have measurements heights between 10 and 87m, and in five of these six events, the wind gusts registered at all heights were higher than 40m/s, being the highest recorded values 45m/s (162km/h) at 86m height at station 11-Pintado as previously mentioned, and 43m/s at 74.5m and at 76.5m height at stations 4-Peralta and 5-Valentines, respectively. Of these four stations, Peralta and Valentines were the only ones that had anemometers installed at 10m height, as indicated in Table 3.1. During the highest event registered in Valentines, a wind gust speed of 40m/s was measured at 10m height, while the event in Peralta registered 39m/s at 10m height.

Finally, data series from stations with anemometers installed at 10m height were analysed to verify that the events presenting $U_{gust\ 10m} \geq$ 80km/h, would have characteristics similar to those found for the events that presented high $U_{gust\ 45m}$. The events at 10m height were identified from spread sheets generated as indicated in paragraph **a)** of the previous sub-section, which contained information of all the events at each station that registered wind gusts higher than 80km/h at any height.

It was found that the characteristics already described for events with $U_{gust\ 45m} \geq$ 80km/h also applied to those with $U_{gust\ 10m} \geq$ 80km/h. The most important conclusion from this analysis is that intense convective activity would also cause the highest wind gust speeds at 10m height.

5.6. Analysis of high 10min mean wind speeds

After the analysis presented in Section 5.5, it was decided to investigate if the highest 10min mean wind speeds would also be mainly caused by intense convective activity, or if events of higher temporal (or length) scale, such as the synoptic events described in Sub-section 2.2.5.2, would be predominant.

5.6.1. Methodology

In order to analyse the events that produced the highest 10min mean wind speeds in Uruguay during the measurement periods indicated in Table 3.1, 10min mean wind speed data series of

each station were again homogenised as in Section 5.5, linearly interpolating at 45m height and studying only complete years.

In this case, the threshold 10min mean wind speed selected for analysis was 60km/h (16.7m/s), and all the events that presented 10min mean wind speed at 45m height ($U_{10min\ 45m}$) higher than that value at each station of the network were analysed. This value was selected under the hypothesis that if the highest 10min mean wind speed values were caused by flows of ABL type, the relationship between gust and 10min mean wind speeds would be expected to be roughly around 1.3, as suggested by results from the previous section, and expected for ABL flows over rural terrains. Therefore, if wind gust speeds of 80km/h represent a threshold for damaging wind events, and they are caused by flows of ABL type, 60km/h would be the 10min mean wind speed corresponding threshold for damaging wind events.

In this sub-section, a high wind event will thus be considered as that with $U_{10min\ 45m} \geq$ 60km/h.

The specific analysis of the events presenting $U_{10min\ 45m} \geq$ 60km/h was carried out following similar methodologies as those described in paragraphs **d), e)** and **f)** of Sub-section 5.5.1.

5.6.2. Results

In a first stage, analogous graphs to the ones presented in Annex A.3 were obtained for the events that presented $U_{10min\ 45m} \geq$ 60km/h at each station. The ones corresponding to station 11-Pintado are shown in Annex A.4.

Looking at figures from different stations, several characteristics could be identified.

Perhaps, one of the most important results was that, although at every station the highest events with $U_{10min\ 45m} \geq$ 60km/h were non-synoptic and presented characteristics typically related to the occurrence of intense convective activity, a higher frequency of occurrence of this type of event was found in the northwest of Uruguay than in its southeast.

In general, the stations located in the northwest and in the centre of Uruguay registered their highest $U_{10min\ 45m}$ events in association with temperature drops and variations in wind direction. Many of these cases presented characteristics similar to those of Figure 5.6(a), but

events similar to those illustrated in Figure 5.6(b) were also found. Also, more cases associated with temperature increases, i.e., increase in wind speed simultaneously occurring with increase in temperature and wind direction change, were identified during this analysis than in that carried out on the highest wind gust speed events, presented in Section 5.5.

For the whole country, the most common non-synoptic wind events with high $U_{10min\ 45m}$ related to severe convection were also similar to those presented in Figure 5.5(b) and Figure 5.6(a), followed by those similar to Figure 5.6(b).

Analysing the figures of station 11-Pintado shown in Annex A.4, it can be noticed that the 5 highest 10min mean wind speed events measured along 4 years would present characteristics compatible with the occurrence of outflow boundaries associated with deep convection, i.e., fast increases of wind gust speeds temperature drops, variations in wind direction and some more abrupt than others. These characteristics were shared with most of the highest $U_{10min\ 45m}$ cases for the stations located in the northwest and in the centre of the country. For station Pintado, for example, the first three cases along 4 years of measurements corresponded to abrupt and significant temperature drops.

On the other hand, in the analysed database, synoptic high wind events appeared more frequently in the events with high 10min mean wind speeds than in those with high wind gust speeds, as expected.

Synoptic high wind events also appeared earlier. For example, for Pintado, the 6th case of those presenting $U_{10min\ 45m} \geq$ 60km/h corresponded to a synoptic event, as shown in Annex A.4, while for the events with $U_{gust\ 45m} \geq$ 80km/h, indicated in Annex A.3, the first synoptic high wind event had been registered as the 11th event.

The previous results suggest that intense convection would tend to generate the highest 10min mean wind speeds in the northwest and centre of the country, while the southeast should be analysed with more detail to arrive at conclusions on the type of wind event that dominates its extreme 10min mean wind speed, as more high wind events with higher temporal (or length) scales would be expected in the southeast than in the northwest of the country.

It was found that several synoptic high $U_{10min\ 45m}$ events were related to the passage of extra-tropical cyclones, others to fast intrusions of cold air masses from the south, while other types of synoptic high wind events would need further analysis in order to be classified.

In addition, it was observed that several high $U_{10min\ 45m}$ events related to decreases or increases in temperature had higher time scales, -i.e., more gradual decreases or increases in temperature associated with more gradual increases in wind speed-, than those identified as high $U_{gust\ 45m}$ presenting decreases or increases in temperature.

In a second part of this analysis, the events with $U_{10min\ 45m} \geq$ 60km/h that took place at each station were characterised with bar graphs and wind roses, indicating their wind speed, seasonal and wind direction distributions for each corresponding analysed period.

The results for station 11-Pintado are presented in Figure 5.16.

Figure 5.16(a) illustrates the frequency of occurrence (in %) of the events with $U_{10min\ 45m}$ ≥60km/h for different values of their 10min mean wind speed (in km/h) along the analysed 4 years of this station. It can be seen that the maximum $U_{10min\ 45m}$ corresponded to a value between 90 and 95km/h (25 and 26.4m/s).

Figure 5.16(b) describes the monthly frequency of occurrence of these events for Pintado. This graph shows that the most frequent occurrence was from October to February, during the analysed period, with a distinctive peak in October. Spring and summer were the seasons with more number of these events. As this seasonal distribution approximately resembles that of severe convection in SESA, as described in Sub-section 5.5.2, this may suggest that intense convective activity would also dominate the extreme 10min mean wind speed climate around Pintado station. However, spring clearly predominated over summer: around 51% of the cases occurred in spring, compared with nearly 23% in summer. Comparing these results with those shown in Figure 5.12(b), it can be observed that spring presents a frequency of events similar to that of Figure 5.12(b), but that in Figure 5.16(b) there are relatively less events in summer, and more in winter.

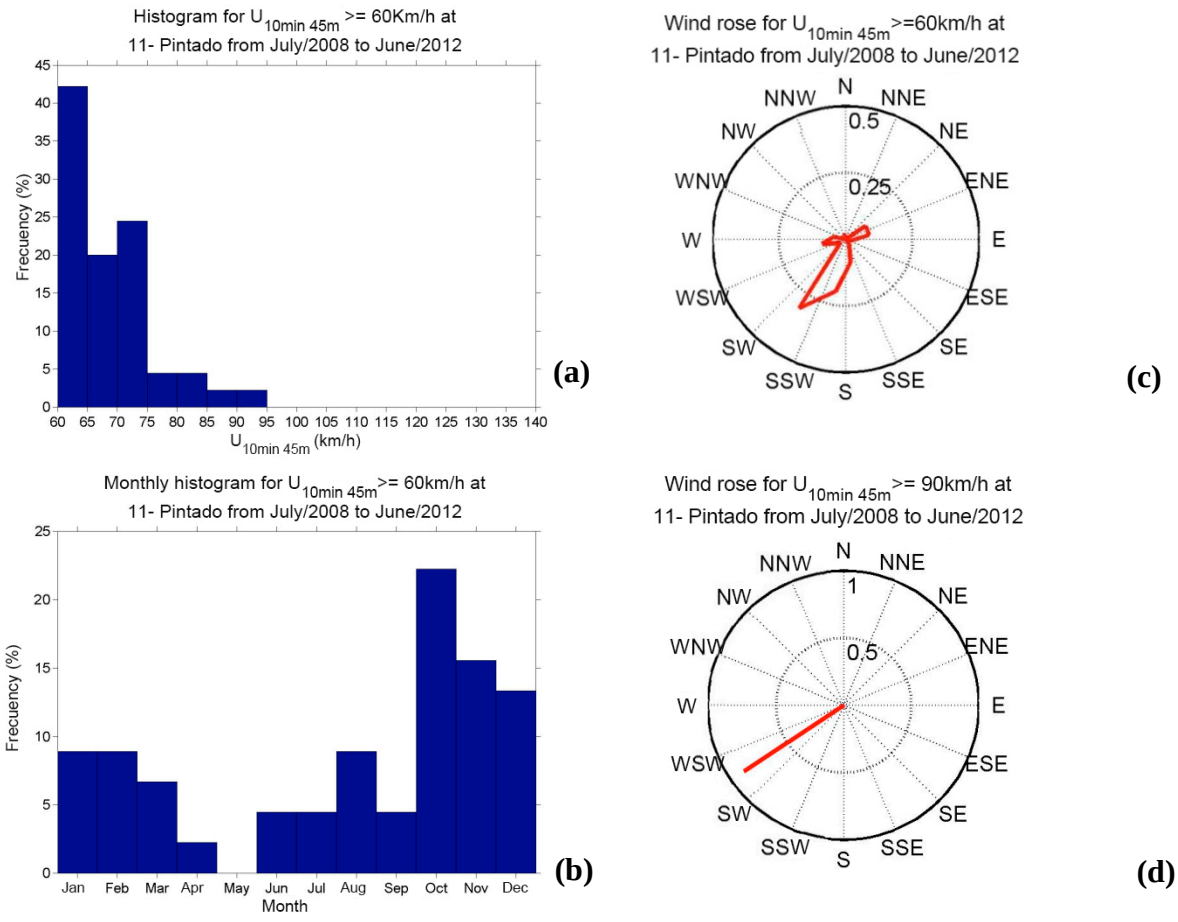


Figure 5.16 Characteristics of high 10min mean wind events at 45m at station 11-Pintado

These results also suggest that the events causing high wind gusts in spring may have a higher time scale than those that take place in summer.

On the other hand, it can be observed that the peak seen in February in Figure 5.12(b) is no longer present in Figure 5.16(b), but the peak shown in August in the first figure is again observed in the latter figure. This might mean that the events that took place in August had a relative higher time scale than those that occurred in February in Pintado. May appears as the month with the lowest frequency of occurrence of high wind events in both figures.

In addition, Figure 5.16(c) and (d) respectively show the wind rose for Pintado station for high $U_{10min\ 45m}$ events, and for the events with $U_{10min\ 45m} \geq$ 90km/h (25m/s), during the analysed period.

Figure 5.16(c) indicates that most of the high $U_{10min\ 45m}$ events registered at Pintado station presented directions from the SW quadrant, especially around the SSW, and that events from the W and from the ENE also took place, while Figure 5.16(d) shows that all the events with $U_{10min\ 45m} \geq$ 90km/h presented wind directions around the SW.

In a third stage of this study, the results obtained from the analyses of all the stations similar to the one shown for Pintado, were summarised in bar graphs and wind roses, describing the typical characteristics of the events found to generate high $U_{10min\ 45m}$ in Uruguay during the analysed period. These results are presented in Figure 5.17(a)-(d).

From Figure 5.17(a), it can be seen that the highest $U_{10min\ 45m}$ registered by the stations of the network corresponded to wind speeds between 100 and 105km/h (27.8 and 29.2m/s). Figure 5.17(b) shares some similar features with Figure 5.16(b): high $U_{10min\ 45m}$ tending to occur more frequently in spring, with the highest frequency in October; higher frequency in August than in July or September, and May as the month with less number of high $U_{10min\ 45m}$ for the whole country in average.

In this case, winter presented a slighter predominance over summer. As intense convective events present a seasonal distribution with a minimum in winter and extra-tropical cyclones would predominate in winter in the region, as presented in Sub-section 2.2.4.2, these results might suggest that in winter, the highest 10min mean wind speed events may be related to the passage of strong extra-tropical cyclones over the country, perhaps together with other synoptic events also capable of causing high mean wind speeds more frequently in winter.

The comparison between Figure 5.17(b) and Figure 5.16(b) might suggest that there would be an area, or areas, in Uruguay, where high wind events dominate the extreme 10min mean wind climate in winter more than in Figure 5.17(b). As indicated before, one of these areas could be the southeast of Uruguay, where more events with higher temporal (length) scales were found.

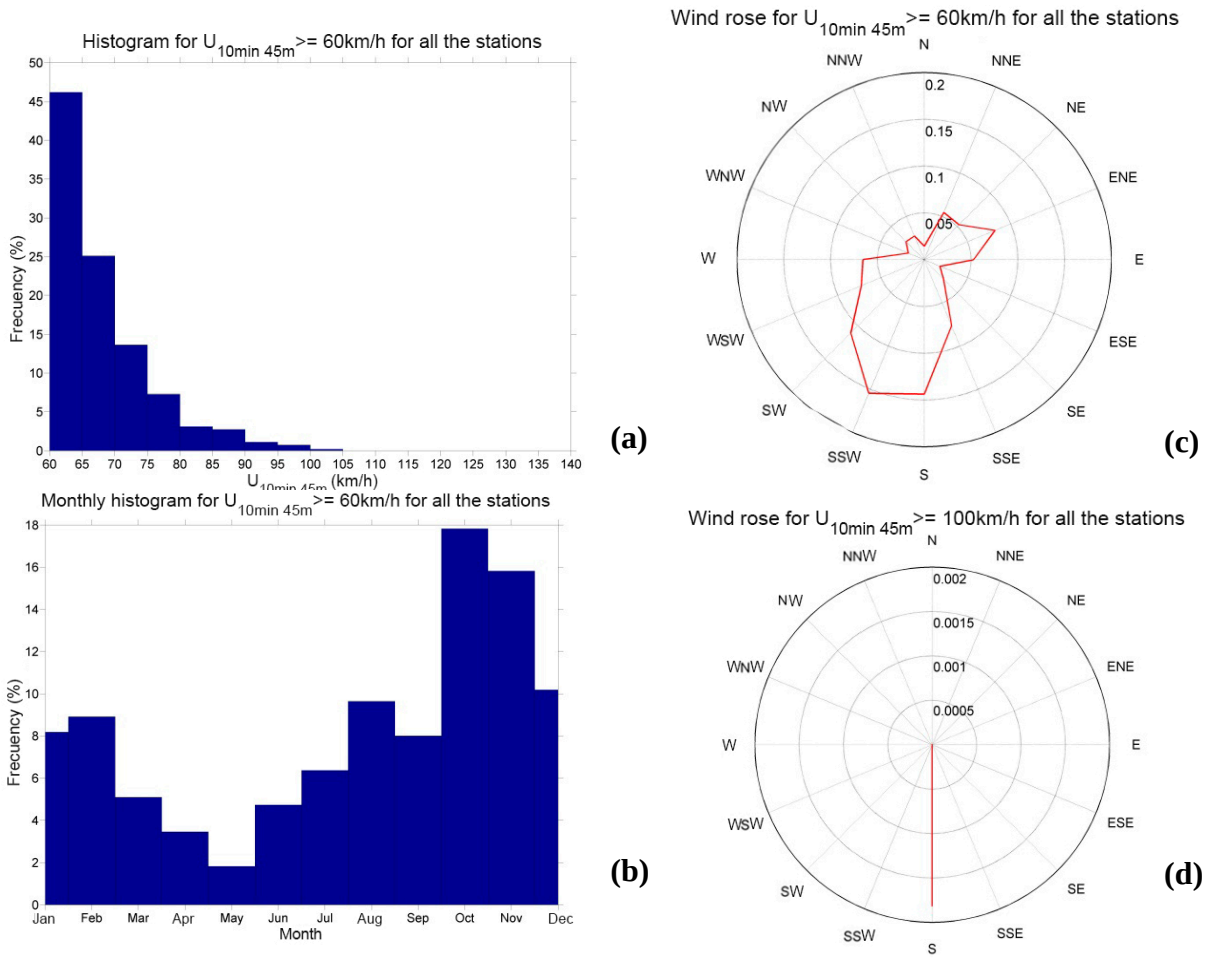


Figure 5.17 Characteristics of high 10min mean wind events at 45m in the network

However, it is again reminded that there were relatively few stations operative toward the northwest of the country than in other areas by the time this analysis was carried out, and that the analysed database was only 4 years long.

Figure 5.17(c) also shows that high $U_{10min\ 45m}$ events registered in the network of automatic stations of UTE during the analysed period mainly presented directions from the SW quadrant, with the highest frequency corresponding again to the SSW direction, followed closely by the S; and that there were some other events from the NE quadrant as in Figure 5.16(c), with a higher predominance over directions from the NW than in Figure 5.17(c). It can also be noticed that Figure 5.17(c) is quite similar to Figure 5.13(a), the latter corresponding to the wind rose for the high $U_{gust\ 45m}$ events analysed from the whole network

(d)

of stations. On the other hand, Figure 5.17(d) indicates that the events with $U_{10min\ 45m} \geq$ 100km/h (27.8m/s) presented directions from the S.

5.7. Discussion

The analysis performed on the database corresponding to the network of automatic meteorological stations of UTE located in open and level terrain until July, 2012, not longer than 4 years, showed that at any station the highest wind gusts corresponded to non-synoptic high wind events with relevant transient characteristics on their wind gust speeds, wind direction and temperature, registered during intense convective activity. In general non-synoptic high wind events, i.e., of temporal scales smaller than few hours, generated higher wind gusts than synoptic high wind events. At every station, when the highest wind gusts registered during the analysed period were ordered in descending order, there were several non-synoptic high wind events before synoptic high wind events started to appear. An example of this characteristic is presented in Annexes A.2 and A.3.

It was also found that non-synoptic high wind events, mostly related to intense convective activity, apart from producing the highest wind gusts across all the country, would also tend to dominate the maxima 10min mean wind speeds, at least in the northwest and centre of the country. More analysis would be needed to conclude on the type of high wind events that would cause the maxima 10min wind speeds in the southeast of Uruguay.

Regarding the geographic distribution of the highest winds, it was found that toward the northwest of the country, higher wind gusts would be measured more frequently than in the southeast, as shown by Figure 5.15. More recently, stations installed in the northwest of Uruguay, and longer records, confirmed this trend (Durañona et al., 2015). On the other hand, in all the analysed stations, the predominant directions registered during the occurrence of the highest wind gust speeds and of the highest 10min mean wind speeds were from the southwest quadrant. Non-synoptic as well as synoptic high wind events would generate most of their highest winds from these directions.

Even with the short length of the records analysed (not greater than 4 years), events producing wind gusts of 40m/s were measured at 4 stations of the network, in the southern centre of the country and twice in two of them.

On the other hand, in two of the six stations that had anemometers installed at around 10m height, wind gusts of about 40m/s were registered at that height during the analysed 4-year period. These stations were located in the centre of the country (4-Peralta and 5-Valentines). The frequency of these higher wind speed values is in accordance with wind speeds already measured in Montevideo in the beginning of last century, as commented in Sub-section 4.5.4.

In general, when wind speed abruptly increases, fast drops in temperature and wind direction changes are measured and the occurrence of intense convective activity over the analysed station can be verified. As mentioned in Sub-section 2.2.3.2.1, these characteristics can be associated with e.g. the passage of cold fronts or squall lines across the country, which produce strong downburst outflows or gust fronts due to the presence of high cumulus nimbus clouds. Although a severe isolated, multicell or super cell storm, or a MCS are all capable of producing strong outflow boundaries associated with deep convection, looking at GOES satellite images and running animations of time evolution of wind gusts, wind direction and temperature measured by UTE stations during several of the most intense of these events, it could be verified that the most intense events would be related to convective activity organised in lines over the country, i.e., cold fronts or squall lines, generally moving from the southwest to the northeast. The passage of cold fronts over Uruguay was already identified by Vieira, 1949 as one of the main meteorological phenomena responsible for the occurrence of high winds in Montevideo. During many of these events, significant temperature drops were registered by the network of stations, verifying this distinctive characteristic of the country, as indicated by Boerger, 1953.

When synoptic weather patterns were found to be responsible for the generation of high wind gusts, no significant changes in wind direction or temperature were usually registered, and the temporal change in wind speed was more gradual. Examples of the meteorological conditions found in these cases were the intensification of extra-tropical cyclones during their passage over Uruguay and fast irruptions of cold air masses from the south, which corresponded to

some of the synoptic weather patterns described in Sub-section 2.2.5.2.1 as causes of synoptic high winds in Uruguay.

From the analysis carried out in a database not longer than 4 years, it could also be concluded that non-synoptic high wind events corresponding to the occurrence of intense convective activity may affect great part of the country with higher wind gusts speeds and more frequently than synoptic high wind events. Although different, both types of events produce their maximum wind gusts from the southwest quadrant.

In addition, it was also found that although synoptic high winds are usually sustained in a particular site during longer periods than high winds due to convective activity, intense convective activity also has an important effect on the registered 10min mean wind speeds.

Under conditions of intense convective activity, gust factors between 2 to 2.5 and greater, defined over 10min periods, were obtained, values similar to those presented in Bradbury and Deaves, 1994, and very different from those corresponding to ABL flows (Cook, 1985). It was then confirmed that this should be taken into account when trying to compare extreme wind maps based on 10min mean wind speed measurements with those based on wind gust measurements, or if extreme wind gusts are estimated from extreme 10min mean wind speeds, especially in regions where severe convective activity is an important feature of the extreme wind climate.

During the analysis presented in this chapter, wind speed measured at heights with only one anemometer were also taken into account. As Table 3.1 showed, most of these anemometers were installed looking to the south or west, directions where the highest winds usually come from in Uruguay, thus, it was assumed that the effect of the tower on these wind speed measurements could be disregarded.

A strong predominance for high wind events to occur mostly between October and February was found, in accordance with the seasonal behaviour of severe convective activity in the region (e.g. Salio et al., 2007).

Given the relatively small area of Uruguay, and the availability of measurements of different meteorological parameters every 10min at 25 stations located across the country, the network of stations of UTE allows the study of the trajectories and time evolutions of different

meteorological phenomena that cause high winds in the country. The fact that anemometers are located at heights between 10 and 100m allows the analysis of the behaviour of high wind events in a wide range of heights.

As the analysed height of 45m is higher than usual meteorological measurements, a study was performed at stations that had anemometers at 10m height, yielding qualitatively similar results for the highest wind gusts, i.e., intense convective activity also dominated the occurrence of the highest wind gust speeds at 10m height.

In order to compare wind gust speed results obtained in this chapter with results obtained from other meteorological stations, precise metadata on instrumentation and recording systems from those stations would be needed. In particular, their wind gust averaging periods would need to be analysed in relation to the ones corresponding to the anemometers from the stations of UTE.

Chapter Six

Extreme wind value analyses of 10min mean wind speed registered at Carrasco station

6.1. Introduction

At present, the station with the longest current wind record corresponds to the INUMET station located at Carrasco airport in Montevideo, whose data and metadata were detailed in Section 3.4.

Although, as presented in Section 2.5, it would be required to perform extreme value analysis on wind gust data in order to adequately describe the extreme wind climate of regions where severe convective activity is frequent, as verified for Uruguay in Chapter 5 of this thesis, it was decided to carry out extreme value analysis on the 10min mean wind speed data of Carrasco station. On the one hand, some wind codes used in the country, as e.g. IEC, 2005, require extreme wind value analysis of 10min mean wind speeds for their application. On the other hand, the short length of wind gust records in Uruguay available at the time of the analysis presented in Chapter 5 was carried out (July, 2012), i.e., less than 5 years, would have required the use of more complex statistical techniques (as indicated in Sub-section 2.4.1) that were outside the scope of this PhD research.

As presented in Section 3.4, Carrasco station has been measuring hourly mean wind speed and direction in the last 10min of each hour since 1960. During this PhD research, wind data measured at this station between 1960 and 2009 and its corresponding metadata were collected and analysed between 2011 and 2012. After discarding years with less than 90% of records, inadequate metadata and/or wind data of dubious quality, the following 35 years of wind measurements were found suitable for extreme wind value analysis: 1960 to 1967, 1969, 1970, 1972 to 1978 and 1992 to 2009.

These years corresponded to the four different periods of measurement indicated in Table 3.3, with the station anemometer installed at different locations and heights.

According to the requirements for wind measurements described in the (WMO)-CIMO Guide and cited in Section 2.3 wind speed should be measured at official stations at 10m height over open and level terrain (with a minimum distance between the anemometer and any obstruction

of 10 times the height of the obstruction). This also means that the type of terrain surrounding the anemometer of the four periods of measurements corresponding to the last two periods (1995-2009) conform to these requirements, as it can be verified looking at Table 3.3 and at Figure 3.16, Figure 3.17, Figure 3.19 and Figure 3.20. These two periods comprise 15 years of wind measurements of adequate quality, while for applying the most recommended technique for extreme wind value analysis, as described in Sub-section 2.4.1, i.e., the classical GEV method, at least 20 years of wind data would be required.

In addition, for both statistical and meteorological reasons, longer records will usually produce more accurate estimates of extreme winds, if causes of possible inhomogeneities in the wind data series are taken into account and corrected (Sub-section 2.4.1).

Considering the restraints already commented, it was decided to use the indicated 35 years of wind data, and compare the results obtained with those obtained using the 15 years of wind data corresponding to the last two periods of measurements, which conform to the rules of the (WMO)-CMO Guide.

This chapter describes the procedure applied to conduct extreme wind value analyses on this database of 35 years of hourly 10min mean wind speeds, and the main results found.

6.2. Wind data homogenisation

In this section, the procedure used to homogenise the 35 years of hourly 10min mean wind speed data already indicated is described.

As described in Section 3.4, wind speed at Carrasco station has been measured at different heights and sites, and with different instruments and units since 1960. As presented in Section 2.3, before conducting any extreme wind value analysis, the available data series needs to be homogenised in order to get rid of any discontinuity it may present due to changes in height, location, surroundings, data acquisition procedure, etc., along time. The importance of evaluating and verifying the homogeneity of wind data, its quality and that of its metadata was stressed in Section 2.3 and it is especially required when extreme wind value analyses are conducted.

The 35 years long data series of hourly 10min mean wind speeds measured at Carrasco station was first homogenised taking into account the original resolution and units of measurement of the instruments used along those years. As presented in Section 3.4, it was found that most of the original readings of the 10min mean wind speeds of Carrasco station had been visually averaged on dials graduated in knots, with a resolution of 1kt, and written down in the books of the station using different units and resolutions along the years. It was then decided to work with the wind speed values converted back to knots, with a resolution of 1kt. More details of this homogenisation can be found in Durañona, 2011a.

When the exposure of a station is not standard, WMO, 2006 recommends applying models of flows of ABL type (Section 2.3) to take into account differences in height and roughness length so as the corrected mean wind speeds measured for all wind directions and strings of anemometer represent wind speeds measured as if the anemometer were surrounded by open and level terrain in all wind directions and placed at 10m height. In spite that Chapter 5 of this thesis indicates that many of the highest 10min mean wind speeds registered in Uruguay would not correspond to flows of ABL type, no other methods are available or universally accepted to take into account these inhomogeneities at the moment.

Therefore it was decided to apply Equation (2.4) to calculate the corresponding wind speed at a height of 10m and a z_0 value of 0.03m, typical of rural terrain, for each 10min mean wind speed data along those years, considering the characteristics of each of the 8 wind direction sectors defined in Table 3.4 for each of the four measurement periods.

The actual z_0 values for each sector and location of the anemometer were visually estimated from the figures presented in Section 3.4, Google Earth images and videos taken during the visit to Carrasco station, as described in that section.

Different recommendations for carrying out visual estimations of z_0, and several sources of information of z_0 values for homogeneous and non-homogeneous terrains were considered during this procedure (e.g., Wieringa, 1992; Wieringa, 1993; Davenport et al., 2000; Aguilar et al., 2003; WMO, 2006).

Due to the inherent uncertainties in the visual estimation of z_0 values, instead of estimating one z_0 value for each wind sector and location of the anemometers in order to apply Equation

(2.4), an upper and a lower bound for z_0 were estimated for each wind sector and site of wind measurement.

Table 6.1 and Table 6.2 respectively show the estimated bounds of z_0 values for each wind sector and for each site (indicated as measurement period in these tables).

Measurement period / Wind sector	1960-1976	1977-1994	1995-2006	2007-2009
1	0.1	0.1	0.25	0.25
2	0.1	0.25	0.25	0.25
3	0.1	0.1	0.25	0.25
4	0.1	0.1	0.25	0.25
5	0.1	0.1	0.1	0.25
6	0.1	0.1	0.1	0.1
7	0.1	0.03	0.03	0.03
8	0.03	0.03	0.03	0.1

Table 6.1 Lower bounds for z_0 ($z_{0\ min}$)

Measurement period / Wind sector	1960-1976	1977-1994	1995-2006	2007-2009
1	0.1	0.25	0.5	0.5
2	0.1	0.5	0. 5	0.5
3	0.25	0.5	0.5	0.5
4	0.25	0.5	0.5	0.5
5	0.25	0.5	0.25	0.5
6	0.25	0.25	0.25	0.25
7	0.1	0.1	0.1	0.1
8	0.1	0.1	0.1	0.25

Table 6.2 Upper bounds for z_0 ($z_{0\ max}$)

The analysed 35 years long 10min mean wind speed data series was then homogenised applying Equation (2.4), considering the actual anemometer height, presented in Section 3.4, and both groups of z_0 values presented in these tables. In this way, two 35 years long 10min mean wind speed data series were obtained, and two sets of 35 homogenised annual maxima 10min mean wind speed values were extracted, each set corresponding to a different group of z_0 values (z_{0min} and z_{0max}). After that, extreme value analyses were carried out on both annual maxima 10min mean wind datasets.

6.3. Extreme wind value analysis

The Generalized Extreme Value (GEV) distribution and the Gumbel (or type I) distribution were selected to test their fit to each of the two datasets of annual maxima 10min mean wind. Speeds, based on the considerations discussed in Section 2.4 when long data series are available. The characteristics of these distributions and the definition of their parameters were presented in that section.

Matlab program allows estimating the parameters of the GEV distribution (k, μ and σ), as well as the parameters of the Gumbel distribution (μ and σ), with k set to zero. In both cases, this program uses the Maximum Likelihood (ML) method for these estimations, which is one of the main methods recommended in Section 2.4. It was then decided to use Matlab routines to estimate the parameters of these extreme statistical distributions.

Table 6.3 presents both the GEV and the Gumbel parameters estimated in this way, for both sets of homogenised 10min mean wind speed annual maxima.

This table also presents the results of statistical tests conducted to verify the hypothesis that these datasets were independent and identically distributed (i.i.d), condition that must be met if the GEV distribution is applied for extreme value analysis (Fisher and Tippett, 1928). The tests selected with this aim were the Spearman rank correlation test and the Up and Down Runs test (Perera, 2000, Durañona and Perera, 2003).

	GEV distribution					Gumbel distribution			
	k	μ	σ	Runs test	Spearman test	μ	σ	K-S test	χ^2 test
z_{0min}	0.2	72.7	8.4	✓	✓	73.8	9.4	✓	✓
z_{0max}	0.0	84.5	12.2	✓	✓	84.4	12.2	✓	✓

Table 6.3 Estimated parameters for the GEV and Gumbel distributions and results of statistical tests, for both sets of homogenised annual maxima 10min mean wind speed from Carrasco station

Usually, the Spearman test detects trends in the data, while the Runs test works better detecting cycles in the data. These tests yield p-values, corresponding to the probability of erroneously rejecting the i.i.d. hypothesis. High p-values do not allow the rejection of the hypothesis made, and this was the case for both tests and datasets tested, as shown in Table 6.3 with a tick, indicating that the corresponding test had been passed. Therefore, the hypothesis that both sets of 35 10min mean wind speeds annual maxima from Carrasco station were i.i.d. would be reasonable according to these results.

On the other hand, two tests were applied to study the goodness of fit of the Gumbel distribution to both datasets: the Kolomogorov-Smirnov (K-S) and the chi-square (χ^2) tests (Perera, 2000; Durañona and Perera, 2003).

The K-S test compares the experimental distribution, obtained from the annual maxima wind datasets, with the selected theoretical distribution, while the χ^2 test compares the experimental and theoretical distributions in association with previously defined wind speed classes. If both distributions are similar, these tests should yield high p-values, which would not reject the hypothesis that the experimental distribution is similar to the theoretical distribution.

Applying both tests to both datasets of 35 annual maxima yielded high p-values, indicating that the hypothesis that the Gumbel distribution with the parameters shown in Table 6.3 would adequately model the experimental statistical distribution for both maxima datasets could not be rejected. This was also indicated in Table 6.3 with ticks.

These results would imply that the underlying extreme distribution of the annual maxima 10min mean wind speeds measured at Carrasco station during the analysed 35 years could be in fact adequately modelled by a Gumbel distribution, with parameters that would depend on the procedure selected for homogenising the hourly 10min mean wind speed data series, i.e., on the estimated z_0 values for each wind sector and site of measurement.

In order to analyse the influence of the non-standard siting of the station anemometer during the two first periods of measurement (1960-1994), i.e., above the control tower of the airport, and above the roof of the station building, on the extreme wind value analysis, it was decided to compare the 10min mean wind speeds that would correspond to return periods (defined in Section 2.4) of 20, 50 and 100 years for four different annual maxima datasets of 10min wind speeds, assuming a Gumbel distribution.

The following datasets were selected:

- the annual maxima 10min mean wind speeds from the 35 years selected from the period 1960-2009 homogenised with z_{0max}
- the annual maxima 10min mean wind speeds from the 15 years selected from the period 1995-2009 homogenised with z_{0max}
- the annual maxima 10min mean wind speeds from the 35 years selected from the period 1960-2009 homogenised with z_{0min}
- the annual maxima 10min mean wind speeds from the 15 years selected from the period 1995-2009 homogenised with z_{0min}

The 10min mean winds speeds corresponding to return periods of 20, 50 and 100 years for each of these four datasets are presented in Table 6.4.

Looking at this table, it can be clearly noticed that the effect of the choice of z_0 values (to homogenise the annual maxima 10min mean wind speeds measured at Carrasco station) is greater than the effect of the choice of the dataset on the 10min mean wind speeds for the three selected return periods.

Dataset	Return period (years)		
	20	**50**	**100**
1960-2009 z_{0max}	121	132	141
1995-2009 z_{0max}	113	122	128
1960-2009 z_{0min}	102	110	117
1995-2009 z_{0min}	96	104	109

Table 6.4 Comparison of 10min mean wind speeds obtained for different return periods, corresponding to different measurement periods and length homogenisations (km/h)

Typical differences in wind speed values obtained for the two different z_0 homogenisations were between 17 and 24km/h for the three return periods considered, while this difference was between 6 and 13km/h for the different datasets chosen (1960 to 2009 and 1995 to 2009).

These results suggest that the choice of z_0 values for homogenisation is a delicate point that should be addressed with care. It is worth pointing out that there exist more modern techniques to assign z_0 values than those presented in Sub-section 2.2.1.3 (e.g. Burlando et al., 2007), as indicated in Solari et al., 2012.

6.4. Seasonal distribution

As the high 10min mean wind speeds measured by the network of stations of UTE presented an evident seasonal behaviour, with higher frequency of occurrence in spring and summer, as shown in Sub-section 5.6.2 of Chapter 5, it was decided to investigate if that was also the case for longer periods, analysing the annual maxima 10min mean wind speeds measured at Carrasco station, which comprised 35 years of data.

In order to analyse this possibility, the annual maxima 10min mean wind speed datasets obtained homogenising the wind speed measurements with both sets of z_0 values presented in Table 6.1 and Table 6.2 were sorted out according to the month they were measured. Figure

6.1 and Figure 6.2 show the monthly distribution of these series of annual maxima, where month 1 corresponds to January, and month 12, to December.

As it can be noticed, both figures show seasonal distributions that are qualitatively similar to those obtained during the analysis presented in Section 5.6 of Chapter 5. The reader is especially referred to Figure 5.17(b), which showed the monthly average frequency of occurrence of all high $U_{10min\ 45m}$ events registered at all the stations from the UTE network, i.e., those that presented 10min mean wind speeds higher than 60km/h at 45m height, and to Figure 5.16(b), which showed the monthly average frequency of occurrence of all high $U_{10min\ 45m}$ events at station 11-Pintado.

These results would suggest that the 10min mean wind speed annual maxima measured at Carrasco station during the analysed period of 35 years may have been mainly caused by the presence of intense convective activity, as similar comments made in Section 5.6 (about Figure 5.17 (b)) apply to this case, and in particular to Figure 6.2, which also "shows that the most frequent occurrence was from October to February (…) with a distinctive peak in October. Spring and summer were the seasons with more number of these events. As this seasonal distribution approximately resembles that of severe convection in SESA, as described in Sub-section 5.5.2, this may suggest that severe convective activity would also dominate the extreme 10min mean wind speed climate" at Carrasco station. (Quite similar comments also apply to Figure 6.1). In both figures (Figure 6.1 and Figure 6.2), many of the events occurring in winter (July, August and September) may have occurred during synoptic high wind events, as intense extra-tropical cyclones and other synoptic weather patterns causing high synoptic winds are more common in winter, as indicated in Sub-section 2.2.5.2.1. Nevertheless, some of them may correspond to convective activity, embedded or not in larger synoptic systems.

It can be noticed in both figures that more 10min mean wind speed annual maxima occurred in spring than in summer, and that more annual maxima occurred in summer than in winter.

The above comments suggest that the 10min mean wind speed annual maxima datasets from Carrasco station may correspond to a mixed series (combining intense convective events with synoptic high winds), where intense convective events would present a higher frequency of occurrence than synoptic high winds.

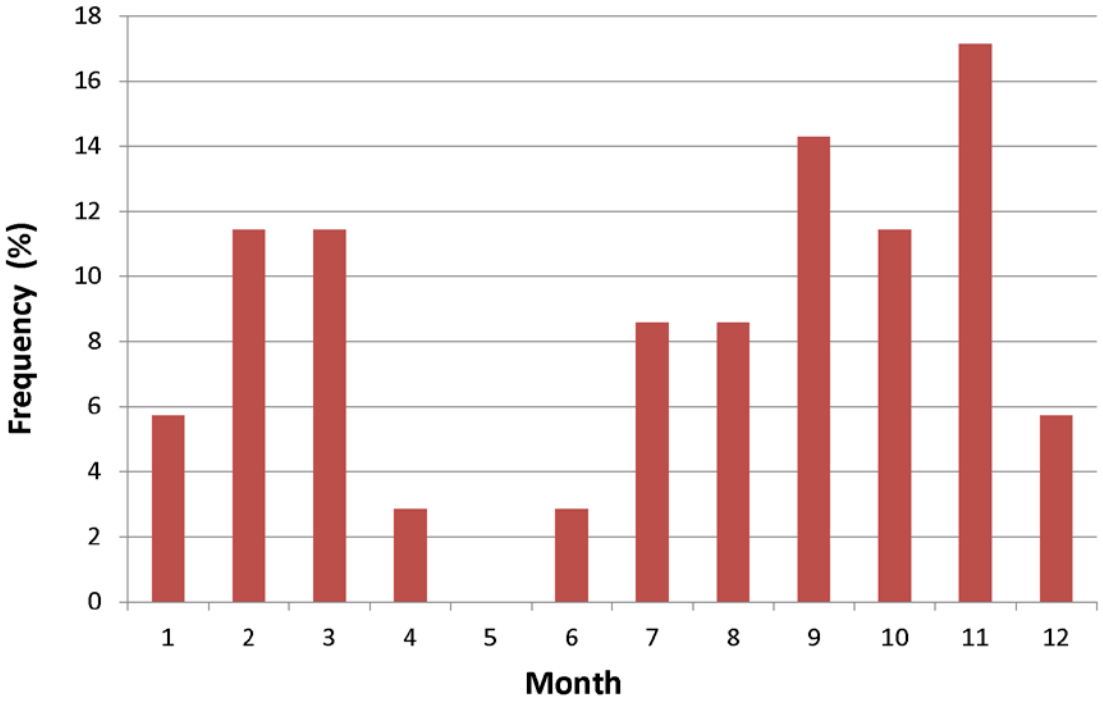


Figure 6.1 Monthly distribution of the 10min mean wind speed annual maxima from Carrasco station, homogenised with z_{0min}

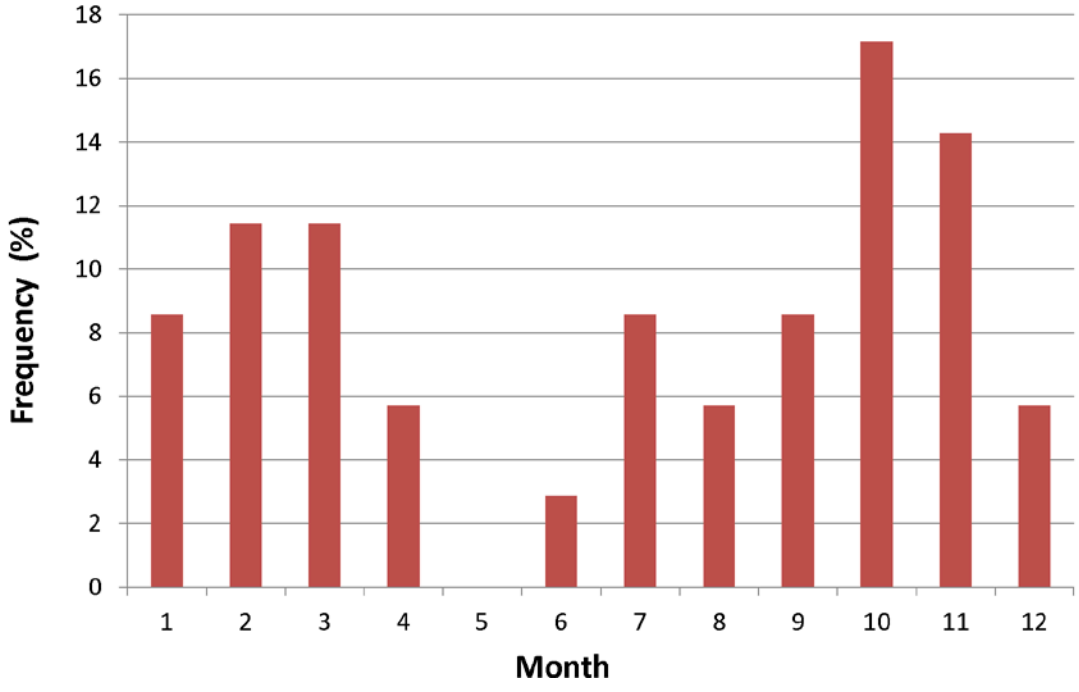


Figure 6.2 Monthly distribution of the 10min mean wind speed annual maxima from Carrasco station, homogenised with z_{0max}

6.5. Discussion

As mentioned before, the use of Equation (2.4) to homogenise the wind speed measurements carried out at Carrasco station implied the hypothesis that the wind flow structure during those measurements corresponded to an ABL flow.

As presented in the previous section, the seasonal distribution of the 10min mean wind speed annual maxima registered at Carrasco station during the analysed period would suggest that these maxima may have been mostly caused by intense convective activity, result that would invalidate the hypothesis indicated above for most of the annual maxima wind speed records. This result would mean that a different law from the one presented in Equation (2.4) should be used in order to homogenise the wind speed data series measured at Carrasco station, or even, that it might not be necessary to take into account the roughness of the surroundings during the homogenisation procedure, as it is believed that outflow boundaries associated with deep convection may not be greatly affected by the roughness of the terrain where they take place. Anyhow, at present there is not a general profile with height for this types of flow, as their actual wind speed variation with height is not known with enough detail yet. Therefore, the uncertainties regarding the homogenisation procedure described in Section 6.2 are quite difficult to be estimated and surpass the scope of this PhD research. Moreover, if most of these 10min mean wind speed annual maxima correspond to intense convective events, the relation between them and their corresponding wind gust speeds could be very variable, as indicated in Sub-section 2.2.1.4.

In relation to the extreme wind value analyses carried out, the result that a Gumbel distribution would adequately model the behaviour of the extreme wind statistics of the 10min mean wind speeds is in accordance with the results of many authors, as presented in Section 2.4, even in this case, where the analysed series of annual maxima may correspond to a mixed series, including non-synoptic as well as synoptic high wind events. However, it would be recommendable to analyse if different extreme wind statistics would be obtained if 10min mean wind speeds annual maxima are classified into synoptic and non-synoptic types of events. In that case, these results should be combined through mixed statistics.

The results obtained from the extreme value analysis presented in Table 6.3 would yield for example, a 10min mean wind speed with a 50-year return period of 132km/h (36.7m/s) for Montevideo, for the annual maxima series of the four periods of measurements homogenised with the upper bound of z_0 (z_{0max}), and modelled by a Gumbel distribution.

The obtained results for Montevideo can also be compared with results presented in the Argentinian wind code CIRSOC 102, which indicate for areas of Argentina near Uruguay, a 3s gust with a 50-year return period between 46 and 48m/s at 10m height. These values would yield gust factors between 1.25 and 1.3 if they are calculated with the 10min mean wind speed of 132km/h (36.7m/s). These gust factor values are lower than those expected for intense convective activity, as concluded in Chapter 5 of this thesis, but match gust factor values expected for ABL flows.

When comparing results obtained from wind gust speeds measured with different instruments and/or recording systems (as when comparing results from Chapter 5 with wind gust measurements in Argentina), the averaging period of the wind gusts should be known or estimated.

On the other hand, the visual average of the 10min mean wind speeds carried out at Carrasco station when the maxima wind speeds were registered during the analysed 35 years might correspond to a wind speed averaged over a shorter period than 10min, due to the usual measurement procedure at stations where averages are taken visually during the last 10min of each hour.

The results obtained in this chapter would also confirm that for Montevideo, more high wind events would be expected to occur in spring and summer, and more in summer than in winter. May would be the month with the smallest probability of registering an annual highest wind speed, in agreement with results shown in Chapter 5 for Pintado station and for all the country.

Due to the seasonal trend found, it seems sensible to work with annual maxima wind speeds if classical extreme value analysis is going to be applied, as e.g. monthly maxima might not be i.i.d. due to the seasonal distributions shown by Figure 6.1 and Figure 6.2.

Gust factors should be applied with care to the annual maxima 10min mean wind speeds registered at Carrasco station, as most of these registers seem to have been recorded during intense convective activity and not during flows of ABL type. As presented in Chapter 5, gust factors during convective activity may vary within a broad range.

Chapter Seven

Review of wind speeds for structural design and extreme wind map of Uruguay, established in the wind code UNIT 50-84

7.1. Introduction

In this chapter, Section 7.2 presents the background and motivation for the analysis of the wind speed values for structural design and of the development of the extreme wind map of Uruguay, both established in the national wind code for actions on structures, UNIT:50-84, 1984. Section 7.3 describes how the values of design winds speeds were set, Section 7.4 summarises the main metadata of Antepuerto station, main data source used for the development of the national wind code, while Section 7.5 focuses on the methodology used to develop the national extreme wind map. Section 7.6 analyses the main hypotheses made, the wind data used for its development, its associated metadata, and the proposed wind profile with height. Finally, Section 7.7 discusses the assumptions made and the quality of the wind data used, applying current knowledge from the wind engineering field, analyses the validity of the proposed extreme wind map and design wind speeds, and proposes some guidelines for future work.

The data and metadata of Antepuerto station and the information on the methodology used to develop the national extreme wind map were collected by the author of this thesis between 2011 and 2012, and the analysis and discussion presented in Sections 7.6 and 7.7 were conducted and organised during 2013 and 2014.

7.2. Background and motivation

The current wind speed values for structural design in Uruguay and the corresponding extreme wind map were established in the national wind code for actions on structures UNIT:50-84, 1984, being since then the official data source for wind loading calculation of any type of structure in the country. If a wind-related failure occurs, the person responsible for the structural design must demonstrate that the calculations comply with this code, and therefore, with its design wind speeds.

However, these wind speed values and extreme wind map deserve several important observations, such as the non-standard exposure of the anemographs whose measurements were the basis for the recommended design wind speed values and extreme wind map; the analysed measurement period that ended in 1969, more than forty years ago; or the assumed probability distribution of the extreme winds, which does not agree with results from more recent extreme wind value analyses for Uruguay, for the region (Riera and Rocha, 1998; Beck and Correa, 2012), or with the wind extreme distribution proposed in recently updated regional wind codes as CIRSOC, 2005b. Other relevant issues that require careful analyses are also commented in the following sections.

During the procedure for the establishment of the design wind speeds and the development of the national extreme wind map, the original creators of this wind code needed to make some assumptions, especially due to the lack of adequate wind data series of enough length and to the state of development of the wind engineering field by that time. Now, 30 years later, more wind data and knowledge on the extreme wind climate of Uruguay became available, as presented in Chapter 5, allowing the hypotheses made to be evaluated.

In particular, due to the differences detected between the characteristics of the geographic distribution of high winds in Uruguay commented in Section 5.7, and the geographic distribution of extreme winds proposed in the national extreme wind map, and the differences between the wind flow structure proposed for the calculation of wind action on structures in Uruguay and the type of wind flow that would take place during most of the high wind events that occur in the country, as discussed in Section 5.7, it was understood that this thesis should include a review of the design wind speeds and of the national extreme wind map presented in the national wind code UNIT:50-84, 1984.

7.3. Wind speeds for structural design

The wind code UNIT:50-84, 1984 defines a characteristic wind speed as the 3s wind gust at 10m height over level and open terrain with a return period of 20 years. The definition of return or recurrence period was presented in Section 2.4.

When extreme winds need to be calculated at other heights or roughness exposures, UNIT:50-84, 1984 proposes corrections to the characteristic wind speed applying power laws as the one presented in Equation (2.5), thus assuming that the flow structure during extreme wind events is that of a flow of ABL type.

The wind speed for structural design at a specific site, with surroundings of certain roughness and topography can be defined as the characteristic wind speed that corresponds to that site, corrected taking into account the differences between the height at which the wind speed needs to be defined for design and the reference height (10m), the differences between the actual and reference roughness, any effect that the topography may exert on the wind speed, and by the dimensions and use of the structure that is being analysed. The type of use of the structure determines the return period that should be used to calculate the design wind speed, which may differ from the reference return period of 20 years associated with the definition of the characteristic wind speed in this code.

The characteristic wind speed for Montevideo was obtained fitting a Type II (Frechet) distribution to the wind gust speed annual maxima measured from 1906 to 1969 at Antepuerto station shown in Figure 7.1.

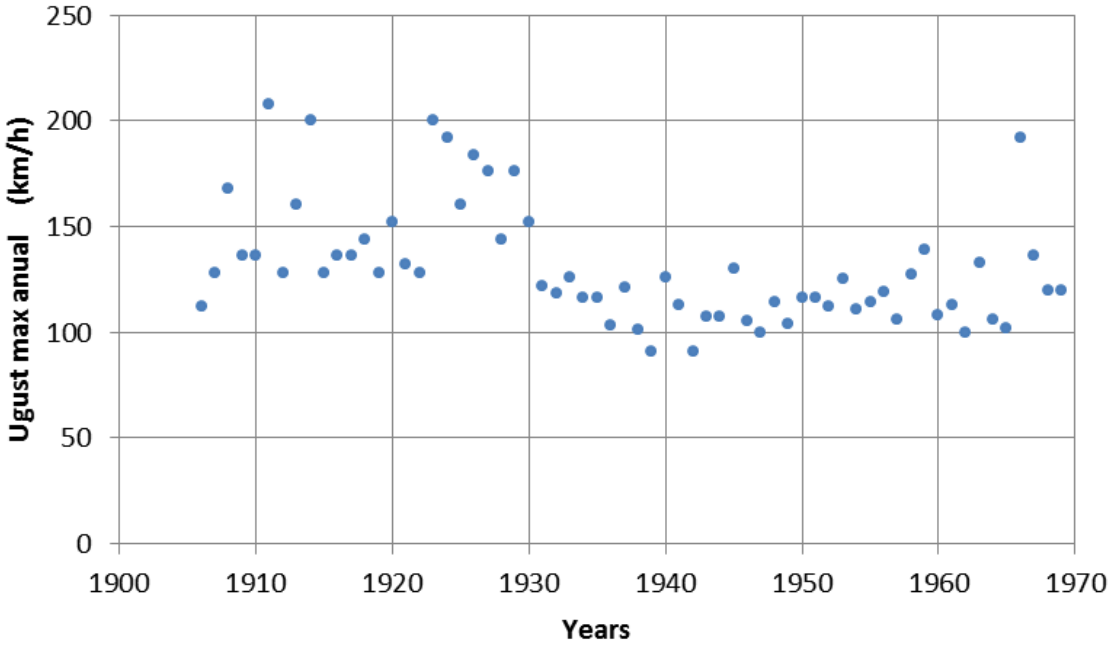


Figure 7.1 Annual maxima wind gust speeds registered at Antepuerto station from 1906 to 1969 (km/h)

This station, whose metadata is described in Section 7.4, was located in front of the port of Montevideo and belonged to the DNM (Ricaldoni, 1979), currently INUMET.

The Frechet distribution was chosen in accordance with the extreme distributions used for the establishment of the characteristic wind speeds in the Argentinian and Brazilian wind codes at that time (IRAM:11-700, 1979; NBR:6123, 1988a), as described in Sub-section 2.5.2.

If a Frechet distribution is assumed, the probability that the annual maximum wind gust speed, v, is higher than v_o can be expressed as (UNIT:50-84, 1984):

$$\mathrm{P}(v \le v_o) = e^{\left[-\left(\frac{\beta}{v_o}\right)^{\gamma}\right]} \tag{7.1}$$

where β, the reference wind speed, and γ, the shape factor, are the parameters of this distribution.

In a first step (Ricaldoni, 1979), the parameters of the Frechet distribution were calculated for the series shown in Figure 7.1, yielding values of β = 32.5m/s and γ = 6.80.

After that, the value of β was corrected in order to represent wind gust speeds at the standard height of 10m, assuming that the wind gust profile could be modelled with a power law as that presented in Equation (2.5). For the whole period of measurement, a power law exponent n of 0.09 was selected assuming that the height of the anemograph had been 45m above ground level during the whole period and taking into account the roughness characteristics of the surfaces associated with wind directions from the port, as the highest wind speeds measured at Antepuerto station came mainly from the port.

After applying this correction, a value of β = 28.3m/s was obtained for Antepuerto station at 10m height. From Equation (7.1), the probability that the annual maximum wind gust speed at 10m height in Montevideo was lower than v_o (in m/s) could be expressed as:

$$\mathrm{P}(v \le v_o) = e^{\left[-\left(\frac{28.3}{v_o}\right)^{6.80}\right]} \tag{7.2}$$

7.4. Metadata of Antepuerto station

Antepuerto station was located in front of the port of Montevideo, with the city centre to the east and the port to the west, as shown with crosses in Figure 7.2 at different scales, The horizontal scale bar in the bottom left of each of these figures is presented in kilometres. The coordinates of this station were 34°55'S latitude and 56°13'W longitude.

In this station, wind gust speeds were continuously registered from 1906 until 1970 with Richard, Fuess, Bondix and Lambrecht cup anemographs. Since 1930's at least two anemographs and a wind vane with graphic register measured simultaneously, according to Battione, 1969.

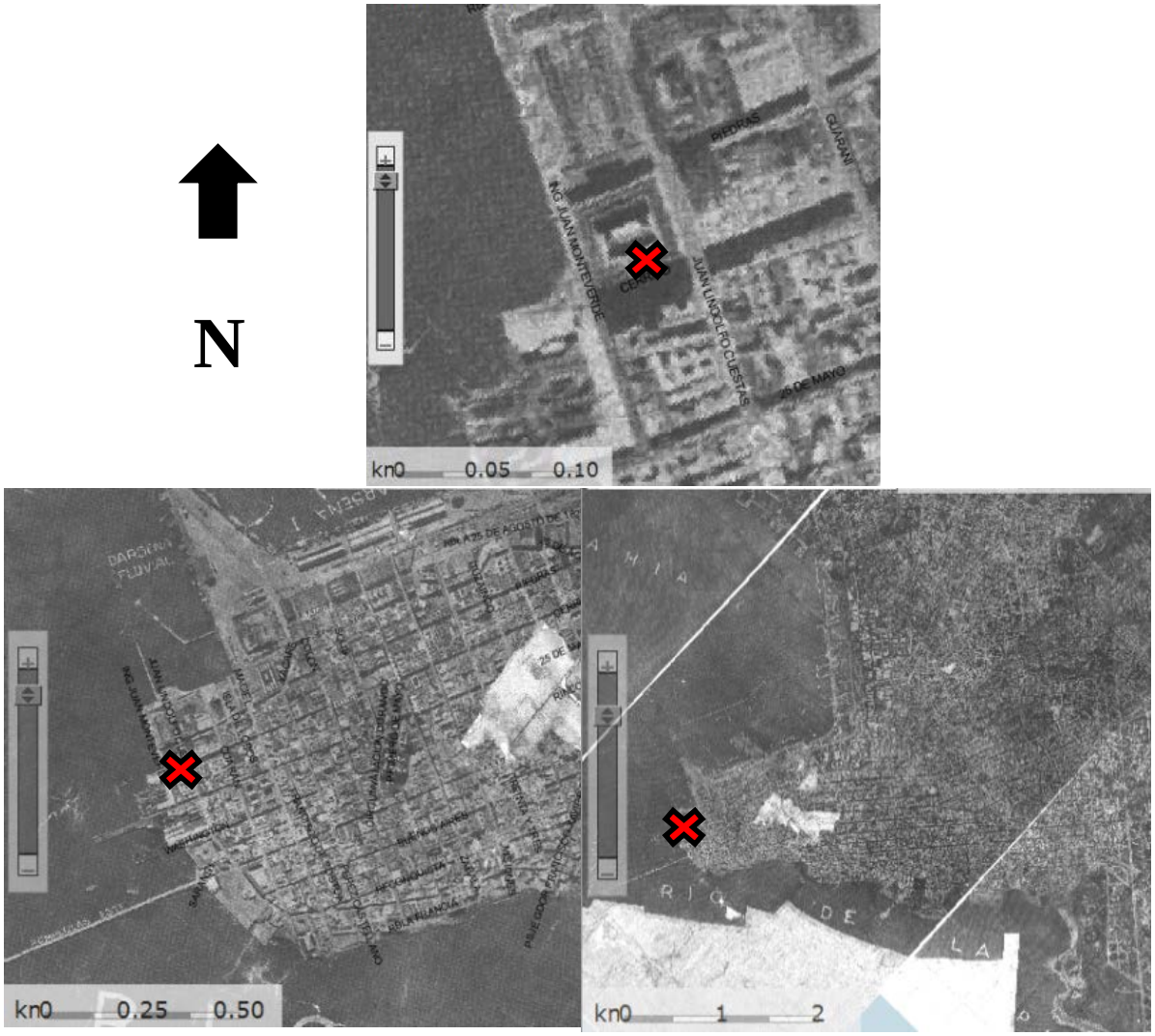


Figure 7.2 Antepuerto station and surroundings (from IMM data)

The sensors of these instruments were located above the roof of a four-storey building. The height of the wind speed sensors was reported to be 45m above ground level and 13m above the roof of the building in Battione, 1969, with the sensors installed on a metallic tower.

As already observed by the creators of the Uruguayan extreme wind map and wind code UNIT:50-84, 1984, the exposure of the sensors at Antepuerto station was not ideal (Ricaldoni, 1979).

7.5. Development of the national extreme wind map

In order to propose a geographic distribution for the extreme wind speeds in Uruguay, some assumptions had to be made due to the lack of wind records of adequate length and quality outside the capital city, Montevideo (Ricaldoni, 1979).

One of these main hypotheses was that the geographic distribution of extreme winds presented a good correlation with the geographic distribution of mean wind speeds across all the country.

Montevideo was chosen as the reference site, due to the temporal length of Antepuerto's series, and mean wind speeds measured during 10 years at other 26 stations across the country were used to correlate the mean wind climate at these sites with the mean wind climate of Montevideo. The same correlation was then assumed to be valid between the extreme wind climate of these sites and the extreme wind climate of Montevideo. Some additional information was used to correct this assumption in regions considered to experience intense extreme winds quite frequently.

Outside Montevideo, it was assumed that the value of the shape factor of the Frechet distribution took the same value as in Montevideo (γ = 6.80), and that the variation of the reference wind speed, β, with location was correlated with the geographic distribution of mean wind speeds (Ricaldoni, 1979). Figure 7.3 presents the proposed geographical distribution of β in the national wind code for actions on structures UNIT:50-84, 1984, still valid for wind loading calculations.

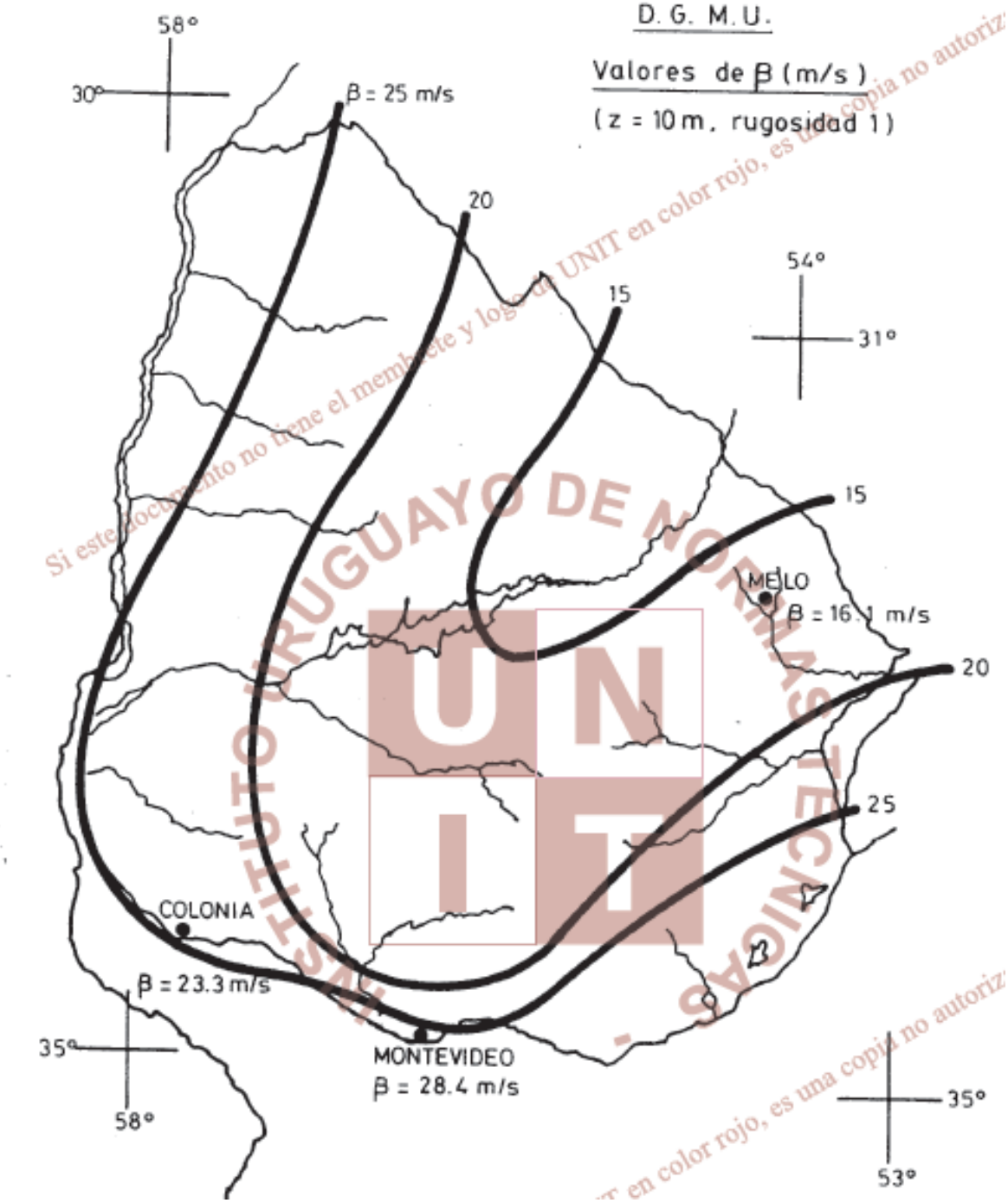


Figure 7.3 Current Uruguayan extreme wind map: values of the reference wind speed (β, in m/s, at 10m height) in the Uruguayan wind code UNIT:50-84

As it can be noticed, this map indicates higher values of β, and thus, higher extreme wind speeds, along the south and south east coastline of Uruguay, as mean wind speeds were found to be higher in that area. The western border of Uruguay with Argentina was considered to be a region where extreme winds occurred rather frequently, and β was consequently increased in that area.

For wind design calculations, the wind code UNIT:50-84, 1984 divides the country into just two regions with distinct values for the reference wind speed, β, and proposes just one value for the shape factor, i.e., γ = 6.80 for all the country. According to this code, the region with the highest extreme wind speeds corresponds to a strip 25km wide along the Río de la Plata and South Atlantic coastlines, i.e., south and south east coastlines, respectively, and along River Uruguay (which determines the western border with Argentina). A value of β of 28.2m/s (101.4km/h) was assigned to this region, while for the rest of the country, a value of β of 24.1m/s (86.6km/h) was proposed.

The characteristic wind speed, defined in Section 7.3 (3s wind gust at 10m height over open and level terrain with a return period of 20 years), takes therefore two possible values: 43m/s in the defined coastal area and 37.5m/s in the rest of the country.

As an example, the extreme wind speeds for structural design at 10m height with a 50 year-return period would respectively correspond to 50.5 and 43.1m/s, if the effect of the topography and size of the structure are disregarded.

7.6. Analysis of the wind data used, procedures and hypotheses made

A first remark that needs to be made is that the annual maxima wind gusts series from Antepuerto station, used to develop the extreme wind statistics for the wind code UNIT:50-84, 1984, presents a clear discontinuity in terms of a sudden drop in the registered wind gusts around 1930 as shown in Figure 7.1. Serrentino, 1981 indicates that the anemograph of Antepuerto station was located at different sites and heights between 1906 and 1969, and that it measured at 39m height between 1906 and 1930, and at 49m between 1940 and 1969. As in several references from 1960's, 49m is mentioned as the height above mean sea level of the

anemograph of this station, and 45m, as its height above ground, the heights mentioned in Serrentino, 1981 may correspond to heights of 35 and 45m above ground, respectively.

Either way, wind gusts would be expected to be higher after 1930, as the height of the anemograph was reported to have increased, but the opposite trend is clearly noticed in Figure 7.1. This behaviour could be related to a previously affected exposure that accelerated the flow, to a sheltered exposure since 1930, to both reasons, or to a bias in wind speed measurement due to e.g. faulty instruments or inadequate calibration, before or after the change in height, as indicated in Section 2.3. In fact, after analysing 50 years of wind data from this station, Battione, 1969 selected the period 1941-1965 for study due to a higher found reliability of its measurements.

The observed discontinuity, which would not correspond to climatic changes, can greatly affect the results obtained by extreme wind value analyses, as indicated in Section 2.3.

A second observation is that the statistical distribution selected to represent the annual extreme wind gusts in Uruguay, the Frechet distribution, is usually indicative of a mixed extreme wind climate, and generally gives higher wind speeds for design than the Gumbel distribution, as presented in Sub-section 2.4.1. The goodness of fit of these distributions to the annual maxima wind gusts measured at Antepuerto station were not compared during the development of this code; the Frechet distribution was selected because that was the extreme statistical distribution that Argentina and Brazil had chosen for their wind codes. It also gives higher design wind speeds, as commented in Sub-section 2.5.2, and in that sense, it would be a conservative choice.

However, it has been found in the last decades that most extreme wind data series are better represented by a Gumbel distribution (e.g. ISO:4354, 2009; Beck and Correa, 2012). In particular, if extreme wind events are classified according to the type of meteorological event that caused them, e.g. intense extra-tropical cyclones or severe convective storms, it has been found that each extreme wind data series, corresponding to just one type of extreme wind event, is better represented by a Gumbel distribution. Even in the case of a mixed extreme wind climate, Gumbel distribution has also yielded the best fit, as presented in Vega and Letchford, 2009. In addition, Durañona and Perera, 2003 and Durañona, 2012b indicate that annual maxima 10min mean wind speeds for Montevideo are also adequately adjusted by a

Gumbel distribution. On the other hand, for the development of the current Argentinian extreme wind map, it was assumed that a Gumbel distribution adjusted the annual maxima wind gusts, and during an analysis carried out for the proposed new extreme wind map for Brazil, it was statistically checked that the Gumbel distribution offered a better fit to the annual maxima wind gusts series of most Brazilian stations.

A third remark is that, although the height of the anemographs of Antepuerto station was considered to be 45m above ground level by most references (e.g. Hernández, 1971; Battione, 1969), current information from local government (IMM) indicates that the height of the building over which the station was located is 17m. Consulted land surveyors analysed historical pictures and also confirmed this approximate height (Casanova, 2013). This building is shown in Figure 7.4, and the arrow in this figure indicates the location of Antepuerto station, which was built over the roof of the main building. Likewise, Figure 7.5 offers a closer view of the station and its sensors, with the arrow indicating the location of the anemometers. This picture was found at the central office of DNM by Met. Mario Bidegain and kindly shared with the author of this thesis.

Looking at Figure 7.4 and Figure 7.5, it would not seem sensible, at least to the author's opinion, that if the building shown in Figure 7.4 is 17m high, the distance between the main roof of this building and the anemometers shown in Figure 7.5 is 28m (or 18m before 1930, according to Serrentino, 1981), as the anemometers should have been located at 45m above ground level (or 35m before 1930, according to Serrentino, 1981).

Fourthly, during the extreme wind speeds calculation for the development of the wind code UNIT:50-84, 1984 it was assumed that the building over which Antepuerto station was located did not have an effect on its wind measurements. However, the registered wind speeds may have been affected by the blocking effect of the building or its surroundings on the wind flow, depending on the location of the anemometers, as commented before.

On the other hand, an ABL flow profile with height was assumed in order to obtain the corresponding wind gust speeds at 10m height from the measured wind gusts, whereas most high winds in Uruguay would be caused by severe convective activity, as suggested in Sub-section 2.2.5.2 and verified in Chapter 5. ABL flows and downdraft outflows present different

profiles with height, as shown by Figure 2.11, and this difference needs to be taken into account when applying a height correction.

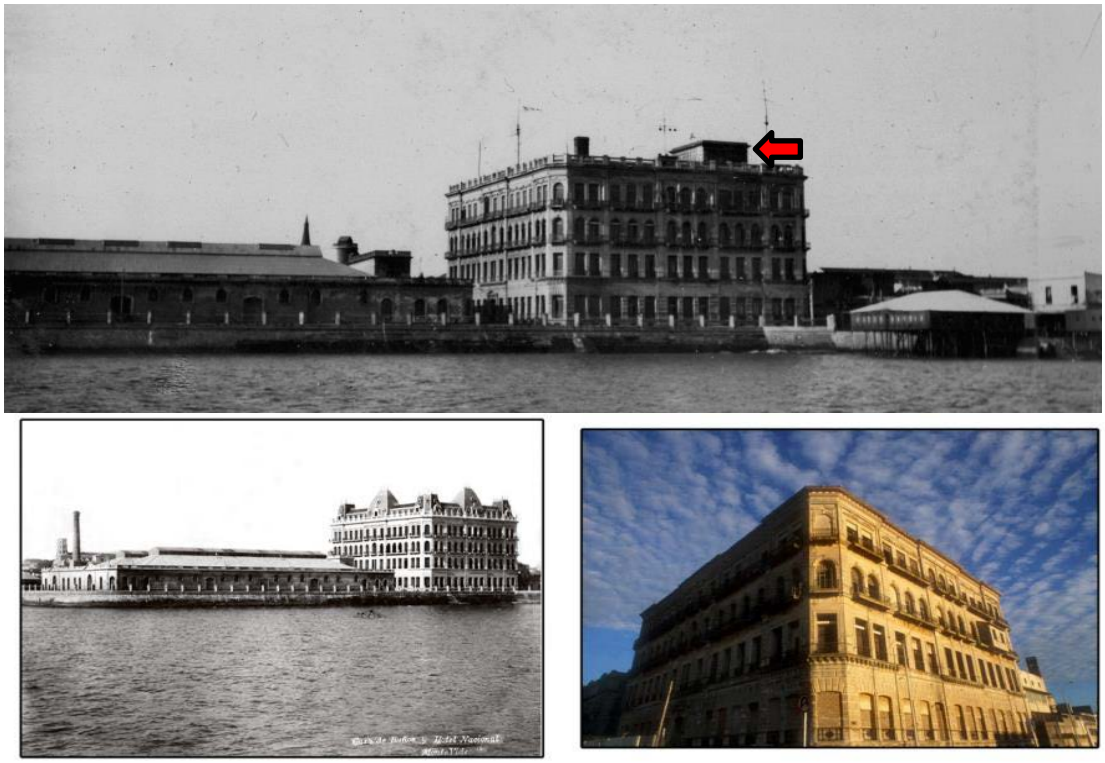


Figure 7.4 Antepuerto station and surroundings

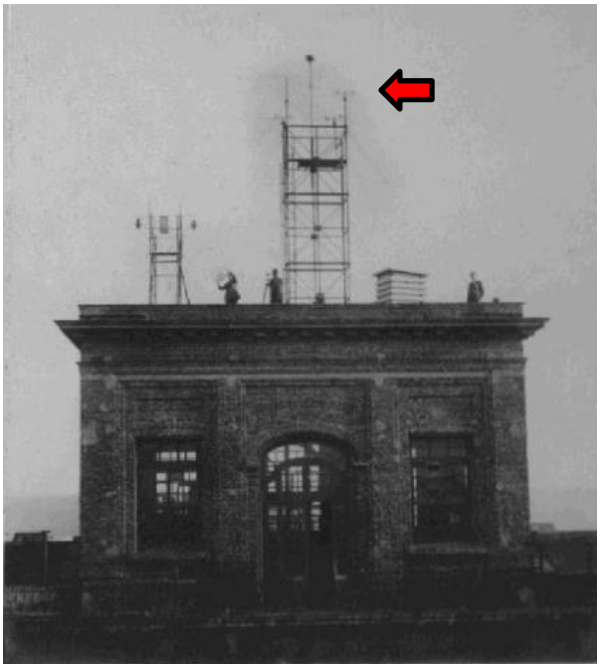


Figure 7.5 Location of anemometers at Antepuerto station (image from DNM)

Finally, the hypothesis that extreme and mean wind climates are correlated across the country is not correct. Mean winds are mainly determined by the South Atlantic anticyclone, the topography and the sea-breeze near the coastline, as presented in Sub-section 2.2.5.1, while the characteristics of high winds are mostly related to the development of severe convective activity over the country, as that associated with the passage of cold fronts or squall lines; as well as with the intensification of extra-tropical cyclones over Uruguay, or the occurrence of other synoptic high winds, as shown in Chapter 5. The geographic distribution of these meteorological high wind events is different from that of the mean winds.

7.7. Discussion

The observations made in the previous section arise sensible doubts on the data quality of the annual maxima wind gusts data series used to obtain the characteristics of the extreme wind climate of Montevideo, from which the extreme wind speeds for structural design for the whole country and the national extreme wind map were mainly derived. To base the establishment of the extreme wind speeds for design for a whole country on wind data from mainly one station is a bit risky, and even more if this station presents a non-standard exposure and an annual maxima wind gust speeds series with a clear discontinuity. Thus, all efforts should be made to verify the wind data quality of this wind speed series in order to apply any result derived from its analysis with certain confidence.

If more metadata from Antepuerto station were available, e.g. details of the different locations, heights, surroundings, models of the anemometers, dates when the sensors were changed or adjusted, calibration reports, etc., it might be possible to evaluate the quality of the wind measurements of this station, as presented in Section 2.3, the possible reason(s) for the drop presented by the annual maxima wind gusts, and the feasibility of correcting its annual maxima wind gusts data series, in particular, the drop that this series presents around 1930.

Knowing the actual location and height of the anemographs that registered wind speed in Antepuerto station from 1906 to 1969 is also required for an adequate calculation of extreme wind speeds at 10m height. Wind speeds measured during periods corresponding to different heights and/or surroundings of the anemometer should be first independently converted to

wind speeds at 10m height over open and level terrain, in order to obtain a homogeneous data series for the whole measurement period. In order to be able to apply results from Fisher and Tippett, 1928, the calculation of the parameters of the statistical distribution that best adjusts the annual maxima wind gusts series should be only carried out once this series is homogenised, as Fisher and Tippett, 1928 requires working with identically distributed data.

Another issue that would need to be investigated is if the presence of Antepuerto building affected the wind gust measurements carried out in this station, and if so, in which way, as well as the law that should be applied for correcting wind gust speeds measured at non-standard heights, to represent measurements at the standard height of 10m. A law for flows of ABL type was assumed for this task, but intense convective activity has been proved to be the cause of the most frequent and highest wind gusts in Uruguay during this PhD research. On the other hand, the interaction of a strong outflow boundary with a building, and especially how the building affects the developed wind flow above it, are topics currently under research for which there would not be a direct answer yet, but that need to be considered for this correction, due to the non-standard location of Antepuerto station, i.e., above the roof of a four-storey building.

If a reliable measurement period can be identified, and wind gust speeds at 10m height can be adequately calculated from the actual measurements, the extreme wind gust statistics for Montevideo could be recalculated. The series from Antepuerto station may be the longest wind gust speed series in Uruguay, and as such, it could be worth exploring the possibility of correcting it.

On the contrary, if more metadata from this station are not found, it would be difficult to evaluate the quality of its wind data, and how well the extreme wind statistics proposed for Montevideo in the national wind code UNIT:50-84, 1984 reflects the actual extreme statistics.

Other options could be using only the period that Battione, 1969 indicates as reliable (1941-1965) to calculate the extreme wind statistics for Montevideo, taking also into account other observations previously made; or performing a search for wind gust speed series of adequate length and quality measured at other meteorological stations of the country.

In this sense, finding reliable wind gust data series of adequate length measured at 10m height could be an easier and better solution. As non-synoptic winds mostly associated with the occurrence of intense convective activity, dominates the extreme wind climate of Uruguay, wind gust speeds measurements are needed to characterise it, as observed before. In that case, extreme wind value analysis should be performed to check the extreme wind gust statistics presented for Montevideo in the national wind code UNIT:50-84, 1984, and/or the statistics for other sites of Uruguay could be calculated without having to assume any correlation between wind gusts at different regions of the country.

On the other hand, it would be good to use more recent wind gust speed measurements, as the ones used to establish the wind speed vales for structural design are more than 40 years old. This has been recently performed for Brazil (Beck and Correa, 2012), and also proposed for Argentina (Natalini and Natalini, 2010). To the author's opinion, it is worth considering the possibility of developing a regional extreme wind map.

If extreme wind maps from neighbouring countries are compared, the gust averaging time used in each country should be known and taken into account; as well as the quality of the data and of the associated metadata. The importance of these issues was stressed in Section 2.3. This comparison should be performed among areas with extreme wind climates of similar characteristics.

If design wind speeds given by the current Argentinian and Uruguayan wind codes for actions on structures (CIRSOC, 2005a and UNIT:50-84, 1984) are compared for the borders between these countries, differences of 5 to 10% would be obtained (e.g. the 3s wind gust of 50-year return period for Argentina is between 46 to 48m/s for that region while for Uruguay corresponds to 50.5m/s).

If the same comparison is made for the borders between Brazil and Uruguay, using the NBR:6123, 1988b wind code and the UNIT:50-84, 1984, the difference between the 3s wind gusts of 50-year return period wold be around 5 to 15%, with the higher values corresponding to Brazil.

On the other hand, results obtained from Chapter 5 indicated that toward the northwest of Uruguay, higher wind gusts would be measured more frequently than in the southeast. This

could imply that design wind speeds should be higher in the northwest than in the southeast of Uruguay. This is not what the current national extreme wind map indicates, as shown in Figure 7.3, where higher design wind gust speeds are proposed along the South Atlantic and the Río de la Plata coastlines, as well as along the border with Argentina, and this difference should be analysed with care. At the time this thesis is being submitted, more years of wind gust measurements from UTE database are available, which would allow applying different statistical techniques to analyse the geographical distribution of extreme winds in the country, as well as proposing design wind speed values for different regions of Uruguay.

Last, but not least, it would be very valuable to analyse which averaging time and sampling frequency would be adequate for wind gust speed measurements in order to develop a new extreme wind map and make all efforts to maintain the measurement procedures and sites. As presented in Holmes and Ginger, 2012 or Lombardo, 2012, changing types of instruments, averaging procedures, etc., may have a significant effect in the calculated extreme winds, e.g. a system with a slower response to high wind gusts may register smaller extreme wind gust speeds.

A prior discussion on how wind gust speeds should be measured to adequately characterise wind loads on structures would be useful. For example, Prof. Giovanni Solari, from the University of Genoa, Italy has been developing lines of research with this aim (e.g. Solari, 2014; Solari et al., 2015a; Solari et al., 2015b). On the other hand, the work presented in Holmes et al., 2014 is also worth taking into account for this discussion.

Chapter Eight

Summary discussion

South Eastern South America (SESA), defined in Figure 2.23 in this thesis, presents a particularly strong extreme wind climate that combines the occurrence of severe convective activity, with the passage of weather fronts and intense extra-tropical cyclones (e.g. Satyamurty et al., 1998, all having the potential of generating high winds, such as.

As described in Sub-section 2.2.4, the development of severe convective activity in SESA in summer and spring would be tightly linked to the strengthening of a LLJS flowing east of the Andes, which transports heat and moisture at low levels from tropical SA to SESA (e.g. Salio et al., 2007, and Veblen et al., 2007), and increases atmospheric convective instability in this region, setting conditions for convection initiation.

This mechanism is illustrated in Figure 8.1 and explains why different types of MCSs, which have the potential to generate different types of outflow boundaries associated with deep convection, downbursts, and sometimes tornadoes, frequently develop in SESA, as shown in Figure 2.19 and Figure 2.20, (and in Figure 2.28 to Figure 2.30 for the case of severe convective storms). This mechanism would be similar to the one that favours the development of MCSs in the Great Plains of USA (Maddox, 1983).

In relation to extra-tropical cyclones in SA, typical trajectories were shown in Figure 2.26, while Necco, 1982b observed that the most intense of these systems tended to move to the southeast while intensifying in their way to the South Atlantic Ocean. On the other hand, Schwarzkopf, 1997 indicates for Argentina that between 35° an 55°S latitude and in its north-central area, strong winds are dominated by extra-tropical cyclones, moving from west to east in the first mentioned area, and toward the south-east in the second case. For the latter case, she indicates that they form mainly in winter and early spring.

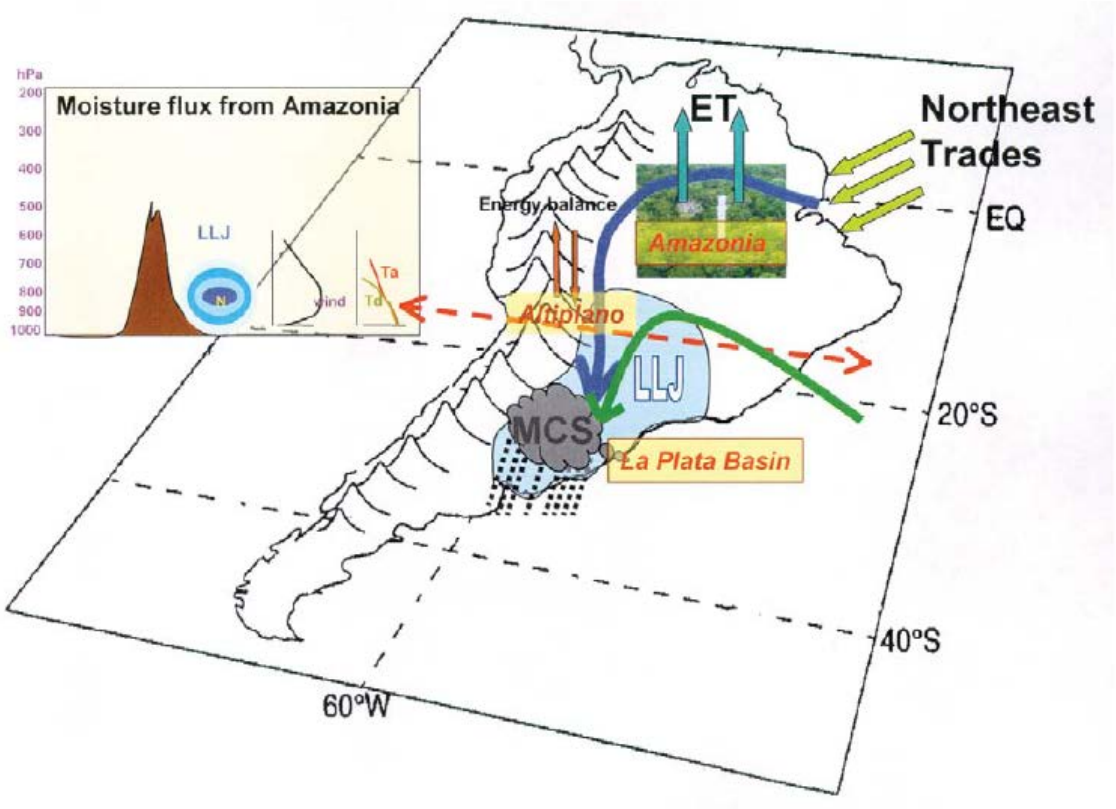


Figure 8.1 Main mechanism for the development of MCSs in SESA (Vera et al., 2006)

Results obtained in Chapter 5 showed that in Uruguay, non-synoptic winds, usually associated with intense convective activity, would dominate the highest wind gust speeds in all the country, with more frequent and more intense events toward the northwest of the country. This geographic behaviour differs from the one proposed in the national wind code for actions on structures, UNIT:50-84, 1984, as indicated in Chapter 7.

Results from Chapter 5 also indicated that with high wind events of larger temporal (and therefore larger length) scales were more frequently found in the southeast than in the northwest of Uruguay. Intensifying extra-tropical cyclones and fast entrances of cold air masses from the south were two of the identified meteorological phenomena of synoptic temporal scales (as measured at fixed locations) causing high winds in Uruguay. Synoptic high wind events were registered with higher frequency of occurrence in the southern and south eastern regions of the country, but with lower frequency of occurrence and corresponding to lower wind gust speeds than non-synoptic high winds events.

The relative significance of these different types of extreme wind events in the extreme wind climate of Uruguay, and the observed main characteristics of the geographic behaviour of high wind events of different temporal (and length) scales over the country analysing UTE data, agree with results from several regional wind engineering and meteorological studies, as those presented in Sub-section 2.2.4.2. As indicated by Natalini et al., 2011, in north eastern Argentina, i.e., to the northwest of Uruguay, virtually all high wind events that produce damage to civil structures are associated with severe convective activity, mainly in the form of MCCs or due to the passage of cold fronts or squall lines with the potential of generating intense convective activity. On the other hand, Lichtenstein and Schwarzkopf, 1970 found a maximum in the geographic distribution of the passage of squall lines in Argentina to the northwest of Uruguay, as shown in Figure 2.33, while Ferreira, 2014 shows for the south of Brazil, an increasing trend in the number of severe convective wind gusts also toward the northwest (reproduced in Figure 2.32). These results, together with those from Gan and Rao, 1991 shown in Figure 2.25 on the geographic distribution of cyclogenesis for SA, would explain the geographic distribution of the high wind gust speeds found for Uruguay, with an increasing trend in frequency and wind speed values toward the northwest of the country, and the fact that more high wind events with higher temporal (and length) scales were found toward the southeast of Uruguay.

The extreme wind climate of Uruguay would then be dominated by non-synoptic high wind events mostly related to intense convective activity, and, in a lesser degree, would be influenced by synoptic high wind events, especially in its south and southeast, in particular due to the intensification of extra-tropical cyclones during their trajectory to the South Atlantic Ocean. The first characteristic can be related to the main features shown in Figure 8.1, and the second one, to the geographic distribution of cyclogenesis events in SA indicated in Figure 2.25. The analysis presented in Chapters 5 and 6 respectively indicate that intense convective activity would dominate the extreme wind climate of Uruguay for short return periods (few years) as well as for longer return periods.

In relation to the seasonal distribution of high wind events, SESA presents more frequent severe convective activity in spring and summer, fact that can be explained by the observation of Veblen et al., 2007 that during the warm season, the deepening of the Chaco low intensifies the transport of moist, warm air from the Amazon basin toward SESA, fuelling severe storms

in the form of prefrontal squall lines or other MCSs, as illustrated in Figure 8.1. Accordingly, the highest wind gust speeds measured by the network of stations of UTE, as shown in Chapter 5, presented higher frequency of occurrence between October and March, i.e., during SH spring and summer.

In particular, the northwest of the country registered more high wind events, i.e., events with $U_{gust\ 45m} \geq$ 80km/h (22.2m/s), in January, while the south and east of the country, in October and November, as shown by Figure 5.14. It should be noticed that in the northwest of Uruguay the network of analysed stations presented less density than in the rest of the country, as indicated by Figure 3.1(b), but more recent analyses have confirmed the trend found for that area (Durañona et al., 2015).

The highest wind events at all the analysed stations across the country presented sudden increases in wind gust speed, sudden changes in wind direction and fast temperature drops, all features compatible with the occurrence of outflow boundaries generated by intense convective activity (e.g. downdraft outflows and gust fronts, among others). As presented in Chapter 2 and verified in Chapter 5, these events tend to present higher gust factors than those expected for ABL flows, with values varying within a wide range.

In particular, in the present research, gust factors defined over 10min periods during convective activity ranged from 2 to 2.5 and above, with a positive trend between the registered wind gust speed and the corresponding gust factor value. The latter would indicate that the highest wind gust speeds tend to occur during convective events of smaller time (and therefore length) scales, corresponding to high wind gust speeds sustained during a small fraction of the corresponding 10min measurement interval. Some gust factors defined over 10min periods were as high as 3.8 at 10m height. As higher gust factor values were found in the northwest of the country than in its southeast, the occurrence of non-synoptic high wind events related to intense convective wind events of smaller time (and therefore length) scale would be expected to be more significant in the northwest of Uruguay than in the rest of the country. The positive relation found between gust factor values and wind gust speeds would be in accordance with results from Fujita, 1985 and other authors, which indicate that the most intense wind events tend to present smaller length scales.

The seasonal behaviour of the high 10min mean wind speed events found also resembles the seasonal characteristics of convective activity in SESA along the year and a monthly frequency of occurrence very similar to that of the highest wind gust speed events, as shown in Chapter 5. This can be easily verified comparing the monthly frequency of occurrence found for the high 10min mean wind speed events measured by the network of UTE during the 4-year analysed period (Figure 5.17 (b)) and the monthly frequency of occurrence found for the 10min mean wind speed annual maxima measured at Carrasco station (Figure 6.1 and/or Figure 6.2), with the monthly frequency of occurrence found for the high wind gust speed events measured by the network of stations of UTE (Figure 5.13(b)).

These results indicate that although it would be difficult to estimate design wind gust speeds from 10min mean wind speed records, the highest 10min mean wind speed values tend to occur also during intense convective activity, and that convective activity would also dominate the 10min mean extreme wind climate of Uruguay for short return periods (few years) as shown in Chapter 5, as well as for longer return periods, as shown in Chapter 6.

These main characteristics can be understood looking for example at Figure 5.6(a), which presents a typical example of a high wind event generated by intense convective activity in Uruguay, as it presents sudden wind speed increase, change of wind direction and temperature drop. As the wind speed of many of the identified non-synoptic high wind events showed a similar pattern to the one illustrated in this figure, i.e., wind speeds did not decrease immediately, but tended to remain high for 1 hour or more instead, they would also be registered as high 10min mean wind speed events.

The main characteristics found for high wind events at 45m height were verified for high wind events at 10m height.

As presented in Chapter 5, during the highest wind gust speed events registered by UTE stations (U_{gust}>40m/s) wind gust speeds registered between 10 and 80m height tended to present quite similar values.

All these characteristics would indicate that the flow during non-synoptic high wind events would considerably differ from an ABL flow. These conclusions raise sensible doubts about the wind flow model that should be considered for wind design of structures in Uruguay, as

well as for the calculation of wind speeds and other flow characteristics at heights different from the measurement height, and have an important and direct implication in the validity of the wind design calculation scheme proposed in the wind code for actions on structures, UNIT:50-84, 1984, as discussed in Chapter 7.

In relation to the wind direction distribution of high wind speeds it was found that around 80% of the high wind gust events occurred with wind directions from the south-west quadrant, as indicated in Chapter 5. Places particularly exposed and/or open to those wind directions should therefore be carefully analysed and/or designed.

Several of the meteorological phenomena that generated some of the most intense wind gust speeds over a series of UTE stations during the same dates moved toward the northeast, with a typical NW-SE orientation. Their time evolution could be analysed running animated sequences of UTE data over a map of Uruguay, and looking at the evolution of intense convection over the country with GOES satellite infrared images, as explained in Chapter 5. Some of these phenomena were identified as cold fronts passing over Uruguay and generating convective high winds along its trajectory, and agree with observations from, for example, Celemín, 1984 on the frequent passage of cold fronts and squall lines in our region, and with the identification of cold fronts as one of the main meteorological mechanisms producing high wind speeds in Montevideo by Vieira, 1949.

Looking at the time evolution of the highest wind speeds across Uruguay, the translational wind speed of these systems could be estimated to be around 60km/h in some of the analysed cases.

On the other hand, as described in Chapter 2, documentation from the beginning of last century already indicated the significance of convective activity in the extreme wind climate of Uruguay (e.g. Morandi, 1901 - 1917; Morandi, 1945; Vieira, 1949; Vieira, 1969, among others). In bulletins from Observatory of Prado station, located in Montevideo and described in Section 3.5, high wind events of relatively short time scale, occurring suddenly and simultaneously with intense rain and/or hail and shifts in wind direction were often reported. The highest wind speeds registered at this station corresponded more frequently to wind events with time scales of several to tens of minutes rather than to typical time scales of synoptic high wind events i.e. of at least several hours, as those illustrated in Figure 2.3. This

is in accordance with results presented in Chapter 5 from the analysis of wind data from the network of stations of UTE: the highest wind speeds were mostly generated by events that usually lasted more than few minutes, but less than 4 hours, and presented sudden increases in wind speed, abrupt wind direction changes and temperature drops.

Frequent and abrupt changes of temperature were also commonly reported in the country during the first half of last century, and considered as one of the main characteristics of the climate of Uruguay (e.g., Boerger, 1953; Morandi, 1952), a feature also found during many of the non-synoptic high wind events identified during this research. Some of these reports can be found in papers from the 'Revista Meteorológica', in periodic bulletins from the Observatory of Prado, as well as in books and papers written by Prof. Morandi (Morandi, 1921) and other authors.

From the previous paragraphs, it can be concluded that the occurrence of non-synoptic high winds generated by intense convective activity would be a significant feature of the extreme wind climate of Uruguay and that their distinct characteristics and flow structure should be further analysed and taken into account for wind loading calculations. Currently, several international lines of research are being developed with that aim, as mentioned in Chapter 7.

As Chapter 5 showed that there is not a direct relationship between the highest wind gusts that occur in Uruguay and their corresponding 10min mean wind speeds, and as high wind gusts of time scales of just few seconds would have flow structures with characteristic lengths of at least tens of meters, extreme value analysis of wind gust series would be required to adequately describe the extreme wind climate of Uruguay for many wind engineering applications, in agreement with results presented by authors such as Riera et al., 1977 or Holmes et al., 2005b, and with the current work of Prof. Solari (e.g. Solari, 2014 and Solari et al., 2015a).

On the other hand, according to Holmes et al., 2005b as presented in Section 2.5, when there is more than one meteorological event that produces high wind speeds in a region, and one of them is clearly more dominating than the others, extreme value analysis without separating into storm types may not introduce significant errors in the estimated extreme wind speeds. As intense convective activity would be responsible for the most frequent and highest wind gusts registered in Uruguay, it might not be required to separate wind gusts according to the

meteorological type of event that generated them, in spite of the existence of other meteorological events producing extreme winds in the country, as e.g. intense extra-tropical cyclones. However this hypothesis should be tested as suggested by e.g. De Gaetano et al., 2014, among others.

The extreme wind value analysis carried out on the 10min mean wind speed series of Carrasco station presented in Chapter 6 would not be the best source for obtaining the extreme statistics of wind gusts for Montevideo, due to the lack of a direct relationship between wind gusts and 10min mean wind speeds.

To accomplish this task, one option could be trying to correct the wind gust series of Antepuerto station presented in Chapter 7, taking into account exposure conditions and checking its metadata. For example, the period indicated by Battione, 1969 as the most reliable could be first analysed to obtain the extreme statistics of wind gusts in Montevideo and compare it with results from other measurement periods from this station. For other regions of the country, extreme value techniques for relatively short wind records, as those mentioned in Sub-section 2.4.1, and others, could be applied to wind gusts series of UTE stations.

If a statistical method that requires extreme data series to be i.i.d., as the classical GEV method, is going to be applied, it is recommended to use annual maxima wind gust speeds due to the seasonal behaviour of the highest wind gusts found for Uruguay, with higher frequencies of occurrence from October to March, and much lower values in May, as shown in Section 5.5.

These seasonal characteristics could be related to the fact that between March and May convection shifts gradually northward toward the equator according to CLIVAR, 2006, as presented in Sub-section 2.2.4.1, and that during April and May, the southward flow of tropical warm and humid air from the Amazonia weakens, as more frequent incursions of drier and cooler air from mid-latitudes begin to occur over the interior of subtropical SA.

As mentioned before, another important finding of this research is that the geographic distribution of the highest wind gusts proposed in the national wind code UNIT:50-84, 1984, would not agree with results obtained in Chapter 5, as the highest wind gusts would not occur

along the South Atlantic and the Río de la Plata coastlines and along all the border with Argentina. Instead, higher and more frequent high wind gusts would be found toward the northwest of the country.

Given these results, the number of incorrect assumptions made, and the wide range of uncertainties regarding the extreme wind time series used for the development of the extreme wind statistics and the national extreme wind map presented in the national wind code UNIT:50-84, 1984, as discussed in Sub-section 7.6, a review and update of the extreme wind statistics and extreme wind map presented in this code are strongly suggested. If this wind code is revised, it would be advisable to analyse the potential effect of the flow structure of non-synoptic high winds, which present significant transient characteristics, on the wind loading of structures. One option for this could be to follow approach suggested by Prof. Solari (e.g. Solari et al., 2015b). A possible revision of the national wind code could also offer the opportunity to establish a benchmark by incorporating downburst wind profiles and wind flow structures into a code or standard.

This issue had already been pointed out by several authors as e.g. Chay et al., 2006a, stressing that most design techniques and wind codes currently evaluate wind loads on structures assuming ABL flows, despite increasing recognition that outflows generated by severe convective activity should be taken into account for calculating design wind speeds in many regions of the world, as mentioned in Section 2.5. More recently, Ponte Jr and Riera, 2010 stated that "in spite of the overwhelming evidence concerning the relevance of thunderstorm winds in structural design, the subject has received due attention only in the area of overhead transmission lines" (AS:1170.2, 2002; AS/NZS:1170.2, 2011; AS/NZS:7000, 2010); Jackson, 1981; ASCE, 1990; CIGRE, 2004; CIGRE, 2008).

To this author's knowledge, the only wind code on wind action of structures that considers and proposes a wind gust profile for downburst winds is ISO:4354, 2009, while Holmes et al., 2005a proposes a wind gust profile to use in wind codes until the required full-scale data is available. Other models are also available, as mentioned in Sub-sections 2.2.1 and 2.2.3.2.

In order to propose an adequate model of the flow structure and time evolution of these events, more non-synoptic high wind events should be measured with higher sample

frequencies, as also pointed out by Solari et al., 2015a, who recommended sampling frequencies of at least 10Hz.

In relation to the time scale during which wind gust speeds usually sustain high values, as presented in Chapter 5, it was found that most of the times it ranged from tens of minutes to few hours.

It needs to be pointed out that most of these conclusions could be arrived at due to the existence of the network of stations of UTE, which presents a relatively high density of meteorological stations, measuring continuously every 10min at heights between 10 and 100m. These features allowed the description of the time evolution of over Uruguay, and of some of their main characteristics.

This network constitutes an important tool for the study of different weather systems that define the extreme wind climate in Uruguay, and as such, it is an extremely valuable source of information for the country in different fields, and for wind engineering applications in particular.

If compared worldwide, the characteristics of this network are quite unique, and together with the relatively high frequency of registers of non-synoptic high wind events related to intense convective activity in Uruguay, as indicated in Chapter 5, offer an interesting opportunity for the study of these events. The need of more full-scale measurements of downburst outflows and non-synoptic high wind events in general has been highlighted over the last decades, especially in the transmission lines and wind engineering fields in mid-latitude regions.

In this sense, and as it was previously observed, it would be very valuable if several stations could be implemented with recording systems that would store data at higher sampling frequencies during high wind events, for a better description of their time evolution and flow structures.

In particular, to ensure public safety, the design of critical structures (such as nuclear plants, high-voltage transmission lines, etc.) requires detailed extreme value analyses and a good knowledge of the geographic distribution and flow structure characterisation of the flows that cause the highest wind gust speeds. In our region, the coordination of a research of this type with Argentina and Brazil seems to be a sensible way to accomplish this task.

On the other hand, the main results presented in Chapter 4 agree with results from regional research and with results presented in other chapters of this PhD thesis:

- In agreement with results for northeaster Argentina presented in Natalini et al., 2011, the most common types of wind damage reported corresponded to fallen branches, uprooted trees, downed electricity poles and blown roofs, and most of these damaging wind events were also found to have been caused by intense convective activity.

- The non-synoptic and transient characteristics of most of the high wind events described in newspaper reports along the analysed 5 years matched the results presented in Section 5.5.

- The geographic behaviour of the dimensions of the affected areas, i.e., bigger areas affected by wind damage reported in the southeast of the country than in its northwest, agrees with the tendency of intense extra-tropical cyclones to produce higher wind speeds in the southeast of Uruguay, and with the fact that convective activity would be relatively more important in the northwest of the country, as expected from Sub-section 2.2.5.2 of the literature review.

- The values of the wind speeds reported during intense convective activity, the typical wind directions cited, the estimated translational speed of those storms, among other characteristics, also agree with results presented in Chapter 5.

During the research outlined in Chapter 4, a preliminary link between reported wind gust speeds and types of wind damage could be found. This type of relation could be used to develop a scale to estimate wind speed from wind damage in the country. With that purpose, the local characteristics of trees, soil, types of constructions, structures, etc. of Uruguay should be taken into account, as it is usually recommended for the development of such scales.

In addition, the investigation of the failures and incidences experienced by the 500kV Palmar-Montevideo transmission lines presented in Section 4.8 showed that most of them occurred when intense convective activity was affecting those areas, sustaining high wind speeds during several minutes.

Traditional design codes calculation underestimates the wind loads acting on these systems, principally due to the hypothesis that the flow that should be considered for design corresponds to an ABL flow, which is less correlated in space than during downdraft outflows. As indicated in Section 4.7, designers of transmission lines have, until recently, applied span reduction factors that are too low for convective downbursts. This example highlights the importance that has the adequate consideration and characterisation of the type of high wind events that dominates the high wind climate of Uruguay, for many other wind engineering applications.

In relation to the passage of intense extra-tropical cyclones over Uruguay, different analysis could also be carried out.

- Section 4.6 presented the study of one of the most intense extra-tropical cyclones that deepened over Uruguay in the last decade, on August 23rd, 2005. As shown in that section, it principally affected the southern and eastern areas of the country along the coast, with a maximum wind gust speed registered in Montevideo, at Carrasco station, of 174km/h (48.3m/s). In that section, it was hypothesised that this high wind gust speed may have corresponded to the occurrence of a sting jet. The corresponding gust factor (2.35) presented a value very different from what it would be expected for a synoptic high wind event of ABL type. Thus, this section showed that high wind gusts measured during the passage of extra-tropical cyclones do not necessarily correspond to synoptic high winds, supporting the concept presented in Sub-section 2.2.1 that circulations of all sizes simultaneously exist within the atmosphere, but as the size of a weather system decrease, the severity of the weather it can create tends to increase. Another example of this concept was the occurrence of a tornado inside an extra-tropical cyclone that generated intense winds in the country on October 23rd, 2012, as shown in Figure 2.52(b).

- During the analysis of the passage over Uruguay of the extra-tropical cyclone of September 19th, 2012 shown in Chapter 5, the behaviour of the values and directions of the highest wind gust speeds recorded at each station showed the expected cyclonic streamlines, and a trajectory and intensification toward the southeast, as illustrated by

Figure 5.10. These characteristics matched those described in Sub-section 2.2.5.2. A translational wind speed of about 50km/h (~14m/s) could also be estimated from this figure, which agrees with results from Sinclair, 1995 mentioned in Sub-section 2.2.4.2.

- Another particular characteristic of this extra-tropical cyclone was that their highest wind speeds along most of the southern Uruguayan coast were registered from the south. In Montevideo, streets that tend to channel the wind flow in this direction represent a threat for the population, as it happened during this event in Ciudad Vieja (Old City), where many of the streets have a south-north orientation and are surrounded by buildings of medium height.

Chapter Nine

Conclusions and recommendations for future work

9.1. Conclusions

The research aims outlined in Section 1.2 were fulfilled: the main types of high wind events that determine the extreme wind climate of the country were identified and characterised, and their relative contribution to it, as well as the most common types of wind damage they produce, evaluated.

On the other hand, several available wind databases and sources of information on high wind events, current as well as historical, were documented and analysed, and the main characteristics of the type of wind measurements required to adequately characterise the extreme wind climate of Uruguay were discussed, and in particular, the one needed to update the national extreme wind map, established in the wind code UNIT:50-84, 1984.

The same comments apply in relation to the objectives: a search and analysis was conducted on available sources of information regarding damaging wind events that occur in Uruguay; a database with the main characteristics of these events and their effects was generated, and a threshold wind speed for wind damage was estimated.

In addition, a search and analysis of available historical and current wind measurements and their corresponding metadata was conducted, and the quality of their data and metadata was analysed. Besides, different types of high wind events that cause wind damage in the country were analysed, and their main characteristics, described, such as typical wind speed evolutions with time, expected wind speed values, frequencies of occurrence, predominant wind directions, gust factor values, wind speed distribution with height, seasonal behaviour typical trajectories, etc. These results were then compared and linked to information presented in historical literature and with national, regional and international research in the fields of meteorology and wind engineering.

An extreme wind value analysis was carried out on a 35-year long database of hourly 10min mean wind speeds measurements from Carrasco station, located in Montevideo and the

frequency of occurrence of potential damaging wind events was estimated from the wind database from the network of UTE stations.

Finally, the characteristics of the wind data, corresponding metadata and procedures applied for determining the design wind speeds for Uruguay and developing the national extreme wind map established in the national wind code UNIT:50-84, 1984 were described and discussed, and the probability and geographic distributions of extreme winds presented in this code were compared and discussed with those obtained from other wind databases studies.

The next paragraphs summarise the main conclusions of this PhD research.

♦ Non-synoptic high winds generated by intense convective activity dominate the extreme wind climate of Uruguay. The analysis presented in Chapter 5 of 4 years of meteorological data from the network of automatic weather stations of UTE described in Section 3.3, showed that the highest wind gusts recorded at all the analysed stations occurred during severe convective activity, while results from Chapter 6 on the seasonal distribution of the annual maxima wind speeds registered at Carrasco station along 35 years suggest convective activity also dominates the extreme wind climate of Uruguay for longer return periods. With lower frequency of occurrence and typically lower wind gust speeds, the passage of intense extra-tropical cyclones and of other synoptic weather systems, such as fast entrances of cold air masses, were other types of meteorological phenomena found to generate high winds in the country.

♦ Distinct and much wider ranges of gust factor values (maximum wind gust speed divided by its corresponding 10min-mean wind speed) were found during non-synoptic high wind events, usually associated to intense convective activity, than during synoptic high wind events. For non-synoptic high winds, gust factors mainly between 2 and 2.5, and greater, were obtained, as shown in Section 5.5. These values are similar to those calculated from Choi's work, as discussed in Sections 4.6 and 5.5, and very different from those corresponding to ABL flows (Cook, 1985) and to synoptic high wind events reported in Solari et al., 2015a.

♦ Gust factor values could therefore help discriminating high winds caused by intense convective activity from those caused by synoptic high winds.

♦ The variability of gust factor values during intense convective activity should warn against estimating extreme wind gusts from extreme 10min mean wind speeds. Instead, the analysis of direct wind gust speed measurements should be preferred.

♦ Wind gust data series should then be used to perform extreme value analysis for wind loading calculations and risk analysis.

♦ To perform these types of analyses, wind data and metadata of good quality are required. The recorded values of wind gust speeds strongly depend on the wind gust averaging period. The sample frequency should also be known and set to ensure that continuous monitoring of the highest wind gusts is taking place. Different averaging periods, and/or sample frequencies may affect the derived extreme wind gust statistics for a site. Solari et al., 2015a, for example, propose to perform these measurements with ultrasonic anemometers with a sampling frequency of 10Hz.

♦ Several historical wind measurements and their metadata were analysed and detailed in this thesis, as presented in Section 3.5 for the Observatory of Prado station, in Section 3.4 for Carrasco station, and in Section 7.4 for Antepuerto station.

♦ As reliable wind gust speed measurements are needed over long periods of time for usual extreme wind value analysis (i.e., 20 to 30 years), it would be very valuable that the criteria for measuring and registering wind gusts at the network of stations of UTE could be maintained along time, as well as the register of their metadata. Improvements such as measuring high wind speed events at a higher sample frequency (e.g. 10 samples per second) at all heights, at least at several stations, and increasing the number of anemometers measuring at 10m height would be extremely valuable for wind loading analysis and calculation. The use of ultrasonic anemometers would also be recommended.

♦ The unique features of the network of stations of UTE allow the characterisation of high wind events that occur in Uruguay as never before, and of their geographic and seasonal behaviours. This knowledge is required for many wind engineering applications, such as research to decrease the number of blown down poles from medium- and low-voltage distribution lines, to adequately calculate wind loads on high-voltage transmission lines, or to select the class of wind turbine for a specific site, just to cite some examples related to the

energy sector. In this sense, the investment needed to maintain or even improve this network of stations would not be significant if compared with short, medium and long-term benefits derived from its existence and use.

♦ Potential damaging wind gust speeds in Uruguay at sites with open and level exposures have an estimated frequency of occurrence of once every one or two months in average along the year, as presented in Figure 5.14.

♦ Although, for uniformity reasons, these numbers were obtained and presented at a height of 45m, during most of the highest wind gust events wind speeds of similar values were also measured at 10m height in stations that had anemometers installed at this lower height. For example, during the analysed period (i.e., not greater than 4 years), six events that produced wind gusts between 40m/s (i.e., 144km/h) and 45m/s (162km/h) at different dates were registered in four stations of UTE network. Three of these six events were registered in two stations that had anemometers at 10m height, and in two of these events, these anemometers measured wind gust speeds of 40m/s. These values of wind gust speeds agree with values already measured in Montevideo at heights around 10m in the beginning of last century. Taking into account historical data, wind gusts of 55m/s could be expected to occur at this height at higher return periods, as illustrated by Figure 2.51(b). Careful extreme value analyses carried out on good quality wind gust speed series would help estimating these higher return periods with adequate confidence intervals. On the other hand, the similarity among wind gust speed values measured at heights between 10 and 80m, and the distinctive transient features of most of the registered high wind events, reinforce the concept that these wind flows do not correspond to ABL flows, and that it should be analysed if a different scheme for wind loading calculations would need to be applied in these cases.

♦ More frequent and higher wind gusts were found to the northwest of Uruguay. Longer data series and more analyses would be needed to improve the preliminary estimation of the geographic behaviour of high wind events in Uruguay presented in Chapter 5. This result is not in accordance with the geographic distribution of extreme winds proposed in the national wind code UNIT:50-84, 1984.

♦ Damaging winds in Uruguay show a seasonal trend similar to that of severe convective activity in South Eastern South America (SESA), as described in Sub-section 5.5.2. They

were found to occur more frequently between October and March, being May the month that presented less number of cases.

♦ In general, when wind speed suddenly increases, i.e., in few minutes, wind direction changes and fast drops in temperature (typically experienced in tens of minutes) occur. As mentioned in Section 2.1, these characteristics may be associated with the occurrence of strong outflow boundaries generated by deep convection, such as strong downdraft outflows or gust fronts, generally related to the presence of high cumulus nimbus clouds, which affect the wind flow structure up to at least 100m high.

♦ Several of the highest wind speed events registered by UTE stations were related to convective activity organised in lines, like along cold fronts with NW-SE orientation moving to the northeast, in accordance with results from, for example, Vieira, 1949 and Celemín, 1984.

♦ Population should be warned when an intense extra-tropical cyclone may cause high wind speeds at main streets parallel to the direction from where the highest wind speeds are expected to come from, as this may cause pedestrian risk during some hours at important places of the city, as it occurred in Montevideo during the passage of an intense extra-tropical cyclone on September 19th, 2012 at certain streets of Ciudad Vieja (Old City). In addition, the coastline tends to be a particularly exposed place for driving during such events, and warnings should be issued if risky conditions may be met.

♦ Although different, intense convective events, strong extra-tropical cyclones and even fast entrances of cold air masses tend to produce their maximum wind gusts from the southwest quadrant. High winds tend to come from the southwest quadrant, as verified in around 80% of the high wind events registered by UTE stations. This simple knowledge may help in the preliminary stages of the design of structures and estimation of wind loadings.

♦ When synoptic weather patterns are responsible for the register of high wind gusts, typically no significant changes in wind direction or temperature are registered, and the increase and decrease of wind speed is more gradual.

♦ Although synoptic high winds are usually sustained at a particular site during longer periods than high winds due to convective activity, intense convective activity also seems to dominate the extreme 10min mean wind climate of Uruguay.

♦ In spite of the mixed extreme climate that Uruguay presents, if typical extreme value analysis is applied, the Gumbel distribution seems to adequately represent the extreme statistics of 10min mean wind speeds, as indicated by the hypothesis tests shown in Chapter 6, and also suggested for example by Holmes et al., 2005b, for regions where one meteorological mechanism is dominant. However, it would be recommendable to analyse if different extreme wind statistics would be obtained if 10min mean wind speeds annual maxima are classified into synoptic and non-synoptic types of events and these results combined through mixed statistics.

♦ Blown roofs, trees and poles are the most common types of reported damage during high wind events.

♦ The research presented in Chapter 7 indicates that the national extreme wind map and the values of the characteristic wind speeds defined in the national wind code for actions on structures UNIT:50-84, 1984 should be revised and updated, for several important reasons:

- they are based on wind measurements performed more than 40 years ago
- they are mainly based on measurements carried out at just one meteorological station, Antepuerto station, extrapolating its derived extreme winds statistics assuming that the geographic distribution of extreme winds correlates well with the geographical distribution of mean winds across the country. Results from this PhD research do not support this hypothesis
- a clear drop on the annual highest wind gusts recorded at this station can be noticed around the year 1930 in the data series used to derive the extreme wind statistics, shown in Figure 7.1. This abrupt change experienced by the wind gusts recorded at this station apparently occurred when the anemograph was relocated and placed at a higher altitude. Extreme statistics are highly dependable on the homogeneity of the analysed data series, as emphasised in Section 2.3, and this type of inhomogeneity can have a great effect in the derived extreme value analysis. After analysing 50 years of wind data from this

station, Battione, 1969 regarded the period 1941-1965, after this relocation, as the most reliable.

- during the development of the extreme wind value analyses, Antepuerto's anemographs were supposed to have measured at 45m height above mean sea level (e.g. Hernández, 1971) and their measurements corrected to represent wind gust speeds measured at 10m height in open and level terrain assuming an ABL profile, without considering any influence of the nearby surroundings, but:
    - it is suspected that actual wind measurements took place at heights lower than 45m, as the building where this station was located is only 17m height according to IMM data.
    - Serrentino, 1981 mentions that wind was measured at different heights and sites at this station, thus the height correction should have been independently made for each measurement period, additionally checking that the new surroundings did not affect wind measurements. Very little information was found on the metadata of this station, and part of it was contradictory.
    - wind speed records may have been affected by the blocking effect of the building above which Antepuerto station was located
    - as results from this PhD research indicate that the non-synoptic winds would dominate the extreme wind climate of Uruguay, an ABL profile height might not be the best choice for correcting high wind speeds measured at non-standard heights (i.e., different from 10m height).

♦ Thorough research to describe the flow structure and turbulent characteristics of non-synoptic high winds associated with intense convective activity in Uruguay should be carried out. In particular, the wind loading calculation method proposed in the national wind code UNIT 50-84 might need to be revised.

♦ More research on the extreme wind climate of Uruguay, both general and specific to any wind engineering application, is needed to adequately prevent and mitigate its effects, by e.g. selecting the design wind speed for any structure in a more appropriate way, reducing the impact in the agronomic sector, providing for the improved management of agroclimatic insurances and the creation of new insurance products, improving existent wind codes that are applied in the country or creating new wind codes that Uruguay may need, to cite some

examples. About the latter issue, it must be taken into account that results from other regions of the world should not be directly extrapolated to our reality before checking that similarity exists between extreme wind climates.

9.2. Recommendations for future work

- Given the significance of non-synoptic high wind events, generally associated with the occurrence of intense convective activity in the extreme wind climate of Uruguay, extensive research on their vertical structure, their evolution with time, typical dimensions of their associated high wind speed areas, their interaction with complex topography, their extreme winds statistics, etc. is needed to adequately characterise the extreme wind climate of our country and its effects for many required wind engineering studies.

- As intense convective activity was proven to cause the highest wind gust speeds and the highest 10min mean wind speeds across all the country, and no relation was found between the maxima 10min mean wind speeds and the maxima wind gust speeds, counting with long databases of wind gust data of proven quality would be very valuable for extreme wind value analyses, as the wind loading of buildings and structures would depend more directly on wind gust speeds than on 10min mean wind speeds. This could involve the continuation of measurements and analyses of wind gust data from stations from UTE network, and the analysis of statistical tools that could allow the use of shorter datasets (i.e., less than 10 years) of wind gust speeds for extreme value analysis than the ML method applied to the GEV distribution. One possibility could be to explore the grouping of records from different stations belonging to regions with homogeneous wind extreme climates.

- If the quality of the wind gust data records registered at Antepuerto station can be verified, or if certain problems are detected and corrected for at least 20 to 30 years of records, then new extreme wind value analyses for Montevideo may be performed using its measurements, and comparisons between these results and others could be made.

- The national wind code, UNIT:50-84, 1984 assumes for wind loading calculations flows of ABL type, while intense convective activity was proven along this thesis to be responsible for

most of the highest wind gusts and 10min mean wind speeds registered across the country. It would be of due importance to investigate on the differences between wind loading generated by ABL flows and by strong outflow boundaries associated to deep convection on different types of structures. For this, more full-scale measurements of this type of events would be needed. As their characteristics depend on a number of factors, which in turn may depend on the particular climate of the region where they occur (e.g. Wakimoto and Bringi, 1988), these measurements should be carried out for national and regional meteorological conditions, in order to asses with more certainty the wind gust speeds that this type of extreme wind events may cause in Uruguay for different return periods and at different heights and how structures are loaded by them. One possible approach for the latter may be the one suggested in Solari et al., 2015b. This generated knowledge should then be incorporated into national wind codes for wind loading calculations, such as the national wind code UNIT:50-84, 1984 and other wind design codes applied in the country.

- It would be very valuable to have at least some automatic stations from UTE measuring and recording wind data at higher sample frequencies (e.g. 10 samples per second as recommended in Solari et al., 2015a) during high winds, and more measurements at 10m height in open and level terrain, thus enabling an easier comparison of high winds measured by conventional meteorological stations at the standard height of 10m with those registered by the network of UTE. Wind measurements carried out with ultrasonic anemometers may offer valuable information.

- When longer data series of wind gust speeds from stations from the network of stations of UTE become available, it would be recommendable to carry out different types of extreme value analyses, and to compare their results among them and with results obtained in neighbouring countries, and especially in their borders with Uruguay. An analysis of the wind gust averaging period of the anemometers of UTE and of other anemometers used during this comparison should be carried out.

- It could be worth analysing the characteristics of the transient forces that sudden increases in wind speeds can exert on buildings and structures, and if these forces should be taken into account for wind loading calculations.

- Performing field surveys when wind damage occurs could improve the current knowledge on the vulnerability of Uruguay to high winds, and on the relationship between wind speed values, type of damage and damage level. In particular, it would be interesting to:

  - conduct this study in collaboration with other research groups that are already performing field surveys in Argentina, as mentioned in Sub-section 2.2.4.2, in order to compare the obtained results. Some people in Uruguay already making individual efforts to describe severe winds could be incorporated to carry out this type of study in Uruguay, with guidelines on how to perform these surveys for wind engineering applications. The participation of regional meteorologists and a better transference of knowledge between the fields of wind engineering and meteorology at regional level would be very valuable.
  - organise a coordinated effort for an improved documentation of severe convective storms along the different South American countries affected by these phenomena (Nascimento and Doswell, 2006).
  - consider training volunteers to spot intense convective storms from their own homes and report the events in a standardised form (Nascimento and Doswell, 2006).
  - organise at national level a systematic documentation of high wind events, which may include damage reports from emergency management teams, the electric public company (UTE), severe weather events from airports, direct field surveys, etc. According to Nascimento and Doswell, 2006 there are several reasons to do this: there exists a synergetic relationship between the (good-quality) reporting of storm events and severe storms research/forecasting; the accurate documentation of different types of severe wind events is needed for developing forecast methodologies that not only identify environments conducive to severe weather in general, but that are also capable of discriminating distinct forms of severe weather. This documentation is also substantial when assessing the accuracy and/or skill of a given convective forecast methodology. Documentation of direct severe weather events from airports contribute to an important convective weather archive to research seeking the identification and prediction of atmospheric conditions favourable to potentially hazardous aviation weather. A study addressing the impact of climate changes upon the frequency of severe convective storms requires background knowledge on the ‘current climatology’

of severe weather events and of the large-scale atmospheric environments in which they develop. The systematic documentation of severe convective storms can play an important role in this sense (Nascimento and Doswell, 2006).

- Regional research programmes and collaboration could help developing a regional extreme wind map. In particular, a more detailed delimitation of the areas more prone to severe convective activity may help improving the awareness of the general public and local governments to these potential threats to human lives and properties, and lead to the improvement of policies for the prevention and management of these risks and economic losses.

List of references

Aguilar, E., Auer, I., Brunet, M., Peterson, T.C. and Wieringa, J., 2003. Guidance on Metadata and Homogenization, WMO.

Ahrens, C.D., 2009. *Meteorology Today: an Introduction to Weather, Climate, and the Environment*, Brooks/Cole, California, USA, 621 pp.

AS/NZS:1170.2, 2011. Australia New Zealand Standards: Structural design actions - Part 2: Wind actions, Standards Australia/New Zealand Standards, Sydney, Australia, pp. 296.

AS/NZS:7000, 2010. Australian New Zealand Standard: Overhead line design, Australian New Zealand Standard, pp. 304.

AS:1170.2, 2002. Australia Standards: Structural design actions - Part 2: Wind actions

ASCE, 1990. *ASCE Manual 74: Guidelines for electrical transmission line structural loading, Committee on Analysis and Design of Structures*, Structural Division, American Society of Civil Engineers.

ASCE:7-10, 2010. ASCE Standard: Minimum design loads for buildings and other structures, *ASCE/SEI 7-10*, American Society of Civil Engineers Standard/Structural Engineering Institute, Virginia, USA, pp. 658.

Baines, P.G., 2003. Density currents, in: J.R. Holton J.A. Curry and J.A. Pyle, eds.: *J.R. Holton J.A. Curry and J.A. Pyle, Encyclopedia of Atmospheric Sciences*, Academic Press, 2002, pp. 625-630.

Bashor, R. and Kareem, A., 2009. Comparative study of major international standards, *Proceedings of the 7th Asia–Pacific Conference on Wind Engineering (APCWE-VII)*, Taipei, pp. 8.

Battione, J.A., 1969. Analysis of 25 years of hourly wind speed measured in Montevideo, *Suplemento de la Revista Meteorológica*, (in Spanish).

Beck, A.T. and Correa, M.R.S., 2012. Proposal of updated basic wind speeds for Brazil, *Revista TECHNE*, pp. 64-67 (in Portuguese).

Beniston, M., Boissonnade, A., Brooks, H., Cutter, S.L., Diaz, H.F., Dlugolecki, A., Dotzek, N., Douville, H., Easterling, D.R., Elsner, J.B., Emrich, C.T., Gall, M., Gershunov, A., Grossi, P., Jagger, T.H., Johnson, M.E., Knap, A., Knutson, T.R., Meehl, G.A., Miller, S., Muir-Wood, R., Murnane, R.J., Saunders, M.A., Stephenson, D.B., Storch, H.v.,

Tebaldi, C., Tuleya, R.E., Walker, E.L.L., Watson, C.C. and Weisse, R., 2008. *Climate Extremes and Society,* Cambridge University Press, New York, USA.

Bidegain, M., 2001. *Final Report of CSIC Project "Characterisation of wind and rain regimes that affect vertical openings in constructions in Uruguay", Annex 1 - Wind regime in Uruguay,* School of Arquitecture, UdelaR and National Directorate of Meteorology, Montevideo, Uruguay, (in Spanish).

Bidegain, M., 2007. *Notes of the course "Introduction to Meteorology", for the Bachelor Degree in Atmospheric Sciences,* School of Sciences, UdelaR, Montevideo, Uruguay, 11 pp. (in Spanish).

Bietry, J., Simiu, E. and Sacre, C., 1978. Mean wind profiles and change of terrain roughness, *Journal of the Structural Division, ASCE,* vol. 104, pp. 1585-1593.

Blackmore, P., 2003. *Report for the BRE: Windstorm damage to buildings and structures in the UK during 2002,* Building Research Establishment, Building Regulations Division, Watford, UK, 19 pp.

BluchannelTV, 2012. Extra-tropical cyclone in spring keeps Uruguay under alert, in: http://www.youtube.com/watch?v=_hOjaSH_ckk. (in Spanish).

Bluestein, H.B., 2003. Tornadoes, in: J.R. Holton J.A. Curry and J.A. Pyle, eds.: *J.R. Holton J.A. Curry and J.A. Pyle, Encyclopedia of Atmospheric Sciences,* Academic Press, 2002, pp. 2290-2297.

Boerger, A., 1946. A remarkable hail storm in 'La Estanzuela' (Uruguay) on January 1st, 1954, *Revista Meteorológica*, vol. 13, pp. 26-33 (in Spanish).

Boerger, A., 1953. Sudden temperature changes registered in 'La Estanzuela' (Uruguay) from 1915 to 1953, *Revista Meteorológica*, vol. 12, pp. 38-47 (in Spanish).

Bradbury, W. and Deaves, D.M., 1994. The dependence of gust factor probabilities on convective activity: Analysis conducted for Eurotunnel, *Meteorological Applications,* vol. 1, pp. 159–164.

Bradbury, W.M.S., Deaves, D.M., Hunt, J.C.R., Kershaw, R., Nakamura, K., Hardman, M.E. and Bearman, P.W., 1994. The importance of convective gusts, *Meteorological Applications,* vol. 1, pp. 365-378.

Brock, F.V. and Richardson, S.J., 2001. *Meteorological measurement systems,* Oxford University Press.

Brooks, H.E., Lee, J.W. and Craven, J.P., 2003. The spatial distribution of severe thunderstorm and tornado environments from global reanalysis data, *Atmospheric Research,* vol. 67, pp. 73-94.

Browning, K.A., 2004. The sting at the end of the tail: Damaging winds associated with extratropical cyclones, *Quarterly Journal of the Royal Meteorological Society,* vol. 130, pp. 375-399.

Bunting, W.F. and Smith, B.E., 1993. *A guide for conducting convective windstorm surveys,* US Department of Commerce, National Oceanic and Atmospheric Administration, National Weather Service, Scientific Services Region, Texas, USA.

Burlando, M., Georgieva, E. and Ratto, C.F., 2007. Parameterisation of the planetary boundary layer for diagnostic wind models, *Boundary-layer meteorology,* vol. 125, pp. 389-397.

Cataldo, J., 2010. *Presentation of the wind map of Uruguay for the Master program on Energy Engineering,* School of Engineering, UdelaR, Montevideo, Uruguay, (in Spanish).

Cataldo, J., 2011. *12th Report for the MIEM: Wind Energy Program in Uruguay,* School of Engineering, UdelaR, Montevideo, Uruguay, 47 pp. (in Spanish).

Cataldo, J. and Durañona, V., 2005. *Report for ANTEL: Diagnosis of the events occurred on August 23rd, 2005 around the Telecommunication Tower of ANTEL,* School of Engineering, UdelaR, Montevideo, Uruguay, 47 pp. (in Spanish).

Cataldo, J. and Durañona, V., 2008. *Report for UTE: Characterisation of downbursts and their impact on high voltage transmission lines,* School of Engineering, UdelaR, 67 pp. (in Spanish).

Cataldo, J., Gutierrez, A., Zeballos, M., Nunes, V. and Cornalino, E., 2010a. *Report for the MIEM: Analysis of the installation of meteorological stations of the network of UTE, Wind Energy Program in Uruguay, Annex 2,* School of Engineering, UdelaR, Montevideo, Uruguay, (in Spanish).

Cataldo, J., Nunes, V., Zeballos, M. and Gutiérrez, A., 2010b. *11th report for the MIEM: Wind Energy Program in Uruguay,* School of Engineering, UdelaR, Montevideo, Uruguay, 67 pp. (in Spanish).

Celemín, A.H., 1984. *Practical Meteorology,* ed.: *A.H. Celemín,* Mar del Plata, Argentina, 313 pp. (in Spanish).

Celemín, A.H., 2008. Blog from the Meteorologist Horacio Celemín, Argentina, in: http://meteo-practica.blogspot.com/. Last accesed: July, 2013 (in Spanish).

Cermak, J.E., 1998. Wind damage mitigation - Wind engineering challenges, *Jubileum Conference on Wind Effects on Buildings and Structures*, Porto Alegre, Brazil, May 25-29, pp. 335-352.

Cermak, J.E., Davenport, A.G., Durgin, F.H., Irwin, P.A., Isyumov, N., Peterka, J.A., Ramsay, S.R., Reinhold, T.A., Scanlan, R.H., Stathopoulos, T., Steckley, A.C., Tieleman, H. and Vickery, P.J., 1998. *Wind Tunnel Studies of Buildings and Structures*, ed.: *Nicholas Isyumov*, American Society of Civil Engineers, Virginia, USA.

Cermak, J.E. and Isyumov, N., 1998. *ASCE Manuals and Reports on Engineering Practice No. 67: Wind tunnel studies of buildings and structures*, American Society of Civil Engineers, 222 pp.

CIGRE, 2004. *TB 256: Report on current practices regarding the frequencies and magnitude of high intensity winds*, International Council on Large Electric Systems (CIGRE).

CIGRE, 2008. *TB 350: How overhead lines respond to localized high intensity winds – Basic understanding*, International Council on Large Electric Systems (CIGRE).

CIRSOC, 2005a. *CIRSOC 102. Argentinian Regulation on Wind Actions on Structures*, CIRSOC, Buenos Aires, Argentina, 115 pp. (in Spanish).

CIRSOC, 2005b. CIRSOC 102. Guide for the Use of the Argentinian Regulation on Wind Action on Structures, INTI, Buenos Aires, Argentina, pp. 130 (in Spanish).

Clark, P.A., Browning, K.A. and Wang, C., 2005. The sting at the end of the tail: Model diagnostics of fine-scale three-dimensional structure of the cloud head, *Quarterly Journal of the Royal Meteorological Society*, vol. 131, pp. 2263-2292.

CLIVAR, 2006. Variability of American monsoon systems, in: http://www.clivar.org/sites/default/files/imported/organization/vamos/Publications/vamos_pg3.htm. Last accesed: August, 2013.

CLIVAR, 2013. About CLIVAR, in: http://www.clivar.org/about/about-clivar. Last accesed: August, 2013.

Colmer, M.J., 1971. *On the character of thunderstorm gust fronts , Technical Report Aero 1316*, Royal Aircraft Establishment, Famborough, UK.

Collier, C.G., Dixon, J., Harrison, M.S.J., Hunt, J.C.R., Mitchell, J.F.B. and Richardson, D.S., 1994. Extreme surface winds in mid-latitude storms: forecasting and changes in climatology, *Journal of Wind Engineering and Industrial Aerodynamics,* vol. 52, pp. 1-27.

Cook, N.J., 1985. *The designer's guide to wind loading of building structures - Part 1: Background, damage survey, wind data and structural classification,* Butterworths (for Building Research Establishment, Department of the Environment), London.

Cotton, W.R., Lin, M.-S., McAnelly, R.L. and Tremback, C.J., 1989. A composite model of mesoscale convective complexes, *Monthly Weather Review,* vol. 117, pp. 765-783.

Counihan, J., 1975. *Adiabatic atmospheric boundary layers: a review and analysis of data from the period 1880-1972,* Atmospheric Environment, vol. 9, 35 pp.

CPTEC/INPE, 2012. Database of GOES 10 and GOES 12 satellite images, synoptic charts and weather reports, Centre for Weather Prediction and Climate Studies from the National Institute for Space Research, in: http://satelite.cptec.inpe.br/acervo/goes_anteriores.jsp?i=es. Last accesed: July-October 2012.

Chamlian, H., 1993. *Comparison among wind speeds adopted by wind codes in the region,* Montevideo, Uruguay, 4 pp. (in Spanish).

Chay, M.T., Albermani, F. and Wilson, R., 2006a. Numerical and analytical simulation of downburst wind loads, *Engineering Structures,* vol. 28, pp. 240-254.

Chay, M.T., Albermani, F.G. and Hawes, H., 2006b. Wind loads on transmission line structures in simulated downbursts, *First World Congress on Asset Management,* July 11-14.

Choi, E.C.C., 1999. Extreme wind characteristics over Singapore–an area in the equatorial belt, *Journal of Wind Engineering and Industrial Aerodynamics,* vol. 83, pp. 61-69.

Choi, E.C.C., 2000. Wind characteristics of tropical thunderstorms, *Journal of Wind Engineering and Industrial Aerodynamics,* vol. 84, pp. 215-226.

Choi, E.C.C., 2004. Field measurement and experimental study of wind speed profile during thunderstorms, *Journal of Wind Engineering and Industrial Aerodynamics,* vol. 92, pp. 275-290.

Choi, E.C.C. and Hidayat, F.A., 2002. Gust factors for thunderstorm and non-thunderstorm winds, *Journal of Wind Engineering and Industrial Aerodynamics*, vol. 90, pp. 1683-1696.

D'Angelo, J., 2013. Blog from Salto bcp station - Meteorology from Uruguay, weather and climate from Salto, Uruguay, in: http://bcpsalto.blogspot.com/. (in Spanish).

Davenport, A.G., Grimmond, C.S.B., Oke, T.R. and Wieringa, J., 2000. Estimating the roughness of cities and sheltered country, *15th Conference on Probability and Statistics in the Atmospheric Sciences - 12th Conference on Applied Climatology*, Ashville, NC, pp. 96-99.

De Gaetano, P., Repetto, M.P., Repetto, T. and Solari, G., 2014. Separation and classification of extreme wind events from anemometric records, *Journal of Wind Engineering and Industrial Aerodynamics*, vol. 126, pp. 132-143.

Deaves, D.M., 1993. Analysis of gust factors for use in assessing wind hazard, *Journal of Wind Engineering and Industrial Aerodynamics*, vol. 45, pp. 175-188.

Decaro, C.O., 2015. Personal communication on characteristics of some meteorological stations from the network of UTE.

DNM, 2002. *Tornado in the Department of Canelones (Uruguay), on March 10th, 2002*, DNM, Montevideo, Uruguay, 4 pp. (in Spanish).

Doswell, C.A., 2003a. Severe storms, in: J.R. Holton J.A. Curry and J.A. Pyle, eds.: *J.R. Holton J.A. Curry and J.A. Pyle, Encyclopedia of Atmospheric Sciences*, Academic Press, 2002, pp. 2054-2061.

Doswell, C.A., 2003b. Severe storms, in: J.R. Holton J.A. Curry and J.A. Pyle, eds.: *J.R. Holton J.A. Curry and J.A. Pyle, Encyclopedia of Atmospheric Sciences*, Academic Press, 2002, pp. 2054-2061.

Doswell, C.A. and Bosart, L.F., 2001. Severe convective storms, in: *Extratropical Synoptic-Scale Processes and Severe Convection*, Meteorological Monographs, American Meteorological Society.

Durañona, V., 2003. *Master Thesis on Applied Fluid Mechanics: "Evaluation of wind tunnels"*, School of Engineering, UdelaR, Montevideo, Uruguay, 137 pp. (in Spanish).

Durañona, V., 2010. Wind extreme events in Uruguay, *Proceedings of the 14th Australasian Wind Eng. Society & Southern Hemisphere Extreme Winds Workshops*, Geoscience Australia, Canberra, Australia, August 4-6, pp. 142-145.

Durañona, V., 2011a. *Report for the DNM: Digitation, analysis and homogenisation of wind data from Carrasco station carried out by the School of Engineering*, School of Engineering, UdelaR, Montevideo, Uruguay, 52 pp. (in Spanish).

Durañona, V., 2011b. Wind impact on Uruguay: vulnerability to extreme winds and estimation of their risk, *13th International Conference on Wind Engineering*, Amsterdam, The Netherlands, July 10-15, pp. 8.

Durañona, V., 2012a. Extreme wind climate of Uruguay and its effect on the selection and operation of wind turbines, *III Jornadas de Energía Eólica (III Workshop on Wind Energy)*, Montevideo, Uruguay, June 14-15, pp. 42. Presentation available online in: http://www.auee.com.uy/pags/viernes/duranona.pdf. Last accessed: August, 2013 (in Spanish).

Durañona, V., 2012b. Update of the extreme wind statistics of Uruguay, *2nd Latin-American Congress on Wind Engineering*, La Plata, Argentina, December 5-7, pp. 16 (in Spanish).

Durañona, V., 2013. Highest wind gusts in Uruguay: characteristics and associated meteorological events, *12th Americas Conference on Wind Engineering*, Seattle, Washington, USA, June 16-20, pp. 20.

Durañona, V., 2014a. High wind events in Uruguay: knowledge and needs for wind engineering applications, *WCRP Conference for Latin America and the Caribbean: Developing,linking and applying climate knowledge*, Montevideo, Uruguay, March 17-21.

Durañona, V., 2014b. Report for UTE: Characterisation and classification of the high wind events that occurred in Uruguay around September, 2012, School of Engineering, UdelaR, Montevideo, Uruguay, (in Spanish).

Durañona, V., 2015. Tesis de Doctorado "Extreme wind climate of Uruguay", Facultad de Ingeniería, UdelaR, Montevideo, Uruguay (en proceso de publicación), pp. 434 (in English).

Durañona, V. and Cataldo, J., 2001. Wind series correction due to sheltering caused by upwind obstacles near a meteorological station, *Americas Conference on Wind Engineering*, Clemson University, Clemson, South Carolina, USA, June 3-6 pp. 10.

Durañona, V. and Cataldo, J., 2007. *Report for the BSE: Description of the extreme wind climate in the metropolitan area (of Uruguay) between October and April and their*

relation with fruit fall, School of Engineering, UdelaR, Montevideo, Uruguay, 59 pp. (in Spanish).

Durañona, V. and Cataldo, J., 2008. *Report for UTE: Characterisation of downbursts and their effect on high voltage transmission lines (in Uruguay)*, School of Engineering, UdelaR, Montevideo, Uruguay, 61 pp. (in Spanish).

Durañona, V. and Cataldo, J., 2009. Analysis of severe storms in Uruguay and their effect on high voltage transmission lines, *11th Americas Conference on Wind Engineering*, San Juan, Puerto Rico, June 22-26.

Durañona, V., Guggeri, A. and Orteli, S., 2015. Advances in the characterization of high wind events in Uruguay, *IX Micrometeorology Brazilian Workshop*, ed.: *Federal University of Santa Maria (UFSM)*, Santa Maria-RS, Brazil, November 11-13.

Durañona, V. and Perera, G., 2003. Extreme wind speed distribution of WSW direction for Montevideo, Uruguay, *11th International Conference on Wind Engineering*, vol. 1, Lubbock, Texas, USA, June 2-5, pp. 229-236.

Durran, D.R., 2003. Downslope winds, in: J.R. Holton J.A. Curry and J.A. Pyle, eds.: *J.R. Holton J.A. Curry and J.A. Pyle, Encyclopedia of Atmospheric Sciences*, Academic Press, 2002, pp. 644-650.

Dyer, R.C., 1991. Considerations on the occurrence of tornadoes in Brazil, Paraguay and Argentina, *Revista Brasileira de Cartografia*, pp. 78 - 94 (in Portuguese).

El País, 2002-2015. Different newspaper reports, in: http://www.elpais.com.uy/ediciones-anteriores/. Last accesed: October, 2005 (in Spanish).

ElUruguayo.com, 2010. Encyclopedia of Uruguay. History, geography, politics and maps of Uruguay, in: http://www.mapasdeluruguay.eluruguayo.com. Last accesed: August, 2013 (in Spanish).

Eurocode1, 2004. BSI Standard: Eurocode 1: Actions on structures — General actions — Part 1-4: Wind actions, BSI, pp. 148.

Ferreira, P., 2007. Verified occurrence of tornadoes in Campinas region (Brazil), in: www.temposeveronors.com. Last accesed: 2011 (in Portuguese).

Ferreira, V., 2014. Bachelor Thesis on Meteorology "Behavior of the meteorological variables under wind gusts generated by convective severe storms registered by the automatic stations of INMET", Federal University of Santa Maria, Centre of Natural and Exact Sciences, Rio Grande do Sul, Brazil, pp. 36 (in Portuguese).

Fisher, R.A.S. and Tippett, L.H.C., 1928. Limiting forms of the frequency distribution of the largest or smallest member of a sample, *Mathematical Proceedings of the Cambridge Philosophical Society*, vol. 24, pp. 180-190.

Franklin, J.L., Black, M.L. and Valde, K., 2003. GPS dropwindsonde wind profiles in hurricanes and their operational implications, *Weather and Forecasting,* vol. 18, pp. 32–44.

Fujita, T.T., 1971. *Proposed characterization of tornadoes and hurricanes by area and intensity*, University of Chicago, Chicago, USA.

Fujita, T.T., 1981. Tornadoes and downbursts in the context of generalized planetary scales, *Journal of the Atmospheric Sciences,* vol. 38, pp. 1511-1534.

Fujita, T.T., 1985. *The downburst. Microburst and macroburst.*, Satellite and Mesometeorology Research Project (SMRP), Chicago, Illinois, USA, 122 pp.

Fujita, T.T., 1990. Downbursts: meteorological features and wind field characteristics, *Journal of Wind Engineering and Industrial Aerodynamics*, vol. 36, pp. 75-86.

Gan, M.A. and Rao, V.B., 1991. Surface cyclogenesis over South America, *Monthly Weather Review*, vol. 119, pp. 1293-1302.

Gan, M.A. and Rao, V.B., 1994. The influence of the Andes Cordillera on transient disturbances, *Monthly Weather Review*, vol. 122, pp. 1141-1157.

García, N.O., 1970. *Elements of climatology,* Universidad Nacional del Litoral, Santa Fe. Argentina, (in Spanish).

Garreaud, R.D., Vuille, M., Compagnucci, R. and Marengo, J., 2009. Present-day South American climate, *Palaeogeography, Palaeoclimatology, Palaeoecology*, vol. 281, pp. 180-195.

Gast, K.D. and Schroeder, J.L., 2003. Supercell rear-flank downdraft as sampled in the 2002 thunderstorm outflow experiment, *Proceedings of the 11th International Conference on Wind Engineering*, Lubbock, Texas, USA, June 2-5, pp. 2233-2240.

Golden, J.H., 2003. Waterspouts, in: J.R. Holton J.A. Curry and J.A. Pyle, eds.: *J.R. Holton J.A. Curry and J.A. Pyle, Encyclopedia of Atmospheric Sciences*, Academic Press, 2002, pp. 2510-2525.

Gomes, L. and Vickery, B.J., 1978. Extreme wind speeds in mixed wind climates, *Journal of Wind Engineering and Industrial Aerodynamics*, vol. 2, pp. 331-344.

Grasso, L.D., 2003. Dryline, in: J.R. Holton J.A. Curry and J.A. Pyle, eds.: *J.R. Holton J.A. Curry and J.A. Pyle, Encyclopedia of Atmospheric Sciences*, Academic Press, 2002, pp. 658-668.

Gringorten, I.I., 1963. A plotting rule for extreme probability paper, *Journal of Geophysical Research*, vol. 68, pp. 813-814.

Guin, J. and Saxena, V., 2002. Extreme losses from natural disasters–earthquakes, tropical cyclones and extratropical cyclones, *Boston: Applied Insurance Research*, pp. 14.

Gunter, W.S. and Schroeder, J.L., 2013. High-resolution full-scale measurements of thunderstorm outflow winds, *12th Americas Conference on Wind Engineering*, Seattle, Washington, USA, June 16-20, pp. 13.

Gunter, W.S. and Schroeder, J.L., 2015. Dual-Doppler Radar and Surface Measurements of Thunderstorm Outflow Winds, *Proceedings of the 14th International Conference on Wind Engineering*, Porto Alegre, Brasil.

Hakim, G.J., 2003. Cyclogenesis, in: J.R. Holton J.A. Curry and J.A. Pyle, eds.: *J.R. Holton J.A. Curry and J.A. Pyle, Encyclopedia of Atmospheric Sciences*, Academic Press, 2002, pp. 589-594.

Harper, B.A., Kepert, J.D. and Ginger, J.D., 2010. *Guidelines for converting between various wind averaging periods in tropical cyclone conditions, WMO/TD-No. 1555,* World Meteorological Organization, TCP Sub-Project Report, 64 pp.

Harris, R.I. and Deaves, D.M., 1980. The structure of strong winds, *Proceedings of the CIRIA Conference: Wind Engineering into the 80s*, London, UK, November 12-13.

Hermant, A., 2000. *Traqueur d'orages,* Nathan, (in French).

Hernández, H.F., 1971. Absolute frequency of wind gusts registered at the meteorological station in front of the Port of Montevideo (1906 - 1970), *Suplemento de la Revista Meteorológica*, pp. 15 (in Spanish).

Hjelmfelt, M.R., 1988. Structure and life cycle of microburst outflows observed in Colorado, *Journal of Applied Meteorology,* vol. 27, pp. 900-927.

Holmes, J.D., 2004. Personal communication of measurements from the Australian Bureau of Meteorology, Richard Weller.

Holmes, J.D., 2007. *Wind Loading of Structures,* Taylor & Francis, U.S.A., 444 pp.

Holmes, J.D., 2010. Rational Wind-Load Design and Wind-Load Factors for Locations Affected by Tropical Cyclones, Hurricanes, and Typhoons, *Structures Congress 2010, ASCE*, pp. 2151-2163.

Holmes, J.D., Allsop, A.C. and Ginger, J.D., 2014. Gust durations, gust factors and gust response factors in wind codes and standards, *Wind & Structures*, vol. 19, pp. 339-352.

Holmes, J.D., Baker, C.J., English, E.C. and Choi, E.C.C., 2005a. Wind structure and codification, *Wind and Structures*, vol. 8, pp. 235-250.

Holmes, J.D. and Ginger, J.D., 2012. The gust wind speed duration in AS/NZS 1170.2, *Australian Journal of Structural Engineering*, vol. 13, pp. 207-216.

Holmes, J.D., Hangan, H.M., Schroeder, J.L., Letchford, C.W. and Orwig, K.D., 2008. A forensic study of the Lubbock-Reese downdraft of 2002, *Wind and Structures*, vol. 11, pp. 137-152.

Holmes, J.D., Kasperski, M., Miller, C.W., Żurański, J. and Choi, E.C.C., 2005b. Extreme wind prediction and zoning, *Wind & Structures*, pp. 269-281.

Holton, J.R., 2003. Dynamic meteorology: overview, in: J.R. Holton J.A. Curry and J.A. Pyle, eds.: *J.R. Holton J.A. Curry and J.A. Pyle, Encyclopedia of Atmospheric Sciences*, Academic Press, 2002, pp. 673-679.

Hoskins, B.H. and Hodges, K.I., 2005. A new perspective on Southern Hemisphere storm tracks, *Journal of Climate*, vol. 18, pp. 4108-4129.

IEC, 2005. IEC 61400-1: Wind Turbines–Part 1: Design Requirements, Ed. 3.0 2005-8, International Electrotechnical Commission, Geneva, Switzerland, pp. 184.

IRAM:11-700, 1979. Argentinian Wind Code for Action on Structures, Part I, IRAM, Buenos Aires, Argentina, (in Spanish).

ISO:4354, 2009. International Standard: Wind Actions on Structures, 2nd ed., International Standards Organization, Switzerland, pp. 76.

Jackson, P.S., 1981. On the displacement height in the logarithmic velocity profile, *J. Fluid Mech*, vol. 111, pp. 15-25.

Johnson, R.H. and Mapes, B.E., 2001. Mesoscale processes and severe convective weather, *Meteorological Monographs*, vol. 28, pp. 71-122.

Joly, A., Ayrault, F. and Malardel, S., 2003. Extra-tropical cyclones, in: J.R. Holton J.A. Curry and J.A. Pyle, eds.: *J.R. Holton J.A. Curry and J.A. Pyle, Encyclopedia of Atmospheric Sciences*, Academic Press, 2002, pp. 594-615.

Karpa, O. and Naess, A., 2013. Extreme value statistics of wind speed data by the ACER method, *Journal of Wind Engineering and Industrial Aerodynamics*, vol. 112, pp. 1-10.

Kingsmill, D. and Wakimoto, R., 1991. Kinematic, dynamic, and thermodynamic analysis of a weakly sheared severe thunderstorm over northern Alabama, *Monthly Weather Review*, vol. 119, pp. 262-297.

Knox, J.A., Frye, J.D., Durkee, J.D. and Fuhrmann, C.M., 2011. Non-convective high winds associated with extratropical cyclones, *Geography Compass*, vol. 5, pp. 63-89.

Kruger, A.C., Goliger, A.M., Retief, J.V. and Sekele, S., 2010. Strong wind climatic zones in South Africa, *Wind and Structures*, vol. 13, pp. 19.

Laing, A.G., 2003. Mesoscale meteorology: mesoscale convective systems, in: J.R. Holton J.A. Curry and J.A. Pyle, eds.: *J.R. Holton J.A. Curry and J.A. Pyle, Encyclopedia of Atmospheric Sciences*, Academic Press, 2002, pp. 1251-1261.

Laing, A.G. and Fritsch, J.M., 1997. The global population of mesoscale convective complexes, *Quarterly Journal of the Royal Meteorological Society*, vol. 123, pp. 389-405.

Larguero, P., 2014. Personal communication on blown-down medium- and low-voltage poles in the northwest of Uruguay.

Letchford, C., 2015. Is codification of non-synoptic wind loads possible?, *Keynote at the 14th International Conference on Wind Engineering*, Porto Alegre, Brazil, June 21-26.

Lichtenstein, E.R. and Schwarzkopf, M.L., 1970. Statistical aspects of squall lines in Argentina, *Meteorologica*, vol. 1, (in Spanish).

Lin, W.E., 2010. *PhD Thesis: Validation of a novel downdraff outflow simulator: A slot jet wind tunnel*, The University of Western Ontario, London, Ontario, Canada, 180 pp.

Lombardo, F.T., 2012. Improved extreme wind speed estimation for wind engineering applications, *Journal of Wind Engineering and Industrial Aerodynamics*, vol. 104, pp. 278-284.

Lombardo, F.T. and Smith, D.A., 2009. Analysis and interpretation of non-stationary wind flow on a bluff body, *11th Americas Conference on Wind Engineering*, San Juan, Puerto Rico, June 22-26, pp. 11.

Loredo-Souza, A.M., 2012. Meteorological events causing extreme winds in Brazil, *Wind and Structures*, vol. 15, pp. 177-188.

Lutgens, F.K., Tarbuck, E.J. and Tasa, D., 2001. *The atmosphere: an introduction to meteorology*, Prentice Hall New Jersey.

Lydolph, P.E., 1985. *The Climate of the Earth*, Rowman and Littlefield Publishers, Inc., Maryland, USA.

Maddox, R.A., 1983. Large-scale meteorological conditions associated with midlatitude, mesoscale convective complexes, *Monthly Weather Review*, vol. 111, pp. 1475-1493.

Markowski, P. and Richardson, Y., 2010. *Mesoscale Meteorology in Midlatitudes*, Wiley-Blackwell, 407 pp.

Marks, F.D., 2003a. Hurricanes, in: J.R. Holton J.A. Curry and J.A. Pyle, eds.: *J.R. Holton J.A. Curry and J.A. Pyle, Encyclopedia of Atmospheric Sciences*, Academic Press, 2002, pp. 942-966.

Marks, F.D., 2003b. Hurricanes, in: J.R. Holton J.A. Curry and J.A. Pyle, eds.: *J.R. Holton J.A. Curry and J.A. Pyle, Encyclopedia of Atmospheric Sciences*, Academic Press, 2002, pp. 942-966.

McDonald, J.R., Mehta, K.C. and Mani, S., 2006. *A recommendation for an enhanced Fujita scale (EF-Scale), revision 2*, Wind Science and Engineering, Texas Tech. Univ., Lubbock, TX, USA, 111 pp.

Morandi, L., 1901. *Meteorological Annual Report of the Municipal Observatory of Prado station (Uruguay)*, Imprenta Artística y Encuadernación de Dornaleche y Reyes, Montevideo, Uruguay, 85 pp. (in Spanish).

Morandi, L., 1901 - 1917. *Monthly and annual meteorological reports from the Municipal Observatory of Prado station (Uruguay)*, Imprenta artística de Dornaleche y Reyes, Montevideo, Uruguay, (in Spanish).

Morandi, L., 1917a. *Monthly Bulletin of March of the National Physics-Climatic Institute (Uruguay)*, Talleres Gráficos Curiel, Montevideo, Uruguay, 15 pp. (in Spanish).

Morandi, L., 1917b. *Summary and discussion of the Meteorological Observations from the Municipal Observatory of Prado station (Uruguay), 1901-1915*, ed.: *National Physic-*

Climatic Institute, Tipografía Moderna de Francisco Arduino, Montevideo, Uruguay, 15 pp. (in Spanish).

Morandi, L., 1921. *Essay on the general climatology of Uruguay,* Physics-Climatic Institute, Montevideo, Uruguay, (in Spanish).

Morandi, L., 1938. *Eight years (1926-1936) of meteorological observations in the militar aeronautic station in Camino Mendoza, Montevideo (Uruguay). First part,* Talleres Gráficos Aeronáutica Militar, Montevideo, Uruguay, 28 pp. (in Spanish).

Morandi, L., 1939. *Averages and main characteristics of climatic parameters of Montevideo (Uruguay) on the basis of 56 years of observation (1883-1938), and wind frequencies from 1929 to 1938, in the militar airport of Camino Mendoza, Montevideo,* ed.: *Instituto de Estudios Superiores,* A Montevideo & Cía. , Montevideo, Uruguay, 24 pp. (in Spanish).

Morandi, L., 1942. Main characteristics of the climate of Montevideo (Uruguay), *Revista Meteorológica,* vol. 1, pp. 38-48 (in Spanish).

Morandi, L., 1944. Tempestuous winds in the estuary of La Plata, *Revista Meteorológica,* vol. 11 (año III), pp. 251-264 (in Spanish).

Morandi, L., 1945. Frequency of hourly wind speeds from 1936 to 1940 observed at the Meteorological Observatory of Prado station, Montevideo (Uruguay), *Revista Meteorológica,* vol. 4, pp. 187-190 (in Spanish).

Morandi, L., 1952. Summary of the main characteristics of the climate of Uruguay, *Revista Meteorológica,* vol. 11, pp. 197-207 (in Spanish).

Muzeau, J.P., Bouchaïr, A., Sesov, V. and Coelho, C., 2007. Presentation of the Working Group 4: Identification and classification of exposure events. Exceptional or infrequent event scenarios, *COST Action C26: Urban habitat constructions under catastrophic events Prague Workshop*, Prague, Czech Republic, March, pp. 63.

Nascimento, E.L. and Doswell, C.A., 2006. The need for an improved documentation of severe thunderstorms and tornadoes in South America, *Symposium on the Challenges of Severe Convective Storms,* Atlanta, USA, pp. 8.

Natalini, B., Lassig, J.L., Natalini, M.B. and Palese, C., 2011. Wind-induced damage in two regions of Argentina, *13th International Conference on Wind Engineering*, Amsterdam, The Netherlands, pp. July 10-15.

Natalini, M.B. and Natalini, B., 2010. Review of extreme wind speeds in three sites of the south of Argentina, *XXXIV South American Workshop on Structural Engineering*, San Juan, Argentina, September 27 - October 1, pp. 15 (in Spanish).

NBR:6123, 1988a. Brazilian Standard: Wind forces on constructions, ABNT-Associação Brasileira de Normas Técnicas, Rio de Janeiro, Brazil, pp. 66 (in Portuguese).

NBR:6123, 1988b. *Brazilian Standard: Wind forces on constructions,* ABNT-Associação Brasileira de Normas Técnicas, Rio de Janeiro, Brazil, 66 pp. (in Portuguese).

Necco, G., 1982a. Behaviour of cyclones in the South American area during the FGGE: Cyclogenesis, *Meteorologica*, vol. 13, pp. 7-20 (in Spanish).

Necco, G., 1982b. Behaviour of cyclones over South America during FGGE: trajectories and developments, *Meteorologica,* vol. 13, pp. 21-34 (in Spanish).

Necco, G., 1988. Meteorological systems: Extra-tropical regions, Southern Hemisphere, *Regional Seminar for Professional Formation of National Instructors of AR III and AR IV*, Asunción, Paraguay, September 19-30, pp. 27 (in Spanish).

Necco, G., 2015. Personal communication on the possible occurrence of a sting jet during the explosive extra-tropical cyclone of August 23rd, 2005 in Montevideo, Uruguay.

Nobre, P., Marengo, J.A., Cavalcanti, I.F.A., Obregon, G., Barros, V., Camilloni, I., Campos, N. and Ferreira, A.G., 2006. Seasonal-to-decadal predictability and prediction of South American climate, *Journal of Climate*, vol. 19, pp. 5988-6004.

Oliveira, I.P.V., 2004. *Analysis of tornado events in Santa Catarina (Brazil): synoptic characterization and evaluation of data*, INPE - National Institute of Space Research, Sao Jose dos Campos, Brazil, 225 pp. (in Portuguese).

Orlanski, I., 1975. A rational subdivision of scales for atmospheric processes, *Bulletin of the American Meteorological Society*, vol. 56, pp. 527-530.

Orwig, K.D. and Schroeder, J.L., 2007. Near-surface wind characteristics of extreme thunderstorm outflows, *Journal of Wind Engineering and Industrial Aerodynamics,* vol. 95, pp. 565-584.

Palutikof, J.P., Brabson, B.B., Lister, D.H. and Adcock, S.T., 1999. A review of methods to calculate extreme wind speeds, *Meteorological Applications,* vol. 6, pp. 119-132.

Perera, G., 2000. *Probability and Statistics. A first encounter,* CEI, School of Engineering, Montevideo, Uruguay, (in Spanish).

Pita, G.L. and de Schwarzkopf, M.L., 2016. Urban downburst vulnerability and damage assessment from a case study in Argentina, *Natural Hazards*, pp. 1-19.

Plate, E.J., 1982. Wind tunnel modelling of wind effects in engineering, *Engineering Meteorology*, pp. 573-639.

Ponte Jr, J. and Riera, J.D., 2010. Simulation of extreme wind series caused by thunderstorms in temperate latitudes, *Structural Safety*, vol. 32, pp. 231-237.

Possia, N., Bibiana Ceme, S. and Campetella, C., 2003. A diagnostic analysis of the Río de la Plata Superstorm, May 2000, *Meteorological Applications,* vol. 10, pp. 87-99.

Possia, N.E., Vidal, L. and Campetella, C.C., 2011. A windstorm in La Plata River, *Meteorologica,* vol. 36, pp. 95-110 (in Spanish).

Prohaska, F., 1976. The climate of Argentina, Paraguay and Uruguay, ed.: *W. Schwerdtfeger,* in: *World Survey of Climatology: Climates of Central and South America*, Elsevier Scientific Publishing Company New York, USA.

Raupach, M.R., Antonia, R.A. and Rajagopalan, S., 1991. Rough-wall turbulent boundary layers, *Appl. Mechanics Revs.*, vol. 44, pp. 1-25.

Ricaldoni, J.A., 1979. Study of winds in Uruguay, *Memoria de las XX Jornadas Sudamericanas de Ingeniería Estructural y VI Simposio Panamericano de Estructuras*, Córdoba, Argentina, July 22-28 pp. 17 (in Spanish).

Riera, J.D., 2013. Personal communication on the Brazilian wind code and extreme wind value analyses carried out in Brazil.

Riera, J.D. and Ponte, J.J., 2012. Recent Brazilian research on thunderstorm winds and their effects on structural design, *Wind and Structures*, vol. 15.

Riera, J.D. and Rocha, M.M., 1998. Load definition for wind design and reliability assessments: Extreme wind climate, *Jubileum Conference on Wind Effects on Buildings and Structures*, ed.: *Riera and Davenport*, Porto Alegre, Brazil, May 25-29, pp. 15-38.

Riera, J.D., Viollaz, A.J. and Reimundin, J., 1977. Some recent results on probabilistic models of extreme wind speeds, *Journal of Wind Engineering and Industrial Aerodynamics*, vol. 2, pp. 271-287.

Rogers, R.R. and Yau, M.K., 1989. *A Short Course in Cloud Physics*, Pergamon Press (Oxford and New York), 293 pp.

Rosso, L.C., Schwarzkopf, M.L. and Armanini, M., 2012. Report for the National Meteorological Service of Argentina "Meteorological phenomenon that caused damage in Great Buenos Aires and in the city of Buenos Aires on April, 4th, 2012", Buenos Aires, Argentina, pp. 30 (in Spanish).

Roth, D.M., 2002. A fifty year history of subtropical cyclones, *Preprints of the 25th Conf. on Hurricanes and Tropical Meteorology,* , vol. 1, San Diego, California, USA.

Rotunno, R., 2003. Gust fronts, in: J.R. Holton J.A. Curry and J.A. Pyle, eds.: *J.R. Holton J.A. Curry and J.A. Pyle, Encyclopedia of Atmospheric Sciences*, Academic Press, 2002, pp. 915-918.

Salio, P., Nicolini, M. and Zipser, E.J., 2007. Mesoscale convective systems over southeastern South America and their relationship with the South American low-level jet, *Monthly Weather Review*, vol. 135, pp. 1290-1309.

Satyamurty, P., Nobre, C.A. and Dias, P.L.S., 1998. South America, in: *Meteorology of the Southern Hemisphere*, Springer, pp. 119-139.

Savory, E., Parke, G.A.R., Zeinoddini, M., Toy, N. and Disney, P., 2001. Modelling of tornado and microburst-induced wind loading and failure of a lattice transmission tower, *Engineering Structures*, vol. 23, pp. 365-375.

Schlichting, H., 1979. *Boundary Layer Theory*, McGraw-Hill, New York, USA.

Schmid, W., Schiesser, H.H., Furger, M. and Jenni, M., 2000. The origin of severe winds in a tornadic bow-echo storm over northern Switzerland, *Monthly Weather Review*, vol. 128, pp. 192-207.

Schott, T., Landsea, C., Hafele, G., Lorens, J., Taylor, A., Thurm, H., Ward, B., Willis, M. and Zaleski, w., 2012. The Saffir-Simpson hurricane wind scale, in: http://www.nhc.noaa.gov/pdf/sshws.pdf. Last accesed: August, 2013.

Schwarzkopf, M.L., 1984-1993. Severe storms and tornadoes - Study of tornadoes in Argentina, *Bulletins of the School of Exact and Natural Sciences*, Universidad de Buenos Aires, Buenos Aires, Argentina, (in Spanish).

Schwarzkopf, M.L., 1997. Internal Report "Meteorological considerations for the drawing of the iso-lines of the basic wind speed, map of figure 4, for the modification of the Argentinian CIRSOC 102 wind code", CIRSOC, Buenos Aires, Argentina, (in Spanish).

Schwarzkopf, M.L., 2010. Presentation of "Tornadoes in Argentina (since 1971) - Schwarzkopf and Rosso", *South American Workshop on Wind Engineering*, University of La Plata, La Plata, Buenos Aires, Argentina, March 4-5, pp. 56 (in Spanish).

Schwarzkopf, M.L., 2015. Severe convection in Argentina, *International Workshop on Severe winds - hazard, vulnerability and risk: Australian experience and its application to Argentina*, La Plata, Argentina, June 15, (in Spanish).

Schwarzkopf, M.L. and Ramis, G., 2010. List with main characteristics of severe storms that occurred in Uruguay from 1942 to 2010, Montevideo, Uruguay, (in Spanish).

Schwarzkopf, M.L. and Rosso, L.C., 1993. *Risk of tornadoes and downbursts in Argentina*, ed.: *INTI - CIRSOC*, Department of Atmospheric Sciences, School of Exact and Natural Sciences, Universidad de Buenos Aires, Buenos Aires, Argentina, 35 pp. (in Spanish).

Schwerdtfeger, W., 1976. Climates of Central and South America, in: *World Survey of Climatology*, Elsevier Scientific Publishing Company Amsterdam.

Seluchi, M., de Calbete, N.O. and Rozante, J.R., 2001. Analysis of a cyclonic development in the eastern coast of South America, *Rev Brasil Meteorol,* vol. 16, pp. 51-65 (in Spanish).

Seluchi, M.E., 1995. Diagnosis and prognosis of synoptic conditions prone to the occurrence of cyclogenesis in eastern South America, *Geofísica Internacional,* vol. 34, pp. 171-186 (in Spanish).

Serrentino, C., 1981. *Report for UNIT: Calculus of values of k (shape parameter) and β (characteristic wind speed) (for the development of the Uruguayan extreme map for the national wind code UNIT 50:84),* Dirección Nacional de Meteorología (DNM), Montevideo, Uruguay, 2 pp. (in Spanish).

Silva, A., 2008. Exceptional hail in San José (Uruguay). Tornado or downburst in Florida (Uruguay)?, Montevideo, Uruguay, (in Spanish).

Silva, A., 2012. *Small supercell in the afternoon of January 24th, 2012,* Sociedad Amigos del Viento, Montevideo, Uruguay, 5 pp. (in Spanish).

Silva, A., Nusa, J. and Bonora, D., 2008. Mesoscale convective system in Uruguay: intense and concentrated downburst, Montevideo, Uruguay, (in Spanish).

Simiu, E. and Scanlan, R.H., 1996. *Wind Effects on Structures: Fundamentals and Applications to Design*, John Wiley & Sons, Inc., U.S.A., 702 pp.

SINAE, 2011. National inventory of meteorological disasters, in: http://www.sinae.gub.uy/index.php?option=com_docman&task=doc_download&gid=119&Itemid=36. Last accesed: 06/08/2013 (in Spanish).

Sinclair, M.R., 1995. A climatology of cyclogenesis for the Southern Hemisphere, *Monthly Weather Review*, vol. 123, pp. 1601-1619.

Sinclair, M.R., 1996. A climatology of anticyclones and blocking for the Southern Hemisphere, *Monthly Weather Review*, vol. 124, pp. 245-264.

Sinclair, R.W., Anthes, R.A. and H.A., P., 1973. *Variation of the low level winds during the passing of a thunderstorm gust front*, NASA Contractor Report No. CR-2289.

Solari, G., 2014. Emerging issues and new frameworks for wind loading on structures in mixed climates, *Wind and Structures*, vol. 19, pp. 295-320.

Solari, G., Burlando, M., De Gaetano, P. and Repetto, M.P., 2015a. Characteristics of thunderstorms relevant to the wind loading of structures, *Wind and Structures*, vol. 20, pp. 763-791.

Solari, G., De Gaetano, P. and Repetto, M.P., 2015b. Thunderstorm response spectrum: Fundamentals and case study, *Journal of Wind Engineering and Industrial Aerodynamics*, vol. 143, pp. 62-77.

Solari, G., Repetto, M.P., Burlando, M., De Gaetano, P., Pizzo, M., Tizzi, M. and Parodi, M., 2012. The wind forecast for safety management of port areas, *Journal of Wind Engineering and Industrial Aerodynamics*, vol. 104, pp. 266-277.

Stensrud, D.J., Brooks, H.E. and Weiss, S.J., 2003. Severe weather forecasting, in: J.R. Holton J.A. Curry and J.A. Pyle, eds.: *J.R. Holton J.A. Curry and J.A. Pyle, Encyclopedia of Atmospheric Sciences*, Academic Press, 2002, pp. 2568-2577.

Stull, R.B., 2000. *Meteorology for Scientists and Engineers: a Technical Companion Book with Ahrens' Meteorology Today*, Brooks/Cole.

Sylvestre, F., 2009. Moisture pattern during the last glacial maximum in South America, in: *Past Climate Variability in South America and Surrounding Regions*, Springer, pp. 3-27.

Taljaard, J.J., 1967. Development, distribution and movement of cyclones and anticyclones in the Southern Hemisphere during the IGY, *Journal of Applied Meteorology*, vol. 6, pp. 973-987.

Torena, F., 2003a. F2 Tornado in Migues, Montevideo, Uruguay, pp. 10 (in Spanish).

Torena, F., 2003b. The tornado of Juanico, in: http://www.tiempo.com/ram/732/el-tornado-de-juanico/. Last accesed: October, 2015 (in Spanish).

Torena, F., 2009. Tornado in Carmelo (Colonia-Uruguay), November 21st, 1985. Study of the case, Montevideo, Uruguay, (in Spanish).

Torena, F., 2011. Tornadoes in Uruguay: science or myth?. Presentation for School N° 207 of Uruguay, Montevideo, Uruguay, (in Spanish).

Torena, F., 2013. Tornadoes in Uruguay, in: http://tornadoseneluruguay.blogspot.com/. Last accesed: August, 2013 (in Spanish).

UdelaR, 2005. Storm in the south of Uruguay, 23rd and 24th of August, 2005, School of Sciences, UdelaR, Montevideo, Uruguay, pp. 11 (in Spanish).

UNIT:50-84, 1984. Uruguayan Standard for Wind Actions on Structures, Instituto Uruguayo de Normas Técnicas (UNIT), Montevideo, Uruguay, pp. 119 (in Spanish).

University_of_Illinois, 2010. The Weather World 2010 Project, in: http://ww2010.atmos.uiuc.edu/%28Gh%29/guides/mtr/hurr/glob.rxml. Last accesed: 08/08/2013.

Veblen, T.T., Young, K.R. and Orme, A.R., 2007. *The physical geography of South America*, Oxford University Press, Oxford, UK.

Vecino, C. and Torena, F., 2008. Tornado in 25 de Mayo (Florida-Uruguay) on August, 11th, 2008. Study of the case, in: http://tornadoseneluruguay.blogspot.com/2009/04/tornado-en-25-de-mayo-florida-11-de.html. Last accesed: 2010 (in Spanish).

Vega, R. and Letchford, C.W., 2009. Extreme wind climatology in mixed climates, *11th Americas Conference on Wind Engineering*, San Juan, Puerto Rico, June 22-26, pp. 3.

Velasco, I. and Fritsch, J.M., 1987. Mesoscale convective complexes in the Americas, *Journal of Geophysical Research*, vol. 92, pp. 9591-9613.

Vera, C., Baez, J., Douglas, M., Emmanuel, C.B., Marengo, J., Meitin, J., Nicolini, M., Nogues-Paegle, J., Paegle, J., Penalba, O., Salio, P., Saulo, C., Silva Dias, M.A., Silva

Dias, P. and Zipser, E., 2006. The South American low-level jet experiment, *Bulletin of the American Meteorological Society,* vol. 87, pp. 63-77.

Vieira, S.E., 1949. Storms in the Río de la Plata, *Revista Meteorológica*, pp. 344-354 (in Spanish).

Vieira, S.E., 1969. *Weather and Climate*, ed.: *D. Aljanati, Benedetto, M., de Marsilio, H.*, Nuestra Tierra, Montevideo, Uruguay, 71 pp. (in Spanish).

Wakimoto, R.M., 2001. Convectively driven high wind events, *Meteorological Monographs,* vol. 28, pp. 255-298.

Wakimoto, R.M. and Bringi, V.N., 1988. Dual-polarization observations of microbursts associated with intense convection: The July 20th storm during the MIST project, *Monthly Weather Review,* vol. 116, pp. 1521-1539.

Walker, G.R., 1992. Wind engineering beyond the boundary layer wind tunnel, *Journal of Wind Engineering and Industrial Aerodynamics,* vol. 41, pp. 93-104.

Wallace, J.M., 2003. General circulation: overview, in: J.R. Holton J.A. Curry and J.A. Pyle, eds.: *J.R. Holton J.A. Curry and J.A. Pyle, Encyclopedia of Atmospheric Sciences*, Academic Press, 2002, pp. 821-829.

Wallace, J.M. and Hobbs, P.V., 2006. *Atmospheric Science: an Introductory Survey*, Elsevier Academic Press.

Weisman, M., 2003a. Bow echos and derecho, in: J.R. Holton J.A. Curry and J.A. Pyle, eds.: *J.R. Holton J.A. Curry and J.A. Pyle, Encyclopedia of Atmospheric Sciences*, Academic Press, 2002, pp. 311-322.

Weisman, M., 2003b. Bow echos and derecho, in: J.R. Holton J.A. Curry and J.A. Pyle, eds.: *J.R. Holton J.A. Curry and J.A. Pyle, Encyclopedia of Atmospheric Sciences*, Academic Press, 2002, pp. 311-322.

Weisman, M., 2003c. Convective storms: overview, in: J.R. Holton J.A. Curry and J.A. Pyle, eds.: *J.R. Holton J.A. Curry and J.A. Pyle, Encyclopedia of Atmospheric Sciences*, Academic Press, 2002, pp. 548-559.

Wieringa, J., 1973. Gust factors over open water and built-up country, *Boundary-Layer Meteorology,* vol. 3, pp. 424-441.

Wieringa, J., 1992. Updating the Davenport roughness classification, *Journal of Wind Engineering and Industrial Aerodynamics,* vol. 41, pp. 357-368.

Wieringa, J., 1993. Representative roughness parameters for homogeneous terrain, *Boundary Layer Meteorology*, vol. 63, pp. 323-363.

Wieringa, J., 1996. Representativity of wind extremes, ed.: *Vijay P. Singh*, in: *Hydrology of Disasters*, Kluwer Academic Publishers, Dordrecht, pp. 19-40.

Wieringa, J. and Rudel, E., 2002. Station exposure metadata needed for judging and improving quality of observations of wind, temperature and other parameters, *WMO Technical Conference on Meteorological and Environmental Instruments and Methods of Observation (TECO-2002)* Bratislava, Slovakia, September 23-25, pp. 5.

WMO, 2002. WMO Technical Document 1125, GCOS-76, World Meteorological Organization.

WMO, 2006. Chapter 5: Measurement of surface wind, ed.: *World Meteorological Organisation,* in: *N° 8 - WMO Guide to Meteorological Instruments and Methods of Observation, draft 7th ed.*, Secretariat of the WMO, pp. 569.

WMO, 2008. Guide to meteorological instruments and methods of observation, 7th ed. WMO Tech. Rep. WMO-8. (https://www.wmo.int/pages/prog/gcos/documents/gruanmanuals/CIMO/CIMO_Guide-7th_Edition-2008.pdf), World Meteorological Organization.

WMO, 2015. RELAMPAGO Project - Remote sensing of Electrification, Lightning, And Meso-scale/micro-scale Processes with Adaptive Ground Observations (translates to lightning flash in Spanish and Portuguese), in: https://www.wmo.int/pages/prog/arep/wwrp/new/documents/SN_PS_RELAMPAGO_WMO_WGNR.pdf. Last accesed: November, 2015.

Wölcken, K., 1954. Some synoptic aspects of rain in Argentina, *METEOROS, Buenos Aires*, vol. 4, pp. 327-366 (in Spanish).

Wood, G.S., Kwok, K., Motteram, N.A. and Fletcher, D.F., 1999. Physical and numerical modelling of thunderstorm downbursts, *10th International Conference on Wind Engineering: Wind Engineering Into the 21th Century*, ed.: *Larose & Livesey Larsen*, vol. 89, Copenhague, Denmark, pp. 1919-1923.

Zipser, E.J., Liu, C., Cecil, D.J., Nesbitt, S.W. and Yorty, D.P., 2006. Where are the most intense thunderstorms on Earth?, *Bulletin of the American Meteorological Society*, vol. 87, pp. 1057-1071.

Annexes

A.1 General circulation of the atmosphere and average sea-level pressures

As the actual flow of air around the world is quite complex, simple models of the atmosphere are used to help understanding its behaviour, gradually incorporating additional variables on which the characteristics of the general circulation of the atmosphere depend.

The more complex model, the more it can resemble the actual general circulation of the atmosphere, and the better it explains the main characteristics of the pressure systems that tend to persist throughout the year. These results, in turn, can explain the main characteristics of the mean wind climate of different regions of the world, and of their extreme wind climates.

A first simple model of the general circulation of the atmosphere can be obtained assuming that the Earth does not rotate and that its surface is uniformly covered with water (Wallace, 2003; Wallace and Hobbs, 2006; Ahrens, 2009). If, at the beginning, the pressure and temperature are horizontally uniform and the sun starts heating, the tropics would begin to warm and the polar regions, to cool. If it is also assumed that the sun is always directly over the equator, seasonal variability can be avoided.

The thermal expansion experienced in the tropics would then cause the pressure surfaces to bulge upward, while cooling of the polar atmosphere would cause the pressure surfaces to bend downward, as illustrated by Figure A.1. The sloping of the pressure surfaces gives rise to a poleward flow at the upper levels, also shown in that figure.

This upper level poleward mass flux causes surface pressures to drop in low latitudes and rise in high latitudes, which in turn produce an equatorward low-level flow, as indicated by Figure A.1(b). Then, the general circulation of the atmosphere on the side of the Earth facing the sun would be similar to that shown by Figure A.1(b), and would consist in a thermally driven convection cell in each hemisphere with rising air near the equator, sinking air over the poles, an equatorward flow of air near the surface, and a return flow aloft. This cell is referred as the Hadley cell.

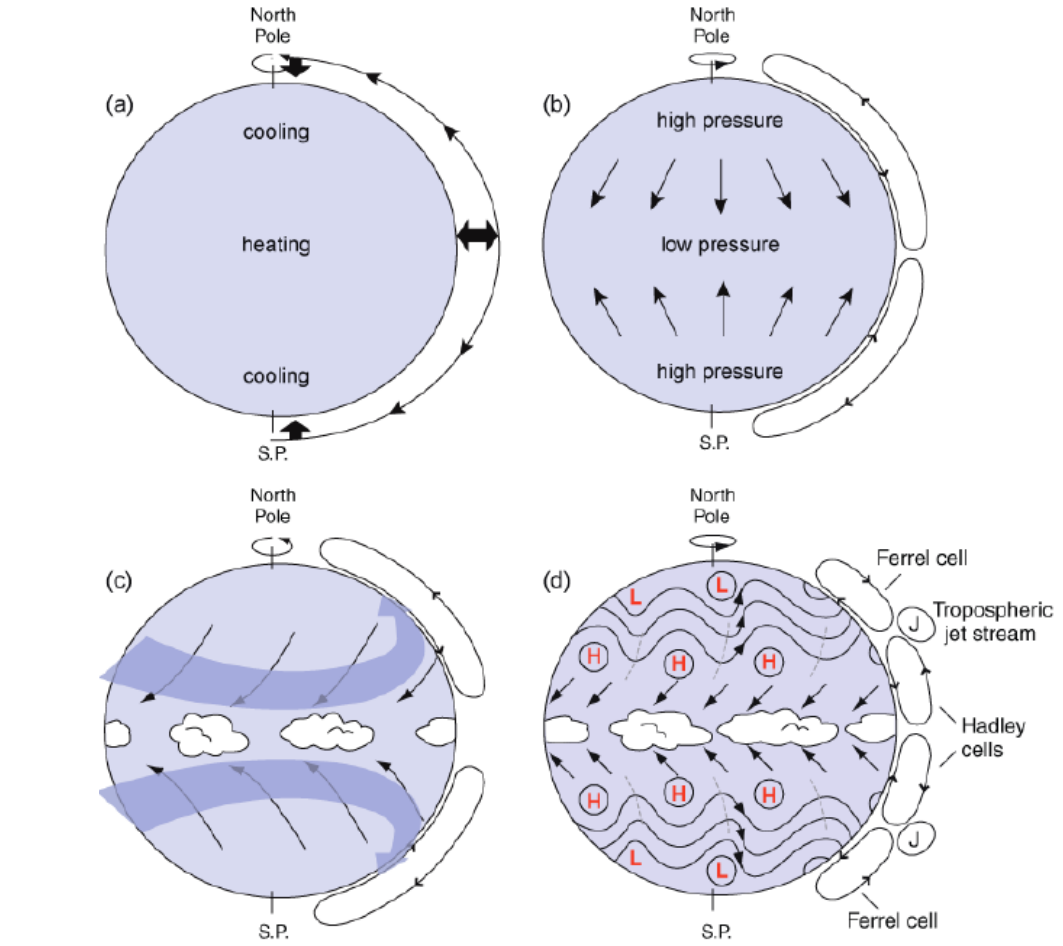


Figure A.1 Evolution of the general circulation of air from a nonrotating to a rotating Earth uniformly covered with water and the with the sun directly above the equator (from Wallace and Hobbs, 2006)

If the Earth starts rotating, in the sense of the small arrows surrounding the poles indicated in Figure A.1(c), Coriolis force would deflect the moving surface air in both hemispheres to the west, producing easterly low level winds at all latitudes, as this figure shows. These surface winds would be moving in the opposite direction to that of the Earth's rotation. Therefore, the equatorward flow in the lower branch of the Hadley cell would have a westward component, while the poleward flow in the upper branch of this cell would have an eastward component in order to conserve angular momentum. This vertical wind shear between the low level easterlies and the upper level westerlies increases in proportion to the strengthening of the temperature gradient between the equator and the poles.

As the model continues running, this wind shear reaches a critical value at which instability in the flow, called baroclinic instability, spontaneously breaks out in mid-latitudes. This is illustrated in Figure A.1(d) and consists in a succession of waves travelling to the east that

modifies the general circulation shown in Figure A.1(c). The low level wind pattern in these baroclinic waves is dominated by rotating low pressure weather systems called extra-tropical cyclones, which are encircled and marked with the letter L in Figure A.1(d).

The term cyclone denotes a closed circulation in which the air spins in the same sense as the Earth's rotation as viewed from above. They rotate clockwise in the Southern Hemisphere (SH) and anticlockwise in the NH (Northern Hemisphere). As a result of these waves, warm, humid mid-latitudes air masses flow poleward ahead of the eastward moving surface cyclones, while cold, dry polar air masses flow equatorward behind these cyclones.

This broad belt of surface westerlies is located poleward of 30° latitude, and its wave-induced heat and momentum fluxes give rise to the observed thermally-indirect mid-latitude Ferrel cell, indicated in Figure A.1(d), in which cooler air rises and warmer air sinks.

The westerlies strengthen with height and peak at the 10km level just poleward of around 30° latitude, in the so-called subtropical or extra-tropical jet streams. These jet streams are found on the poleward sides of the Hadley cells as shown in Figure A.1(d) and in Figure A.2.

These jet streams are swiftly flowing air currents thousands of kilometres long, a few hundred kilometres wide and only a few kilometres thick, which often flow in a wavy west-to-east pattern. They exist where strong winds become concentrated in narrow bands. Although they are usually shown as a continuous river of air, in reality they are discontinuous, and their position can vary from one day to the next. There are several types of jet streams, usually found at elevations between 10 and 15km, although they may occur at both higher and lower altitudes. Jet streaks is the term used to refer to localised wind speed maxima found along the axis of a jet stream, which play an important role in the development and behaviour of extra-tropical cyclones and MCSs. Wind speeds in the central core of a jet stream often exceed 180km/h (50m/s) and may occasionally exceed 370km/h (103m/s).

Another important jet stream is the polar jet stream, associated with the polar front of each hemisphere of the Earth, shown for the NH in Figure A.3. Figure A.2 illustrates its average position for the NH during its winter. The polar jet stream becomes strongest in winter, when the temperature contrast along the polar front is greatest, and its looping nature has an important role in the development of extra-tropical cyclones.

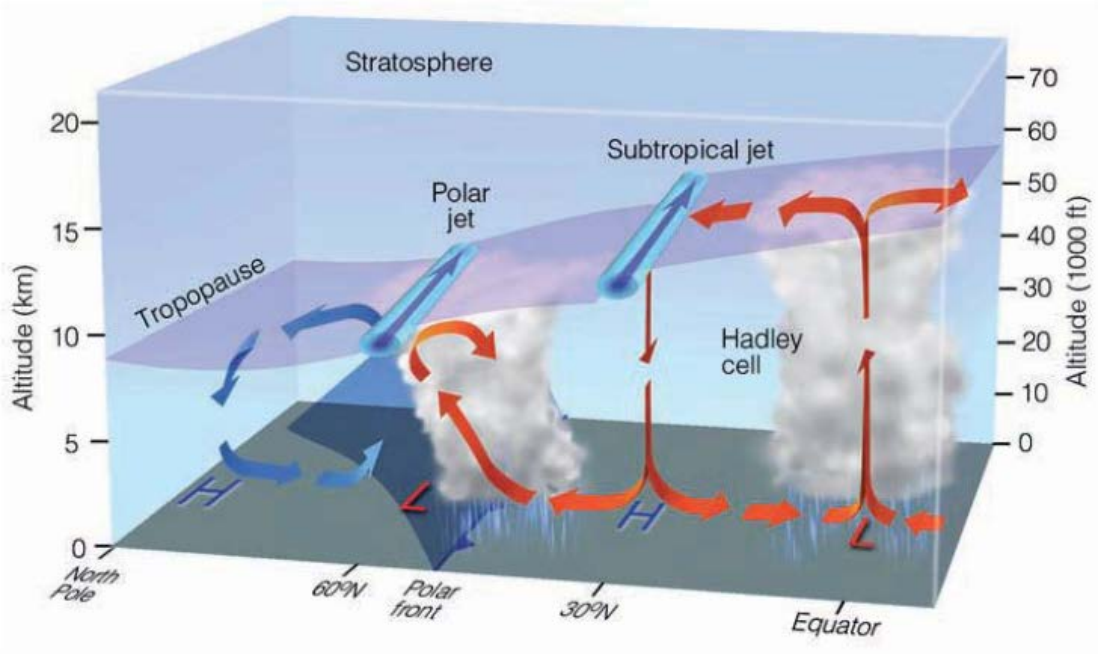


Figure A.2 Average position of the subtropical and polar jet streams for the NH during its winter (from Ahrens, 2009) [2]

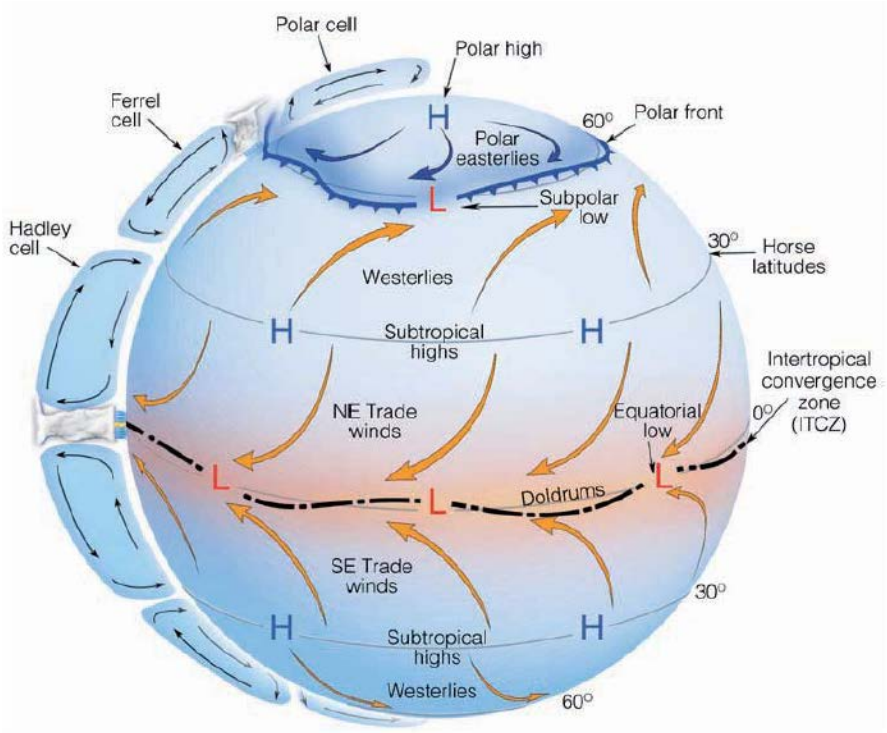


Figure A.3 Idealised wind and surface-pressure distribution over a uniformly water-covered rotating Earth (from Ahrens, 2009)

[2] For a definition of the layers of the atmosphere (as related to the average profile of air temperature above the Earth's surface), the reader can be directed to e.g. Ahrehns, 2009, among other texts.

Jet streams form near the Earth's surface as well, being usually called low level jet streams (LLJSs). Topography can affect their direction, as the presence of the Rocky Mountains or the Andes Cordillera in America, which due to their general north-south trending in both cases tend to funnel the air in this direction, and poleward. One such jet occasionally develops over the Great Plains of USA, which can attain speeds of 110km/h (30.6m/s) several hundred meters above the surface. When this LLJS is present in summer, severe convection is usually found over this area (Ahrens, 2009). A similar mechanism takes place in a region of South America (SA), as mentioned in Sub-section 2.2.4. The latter LLJS originates in a low pressure area over the northern Andes. It operates as a localised wind maximum within the lower 1-2km of the atmosphere, channelled by the Andes and terminating in SESA region, which mainly coincides with the plain areas of north eastern Argentina, Uruguay, southern Brazil and southern Paraguay, called the Pampas (Lydolph, 1985).

It is also worth mentioning that major winter cyclogenesis[3] events involving severe convection seem to show a preference for poleward jet exit regions, too (Doswell and Bosart, 2001).

Finally, the tropical easterlies and the extra-tropical westerlies are separated by a belt of relatively high sea-level pressure weather systems, indicated in Figure A.1(d) by circles containing the letter H. These closed circulations are called anticyclones and, in them, the air spins in the opposite sense as the Earth's rotation as viewed from above; therefore, they rotate anticlockwise in the SH and clockwise in the NH.

Figure A.3 illustrates the wind patterns that would prevail on an idealised Earth, without continents and seasons, and present some additional details that Figure A.1(d) does not show.

Figure A.3 shows that in each hemisphere, three cells instead of one have the task of energy distribution. A Hadley cell extends from the equator to about latitude 30°; a Ferrel cell, from approximately latitude 30° to latitude 60°, and from latitude 60° to the poles there would be a polar cell, similar to the Hadley cell, although weaker.

Over equatorial waters the air is warm, horizontal pressure gradients are weak and winds are light. The intertropical convergence zone (ITCZ), shown in Figure A.3, is part of this region,

[3] Cyclogenesis can be defined as the formation and amplification of extra-tropical cyclones (Hakim, 2003).

which is sometimes referred to as the doldrums. Here warm air rises, often condensing into huge cumulus clouds that liberate enormous amount of latent heat. This heat makes the air more buoyant and provides energy to drive the Hadley cell. The rising air reaches the tropopause, which acts like a barrier, causing the air to move laterally toward the poles. Coriolis force deflects this poleward flow providing westerly winds aloft in the tropics.

As air aloft moves poleward from the tropics, it begins to converge as it approaches mid-latitudes, producing belts of high pressure at the surface near latitude 30°, usually referred to as subtropical highs. These subtropical highs are directly below the subtropical jet streams and below the descending branches of the Hadley cells, as shown in Figure A.1(d), Figure A.2 and Figure A.3. Over the ocean, the weak pressure gradients in the centre of the highs produce only weak winds. The regions corresponding to the subtropical highs are sometimes called the horse latitudes.

Figure A.3 illustrates how from the subtropical highs, some of the surface air moves back toward the equator. Coriolis force deflects the air, causing NE and SE trade winds in the NH and SH, respectively. Near the equator, the NE trades converge with the SE trades along the ITCZ. In this region of surface convergence, air rises and continues its cellular journey.

Also from the subtropical highs, part of the surface air moves toward the poles and deflects toward the east, resulting in a more or less westerly air flow, called the westerlies. As this mild air travels poleward, it encounters cold air moving out from the poles. These two air masses of contrasting temperature do not readily mix. They are separated by a boundary called the polar front, where a zone of low pressure, the subpolar low, is located. Here surface air converges and rises, and storms and clouds develop. Some of the rising air returns at high levels to the subtropical highs, where it sinks back to the surface, completing the Ferrel cell.

Figure A.3 shows for the NH, how the cold air from the poles is deflected by the Coriolis force, so that the general flow of air behind the polar front is from the northeast. This corresponds to the region of the polar easterlies. Along this front, a portion of the rising air moves poleward, and the Coriolis force deflects the air into a westerly wind at high levels. Air aloft eventually reaches the poles slowly sinks to the surface, and flows back toward the polar front, completing the weak polar cell.

The real world, with its seasons, continents and oceans, mountains and ice fields presents some discrepancies with the model presented, although the actual winds and pressure distributions at the surface agree with its main characteristics.

Some of these differences are listed below:

- surface winds tend to be much stronger over the oceans than over land
- the ITCZ is not located along the equator; it is considered to be situated in average along about 7°N latitude. This asymmetry is believed to be a consequence of the asymmetry presented by the land-sea distribution between both hemispheres (Wallace and Hobbs, 2006)
- the rising branches of the Hadley cells are located in tropical latitudes of the summer hemisphere, while their sinking branches are at cooler mid-latitudes of the winter hemisphere
- the subtropical high pressure belts, instead of being continuous, form distinct high pressure centres over the Atlantic and Pacific Oceans, referred to as subtropical anticyclones
- the extra-tropical westerly winds, centred around 45°N and 50°S latitudes, are not constant as in the model, as migrating highs and lows break up the surface flow pattern due to the eastward migrating baroclinic waves shown in Figure A.1(d). In the SH mid-latitudes, where the surface is mostly water, winds blow more steadily from the west, where they are not influenced by topography. The tropospheric jet streams indicated in Figure A.2 are also disturbed by the succession of baroclinic waves
- the subpolar low pressure belt illustrated in Figure A.3 manifests itself in the NH as mid-ocean cyclones
- in winter, the polar fronts with their cold air can move into subtropical latitudes, producing cold polar outbreaks
- the subtropical anticyclones are most pronounced during summer, whereas the subpolar lows are most pronounced during winter. The strength of the tropospheric jet streams varies with season: they are strongest during winter, when the pole-equator temperature gradient is strongest.

Most of the previously mentioned features are illustrated in Figure A.4, already shown in Figure 2.5 in Sub-section 2.2.2. In this figure, actual average distributions of sea-level pressure and winds for January and July are respectively shown. The pressure field is represented as isobars, and local maxima are referred to as high pressure areas or simply

'highs' (H) and minima, as 'lows' (L). It can be seen that, with the exception of the equatorial belt (10°S-10°N), the wind in the Earth's atmosphere is quite parallel to the isobars.

Figure A.4 shows regions where pressure systems appear to persist throughout the year. These systems are referred to as semi-permanent highs and lows, as they move only slightly during the course of a year.

The mid-latitudes anticyclones that develop in response to the convergence of air aloft near the subtropical jet streams (see e.g. Figures A.3 and A.4) can be located between latitudes 25° and 35° in Figure A.4 in both hemispheres. Since surface winds rotate anticlockwise in the SH around these systems, and clockwise in the NH, there are trade winds equatorward from these systems and prevailing westerlies poleward. In the SH, where there is relatively less land area, there is less contrast between land and water, and the subtropical highs show up as well-developed systems with a more clearly defined circulation.

Figure A.4 also shows for the SH, how the subpolar low completely encircles the globe, while in the NH, instead of the polar front, there are two semipermanent subpolar lows between latitudes 40° and 65° (Aleutian and Icelandic lows). In these zones of cyclonic activity, numerous storms, having travelled eastward, tend to converge especially in winter.

There would be different mechanisms for generating extra-tropical cyclones, being the most common the action of the baroclinic waves that form along the polar front, near the location of the tropospheric jet streams, and move to the east (Joly et al., 2003). As the polar front separates warm air to the equator from cold air to the pole, when an extra-tropical cyclone intensifies, both cold and warm fronts become better organised.

Other mechanism for the generation of extra-tropical cyclones would be the interaction of a pre-existing weather feature, such as a front, with the orography, which tends to generate cyclones in the lee of large-scale orographic barriers (Joly et al., 2003), which then move downwind (Hakim, 2003).

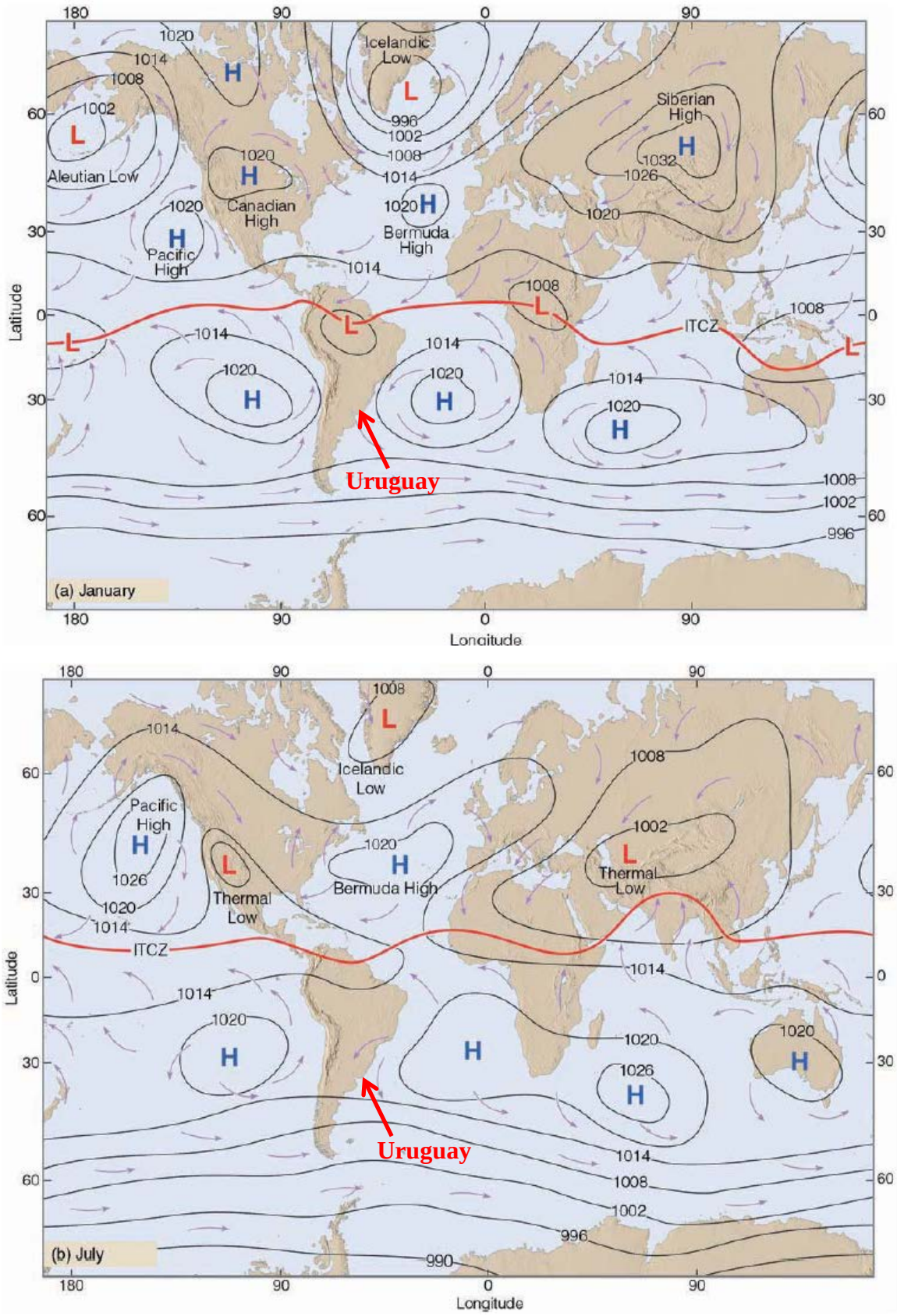


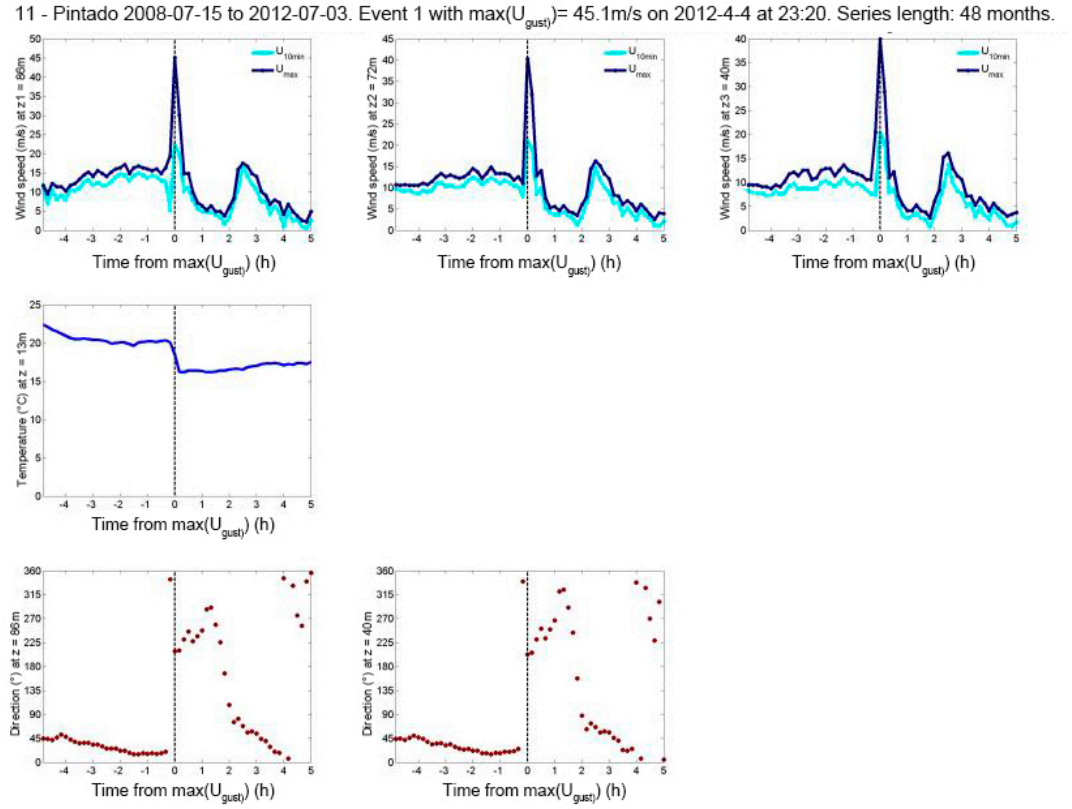
Figure A.4 Average sea-level pressure distribution and surface wind-flow patterns for (a) January and (b) July (adapted from Ahrens, 2009)

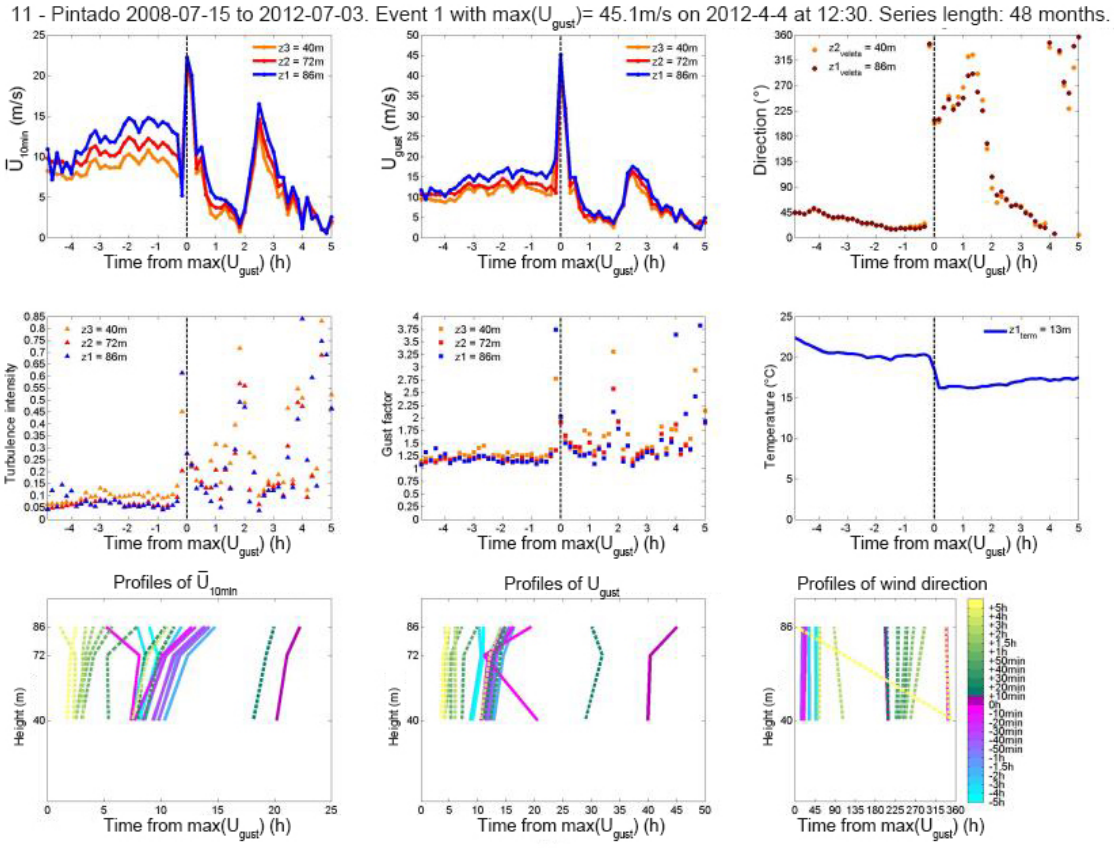
Comparing Figure A.4(a) and (b), several seasonal changes can be noticed: in summer (winter) some pressure systems that are not semipermanent form because of surface low (high) pressures appear over warm (cool) lands. These are called thermal lows (highs). Regarding semipermanent pressure systems, strong subpolar lows so well developed in January over the NH (Figure A.4(a)) are hardly discernible on the July map (Figure A.4(b)). The subtropical highs, however, remain dominant in both seasons.

As the sun is overhead in the SH in January, and overhead in the NH in July, the zone of maximum surface heating shifts seasonally. In response to this shift, the major pressure systems, wind belts and ITCZ (red line in Figure A.4) shift toward the south in January and toward the north in July. Consequently, in Figure A.4(b), the main features of the general circulation have been displaced northward with respect to Figure A.4(a). For example, the South Pacific high tends to move to the north during SH winter. This in turn, together with its decrease in intensity, has an effect on the extreme wind climate of SA, as it is described in Sub-section 2.2.4.2.1.1.

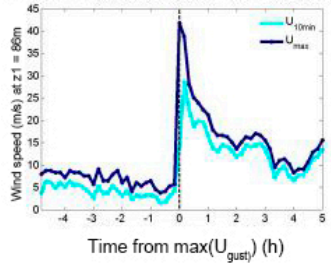
Also, due to this northward shift, the southern centre of SA does not receive so much warm and humid air from the tropical Atlantic Ocean as in the SH summer, which also has a consequence on its extreme wind climate.

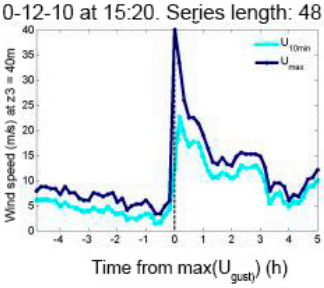
A.2 10 highest wind gust events registered at Pintado station

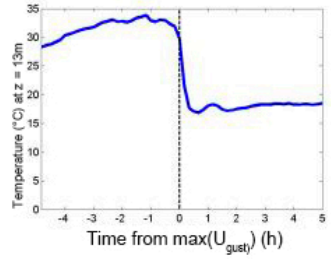


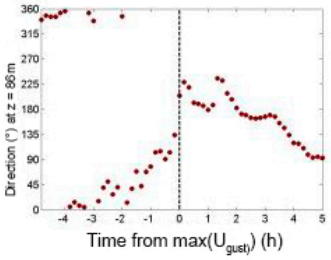


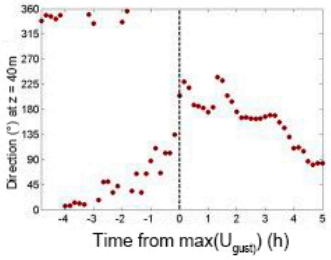
11 - Pintado 2008-07-15 to 2012-07-03. Event 2 with max(U_{gust})= 41.8m/s on 2010-12-10 at 15:20. Series length: 48 months.



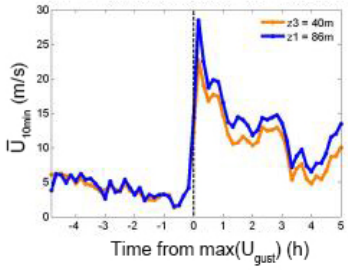


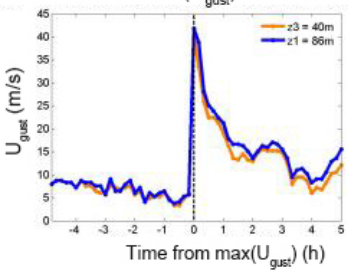


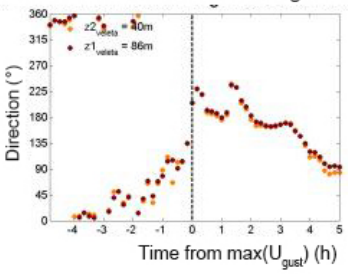


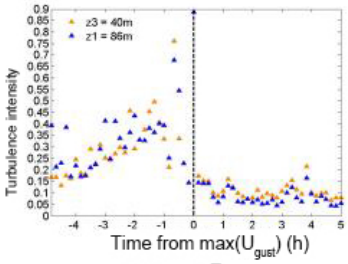


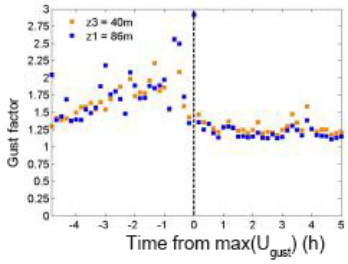
11 - Pintado 2008-07-15 to 2012-07-03. Event 2 with max(U_{gust})= 41.8m/s on 2010-12-10 at 15:20. Series length: 48 months.

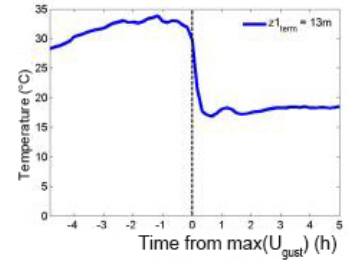




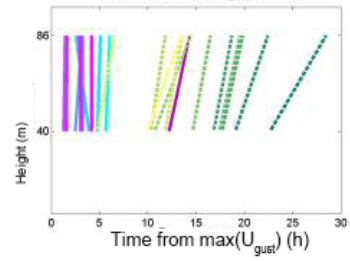




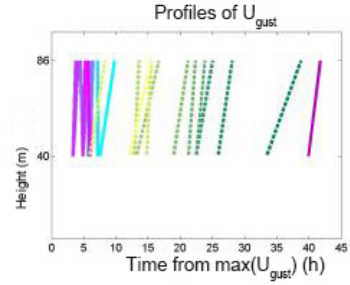




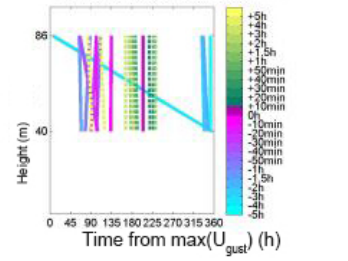
Profiles of $\bar{U}_{10min}$



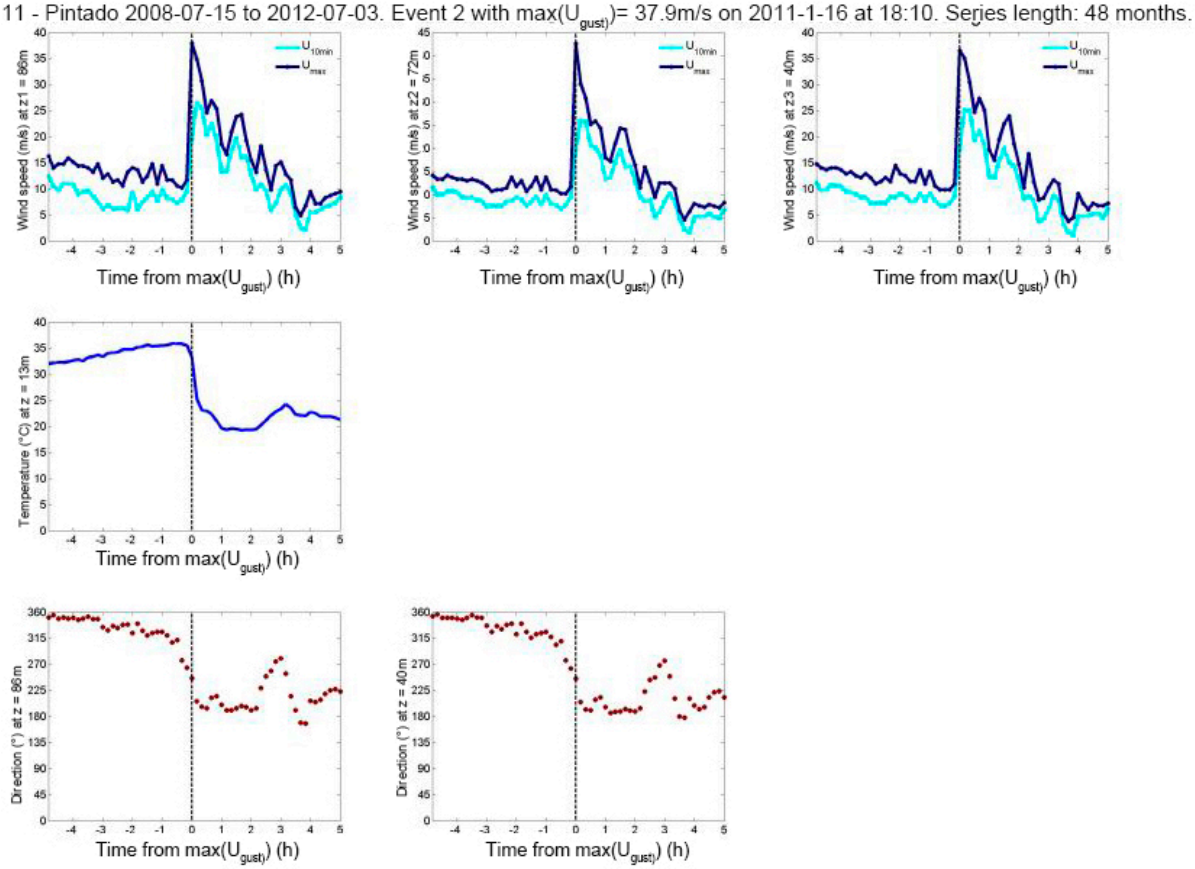
Profiles of U_{gust}



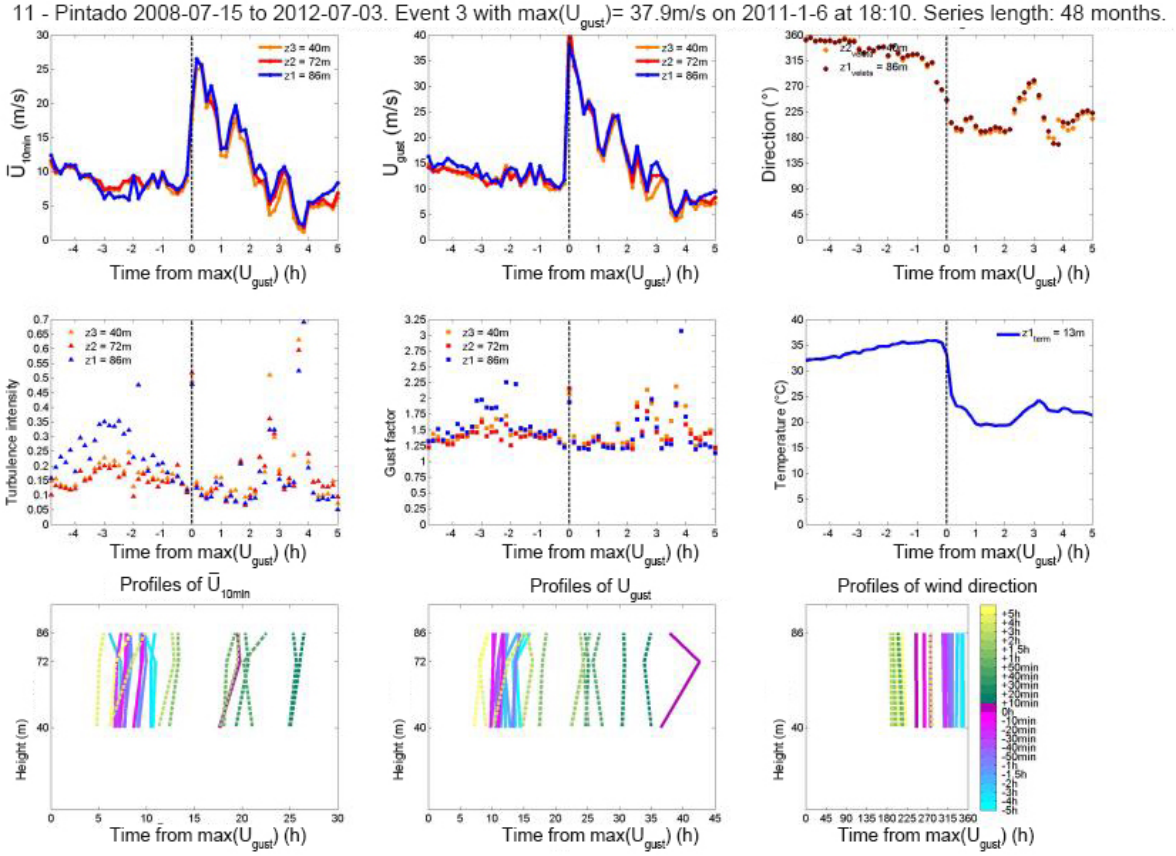
Profiles of wind direction

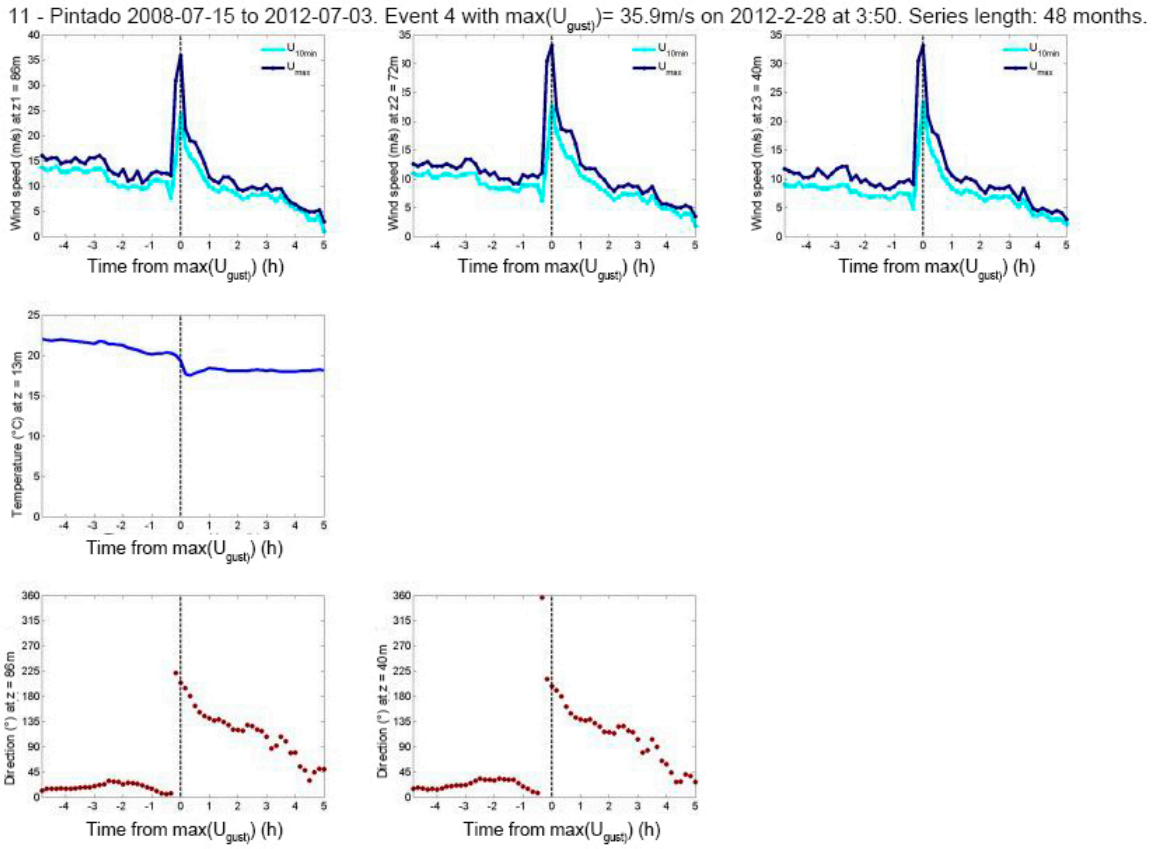


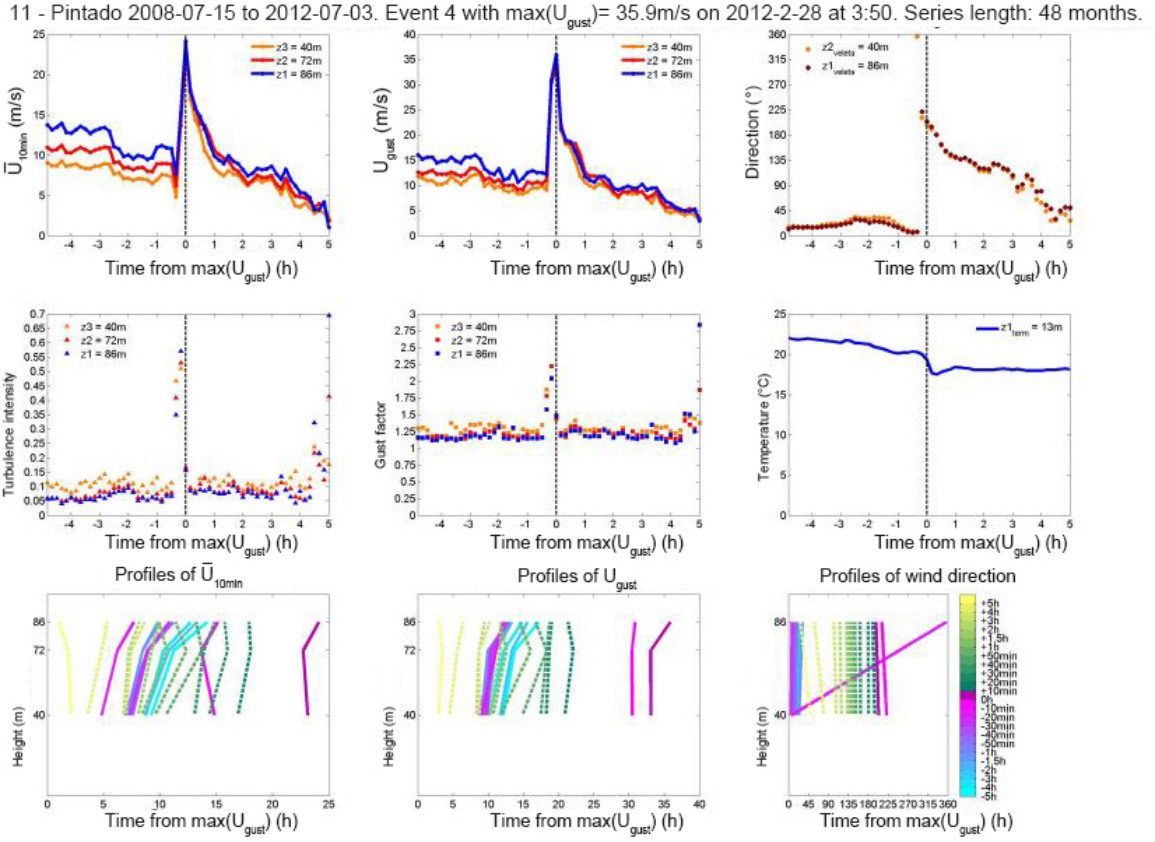
11 - Pintado 2008-07-15 to 2012-07-03. Event 2 with max(U_{gust})= 37.9m/s on 2011-1-16 at 18:10. Series length: 48 months.

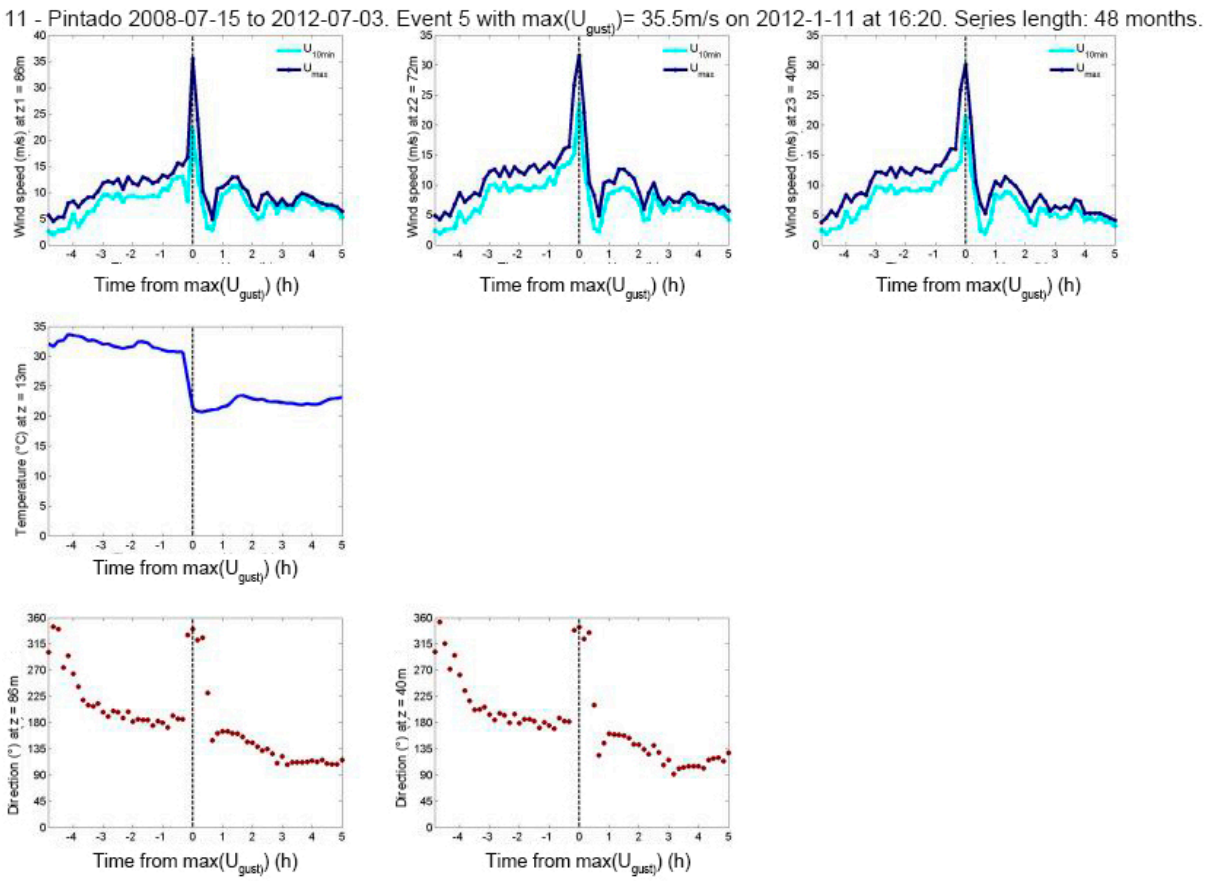


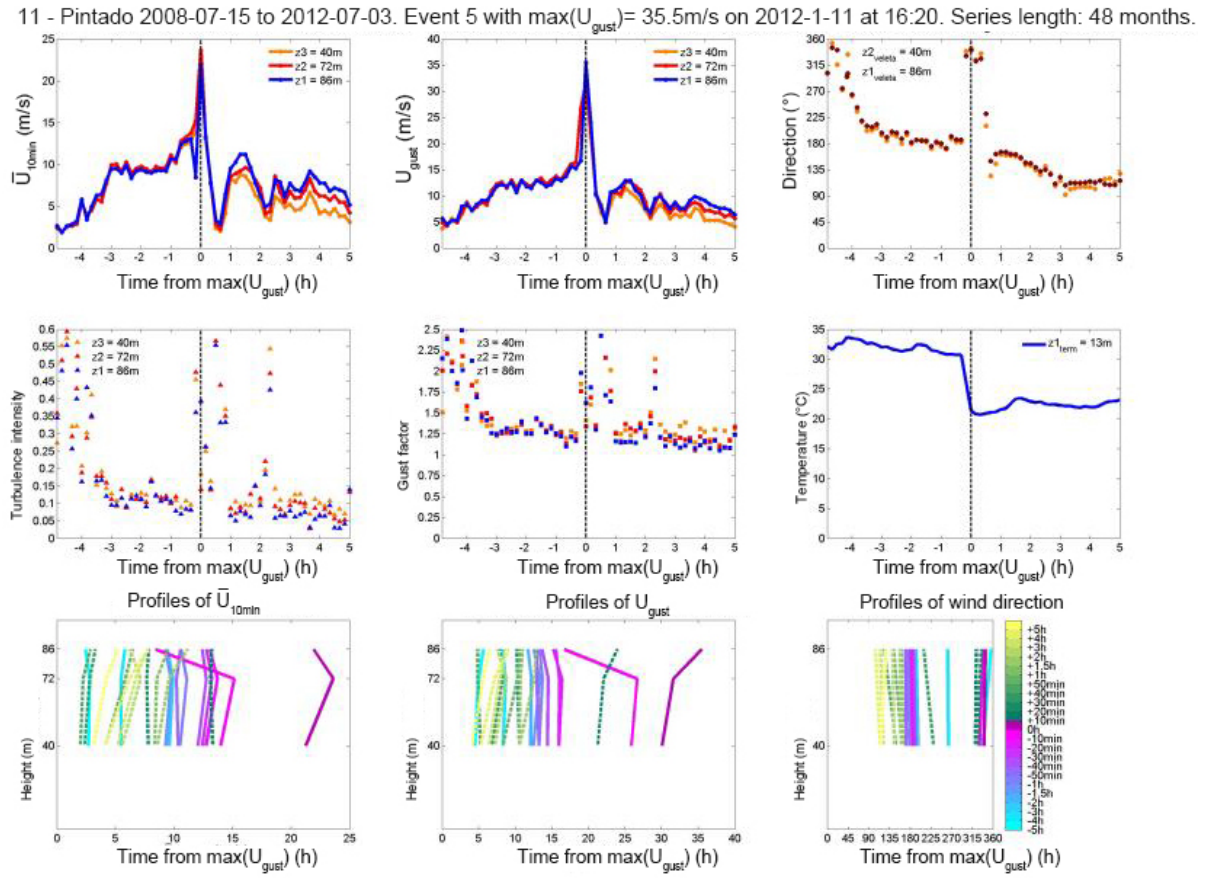
11 - Pintado 2008-07-15 to 2012-07-03. Event 3 with max(U_{gust})= 37.9m/s on 2011-1-6 at 18:10. Series length: 48 months.

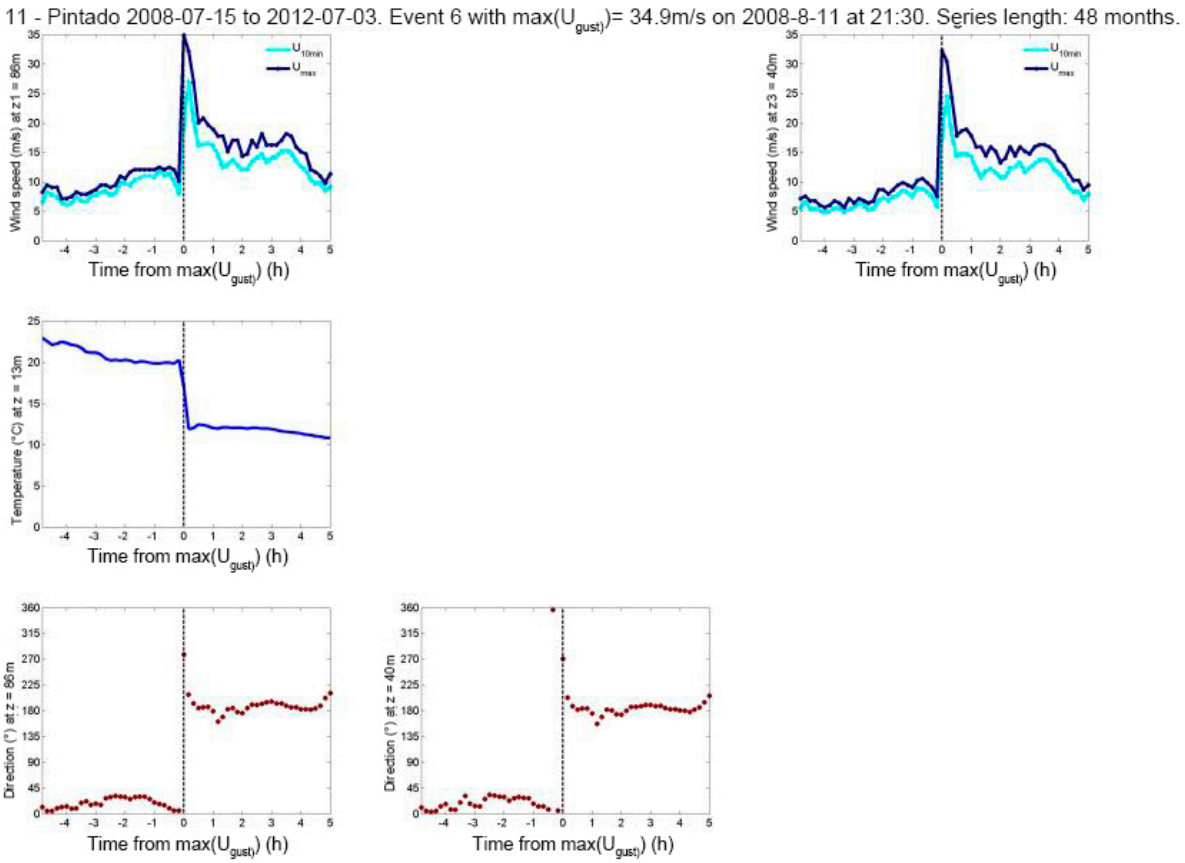


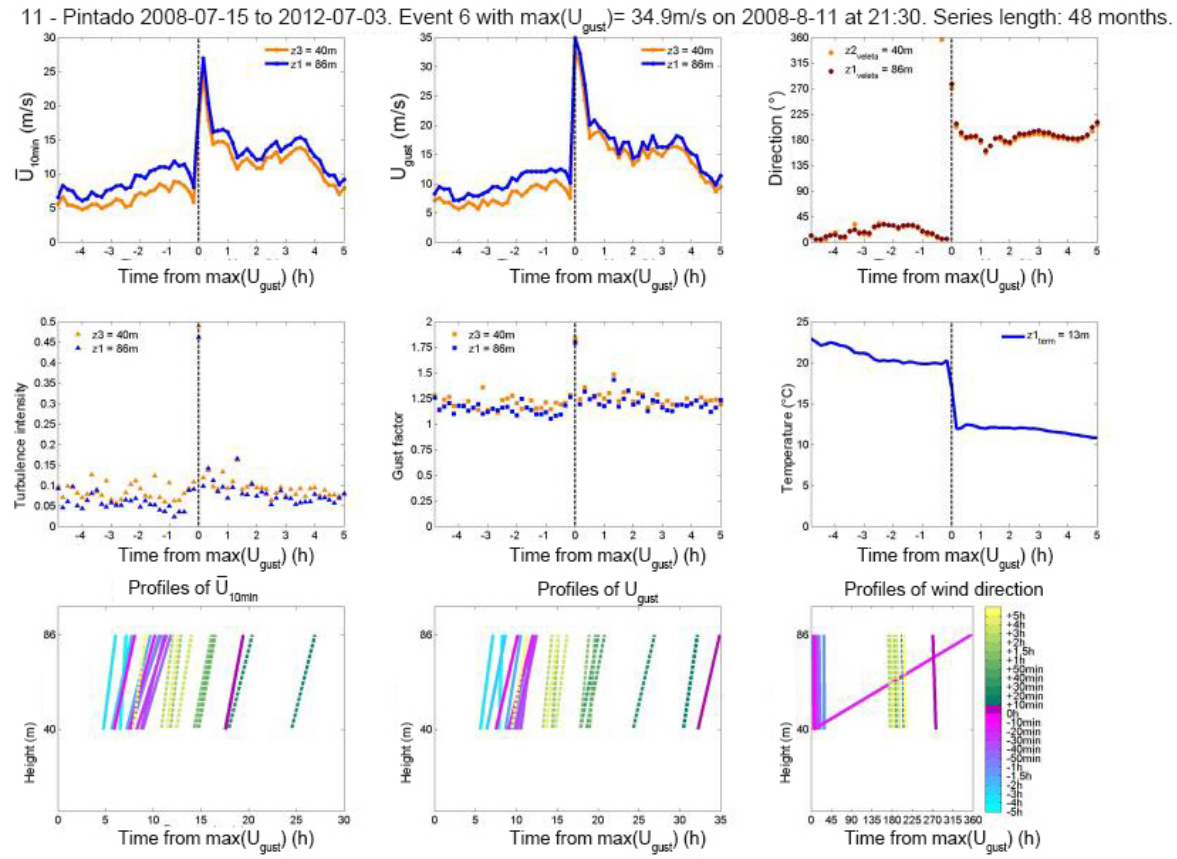

11 - Pintado 2008-07-15 to 2012-07-03. Event 4 with max(U_gust)= 35.9m/s on 2012-2-28 at 3:50. Series length: 48 months.
Wind speed (m/s) at z1 = 86m
Wind speed (m/s) at z2 = 72m
Wind speed (m/s) at z3 = 40m
Temperature (°C) at z = 13m
Direction (°) at z = 86m
Direction (°) at z = 40m
Time from max(U_gust) (h)

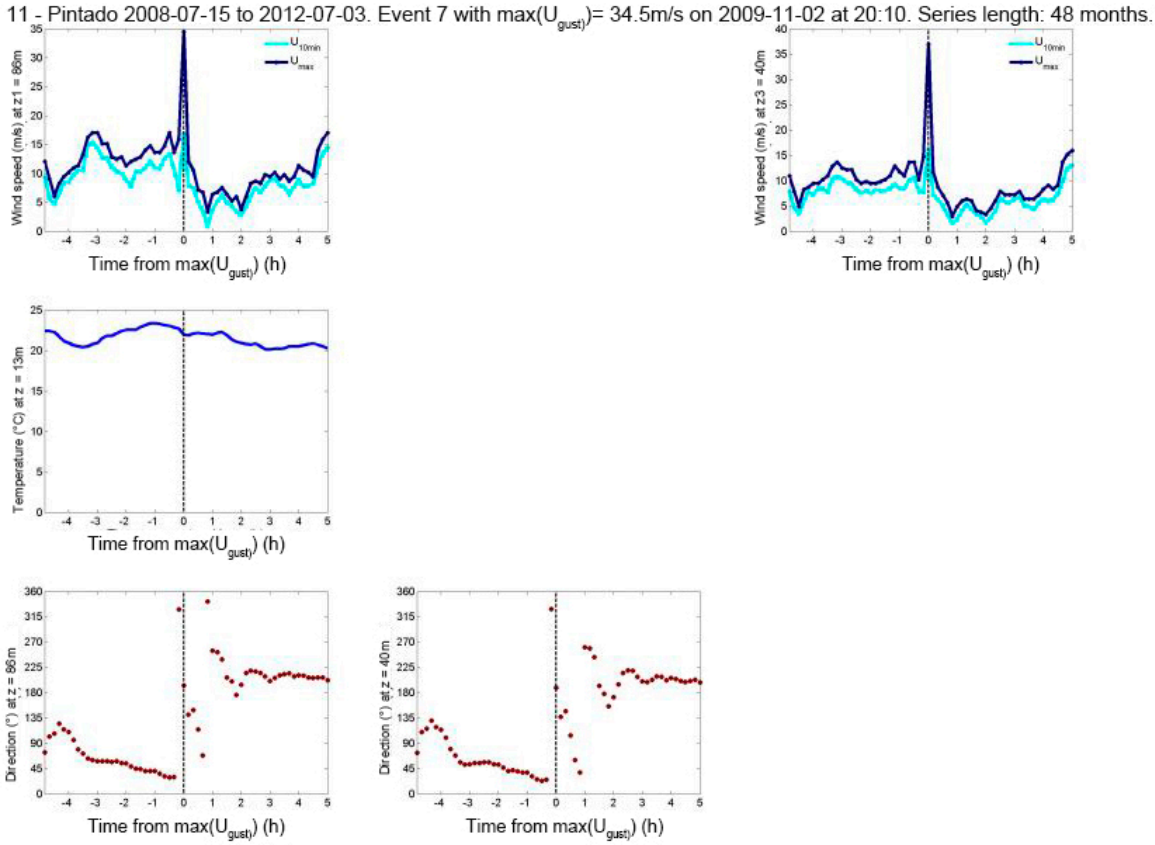

11 - Pintado 2008-07-15 to 2012-07-03. Event 4 with max(U_gust)= 35.9m/s on 2012-2-28 at 3:50. Series length: 48 months.
z3 = 40m
z2 = 72m
z1 = 86m
Turbulence intensity
Gust factor
Temperature (°C)
Direction (°)
Profiles of Ū10min
Profiles of Ugust
Profiles of wind direction
Height (m)
Time from max(U_gust) (h)

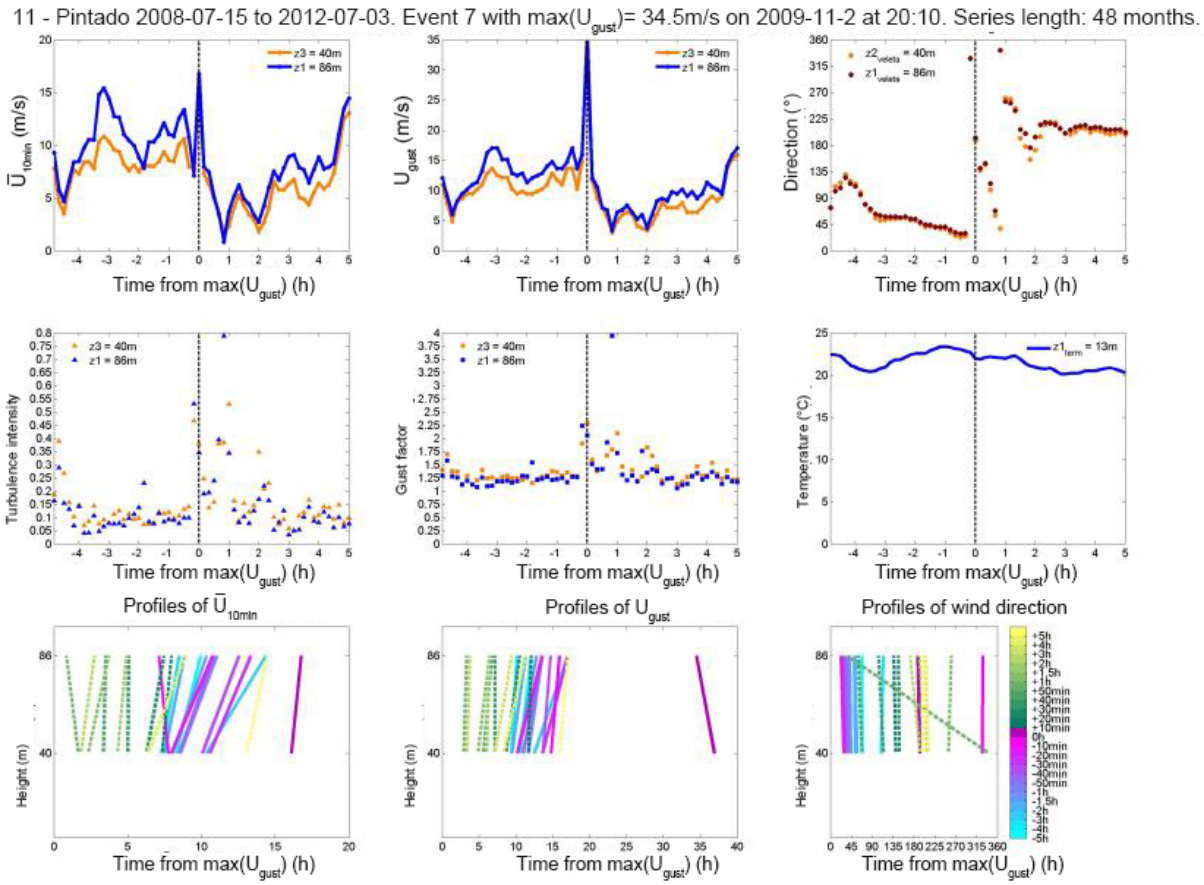

11 - Pintado 2008-07-15 to 2012-07-03. Event 5 with max(U_gust)= 35.5m/s on 2012-1-11 at 16:20. Series length: 48 months.
Wind speed (m/s) at z1 = 86m
Wind speed (m/s) at z2 = 72m
Wind speed (m/s) at z3 = 40m
U10min
Umax
Temperature (°C) at z = 13m
Direction (°) at z = 86m
Direction (°) at z = 40m
Time from max(U_gust) (h)


11 - Pintado 2008-07-15 to 2012-07-03. Event 5 with max(U_gust)= 35.5m/s on 2012-1-11 at 16:20. Series length: 48 months.
z3 = 40m
z2 = 72m
z1 = 86m
Ū10min (m/s)
Ugust (m/s)
Direction (°)
Turbulence intensity
Gust factor
Temperature (°C)
Profiles of Ū10min
Profiles of Ugust
Profiles of wind direction
Height (m)
Time from max(U_gust) (h)

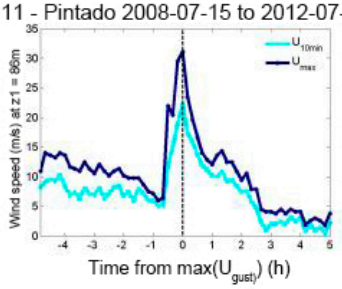

11 - Pintado 2008-07-15 to 2012-07-03. Event 6 with max(U_gust)= 34.9m/s on 2008-8-11 at 21:30. Series length: 48 months.
Wind speed (m/s) at z1 = 86m
Wind speed (m/s) at z3 = 40m
Temperature (°C) at z = 13m
Direction (°) at z = 86m
Direction (°) at z = 40m
Time from max(U_gust) (h)

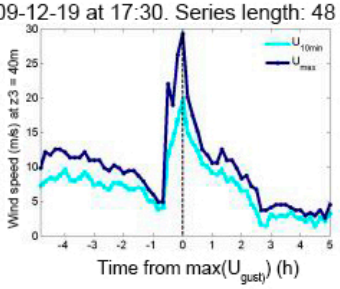

11 - Pintado 2008-07-15 to 2012-07-03. Event 6 with max(U_gust)= 34.9m/s on 2008-8-11 at 21:30. Series length: 48 months.
Turbulence intensity
Gust factor
Temperature (°C)
Direction (°)
Profiles of Ū10min
Profiles of U_gust
Profiles of wind direction
Height (m)
Time from max(U_gust) (h)

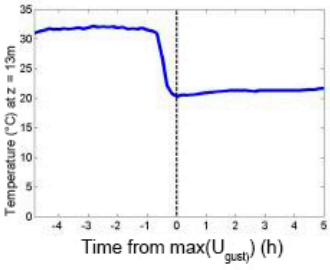

11 - Pintado 2008-07-15 to 2012-07-03. Event 7 with max(U_gust)= 34.5m/s on 2009-11-02 at 20:10. Series length: 48 months.
Wind speed (m/s) at z1 = 86m
Wind speed (m/s) at z3 = 40m
Temperature (°C) at z = 13m
Direction (°) at z = 86m
Direction (°) at z = 40m
Time from max(U_gust) (h)

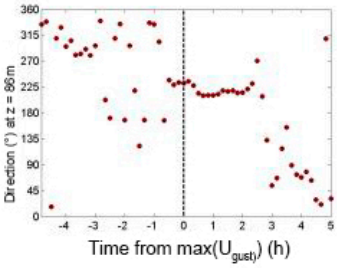

11 - Pintado 2008-07-15 to 2012-07-03. Event 7 with max(U_gust)= 34.5m/s on 2009-11-2 at 20:10. Series length: 48 months.
z3 = 40m
z1 = 86m
Turbulence intensity
Gust factor
Temperature (°C)
Direction (°)
Profiles of Ū10min
Profiles of Ugust
Profiles of wind direction
Height (m)
Time from max(U_gust) (h)

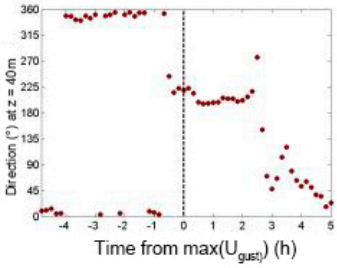
11 - Pintado 2008-07-15 to 2012-07-03. Event 8 with max(U_{gust})= 31.1m/s on 2009-12-19 at 17:30. Series length: 48 months.



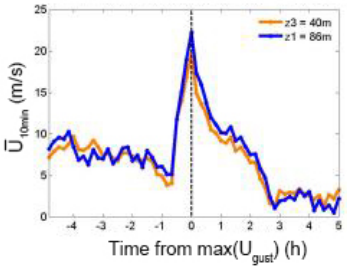


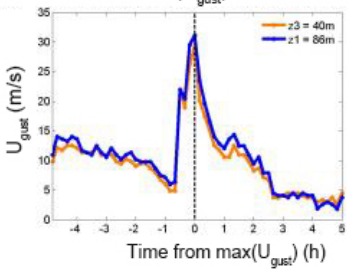


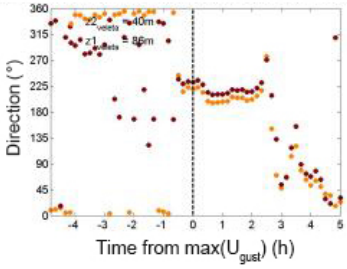


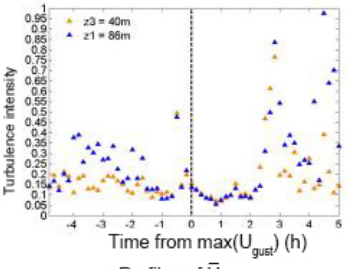


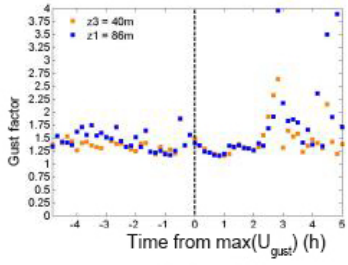
11 - Pintado 2008-07-15 to 2012-07-03. Event 8 with max(U_{gust})= 31.1m/s on 2009-12-19 at 17:30. Series length: 48 months.

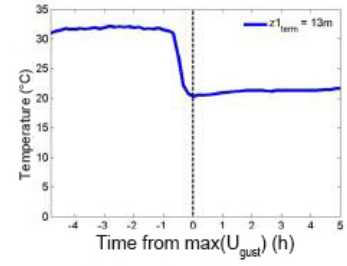




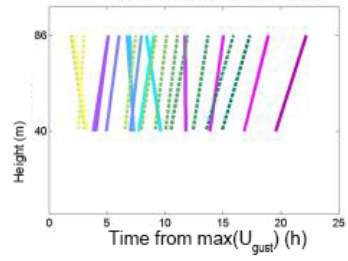




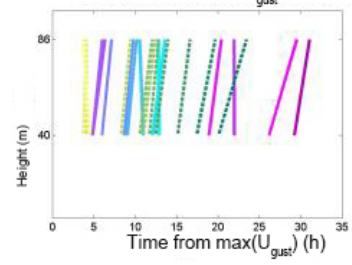




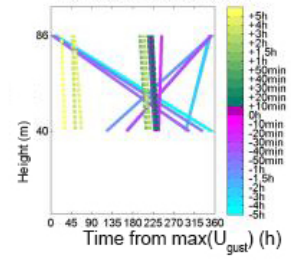
Profiles of $\bar{U}_{10min}$

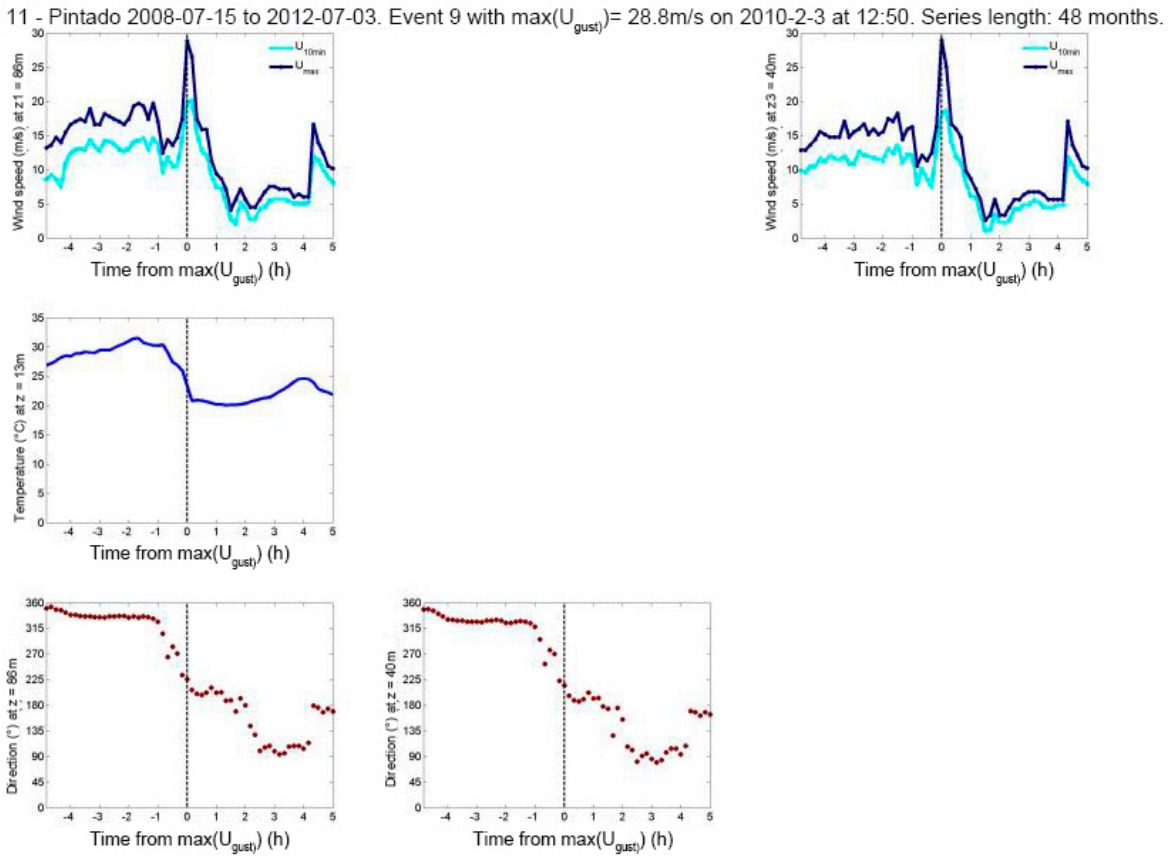


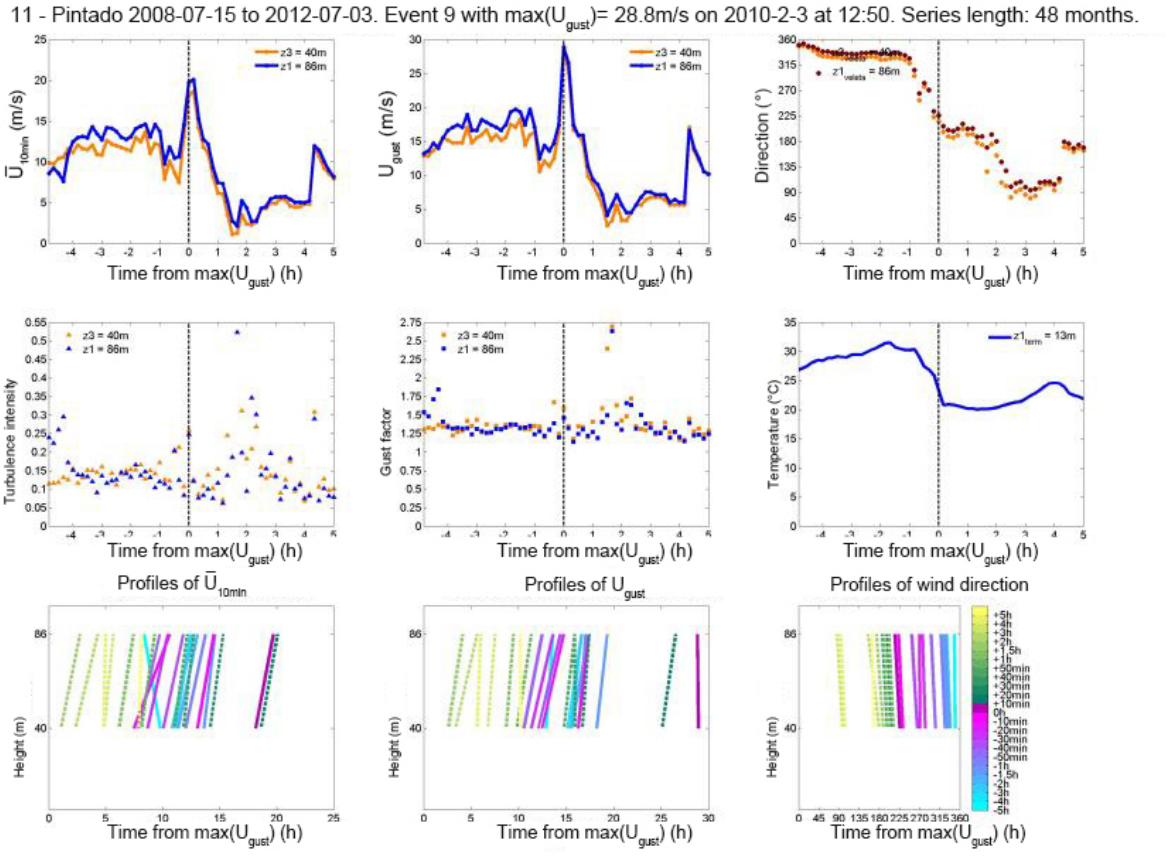
Profiles of U_{gust}



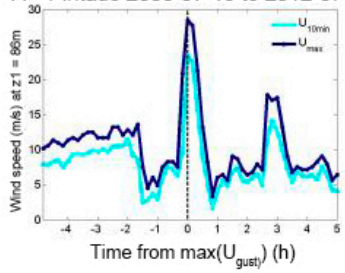
Profiles of wind direction

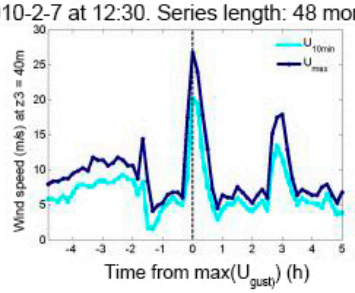


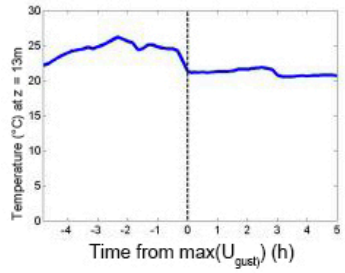

11 - Pintado 2008-07-15 to 2012-07-03. Event 9 with max(U_gust)= 28.8m/s on 2010-2-3 at 12:50. Series length: 48 months.
Wind speed (m/s) at z1 = 86m
Wind speed (m/s) at z3 = 40m
Temperature (°C) at z = 13m
Direction (°) at z = 86m
Direction (°) at z = 40m
Time from max(U_gust) (h)

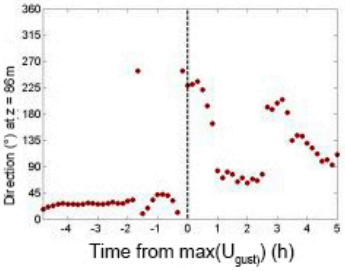

11 - Pintado 2008-07-15 to 2012-07-03. Event 9 with max(U_gust)= 28.8m/s on 2010-2-3 at 12:50. Series length: 48 months.
z3 = 40m
z1 = 86m
Turbulence intensity
Gust factor
Temperature (°C)
Direction (°)
Profiles of Ū10min
Profiles of U_gust
Profiles of wind direction
Height (m)
Time from max(U_gust) (h)

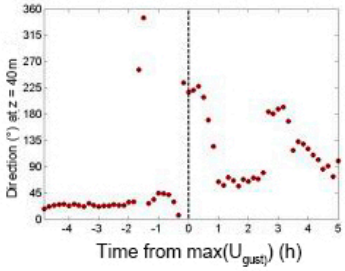
11 - Pintado 2008-07-15 to 2012-07-03. Event 10 with max(U_{gust})= 28.5m/s on 2010-2-7 at 12:30. Series length: 48 months.



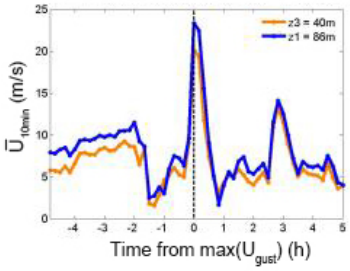


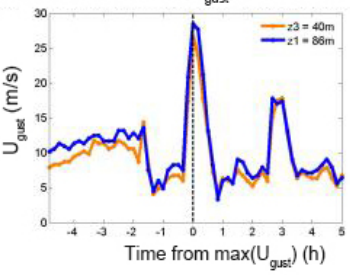


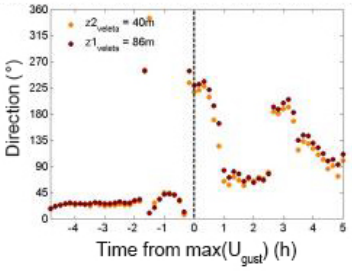


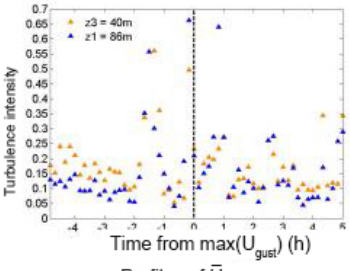


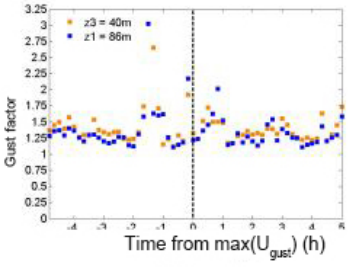
11 - Pintado 2008-07-15 to 2012-07-03. Event 10 with max(U_{gust})= 28.5m/s on 2010-2-7 at 12:30. Series length: 48 months.

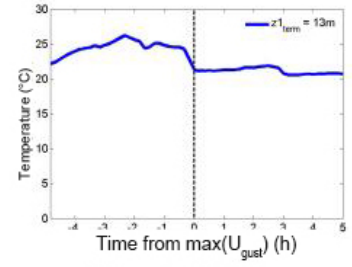




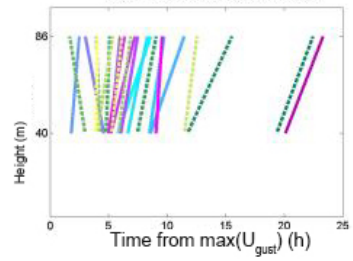




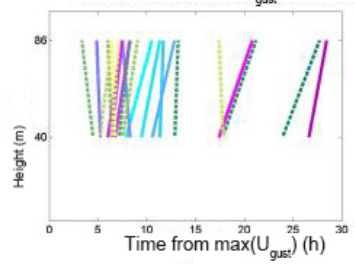




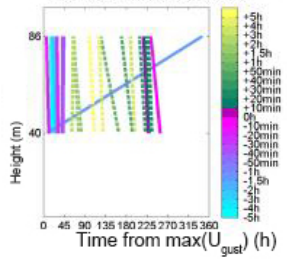
Profiles of $\bar{U}_{10min}$



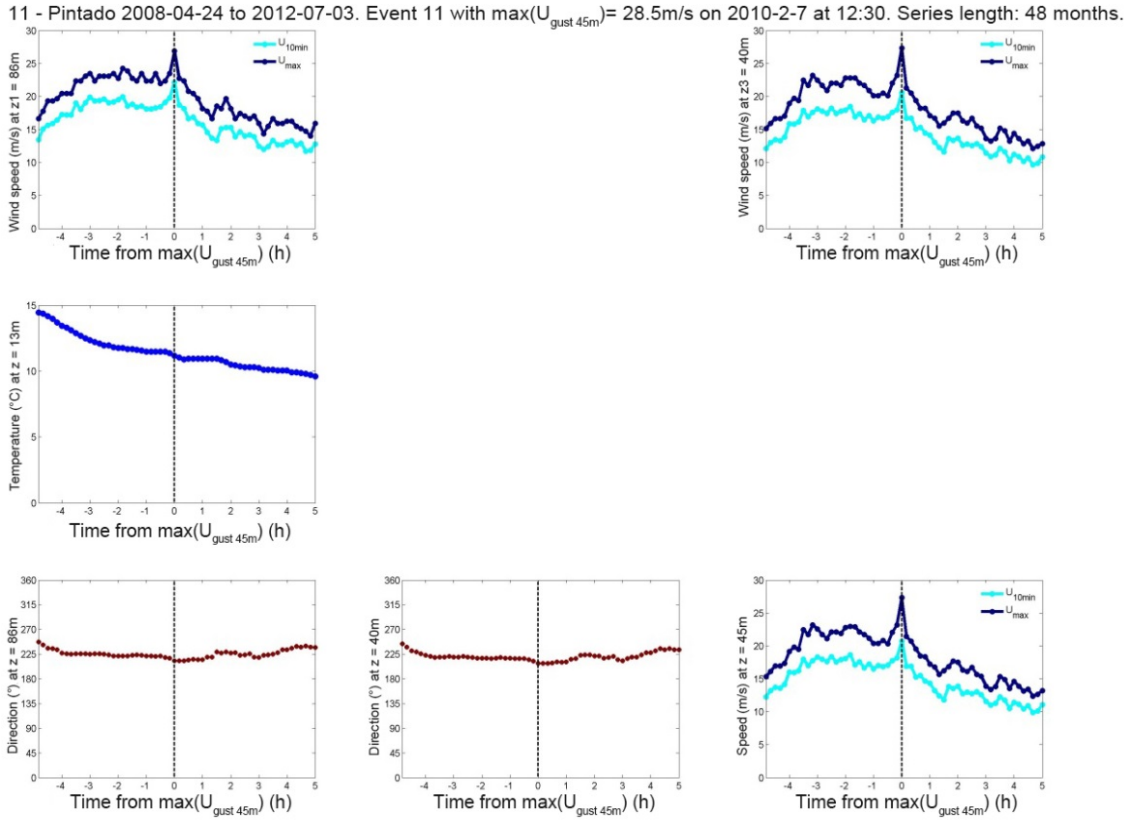
Profiles of U_{gust}

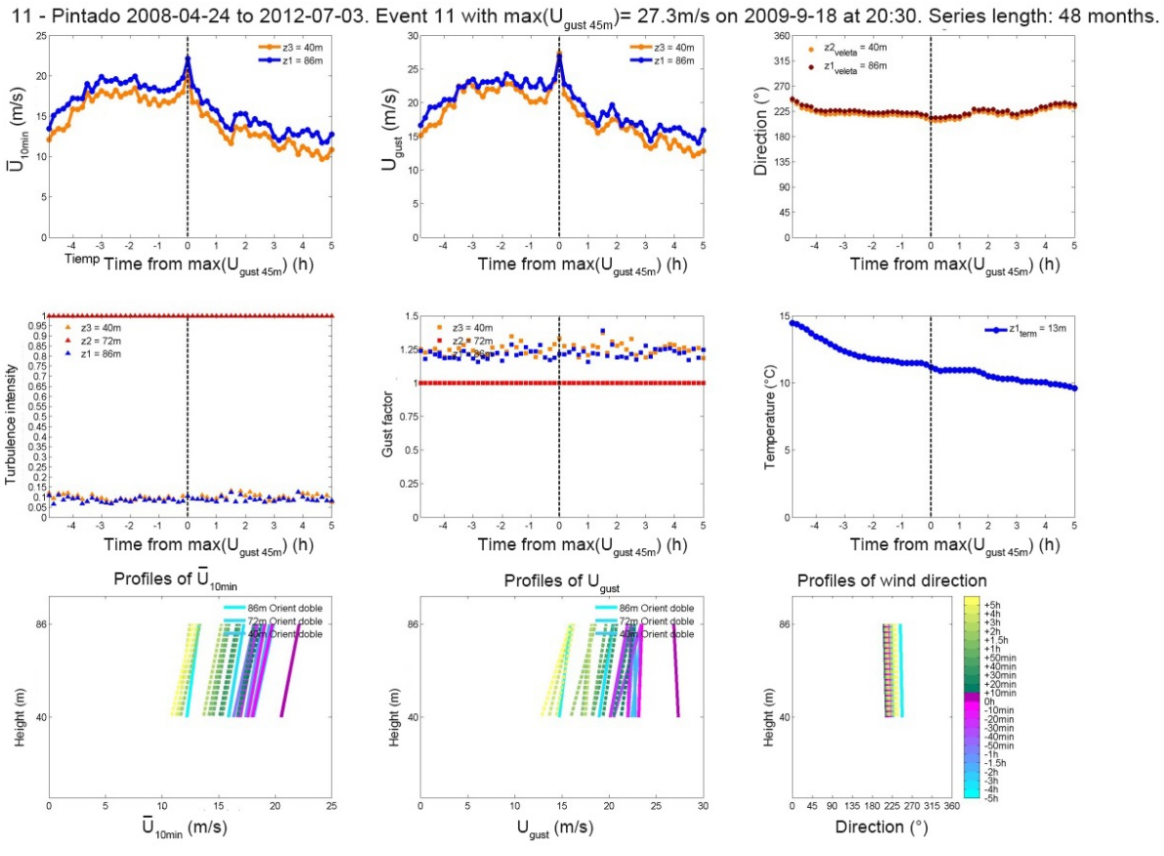


Profiles of wind direction

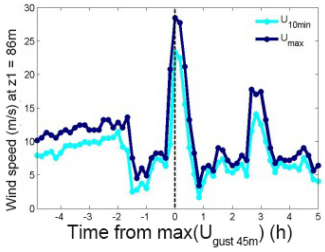


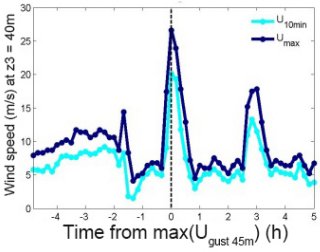
A.3 Highest wind gust events at Pintado at 45m, complete years, from the 11th case

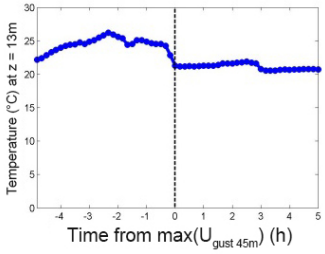


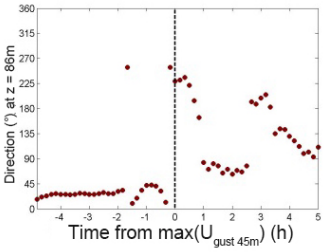


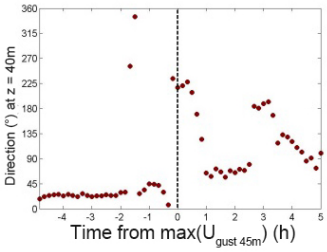
11 - Pintado 2008-04-24 to 2012-07-03. Event 12 with max($U_{gust\ 45m}$)= 26.8m/s on 2010-2-7 at 12:30. Series length: 48 months.

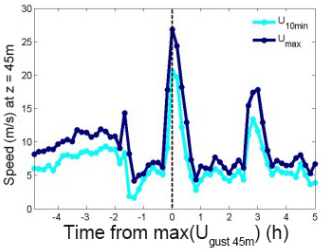




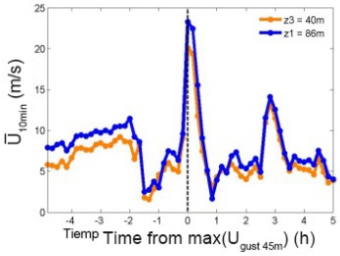


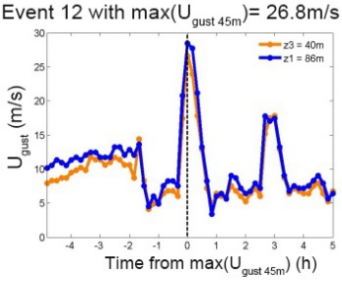


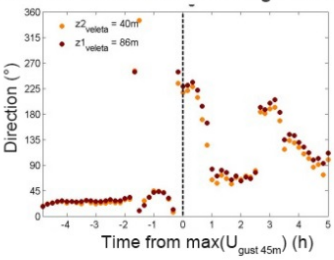


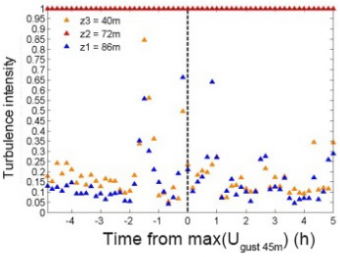


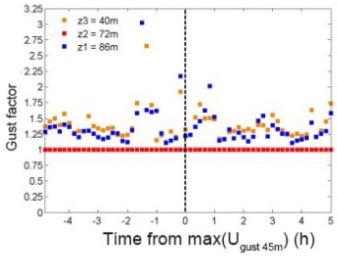
11 - Pintado 2008-04-24 to 2012-07-03. Event 12 with max($U_{gust\ 45m}$)= 26.8m/s on 2010-2-7 at 12:30. Series length: 48 months.

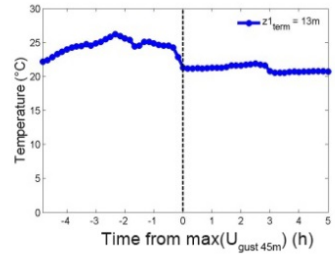


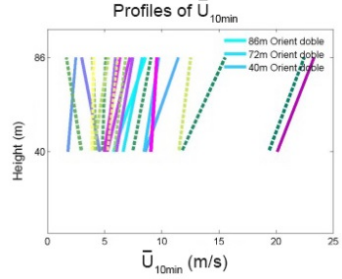


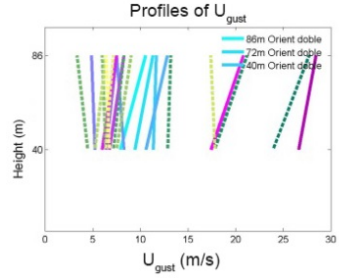


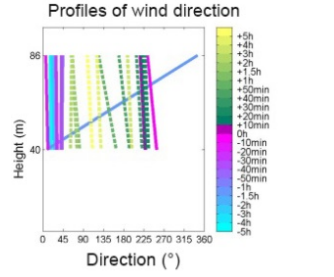




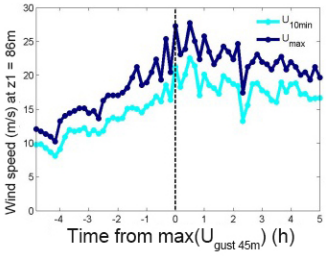


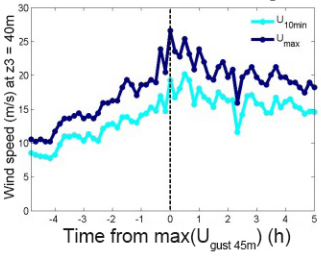


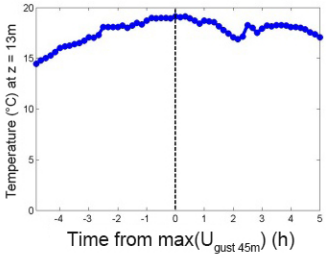


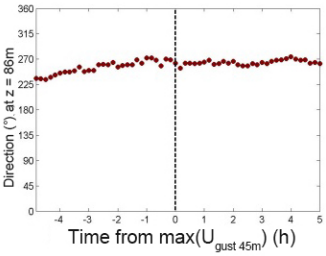


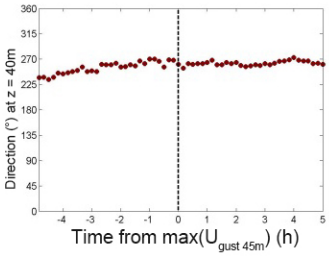
11 - Pintado 2008-04-24 to 2012-07-03. Event 13 with max($U_{gust\ 45m}$)= 26.7m/s on 2010-10-30 at 13:30. Series length: 48 months.

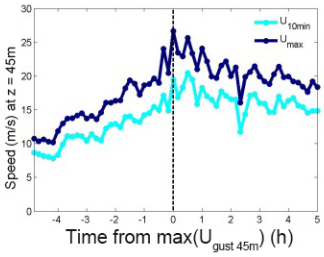




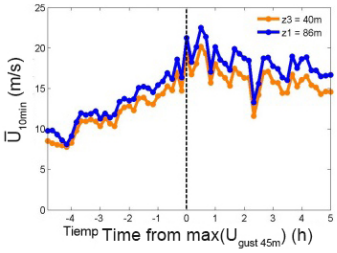


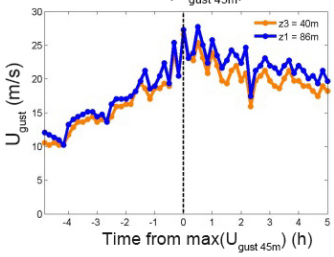


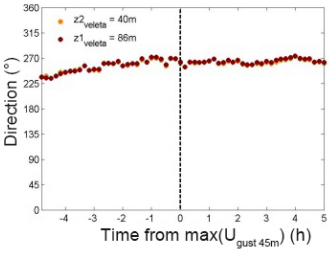


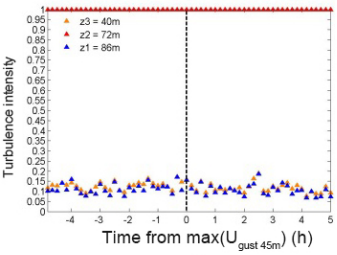


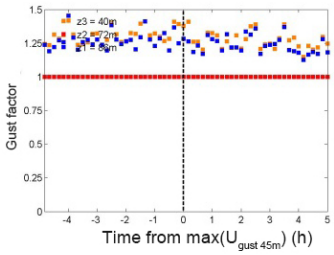
11 - Pintado 2008-04-24 to 2012-07-03. Event 13 with max($U_{gust\ 45m}$)= 26.7m/s on 2010-10-30 at 13:30. Series length: 48 months.

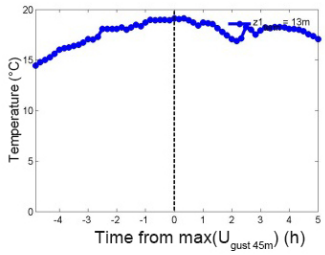


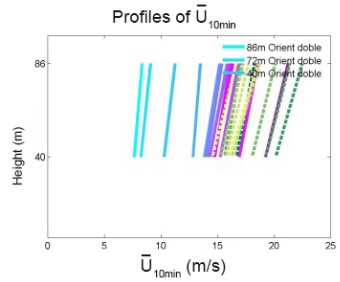


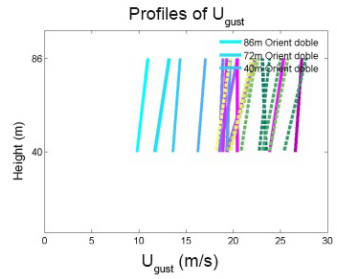


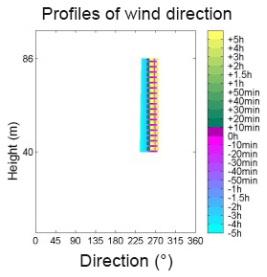




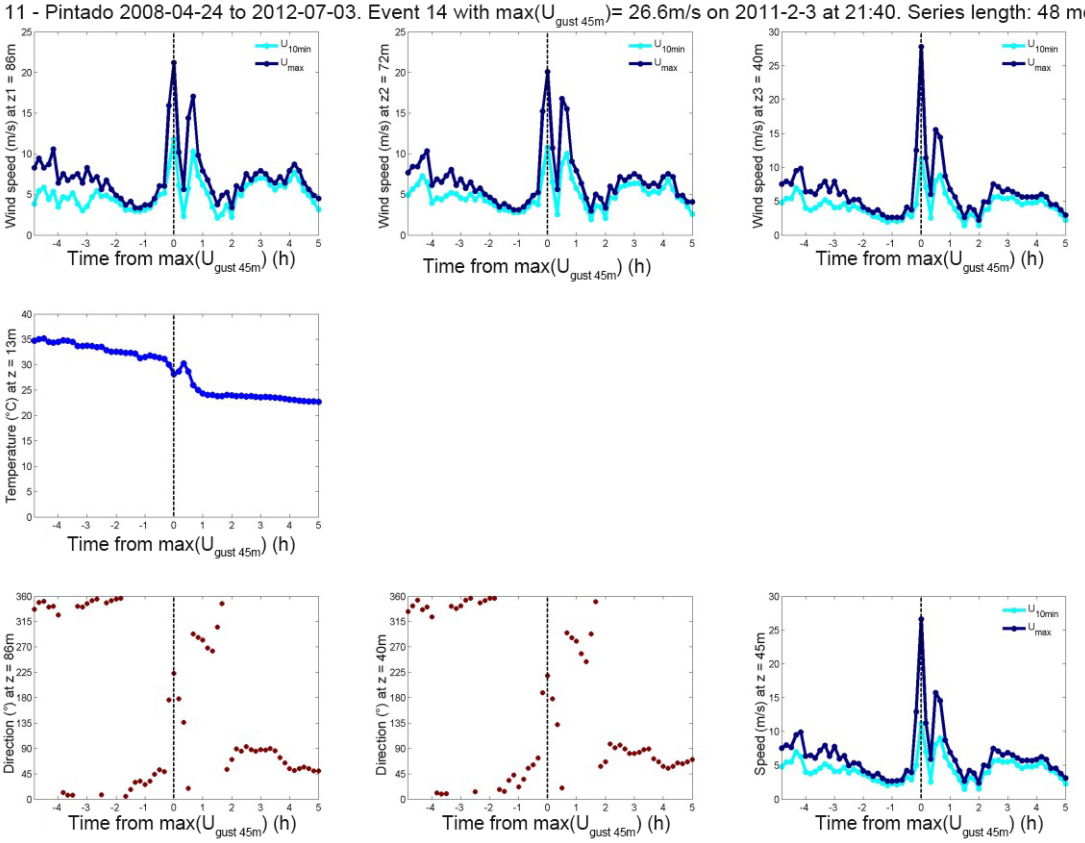




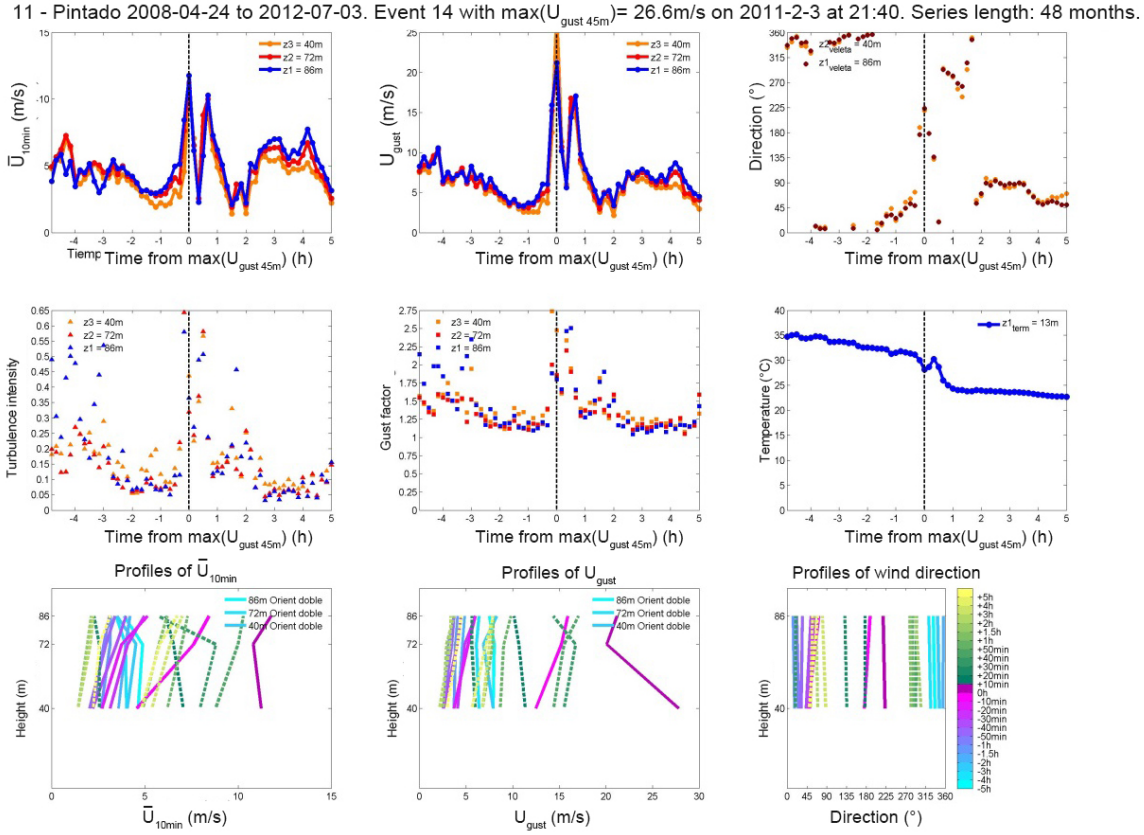




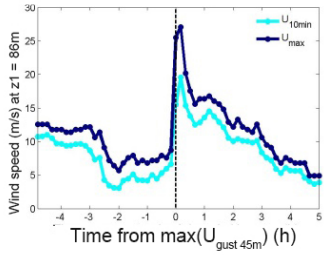
11 - Pintado 2008-04-24 to 2012-07-03. Event 14 with max($U_{gust\ 45m}$)= 26.6m/s on 2011-2-3 at 21:40. Series length: 48 months.

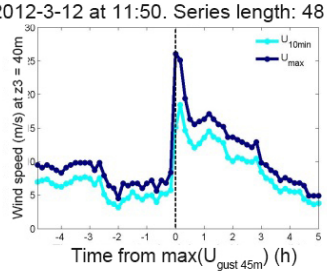


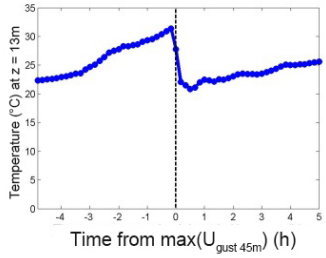
11 - Pintado 2008-04-24 to 2012-07-03. Event 14 with max($U_{gust\ 45m}$)= 26.6m/s on 2011-2-3 at 21:40. Series length: 48 months.

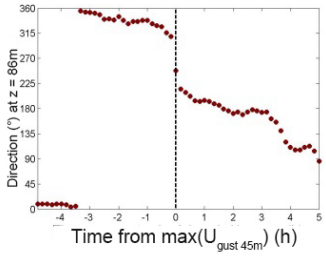


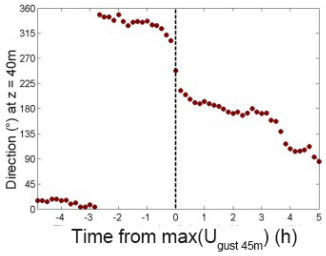
11 - Pintado 2008-04-24 to 2012-07-03. Event 15 with max($U_{gust\ 45m}$)= 26.4m/s on 2012-3-12 at 11:50. Series length: 48 months.

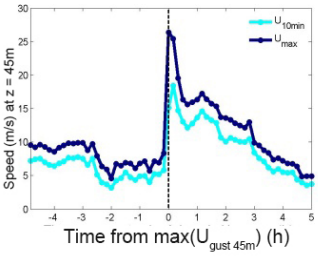




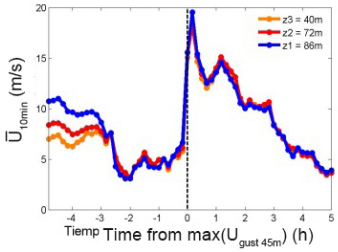


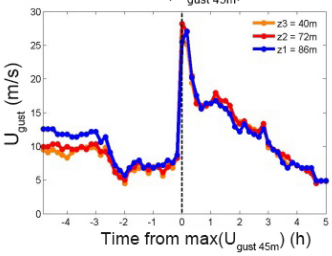


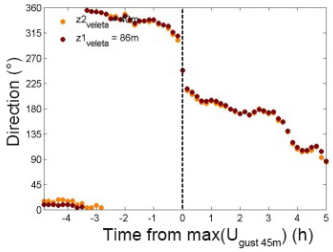


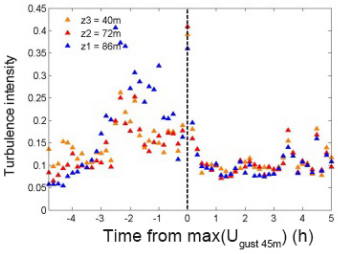


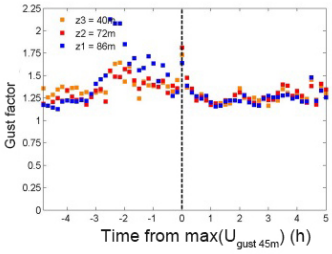
11 - Pintado 2008-04-24 to 2012-07-03. Event 15 with max($U_{gust\ 45m}$)= 26.4m/s on 2012-3-12 at 11:50. Series length: 48 months.

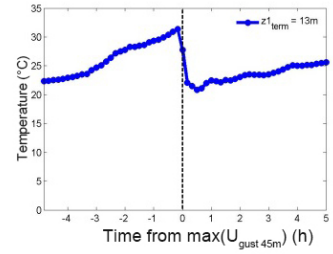


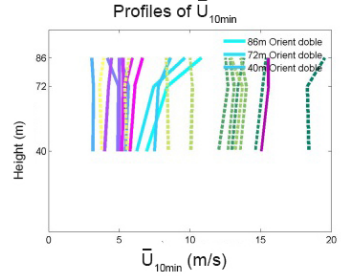


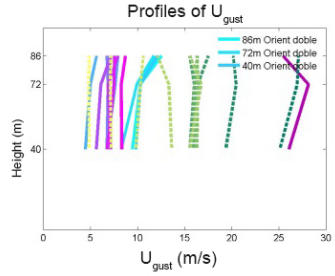


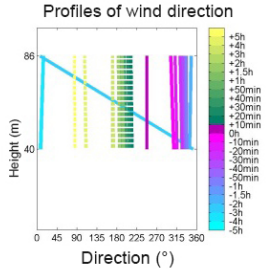




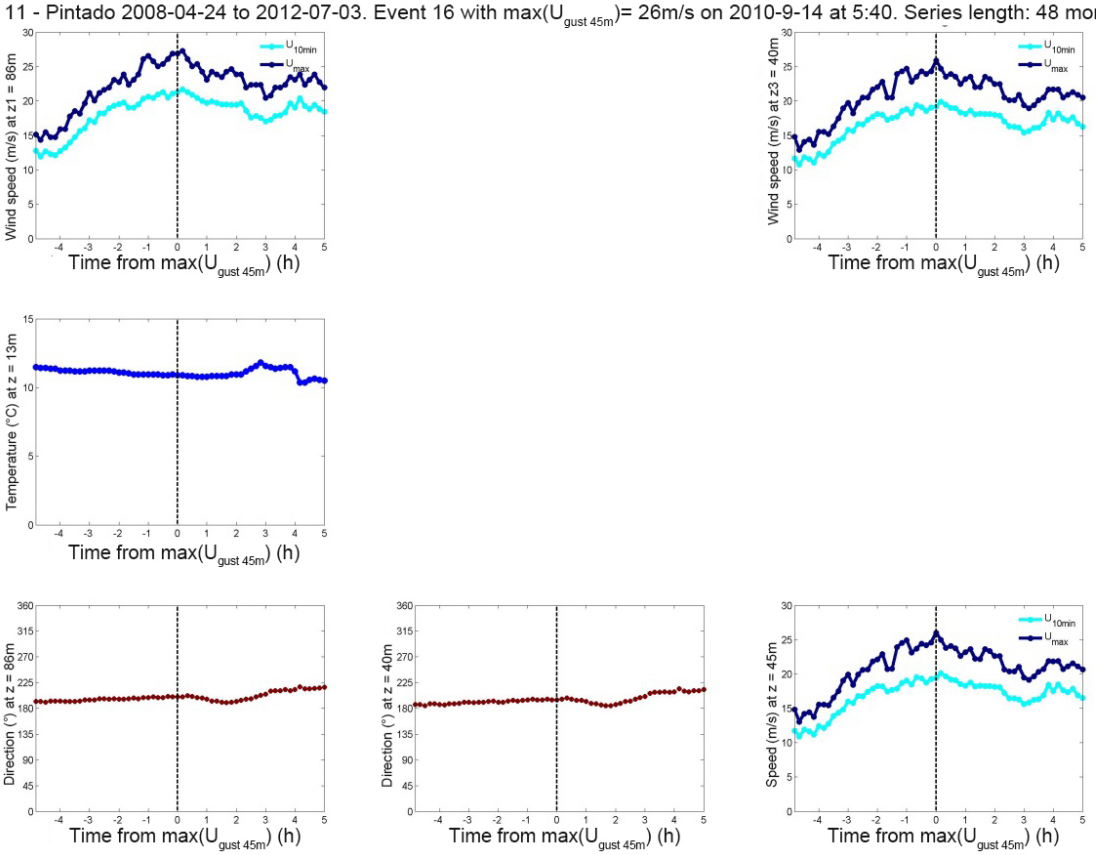




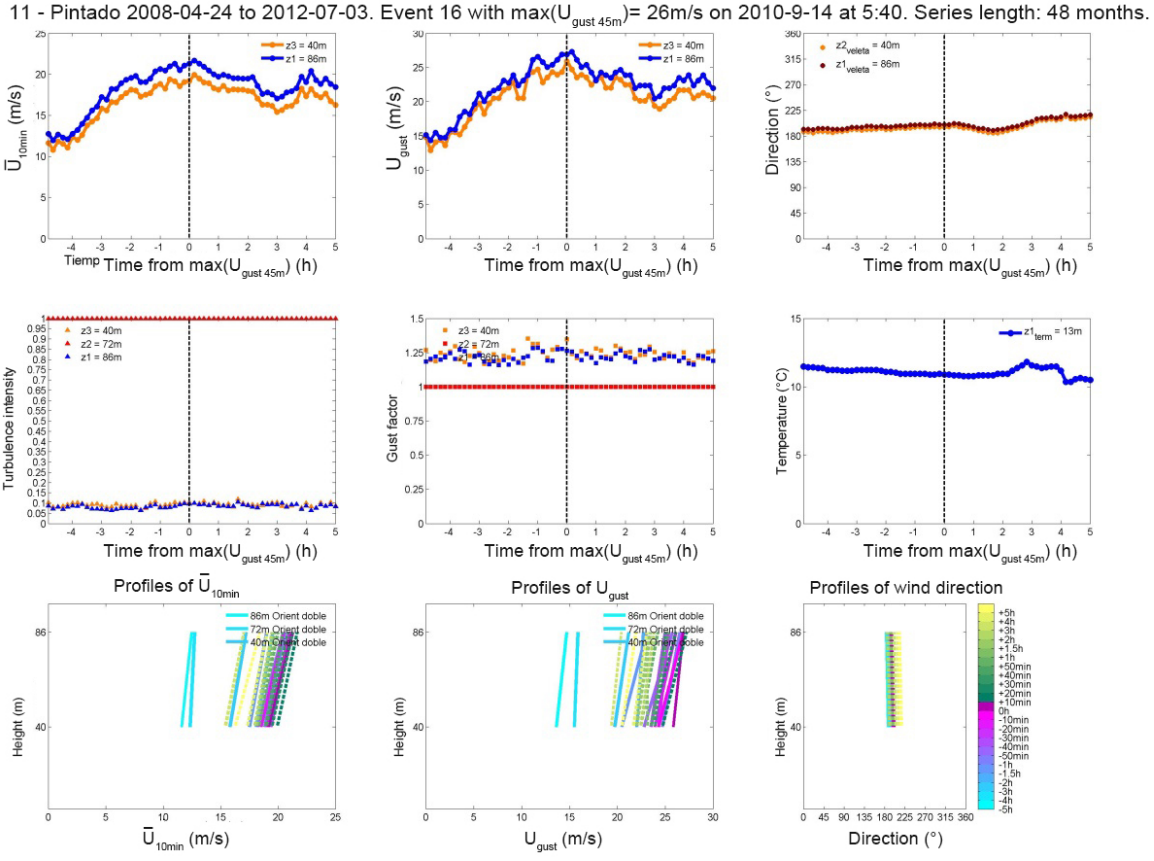




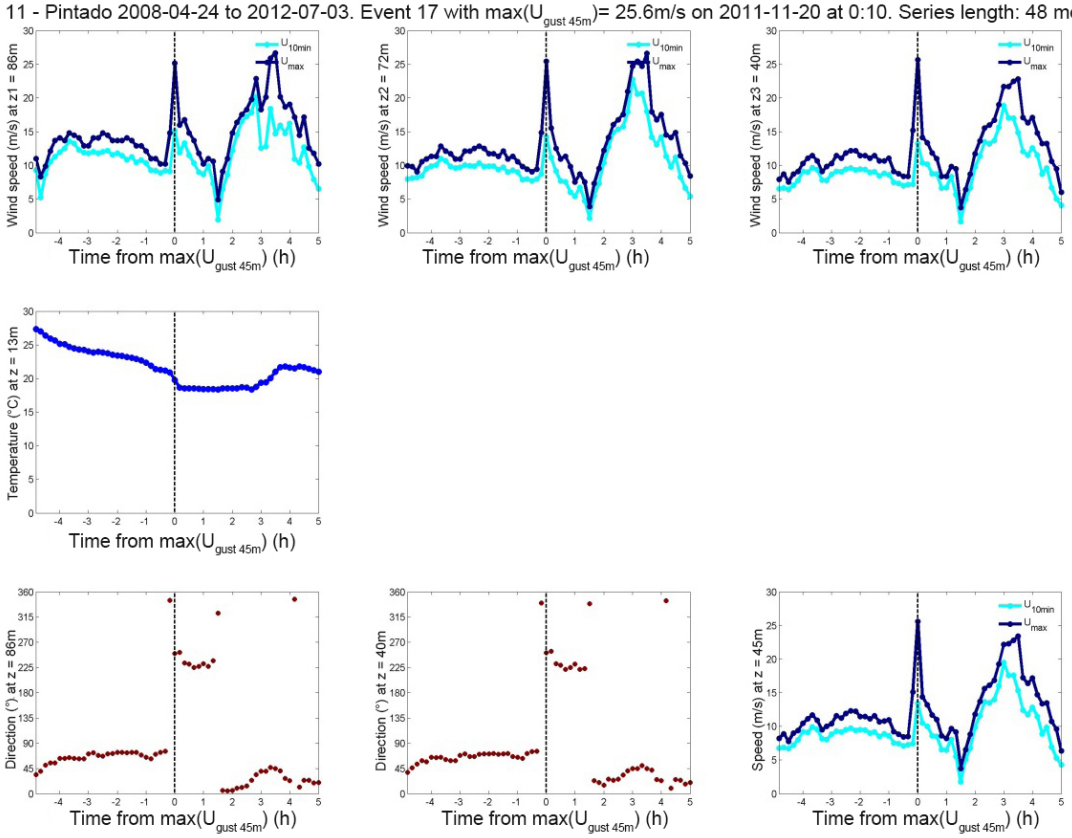
11 - Pintado 2008-04-24 to 2012-07-03. Event 16 with max($U_{gust\ 45m}$)= 26m/s on 2010-9-14 at 5:40. Series length: 48 months.



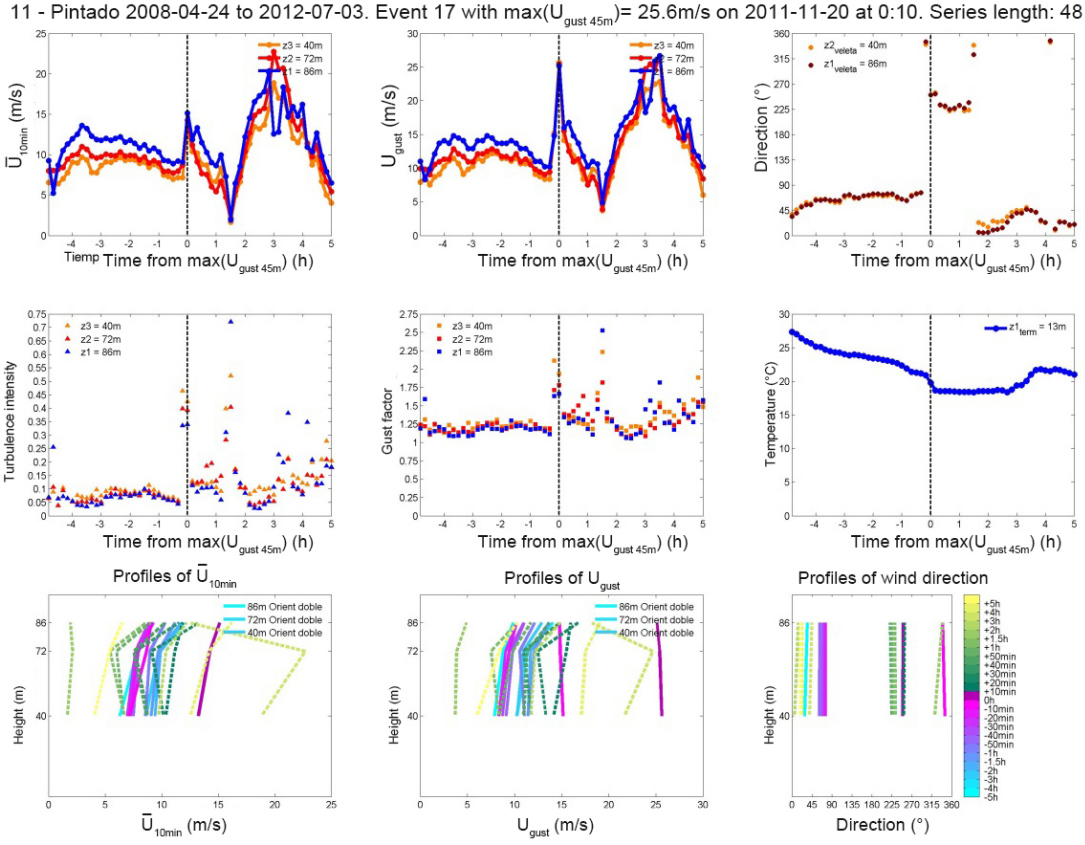
11 - Pintado 2008-04-24 to 2012-07-03. Event 16 with max($U_{gust\ 45m}$)= 26m/s on 2010-9-14 at 5:40. Series length: 48 months.



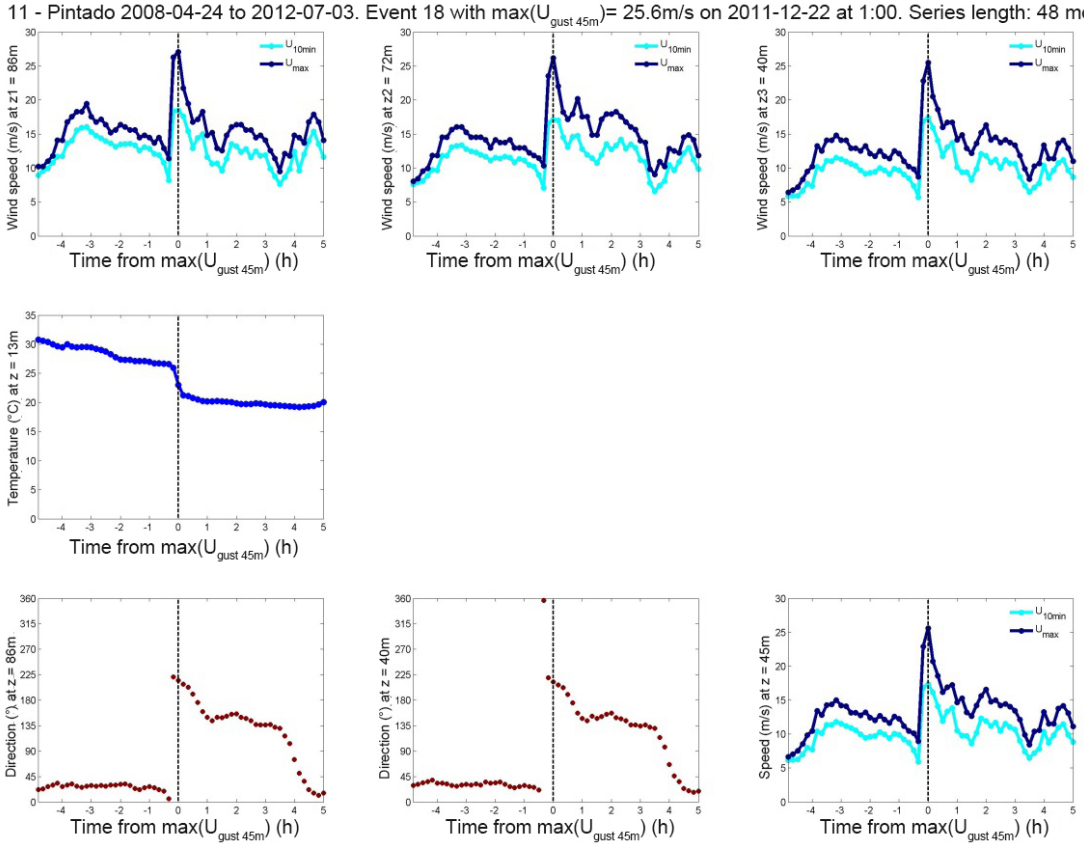
11 - Pintado 2008-04-24 to 2012-07-03. Event 17 with max($U_{gust\ 45m}$)= 25.6m/s on 2011-11-20 at 0:10. Series length: 48 months.



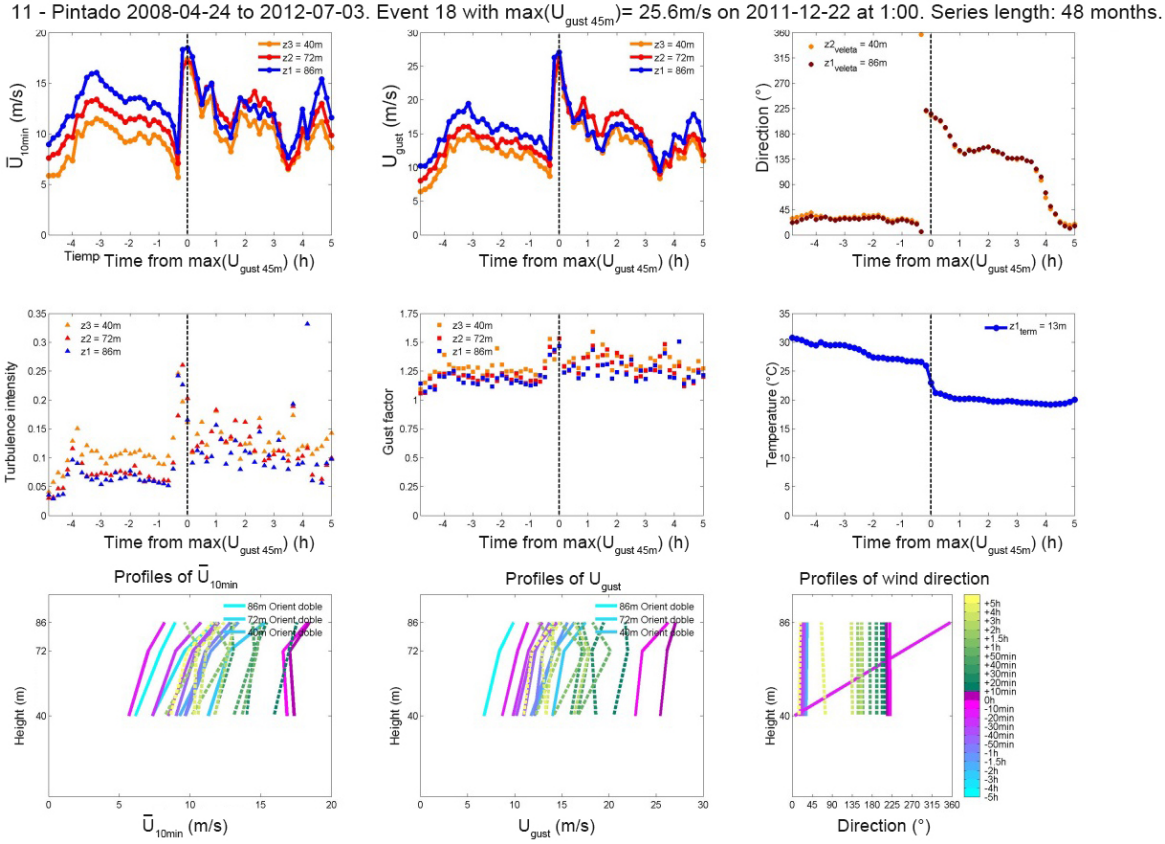
11 - Pintado 2008-04-24 to 2012-07-03. Event 17 with max($U_{gust\ 45m}$)= 25.6m/s on 2011-11-20 at 0:10. Series length: 48 months



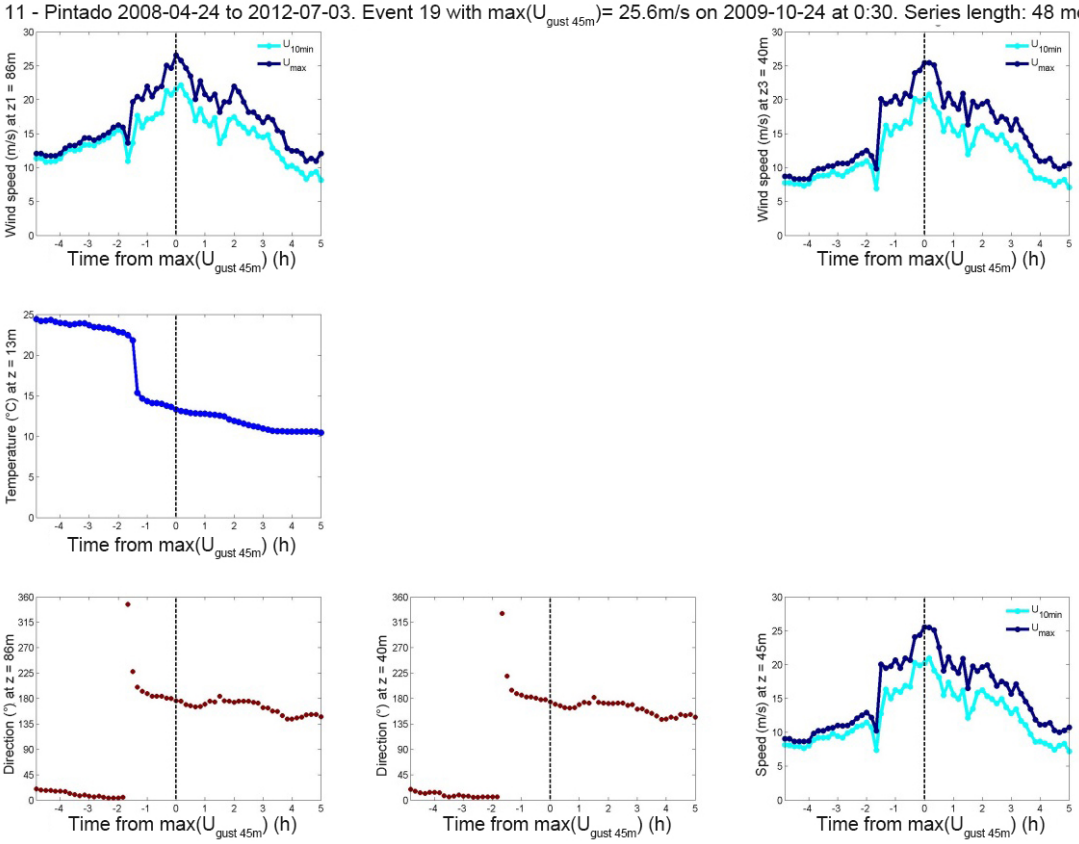
11 - Pintado 2008-04-24 to 2012-07-03. Event 18 with max($U_{gust\ 45m}$)= 25.6m/s on 2011-12-22 at 1:00. Series length: 48 months.



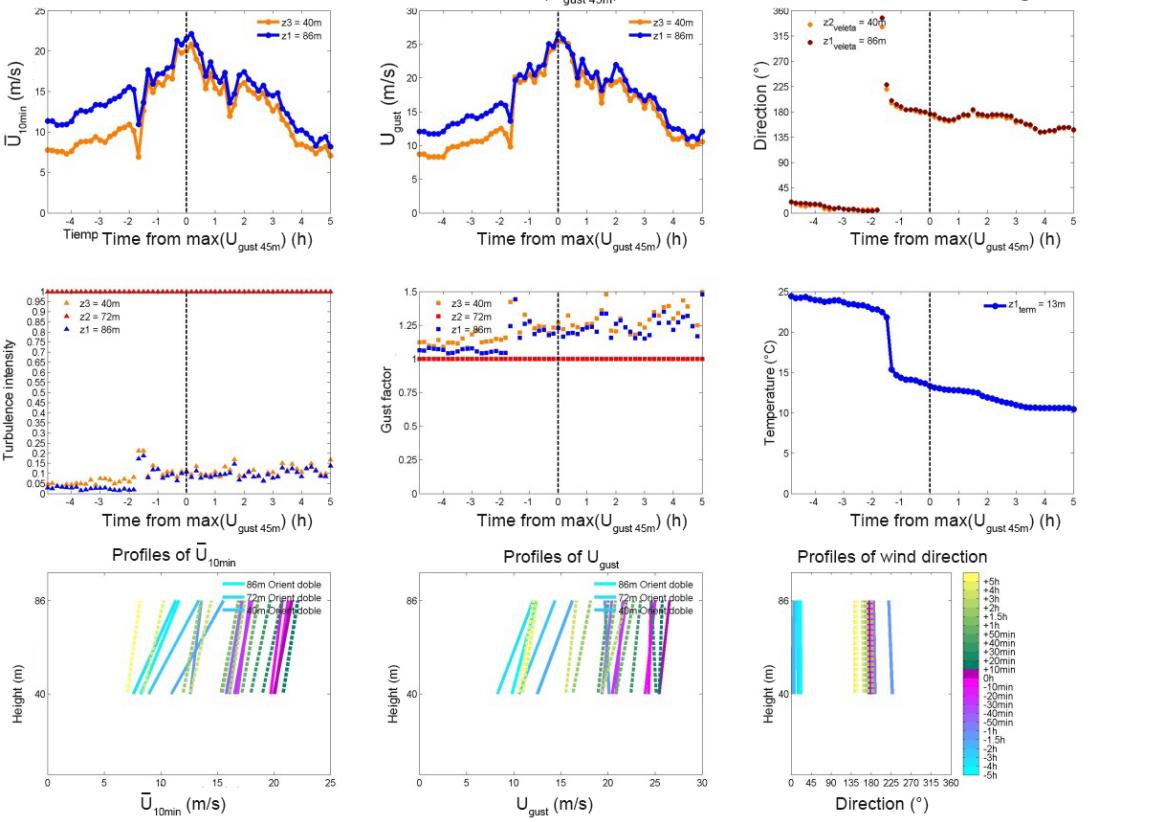
11 - Pintado 2008-04-24 to 2012-07-03. Event 18 with max($U_{gust\ 45m}$)= 25.6m/s on 2011-12-22 at 1:00. Series length: 48 months.



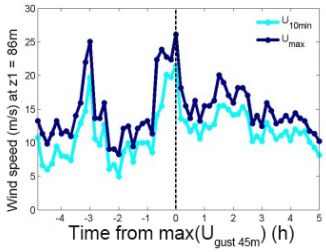
11 - Pintado 2008-04-24 to 2012-07-03. Event 19 with max($U_{gust\ 45m}$)= 25.6m/s on 2009-10-24 at 0:30. Series length: 48 months.

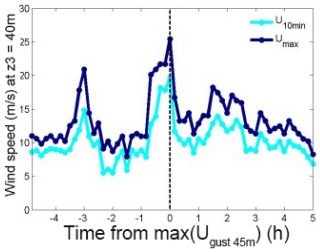


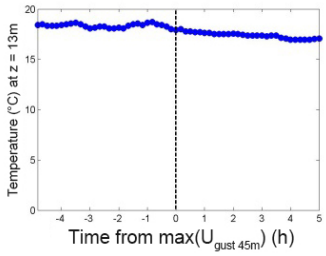
11 - Pintado 2008-04-24 to 2012-07-03. Event 19 with max($U_{gust\ 45m}$)= 25.6m/s on 2009-10-24 at 0:30. Series length: 48 months.

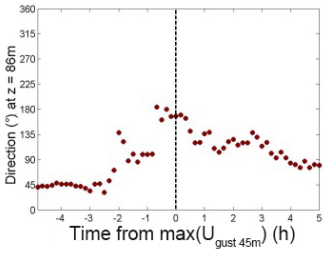


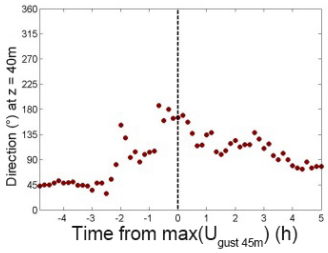
11 - Pintado 2008-04-24 to 2012-07-03. Event 20 with max($U_{gust\ 45m}$)= 25.5m/s on 2009-10-5 at 6:20. Series length: 48 months.

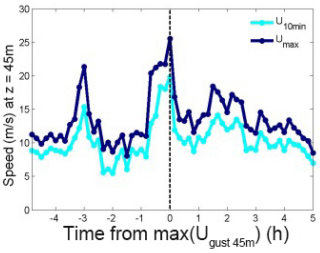




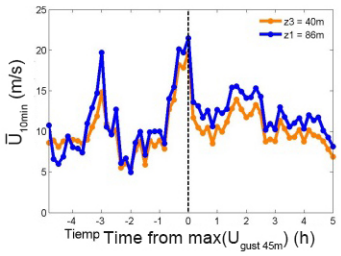


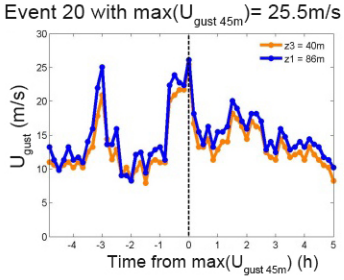


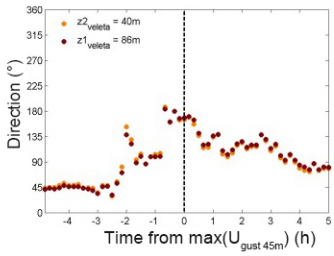


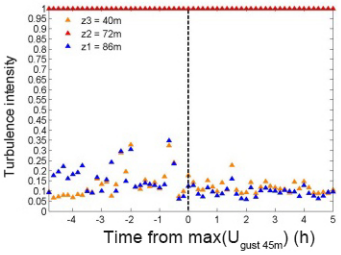


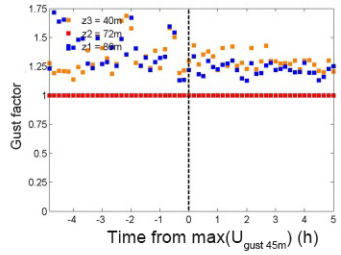
11 - Pintado 2008-04-24 to 2012-07-03. Event 20 with max($U_{gust\ 45m}$)= 25.5m/s on 2009-10-5 at 6:20. Series length: 48 months.

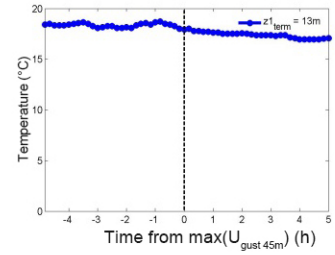


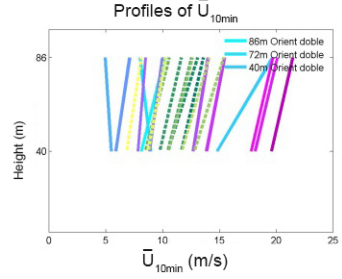


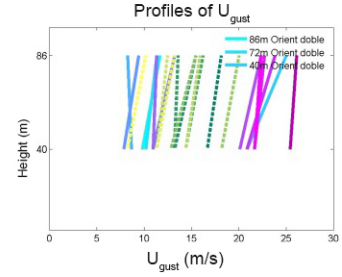


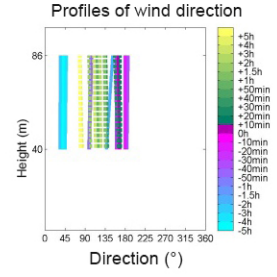




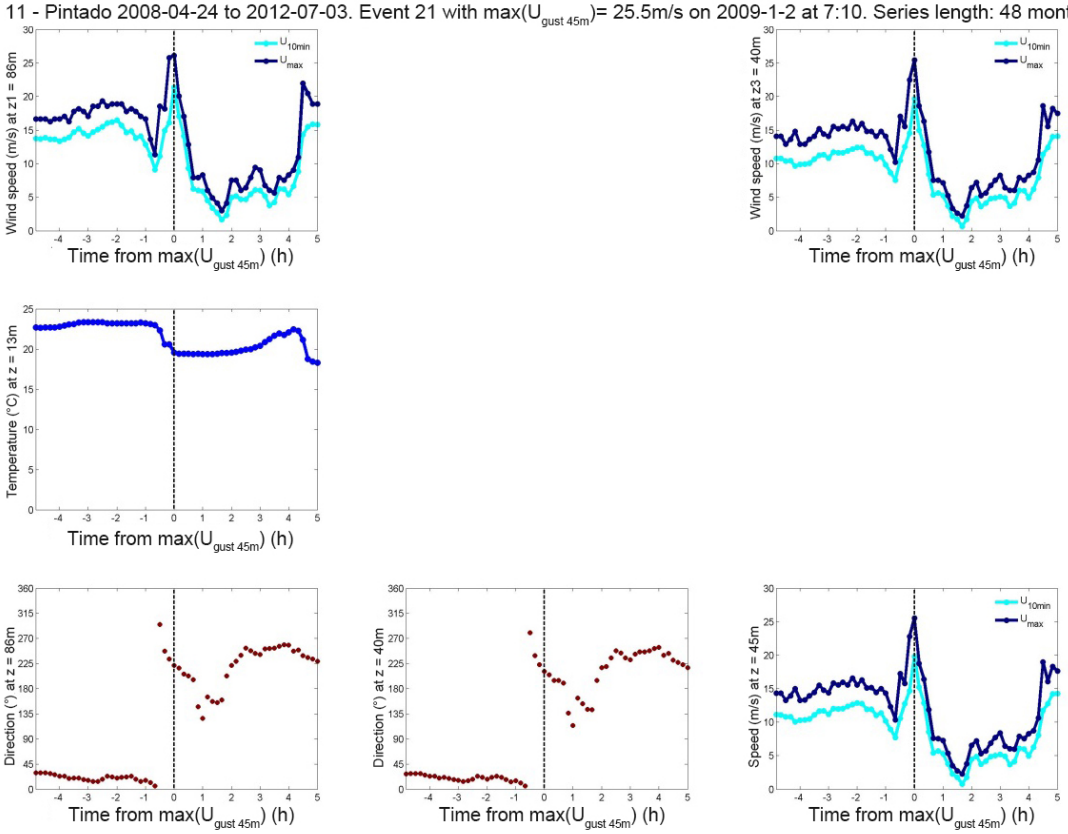




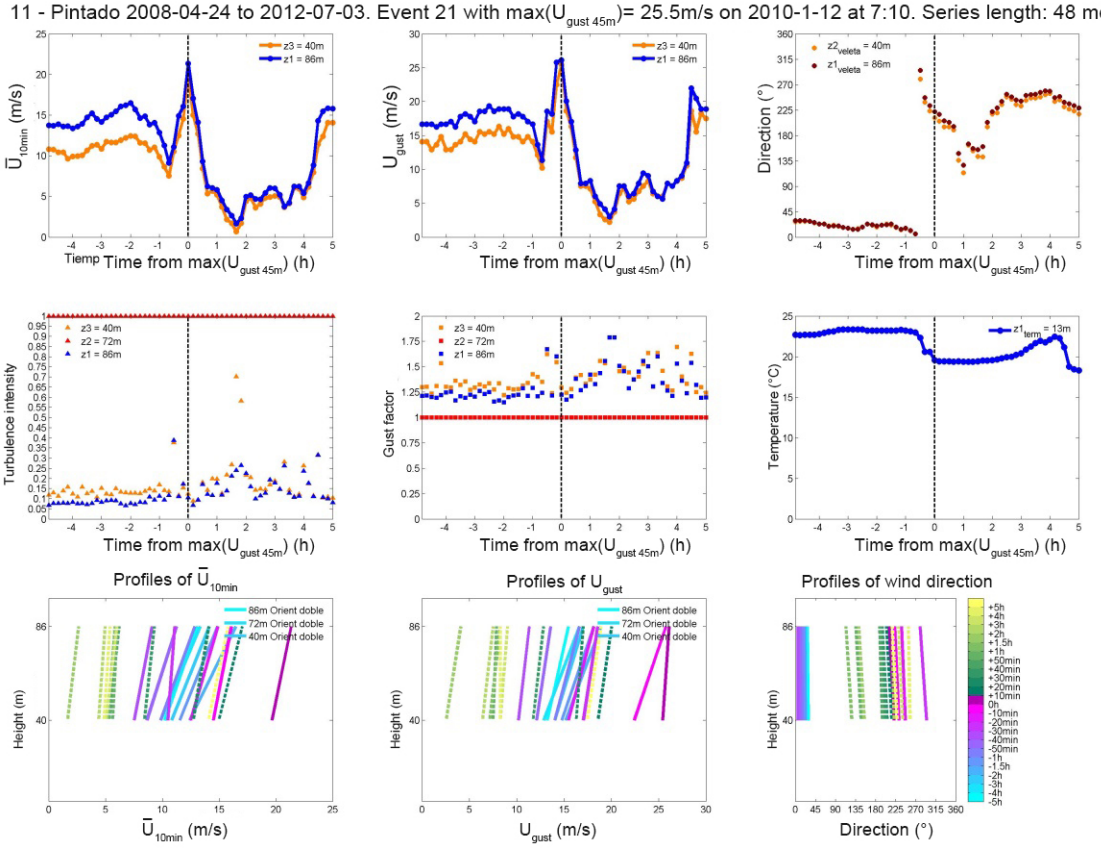




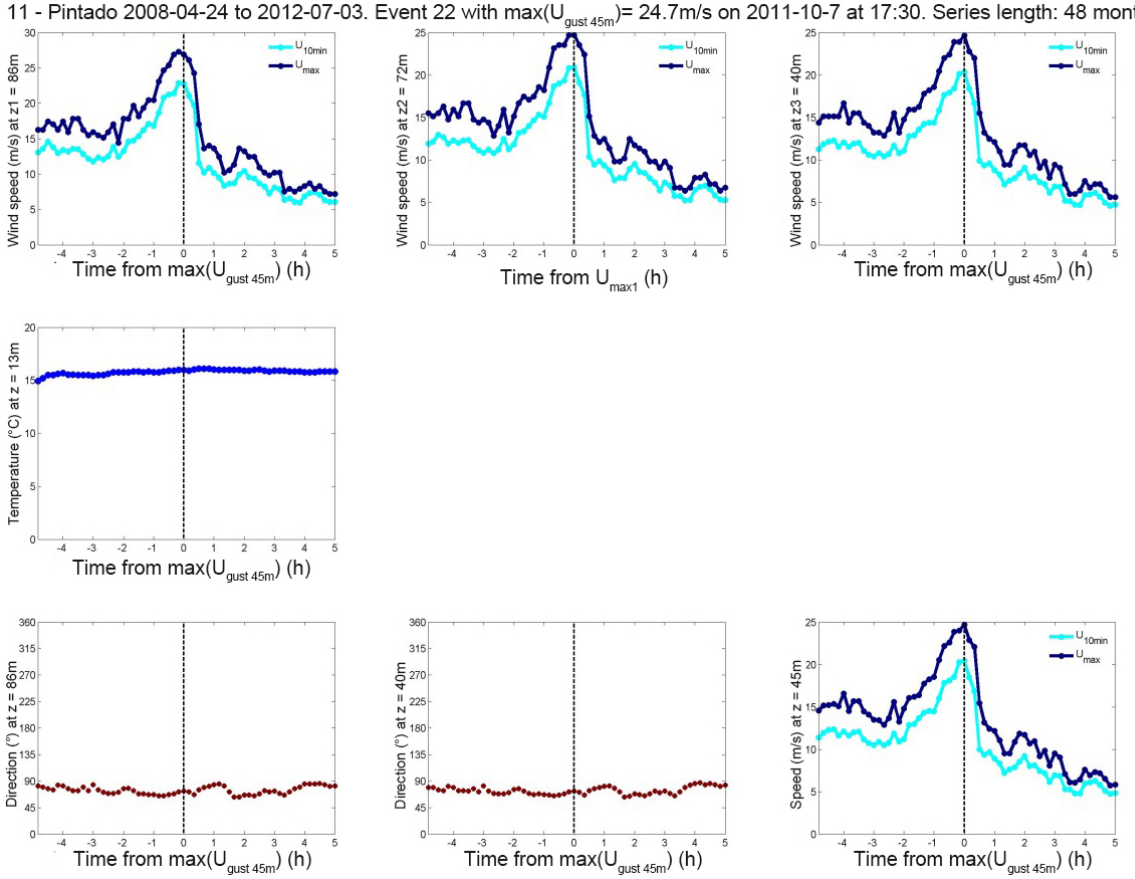
11 - Pintado 2008-04-24 to 2012-07-03. Event 21 with max($U_{gust\ 45m}$)= 25.5m/s on 2009-1-2 at 7:10. Series length: 48 months.



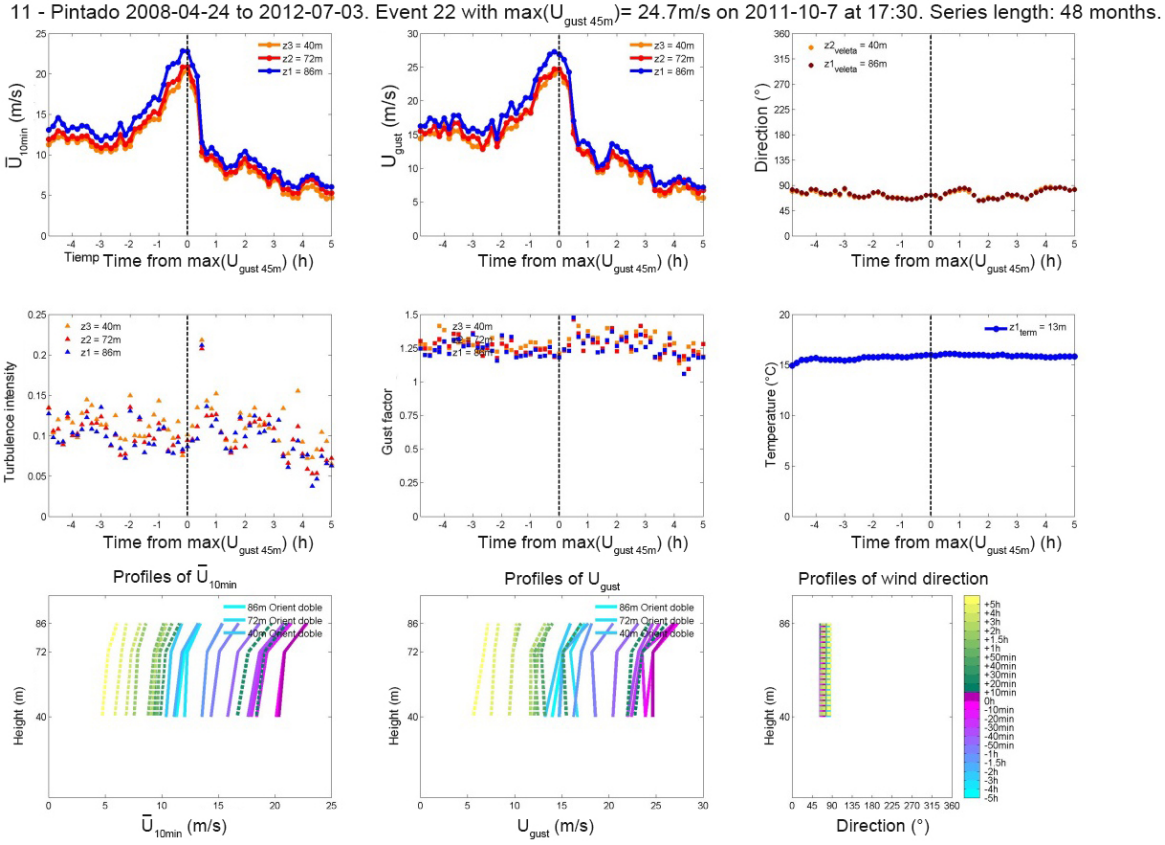
11 - Pintado 2008-04-24 to 2012-07-03. Event 21 with max($U_{gust\ 45m}$)= 25.5m/s on 2010-1-12 at 7:10. Series length: 48 months.



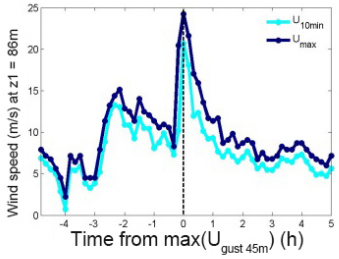
11 - Pintado 2008-04-24 to 2012-07-03. Event 22 with max($U_{gust\ 45m}$)= 24.7m/s on 2011-10-7 at 17:30. Series length: 48 months.

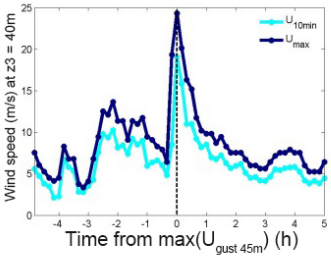


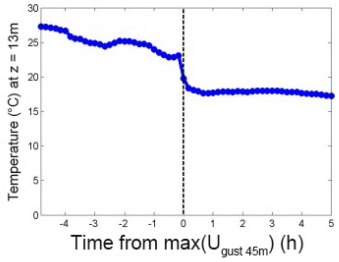
11 - Pintado 2008-04-24 to 2012-07-03. Event 22 with max($U_{gust\ 45m}$)= 24.7m/s on 2011-10-7 at 17:30. Series length: 48 months.

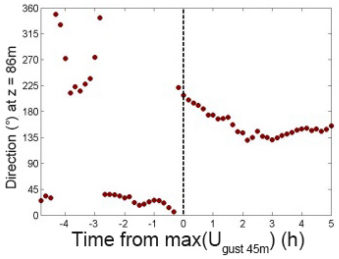


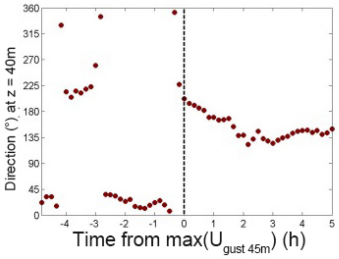
11 - Pintado 2008-04-24 to 2012-07-03. Event 23 with max($U_{gust\ 45m}$)= 24.3m/s on 2009-11-29 at 21:40. Series length: 48 months.

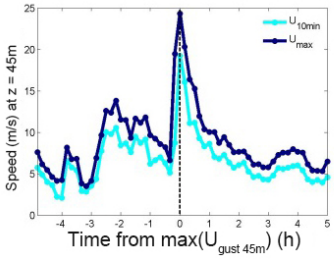




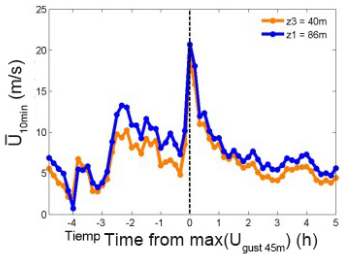


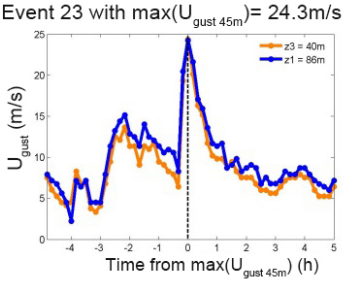


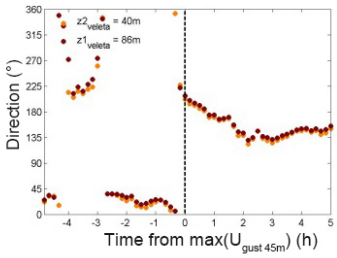


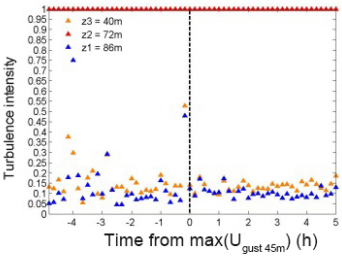


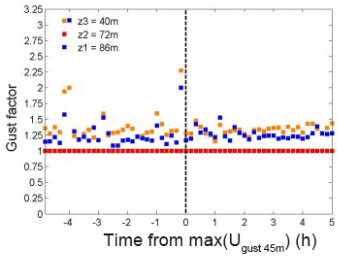
11 - Pintado 2008-04-24 to 2012-07-03. Event 23 with max($U_{gust\ 45m}$)= 24.3m/s on 2009-11-29 at 21:40. Series length: 48 months.

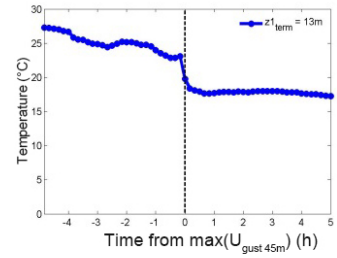


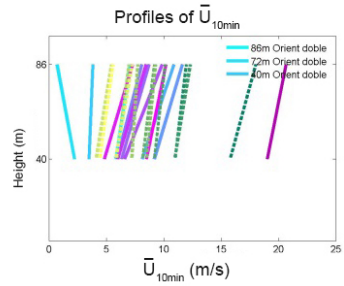


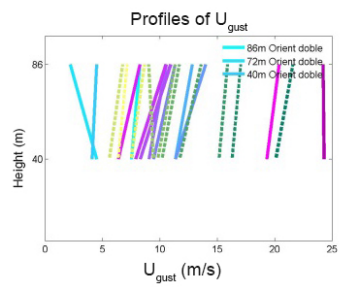


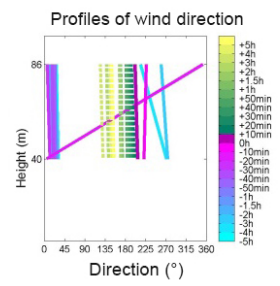




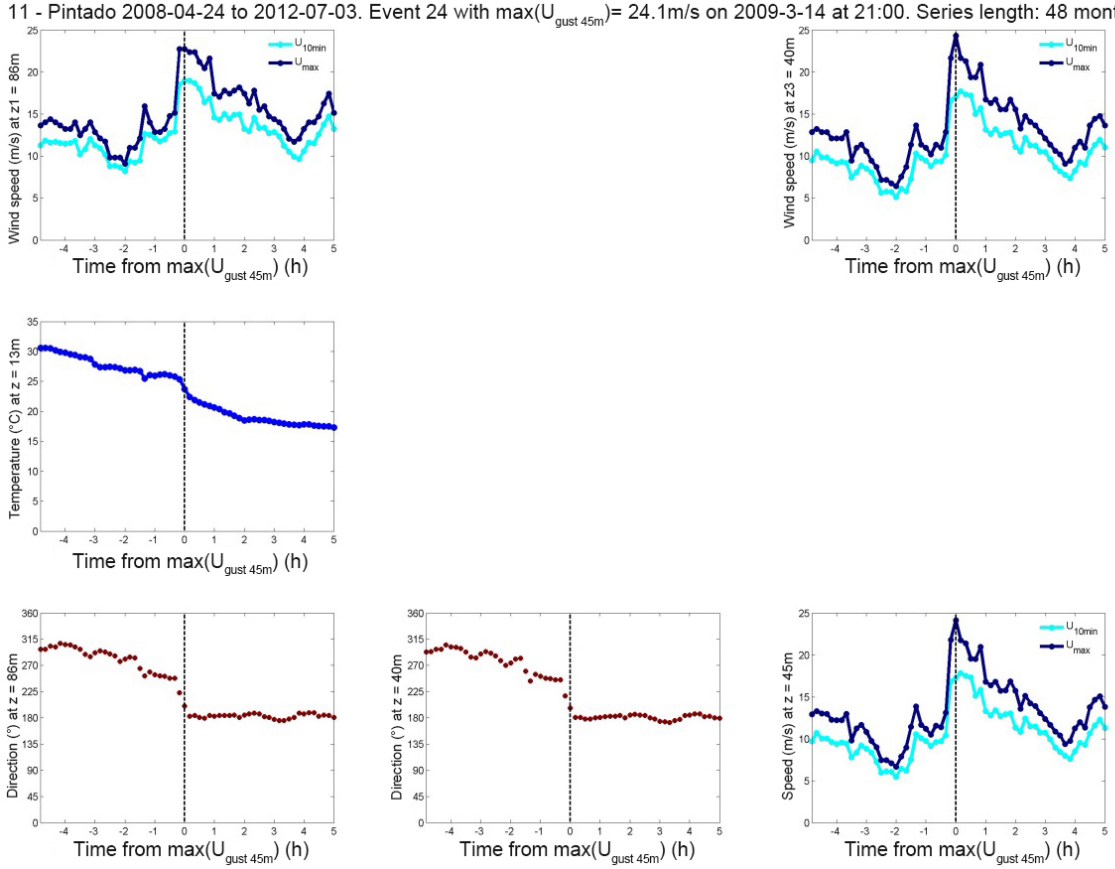




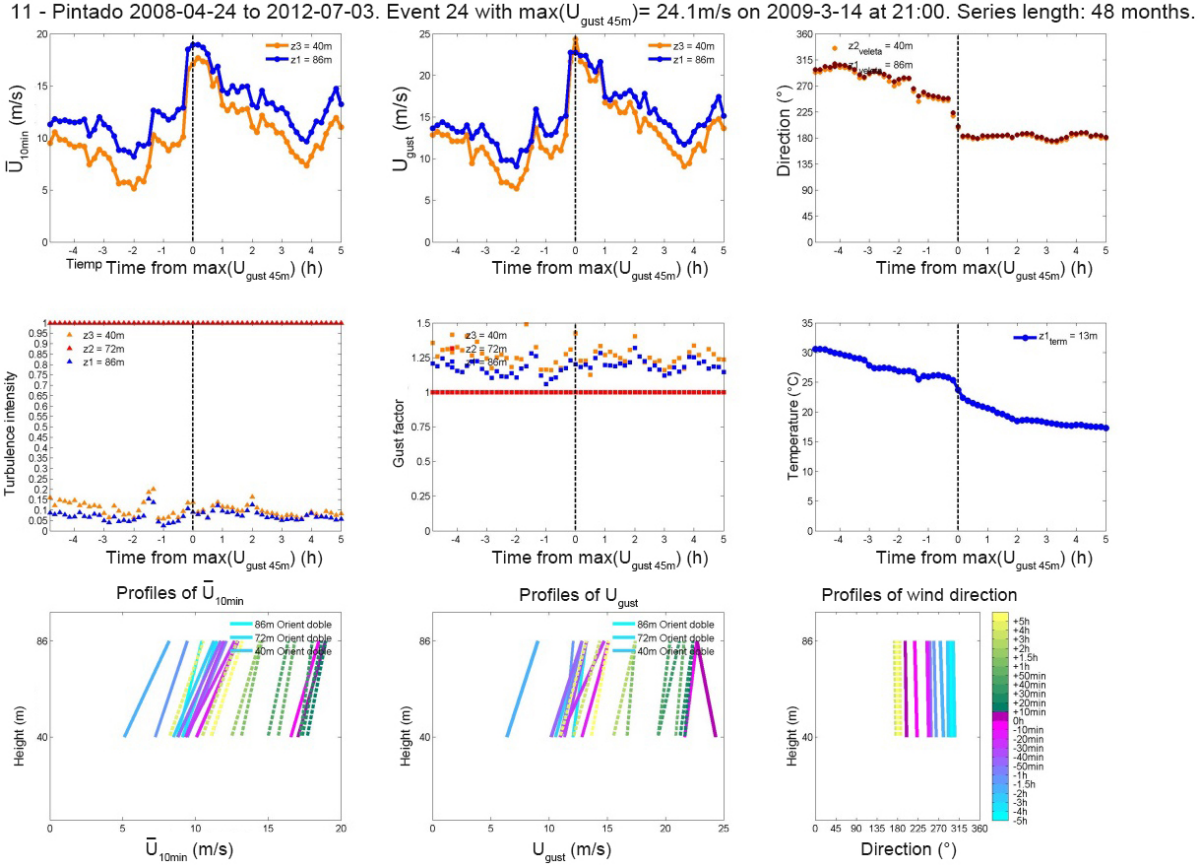




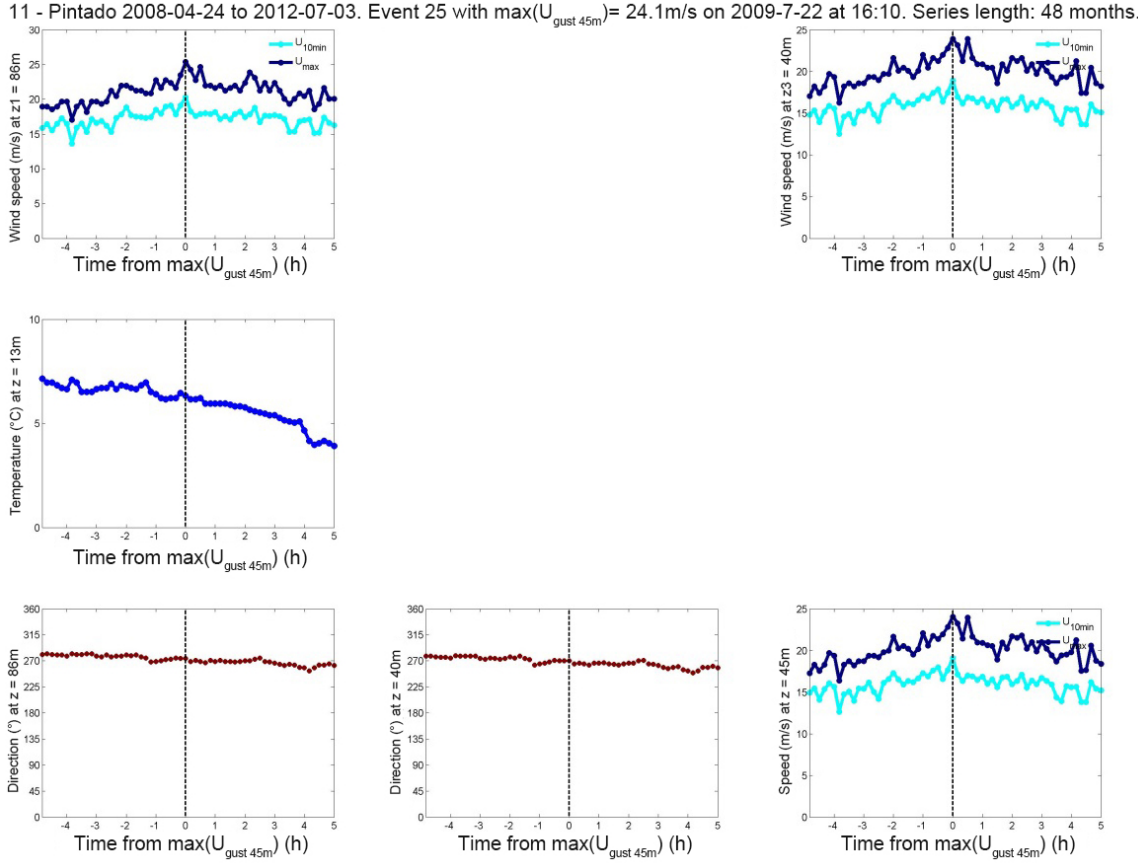
11 - Pintado 2008-04-24 to 2012-07-03. Event 24 with max($U_{gust\ 45m}$)= 24.1m/s on 2009-3-14 at 21:00. Series length: 48 months.



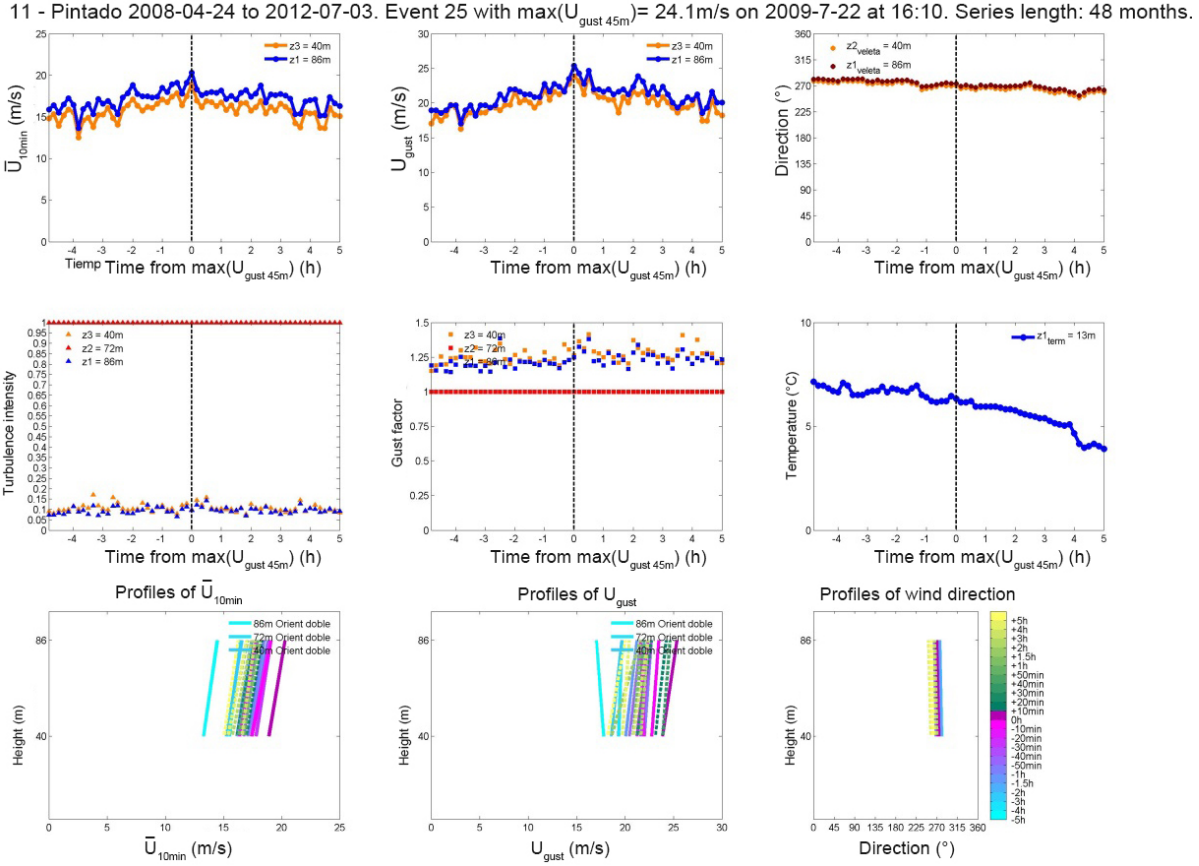
11 - Pintado 2008-04-24 to 2012-07-03. Event 24 with max($U_{gust\ 45m}$)= 24.1m/s on 2009-3-14 at 21:00. Series length: 48 months.



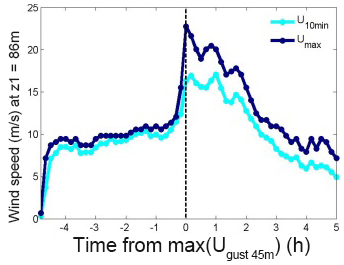
11 - Pintado 2008-04-24 to 2012-07-03. Event 25 with max($U_{gust\ 45m}$)= 24.1m/s on 2009-7-22 at 16:10. Series length: 48 months.

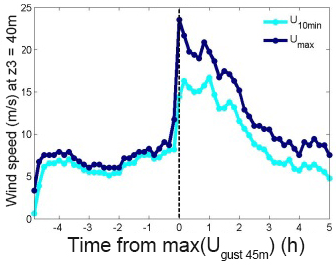


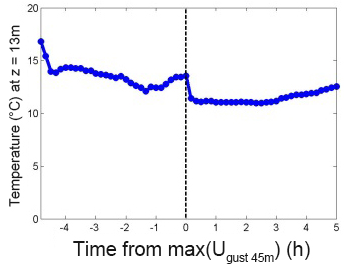
11 - Pintado 2008-04-24 to 2012-07-03. Event 25 with max($U_{gust\ 45m}$)= 24.1m/s on 2009-7-22 at 16:10. Series length: 48 months.

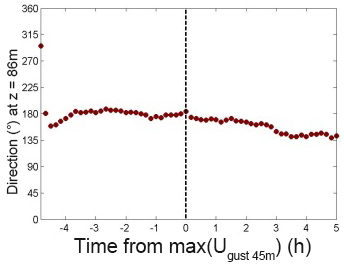


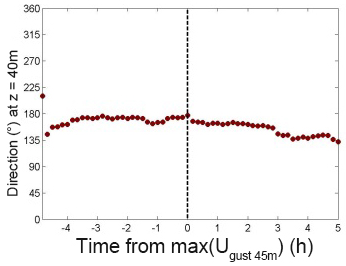
11 - Pintado 2008-04-24 to 2012-07-03. Event 26 with max($U_{gust\ 45m}$)= 23.5m/s on 2010-8-29 at 5:10. Series length: 48 months.

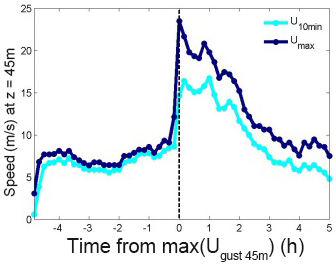




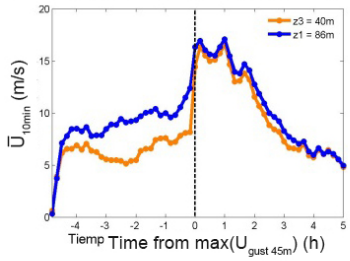


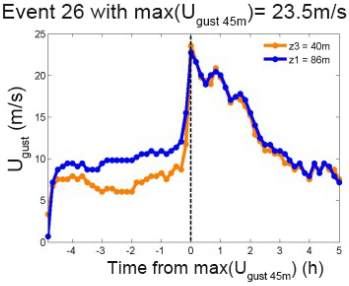


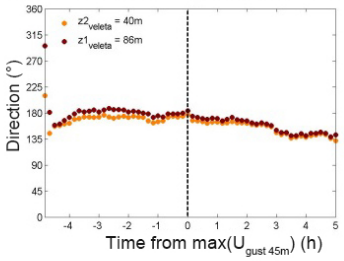


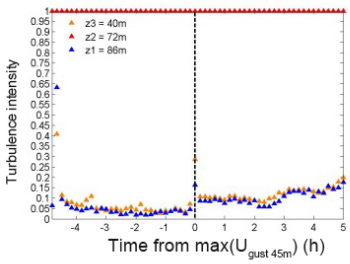


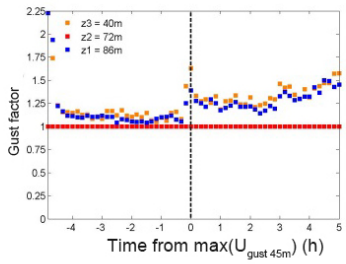
11 - Pintado 2008-04-24 to 2012-07-03. Event 26 with max($U_{gust\ 45m}$)= 23.5m/s on 2010-8-29 at 5:10. Series length: 48 months.

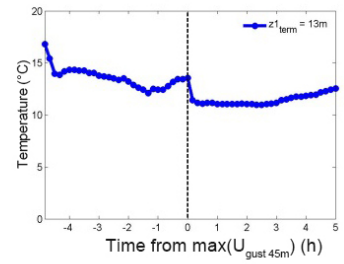




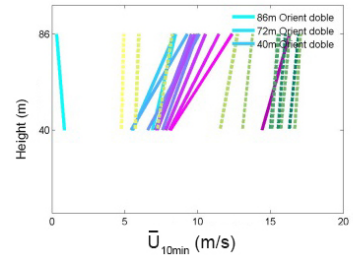




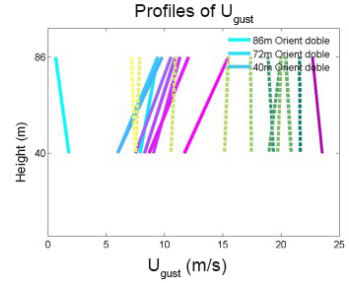




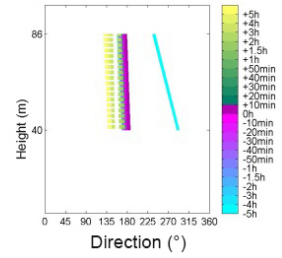
Profiles of $\bar{U}_{10min}$

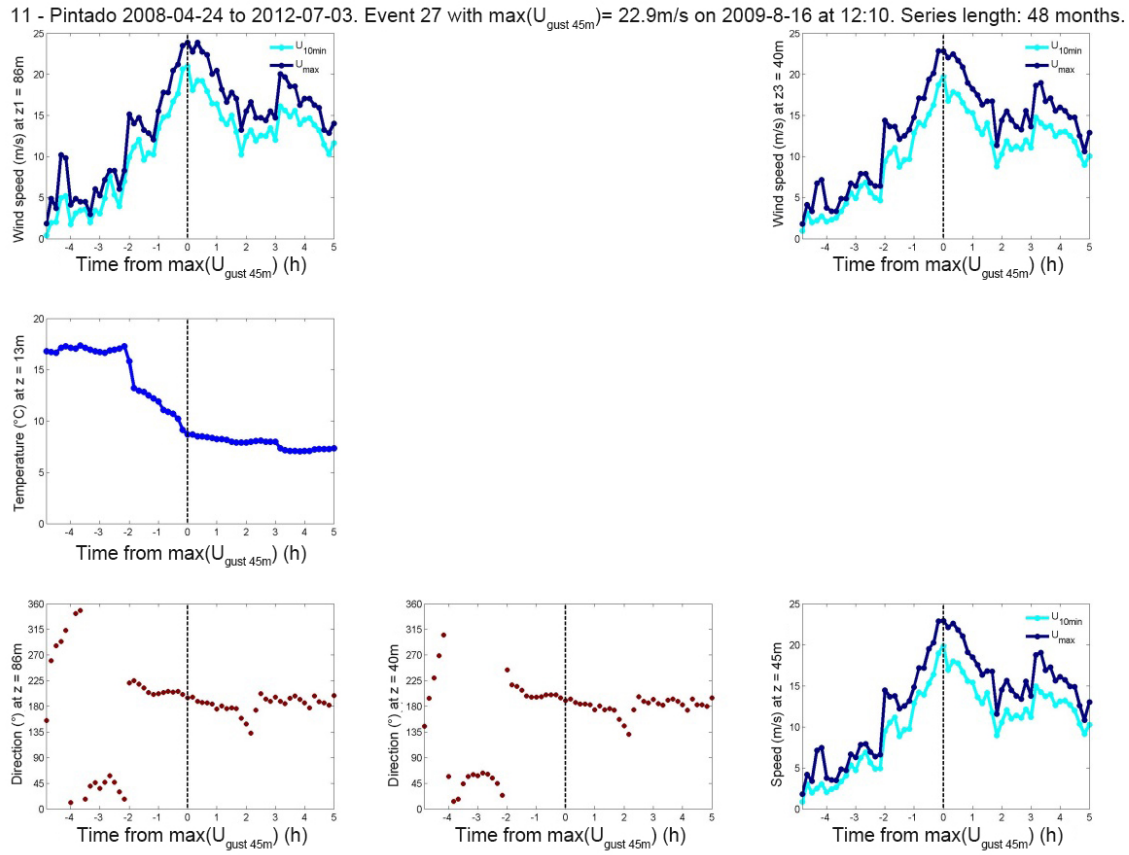


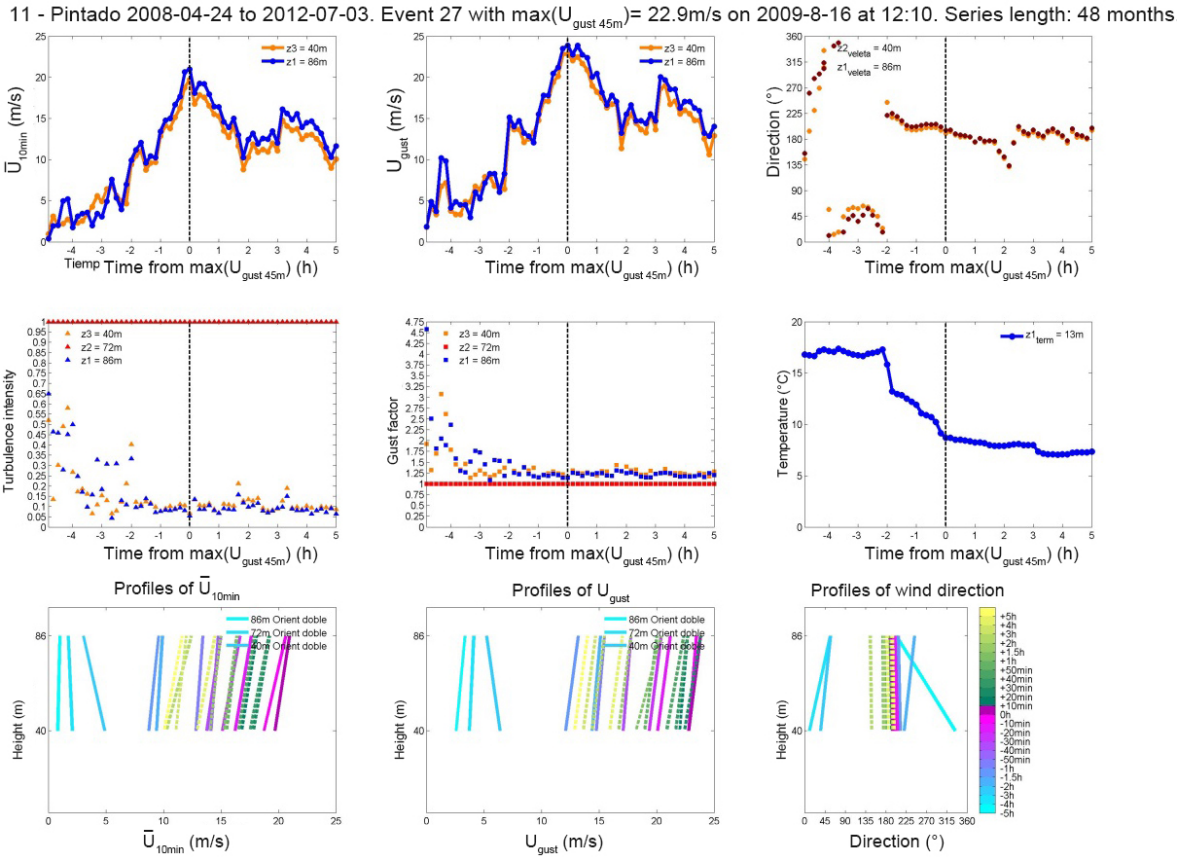
Profiles of U_{gust}



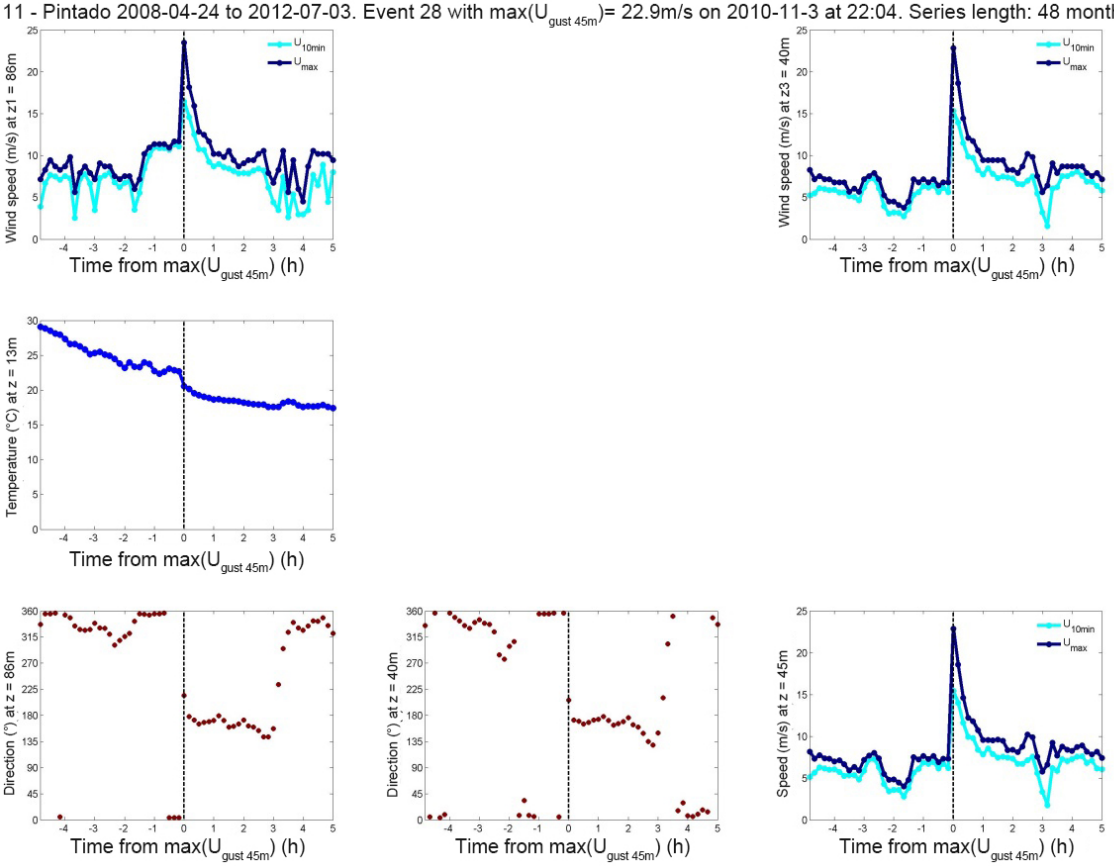
Profiles of wind direction



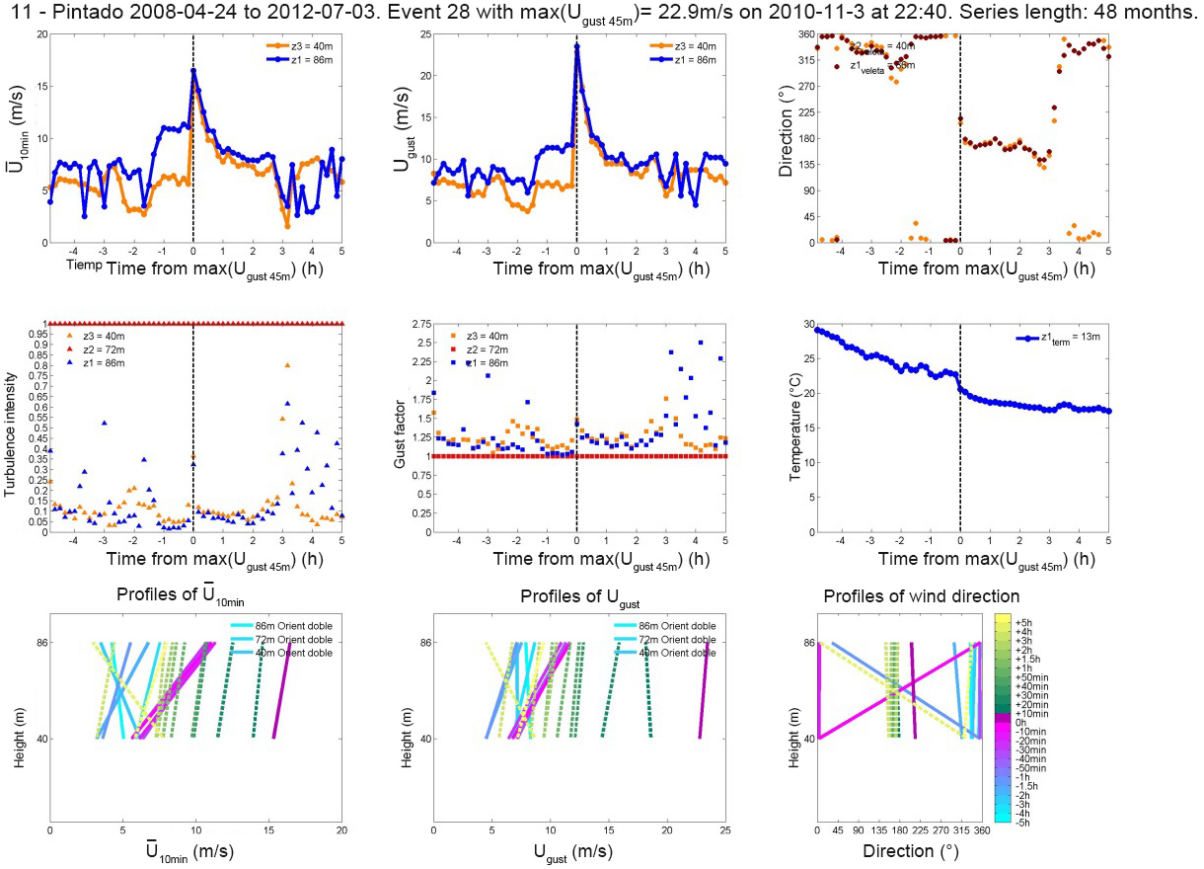

11 - Pintado 2008-04-24 to 2012-07-03. Event 27 with max(U gust 45m)= 22.9m/s on 2009-8-16 at 12:10. Series length: 48 months.
Wind speed (m/s) at z1 = 86m
Wind speed (m/s) at z3 = 40m
Temperature (°C) at z = 13m
Direction (°) at z = 86m
Direction (°) at z = 40m
Speed (m/s) at z = 45m
U 10min
U max
Time from max(U gust 45m) (h)

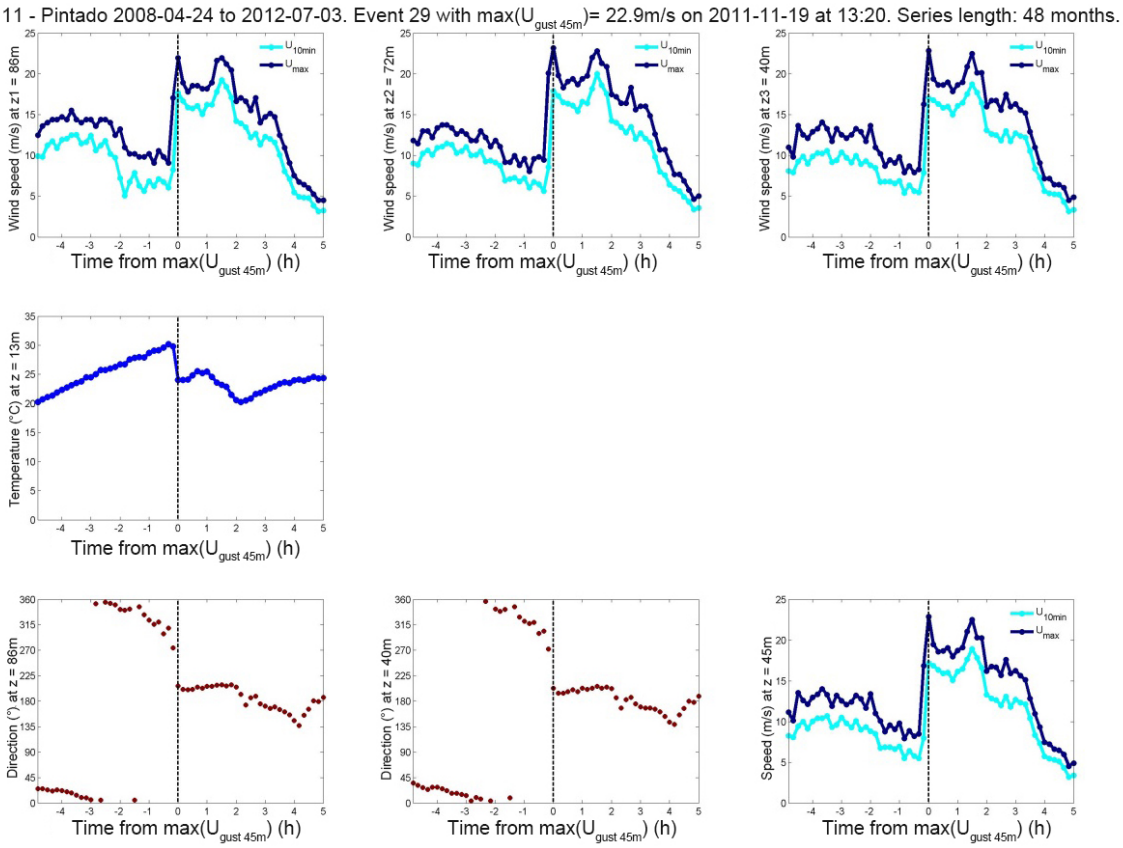

11 - Pintado 2008-04-24 to 2012-07-03. Event 27 with max(U gust 45m)= 22.9m/s on 2009-8-16 at 12:10. Series length: 48 months
z3 = 40m
z1 = 86m
z2 = 72m
Tiemp
Direction (°)
Turbulence intensity
Gust factor
Temperature (°C)
Profiles of U 10min
Profiles of U gust
Profiles of wind direction
Height (m)
86m Orient doble
72m Orient doble
40m Orient doble
Time from max(U gust 45m) (h)

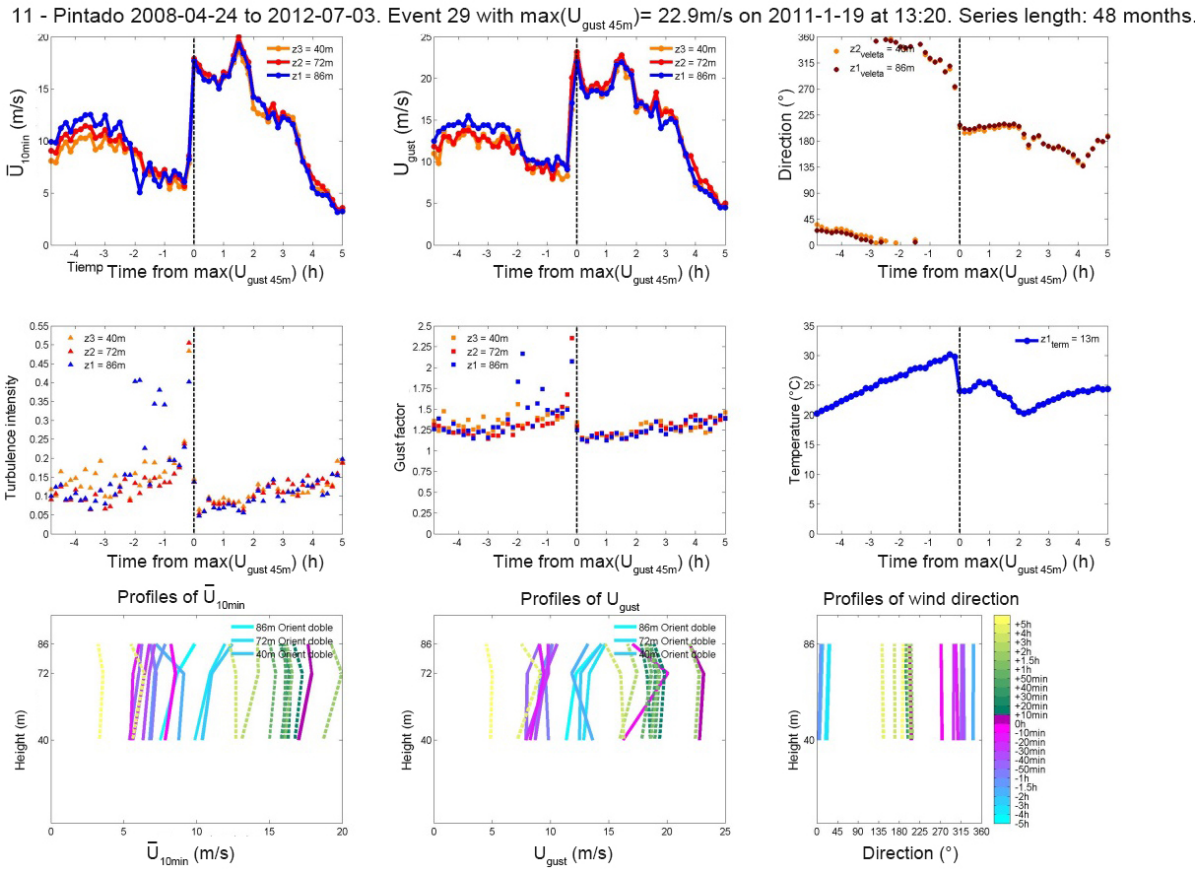
11 - Pintado 2008-04-24 to 2012-07-03. Event 28 with max($U_{gust\ 45m}$)= 22.9m/s on 2010-11-3 at 22:04. Series length: 48 months.



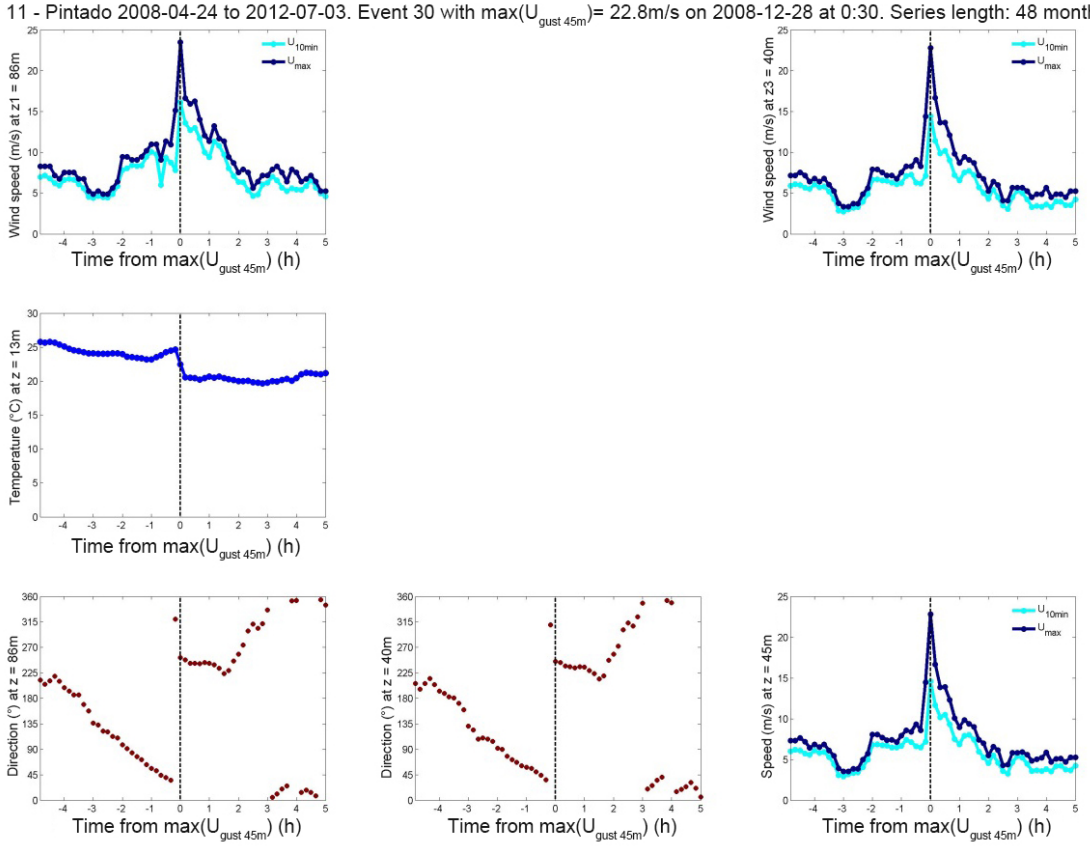
11 - Pintado 2008-04-24 to 2012-07-03. Event 28 with max($U_{gust\ 45m}$)= 22.9m/s on 2010-11-3 at 22:40. Series length: 48 months.



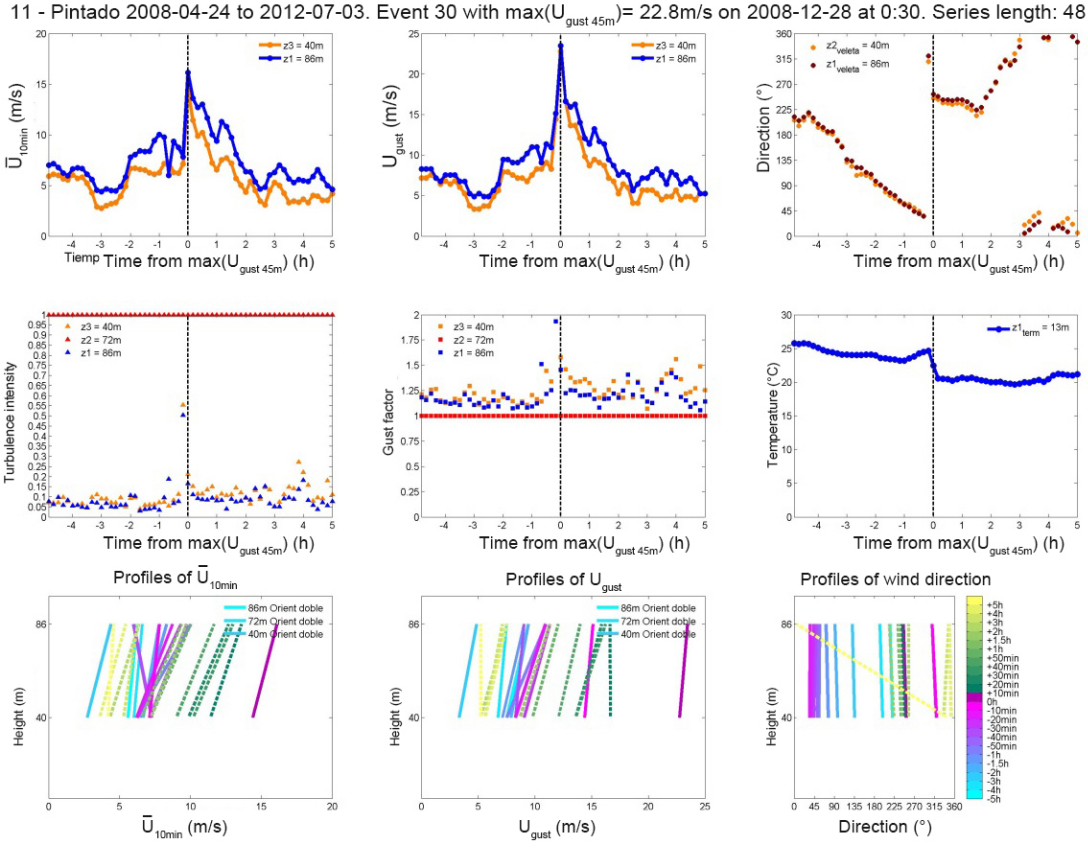

11 - Pintado 2008-04-24 to 2012-07-03. Event 29 with max(U gust 45m)= 22.9m/s on 2011-11-19 at 13:20. Series length: 48 months.
Wind speed (m/s) at z1 = 86m
Wind speed (m/s) at z2 = 72m
Wind speed (m/s) at z3 = 40m
U10min
Umax
Time from max(U gust 45m) (h)
Temperature (°C) at z = 13m
Direction (°) at z = 86m
Direction (°) at z = 40m
Speed (m/s) at z = 45m


11 - Pintado 2008-04-24 to 2012-07-03. Event 29 with max(U gust 45m)= 22.9m/s on 2011-1-19 at 13:20. Series length: 48 months.
z3 = 40m
z2 = 72m
z1 = 86m
Time from max(U gust 45m) (h)
Direction (°)
Turbulence intensity
Gust factor
Temperature (°C)
Profiles of U10min
Profiles of U gust
Profiles of wind direction
Height (m)
U10min (m/s)
U gust (m/s)
Direction (°)

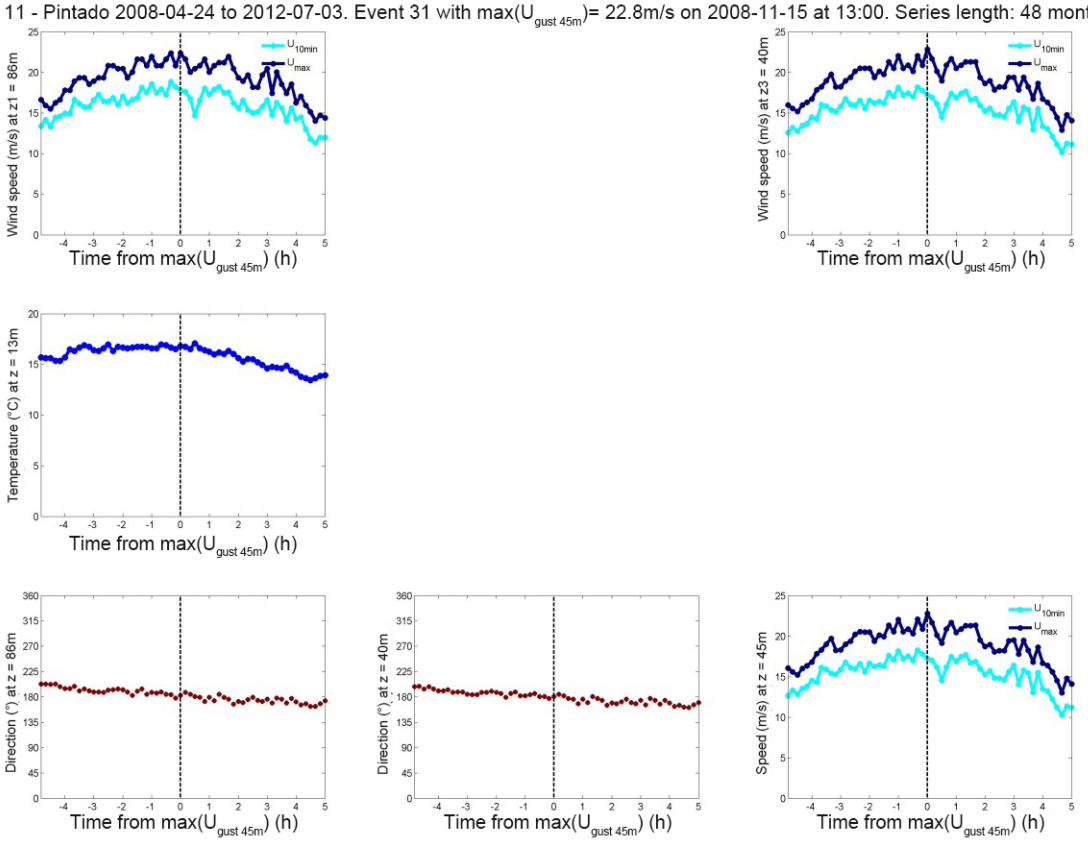
11 - Pintado 2008-04-24 to 2012-07-03. Event 30 with max($U_{gust\ 45m}$)= 22.8m/s on 2008-12-28 at 0:30. Series length: 48 months.



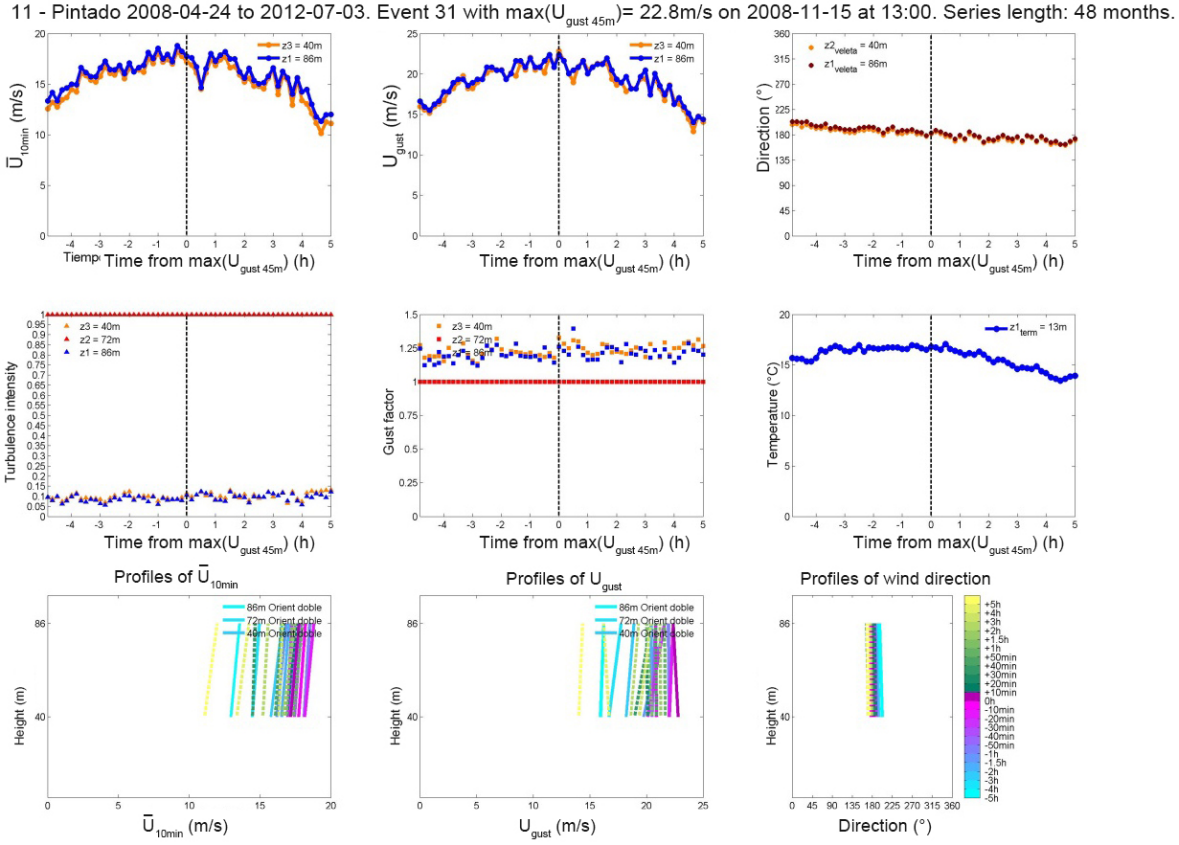
11 - Pintado 2008-04-24 to 2012-07-03. Event 30 with max($U_{gust\ 45m}$)= 22.8m/s on 2008-12-28 at 0:30. Series length: 48 months.

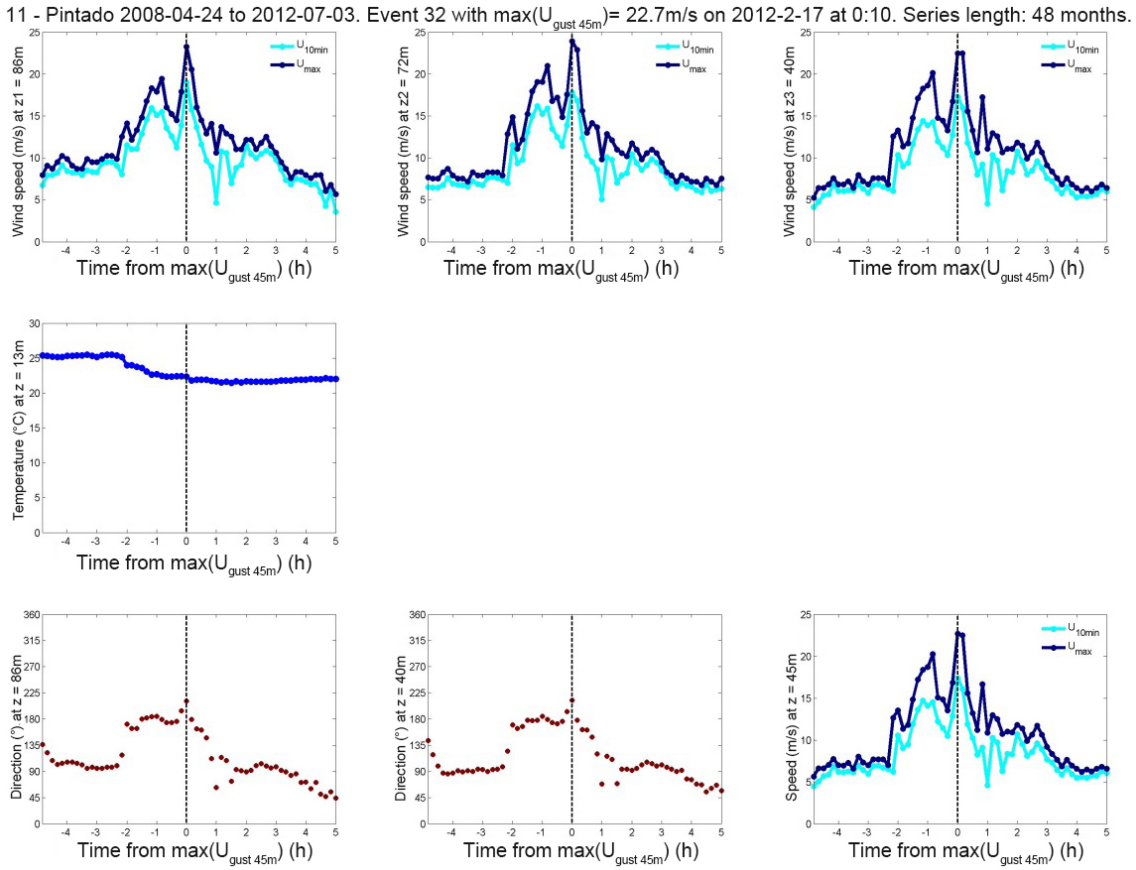


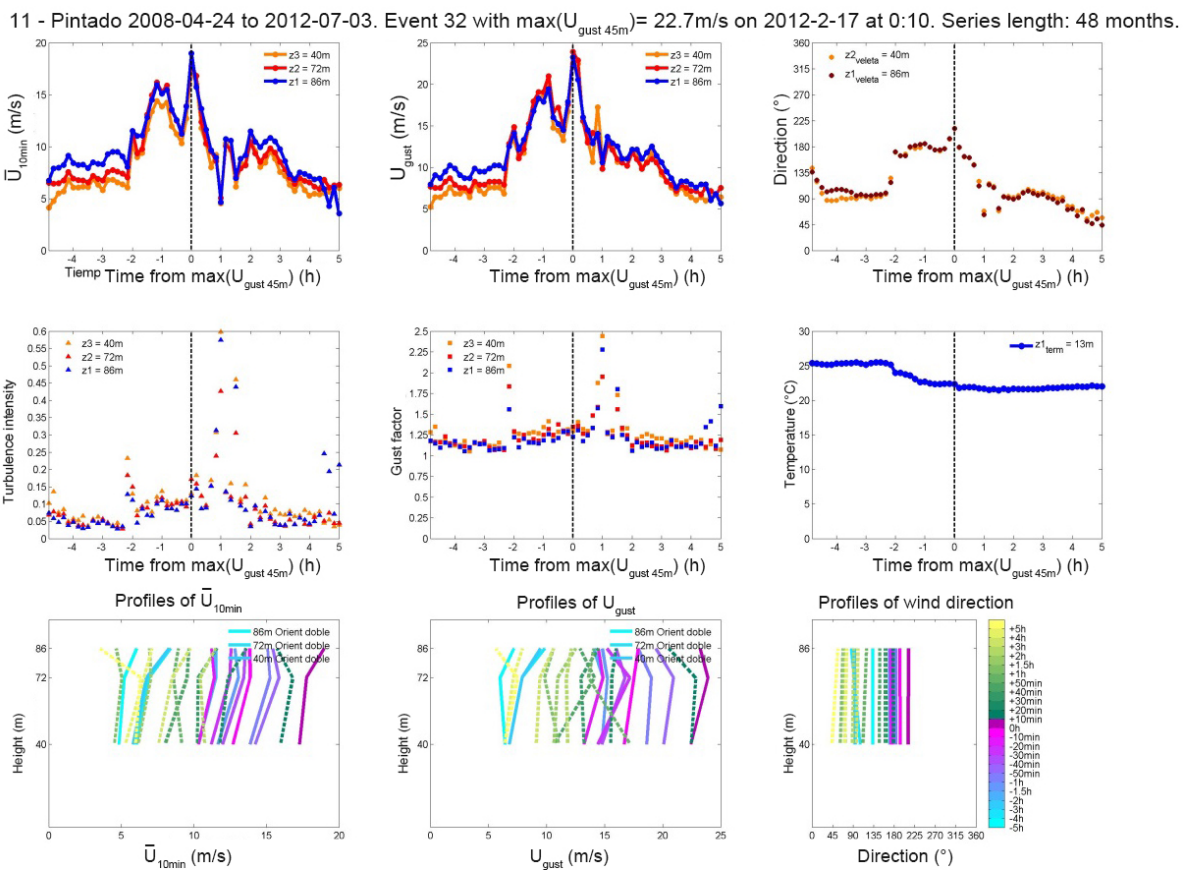
11 - Pintado 2008-04-24 to 2012-07-03. Event 31 with max($U_{gust\ 45m}$)= 22.8m/s on 2008-11-15 at 13:00. Series length: 48 months.

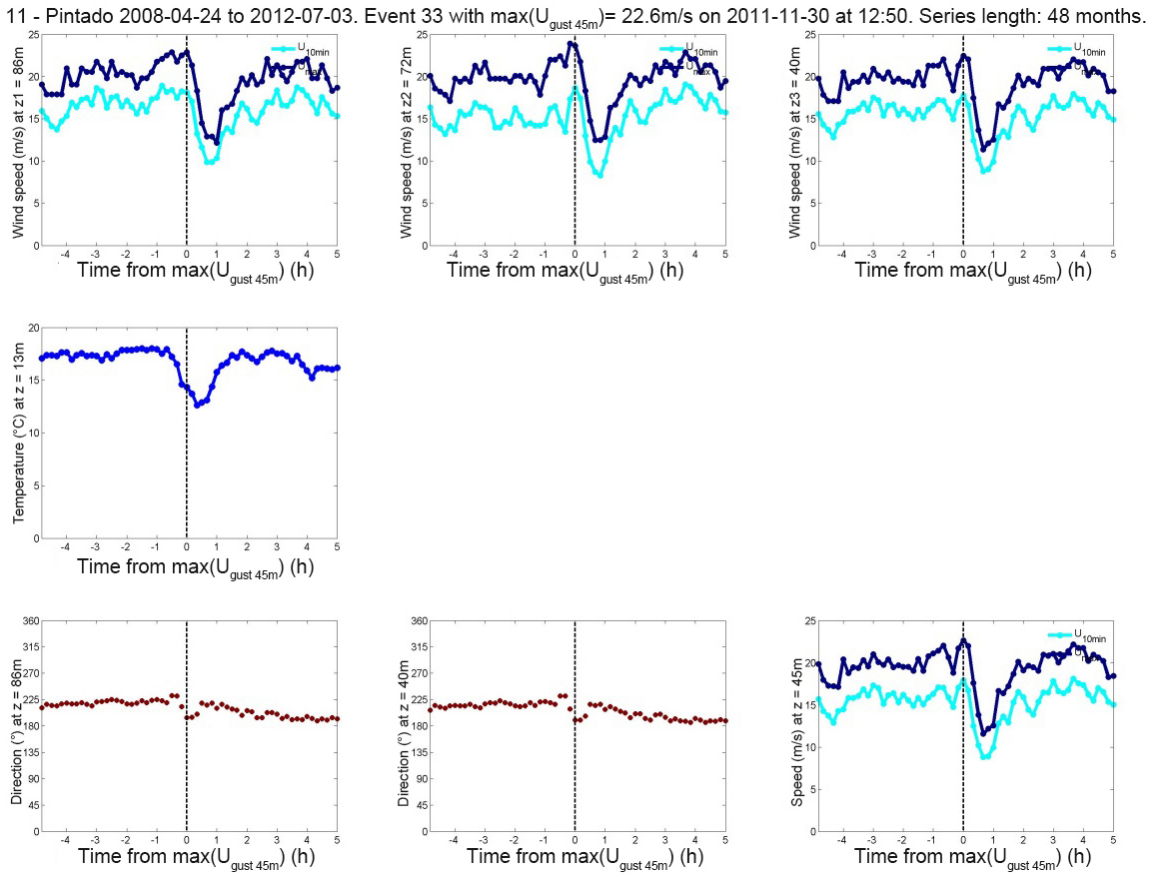


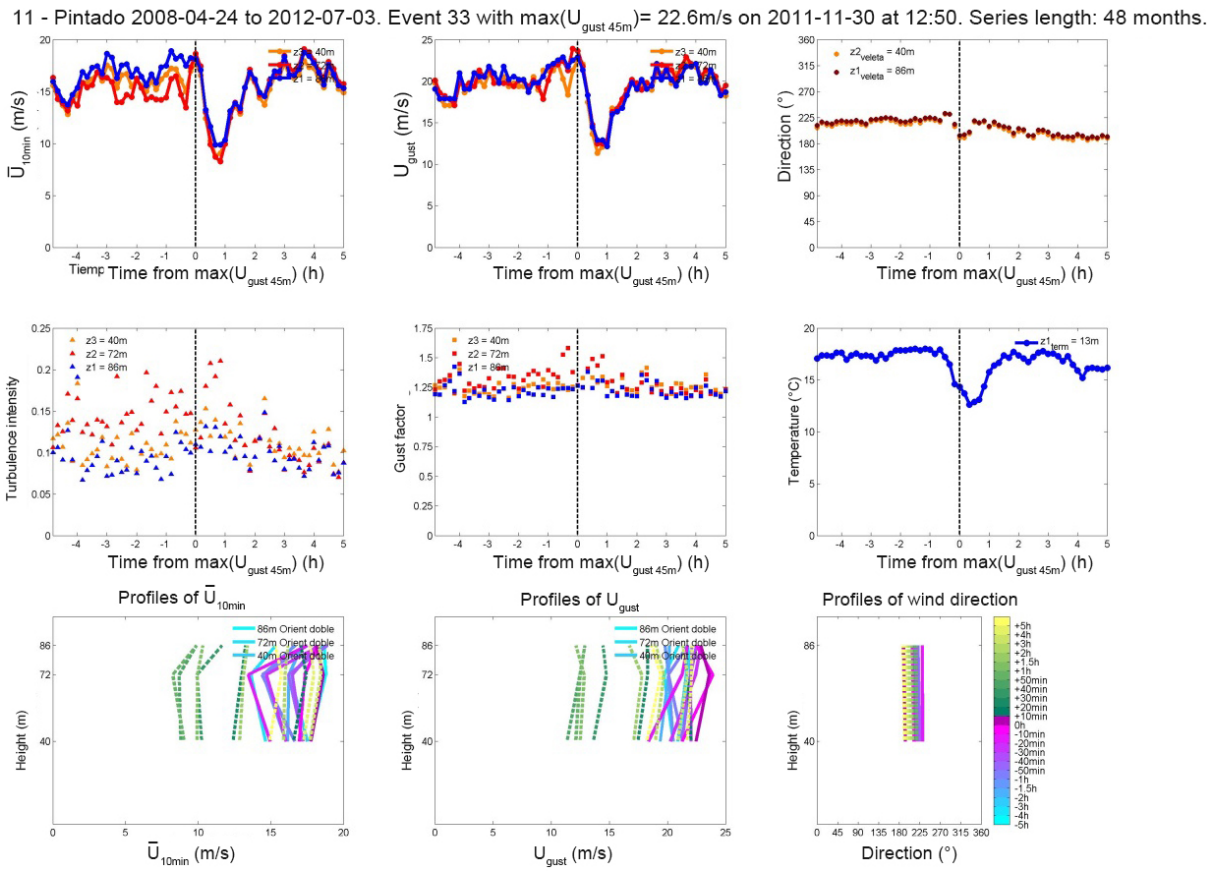
11 - Pintado 2008-04-24 to 2012-07-03. Event 31 with max($U_{gust\ 45m}$)= 22.8m/s on 2008-11-15 at 13:00. Series length: 48 months.

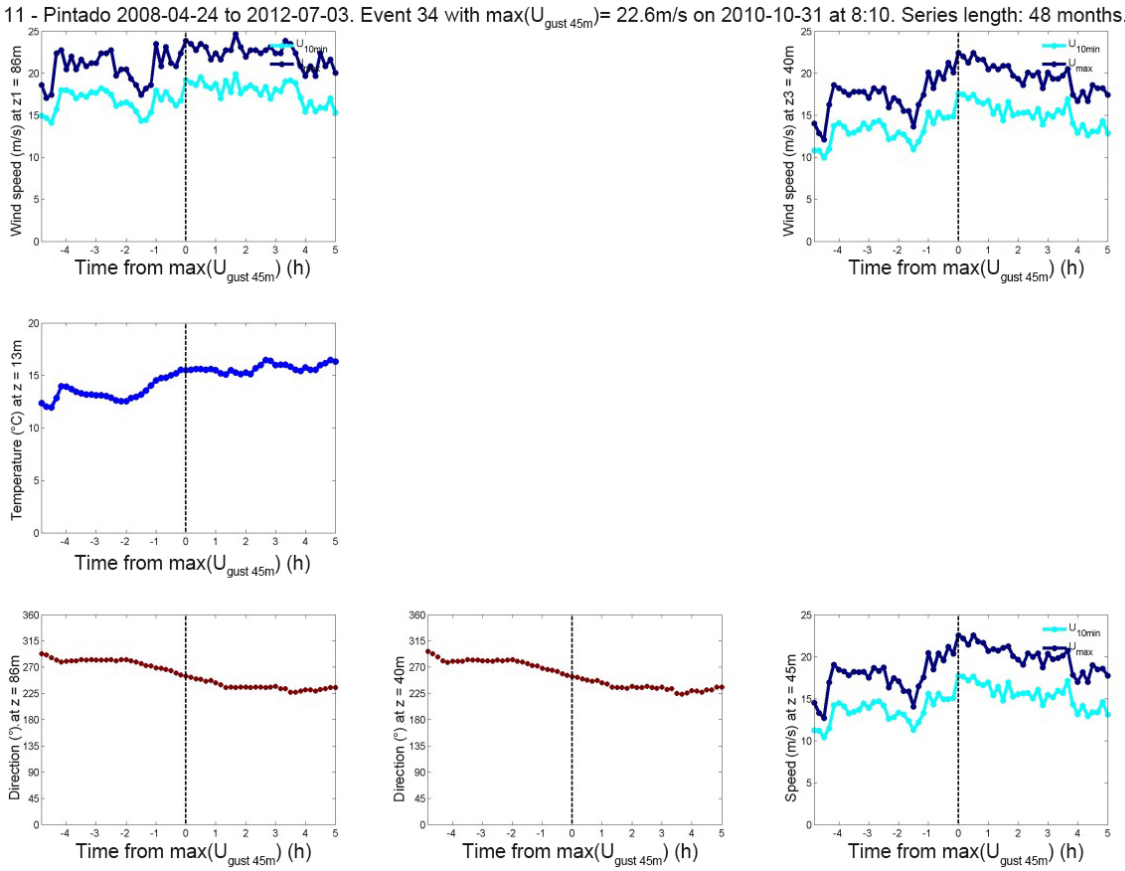


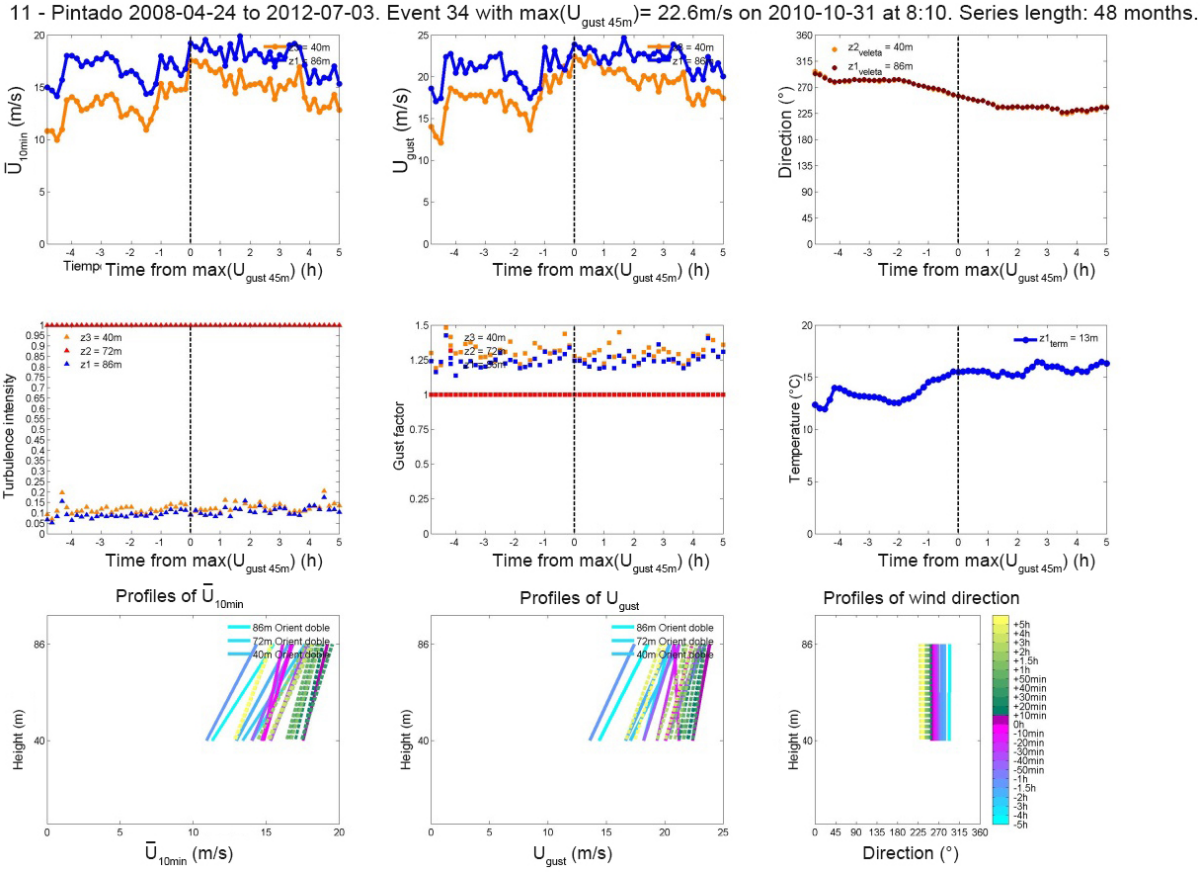

11 - Pintado 2008-04-24 to 2012-07-03. Event 32 with max(U gust 45m)= 22.7m/s on 2012-2-17 at 0:10. Series length: 48 months.
Wind speed (m/s) at z1 = 86m
Wind speed (m/s) at z2 = 72m
Wind speed (m/s) at z3 = 40m
U10min
Umax
Temperature (°C) at z = 13m
Direction (°) at z = 86m
Direction (°) at z = 40m
Speed (m/s) at z = 45m
Time from max(U gust 45m) (h)


11 - Pintado 2008-04-24 to 2012-07-03. Event 32 with max(U gust 45m)= 22.7m/s on 2012-2-17 at 0:10. Series length: 48 months.
z3 = 40m
z2 = 72m
z1 = 86m
Turbulence intensity
Gust factor
Direction (°)
Temperature (°C)
Time from max(U gust 45m) (h)
Profiles of U10min
Profiles of Ugust
Profiles of wind direction
Height (m)
86m Orient doble
72m Orient doble
40m Orient doble
U10min (m/s)
Ugust (m/s)
Direction (°)

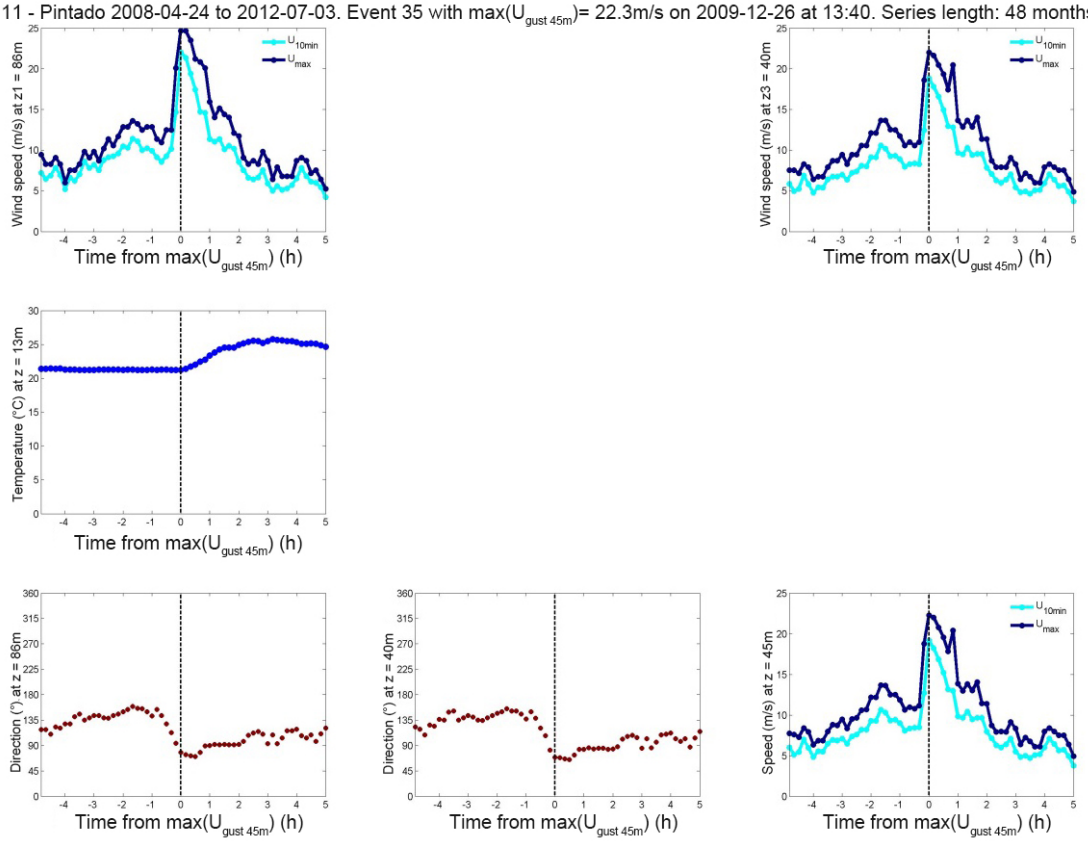

11 - Pintado 2008-04-24 to 2012-07-03. Event 33 with max(U gust 45m)= 22.6m/s on 2011-11-30 at 12:50. Series length: 48 months.
Wind speed (m/s) at z1 = 86m
Wind speed (m/s) at z2 = 72m
Wind speed (m/s) at z3 = 40m
Temperature (°C) at z = 13m
Direction (°) at z = 86m
Direction (°) at z = 40m
Speed (m/s) at z = 45m
Time from max(U gust 45m) (h)


11 - Pintado 2008-04-24 to 2012-07-03. Event 33 with max(U gust 45m)= 22.6m/s on 2011-11-30 at 12:50. Series length: 48 months.
Ū 10min (m/s)
U gust (m/s)
Direction (°)
Turbulence intensity
Gust factor
Temperature (°C)
Time from max(U gust 45m) (h)
Profiles of Ū 10min
Profiles of U gust
Profiles of wind direction
Height (m)
Ū 10min (m/s)
U gust (m/s)
Direction (°)

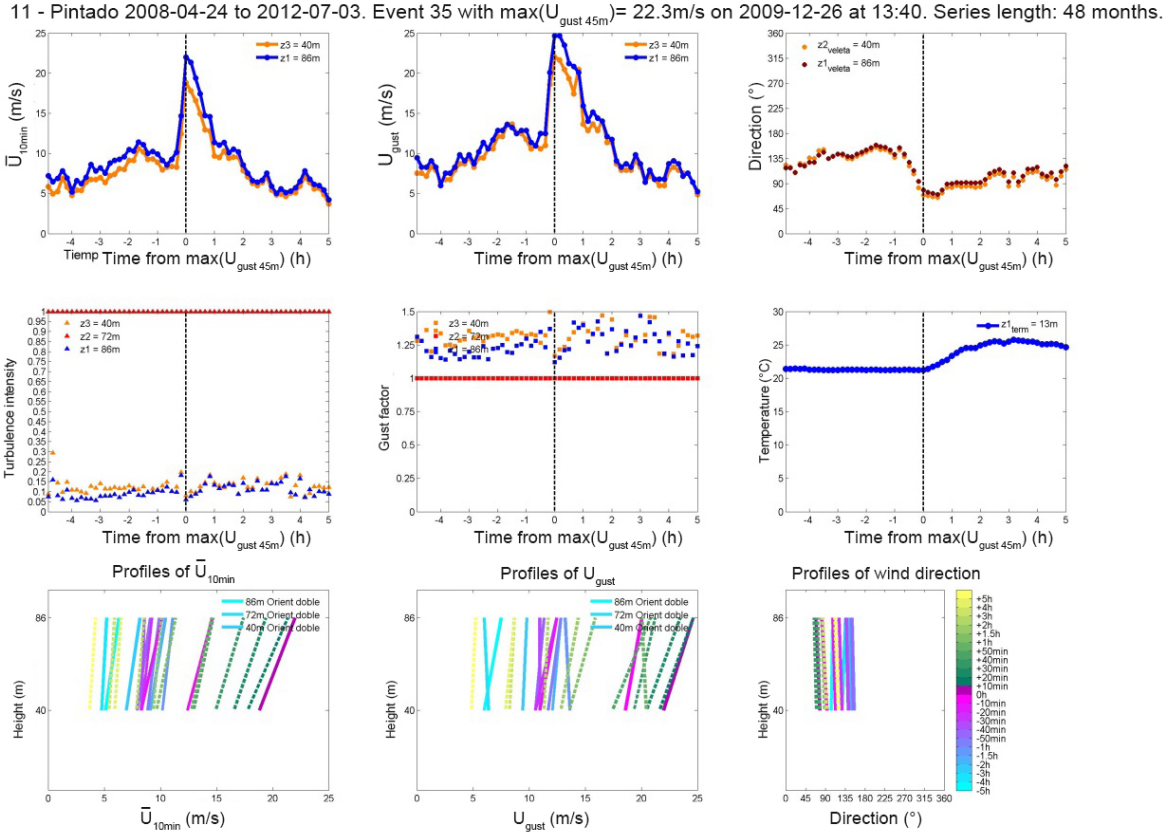

11 - Pintado 2008-04-24 to 2012-07-03. Event 34 with max(U gust 45m)= 22.6m/s on 2010-10-31 at 8:10. Series length: 48 months.
Wind speed (m/s) at z1 = 86m
Wind speed (m/s) at z3 = 40m
Temperature (°C) at z = 13m
Direction (°) at z = 86m
Direction (°) at z = 40m
Speed (m/s) at z = 45m
Time from max(U gust 45m) (h)


11 - Pintado 2008-04-24 to 2012-07-03. Event 34 with max(U gust 45m)= 22.6m/s on 2010-10-31 at 8:10. Series length: 48 months.
Direction (°)
Turbulence intensity
Gust factor
Temperature (°C)
Time from max(U gust 45m) (h)
Profiles of U 10min
Profiles of U gust
Profiles of wind direction
Height (m)

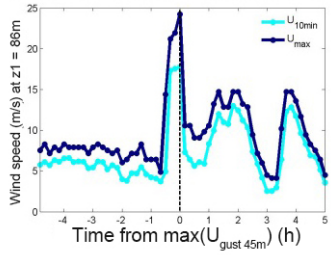
11 - Pintado 2008-04-24 to 2012-07-03. Event 35 with max($U_{gust\ 45m}$)= 22.3m/s on 2009-12-26 at 13:40. Series length: 48 months.

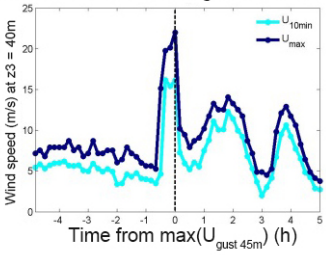


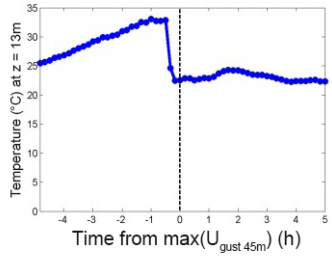
11 - Pintado 2008-04-24 to 2012-07-03. Event 35 with max($U_{gust\ 45m}$)= 22.3m/s on 2009-12-26 at 13:40. Series length: 48 months.

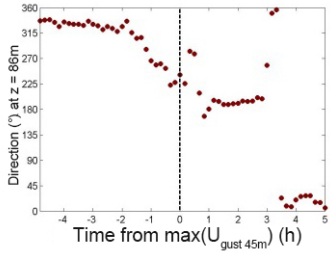


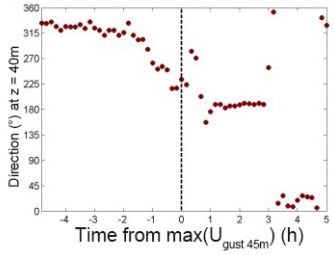
11 - Pintado 2008-04-24 to 2012-07-03. Event 36 with max($U_{gust\ 45m}$)= 22.2m/s on 2009-2-20 at 14:10. Series length: 48 months.

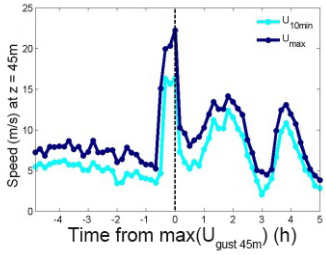




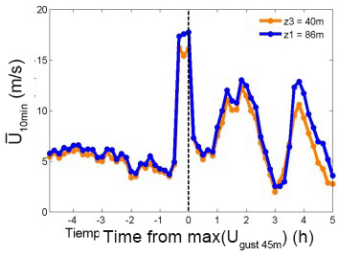


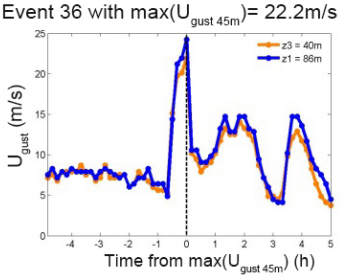


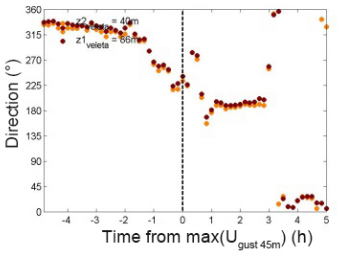


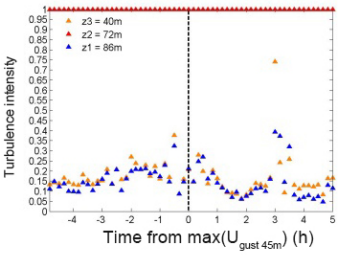


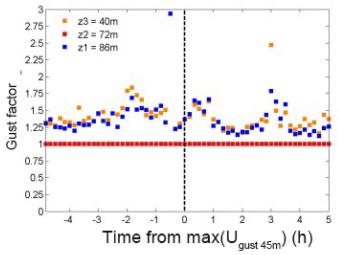
11 - Pintado 2008-04-24 to 2012-07-03. Event 36 with max($U_{gust\ 45m}$)= 22.2m/s on 2009-2-20 at 14:10. Series length: 48 months.

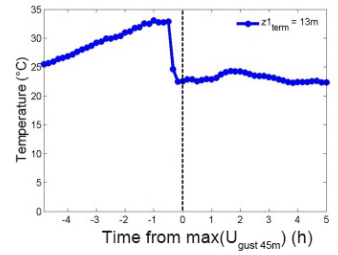


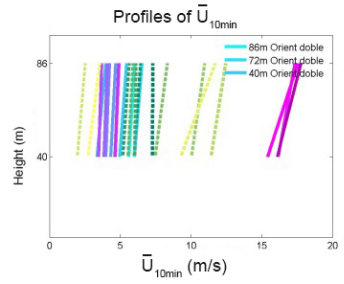


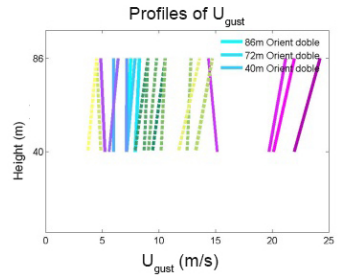


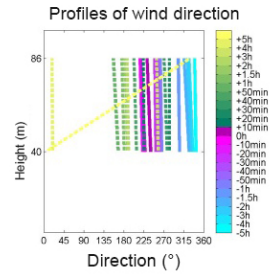




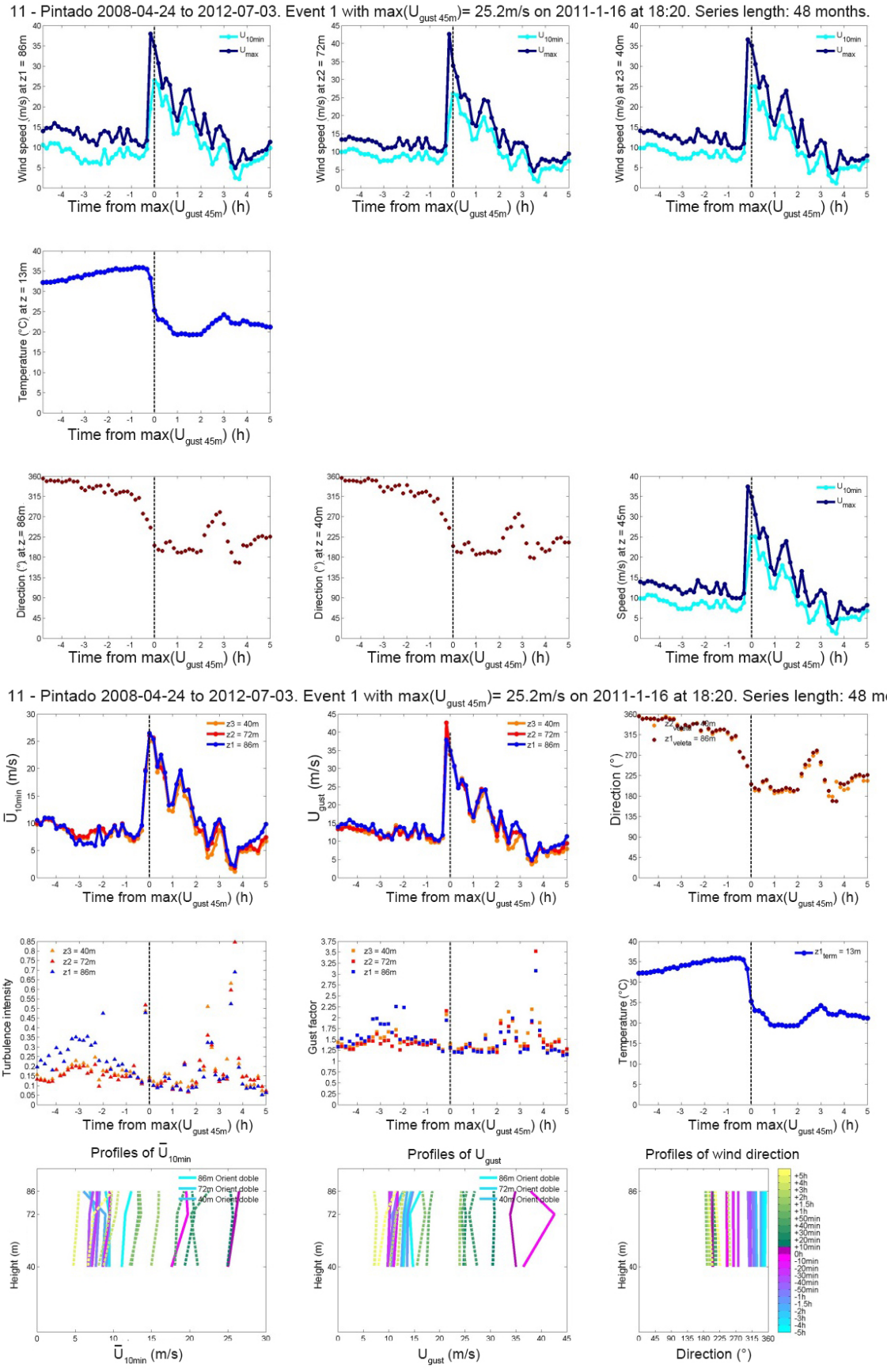




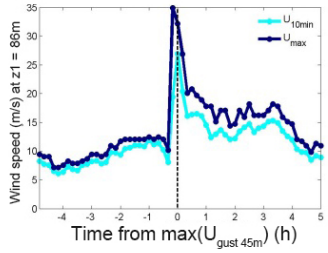


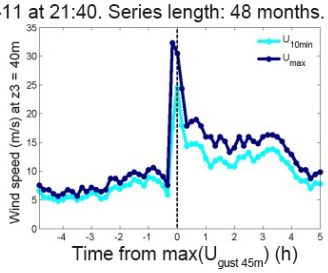


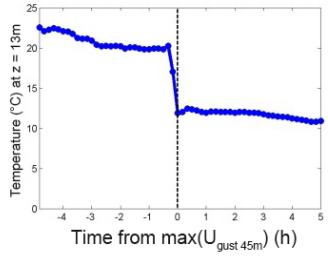
A.4 Highest 10min mean wind events at Pintado at 45m, complete years

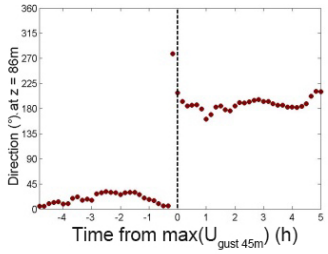


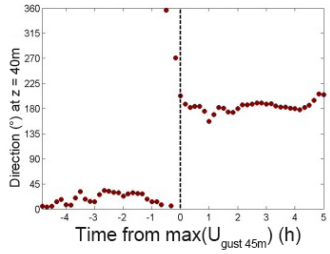
11 - Pintado 2008-04-24 to 2012-07-03. Event 2 with max($U_{gust\ 45m}$)= 24.8m/s on 2008-8-11 at 21:40. Series length: 48 months.

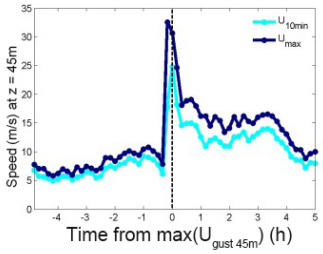




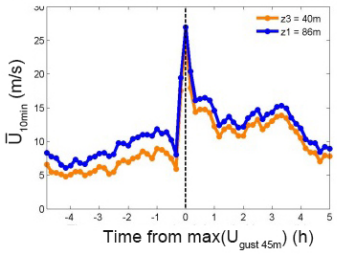


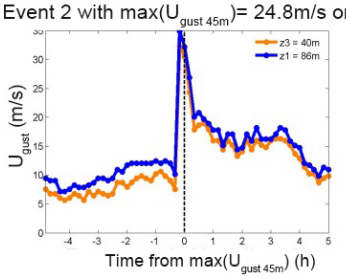


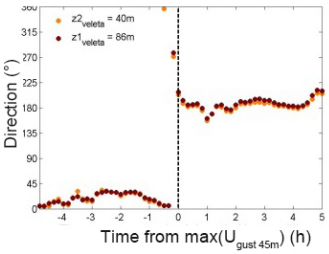


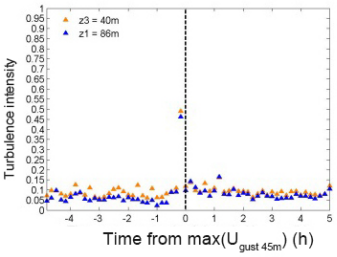


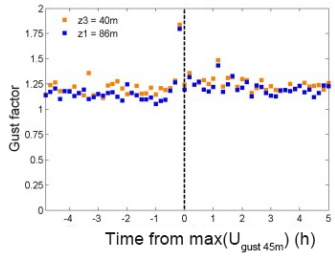
11 - Pintado 2008-04-24 to 2012-07-03. Event 2 with max($U_{gust\ 45m}$)= 24.8m/s on 2008-8-11 at 21:40. Series length: 48 months.

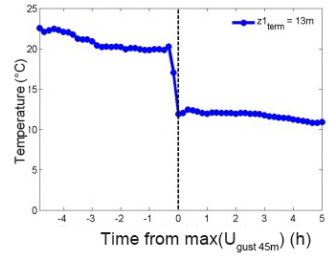


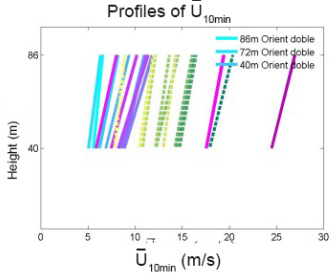


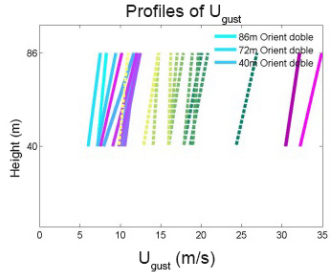


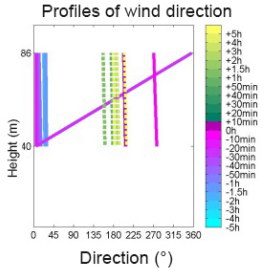




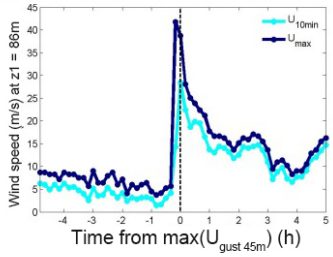


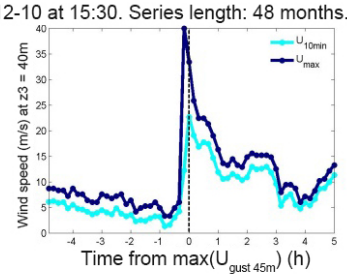


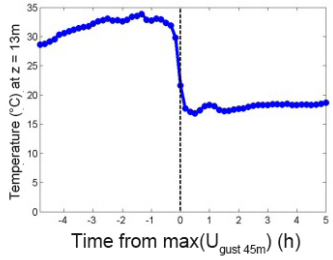


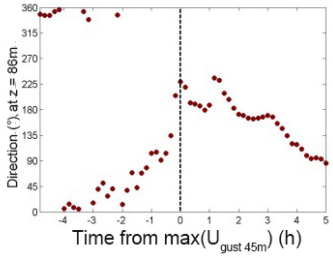


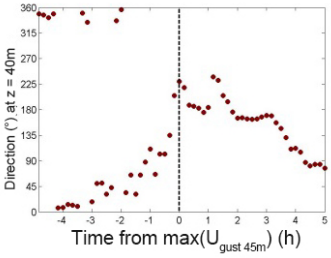
11 - Pintado 2008-04-24 to 2012-07-03. Event 3 with max($U_{gust\ 45m}$)= 23.3m/s on 2010-12-10 at 15:30. Series length: 48 months.

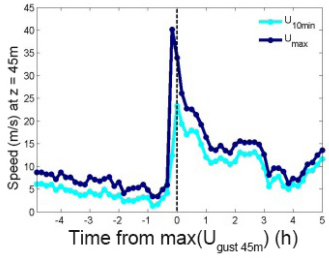




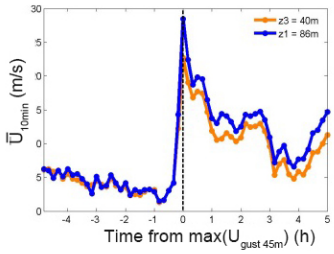


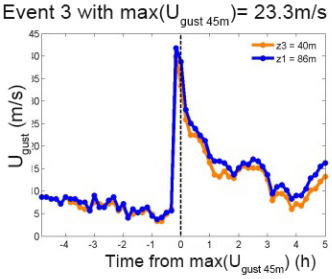


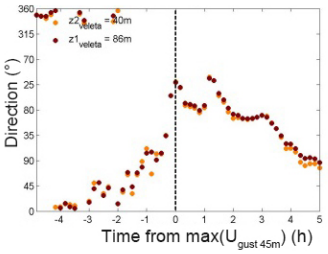


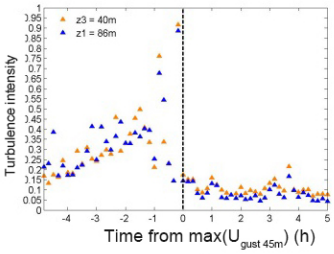


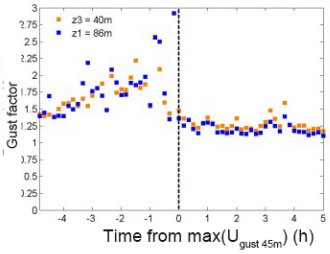
11 - Pintado 2008-04-24 to 2012-07-03. Event 3 with max($U_{gust\ 45m}$)= 23.3m/s on 2010-12-10 at 15:30. Series length: 48 months.

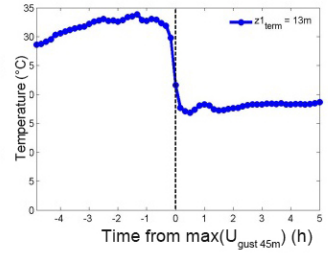


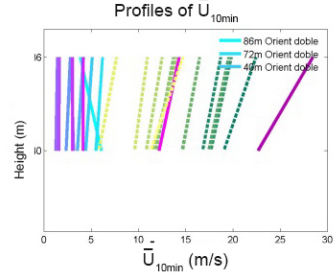


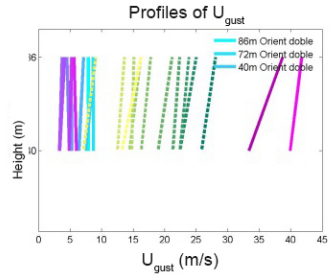


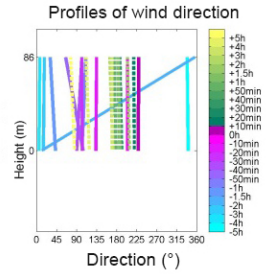




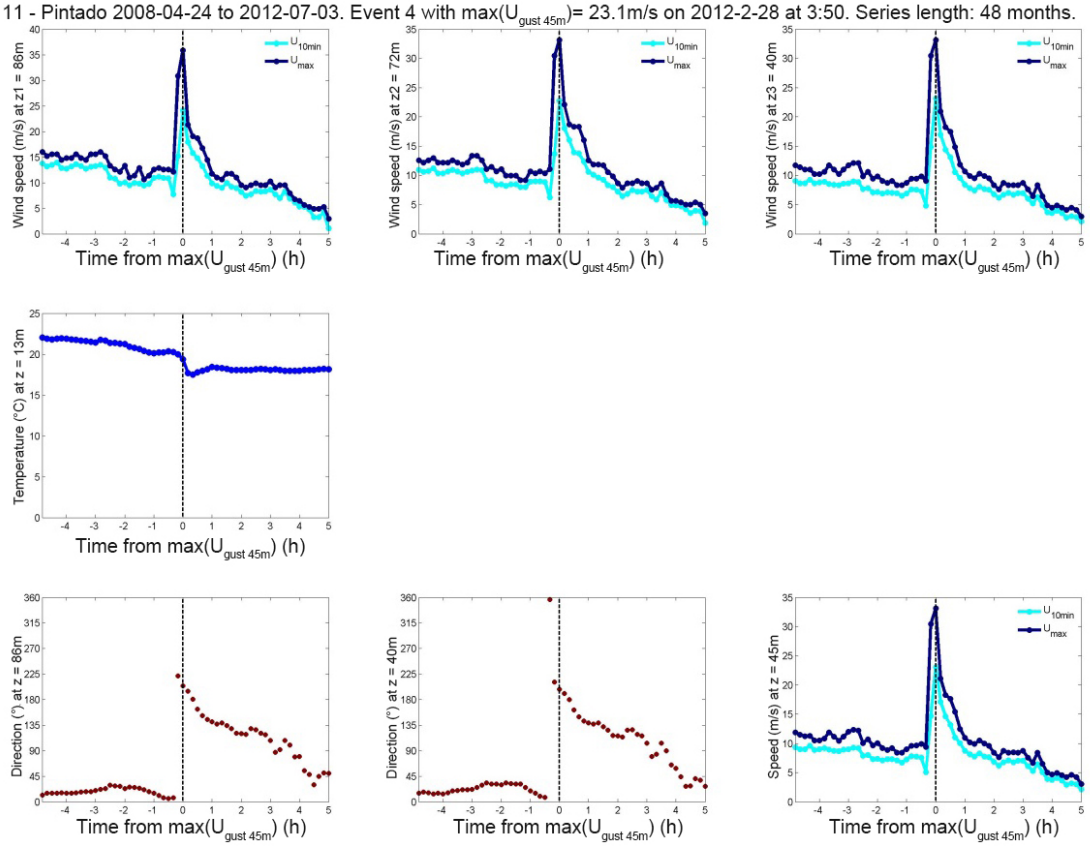




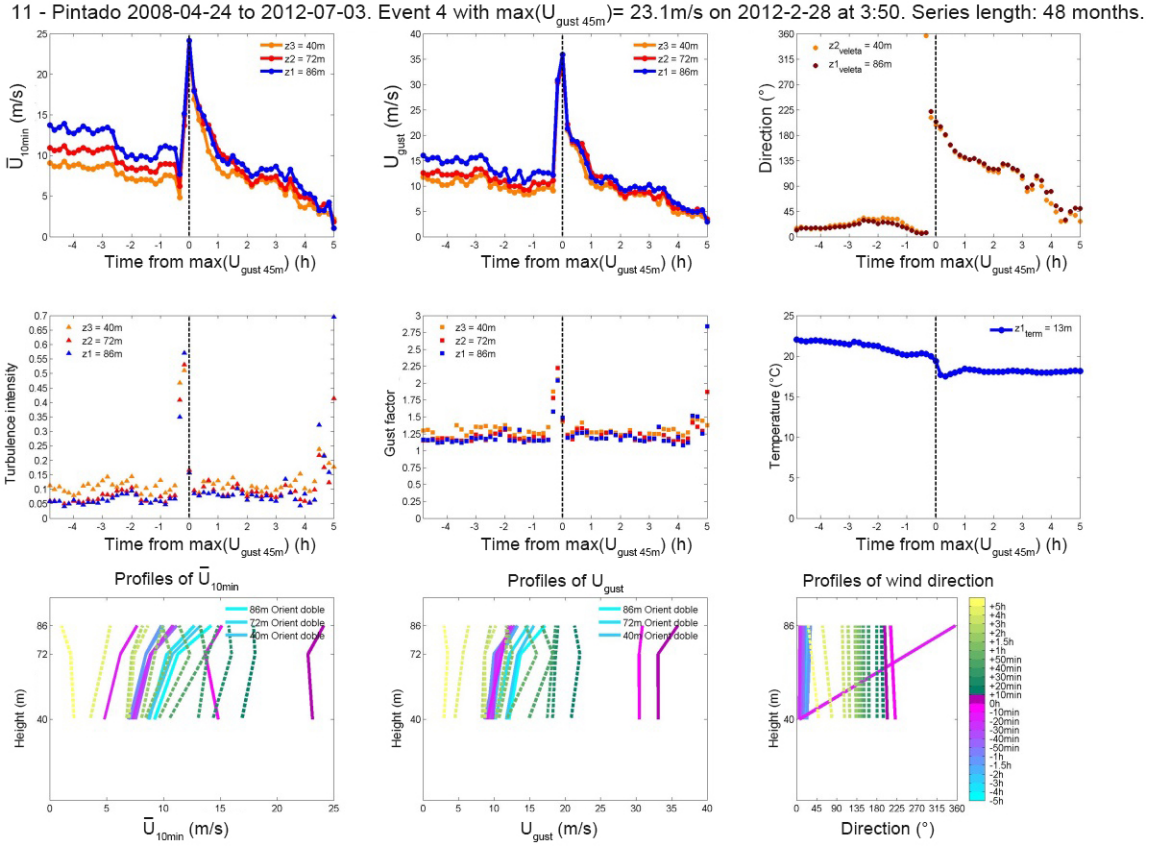




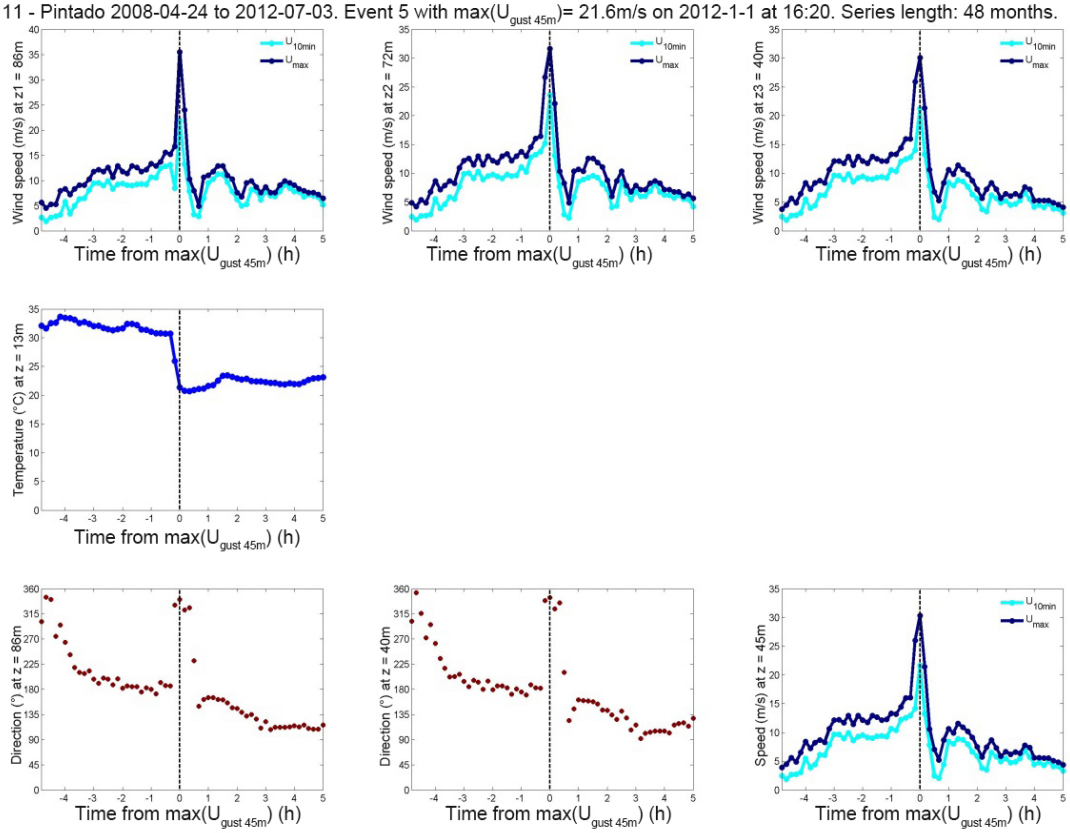
11 - Pintado 2008-04-24 to 2012-07-03. Event 4 with max($U_{gust\ 45m}$)= 23.1m/s on 2012-2-28 at 3:50. Series length: 48 months.



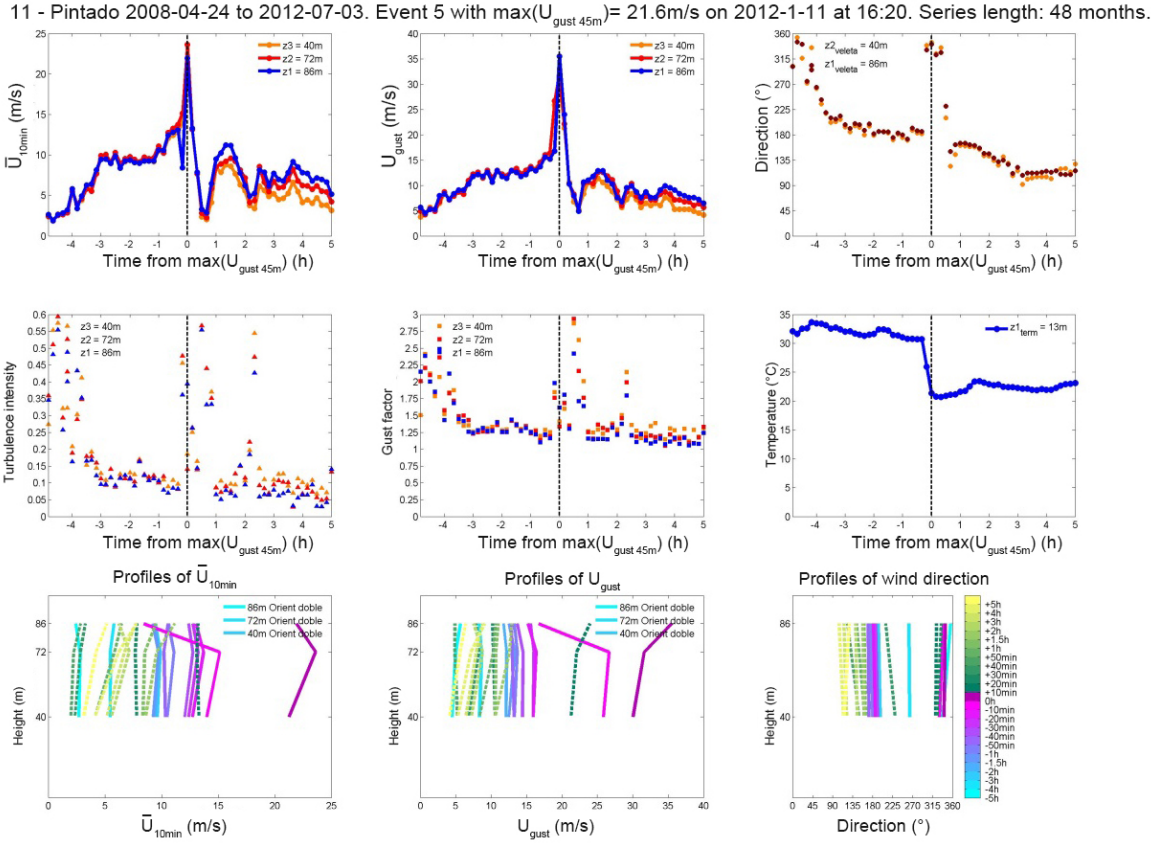
11 - Pintado 2008-04-24 to 2012-07-03. Event 4 with max($U_{gust\ 45m}$)= 23.1m/s on 2012-2-28 at 3:50. Series length: 48 months.



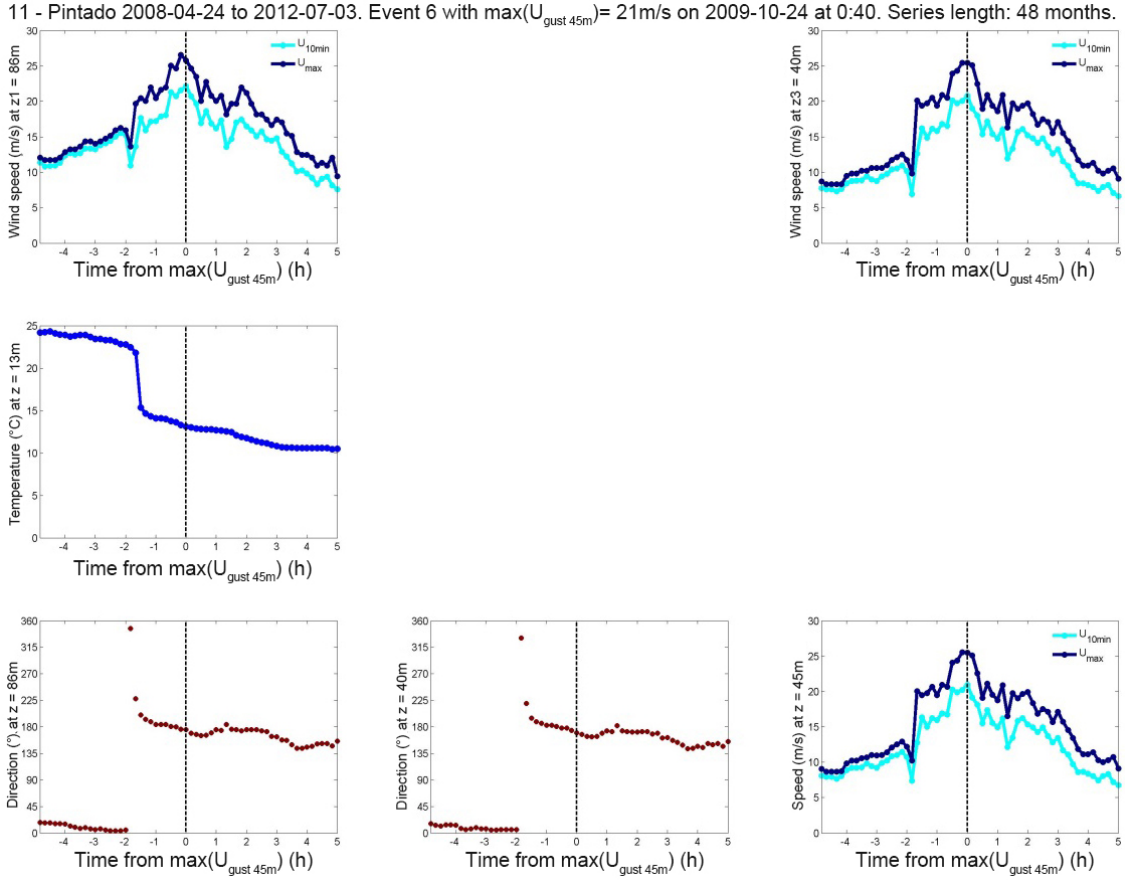
11 - Pintado 2008-04-24 to 2012-07-03. Event 5 with max($U_{gust\ 45m}$)= 21.6m/s on 2012-1-1 at 16:20. Series length: 48 months.



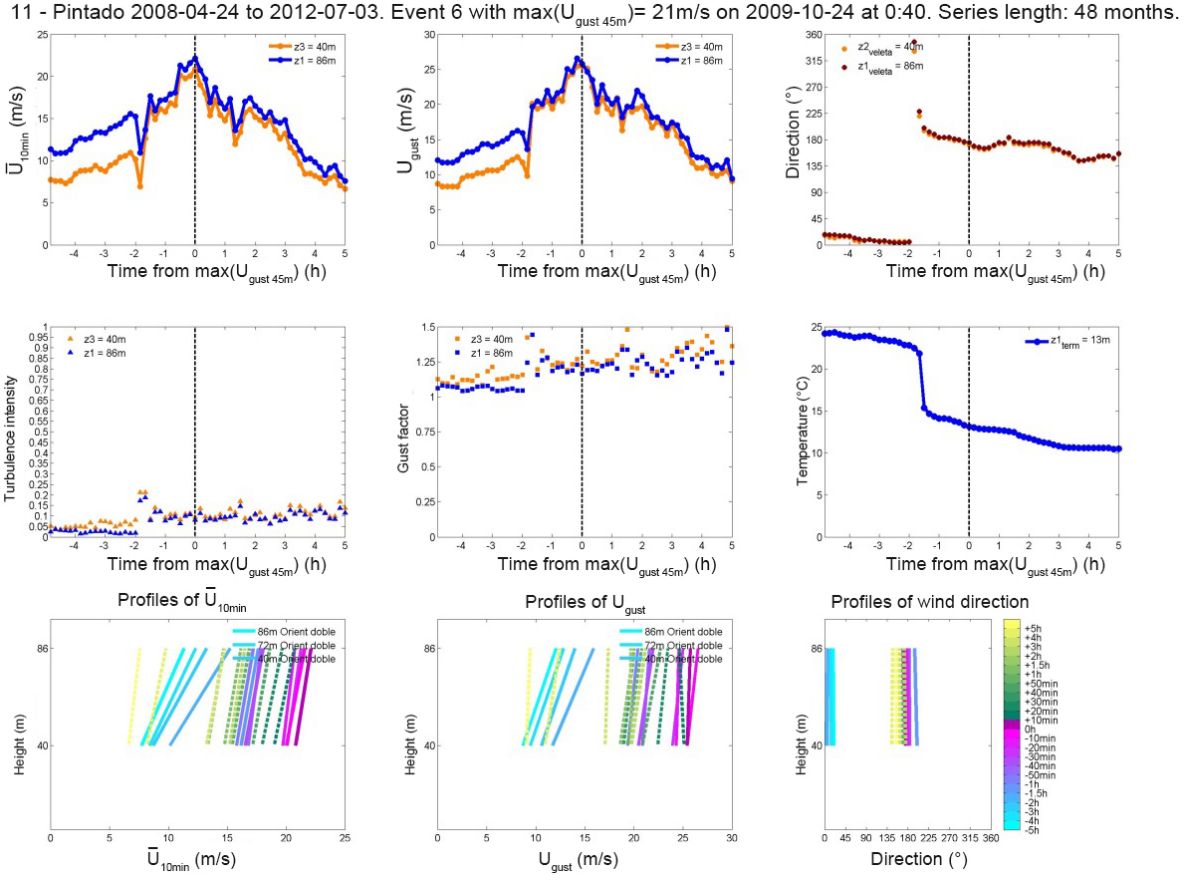
11 - Pintado 2008-04-24 to 2012-07-03. Event 5 with max($U_{gust\ 45m}$)= 21.6m/s on 2012-1-11 at 16:20. Series length: 48 months.



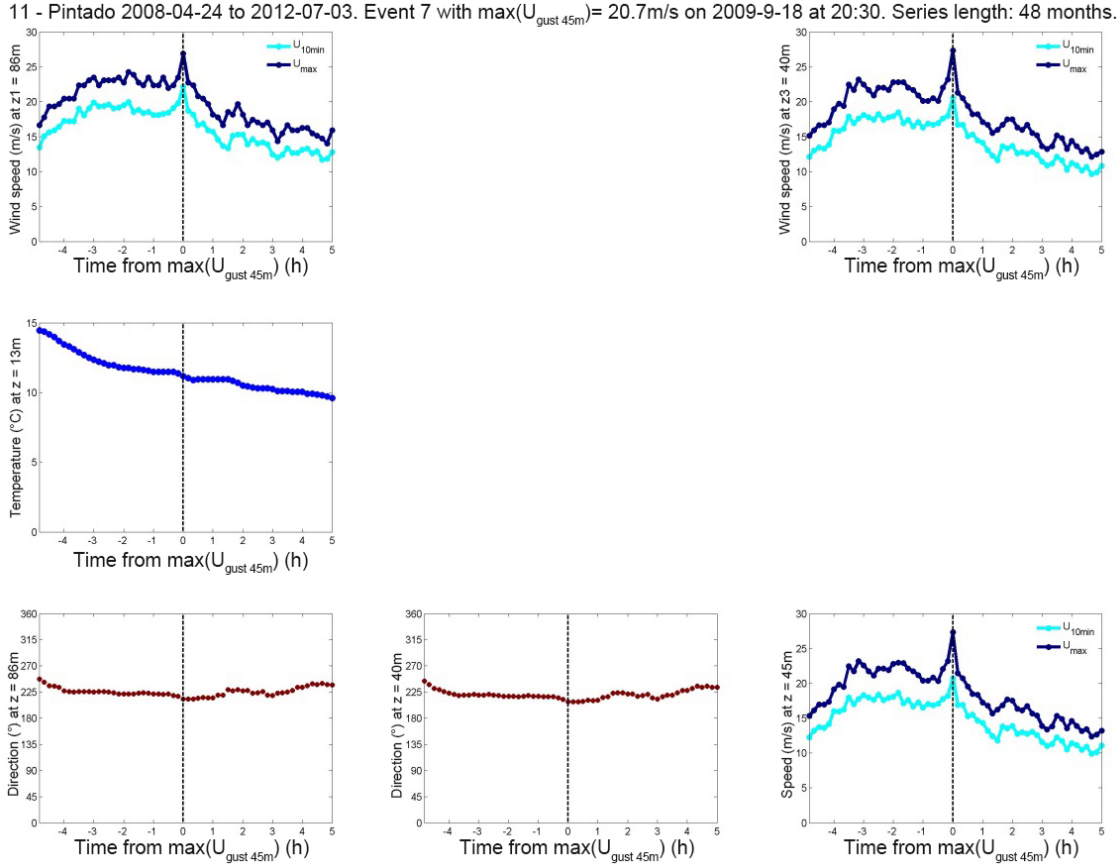
11 - Pintado 2008-04-24 to 2012-07-03. Event 6 with max($U_{gust\ 45m}$)= 21m/s on 2009-10-24 at 0:40. Series length: 48 months.



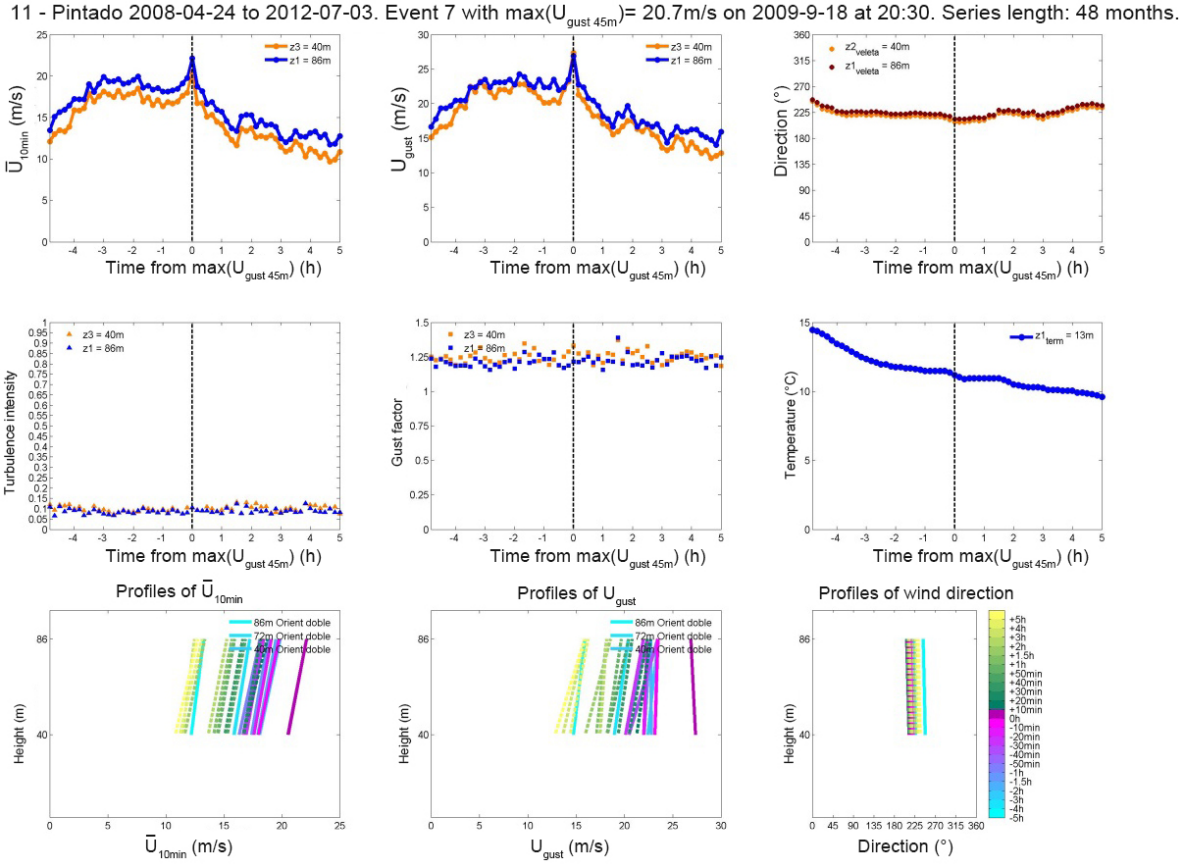
11 - Pintado 2008-04-24 to 2012-07-03. Event 6 with max($U_{gust\ 45m}$)= 21m/s on 2009-10-24 at 0:40. Series length: 48 months.



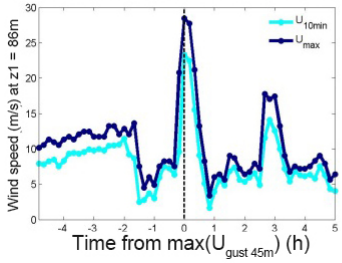
11 - Pintado 2008-04-24 to 2012-07-03. Event 7 with max($U_{gust\ 45m}$)= 20.7m/s on 2009-9-18 at 20:30. Series length: 48 months.

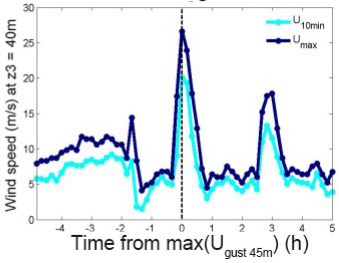


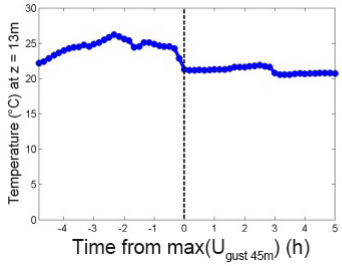
11 - Pintado 2008-04-24 to 2012-07-03. Event 7 with max($U_{gust\ 45m}$)= 20.7m/s on 2009-9-18 at 20:30. Series length: 48 months.

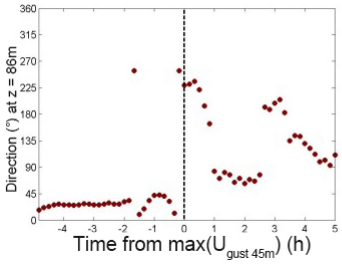


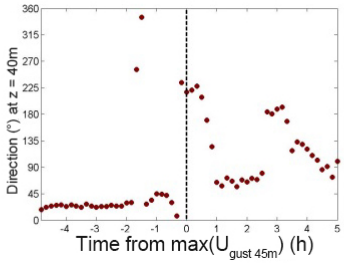
11 - Pintado 2008-04-24 to 2012-07-03. Event 8 with max($U_{gust\ 45m}$)= 20.5m/s on 2010-2-7 at 12:30. Series length: 48 months.

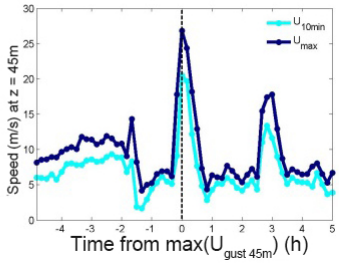




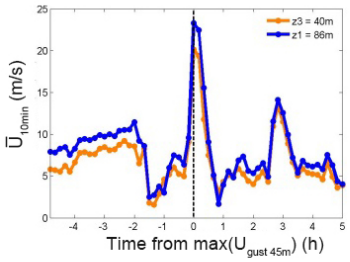


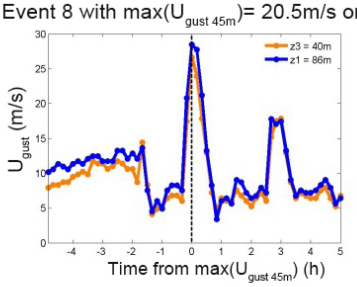


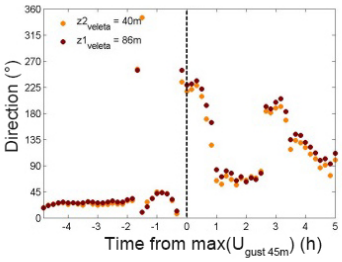


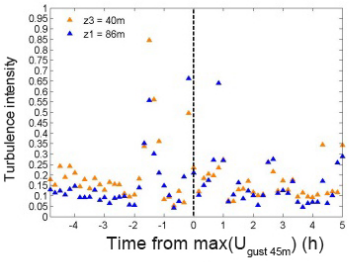


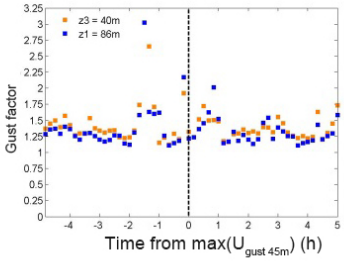
11 - Pintado 2008-04-24 to 2012-07-03. Event 8 with max($U_{gust\ 45m}$)= 20.5m/s on 2010-2-7 at 12:30. Series length: 48 months.

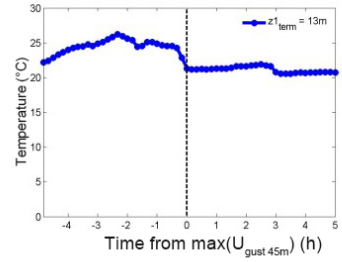


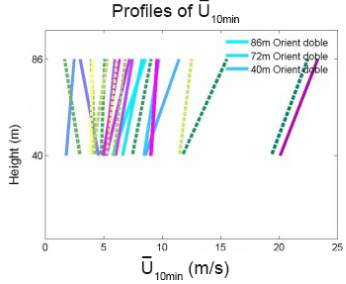


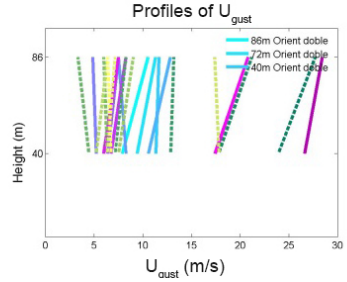


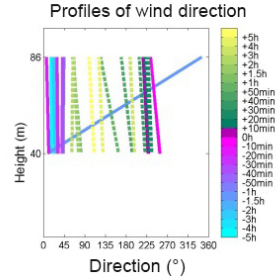




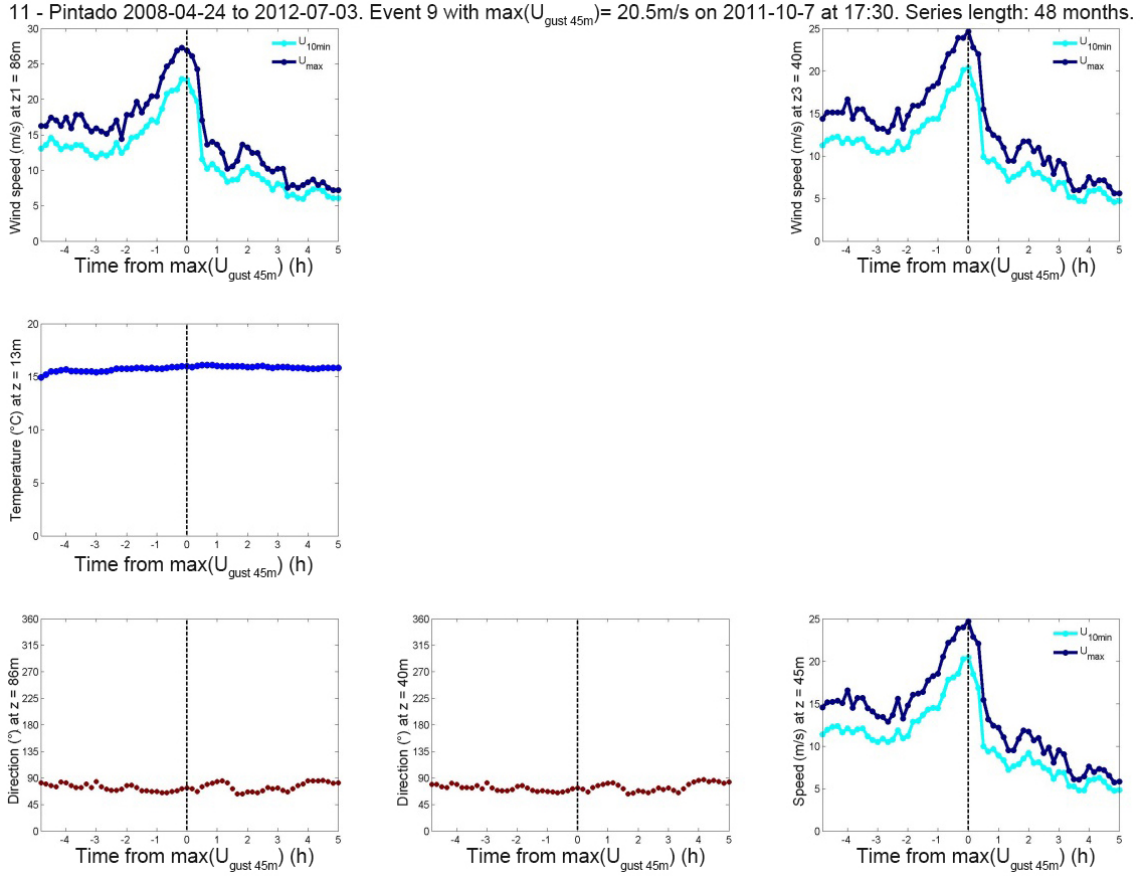




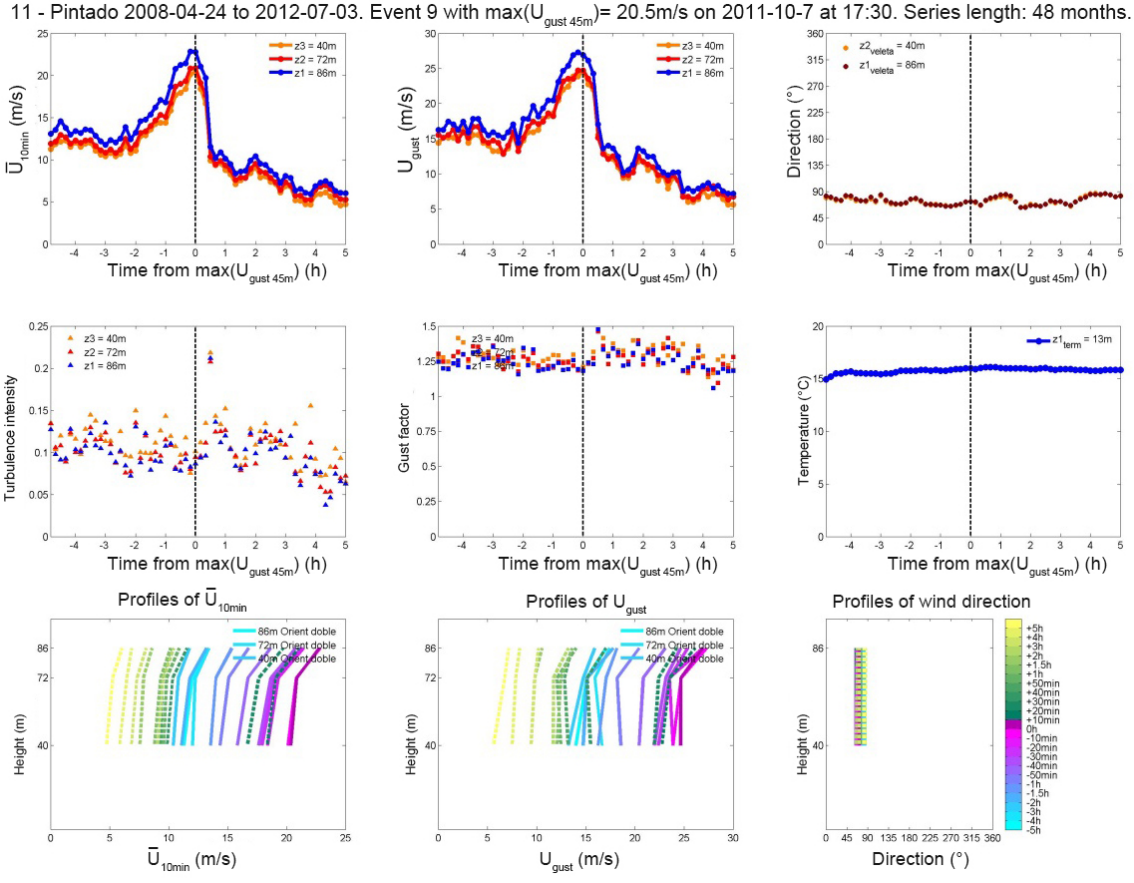




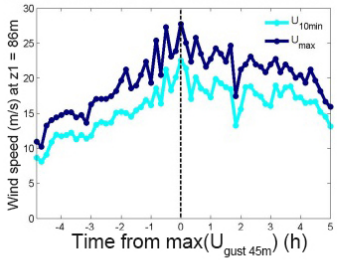
11 - Pintado 2008-04-24 to 2012-07-03. Event 9 with max($U_{gust\ 45m}$)= 20.5m/s on 2011-10-7 at 17:30. Series length: 48 months.

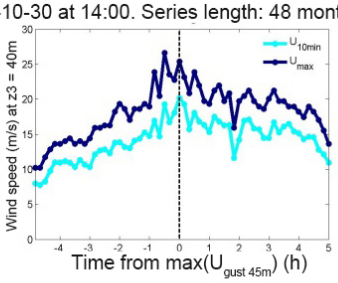


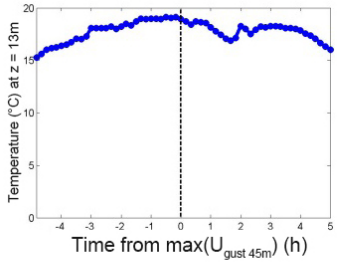
11 - Pintado 2008-04-24 to 2012-07-03. Event 9 with max($U_{gust\ 45m}$)= 20.5m/s on 2011-10-7 at 17:30. Series length: 48 months.

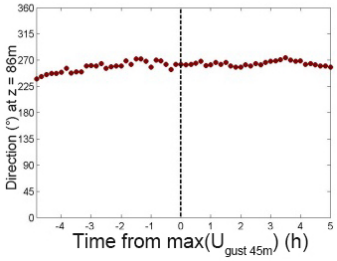


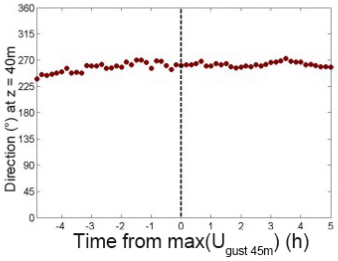
11 - Pintado 2008-04-24 to 2012-07-03. Event 10 with max($U_{gust\ 45m}$)= 20.4m/s on 2010-10-30 at 14:00. Series length: 48 months.

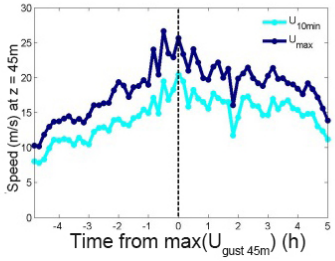




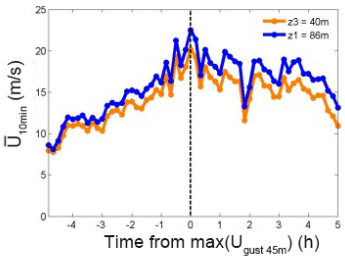


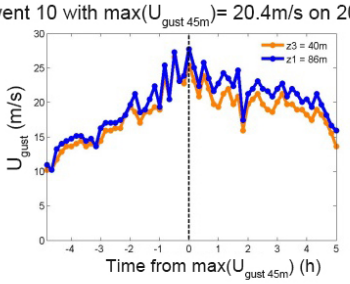


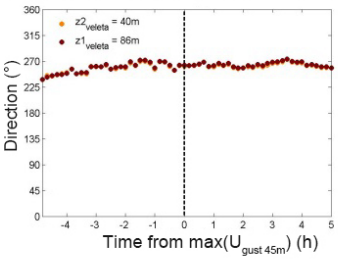


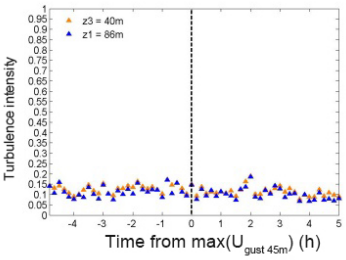


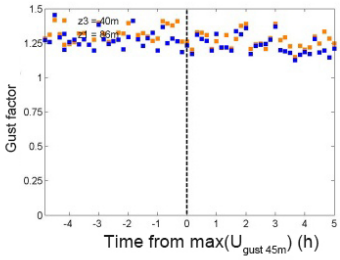
11 - Pintado 2008-04-24 to 2012-07-03. Event 10 with max($U_{gust\ 45m}$)= 20.4m/s on 2010-10-30 at 14:00. Series length: 48 months.

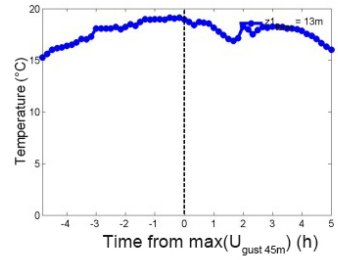


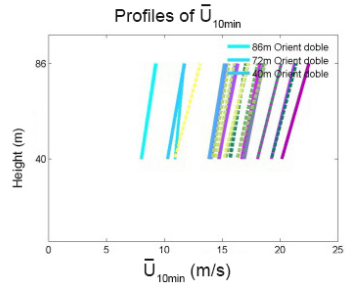


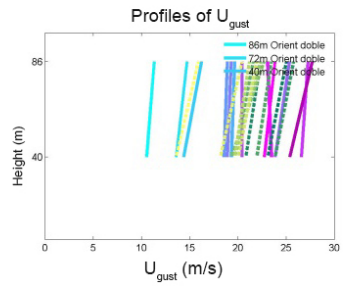


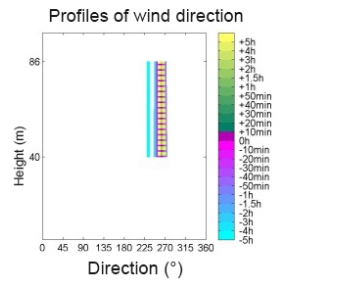


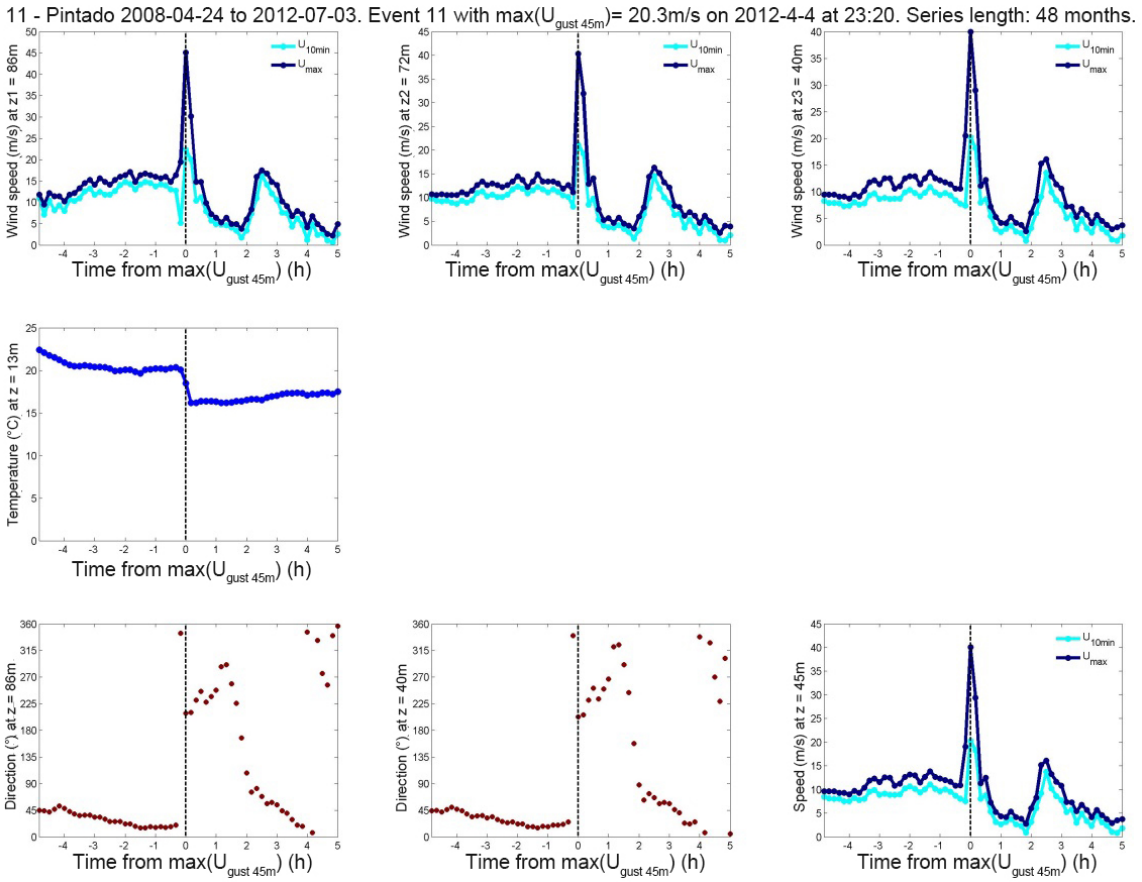


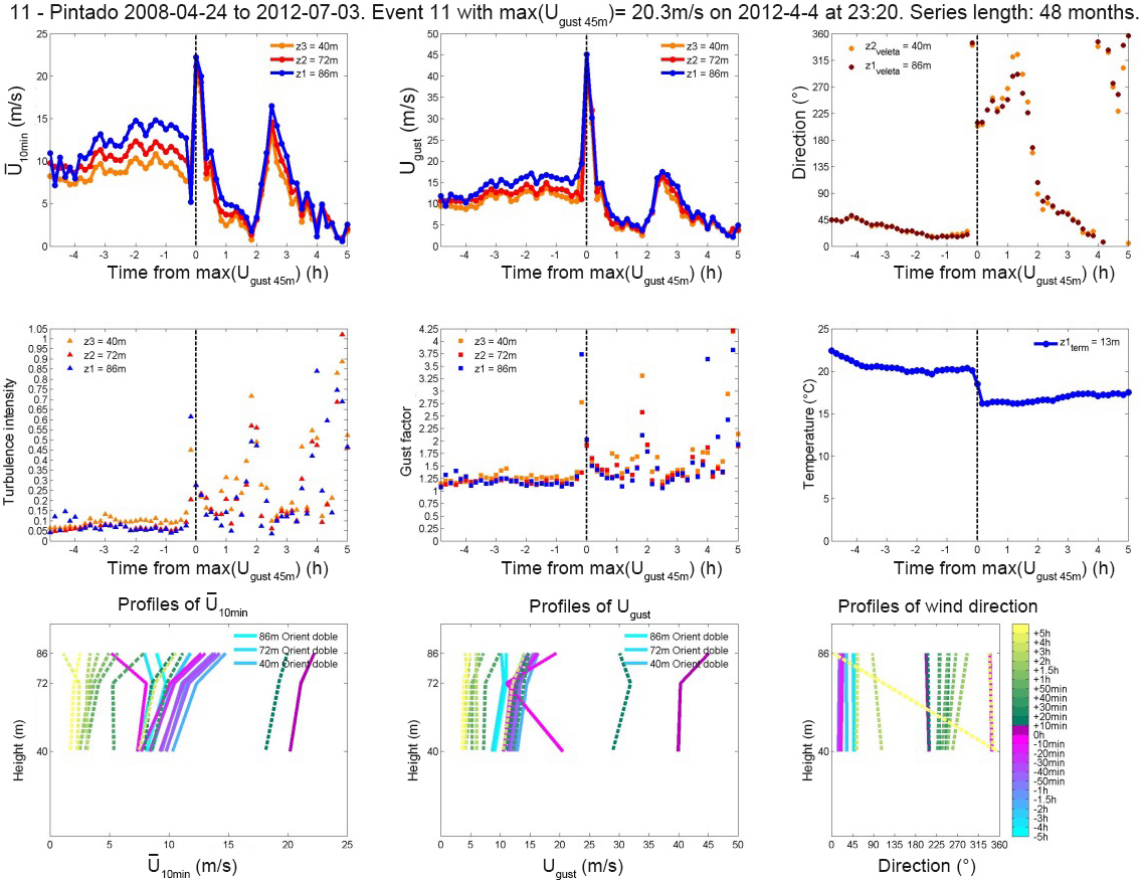


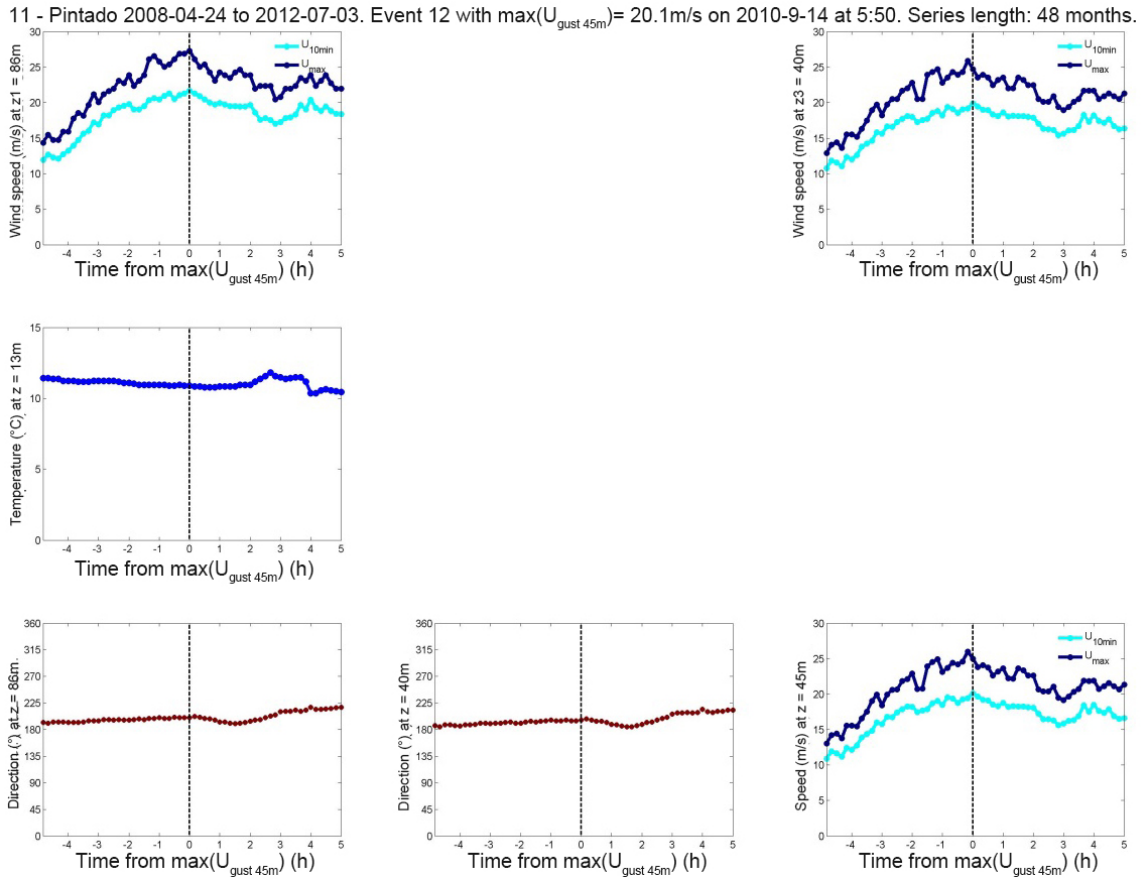


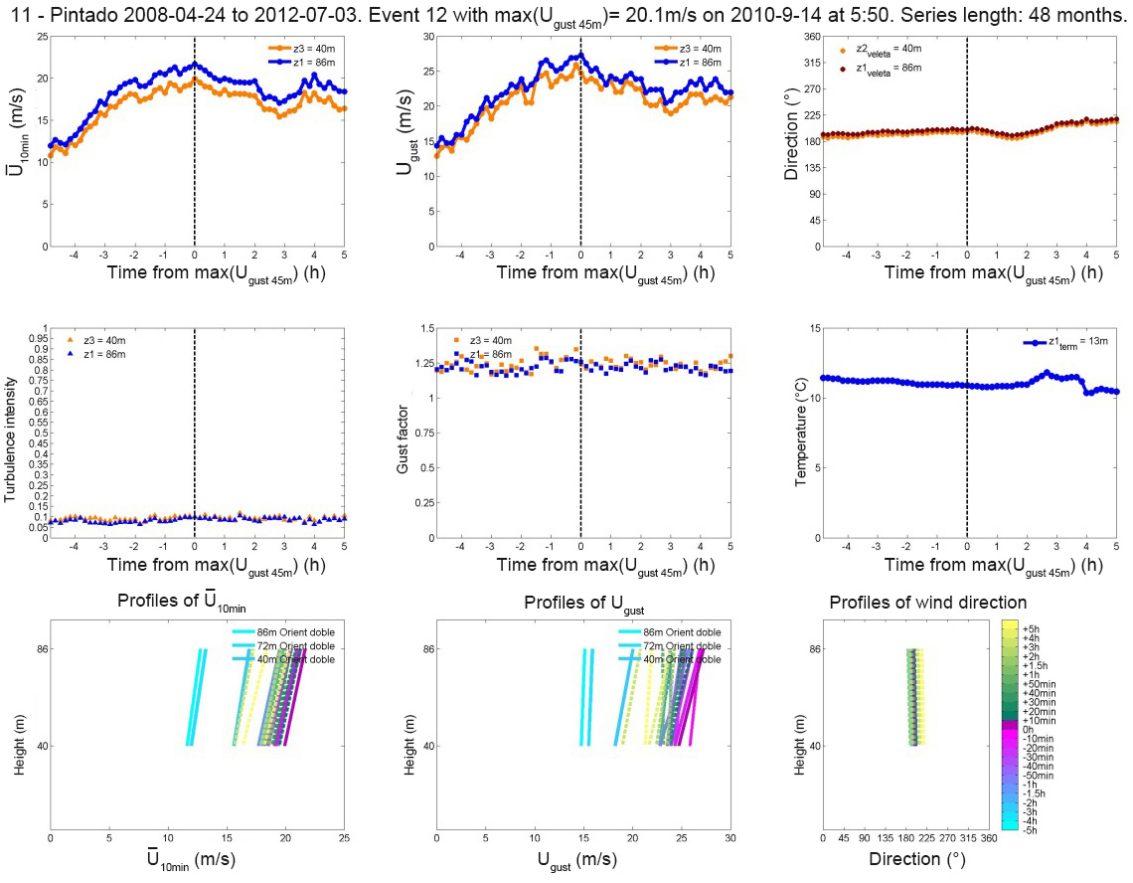




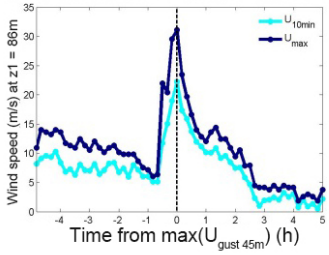

11 - Pintado 2008-04-24 to 2012-07-03. Event 11 with max(U gust 45m)= 20.3m/s on 2012-4-4 at 23:20. Series length: 48 months.
Wind speed (m/s) at z1 = 86m
Wind speed (m/s) at z2 = 72m
Wind speed (m/s) at z3 = 40m
U 10min
U max
Temperature (°C) at z = 13m
Direction (°) at z = 86m
Direction (°) at z = 40m
Speed (m/s) at z = 45m
Time from max(U gust 45m) (h)

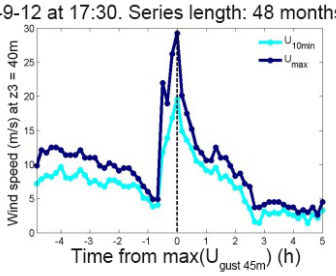

11 - Pintado 2008-04-24 to 2012-07-03. Event 11 with max(U gust 45m)= 20.3m/s on 2012-4-4 at 23:20. Series length: 48 months.
z3 = 40m
z2 = 72m
z1 = 86m
Ū 10min (m/s)
U gust (m/s)
Direction (°)
z2 veleta = 40m
z1 veleta = 86m
Turbulence intensity
Gust factor
Temperature (°C)
z1 term = 13m
Time from max(U gust 45m) (h)
Profiles of Ū 10min
Profiles of U gust
Profiles of wind direction
86m Orient doble
72m Orient doble
40m Orient doble
Height (m)
Ū 10min (m/s)
U gust (m/s)
Direction (°)

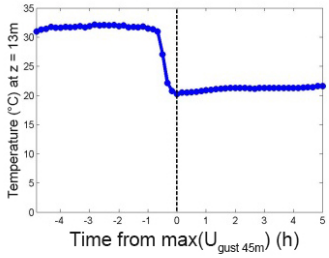

11 - Pintado 2008-04-24 to 2012-07-03. Event 12 with max(U gust 45m)= 20.1m/s on 2010-9-14 at 5:50. Series length: 48 months.
Wind speed (m/s) at z1 = 86m
Wind speed (m/s) at z3 = 40m
Temperature (°C) at z = 13m
Direction (°) at z = 86m
Direction (°) at z = 40m
Speed (m/s) at z = 45m
U10min
Umax
Time from max(U gust 45m) (h)

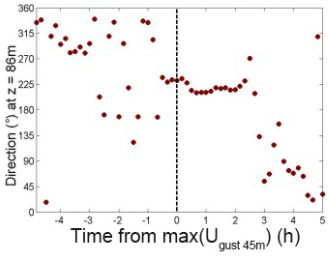

11 - Pintado 2008-04-24 to 2012-07-03. Event 12 with max(U gust 45m)= 20.1m/s on 2010-9-14 at 5:50. Series length: 48 months.
z3 = 40m
z1 = 86m
z2veleta = 40m
z1veleta = 86m
z1term = 13m
Turbulence intensity
Gust factor
Temperature (°C)
Direction (°)
Time from max(U gust 45m) (h)
Profiles of Ū10min
Profiles of U gust
Profiles of wind direction
86m Orient doble
72m Orient doble
40m Orient doble
Height (m)
Ū10min (m/s)
U gust (m/s)

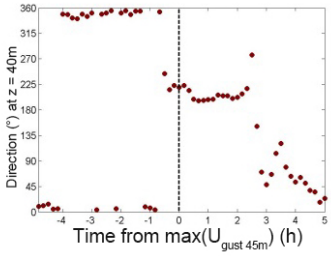
11 - Pintado 2008-04-24 to 2012-07-03. Event 13 with max($U_{gust\ 45m}$)= 19.9m/s on 2009-9-12 at 17:30. Series length: 48 months.

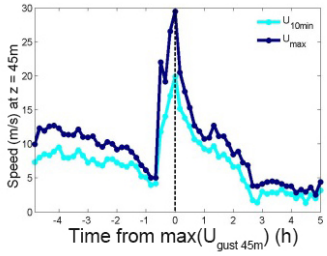




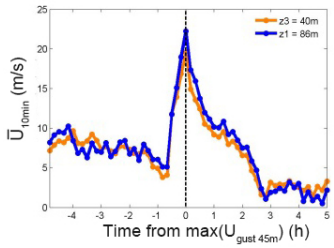


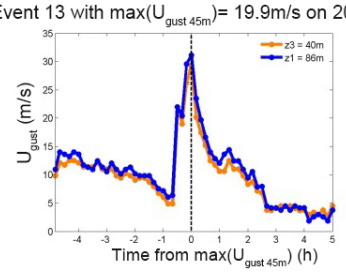


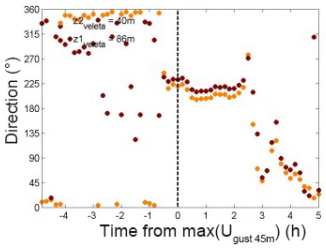


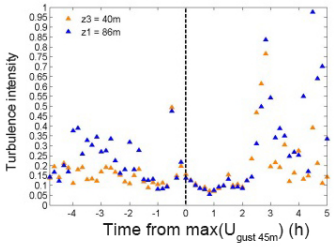


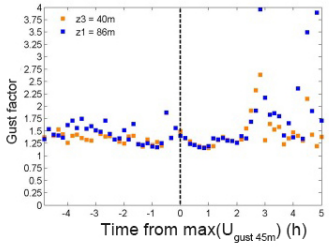
11 - Pintado 2008-04-24 to 2012-07-03. Event 13 with max($U_{gust\ 45m}$)= 19.9m/s on 2009-12-19 at 17:30. Series length: 48 months.

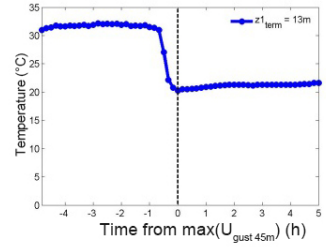


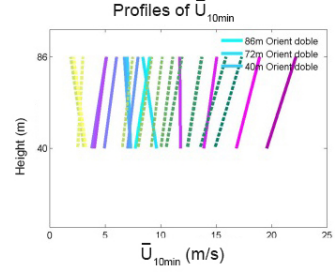


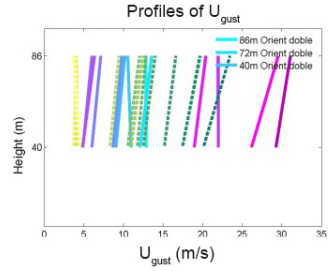


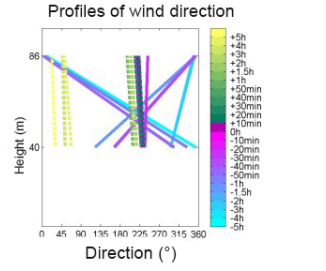




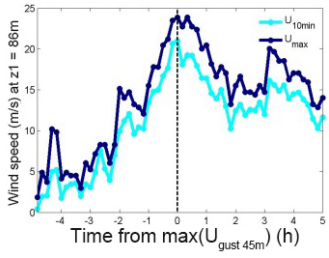


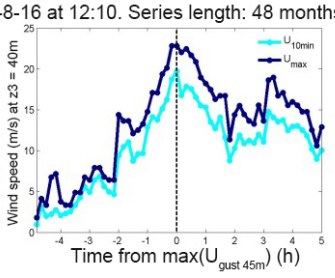


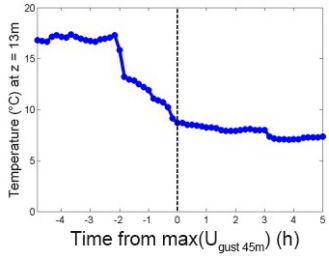


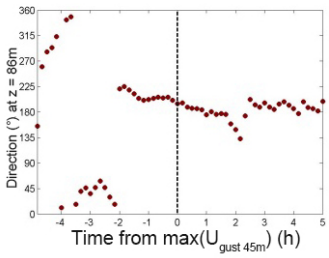


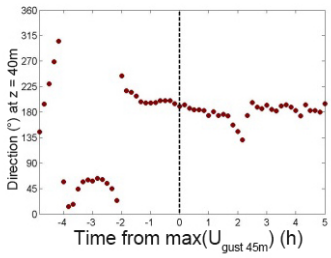
11 - Pintado 2008-04-24 to 2012-07-03. Event 14 with max($U_{gust\ 45m}$)= 19.8m/s on 2009-8-16 at 12:10. Series length: 48 months.

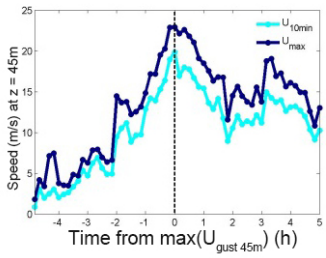




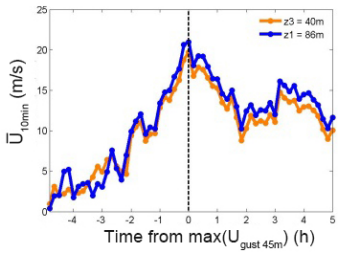


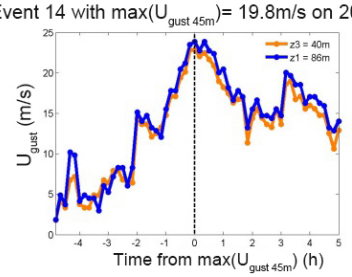


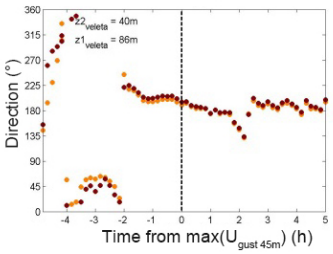


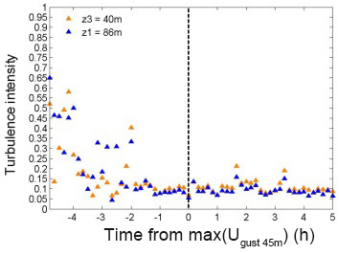


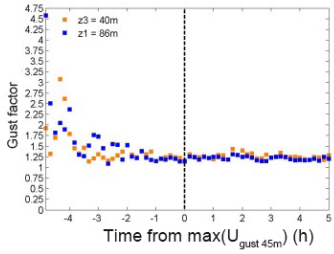
11 - Pintado 2008-04-24 to 2012-07-03. Event 14 with max($U_{gust\ 45m}$)= 19.8m/s on 2009-8-16 at 12:10. Series length: 48 months.

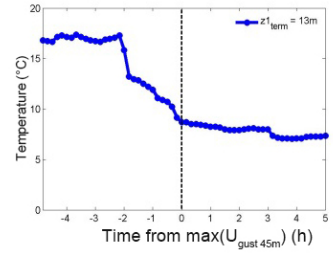


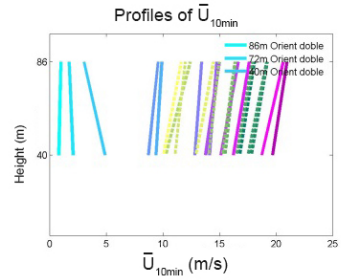


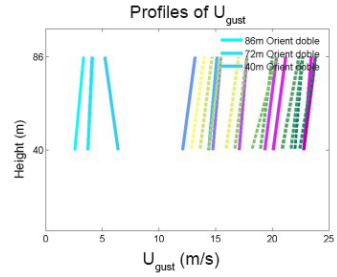


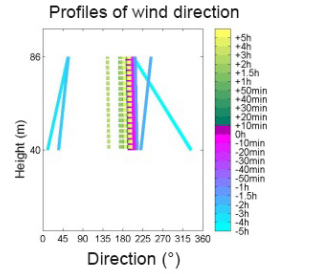


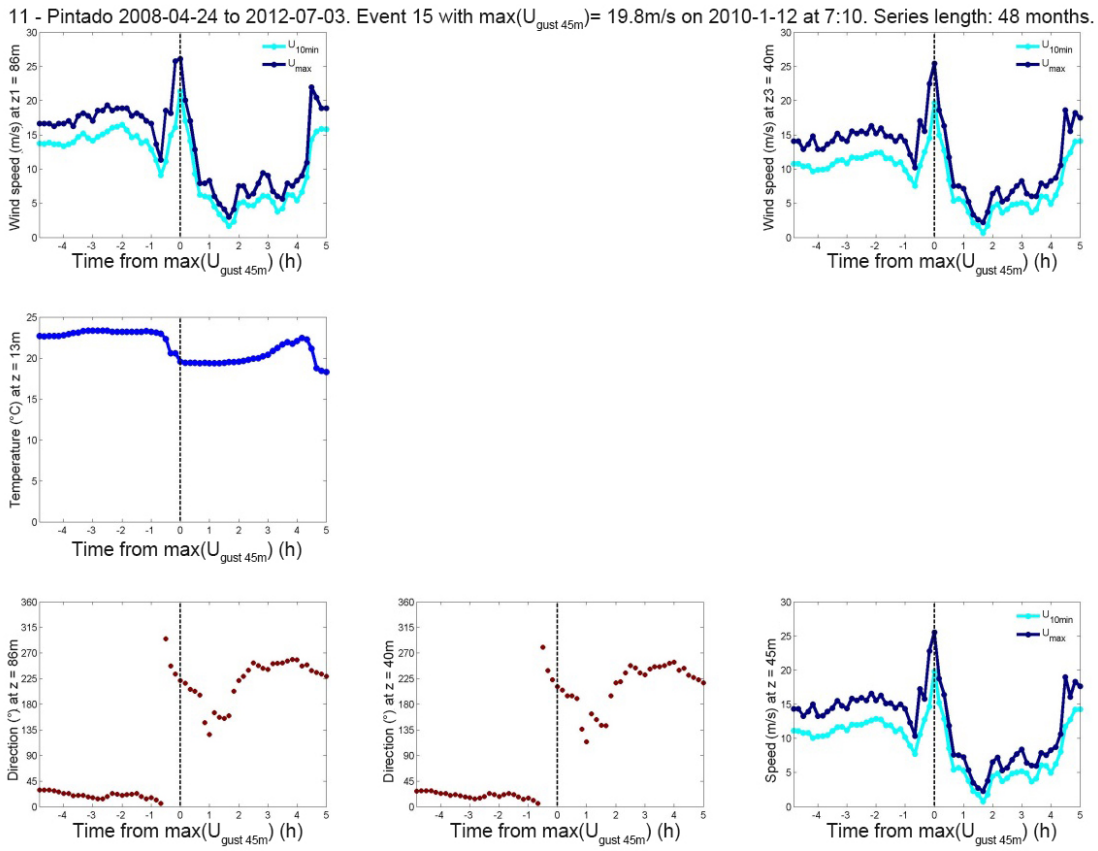


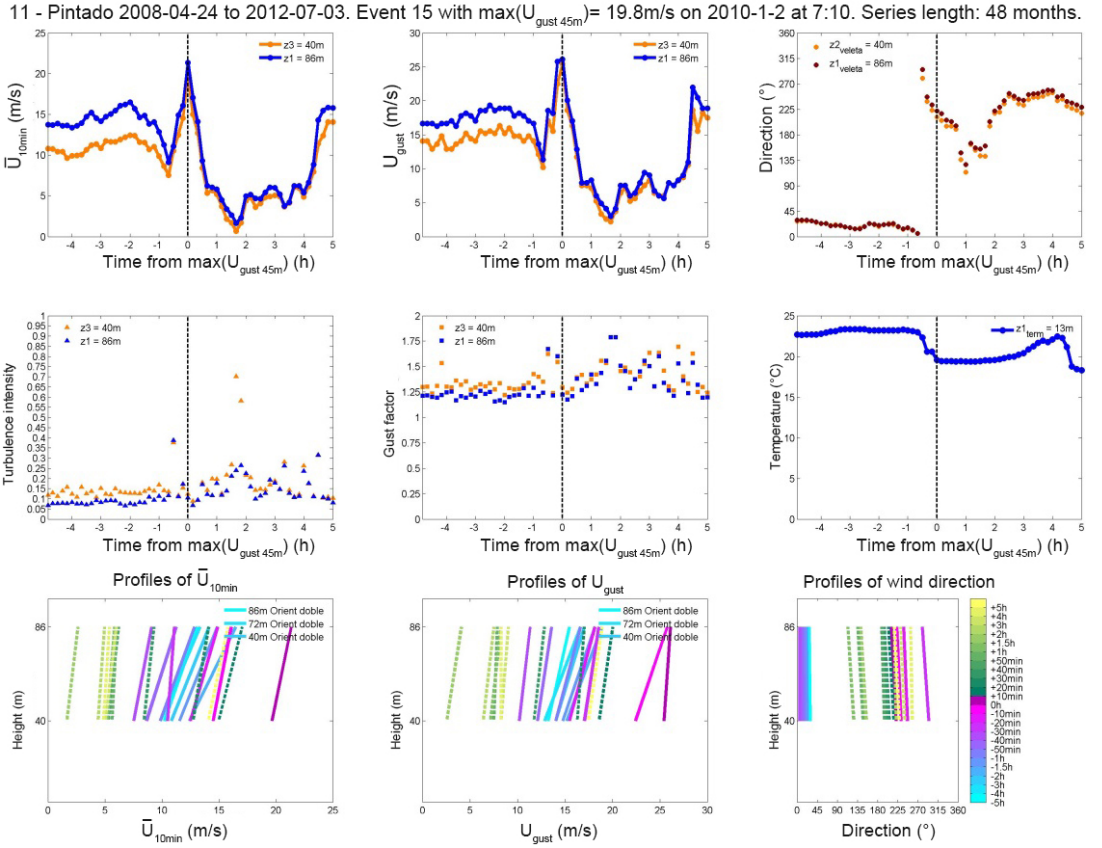




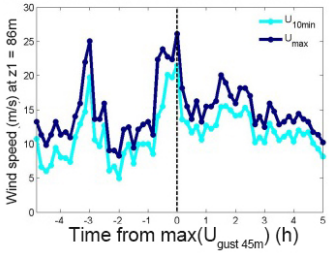


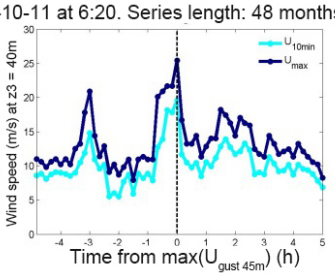


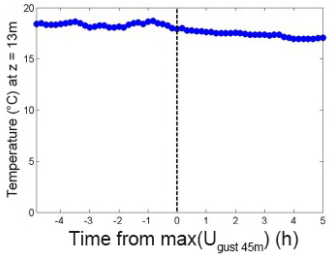

11 - Pintado 2008-04-24 to 2012-07-03. Event 15 with max(U gust 45m)= 19.8m/s on 2010-1-12 at 7:10. Series length: 48 months.
Wind speed (m/s) at z1 = 86m
Wind speed (m/s) at z3 = 40m
Temperature (°C) at z = 13m
Direction (°) at z = 86m
Direction (°) at z = 40m
Speed (m/s) at z = 45m
U 10min
U max
Time from max(U gust 45m) (h)

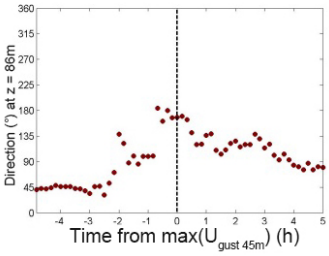

11 - Pintado 2008-04-24 to 2012-07-03. Event 15 with max(U gust 45m)= 19.8m/s on 2010-1-2 at 7:10. Series length: 48 months.
z3 = 40m
z1 = 86m
z2 veleta = 40m
z1 veleta = 86m
z1 term = 13m
Turbulence intensity
Gust factor
Temperature (°C)
Direction (°)
Time from max(U gust 45m) (h)
Profiles of Ū 10min
Profiles of U gust
Profiles of wind direction
86m Orient doble
72m Orient doble
40m Orient doble
Height (m)
Ū 10min (m/s)
U gust (m/s)

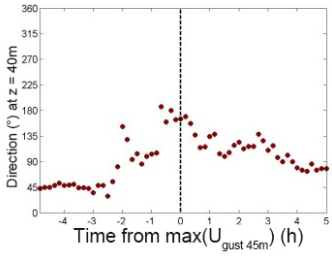
11 - Pintado 2008-04-24 to 2012-07-03. Event 16 with max($U_{gust\ 45m}$)= 19.8m/s on 2009-10-11 at 6:20. Series length: 48 months.

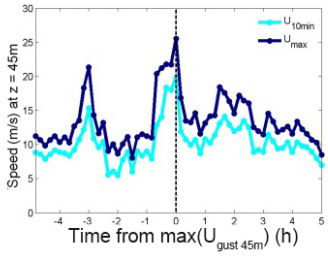




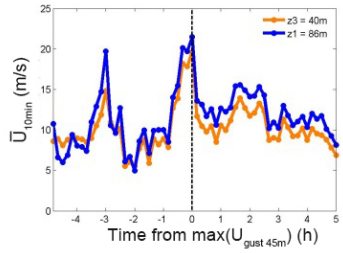


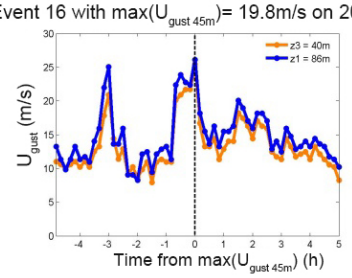


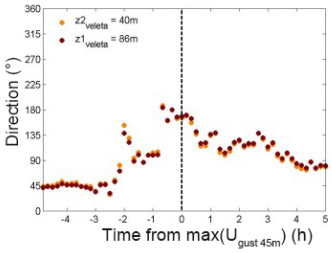


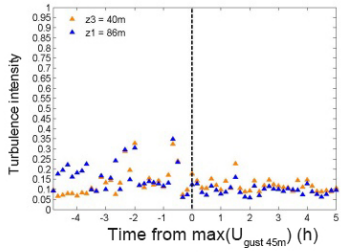


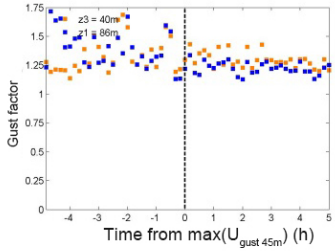
11 - Pintado 2008-04-24 to 2012-07-03. Event 16 with max($U_{gust\ 45m}$)= 19.8m/s on 2009-10-5 at 6:20. Series length: 48 months.

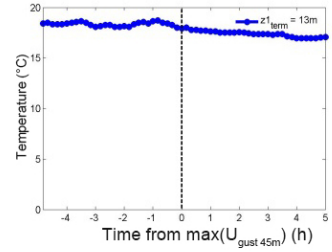




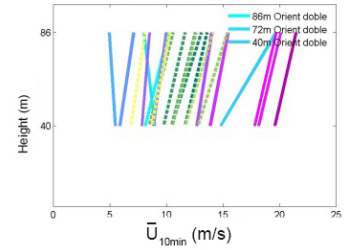




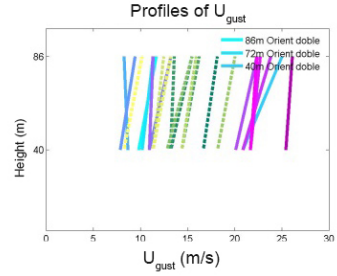




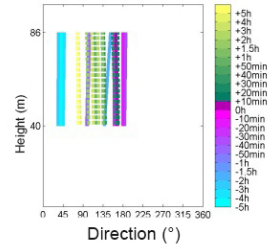
Profiles of $\bar{U}_{10min}$



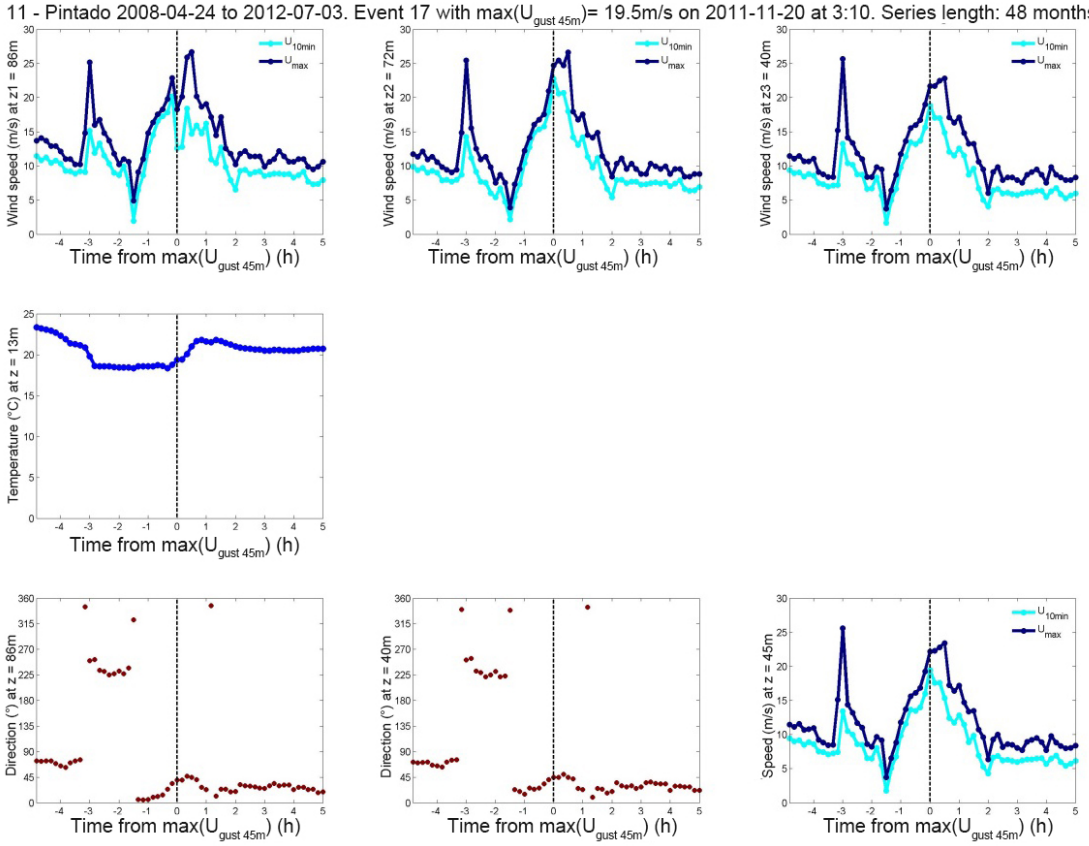
Profiles of U_{gust}



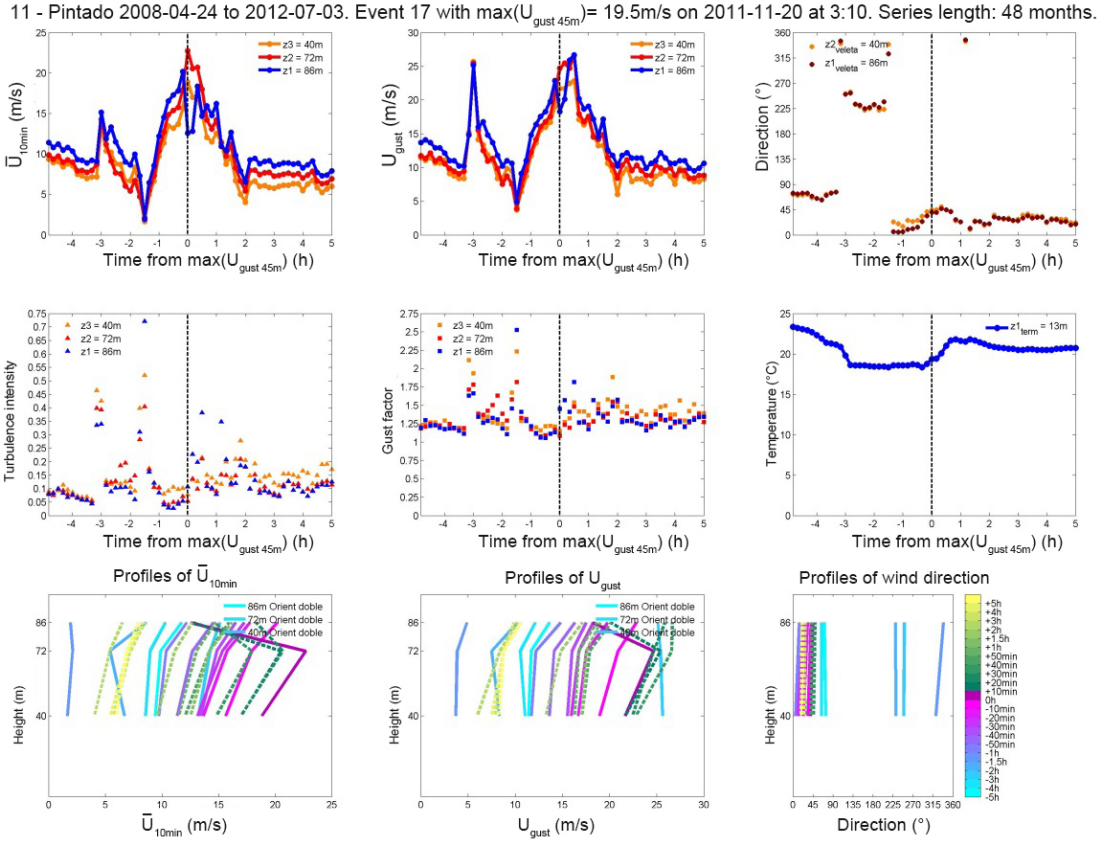
Profiles of wind direction



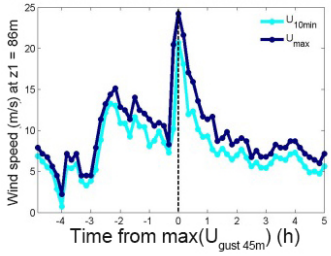
11 - Pintado 2008-04-24 to 2012-07-03. Event 17 with max($U_{gust\ 45m}$)= 19.5m/s on 2011-11-20 at 3:10. Series length: 48 months.

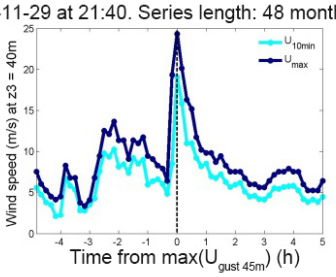


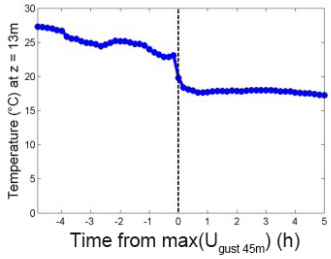
11 - Pintado 2008-04-24 to 2012-07-03. Event 17 with max($U_{gust\ 45m}$)= 19.5m/s on 2011-11-20 at 3:10. Series length: 48 months.

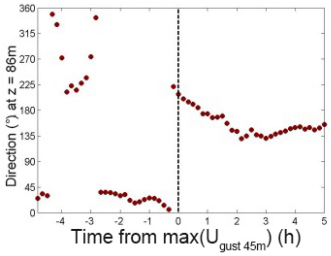


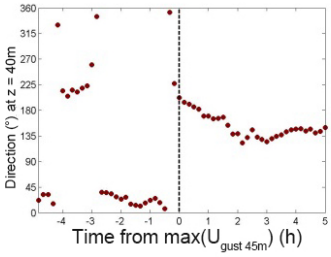
11 - Pintado 2008-04-24 to 2012-07-03. Event 18 with max($U_{gust\ 45m}$)= 19.2m/s on 2009-11-29 at 21:40. Series length: 48 months.

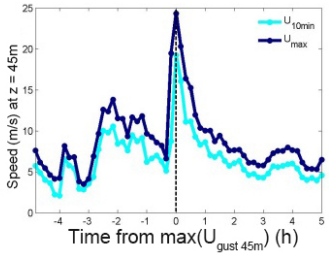




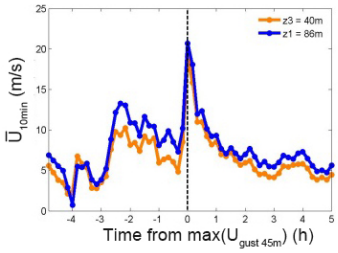


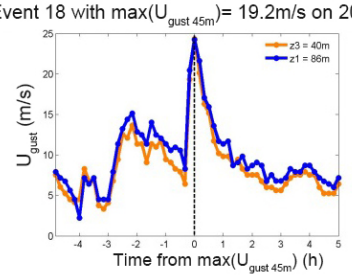


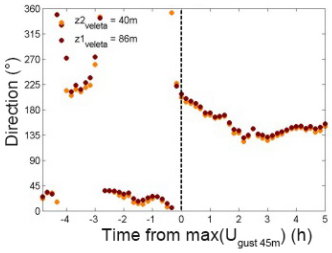


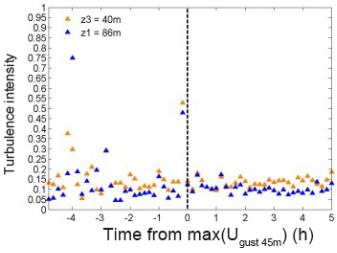


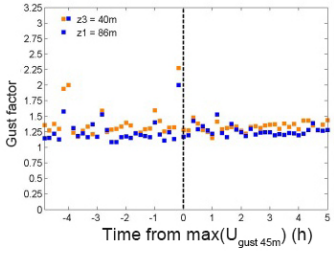
11 - Pintado 2008-04-24 to 2012-07-03. Event 18 with max($U_{gust\ 45m}$)= 19.2m/s on 2009-11-29 at 21:40. Series length: 48 months.

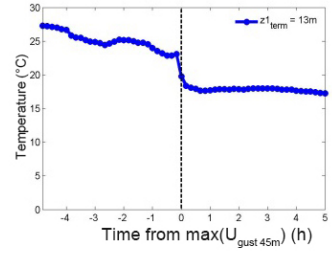


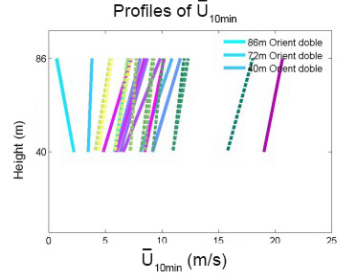


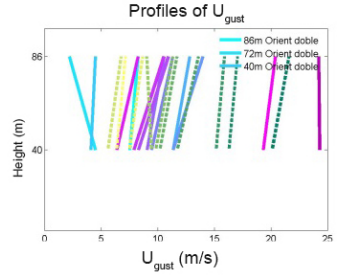


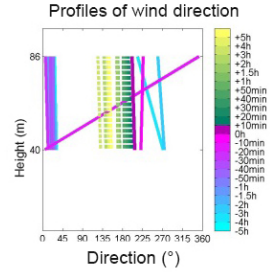




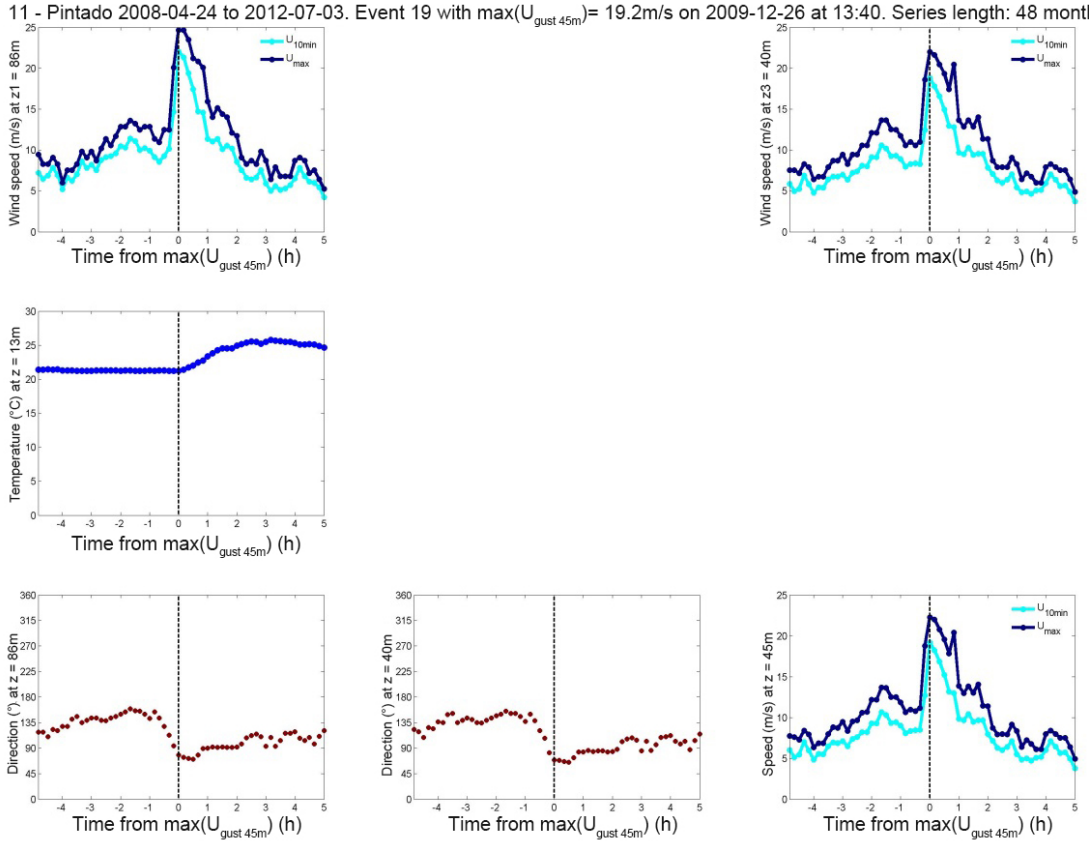




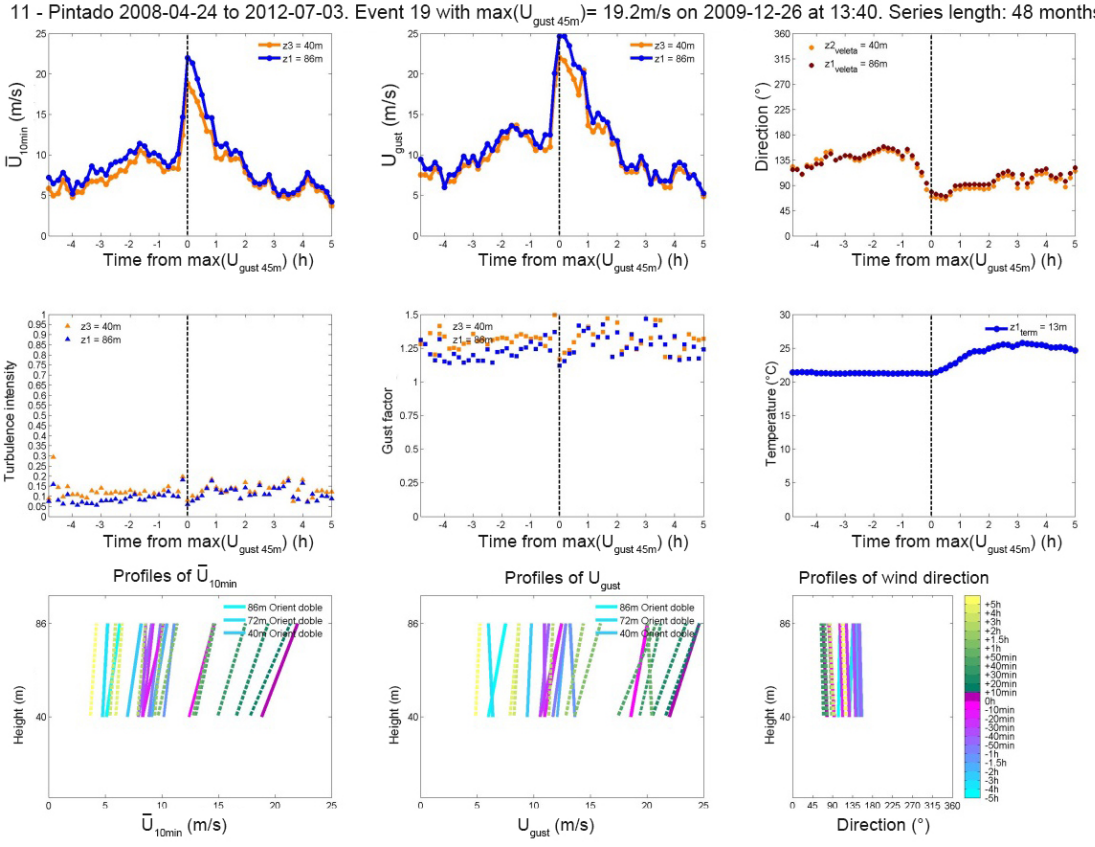




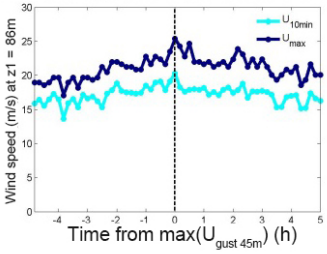
11 - Pintado 2008-04-24 to 2012-07-03. Event 19 with max($U_{gust\ 45m}$)= 19.2m/s on 2009-12-26 at 13:40. Series length: 48 months.

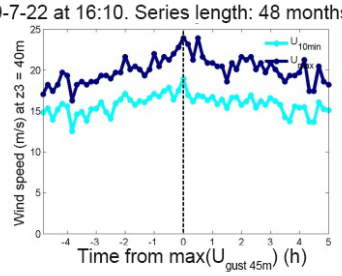


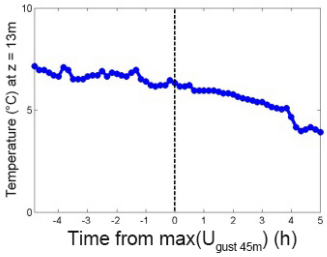
11 - Pintado 2008-04-24 to 2012-07-03. Event 19 with max($U_{gust\ 45m}$)= 19.2m/s on 2009-12-26 at 13:40. Series length: 48 months.

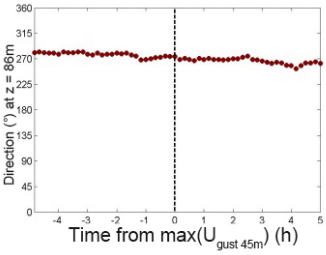


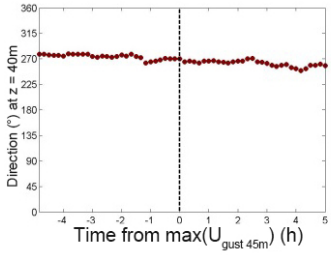
11 - Pintado 2008-04-24 to 2012-07-03. Event 20 with max($U_{gust\ 45m}$)= 19.1m/s on 2009-7-22 at 16:10. Series length: 48 months.

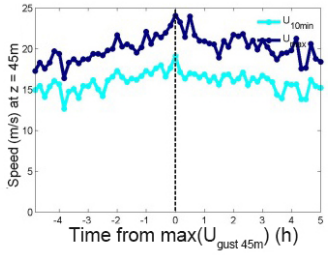




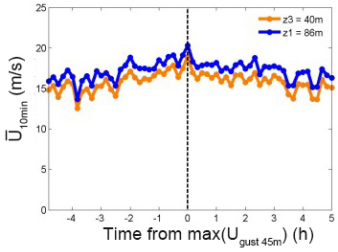


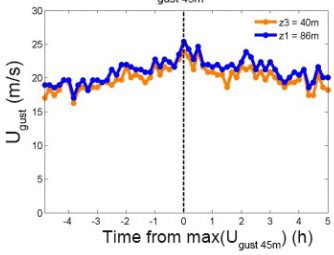


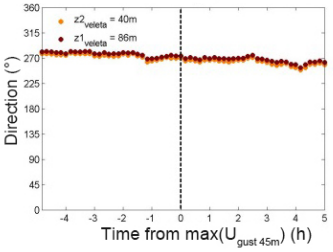


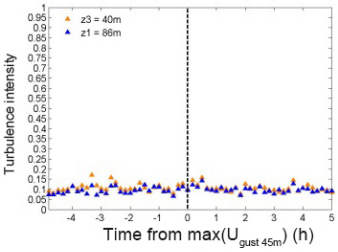


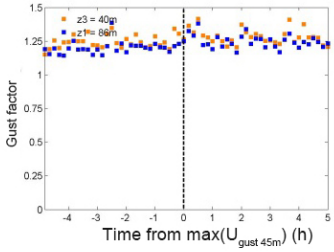
11 - Pintado 2008-04-24 to 2012-07-03. Event 20 with max($U_{gust\ 45m}$)= 19.1m/s on 2009-7-22 at 16:10. Series length: 48 months.

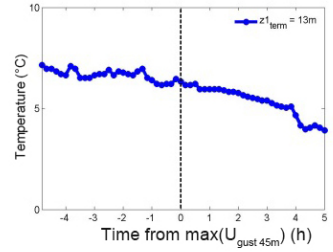


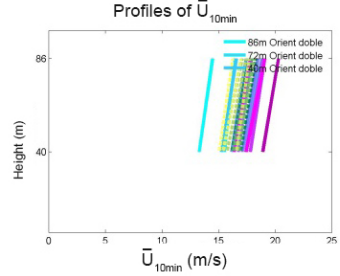


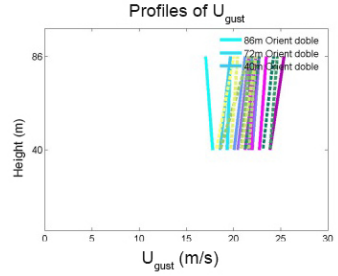


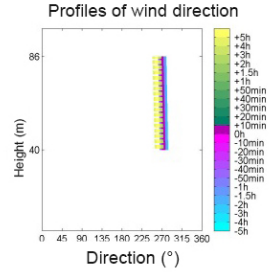




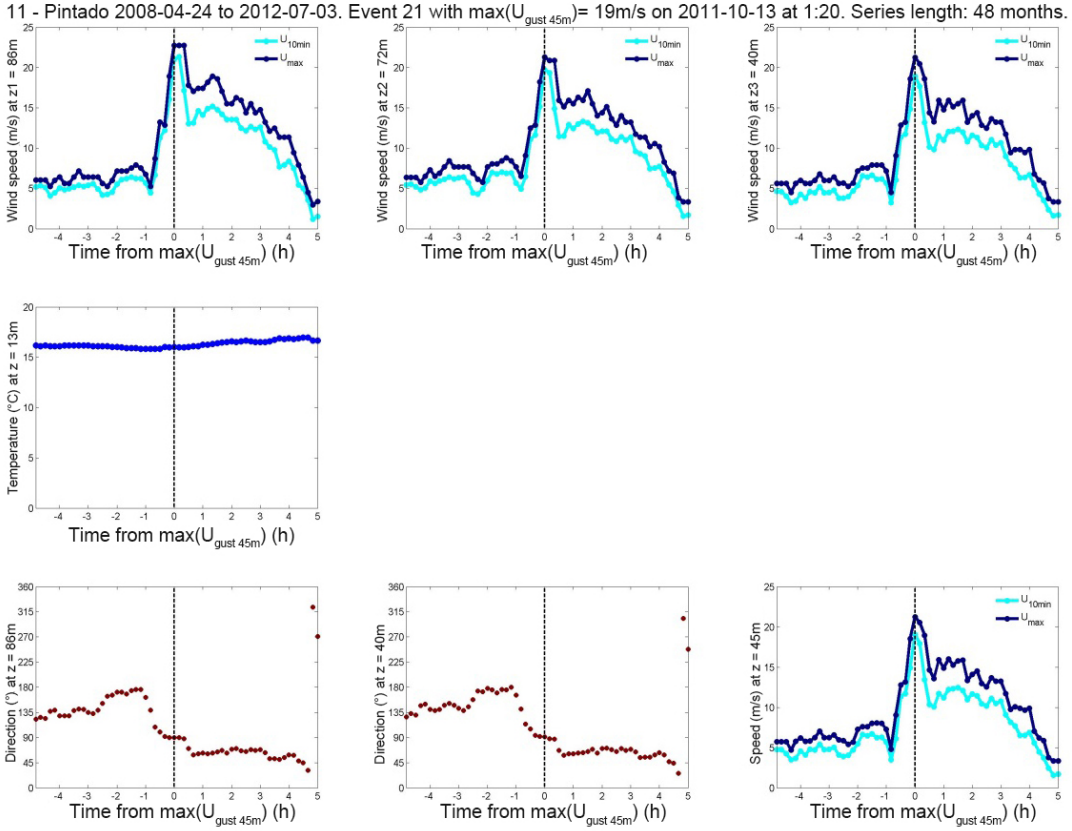




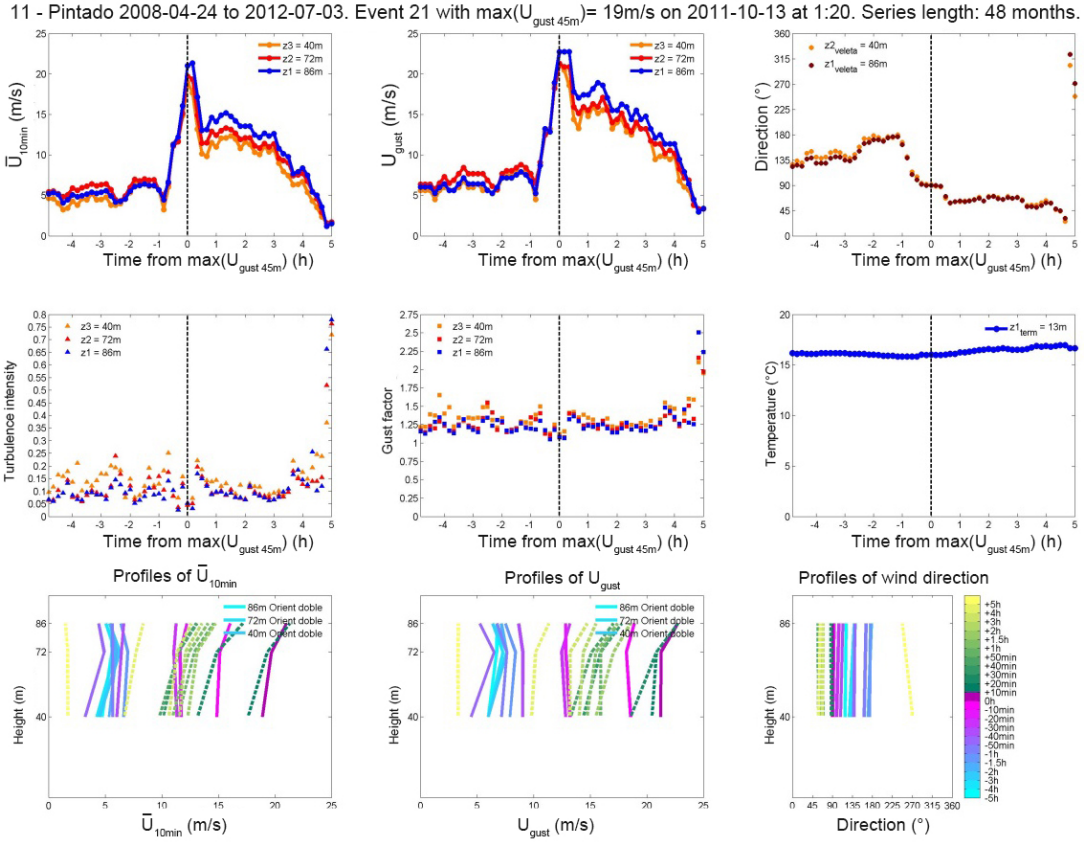


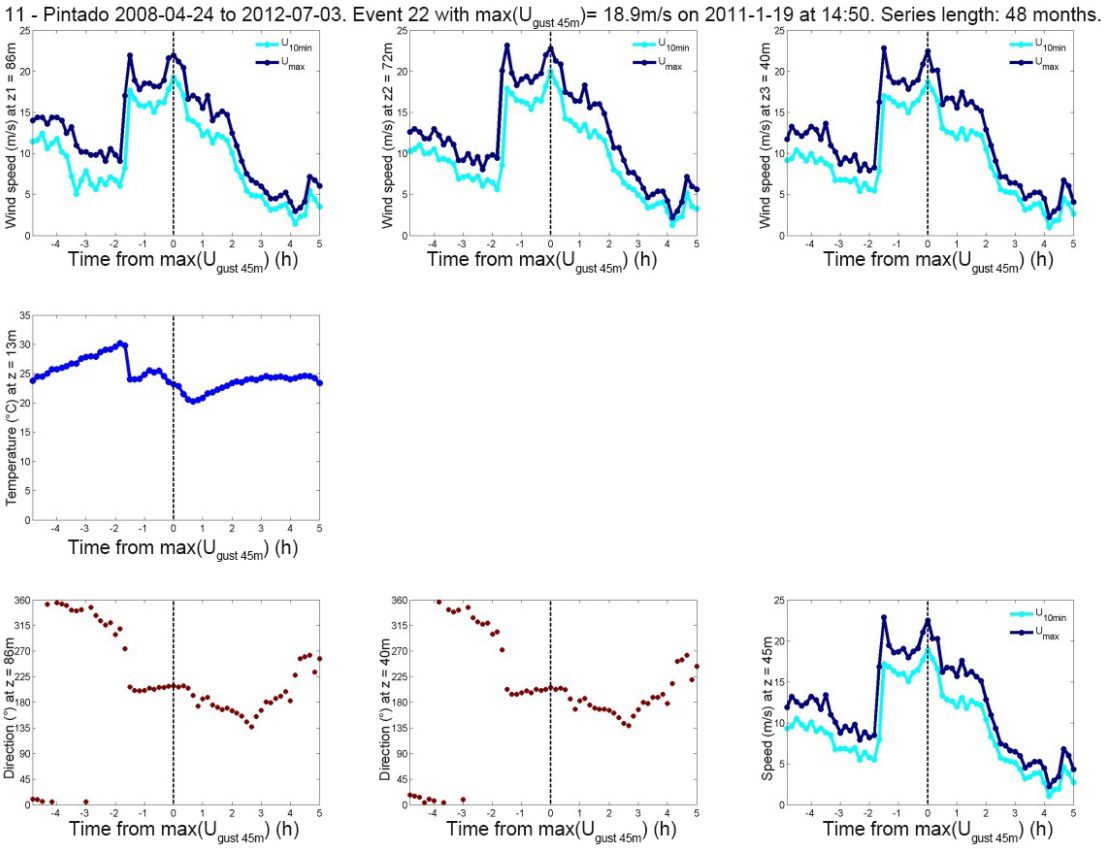


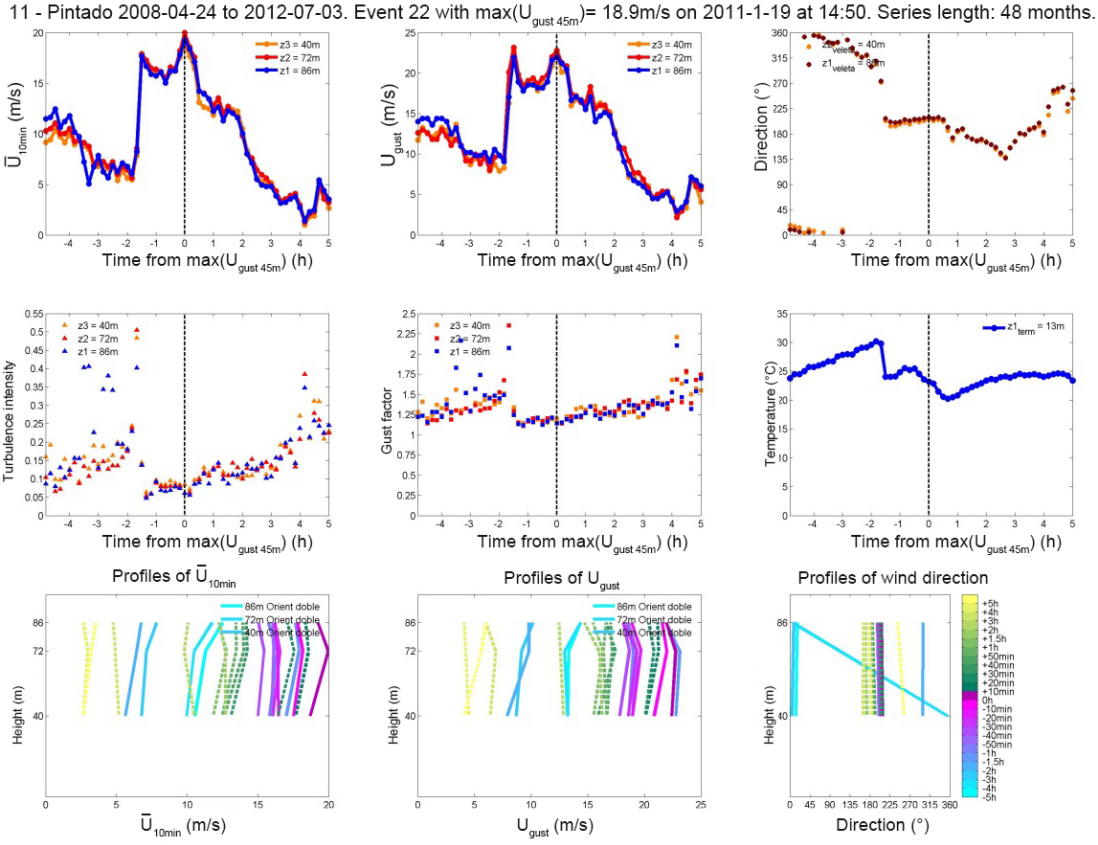
11 - Pintado 2008-04-24 to 2012-07-03. Event 21 with max($U_{gust\ 45m}$)= 19m/s on 2011-10-13 at 1:20. Series length: 48 months.



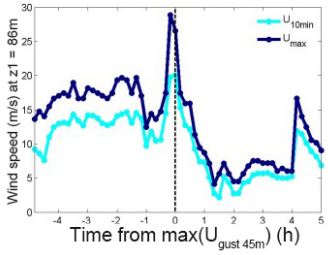
11 - Pintado 2008-04-24 to 2012-07-03. Event 21 with max($U_{gust\ 45m}$)= 19m/s on 2011-10-13 at 1:20. Series length: 48 months.

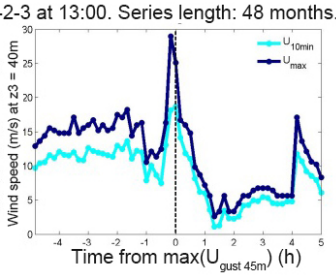


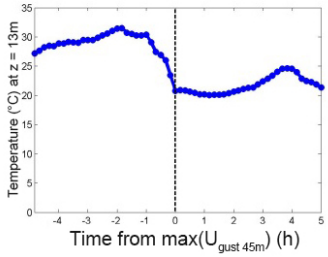

11 - Pintado 2008-04-24 to 2012-07-03. Event 22 with max(U gust 45m)= 18.9m/s on 2011-1-19 at 14:50. Series length: 48 months.
Wind speed (m/s) at z1 = 86m
Wind speed (m/s) at z2 = 72m
Wind speed (m/s) at z3 = 40m
U10min
Umax
Temperature (°C) at z = 13m
Direction (°) at z = 86m
Direction (°) at z = 40m
Speed (m/s) at z = 45m
Time from max(U gust 45m) (h)

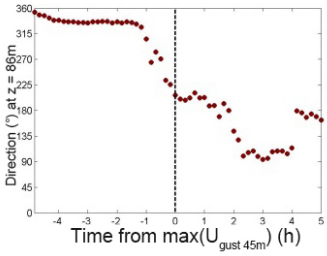

11 - Pintado 2008-04-24 to 2012-07-03. Event 22 with max(U gust 45m)= 18.9m/s on 2011-1-19 at 14:50. Series length: 48 months.
z3 = 40m
z2 = 72m
z1 = 86m
Turbulence intensity
Gust factor
Temperature (°C)
Direction (°)
Time from max(U gust 45m) (h)
Profiles of U10min
Profiles of Ugust
Profiles of wind direction
Height (m)
U10min (m/s)
Ugust (m/s)
86m Orient doble
72m Orient doble
40m Orient doble

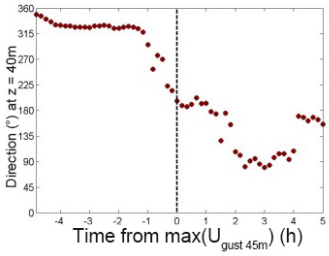
11 - Pintado 2008-04-24 to 2012-07-03. Event 23 with max($U_{gust\ 45m}$)= 18.9m/s on 2010-2-3 at 13:00. Series length: 48 months.

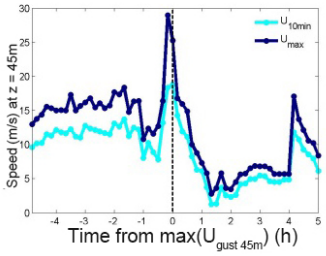




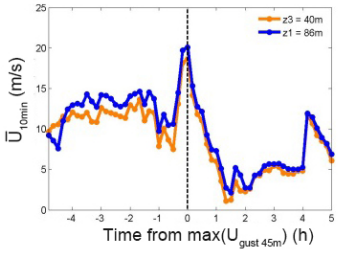


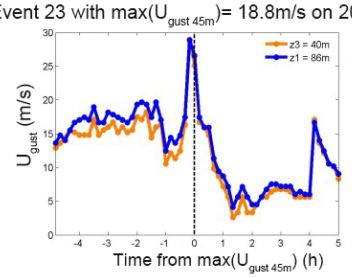


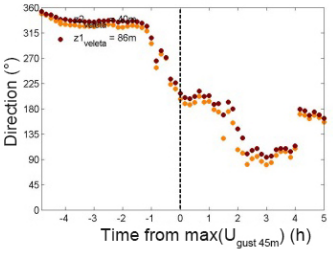


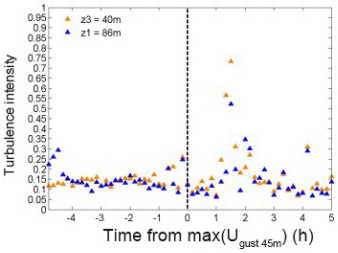


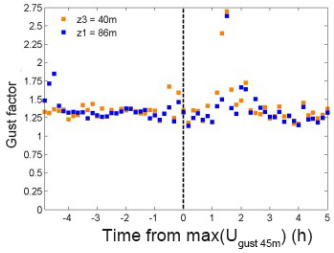
11 - Pintado 2008-04-24 to 2012-07-03. Event 23 with max($U_{gust\ 45m}$)= 18.8m/s on 2010-2-3 at 13:00. Series length: 48 months.

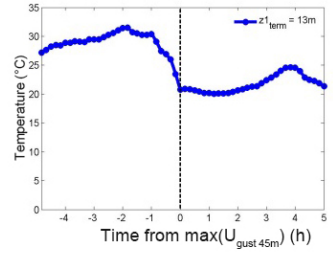


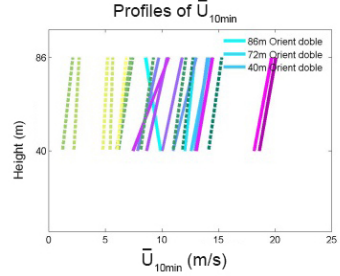


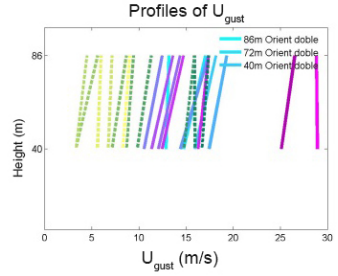


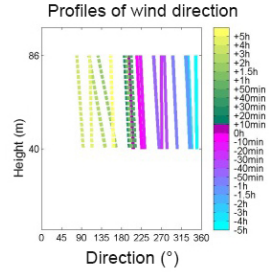




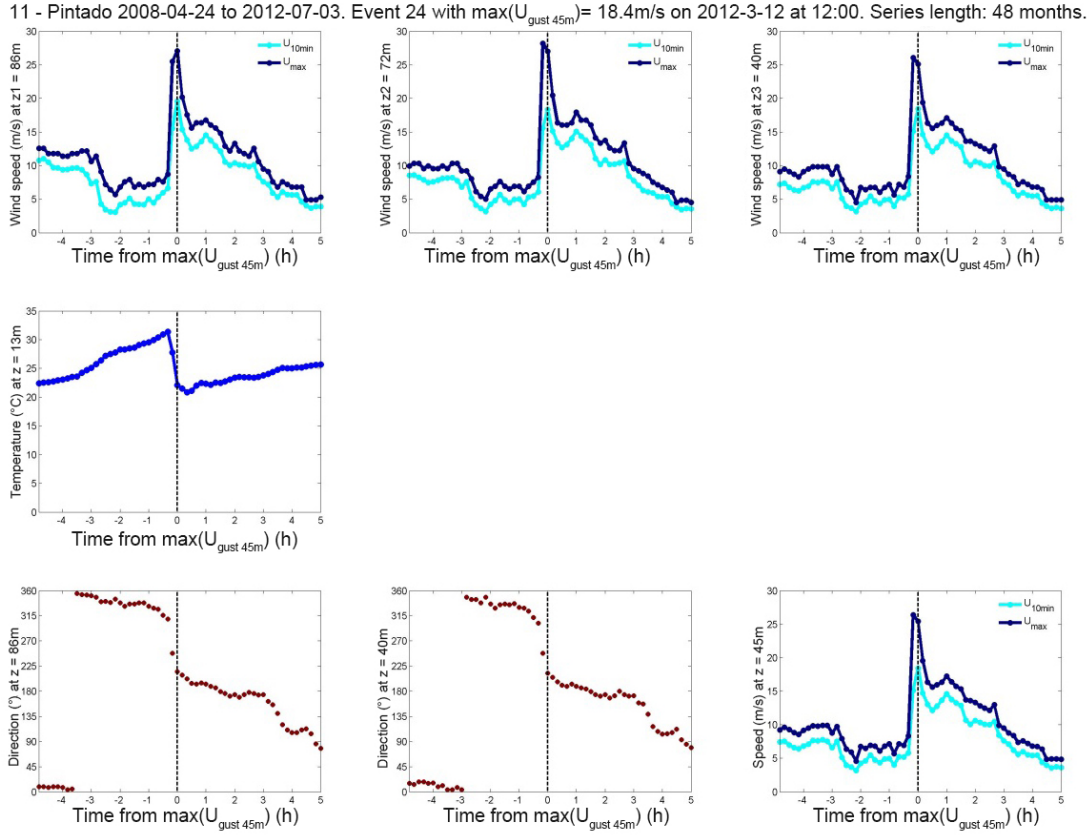




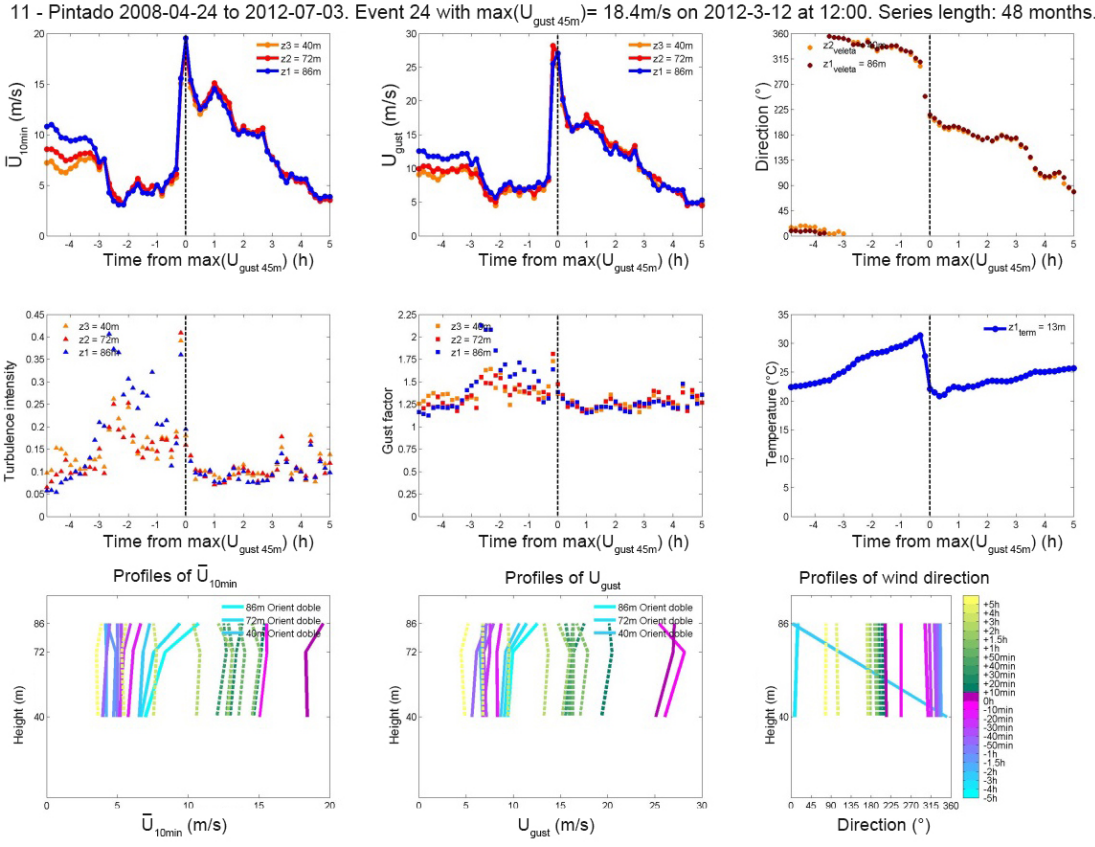




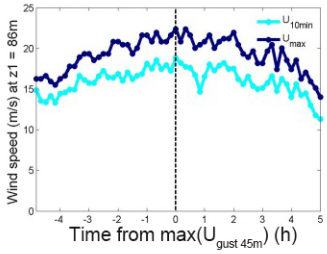
11 - Pintado 2008-04-24 to 2012-07-03. Event 24 with max($U_{gust\ 45m}$)= 18.4m/s on 2012-3-12 at 12:00. Series length: 48 months.

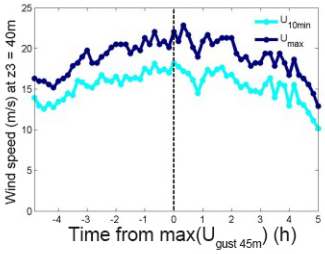


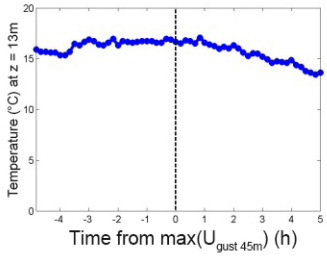
11 - Pintado 2008-04-24 to 2012-07-03. Event 24 with max($U_{gust\ 45m}$)= 18.4m/s on 2012-3-12 at 12:00. Series length: 48 months.

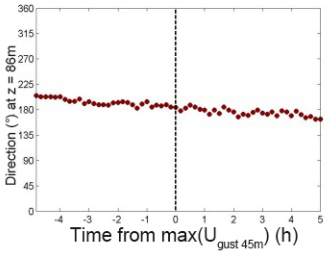


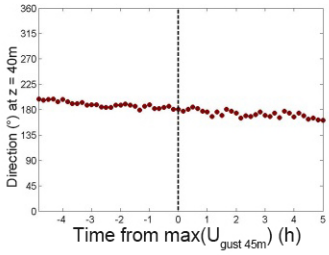
11 - Pintado 2008-04-24 to 2012-07-03. Event 25 with max($U_{gust\ 45m}$)= 18.2m/s on 2008-11-15 at 12:40. Series length: 48 months.

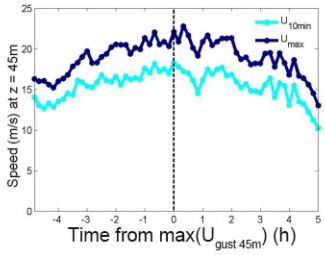




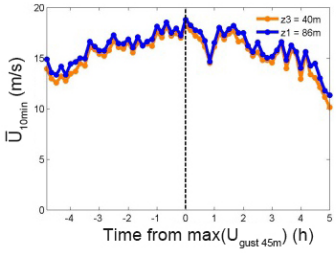


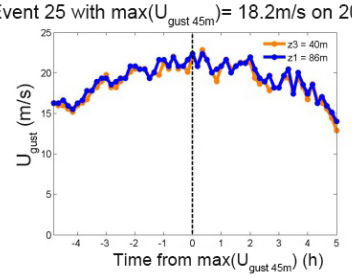


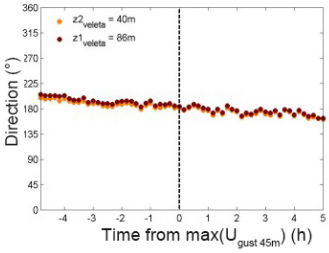


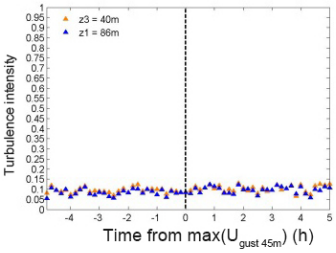


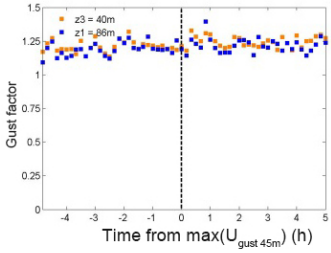
11 - Pintado 2008-04-24 to 2012-07-03. Event 25 with max($U_{gust\ 45m}$)= 18.2m/s on 2008-11-15 at 12:40. Series length: 48 months.

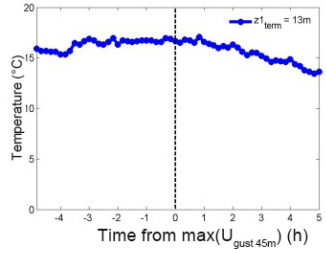


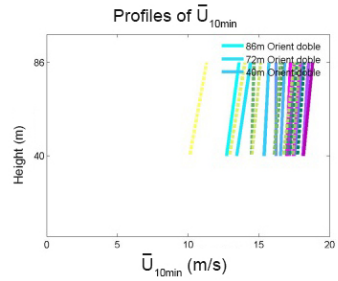


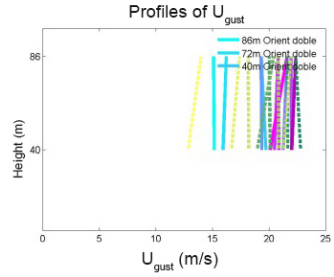


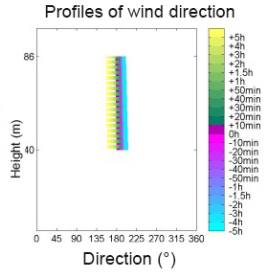


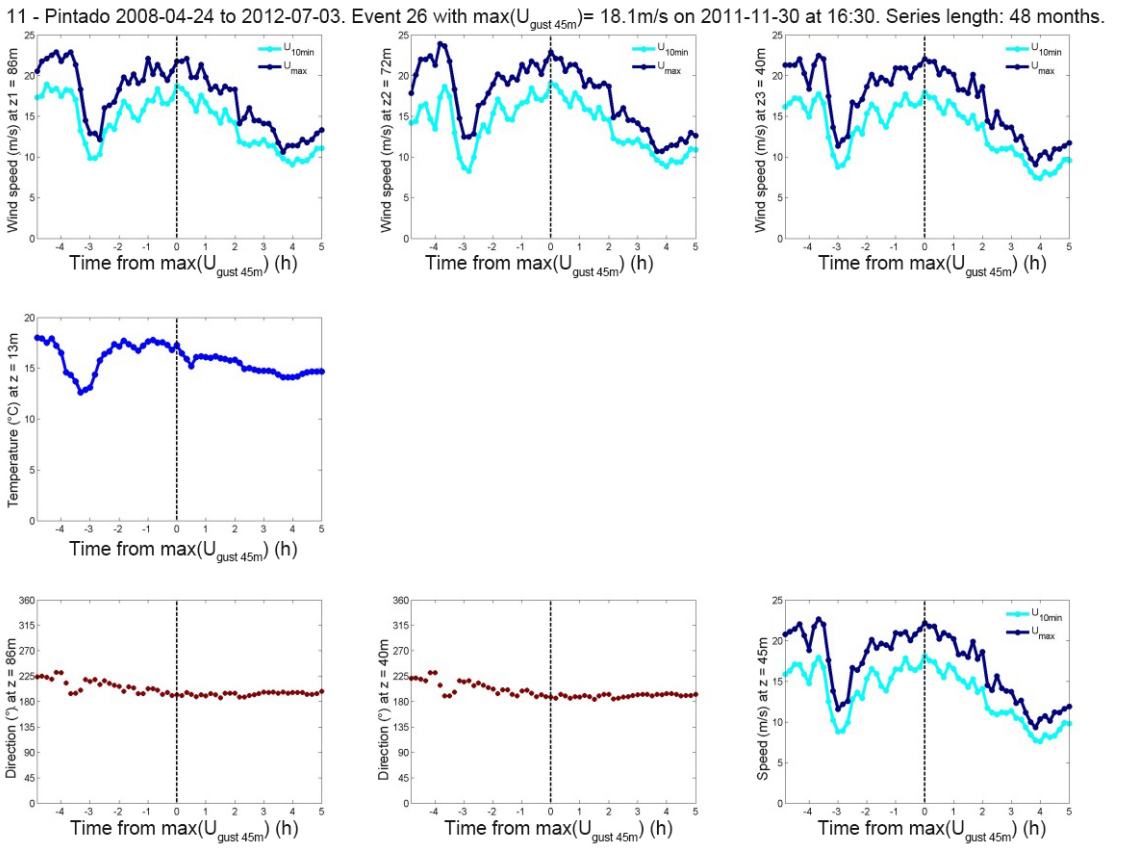


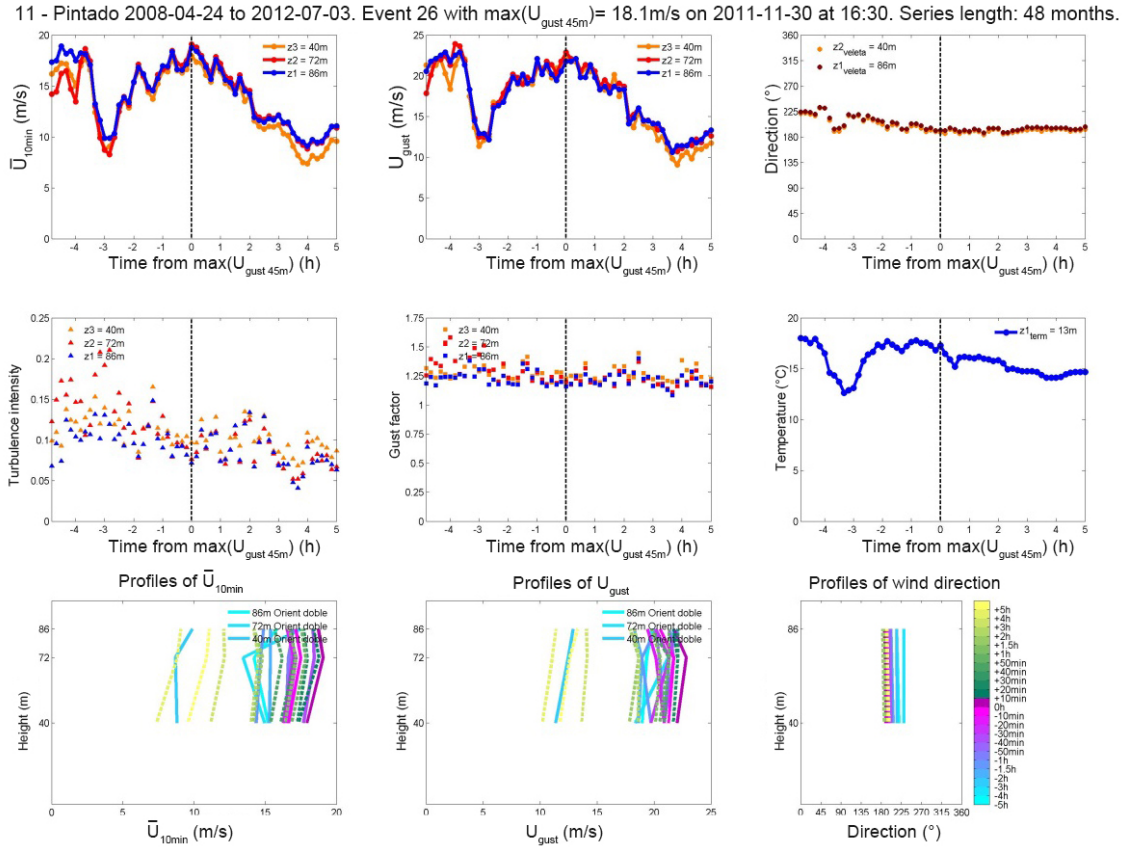




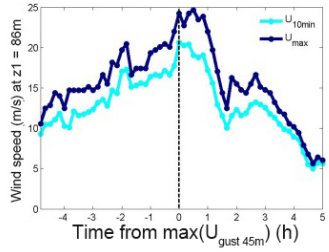


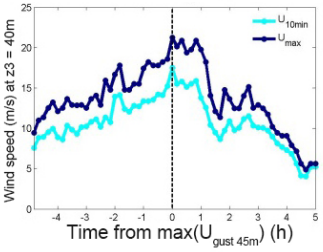


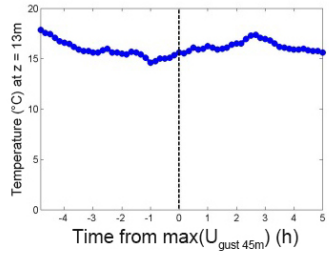

11 - Pintado 2008-04-24 to 2012-07-03. Event 26 with max(U gust 45m)= 18.1m/s on 2011-11-30 at 16:30. Series length: 48 months.
Wind speed (m/s) at z1 = 86m
Wind speed (m/s) at z2 = 72m
Wind speed (m/s) at z3 = 40m
U10min
Umax
Temperature (°C) at z = 13m
Direction (°) at z = 86m
Direction (°) at z = 40m
Speed (m/s) at z = 45m
Time from max(U gust 45m) (h)

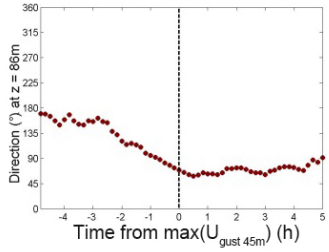

11 - Pintado 2008-04-24 to 2012-07-03. Event 26 with max(U gust 45m)= 18.1m/s on 2011-11-30 at 16:30. Series length: 48 months.
z3 = 40m
z2 = 72m
z1 = 86m
Direction (°)
Turbulence intensity
Gust factor
Temperature (°C)
Time from max(U gust 45m) (h)
Profiles of U10min
Profiles of U gust
Profiles of wind direction
Height (m)
86m Orient doble
72m Orient doble
40m Orient doble
U10min (m/s)
U gust (m/s)
Direction (°)

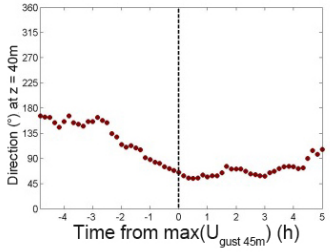
11 - Pintado 2008-04-24 to 2012-07-03. Event 27 with max($U_{gust\ 45m}$)= 17.9m/s on 2009-11-27 at 21:20. Series length: 48 months.

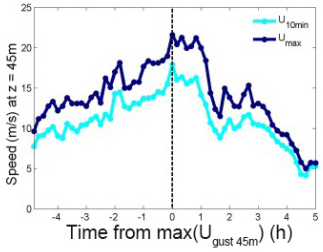




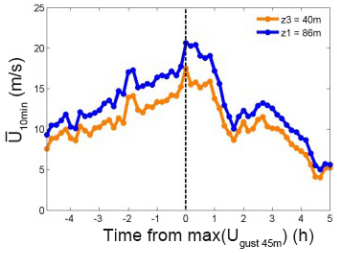


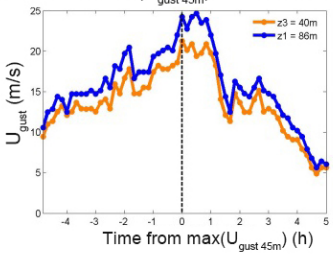


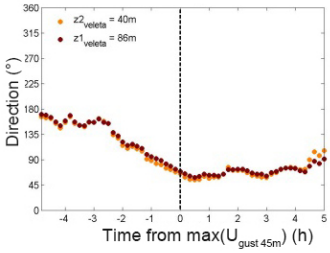


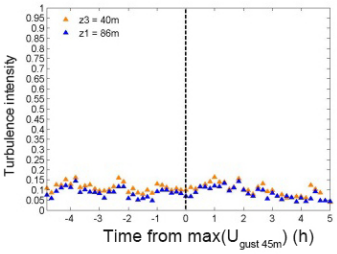


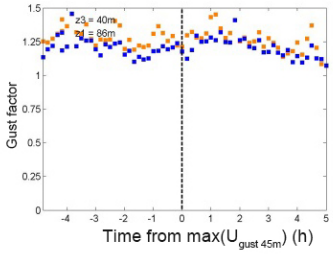
11 - Pintado 2008-04-24 to 2012-07-03. Event 27 with max($U_{gust\ 45m}$)= 17.9m/s on 2009-11-27 at 21:20. Series length: 48 months.

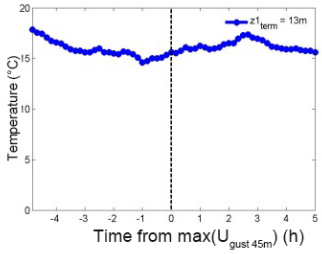


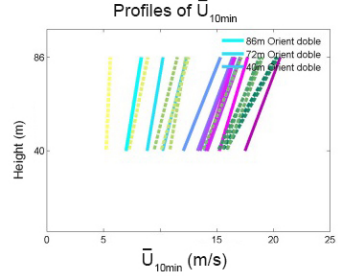


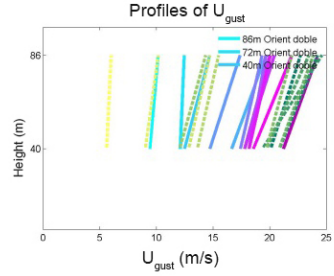


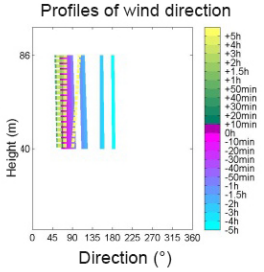


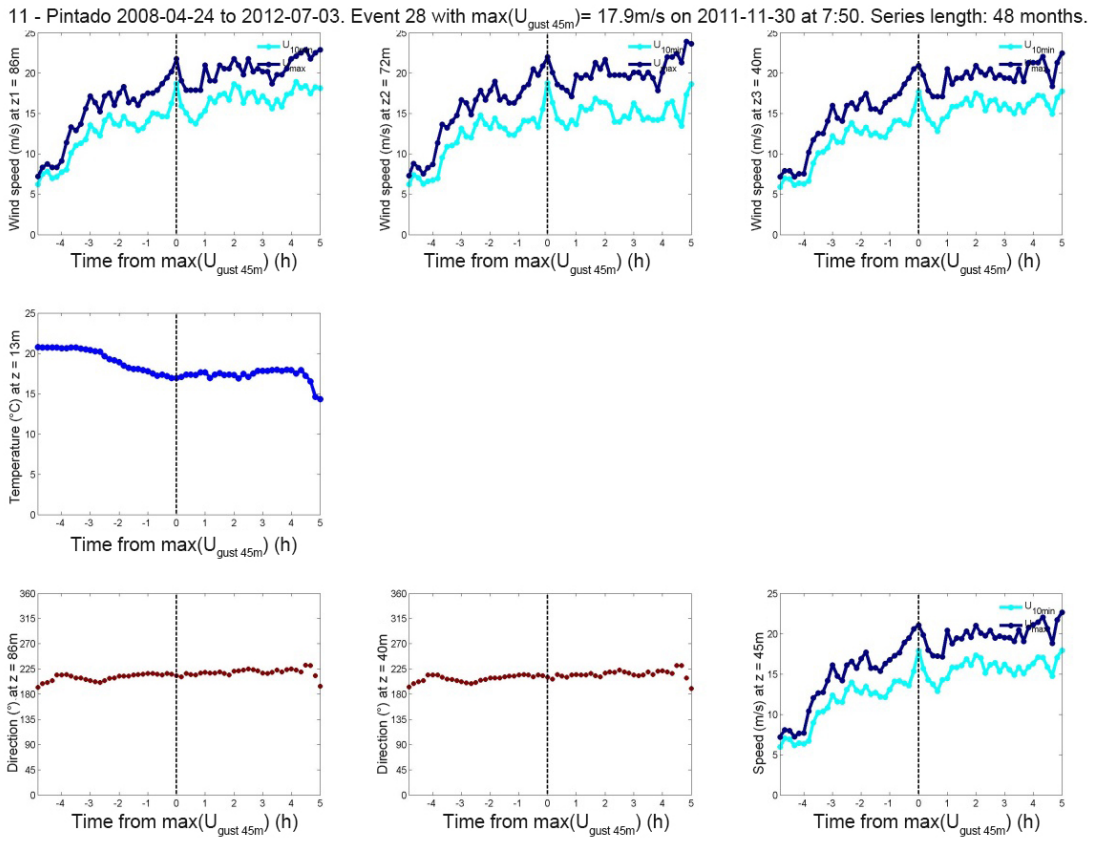


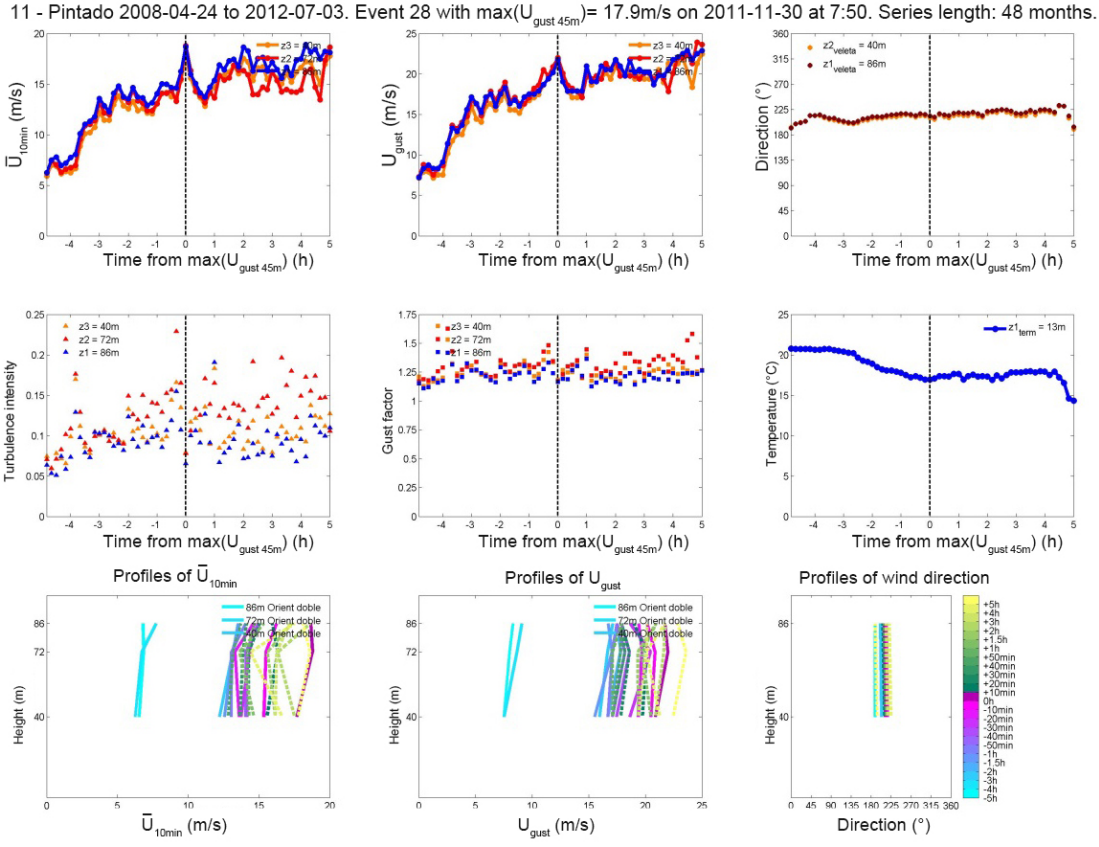




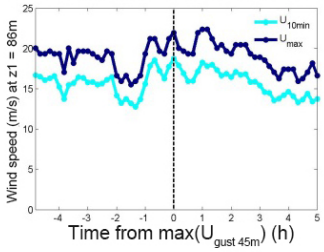


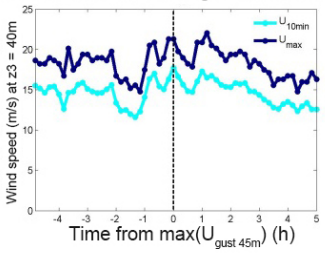


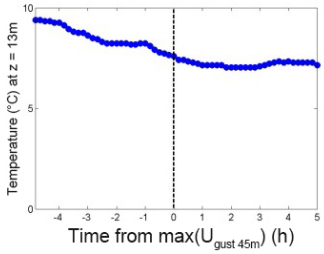

11 - Pintado 2008-04-24 to 2012-07-03. Event 28 with max(U gust 45m)= 17.9m/s on 2011-11-30 at 7:50. Series length: 48 months.
Wind speed (m/s) at z1 = 86m
Wind speed (m/s) at z2 = 72m
Wind speed (m/s) at z3 = 40m
Temperature (°C) at z = 13m
Direction (°) at z = 86m
Direction (°) at z = 40m
Speed (m/s) at z = 45m
Time from max(U gust 45m) (h)

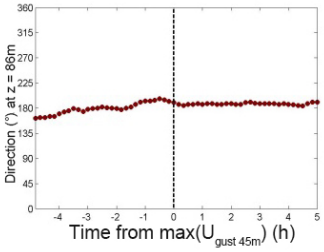

11 - Pintado 2008-04-24 to 2012-07-03. Event 28 with max(U gust 45m)= 17.9m/s on 2011-11-30 at 7:50. Series length: 48 months.
Ū 10min (m/s)
U gust (m/s)
Direction (°)
Turbulence intensity
Gust factor
Temperature (°C)
Time from max(U gust 45m) (h)
Profiles of Ū 10min
Profiles of U gust
Profiles of wind direction
Height (m)
Ū 10min (m/s)
U gust (m/s)
Direction (°)

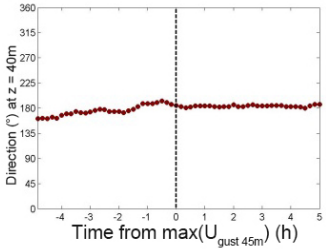
11 - Pintado 2008-04-24 to 2012-07-03. Event 29 with max($U_{gust\ 45m}$)= 17.8m/s on 2010-8-13 at 1:30. Series length: 48 months.

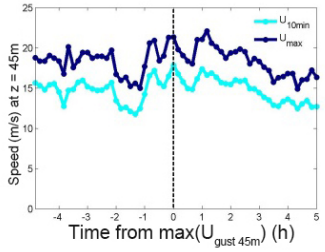




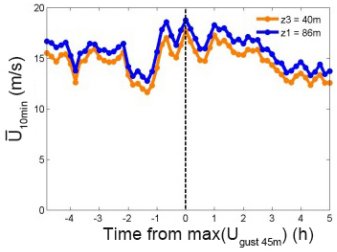


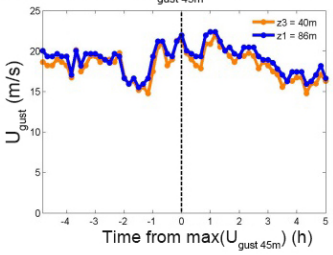


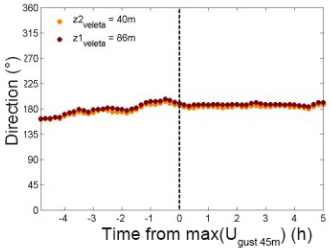


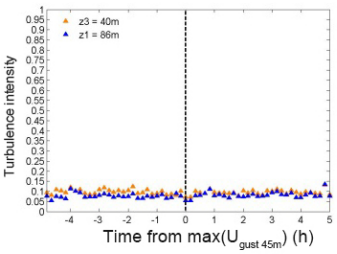


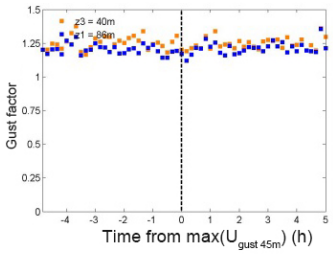
11 - Pintado 2008-04-24 to 2012-07-03. Event 29 with max($U_{gust\ 45m}$)= 17.8m/s on 2010-8-13 at 1:30. Series length: 48 months.

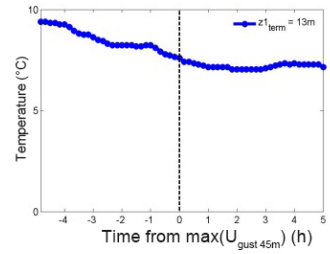


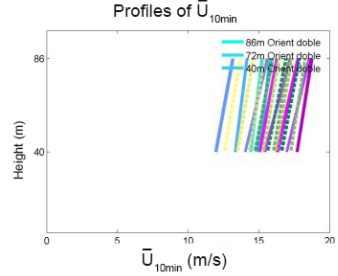


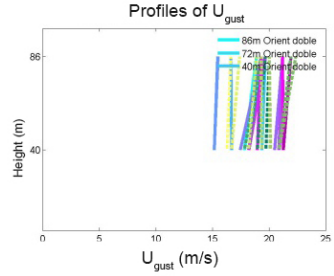


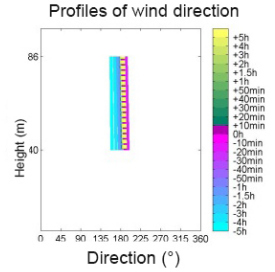




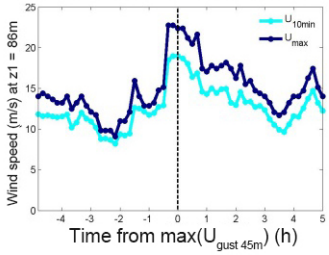


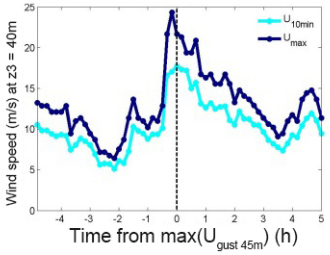


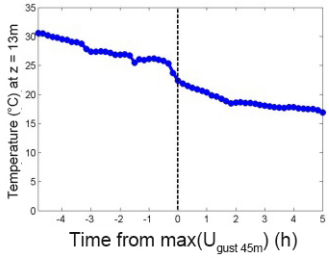


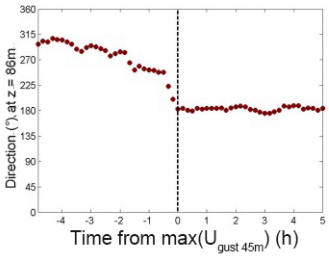


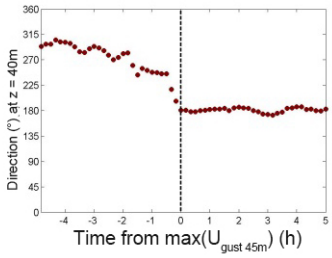
11 - Pintado 2008-04-24 to 2012-07-03. Event 29 with max($U_{gust\ 45m}$)= 17.8m/s on 2010-8-13 at 1:30. Series length: 48 months.

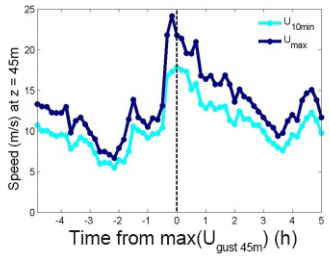




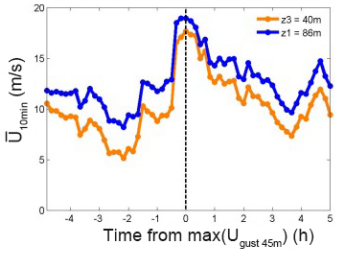


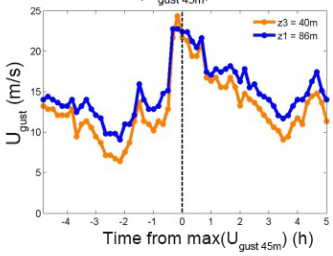


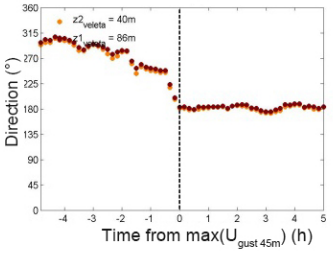


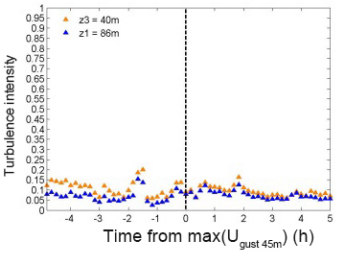


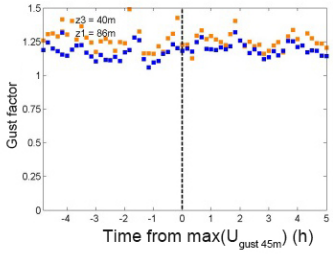
11 - Pintado 2008-04-24 to 2012-07-03. Event 30 with max($U_{gust\ 45m}$)= 17.8m/s on 2009-3-14 at 21:10. Series length: 48 months.

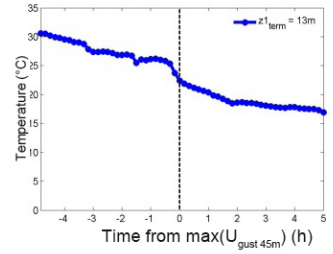


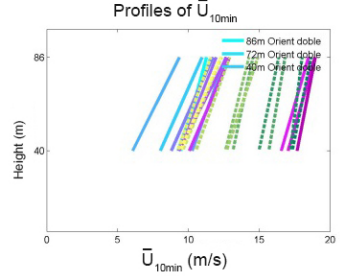


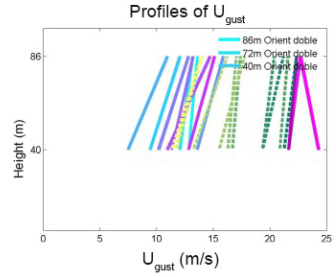


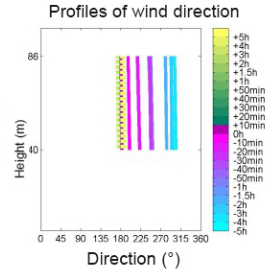




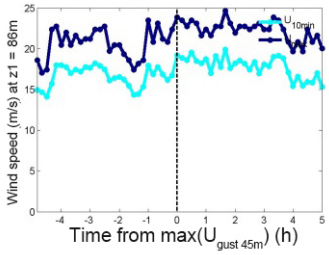


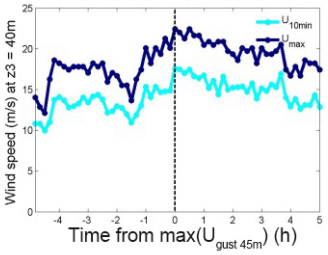


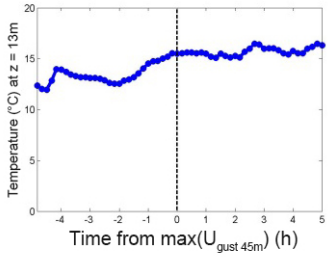


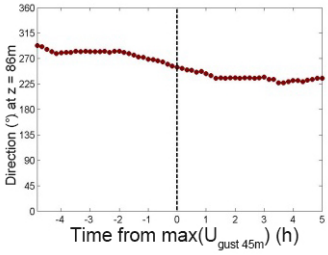


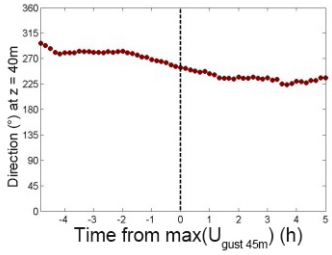
11 - Pintado 2008-04-24 to 2012-07-03. Event 31 with max($U_{gust\ 45m}$)= 17.7m/s on 2010-10-31 at 8:10. Series length: 48 months.

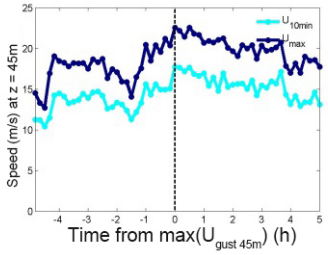




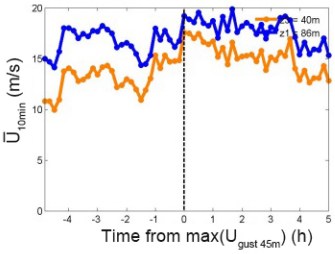


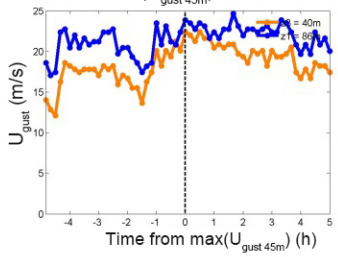


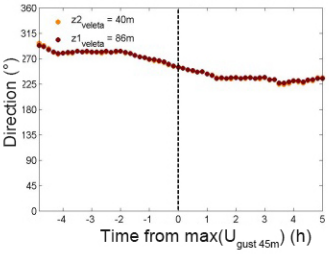


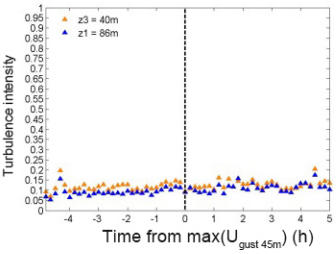


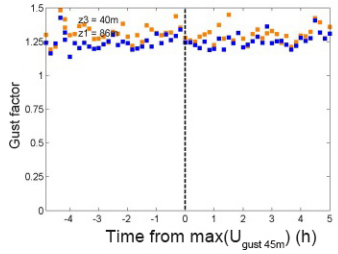
11 - Pintado 2008-04-24 to 2012-07-03. Event 31 with max($U_{gust\ 45m}$)= 17.7m/s on 2010-10-31 at 8:10. Series length: 48 months.

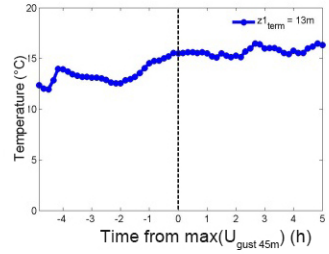


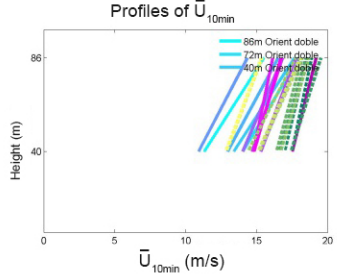


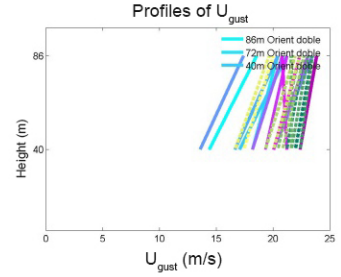


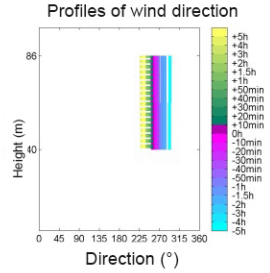




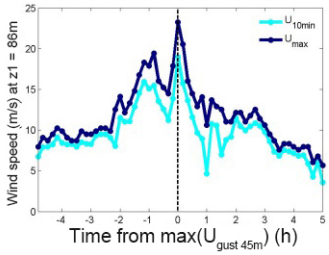


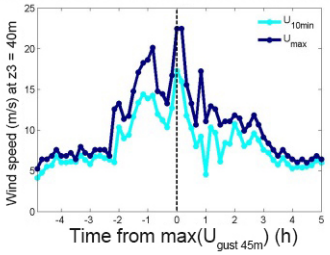


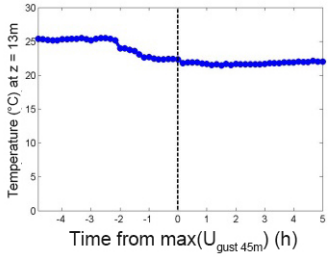


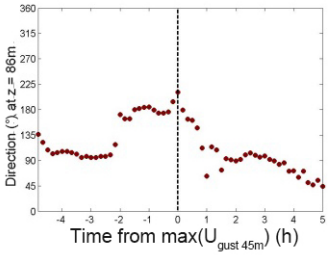


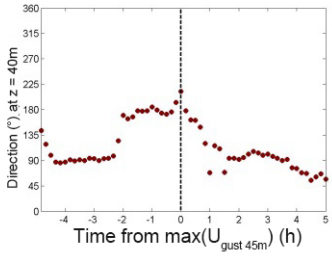
11 - Pintado 2008-04-24 to 2012-07-03. Event 32 with max($U_{gust\ 45m}$)= 17.4m/s on 2012-2-17 at 0:10. Series length: 48 months.

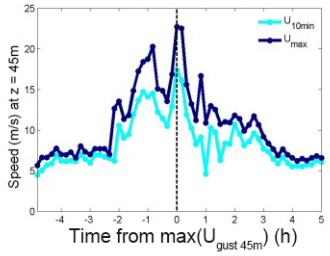




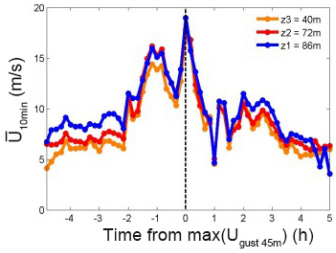


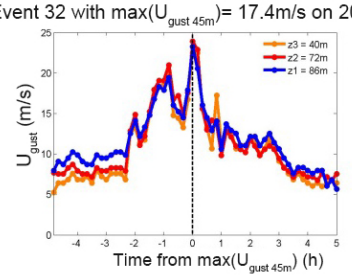


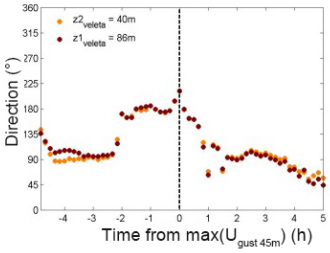


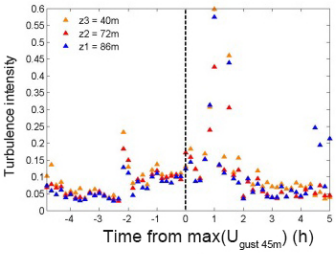


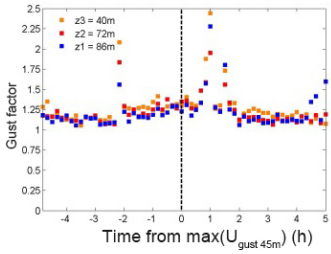
11 - Pintado 2008-04-24 to 2012-07-03. Event 32 with max($U_{gust\ 45m}$)= 17.4m/s on 2012-2-17 at 0:10. Series length: 48 months.

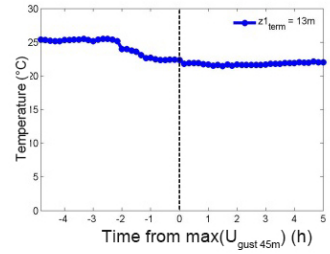


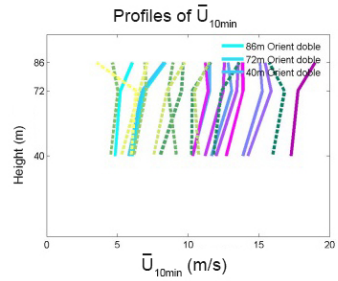


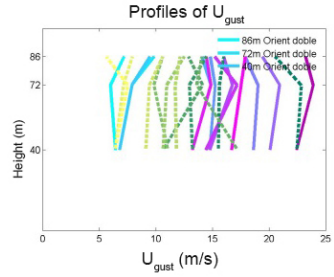


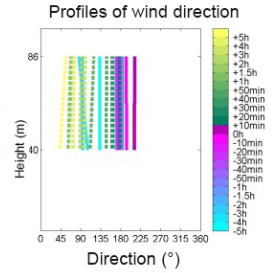




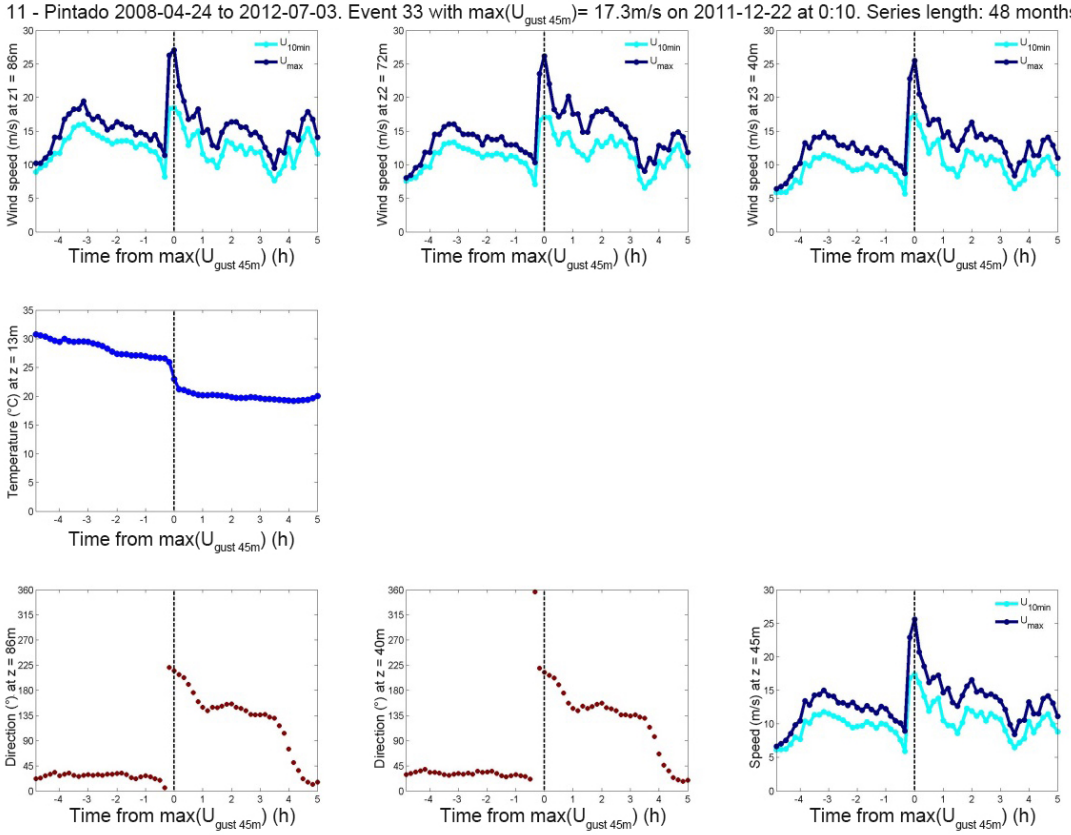




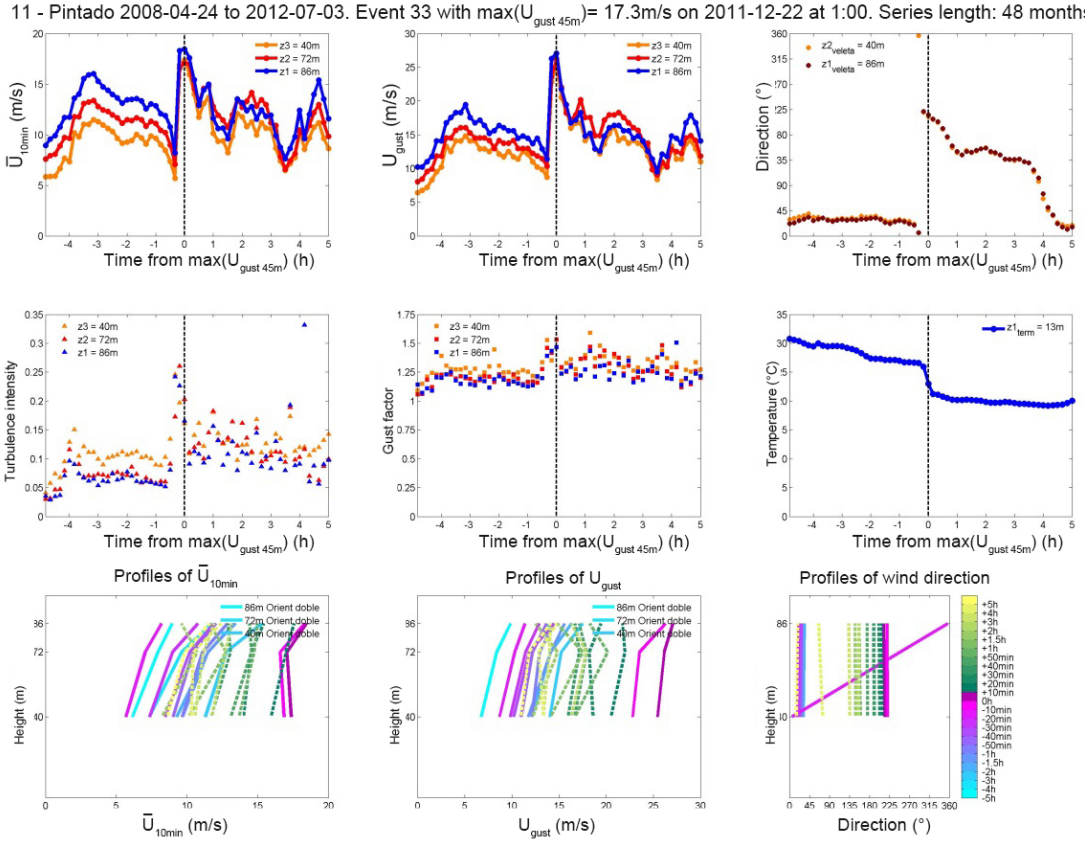




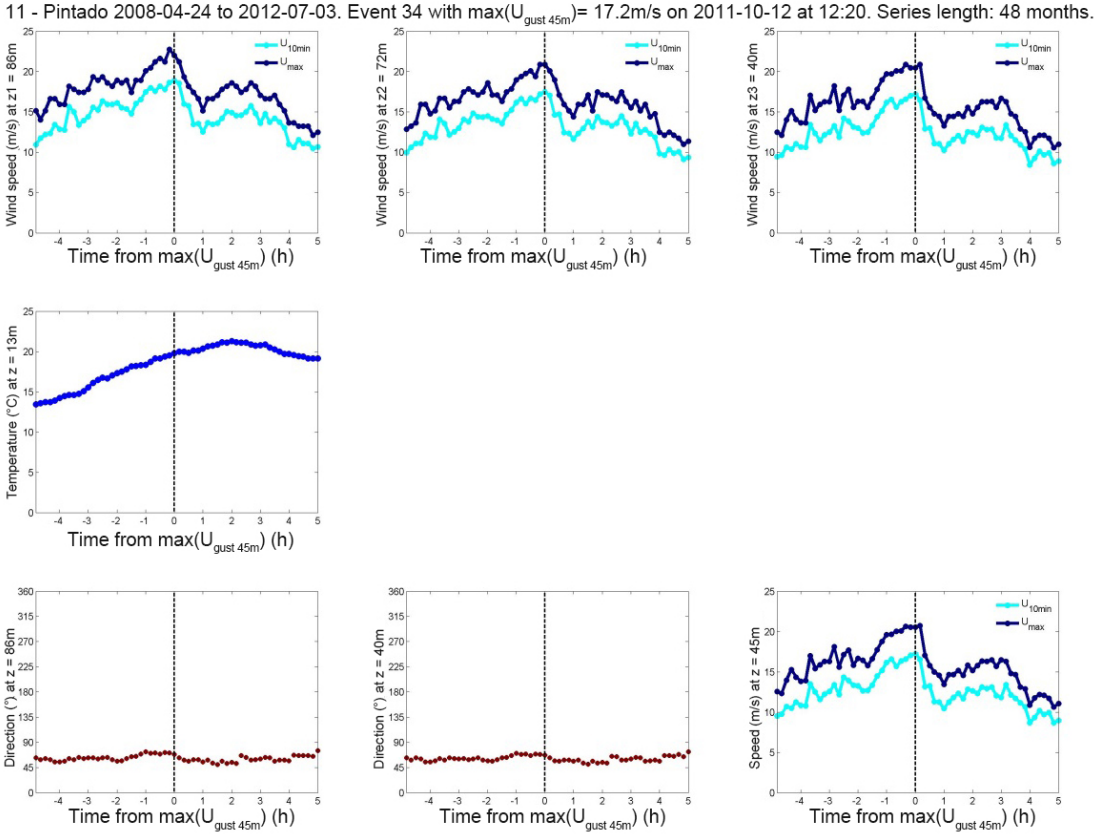
11 - Pintado 2008-04-24 to 2012-07-03. Event 33 with max($U_{gust\ 45m}$)= 17.3m/s on 2011-12-22 at 0:10. Series length: 48 months.



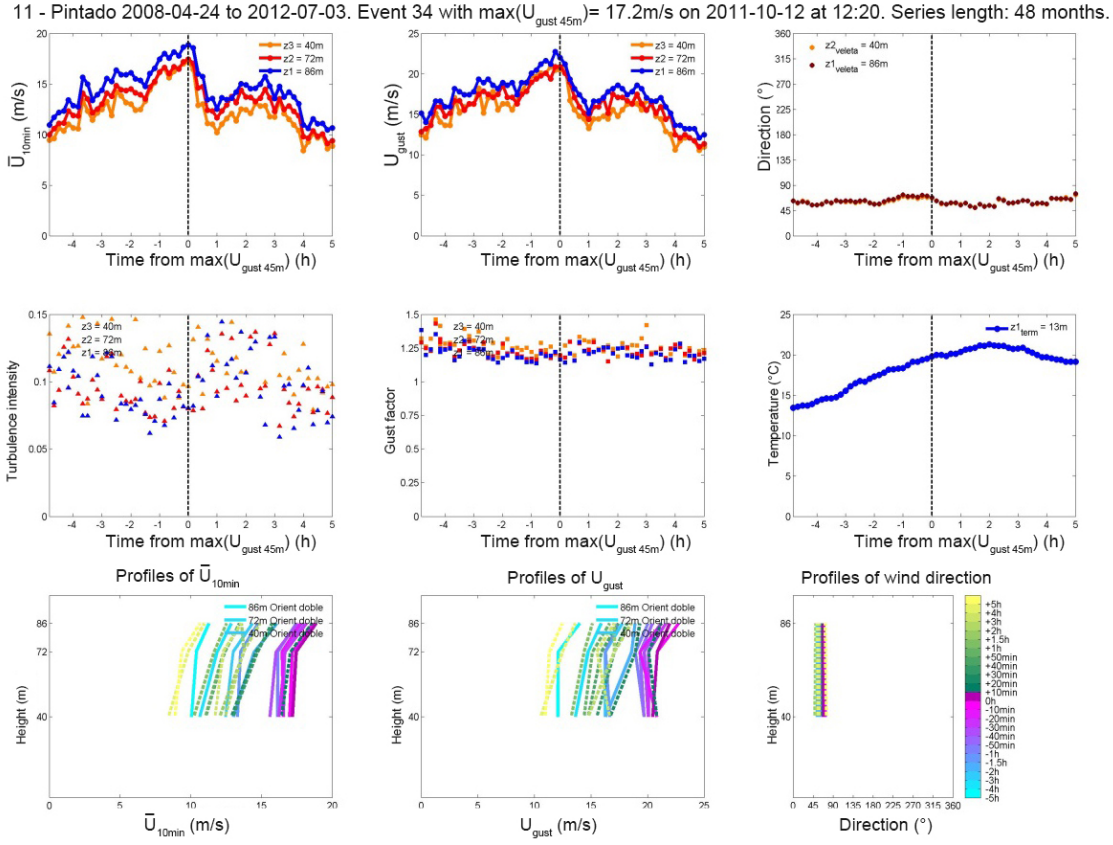
11 - Pintado 2008-04-24 to 2012-07-03. Event 33 with max($U_{gust\ 45m}$)= 17.3m/s on 2011-12-22 at 1:00. Series length: 48 months.



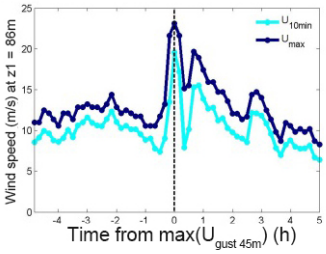
11 - Pintado 2008-04-24 to 2012-07-03. Event 34 with max($U_{gust\ 45m}$)= 17.2m/s on 2011-10-12 at 12:20. Series length: 48 months.

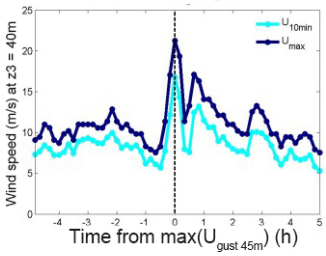


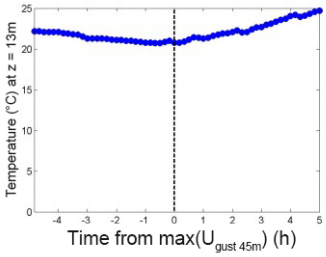
11 - Pintado 2008-04-24 to 2012-07-03. Event 34 with max($U_{gust\ 45m}$)= 17.2m/s on 2011-10-12 at 12:20. Series length: 48 months.

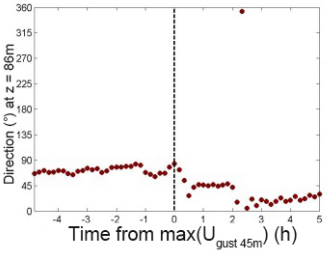


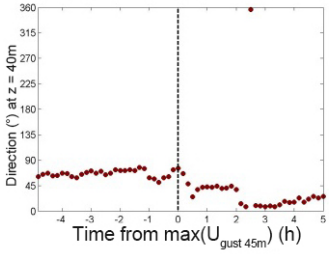
11 - Pintado 2008-04-24 to 2012-07-03. Event 35 with max($U_{gust\ 45m}$)= 17.1m/s on 2009-12-23 at 8:50. Series length: 48 months.

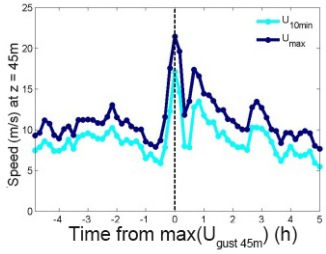




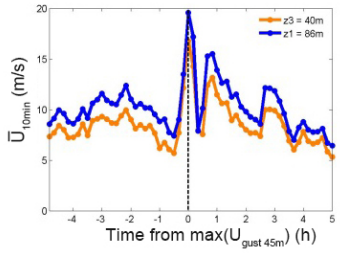


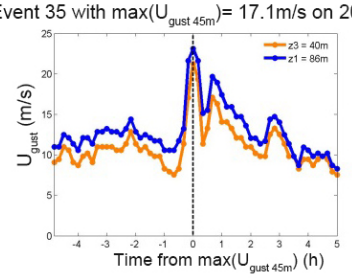


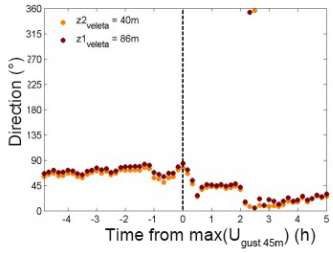


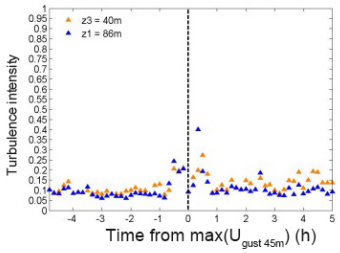


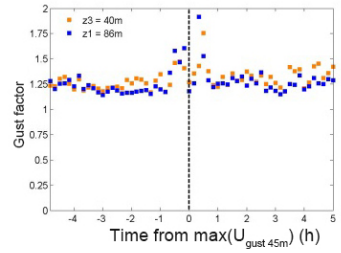
11 - Pintado 2008-04-24 to 2012-07-03. Event 35 with max($U_{gust\ 45m}$)= 17.1m/s on 2009-12-23 at 8:50. Series length: 48 months.

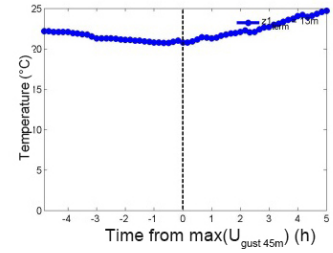




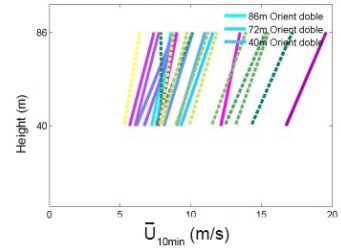




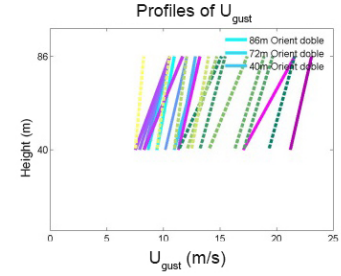




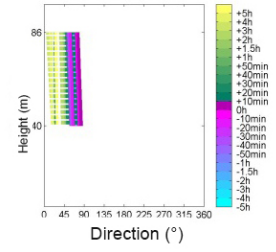
Profiles of $\bar{U}_{10min}$



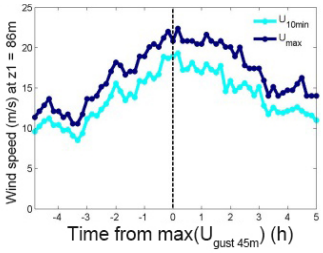
Profiles of U_{gust}

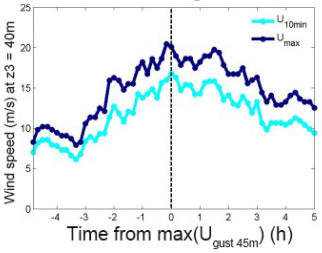


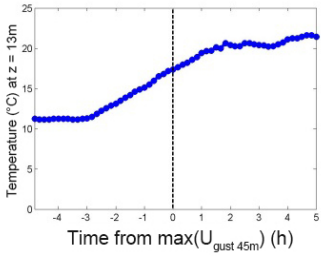
Profiles of wind direction

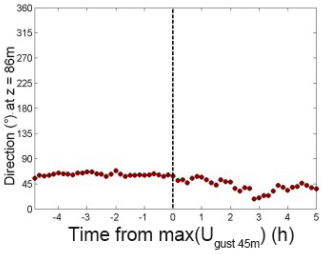


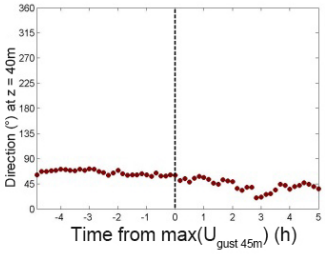
11 - Pintado 2008-04-24 to 2012-07-03. Event 36 with max($U_{gust\ 45m}$)= 17m/s on 2010-10-29 at 9:10. Series length: 48 months.

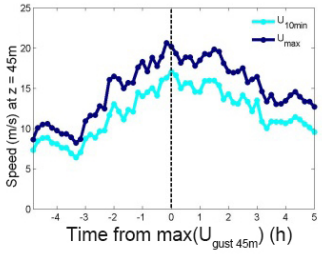




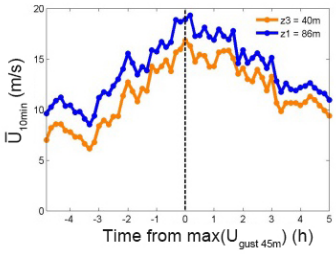


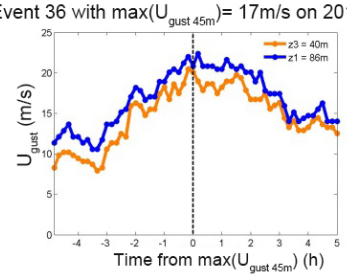


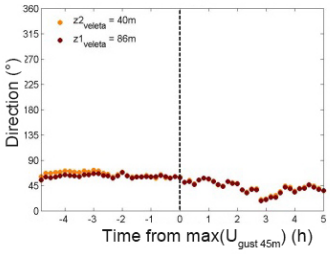


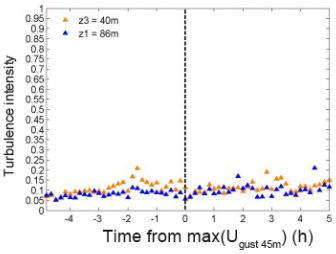


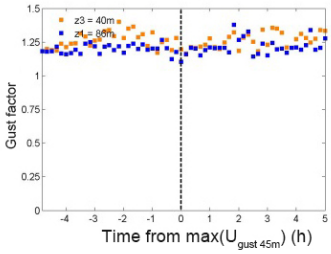
11 - Pintado 2008-04-24 to 2012-07-03. Event 36 with max($U_{gust\ 45m}$)= 17m/s on 2010-10-29 at 9:10. Series length: 48 months.

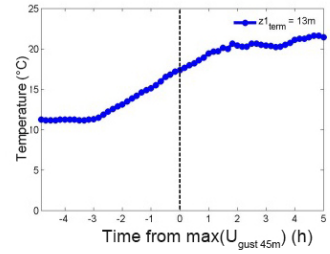


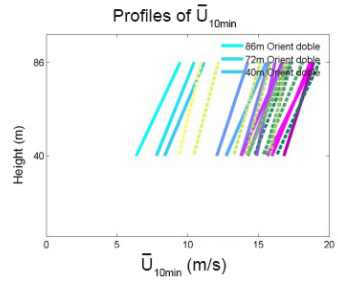


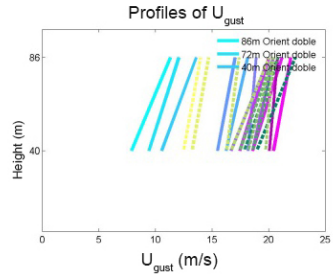


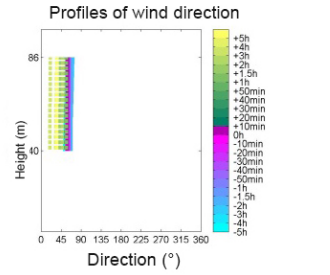




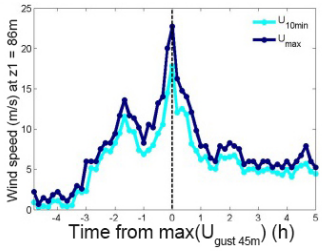


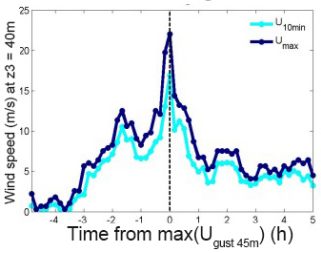


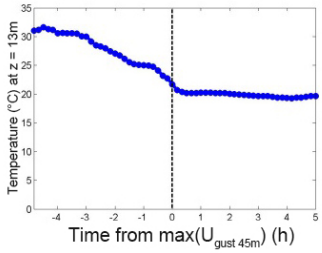


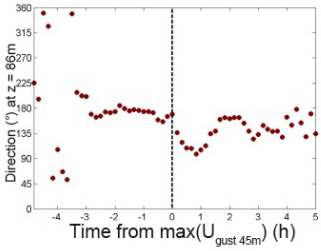


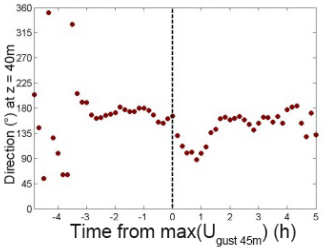
11 - Pintado 2008-04-24 to 2012-07-03. Event 37 with max($U_{gust\ 45m}$)= 17m/s on 2009-11-25 at 21:20. Series length: 48 months.

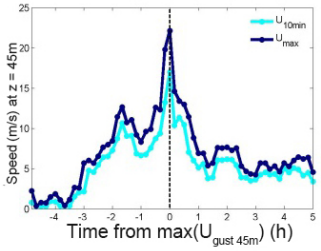




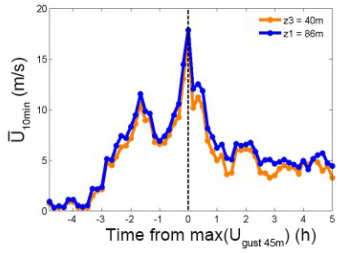


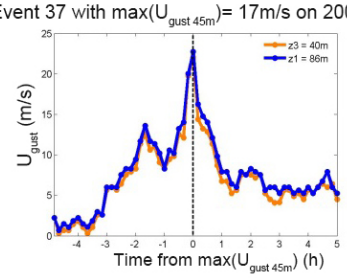


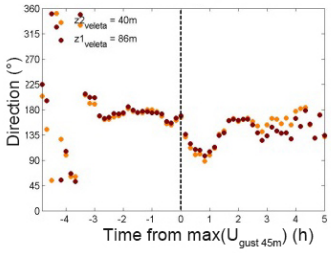


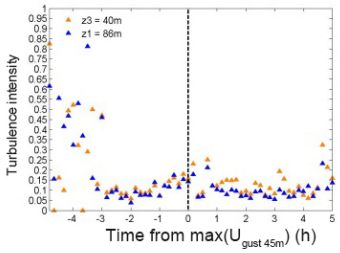


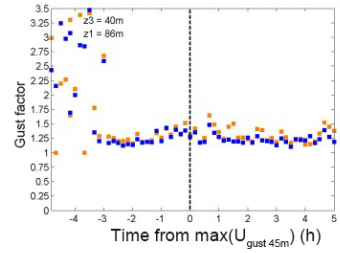
11 - Pintado 2008-04-24 to 2012-07-03. Event 37 with max($U_{gust\ 45m}$)= 17m/s on 2009-11-25 at 21:20. Series length: 48 months.

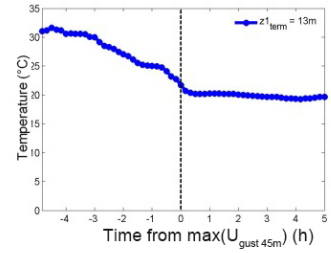


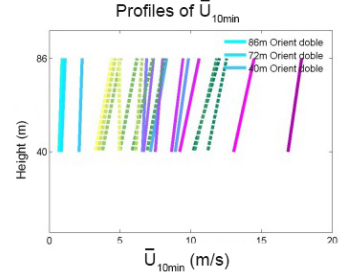


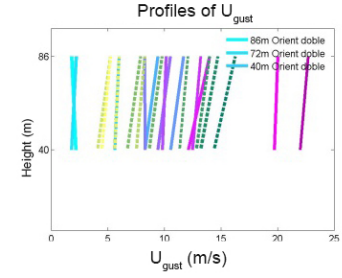


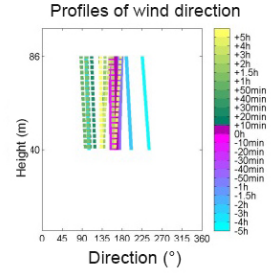




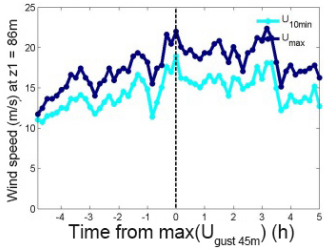


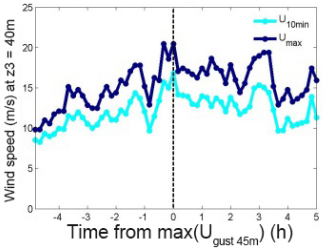


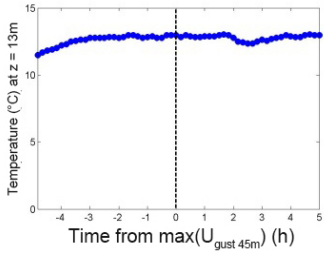


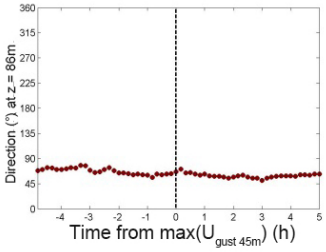


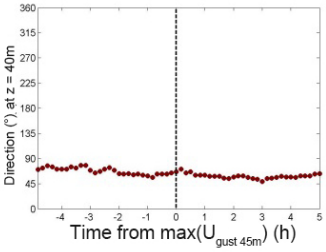
11 - Pintado 2008-04-24 to 2012-07-03. Event 38 with max($U_{gust\ 45m}$)= 17m/s on 2006-2-28 at 23:40. Series length: 48 months.

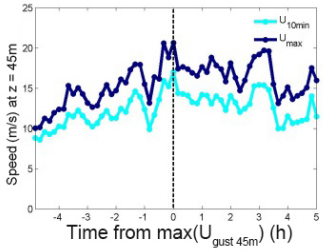




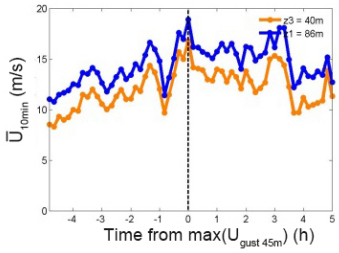


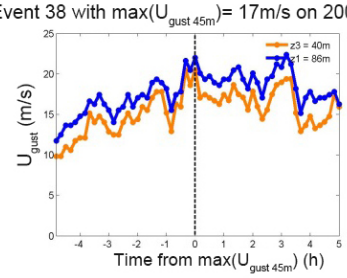


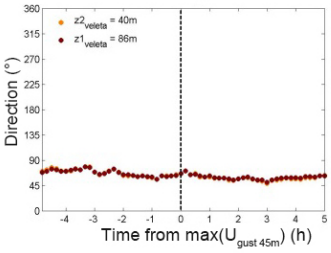


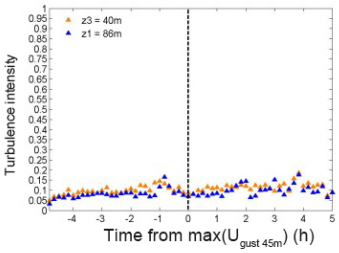


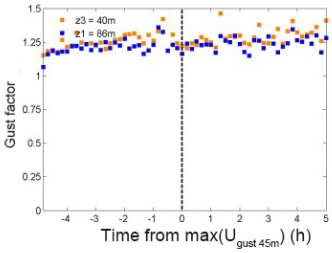
11 - Pintado 2008-04-24 to 2012-07-03. Event 38 with max($U_{gust\ 45m}$)= 17m/s on 2009-6-28 at 23:40. Series length: 48 months.

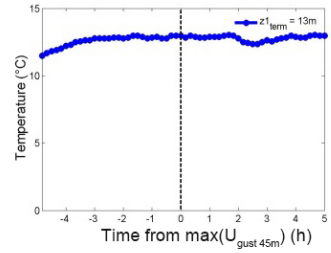




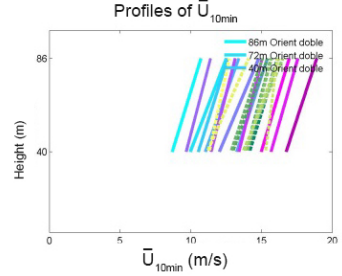




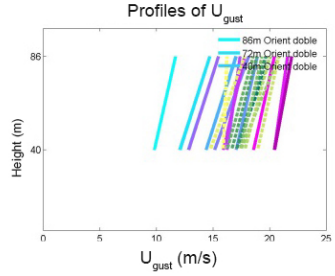




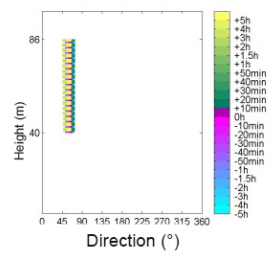
Profiles of $\bar{U}_{10min}$



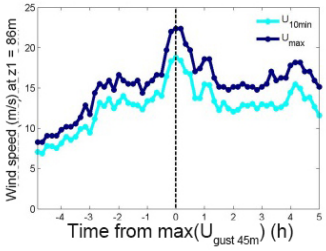
Profiles of U_{gust}

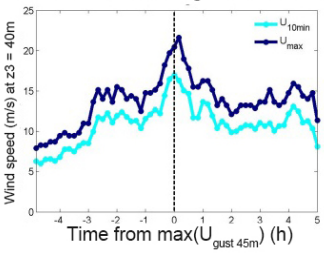


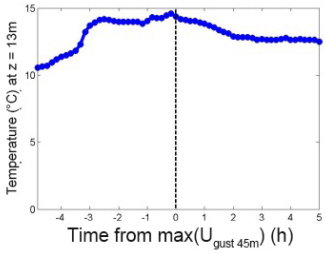
Profiles of wind direction

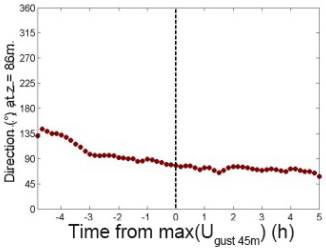


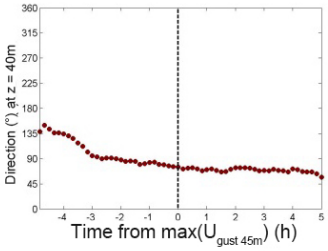
11 - Pintado 2008-04-24 to 2012-07-03. Event 39 with max($U_{gust\ 45m}$)= 17m/s on 2011-7-18 at 15:50. Series length: 48 months.

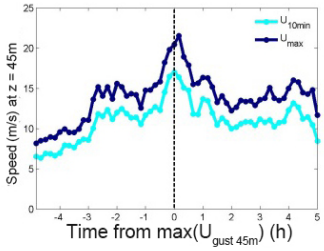




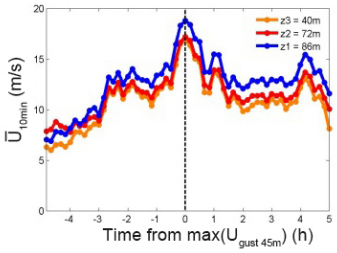


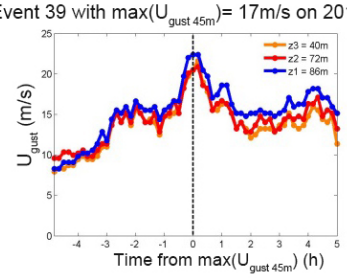


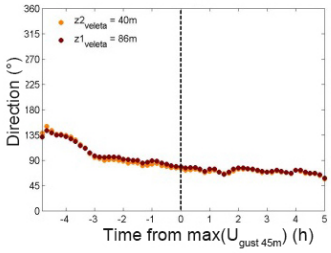


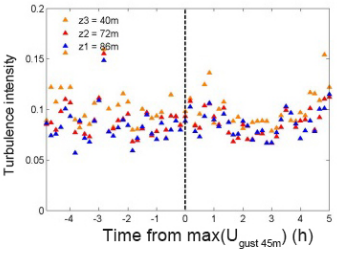


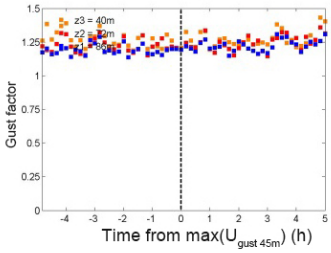
11 - Pintado 2008-04-24 to 2012-07-03. Event 39 with max($U_{gust\ 45m}$)= 17m/s on 2011-7-18 at 15:50. Series length: 48 months.

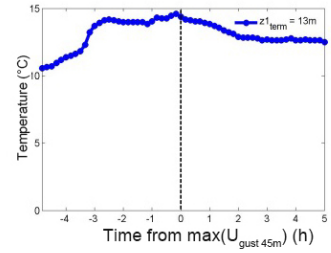


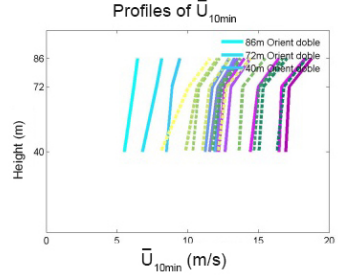


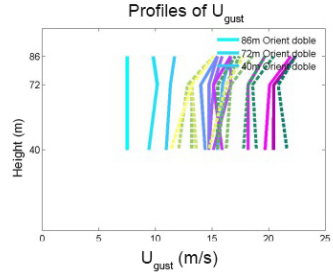


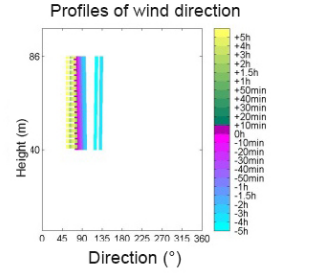




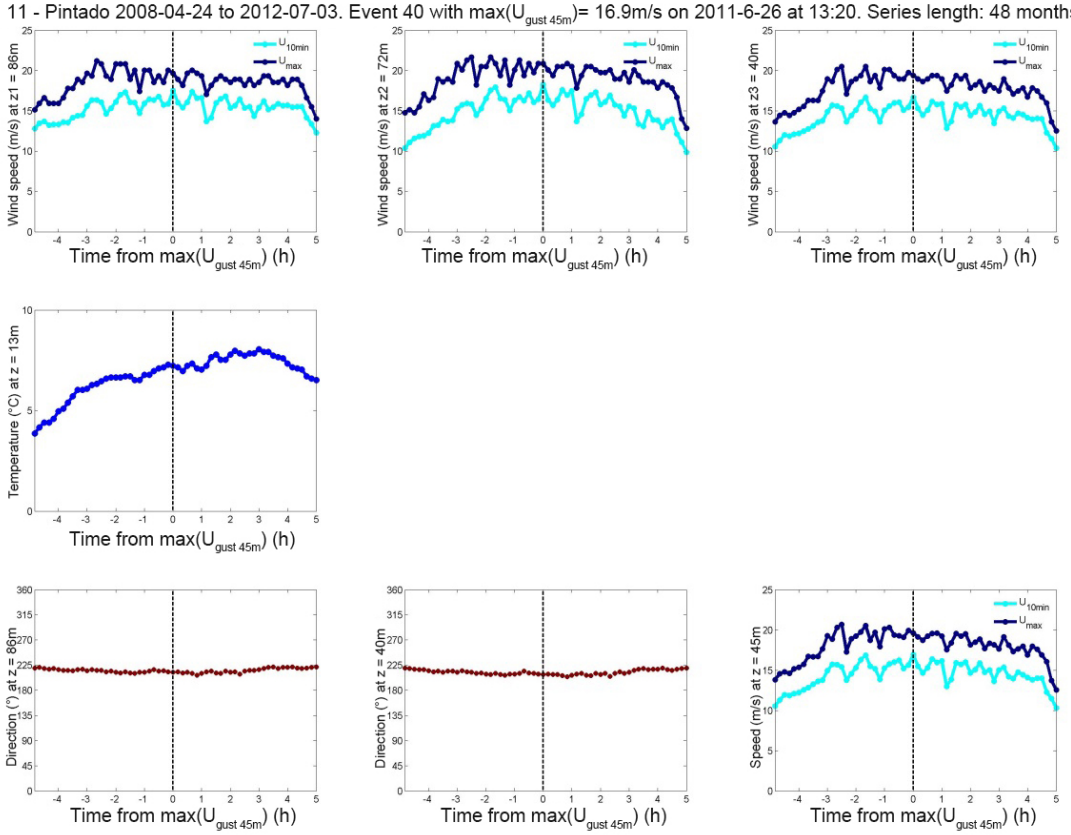




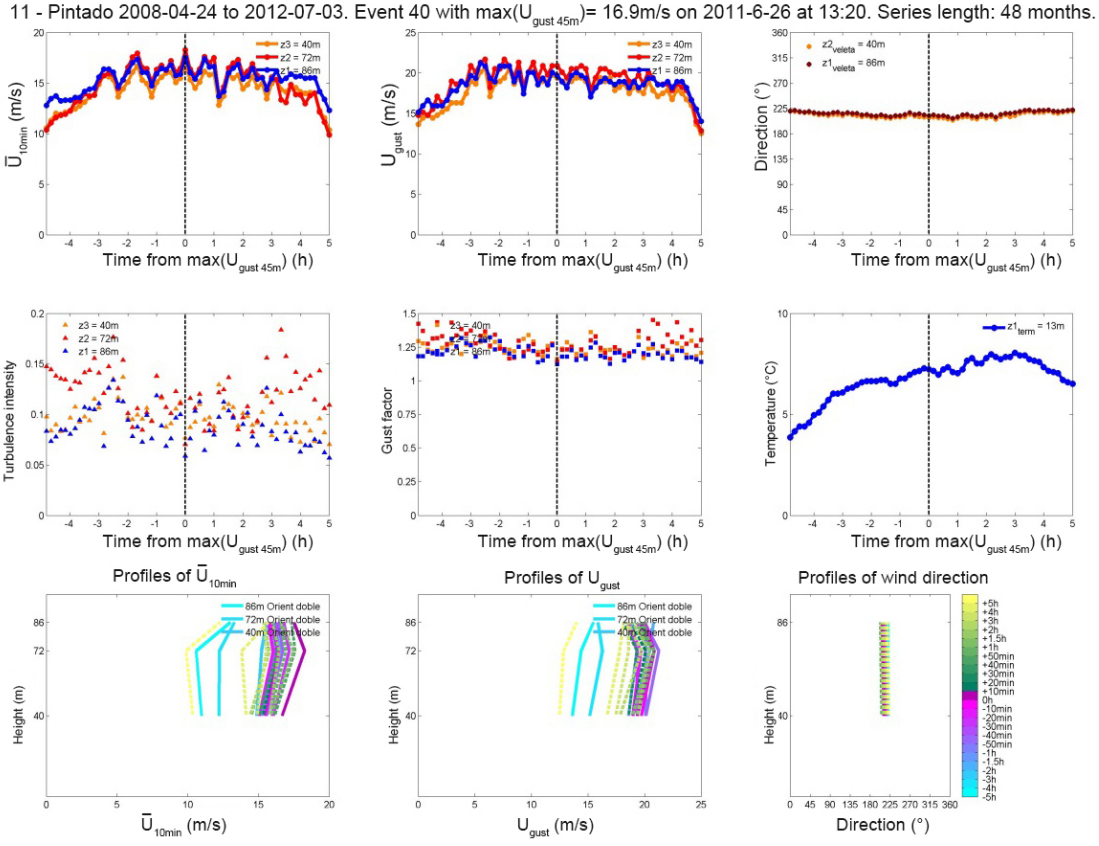




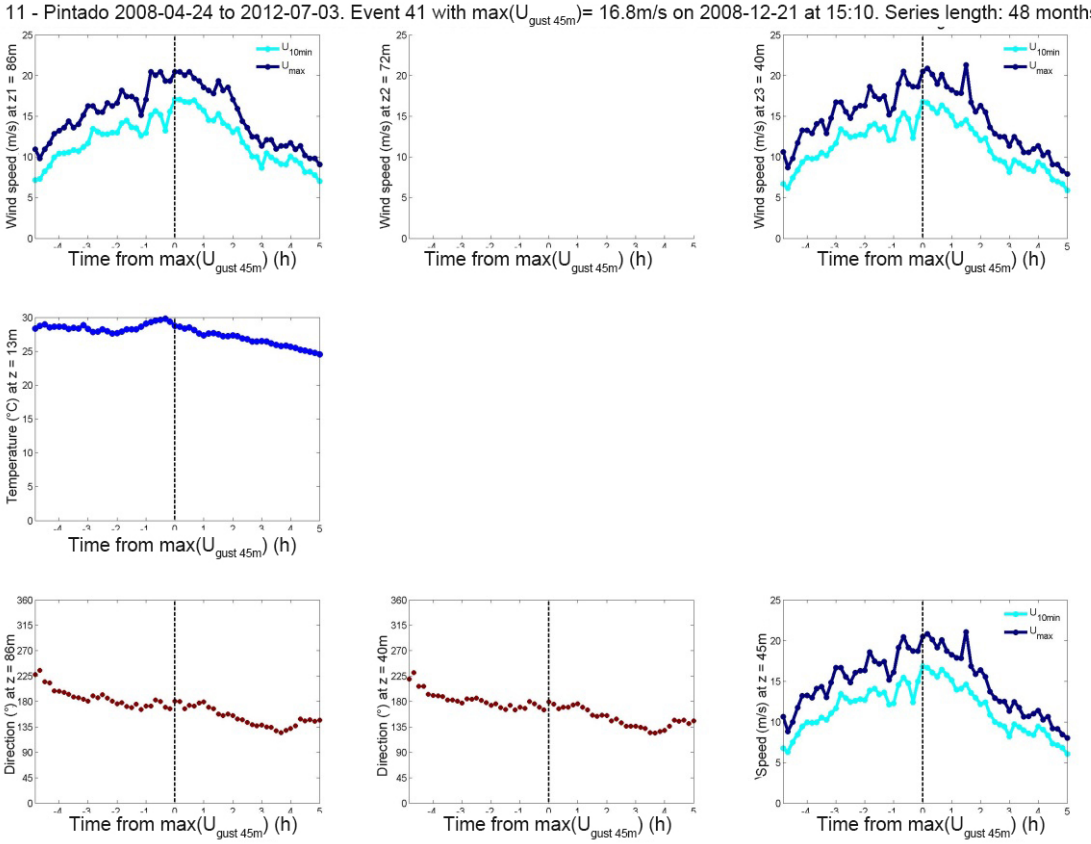
11 - Pintado 2008-04-24 to 2012-07-03. Event 40 with max($U_{gust\ 45m}$)= 16.9m/s on 2011-6-26 at 13:20. Series length: 48 months.



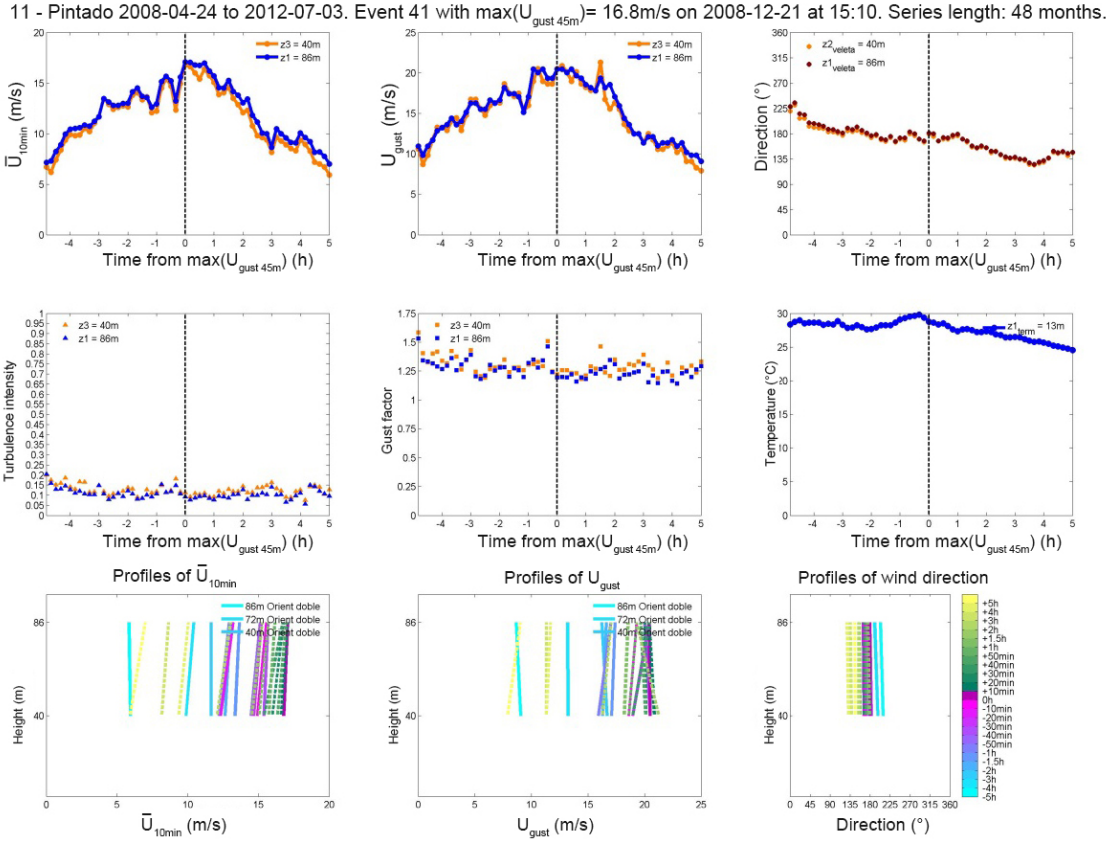
11 - Pintado 2008-04-24 to 2012-07-03. Event 40 with max($U_{gust\ 45m}$)= 16.9m/s on 2011-6-26 at 13:20. Series length: 48 months.



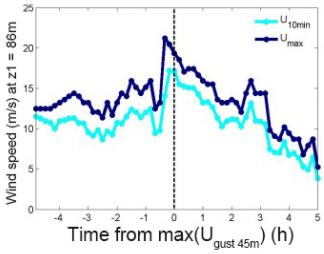
11 - Pintado 2008-04-24 to 2012-07-03. Event 41 with max($U_{gust\ 45m}$)= 16.8m/s on 2008-12-21 at 15:10. Series length: 48 months.

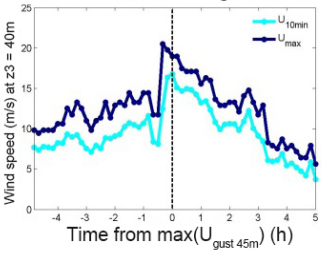


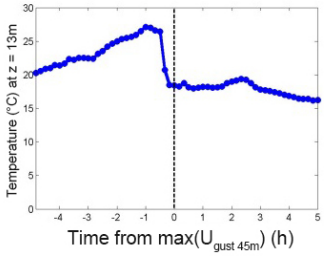
11 - Pintado 2008-04-24 to 2012-07-03. Event 41 with max($U_{gust\ 45m}$)= 16.8m/s on 2008-12-21 at 15:10. Series length: 48 months.

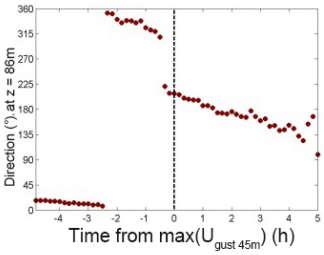


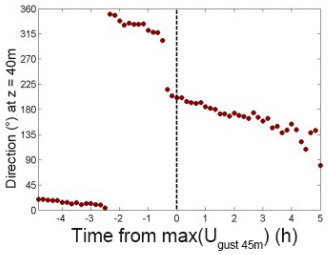
11 - Pintado 2008-04-24 to 2012-07-03. Event 42 with max($U_{gust\ 45m}$)= 16.8m/s on 2008-10-21 at 11:50. Series length: 48 months.

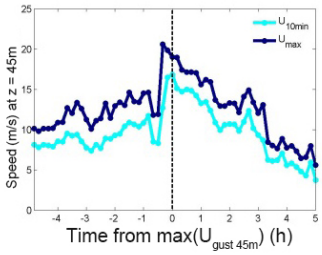




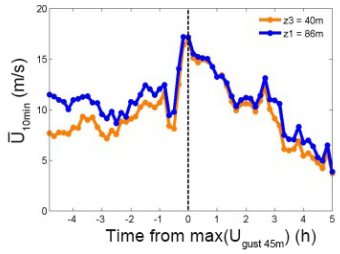


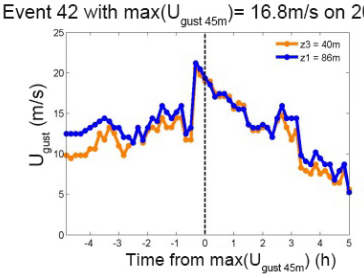


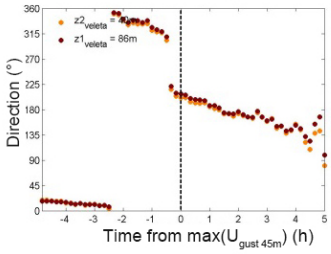


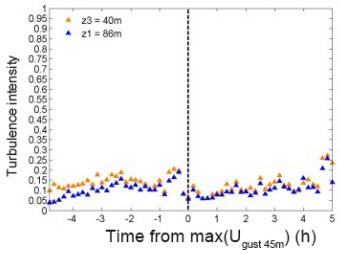


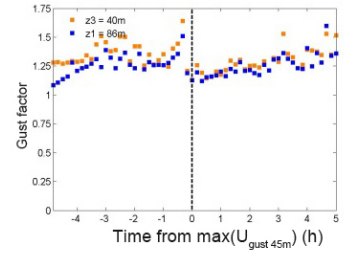
11 - Pintado 2008-04-24 to 2012-07-03. Event 42 with max($U_{gust\ 45m}$)= 16.8m/s on 2008-10-21 at 11:50. Series length: 48 months.

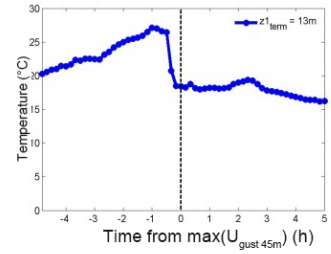


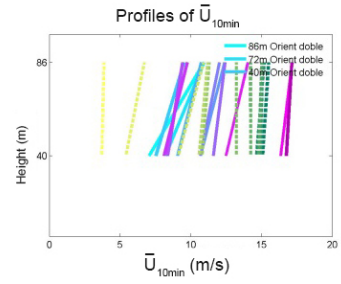


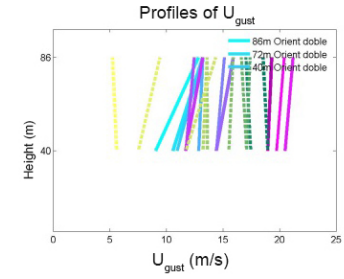


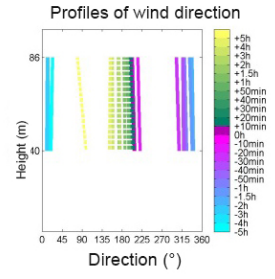




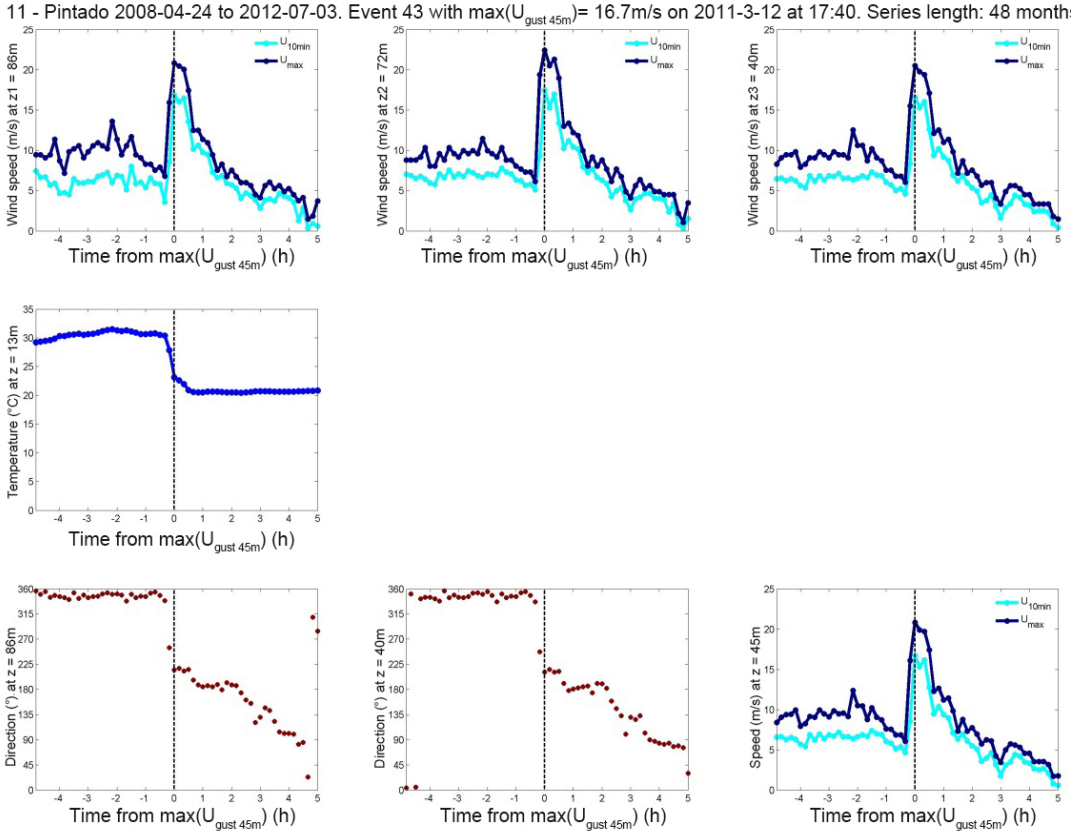




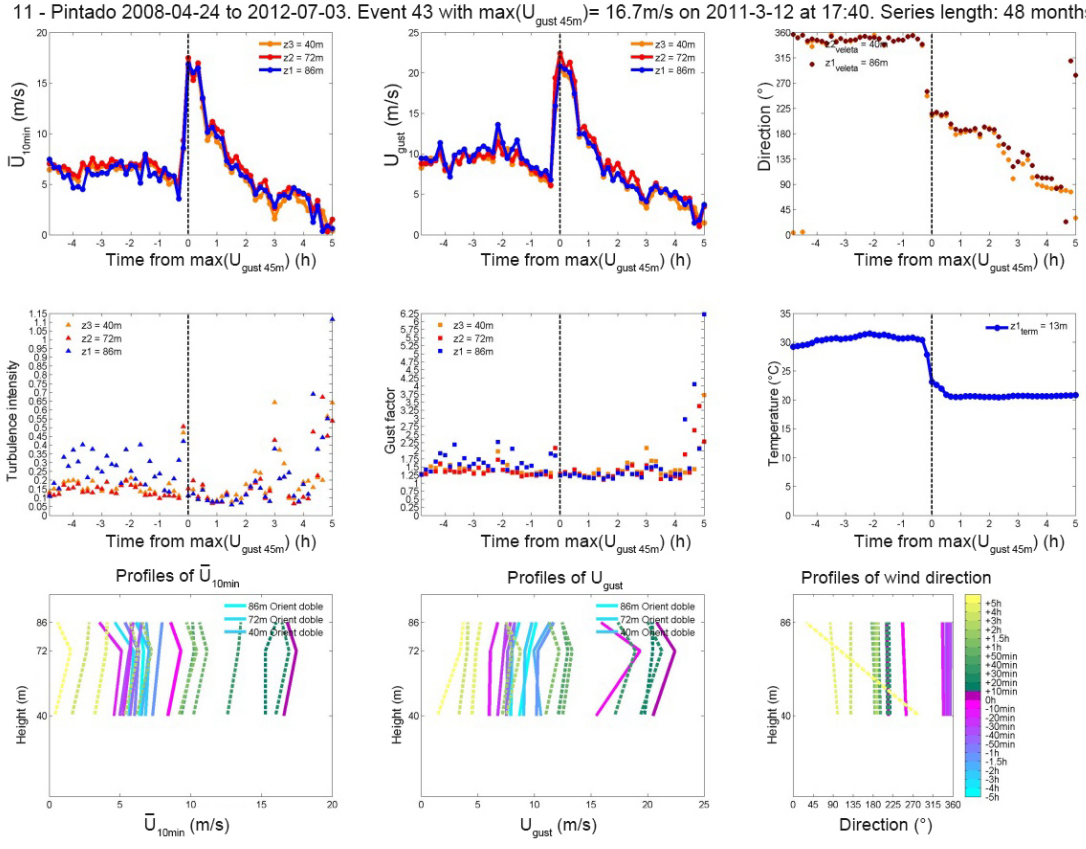




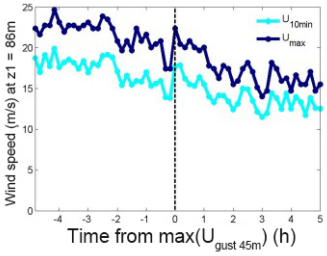
11 - Pintado 2008-04-24 to 2012-07-03. Event 43 with max($U_{gust\ 45m}$)= 16.7m/s on 2011-3-12 at 17:40. Series length: 48 months.

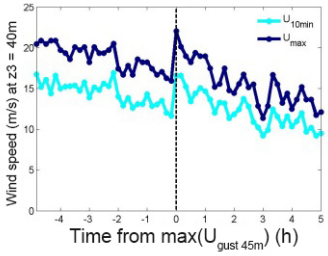


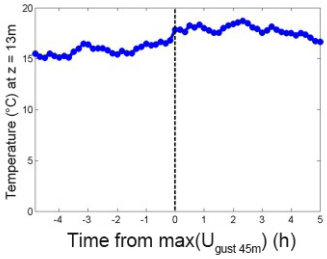
11 - Pintado 2008-04-24 to 2012-07-03. Event 43 with max($U_{gust\ 45m}$)= 16.7m/s on 2011-3-12 at 17:40. Series length: 48 months.

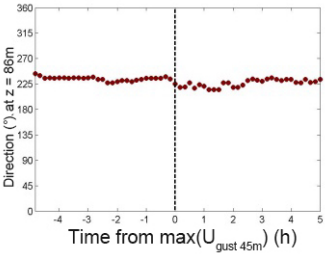


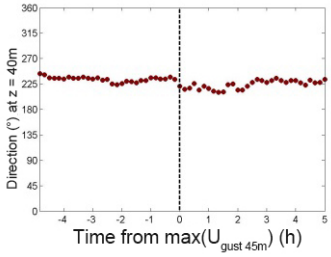
11 - Pintado 2008-04-24 to 2012-07-03. Event 44 with max($U_{gust\ 45m}$)= 16.7m/s on 2010-10-31 at 14:00. Series length: 48 months.

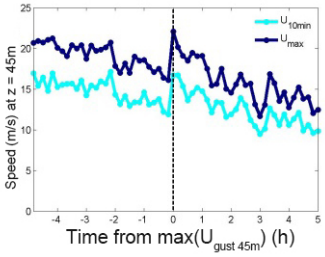




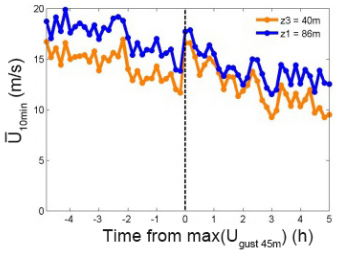


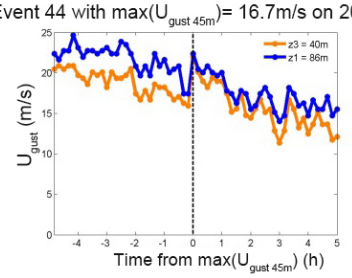


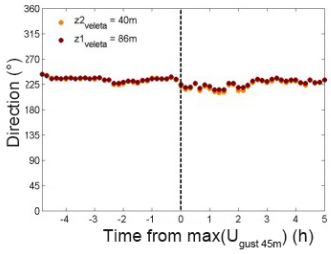


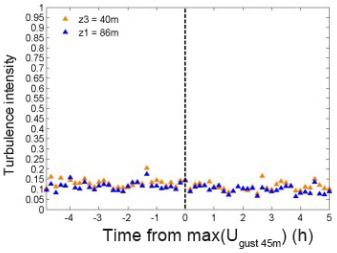


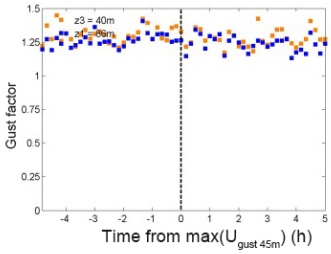
11 - Pintado 2008-04-24 to 2012-07-03. Event 44 with max($U_{gust\ 45m}$)= 16.7m/s on 2010-10-31 at 14:00. Series length: 48 months.

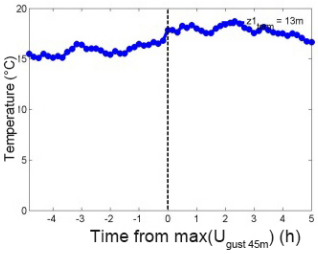


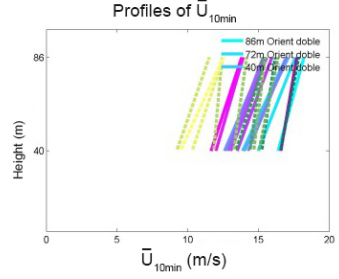


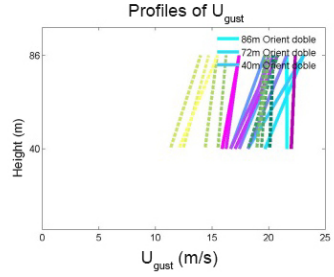


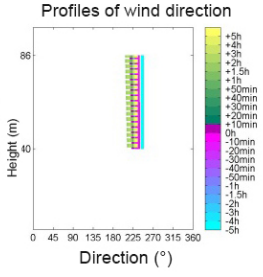




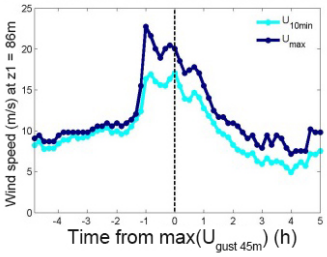


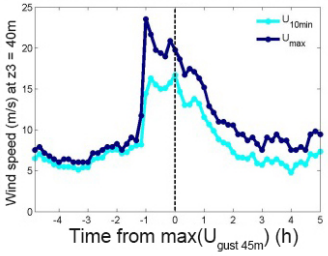


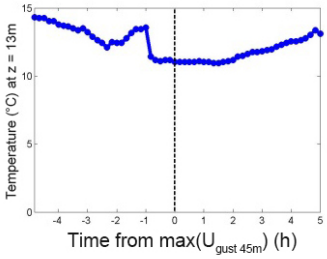


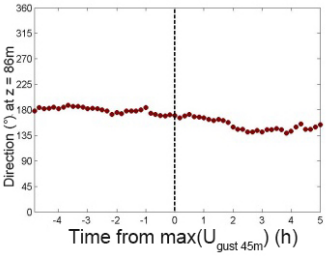


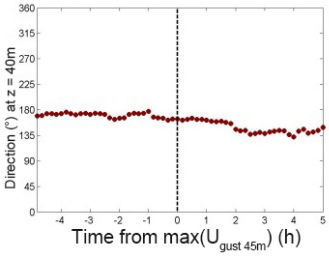
11 - Pintado 2008-04-24 to 2012-07-03. Event 45 with max($U_{gust\ 45m}$)= 16.7m/s on 2010-8-29 at 6:10. Series length: 48 months.

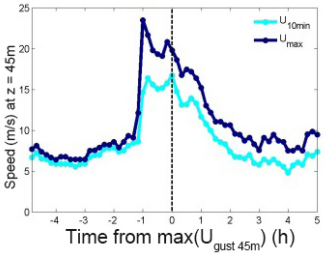












11 - Pintado 2008-04-24 to 2012-07-03. Event 45 with max($U_{gust\ 45m}$)= 16.7m/s on 2010-8-29 at 16:10. Series length: 48 months.

